STUDIES ON CALCIUM SIGNALING GENES *PHOSPHOLIPASE C-1*, *SECRETORY PHOSPHOLIPASE A2*, AND *CALCIUM PROTON EXCHANGER-1* IN *NEUROSPORA CRASSA*

A

thesis submitted in partial fulfillment of the

requirements for the award of the degree of

DOCTOR OF PHILOSOPHY

by

ANANYA BARMAN

Department of Biosciences and Bioengineering

Indian Institute of Technology

Guwahati, Assam, India

Pin-781039

June 2017

भारतीय प्रौद्योगिकी संस्थान गुवाहाटी
INDIAN INSTITUTE OF TECHNOLOGY GUWAHATI
Department of Biosciences and Bioengineering
Guwahati- 781 039

DECLARATION

I do hereby declare that the content embodied in this thesis entitled "Studies on calcium signaling genes *phospholipase C-1*, *secretory phospholipase A2*, and *calcium proton exchanger-1* in *Neurospora crassa*" is the result of investigations carried out by me in the Department of Biosciences and Bioengineering, Indian Institute of Technology Guwahati, for the award of degree of Doctor of Philosophy, under the supervisions of **Dr. Ranjan Tamuli** and **Prof. Utpal Bora**. The research presented in this thesis is original and has not been submitted in part or full for any degree or diploma to any other institute or university to the best of my knowledge and belief.

Guwahati
June, 2017

ANANYA BARMAN
(Roll No. 11610630)

भारतीय प्रौद्योगिकी संस्थान गुवाहाटी
INDIAN INSTITUTE OF TECHNOLOGY GUWAHATI
Department of Biosciences and Bioengineering
Guwahati- 781 039

CERTIFICATE

This is to certify that the research work in this thesis entitled "Studies on calcium signaling genes *phospholipase C-1*, *secretory phospholipase A2*, and *calcium proton exchanger-1* in *Neurospora crassa*" has been carried out at the Indian Institute of Technology Guwahati, by Ananya Barman (Roll No. 11610630), for the award of degree of Doctor of Philosophy in Biosciences and Bioengineering, under our supervision. The outcome of the research work presented in this thesis is original and has not been submitted in part or full for any degree or diploma to any other institute or university.

Guwahati
June, 2017

Thesis Supervisor: Dr. Ranjan Tamuli
Associate Professor
Department of Biosciences & Bioengineering

Thesis Co-Supervisor: Prof. Utpal Bora
Professor
Department of Biosciences & Bioengineering

List of Figures

List of Tables

List of Abbreviations

A	absorbance
ANOVA	analysis of variance
bp	base pair
BLAST	basic local alignment search tool
Ca^{2+}	calcium
cAMP	3′, 5′ cyclic adenosine monophosphate
CDD	conserved domain database
CFW	calcoflour white
CoA	coenzyme A
CPE-1	Ca^{2+}/H^{+} exchanger-1
CTC	chlortetracycline hydrochloride
°C	degree Celsius
cm	centimeter
DAG	diacylglycerol
DCFH-DA	2', 7'- dichlorofluorescein-diacetate
DiBAC	bis (1,3-dibutylbarbituric acid) trimethine oxonol
DNA	deoxyribonucleic acid
FGSC	Fungal Genetics Stock Center
λ_{ex}	fluorescence excitation wavelength
λ_{em}	fluorescence emission wavelength
g	gram
GFP	green fluorescent protein
GPCRs	G-protein-coupled receptors
GPI	glycophosphatidylinositol
h	hour
hph	hygromycin B resistance gene
IP_3	inositol-1, 4, 5-trisphosphate
J/m^2	joule per square meter
K	Kelvin
kb	kilobase

kPa	kilopascal
KV	kilovolt
LG	linkage group
M	Molar
MAPK	mitogen-activated protein kinase A
MEGA	molecular evolutionary genetic analysis version
µF	microfarad
µg	microgram
µl	microliter
mg	milligram
ml	milliliter
mM	millimolar
mm	millimeter
ms	milliseconds
min	minute
N	normal
NAC	N-Acetyl-L-cysteine
NADPH	nicotinamide adenine dinucleotide phosphate
NAG	N-acetylglycine
NCBI	National Center for Biotechnology Information
NCU	*Neurospora crassa* unit
NIH	National Institute of Health
NLS	nuclear localization signal
NPN	1-N-Phenylnaphthylamine
ng	nanogram
nm	nanometer
Ω	ohms
OD	optical density
ORF	open reading frame
P	probability
PCR	polymerase chain reaction

PH	pleckstrin homology
PHS	phytosphingosine
PLC-1	phospholipase C-1
psi	Pounds per square inch
RIP	repeat-induced point mutation
RNA	ribonucleic acid
ROS	reactive oxygen species
RT-PCR	reverse transcriptase polymerase chain reaction
rpm	revolutions per minute
qPCR	quantitative real time polymerase chain reaction
SCM	synthetic crossing medium
sec	second
sPLA2	secretory phospholipase A2
STRING	search tool for the retrieval of interacting genes/proteins
UV	ultraviolet
v/v	volume/volume
V/cm	Volt per centimeter
VGM	Vogel's glucose medium
w/v	weight/volume

Acknowledgements

First and foremost, I owe my deepest gratitude to my supervisor, Dr. Ranjan Tamuli, who introduced me to the fascinating world of Neurospora crassa. Words are less to express my gratitude towards him for his constant guidance and support throughout my PhD. I am grateful to him for patiently going through the various versions of my thesis. I also thank my co-supervisor, Prof. Utpal Bora, for his mentorship and support throughout my research time at the IITG.

I would like to express my sincere regards to all my doctoral committee members Prof. Aiyagari Ramesh, Dr. Anil Mukund Limaye and Prof. Gopal Das for their noble suggestions and constructive criticisms on my work that has eventually helped me for successful completion of my thesis.

I would take this opportunity to thank the present and previous Directors of IITG and Head of the Department of Biosciences and Bioengineering for providing me all the necessary facilities and support. I specially acknowledge the financial support from MHRD for providing me fellowship to successfully carry out my research work.

I am ever so grateful to the Fungal Genetics Stock Centre (FGSC), University of Missouri, Kansas city, USA, for readily providing Neurospora strains, charges of which were generously waived.

Lab is like a family and the warmth of this is provided by the lab members. I am grateful to all my present RT lab members Anand Sir, Dibakar, Ajeet, Avishek, Christy, Darshana and Serena for their warmth, suggestions, continuous support, and help. I sincerely like to thank my previous lab members Rekha Di, Ravi Bhaiya, Vijya, Upasana, Ravi Gedela, Yutika, Jagadeesh, Rimlee, Mayurakhi, Vishakha and Manju for helping me in countless number of ways.

I thank all my friends in IITG especially Manash, Prakash, Ruchi, Neha and Thyahoo who have always brightened my days and cheered my heart during my hard days making my stay in IITG a memorable one. I offer my regards to my close friends Mayurakshi, Seemana, Bhargav and Uttam for supporting me during the completion of my PhD.

I would like to pay my heartiest regards and love to my father, my mother, my elder brother, my sister-in-law and my younger sister for believing in me and showering their love towards me which motivated me for successful completion of my PhD. Thank you Maa and Deuta.

Above all, praises and thanks to the God, the Almighty, for His showers of blessings throughout my research work to complete the research successfully.

Finally, my thanks go to all the wonderful people who have supported me to complete the research work directly or indirectly.

June, 2017 *Ananya Barman*

Synopsis

The ascomycete *Neurospora crassa* is a naturally occurring filamentous fungus typically found in tropical and subtropical areas, mainly on dead and burned vegetation (Luque et al. 2012). *N. crassa* has been established as an excellent eukaryotic model organism and used extensively to understand different aspects of complex biological processes including the calcium (Ca^{2+}) signaling machinery. Ca^{2+} has evolved as a universal second messenger and plays a central role in intracellular signaling in eukaryotes, yet little is known about the Ca^{2+} signaling mechanism in *N. crassa* or any other related fungi in comparison to plants and animals. In *N. crassa*, Ca^{2+} signaling regulates a variety of processes such as Ca^{2+} stress tolerance, the circadian clock, growth, hyphal tip branching, ion transport, ultraviolet (UV) survival, and sexual development (Deka et al. 2011; Deka and Tamuli 2013; Tamuli et al. 2011; 2013; Kumar and Tamuli 2014). The predicted Ca^{2+} signaling machinery of *N. crassa* is complex and comprises of 48 mostly uncharacterized Ca^{2+} signaling proteins, including three Ca^{2+} channel proteins, nine Ca^{2+}/cation- ATPases, six recognizable Ca^{2+}/H^{+} exchangers, two novel putative Ca^{2+}/Na^{+} exchangers, four novel phospholipase C-δ subtype (PLC- δ) proteins, 23 Ca^{2+} and/or calmodulin (CaM) binding proteins, and one CaM, and these proteins effectively coordinate for triggering a range of cellular responses (Galagan et al. 2003; Borkovich et al. 2004; Zelter et al. 2004). In *N. crassa*, the release of Ca^{2+} from intracellular Ca^{2+} stores, which differs significantly from plants and animals, remains to be identified, and knowledge about this might provide novel antifungal targets for drug discovery (Galagan et al. 2003; Borkovich et al. 2004; Zelter et al. 2004).

Chapter 1 briefly describes about the history and life cycle of *N. crassa* and overview of Ca^{2+} signaling in *N. crassa*. In eukaryotes, the resting cytosolic free calcium concentration ($[Ca^{2+}]_c$) is ~100 nm and its increase is detected by specific Ca^{2+}-sensing proteins that initiate the Ca^{2+} signaling process (Chin and Means 2000; Bootman et al. 2001). In *N. crassa*, several Ca^{2+} signaling proteins, including the phospholipase C (PLC), secretory phospholipase A_2 ($sPLA_2$), and Ca^{2+} exchangers are involved in sensing the increase in $[Ca^{2+}]_c$ (Galagan et al. 2003; Borkovich et al. 2004; Barman and Tamuli 2017). The PLC and $sPLA_2$ belong to the phospholipase superfamily of proteins. The phosphoinositide-specific PLC catalyses the hydrolysis of phosphatidylinositol-4, 5-bisphosphate (PIP_2) into two second messengers, inositol-1, 4, 5-trisphosphate (IP_3) that induces Ca^{2+} release from intracellular Ca^{2+} stores via IP_3 receptors to modulate Ca^{2+} and calmodulin regulated pathways, and diacylglycerol (DAG) that binds at Ca^{2+} dependent C2 domain

and activates protein kinase C (PKC) protein (Clapham 2007). Interestingly, no recognizable IP_3 receptors have been identified so far in *N. crassa* and both of its PKC proteins lack a C2 domain with Ca^{2+} binding sites (Galagan et al. 2003; Borkovich et al. 2004). The majority of eukaryotic PLCs consists of two catalytic domains X and Y, an N-terminal pleckstrin homology (PH) domain for interaction with membrane phospholipid, a C-terminal Ca^{2+} dependent C2 domain for phospholipid binding, and an EF-hand motif for Ca^{2+} binding and interaction of PH with phospholipid (Bristol et al. 1988; Watson and Arkinstall 1994; Sutton et al. 1995; Rhee and Bae 1997; Yamamoto et al. 1999). *N. crassa* possesses four novel PLC-δ subtype proteins, including the PLC-1 that lacks the PH domain, but consists of catalytic X and Y domains, and a C2-like domain (Borkovich et al. 2004; Gavric et al. 2007; Barman and Tamuli 2015). PLC regulates a number of biological functions in different organisms ranging from yeast, filamentous fungi to animals. In addition, the relatively low molecular weight $sPLA_2$ proteins are Ca^{2+} dependent extracellular secretory enzymes with a highly conserved region that contains His-Asp dyad sequence responsible for catalytic activity and a number of unique disulfide bonded Cys residues required for the stability of these enzymes (Murakami and Kudo 2004; Schaloske and Dennis 2006; Nakahama et al. 2010). A majority of eukaryotic $sPLA_2$ enzymes also have an N terminal signal peptide for secretion that is cleaved upon internalization into the endoplasmic reticulum or into the periplasm as in bacteria and a catalytic center, which contains a tightly bound water molecule that acts as a potential nucleophile (Verheij et al. 1980; Pickard et al. 1996; Dennis et al. 2011; Cavazzini et al. 2013). This family of enzymes regulate a number of biological processes such as atherosclerosis, eicosanoid biosynthesis, host defense, and inflammation in various organisms (Murakami and Kudo 2004; Boilard et al. 2010; Dennis et al. 2011). In contrast to other fungi, little is known about the *N. crassa* homologues of the PLC and $sPLA_2$, therefore, I studied the role of these two Ca^{2+} signaling genes in regulating various cell functions in *N. crassa* (Barman and Tamuli 2015; 2017). I also studied the cellular role of a unique Ca^{2+}/H^+ exchanger (CPE-1) that shows significant difference from its homologues found in *Saccharomyces cerevisiae* and *Magnaporthe grisea* in a phylogenetic analysis (Zelter et al. 2004; Barman and Tamuli 2015). I also investigated double mutants of the *N. crassa* strains involving the *plc-1*, *splA2*, and *cpe-1* genes to understand the significance of genetic interactions of these loci in regulating vegetative growth and sexual development in *N. crassa* (Barman and Tamuli 2017).

Chapter 2 describes materials and methods used in my thesis work. Growth, maintenance, and crosses of *N. crassa* strains were essentially as described previously (Westergaard and Mitchell 1947; Davis and de Serres 1970). The *N. crassa* strains used in this study were either obtained from the Fungal Genetics Stock Center (FGSC, Manhattan, KS) or generated in our laboratory. Chemicals and reagents were procured from the standard suppliers, and used after autoclave or filter sterilization whenever required. Cloning, PCR, Reverse Transcriptase PCR, Real Time PCR, and other molecular biology experiments were performed by using the standard protocols essentially as described by Sambrook and Russell (2001) or according to manufacturer's instructions.

Chapter 3 describes the cellular roles of PLC-1, sPLA2, and CPE-1 in *N. crassa*. The *N. crassa* strains lacking *plc-1*, *splA2*, and *cpe-1* exhibited growth defects in response to increase in cytosolic $[Ca^{2+}]_c$ induced by the divalent ionophore A23187, suggesting a role for these genes in maintaining $[Ca^{2+}]_c$. The knockout mutants of the *plc-1*, *splA2*, and *cpe-1* genes also showed significantly higher carotenoid content at 8, 22, and 30°C and increased UV survival under conditions that induced carotenoid accumulation. In addition, the *plc-1*, *splA2*, and *cpe-1* knockout mutant strains showed reduced survival in hydrogen peroxide induced oxidative stress and induced thermotolerance after exposure to heat shock temperatures. The Δ*plc-1,* Δ*splA2*, and Δ*cpe-1* mutants carrying the *plc-1*, s*plA2*, and *cpe-1* transgenes complemented the carotenoid accumulation, oxidative stress, and thermotolerance phenotypes of the respective mutants. Therefore, this study revealed multiple cellular roles of *plc-1*, *splA2*, and *cpe-1* genes in the regulation of $[Ca^{2+}]_c$, carotenoid accumulation, survival under stress conditions, and acquisition of induced thermotolerance.

Chapter 4 describes the genetic interactions of the *plc-1*, *splA2*, and *cpe-1* genes. I generated and studied the phenotypes of the double mutants of *plc-1*, *splA2*, and *cpe-1* genes to understand the genetic interactions between these loci. The Δ*plc-1*; Δ*splA2*, Δ*plc-1*; Δ*cpe-1*, and Δ*cpe-1*; Δ*splA2* double mutants were generated by crossing the respective single mutant strains of opposite mating types. The Δ*plc-1*; Δ*splA2* and Δ*plc-1*; Δ*cpe-1* double mutants showed colonial morphology, aberrant hyphal branching, slower growth rate, shorter aerial hyphae, reduced biomass accumulation, early conidiation with delayed germination, inappropriate conidiation of submerged cultures, and slower carotenoid accumulation. In addition, crosses involving the Δ*plc-1*; Δ*splA2* and Δ*plc-1*; Δ*cpe-1* double mutants as the female parent with the respective double or

parental single mutants and wild type strains of opposite mating type as the male parent showed complete absence of perithecia and resulted in a sterile phenotype. Interestingly, higher carotenoid accumulation in the Δ*plc-1*, Δ*splA2*, and Δ*cpe-1* mutants were linked to an increased level of intracellular reactive oxygen species (ROS). The Δ*plc-1*; Δ*splA2* and Δ*plc-1*; Δ*cpe-1* double mutants also showed aberrant hyphal morphology on medium treated with the ionophore A23187, and showed increased sensitivity to Ca^{2+} and UV stress and decreased survival percentage in oxidative stress and acquisition of thermotolerance induced by heat shock. However, the Δ*cpe-1*; Δ*splA2* double mutant did not show any synthetic effect on growth, sexual development, Ca^{2+} and UV stress, indicating no genetic interaction between *cpe-1* and *splA2*. Therefore, this study revealed that genetic interactions between *plc-1*, *splA2*, and *cpe-1* loci plays a crucial role for normal vegetative and sexual development in *N. crassa*.

Chapter 5 describes studies to understand the molecular basis of the *plc-1*, *splA2*, and *cpe-1* functions, and a possible mechanistic model. Ca^{2+} signaling machinery acts in coordination with other signaling pathways for regulation of cellular processes that result in crosstalk between the signaling pathways (Sanders et al. 2002; Berridge et al. 2003). The crosstalk between the cAMP and Ca^{2+} signaling pathways has been well studied in plant and animal cells including the filamentous fungus *Aspergillus niger* (DeBernardi and Brooker 1996; Moore et al. 1998; Volotovski et al. 1998; Gorbunova and Spitzer 2002; Zaccolo and Pozzan 2003; Benčina et al. 2005). However, I found that the addition of cAMP did not rescue the phenotypes of the Δ*plc-1*, Δ*splA2*, and Δ*cpe-1* and their double mutants. This result indicates that the Ca^{2+} signaling responses mediated by the *plc-1*, *splA2*, and *cpe-1* genes occur via a cAMP independent mechanism. In addition, chlortetracycline hydrochloride (CTC) staining of Δ*plc-1*; Δ*splA2* and Δ*plc-1*; Δ*cpe-1* double mutants showed depleted Ca^{2+}gradient, indicating that the double deletion of the *plc-1* and *splA2*, and *plc-1* and *cpe-1* causes disruption of Ca^{2+} homeostasis resulting in phenotypic abnormalities. I also performed quantitative real time PCR (qRT-PCR) and determined fold change expression of some of the important genes such as conidiation specific gene *con-10*, carotenoid biosynthetic genes *al-1*, *al-2*, and *al-3*, and the pheromone signaling genes *ccg-4*, *mfa-1*, and *fmf-1*, and found that the product of these genes regulate the conidiation, carotenoid accumulation, and pheromone signaling of the *plc-1*, *splA2*, and *cpe-1* genes. Taken together, these findings suggest that the Ca^{2+} release from intracellular stores, which is induced by IP_3 generated by the PLC-1, and/or activated PKC might be necessary for the sPLA2 mediated signaling for

normal growth and development in *N. crassa*. In addition, under the conditions inducing sexual development, release of Ca^{2+} mediated by the PLC-1 and the $[Ca^{2+}]_c$ buffering activity of the CPE-1 Ca^{2+}/H^+ exchanger might be important in the regulation of the pheromone signaling genes necessary for fertility.

Thus, in this study, I determined multiple cellular roles of *plc-1*, *splA2*, and *cpe-1* in regulation of $[Ca^{2+}]_c$, carotenoid accumulation, survival under stress conditions, and acquisition of thermotolerance induced by heat shock. Moreover, I found that interaction of *plc-1* with *splA2*, and *plc-1* with *cpe-1* is essential for maintaining Ca^{2+} homeostasis. In addition, I found that the interactions between the *plc-1*, *splA2*, and *cpe-1* loci play an important role in both vegetative and sexual developments in *N. crassa*. Furthermore, I found that Ca^{2+} signaling mediated by *plc-1*, *splA2*, and *cpe-1* is regulated by few developmentally important genes such as *con-10*, *ccg-4*, *mfa-1*, and *fmf-1*. Therefore, this study revealed the cellular functions, genetic interactions, and molecular targets of the Ca^{2+} signaling genes *plc-1*, *splA2*, and *cpe-1* in *N. crassa*.

Dedicated

to

my parents

Dr. Atul Kumar Barman

&

Mrs. Bharati Barman

Chapter 1

An introduction to Neurospora crassa and calcium signaling

1.1 Introduction to *Neurospora crassa*

1.1.1 The biology of *N. crassa*

Neurospora, meaning 'nerve spores' due to characteristics nerve like stripes in its sexual spores, is a filamentous fungus extensively used as a model organism for several decades for understanding numerous aspects of eukaryotic cell biology, genetics, biochemistry, and molecular biology (Perkins 1992; Davis 2000; Davis and Perkins 2002; Galagan et al. 2003). *Neurospora crassa* belongs to the phylum Ascomycota and it was originally discovered as the causative organism of orange bread mould infestations in French bakeries and was independently reported as *Oidium aurantiacum* (Payen 1843) and *Penicillium sitophilum* (Montagne 1843). In mid 1920s, Dodge and Shear identified *N. crassa* as a heterothallic fungus comprising of two mating types, *A* and *a* with eight ordered asci while Bernard Lodge and Carl Lindegren together demonstrated Mendelian inheritance in individual asci (Shear and Dodge 1927; Dodge 1939; Perkins 1992). In addition, genetic map of the sex chromosome of *N. crassa* was the first fungus chromosomal map to be reported by Lindegren (Lindegren 1936). Subsequent work on Neurospora by Beadle and Tatum introduced the 'one gene one enzyme' hypothesis (Beadle and Tatum 1941) for which they were awarded the Nobel Prize in "Physiology or Medicine" in 1958 for their discovery that the characteristic function of a gene is to control the synthesis of a particular enzyme. Thus, *N. crassa* has emerged as an excellent eukaryotic model organism and contributed significantly in understanding various aspects of biological processes such as cellular differentiation and development, DNA methylation and repair, genome defense mechanisms, mitochondrial transport, and post transcriptional gene silencing (Davis 2000; Davis and Perkins 2002; Galagan et al. 2003). *N. crassa* is a simple, multicellular, heterothallic, haploid organism. The genome of *N. crassa* is 43 Mb in size that contains 10,082 protein coding genes and is divided into seven linkage group (LG I-VII, ranging in size from 4 to 10.3 Mb each; Davis and de Serres 1970; Davis and Perkins 2000; Galagan et al. 2003). As a heterotrophic organism, *N. crassa* utilizes carbon and nitrogen, few simple salts, trace elements, biotin, and a single vitamin for its growth while depending on growth conditions, it propagates asexually or reproduces sexually. It is a saprophyte, exclusively found growing on dead and decomposed organic substrates. Neurospora possesses the widest array of genome defense mechanisms that operates in distinct phases of its life cycle, a reversible post transcriptional gene silencing (PTGS) mechanism known as 'quelling' (Romano and Macino 1992) occurs in its vegetative phase, and a transcriptional gene silencing (TGS) mechanism known

as ‘repeat-induced point mutation-RIP’ (Cambareri et al 1989) unique to fungi and meiotic silencing, a PTGS mechanism (Shiu et al. 2001) occurs during its sexual phase.

1.1.2 The life cycle of *N. crassa*

N. crassa is a multicellular fungus with a complex life cycle consisting of both asexual (vegetative) and sexual phase (Raju 1992; Springer 1993). In the presence of abundant nutrients, *N. crassa* enters the asexual cycle whereby it forms multinucleate branched filaments or vegetative hyphae that extends parallel to the surface of the solid medium (Springer 1993). Continued hyphal growth and branching forms the multicellular mycelium (Springer 1993). The hyphae are segmented by internal cross walls or septa that allows the movement of mitochondria, organelles, and other inclusions between cells. Under conditions of nutrient limitations or in the presence of an air-water interface, specialized aerial hyphae develops from the mycelium that give rise to conidiophores and subsequently produces multinucleate asexual spores called macroconidia or uninucleate microconidia (Springer 1993). Macroconidia are primarily used as inoculum for vegetative cultures and also serve as a fertilizing male parent in a sexual cross. Submerged cultures of *N. crassa* normally maintains vegetative non-conidiating hyphae, however, certain environmental cues such as carbon or nitrogen starvation and exposure to high temperatures can also produce conidiophores or conidia in submerged cultures (Cortat and Turian 1974; Guignard et al. 1974; Plesofsky-Vig et al. 1983; That and Turian 1978).

N. crassa is a heterothallic filamentous fungus with two nonswitching mating types that are determined by alternative DNA sequence called idiomorphs at one mating type locus, *mat A* and *mat a*. Nitrogen starvation, light, and low temperature initiates the sexual cycle that results in the formation of female reproductive structures termed protoperithecia (Raju 1992). A specialized hyphae (trichogyne) originating from the protoperithecium undergoes chemotropic growth towards a male cell of opposite mating type that is typically a hyphal fragment, macroconidium, or microconidium. Fusion between the trichogyne and the conidium is followed by transport of the male nucleus to the protoperithecium that initiates development of the multicellular sexual apparatus called ‘perithecium’ (matured protoperithecium). The male and female nuclei do not fuse immediately rather coexist as a dikaryon in specialized structures called ascogenous hyphae. The paired male and female nuclei then undergoes a series of synchronous mitotic divisions at the tip of a specialized hook shaped structure called the crozier. During karyogamy, nuclei of the

opposite mating type fuse to form a diploid zygote which immediately undergo two meiotic divisions and a post meiotic mitosis yielding an octad of eight spindle shaped sexual spores called ascospores that are packaged in a linear order in the narrow ascus. Once matured, the ascospores are eventually ejected through a beak (ostiole) at the tip of the perithecium in the direction of blue light. In the presence of suitable nutrients, the released ascospores eventually germinate and produce their own vegetative hyphae (Figure 1.1; Raju 1980; 1992; Springer 1993; Kim et al. 2012).

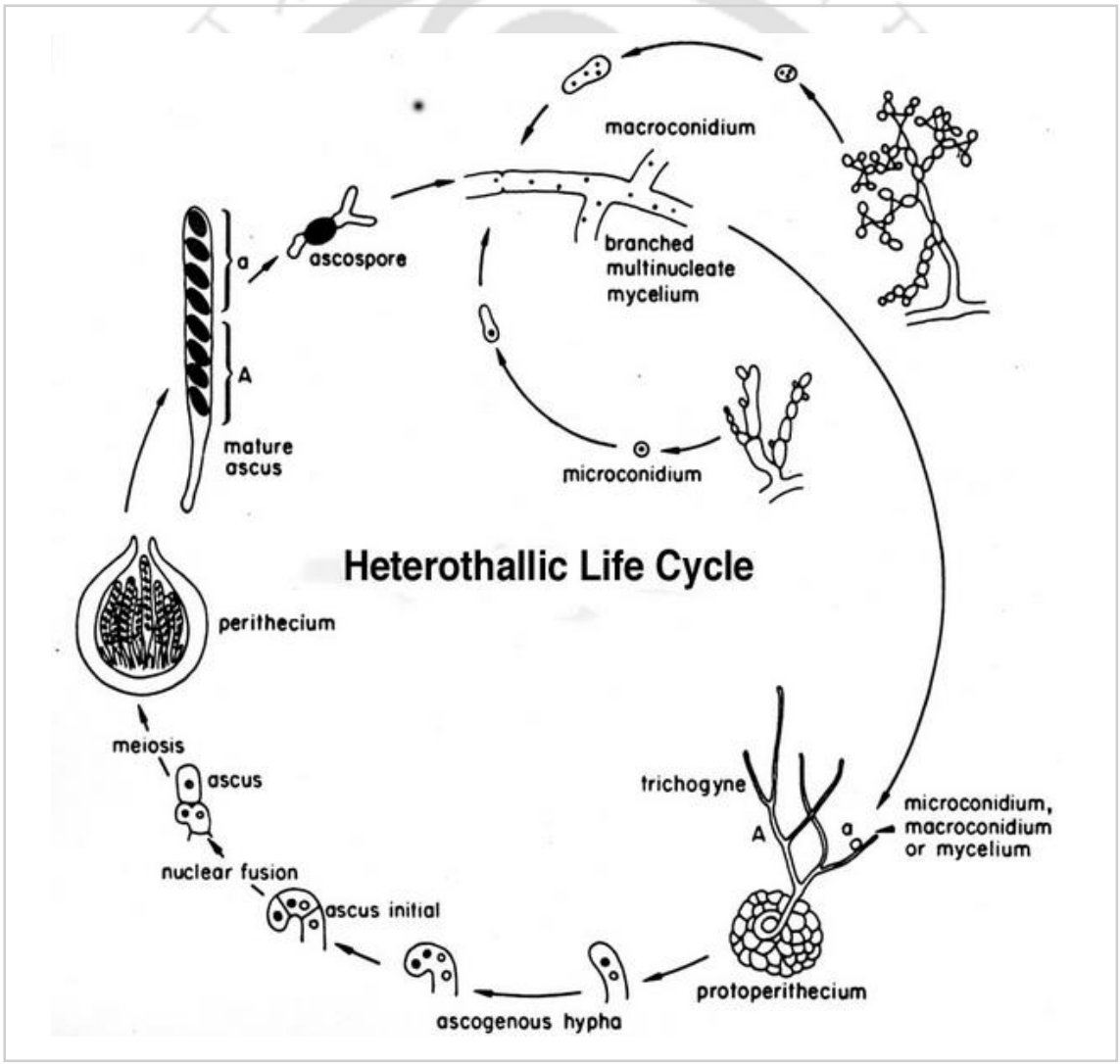

Figure 1.1: The life cycle of *N. crassa*. In the asexual cycle, the branched multinucleate vegetative mycelium develops into aerial hyphae and forms multinucleate asexual spores called macroconidium or uninucleate microconidium that eventually germinate to form new mycelium.

Sexual cycle begins with the formation of a female reproductive structure called protoperithecium and is fertilized by a conidium or mycelium of opposite mating type of a male parent. The fertilized protoperithecium (matured perithecium) undergoes a series of mitotic and meiotic divisions forming eight linearly ordered ascospores within an ascus. Once released, the matured multinucleate and pigmented ascospores develops into new hyphae and forms the multicellular mycelium to complete the asexual cycle or serves as male or a female parent and undergo the sexual cycle. Adapted from FGSC (http://www.fgsc.net/Neurospora/sectionB2.htm).

1.2 Calcium signaling in *N. crassa*

N. crassa possesses a wide array of environmental sensory capabilities and therefore, serves as an outstanding model organism for investigations of signaling. The intracellular signaling pathways that operate in *N. crassa* includes signaling mediated by G-protein-coupled receptors (GPCRs), signaling mediated by mitogen-activated protein kinase (MAPK), and signaling mediated by intracellular calcium (Ca^{2+}; Figure 1.2).

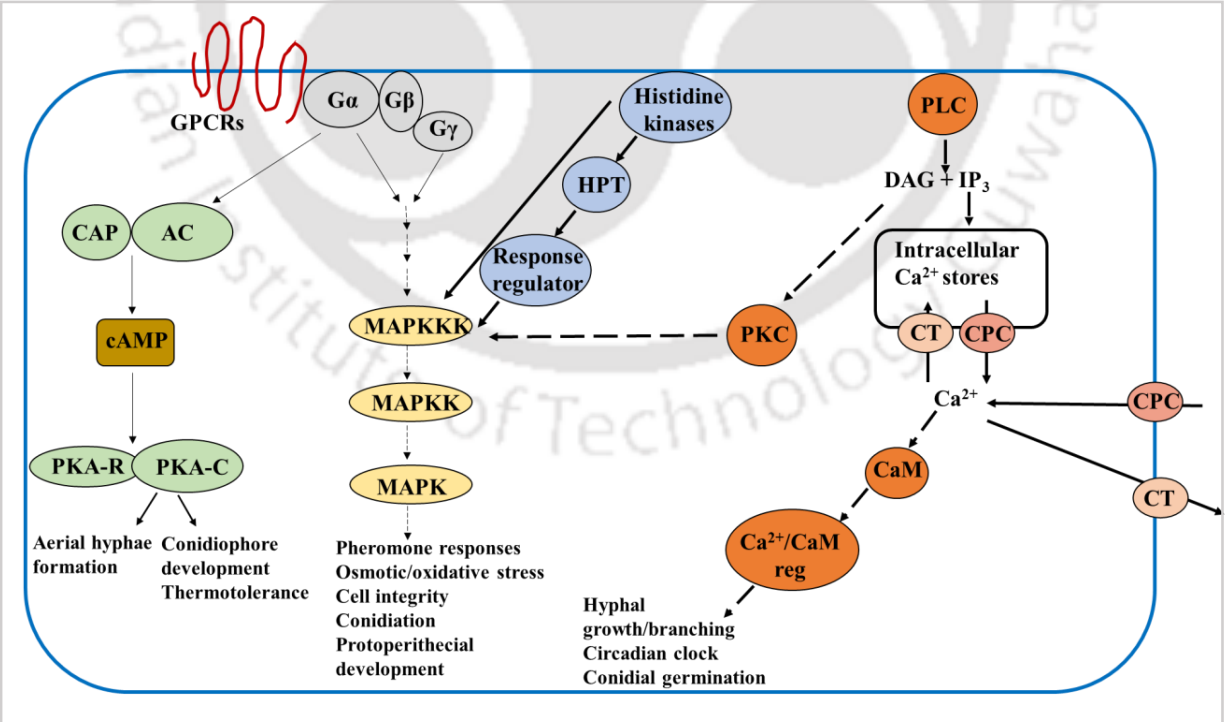

Figure 1.2: Overview of the major intracellular signaling pathways in *N. crassa*. AC: adenylyl cyclase; CaM: calmodulin; Ca^{2+}/CaM reg: calcium and calmodulin regulated protein; CAP:

cyclase-associated protein; CT, Ca^{2+}-transport protein; CPC: Ca^{2+}-permeable channel protein; GPCR: G-protein-coupled receptor; Gα: G-protein α subunit; Gβ: G-protein β subunit; Gγ: G-protein γ subunit; HPT: histidine-containing phosphotransfer domain protein; MAPK: mitogen activated protein kinase; MAPKK: MAPK kinase; MAPKKK: MAPKK kinase; PKA-R: protein kinase A regulatory subunit; PKA-C: protein kinase A catalytic subunit; PLC: phospholipase C; PKC: protein kinase C. The intracellular second messenger molecules cAMP: 3′, 5′-cyclic adenosine monophosphate; DAG: diacylglycerol; IP_3: inositol-1, 4, 5-trisphosphate are also shown. Adapted from Galagan et al. 2003.

To adapt to changing environments, cells must signal. Signaling requires messengers whose concentration varies with time and space (Berridge et al. 2003). Filling this role, Ca^{2+} have come to rule cell signaling (Clapman 2007). It is a ubiquitous second messenger molecule that plays a versatile role in intracellular signaling in all cell types and tissue. Binding of Ca^{2+} changes protein conformation and charge, which are the two universal signaling tools of signal transduction and thus govern protein functions (Clapman 2007). For example, Ca^{2+} triggers life at fertilization and controls the development and differentiation of cells into specialized types and several other cellular activities including cell death (Berridge et al. 2000; Tamuli et al. 2013). The ubiquitous role of Ca^{2+} lies in its chemistry that involves its molecular structure, balance state, binding strength, ionization potential, and kinetic parameters in the biological reactions. The Ca^{2+} ion typically exhibits high coordination numbers (6–8) and can accommodate 4-12 oxygen atoms in its primary coordination sphere. The coordination geometry of Ca^{2+} is often irregular (i.e. protein induced) due to its favourable ionic radius (100–120 pm) and its electronic structure (Swain and Amma 1989; Carugo et al. 1993; Jaiswal 2001). Typically, Ca^{2+} ion is coordinated by 6-7 oxygen atoms in a pentagonal bipyramidal manner or in a trigonal manner (Swain and Amma 1989). The Ca^{2+} ion has maximum affinity for carboxylate oxygen and interestingly, acidic amino acids like aspartic acid and glutamic acid that contain the carboxylate oxygen occur more frequently in proteins. Like other organisms, *N. crassa* is also subjected to various environmental stimuli, and its Ca^{2+} signaling machinery plays an important role in perceiving these extracellular environmental changes to thrive in diverse environments (Li and Borkovich 2006; Tamuli et al. 2013; Kumar and Tamuli 2014). In *N. crassa*, Ca^{2+} is mainly stored in the intracellular stores such as vacuoles (>90% of Ca^{2+} is sequestered in the vacuoles), Golgi, endoplasmic reticulum, plasma membrane vesicles, microsomes, and mitochondria; and only a small amount of Ca^{2+} (~100 nM)

is present freely in the cytosol ($[Ca^{2+}]_c$; Bowman et al. 2011). This low level of $[Ca^{2+}]_c$ is maintained by the Ca^{2+} pumps and the Ca^{2+} transporters and the Ca^{2+} buffering capacity of the cytoplasm. However, $[Ca^{2+}]_c$ becomes an intracellular signal when its concentration is transiently increased (500-1000 nM) by the activation of the Ca^{2+} permeable channels that allows Ca^{2+} to flow down a concentration gradient into the cytoplasm. $[Ca^{2+}]_c$ recovers to its original resting level by the increased activity of the Ca^{2+} pumps and the Ca^{2+} transporters (Zelter et al. 2004).

The filamentous fungus *N. crassa* has been established as an excellent eukaryotic model organism that can be utilized to investigate the complex Ca^{2+} signaling processes. *N. crassa* has 48 Ca^{2+}-signaling proteins that comprises of three Ca^{2+} channel proteins, nine Ca^{2+}/cation-ATPases, six recognizable Ca^{2+}/H^+ exchangers, two novel putative Ca^{2+}/Na^+ exchangers, four novel phospholipase C-δ subtype proteins, 23 Ca^{2+}/calmodulin regulated proteins, and one calmodulin (Figure 1.3, Table 1.1; Borkovich et al. 2004; Tamuli et al. 2013). The unique Ca^{2+} signaling machinery of *N. crassa* varies significantly from plant and animal cells especially in relation to second messenger systems involved in Ca^{2+} release from the internal stores (Galagan et al. 2003). *N. crassa* lacks inositol-1, 4, 5- trisphosphate (IP_3) receptors including ADP ribosyl cyclase and ryanodine receptor proteins which are the key components of Ca^{2+} release mechanisms from internal stores in plants and animal cells and also lacks extracellular Ca^{2+} sensing receptor proteins reported in animal cells for sensing changes in the extracellular concentration of Ca^{2+} (Brown et al. 1993; Galagan et al. 2003; Borkovich et al. 2004). In addition, *N. crassa* possesses both Ca^{2+}/H^+ and Ca^{2+}/Na^+ exchangers, while plants possess only Ca^{2+}/H^+ exchangers, and animals possess only Ca^{2+}/Na^+ exchangers (Borkovich et al. 2004). Thus, *N. crassa* possesses intracellular Ca^{2+} release mechanisms that has yet to be identified. Also these findings suggest that the Ca^{2+} signaling machinery in *N. crassa* might provide novel antifungal targets for drug discovery (Borkovich et al. 2004; Nelson et al. 2004). Below, I give a brief description of the Ca^{2+} signaling proteins in *N. crassa*.

1.2.1 Ca^{2+}-permeable channels: Ca^{2+}-permeable channels are localized across cell membranes and they regulate passive flow of Ca^{2+} across the membranes into the cytoplasm (Bootman et al. 2001; Zelter et al. 2004; Tamuli et al. 2011). The NCU02762, NCU06703, and NCU11680 are three distinct Ca^{2+}-permeable channel proteins classified as group I, II, and III respectively (Zelter et al. 2004; Tamuli et al. 2011). The MID-1 (mating induced death-1) protein encoded by

NCU06703 is a stretch activated Ca^{2+}-permeable channel involved in regulation of ion transport via Ca^{2+} homeostasis (Lew et al. 2008).

1.2.2 Ca^{2+} and cation-ATPases: The ATP driven plasma membrane and organelle membrane localized Ca^{2+} and cation-ATPases mediate Ca^{2+} uptake across cell membranes into the cytoplasm. *N. crassa* contains seven Ca^{2+} and cation-ATPases and two cation-ATPases. NCA-1, NCA-2, NCA-3, PMR-1, and PH-7 ATPases are encoded by NCU03305, NCU04736, NCU05154, NCU03292, and NCU08147 genes, respectively (Benito et al. 2000). While lack of NCA-1 and NCA-3 do not show any defect in growth or Ca^{2+} distribution, however, strains lacking NCA-2 displays slower growth, Ca^{2+} sensitivity, and female sterility and accumulates higher Ca^{2+} than the wild type which indicates it functions to pump Ca^{2+} out of the cell (Bowman et al. 2011; Laxmi and Tamuli 2015). One of the cation-ATPases *trm-9* encoded byNCU04898 was found to play role in growth, Ca^{2+} sensitivity, and acquisition of thermotolerance induced by heat shock temperatures in *N. crassa* (Laxmi and Tamuli 2015).

1.2.3 Ca^{2+}/H^{+} exchangers: The Ca^{2+}/H^{+} exchangers pump Ca^{2+} ions out of the cell and transport Ca^{2+} into the intracellular Ca^{2+} storing organelles to reduce high $[Ca^{2+}]_c$ into resting levels, a process driven by ATP hydrolysis (Zelter et al. 2004). In *N. crassa*, two H^{+} ions are exchanged per Ca^{2+} ion across membranes (Miller et al. 1990). Genome analysis identified six Ca^{2+}/H^{+} exchangers encoded by the NCU07075, NCU00916, NCU00795, NCU06366, NCU07711, and NCU05360 genes in *N. crassa* (Galagan et al. 2003; Borkovich et al. 2004).

1.2.4 Ca^{2+}/Na^{+} exchangers: Ca^{2+}/Na^{+} exchangers transports Ca^{2+} from the cytoplasm and also facilitate Ca^{2+} entry into the cell (Lytton et al. 2007). *N. crassa* possesses two Ca^{2+}/Na^{+} exchangers encoded by NCU02826 and NCU08490 genes.

1.2.5 Phospholipase C-δ subtype proteins: *N. crassa* possesses four novel phospholipase C-δ subtype proteins (PLC-δ) encoded by genes NCU01266, NCU02175, NCU06245, and NCU11415 (Galagan et al. 2003; Borkovich et al. 2004). The phosphoinositide-specific PLC-δ catalyses the hydrolysis of plasma membrane phospholipid phosphatidylinositol-4, 5-bisphosphate (PIP_2) into IP_3 which induces Ca^{2+} release from intracellular Ca^{2+} stores and diacylglycerol (DAG) that

activates protein kinase C (PKC; Berridge 1987; 1993; Cornelius 1989). Interestingly, *N. crassa* lacks any recognizable IP_3 receptors and both of its PKC proteins lack a C2 domain with Ca^{2+} binding sites (Galagan et al. 2003; Borkovich et al. 2004). The *plc-1* encoded by NCU06245 exhibits a high incidence of polymorphism among the natural isolates of *N. crassa* with a unique coding sequence change at the amino acid positions 200-250 (Gavric et al. 2007). The RIP induced mutant of *plc-1* displayed colonial morphology with defects in growth rate, hyphal size, proportion, and branching which indicated role of *plc-1* for normal growth (Garnjobst and Tatum 1967; Gavric et al. 2007).

1.2.6 Ca^{2+} and/or calmodulin binding proteins and calmodulin: The Ca^{2+} and/or calmodulin (CaM) binding proteins are primarily involved in regulation of $[Ca^{2+}]_c$ and they possess several conserved domains like N-terminal catalytic domain, EF-hand domain with Ca^{2+} binding sites, autoinhibitory, and overlapping CaM binding domain. *N. crassa* possesses four Ca^{2+}/CaM-dependent kinases, Ca^{2+}/CaMK-1 to 4, encoded by the genes NCU09123, NCU02283, NCU06177, and NCU09212, respectively (Galagan et al. 2003). Knockout mutant of CaMK-1 show phase delay, a small period lengthening, light-induced phase shifting of the circadian conidiation rhythm, and a transient slow growth phenotype (Yang et al. 2001). The CaMK-1, 2, 3, and 4 are involved in growth, thermotolerance, oxidative stress survival, and sexual development in *N. crassa* as revealed by respective studies in our lab (Deka et al. 2011; Tamuli et al. 2013; Kumar and Tamuli 2014). The Ca^{2+} and/or CaM binding neuronal calcium sensor-1, NCS-1, encoded by NCU04379 has a role in growth, Ca^{2+} stress tolerance, and ultraviolet (UV) survival (Deka et al. 2011). The highly conserved heterodimer calcineurin is a Ca^{2+} /CaM regulated serine/threonine protein phosphatase composed of a catalytic subunit (calcineurin A, CNA-1) that binds to CaM and a regulatory subunit (calcineurin A; CNB-1) that binds to Ca^{2+} (Klee 1979; Winkler et al. 1984). Induction of antisense RNA expression for the *cna-1* indicated essential role of *cna-1* for growth of *N. crassa* as conditional expression caused extensive hyphal branching, altered hyphal morphology, loss of the apical tip-high Ca^{2+} gradient, and eventually growth arrest (Prokisch et al. 1997). Calcineurin B mutant, *cnb-1*, displays an abnormal morphology indicating that calcineurin regulatory subunit B is required for normal vegetative growth in *N. crassa* (Kothe and Free 1998). The NDE-1 protein encoded by NCU08980 is an external NADPH dehydrogenase of *N. crassa* mitochondria (Melo et al. 1999; 2001; Borkovich et al. 2004; Carneiro et al. 2007). It contains a

potential Ca^{2+} binding motif and the NADPH oxidation activity of the NDE-1 protein is Ca^{2+}-dependent (Melo et al. 1999; 2001). *N. crassa* encodes one CaM protein, NCU04120, that appears to be essential for viability and it plays role in various cellular processes including circadian clock, activation of chitin synthase and modulating DNA repair, DNA synthesis, and cell proliferation in both CHO and human cell lines (Chafouleas et al. 1984; Pavelic 1987; Chard 1987; Capelli et al. 1993; Mirzayans et al. 1995; Sadakane and Nakashima 1996; Suresh and Subramanyan 1997; Galagan et al. 2003; Borkovich et al. 2004). Experiments in our lab indicated that the *Cmd* gene play role in vegetative growth, sexual development, UV survival, and survival in stress conditions (Laxmi and Tamuli 2015; 2016).

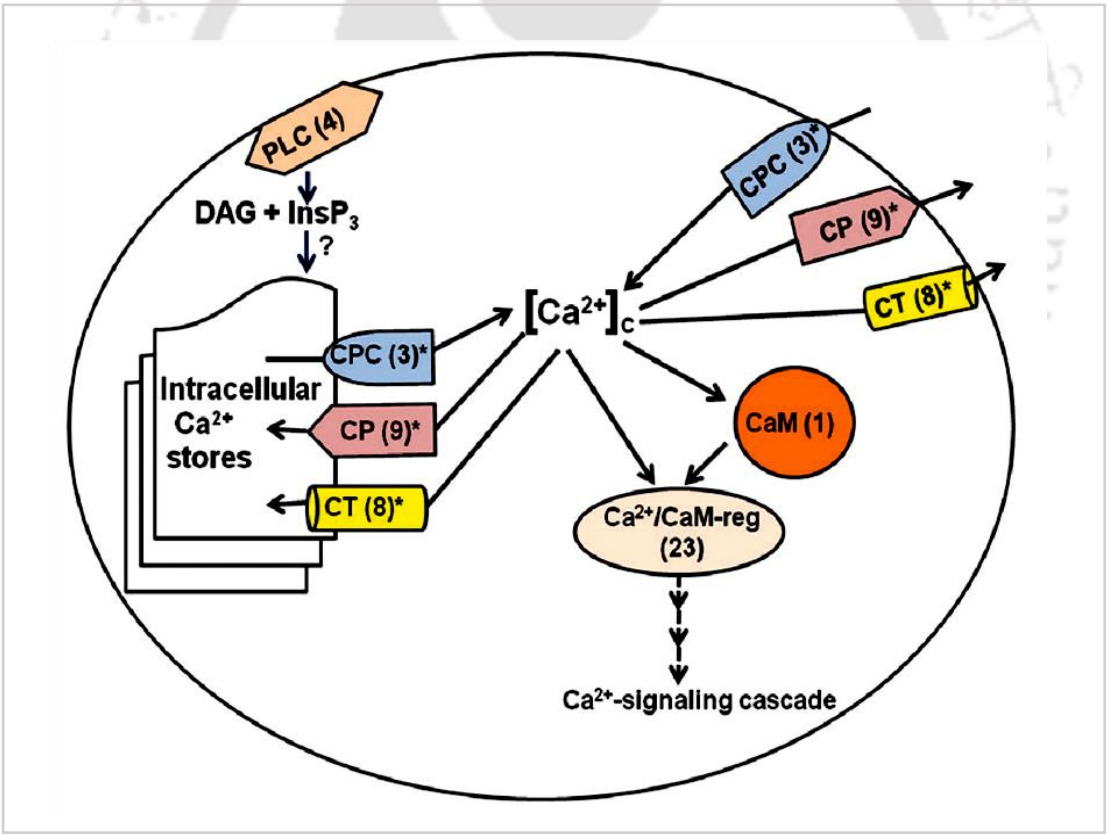

Figure 1.3: Overview of Ca^{2+} signaling system in *N. crassa*. The Ca^{2+} signaling proteins are CPC: Ca^{2+}-permeable channel; CP: Ca^{2+}-and cation-ATPases; CT: Ca^{2+}/H^{+} and Ca^{2+}/Na^{+} exchanger: CaM: calmodulin; Ca^{2+}/CaM-reg: calcium- and calmodulin regulated proteins; and PLC: phospholipase C. The intracellular second messenger molecules DAG: diacylglycerol and

IP_3: inositol-1, 4, 5-trisphosphate are also shown. Changes in $[Ca^{2+}]_c$ triggers a Ca^{2+} signaling cascade via Ca^{2+}/CaM-reg proteins. Numbers in parentheses indicate the number of genes identified in that class and asterisk indicates that the location in the plasma membrane and/or organelle membranes are not determined (Galagan et al. 2003; Borkovich et al. 2004; Zelter et al. 2004). Adapted from Tamuli et al. 2013.

Table 1.1[a]: Ca^{2+} signaling proteins in *N. crassa*

Sl. No.	NCU No.	Name	Type of Protein	Best overall[b] (*e*-value; organism; protein name; accession number)
1	02762.7		Ca^{2+} permeable channel	0; *Verticillium dahlia* (cch1); EGY18507.1
2	06703.7		Ca^{2+} permeable channel	2*e*-97; *Paracoccidioides brasiliensis* (MID1); EEH23338.1
3	11680.7[c]		Ca^{2+} permeable channel	0; *Ajellomyces dermatitidis* (Yvc1); EGE78766.1
4	03305.7	NCA1	Ca^{2+} -ATPase	0; *Trichophyton tonsurans* (SCA-1); EGD96734.1
5	04736.7	NCA2	Ca^{2+} -ATPase	0; *M. oryzae* (Plasma membrane calcium-transporting ATPase 3); EHA56671.1
6	05154.7	NCA3	Ca^{2+} -ATPase	0; *Glomerella graminicola* (Calcium translocating P-type ATPase); EFQ29373.1
7	03292.7	PMR1	Ca^{2+} -ATPase	0; *Uncinocarpus reesii* (PMR1); XP_002541437.1

8	08147.7	PH-7	Ca^{2+} -ATPase	0; *G. graminicola* (Potassium/sodium efflux P-type ATPase); EFQ36596.1
9	04898.7		Ca^{2+} -ATPase	0; *Cordyceps militaris* (Cation transporting ATPase 4); EGX91104.1
10	03818.7		Ca^{2+} -ATPase	0; *V. dahlia* (Neo1p); EGY18069.1
11	07966.7		Cation-ATPase	0; *T. tonsurans* (Cta3p); EGD97988.1
12	10143.7[d]		Cation-ATPase	0; *C. militaris* (ATPase type 13A2); EGX92563.1
13	07075.7	CAX	Ca^{2+} /H^{+} exchanger	0; *G. graminicola* (Calcium/proton exchanger); EFQ30300.1
14	00916.7		Ca^{2+} /H^{+} exchanger	2*e*-176; *A. fumigatus* (Membrane bound cation transporter); XP_001481534.1
15	00795.7		Ca^{2+} /H^{+} exchanger	1e-149; *A. niger* (Membrane bound cation transporter); XP_001400827.2
16	06366.7		Ca^{2+} /H^{+} exchanger	0; *Sclerotinia sclerotiorum* (Ca^{2+}/H^{+} antiporter); XP_001589752.1
17	07711.7		Ca^{2+} /H^{+} exchanger	4*e*-160; *T. tonsurans* (Vacuolar calcium ion transporter/H^{+} exchanger); EGD98067.1
18	05360.7		Ca^{2+} /H^{+} exchanger	0; *Metarhizium anisopliae* (Calcium Permease); EFY95914.1

19	02826.7		Ca^{2+}/ Na^{+} exchanger	0; *V. albo-atrum* (Sodium/calcium exchanger protein); XP_003004985.1
20	08490.7		Ca^{2+} /H^{+} exchanger	1*e*-83; *A. niger* (Sodium/calcium transporter); XP_001397155.1
21	01266.7		Phospholipase C	0; *Sordaria macrospora* (Phosphoinositide-specific phospholipase C); XP_003348116.1
22	06245.7	PLC-1	Phospholipase C	0; *G. graminicola* (Phosphatidylinositol-specific phospholipase C); EFQ28596.1
23	11415.7[e]		Phospholipase C	0; *G. graminicola* (Phosphatidylinositol-specific phospholipase C); EFQ31595.1
24	02175.7		Phospholipase C	3*e*-125; *Botryotinia fuckeliana* (BcPLC2); CCD34776.1
25	04120.7	CaM	Calmodulin	1*e*-103; *Gibberella zeae* (CaM); XP_382067.1
26	03804.7	CNA-1	Calcineurin catalytic subunit	0; *S. macrospora* (Serine/threonine-protein phosphatase 2B catalytic subunit protein); XP_003352213.1
27	03833.7	CNB-1	Calcineurin regulatory subunit /variant	2*e*-119; *Trichoderma reesei* (Calcineurin beta subunit); EGR44907.1
28	09265.7		Calnexin	0; *S. macrospora* (cnx1);

				XP_003347545.1
29	05225.7[f]		Ca^{2+} and/or CaM binding protein	0; *M. oryzae* (Mitochondrial NADH dehydrogenase); EHA47323.1
30	02115.7		Ca^{2+} and/or CaM binding protein	0; *M. oryzae* (EF hand domain containing protein); EHA48778.1
31	01564.7		Ca^{2+} and/or CaM binding protein	0; *M. oryzae* (Calcium dependent mitochondrial carrier protein); EHA48778.1
32	06948.7		Ca^{2+} and/or CaM binding protein	2*e*-54; *Mycosphaerella graminicola* (Calcium ion binding, calmodulin); EGP88834.1
33	04379.7	NCS-1	Ca^{2+} and/or CaM binding protein	4*e*-126; *Grosmannia clavigera* (Neuronal calcium sensor 1); EFX03580.1
34	02738.7	PEF-1	Ca^{2+} and/or CaM binding protein	2*e*-130; *V. dahlia* (Peflin); EGY21808.1
35	09871.7		Ca^{2+} and/or CaM binding protein	4*e*-33; *V. dahlia* (Centrin-3); EGY16271.1
36	01241.7		Ca^{2+} and/or CaM binding protein	0; *T. reesei* (Mitochondrial carrier protein); EGR44893.1
37	06347.7		Ca^{2+} and/or CaM binding protein	0; *S. macrospora* (Actin cytoskeleton-regulatory complex protein); XP_003350109.1
38	06617.7		Ca^{2+} and/or CaM binding protein	7*e*-93; *V. albo-atrum* (Myosin regulatory light chain cdc4); XP_003009631.1

39	03750.7		Ca^{2+} and/or CaM binding protein	8*e*-74; *B. fuckeliana* (Calmodulin); XP_001560827.1
40	08980.7	NDE-1	Ca^{2+} and/or CaM binding protein	0; *G. clavigera* (Alternative NADH-dehydrogenase); EFX03867.1
41	02283.7		Ca^{2+} and/or CaM binding protein	0; *S. macrospora* (Calcium/calmodulin-dependent protein kinase type I); XP_003344498.1
42	09123.7		Ca^{2+} and/or CaM binding protein	0; *Sporothrix schenckii* (Calcium/calmodulin-dependent kinase); AAV80434.1
43	09212.7		Ca^{2+} and/or CaM binding protein	0; *V. dahlia* (Serine/threonine-protein kinase srk1); EGY15110.1
44	02814.7	PRD-4	Ca^{2+} and/or CaM binding protein	0; *G. clavigera* (Serine/threonine-protein kinase chk2); EFX01629.1
45	06650.7		Ca^{2+} and/or CaM binding protein	3*e*-61; *Nectria haematococca* (Phospholipase A2); XP_003042542.1
46	02411.7		Ca^{2+} and/or CaM binding protein	0; *G. graminicola* (Microtubule associated protein); EFQ31793.1
47	06177.7		Ca^{2+} and/or CaM binding protein	0; *M. grisea* (CMKK2); ACM41720.1
48	04265.7		Ca^{2+} and/or CaM binding protein	7*e*-85; *Bacillus megaterium* (Betafructosidase FruA); AEN90524.1

[a]Adapted from Tamuli et al. 2013

[b]BLASTP search at the NCBI (http://blast.ncbi.nlm.nih.gov/Blast.cgi; Altschul et al. 1990; 1997; 2005) with the default parameters for each of the 48 Ca^{2+} signaling proteins against the non-redundant protein sequence databases has been indicated the respective best overall match in other organisms.

[c]Split from NCU07605.1

[d]Split from NCU01437.1

[e]Split from NCU09655.1

[f]NCU05225.5 (was indicated as NCU08980.1 in Borkovich et al. 2004)

1.3 The Ca^{2+} signaling proteins important for maintaining $[Ca^{2+}]_c$ level

In *N. crassa*, cytosolic Ca^{2+} plays a central role as an intracellular signal, however, increase in cytosolic Ca^{2+} levels are noxious to the cell, and therefore, $[Ca^{2+}]_c$ is effectively regulated (Cornelius and Nakashima 1987; Berridge et al. 1998; Sanders et al. 2002). Changes in cytosolic Ca^{2+} levels are detected by three important classes of Ca^{2+} signaling proteins in *N. crassa* which includes novel PLC-δ subtype proteins, Ca^{2+} and/or CaM binding secretory phospholipase A_2 proteins ($sPLA_2$), and Ca^{2+} exchangers. PLC and $sPLA_2$ regulates important cell functions in different organisms including the model filamentous fungi *N. crassa* (Barman and Tamuli 2015; 2017). Below, I briefly describe the structure and functions of PLC, $sPLA_2$, and Ca^{2+} exchangers in fungi.

1.3.1 Phospholipase C

Phospholipases are ubiquitous enzymes which catalyses the hydrolysis of phospholipids yielding free fatty acids and a number of lipophilic signaling molecules such as DAG, free fatty acids (FFAs), phosphatidic acid (PA), and lysophospholipids (Köhler et al. 2006; Hong et al. 2016). Depending on the type of cleavage of an ester linkage within a phospholipid molecule, phospholipases are classified as phospholipase A (PLA_1 and PLA_2), phospholipase B (PLB), phospholipase C (PLC), and phospholipase D (PLD) (Figure 1.4 A; Köhler et al. 2006). The membrane bound phosphoinositide-specific PLC hydrolyses PIP_2 into two important second messengers, IP_3 and DAG. The IP_3 induces release of Ca^{2+} from intracellular Ca^{2+} stores whereas DAG binds to Ca^{2+} dependent C2 domain and in turn activates PKC enzyme (Figure 1.4 B;

Berridge and Irvin 1984; Nishizuka 1984; Clapham 2007). Majority of eukaryotic PLCs comprises of five conserved domains which includes two catalytic domains X and Y, an N-terminal pleckstrin homology (PH) domain for membrane phospholipid interaction, a C-terminal Ca^{2+} dependent C2 domain for phospholipid binding, and an EF-hand motif for Ca^{2+} binding and interaction of PH with phospholipid (Figure 1.4 C; Bristol et al. 1988; Watson and Arkinstall 1994; Sutton et al. 1995; Yamamoto et al. 1999). PLC is involved in the regulation of numerous cellular and biological functions in a variety of organisms including yeast, mold, and filamentous fungi.

***Alternaria alternata*:** The opportunistic fungal pathogen *A. alternata*, causes brown spot disease in citrus plants and is also responsible for respiratory tract infections in humans (Akimitsu et al. 2003; Salo et al. 2006). It comprises of a PLC1 gene that encodes an 1104 amino acid protein and possesses all the known eukaryotic PLC conserved domains (Tsai et al. 2014). The *plc1* deleted strain showed severe morphological abnormalities including vegetative growth defect, swollen hyphae, and reduced sporulation with delayed germination as well as disruption of Ca^{2+} homeostasis (Tsai et al. 2014). Also the *plc1* mutants produced small or almost no necrosis on detached citrus leaves indicating a possible role of *plc-1* in pathogenicity (Tsai et al. 2014). Therefore, PLC1 protein regulates developmental and pathological processes in *A. alternata* (Tsai et al. 2014).

***Botrytis cinerea*:** The air borne plant pathogen *B. cinerea* infects dicotyledonous host plant via extracellular cell wall-degrading enzymes, non-specific phytotoxic metabolites, and generation of reactive oxygen species (ROS; Nakajima and Akutsu 2014). The genome of *B. cinerea* comprises of two PLC proteins, BcPL1 and BcPLC2 and contains conserved catalytic X and Y domains, a C-terminal Ca^{2+} binding motif while the N-terminal PH domain typically found in majority of eukaryotic PLCs is present only in BcPL1 (Schumacher et al. 2008). The knock down mutants of *bcplc1* generated by RNA-mediated gene silencing displayed various morphological defects including formation of small compact colonies, fewer aerial hyphae with altered hyphal morphology, and significantly decreased conidiation with reduced rate of germination (Schumacher et al. 2008). The *bcplc1* deleted strain also formed small non-expanding necrotic lesions carried out with excised bean leaves inoculated with conidia whereas inoculation with mycelium completely infected the bean leaves due to formation of expanding necrotic lesions

(Schumacher et al. 2008). Also down regulation of a number of BCG-1 (encoding GTP binding α subunit) and CN (encoding calcineurin) dependent genes were observed in *bcplc1* knock down mutants which suggested involvement of BcPLC1 in BCG-1 and CN dependent signaling pathways (Schumacher et al. 2008). Thus, BcPLC1 plays an essential role in growth, hyphal development, conidiation, conidiospore germination, virulence, and regulates the transcription of BCG-1 and CN encoding genes.

***Candida albicans*:** The genome of one of the most important opportunistic human pathogen *C. albicans* that causes significant morbidity and mortality in immunocompromised individuals encodes three putative PI-PLC proteins, *CaPLC1*, *CaPLC2*, and *CaPLC3* with *CaPLC1* closely resembles mammalian PI-PLC δ isoform while *CaPLC2* and *CaPLC3* resembles bacterial PI-PLCs (Bennett et al. 1998; Andaluz et al. 2001). *CAPLC1* encodes a putative 1099 amino acid protein (Mw: 124.6 kDa) that contains the conserved X and Y domains, 16 predicted glycosylation sites, and an extended N-terminus but lacks the Ca^{2+} binding EF hand domain (Bennett et al. 1998). The X domain possesses conserved Asn, Gln, and Asp residues essential for Ca^{2+} binding and an additional stretch of 18-19 highly hydrophilic amino acid residues with two conserved His residues required for its catalytic activity (Bennett et al. 1998). The Y domain contains conserved Ser, Arg, and Tyr residues required for catalysis and substrate specificity (Bennett et al. 1998). *CaPLC2* and *CaPLC3* each encode a 343 amino acid protein and both share 99% sequence identity but without any significant similarity to *CaPLC1* (Andaluz et al. 2001; Knechtle et al. 2005). The *CaPLCs* do not contain any N-terminal signal peptide, transmembrane region, or glycophosphatidylinositol (GPI) anchor attachment sites while *CaPLC1* possesses a putative nuclear localization signal (NLS) within the X/Y domains and therefore the three *CaPLCs* are either cytoplasm or nucleus localized (Kunze et al. 2005). *CaPLC1* is an essential gene since targeted disruption of *CaPLC1* could not generate any null mutant and in presence of PI-PLC specific inhibitor 1-O-octadecyl-2-O-methyl-rac-glycero-3-phosphorylcholine (ET-18) completely prevented the growth of *C. albicans* cells (Kunze et al. 2005). The conditional mutants of *CaPLC1* showed phenotypes similar to *S. cerevisiae Plc1p* including osmosensitivity (high concentration of sorbitol or NaCl), sensitivity to lower (18°C) or elevated temperatures (43°C), reduced growth in non-glucose carbon sources (such as galactose), sensitivity to nocodazole that inhibits chromosome segregation as well as reduced growth in filamentous growth inducing conditions and on media containing only Arg

as the sole nitrogen source (Kunze et al. 2005). *CaPLC1* modulates various cellular functions in *C. albicans* as expression profile of different cellular genes were found to be transcriptionally regulated by *CaPLC1* (Kunze et al. 2005). Both the *CaPLC2* and *CaPLC3* genes were found to be non-essential for growth as loss of *Caplc2* and *Caplc3* did not show any phenotypic defects under different growth and stress inducing conditions (Knechtle et al. 2005; Kunze et al. 2005). The *Caplc2* and *Caplc3* mutants showed similar survival rate like the wild type in a mouse model of systemic infection which indicated both *Caplc2* and *Caplc3* were dispensable for virulence (Knechtle et al. 2005; Kunze et al. 2005). Thus, *C. albicans* possesses two different classes of PLC having significantly different functional role.

***Cryptococcus neoformans*:** The basidiomycete *C. neoformans* is a potential human pathogen that causes severe neurological disorders such as meningoencephalitis in immunocompromised hosts. *C. neoformans* possesses two putative *PLC* genes, *CnPLC1* and *CnPLC2* that encodes putative 609 and 430 amino acid proteins, respectively (Chayalkulkeeree et al. 2006). The conserved catalytic X and Y domains and the Ca^{2+} binding C2 domain are present only in CnPLC1 while CnPLC2 contains only the X domain in its predicted amino acid sequence (Chayalkulkeeree et al. 2008). Disruption of *CnPLC1* completely abolished the three major cryptococcal virulence traits including decreased expression of melanin-producing laccase 1 (*Lac*1), growth at the host physiological temperature (37°C), and secretion of cell-associated CnPlb1 and also showed reduced virulence in a murine model of cryptococcal infection and exhibited attenuated killing of *Caenorhabditis elegans* at 25°C (Chayalkulkeeree et al. 2006). The *Cnplc1* mutant formed defective cell walls, abnormal cell morphology, and clumped cells with numerous bud septa and was unable to activate MAPK in the presence of cell-wall perturbing agents (Chayalkulkeeree et al. 2006). In contrast, deletion of *Cnplc2* did not show any phenotypic changes in *C. neoformans* and exhibited virulence similar to wild type in a murine model of cryptococcosis (Chayalkulkeeree et al. 2006). In presence of the PLC inhibitor U73122, growth was inhibited in the wild type strain of *C. neoformans* while notably significant reduction in MICs (minimum inhibitory concentrations) of the azole drugs, amphotericin B, and flucytosine was observed in *plc1* deleted strain which suggests *plc1* can be a potential antifungal drug target (Chayalkulkeeree et al. 2006). Thus, *C. neoformans* Plc1 is essential for expression of certain cryptococcal virulence traits such as melanin production, growth at elevated temperatures, release and secretion of Plb1 from its GPI

anchored site in the plasma membrane, and is involved in maintenance of normal cell morphology, cell wall integrity, and activation of PKC/MAPK signaling pathway.

***Coprinopsis cinerea*:** The small ink-cap mushroom *C. cinerea* is an ideal eukaryotic model organism for genetic and cytological studies (Burns et al. 2010; Pukkila 2011). It encodes three putative *PLC* genes, *CcPLC1*, *CcPLC2*, and *CcPLC3* and shares significant homology to corresponding *PLC1* of *S. cerevisiae* (Oh et al. 2012). The two *PLC* genes, *CcPLC1* and *CcPLC2* encode corresponding putative proteins of 881 and 1036 amino acids, respectively and comprises a PH domain, X and Y catalytic domains, and a C2 domain while *CcPLC3* which encodes a putative protein of 659 amino acid lacks the PH domain (Oh et al. 2012). All three *CcPLC*s are differentially expressed during various stages of *C. cinerea* lifecycle. The wild type *C. cinerea* strain exhibit several phenotypic defects in response to the PLC inhibitor U73122 such as inhibition of oidia and basidiospores germination, reduced hyphal growth with irregular hyphal tips, open clamp connections with aberrant clamp cells (branch like structures), and protoplast inhibition (Oh et al. 2012). Thus, *CcPLC*s play critical role in growth and development of *C. cinerea* (Oh et al. 2012).

***Cryphonectria parasitica*:** The plant pathogen *C. parasitica* causes chestnut blight, a destructive disease that forms 'sunker cankers' in the barks of healthy chestnut trees (MacDonald and Fulbright 1991). However, in presence of a double stranded (ds) RNA virus *Cryphonectria* hypovirus1 (CHV1), certain strains of *C. parasitica* exhibits characteristic symptoms of reduced virulence due to down regulation of expression of extracellular *lac*1 gene via interference of IP_3 mediated Ca^{2+} signal (Anagnostakis et al. 1982; Van Alfen et al. 1975; Larson et al. 1992; Nuss et al. 1992). The corresponding PLC gene of *C. parasitica*, *CPLC1*, encodes a polypeptide of 736 amino acids (Mw: 79.8 kDa) that shares homology to the fungal PLC genes from *S. cerevisiae*, *S. pombe*, *C. albicans*, and *Botryotinia fuckeliana* (Chung et al. 2006). The predicted polypeptide of *CPLC1* contains the catalytic X and Y domains which constitute the triosephosphate isomerase like domain (TIM-barrel), characteristic of mammalian PI-PLC δ isoform with a unique 133 amino acids extended segment starting from the second β-strand (Tβ2) to α-helix (Tα2) of the TIM barrel and a C2 domain but lacks the N-terminal PH domain and the EF-hand motifs (Essen et al. 1996; Chung et al. 2006). The *cplc1* null mutant exhibited a few morphological changes such as bright

orange pigmented colonies with slower mycelial growth and no aerial mycelium, thinner and abrupt vegetative hyphae, and reduced conidiation but showed no temperature sensitivity or osmosensitivity (Chung et al. 2006). Moreover, disruption of *cplc1* did not show any *lac*1 transcript accumulation which indicated wild type *cplc1* play a pivotal role in *lac*1 gene expression (Chung et al. 2006). Also, the *cplc1* null mutant and the hypovirulent strain showed similar lowered necrosis on excised chestnut tree bark which suggested no possible role of *cplc1* in pathogenicity (Chung et al. 2006). Thus, *cplc1* gene is essential for growth and *lac*1 gene expression in *C. parasitica*.

***Fusarium graminearum*:** *F. graminearum* is the causative agent of Fusarium head blight (FHB) disease that affects many cereal crops including barley, maize, oats, rice, and wheat and also affects humans and animals due to its ability to synthesize various trichothecene mycotoxins (Bennett and Klich 2003; Goswami and Kistler 2004; Osborne and Stein 2007). Genome of *F. graminearum* comprises of six putative PLC encoding genes, *FgPLC1*, *FgPLC2*, *FgPLC3*, *FgPLC4*, *FgPLC5*, and *FgPLC6*, and all six *FgPLCs* are differentially expressed in the mycelia (Zhu et al. 2015). In response to U73122, wild type *F. graminearum* exhibited dose dependent reduction in mycelial growth, colony formation, reduction in conidiation and conidial germination, inhibition of perithecium, and showed down regulation of trichothecene biosynthetic *Tri5* and *Tri6* genes in the mycelia (Zhu et al. 2015). Thus, FgPLCs are essential to *F. graminearum* in its growth and development and trichothecene biosynthesis.

***Magnaporthe oryzae*:** The filamentous ascomycete *M. oryzae* is responsible for causing rice blast, one of the most destructive diseases affecting cereal crops particularly cultivated rice (Ou 1985). Its genome comprises of five PLC encoding genes, mainly *MoPLC1*, *MoPLC2*, *MoPLC3*, *MoPLC4*, and *MoPLC5* (Rho et al. 2009). The intron less *MoPLC1* encodes a polypeptide of 847 amino acids that contains the conserved catalytic X and Y domains, PH domain, EF hand domain, and a C2 domain similar to mammalian PLC-δ isoform (Rho et al. 2009). The remaining four *MoPLCs* also contain X/Y domains but lack the PH and EF hand domains while only *MoPLC2* and *MoPLC3* comprises of the C2 domain (Choi et al. 2011). The PLC specific inhibitor, neomycin, causes inhibition of Ca^{2+} influx at the germ tubes apex and appressoria that suggest a possible role of *PLC* in intracellular Ca^{2+} ($[Ca^{2+}]_{int}$) regulation (Rho et al. 2009). Targeted

disruption of *MoPLC1* showed various phenotypic alterations such as reduced growth rate, osmosensitivity (glycerol or NaCl), decreased conidiation with altered conidial morphology, inhibition of perithecium formation, and abnormal appressoria development (Rho et al. 2009). In contrast, the *MoPLC2* and *MoPLC3* deleted strains showed normal vegetative growth, conidium and appressorium morphology, however, conidia production was significantly reduced while multiple appressoria on separate germ tubes were formed from a single conidium probably caused due to a defect in cell wall integrity (Choi et al. 2011). Fewer under developed lesions were observed on excised rice leaves sprayed or injected with conidial suspension of *MoPLC1*, *MoPLC2*, and *MoPLC3* mutants in contrast numerous well-developed spindle shaped lesions were formed by the wild type isogenic strain (Rho et al. 2009; Choi et al. 2011). Also, the abnormal appressoria of *MoPLC1*, *MoPLC2*, and *MoPLC3* mutants failed to penetrate plant epidermal cells and lacked any invasive hyphae whereas the well-developed appressoria of the wild type isogenic strain formed swollen bulbous invasive hyphae that could penetrate plant cells (Rho et al. 2009; Choi et al. 2011). Complementation with a wild type allele of *MoPLC1* and a mouse *PLC-δ1* gene individually recovered most of the defective phenotypes and thus indicated functional conservation of PLC as a regulator of Ca^{2+} flux between two different kingdoms (Rho et al. 2009). The phenotypic abnormalities of *MoPLC2* and *MoPLC3* deleted strains were also complemented by the wild type alleles of *MoPLC2* and *MoPLC3* genes (Choi et al. 2011). Therefore, *M. oryzae* consists of a PLC superfamily that has inter-related but significantly distinct roles in development as well as pathogenesis.

***Saccharomyces cerevisiae*:** The budding or the baker's yeast *S. cerevisiae* has a putative *PLC1* gene (*Plc1p*) that encodes an 869 amino acid protein (Mw: 101 kDa) highly homologous to mammalian PI-PLC δ isoform (Yoko-o et al. 1993). The conserved C-terminal catalytic X and Y region separated by a stretch of 75 amino acid residues forming a PEST motif that is rich in Pro, Glu (and Asp), Ser, and Thr residues and a putative N-terminal Ca^{2+} binding EF-hand motif are present in the deduced amino acid sequence of Plc1p, with both X and Y showing high sequence identity to mammalian PI-PLC δ isoform (Flick and Thorner 1993; Payne and Fitzgerald-Hayes 1993; Yoko-o et al. 1993). The activity of Plc1p is strictly Ca^{2+} dependent and it specifically hydrolyzes PIP_2 at the physiological [Ca^{2+}] of 0.5μM (Flick and Thorner 1993). Mutants of *Plc1p* were viable but exhibited a few phenotypic defects such as slower growth at restricted temperatures

(23°C) or were lethal with multiple morphological aberrations at nonpermissive temperatures (above 35°C) or on synthetic media or media with a high concentration of fermentable carbon source (Flick and Thorner 1993; Payne and Fitzgerald-Hayes 1993; Yoko-o et al. 1993). The *Plc1p* mutants also showed osmosensitivity and sensitivity to nitrogen starvation and were defective in utilizing non-fermentable carbon sources other than glucose at permissive temperatures (23 to 30°C; Flick and Thorner 1993). Insertion of rat PLC-δ1 complemented the growth defect of *Plc1p* mutants which indicated possible role of *PLC1* in growth, nutritional, and stress related responses (Yoko-o et al. 1993). *Plc1p* was also shown to be essential for glucose induced phosphatidylinositol (PtdIns) turnover and subsequent activation of plasma membrane H^+-ATPases and transduction of glucose mediated calcium signaling (Coccetti et al. 1998; Tisi et al. 2002). Plc1p activity is also required for the generation of inositol hexakisphosphate (IP_6) which facilitate mRNA export from the nucleus, for oxidative stress induced degradation of the yeast C-type cyclin Ume3p, increased expression of glycerol P dehydrogenase (GPD1), enhanced intracellular accumulation of glycerol, and osmoresistance (Cooper et al. 1999; York et al. 1999; Lin et al. 2002). Plc1p interacts with Tor2p, a putative PtdIns kinase homolog involved in regulation of translation, cell cycle progression, and actin-cytoskeleton distribution and with Sgd1p, a novel nuclear protein, that affects the expression of GPD1 (Lin et al. 1998; Akhtar et al. 2000; Lin et al. 2002). Interaction of Plc1p with the putative GPCR Gpr1p, as a component of nitrogen signaling pathway, induces morphogenetic transition from yeast to pseudohyphae in *S. cerevisiae* (Ansari et al. 1999). Also Plc1p was shown to interact physically with Ndc10p and Cep3p, components of the kinetochore complex CBF3, as deletion of *PLC1* abolished this interaction causing a few kinetochores associated defects such as cell cycle delay, hypersensitivity to microtubule (MT) depolymerizing drug nocodazole, higher frequency of chromosome missegregation, and increased instability of minichromosomes that resulted in reduced MTs binding ability (Lin et al. 2000). Thus, *S. cerevisiae* Plc1p plays a key role in the regulation of numerous physiological processes.

***Schizosaccharomyces pombe*:** The genome of the fission yeast *S. pombe* encodes a putative *PLC1-1* protein of 899 amino acid residues (Mw: 102.5 kDa) and is a homologue of mammalian PI-PLC δ isoform and *PLC1* of *S. cerevisiae* (Fankhauser et al. 1995). Like all eukaryotic PLC, it also possesses the characteristics X and Y domain at the C-terminal and an EF hand motif with Ca^{2+}

binding site at the N-terminal (Fankhauser et al. 1995). Strains lacking *plc1-1* displayed defective growth with morphologically aberrant cells in normal minimal media (MM; Fankhauser et al. 1995). Growth defect was partially suppressed in low inositol and low phosphate MM containing high concentration of nitrogen which suggests a potential role of *plc1-1* in the mechanism of ammonium sensing (Fankhauser et al. 1995).

A)

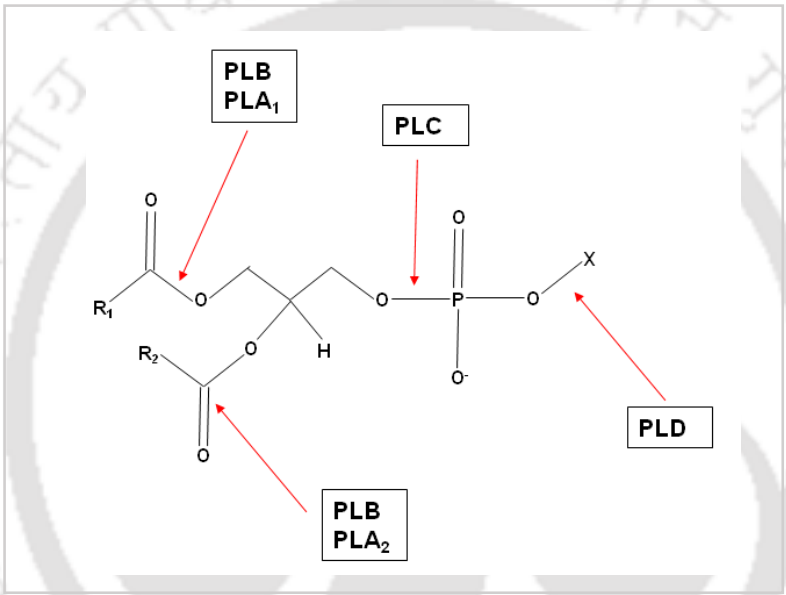

B)

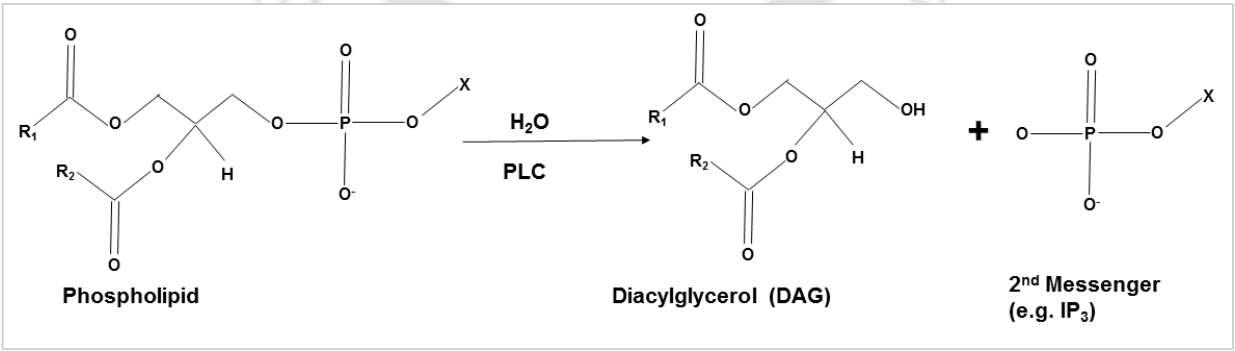

C)

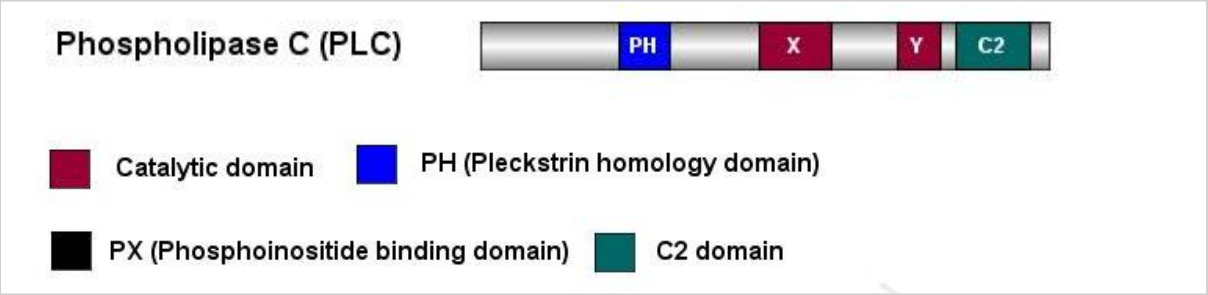

Figure 1.4: Schematics of PLC mechanism of action and domain organization. (A) Phospholipase A_1 (PLA_1), phospholipase A_2 (PLA_2), phospholipase B (PLB), phospholipase C (PLC), and phospholipase D (PLD) hydrolyses different carbon atoms on a phospholipid backbone. The site of action of phospholipases PLA_1, PLA_2, PLB, PLC, and PLD on a phospholipid are shown with red arrow (Köhler et al. 2006). X indicates polar head groups (e.g. choline, serine etc.). **(B)** PLC hydrolyzes the phosphatidylinositol-4, 5-bisphosphate (PIP_2) to inositol-1, 4, 5-trisphosphate (IP_3) and diacylglycerol (DAG). **(C)** Domain organization of PLC using the IBS Illustrator software (Liu et al. 2015).

1.3.2 Secretory phospholipase A_2

The phospholipase A (PLA) superfamily that catalyzes the hydrolysis of membrane phospholipids into FFAs and other lipid soluble molecules can be classified into two types based on their site of cleavage of ester linkages; PLA_1 cleaves at the *sn-1* ester linkage while PLA_2 cleaves at the *sn-2* ester bond of glycerophospholipids (Figure 1.4 A; Ghannoum 2000; Arioka et al. 2005; Köhler et al. 2006). One of the members of PLA_2 superfamily are the low molecular weight (13-19 KDa) Ca^{2+} dependent extracellular secretory proteins ($sPLA_2$). They are secretory enzymes that are involved in regulation of a number of biological processes in a range of organisms starting from bacteria to fungi, plants, and animals (Murakami and Kudo 2002; Boilard et al. 2010; Dennis et al. 2011). They were first reported in mammalian pancreatic juice and cobra venoms but later were also identified in reptiles, insects, plants, bacteria, viruses as well as fungi (Nakashima et al. 2003; Nevaleinen et al. 2012; 2013). The primary amino acid sequence of $sPLA_2$ comprises of a highly conserved His-Asp dyad sequence essential for its catalysis, a number of unique disulfide bonded Cys residues that contributes to stability of these enzymes and an N terminal signal peptide residue for secretion (Murakami and Kudo 2004; Schaloske and Dennis 2006; Nakahama et al. 2010;

Dennis et al. 2011; Cavazzini et al. 2013). Also included in its catalytic center is a tightly bound water molecule that acts as a potential nucleophile (Verheij et al. 1980; Scott et al. 1990; Pickard et al. 1996).

***Tuber borchii*:** In fungal species, $sPLA_2$ activity have been first identified and described in the ascomycete *T. borchii* (TbSP1; Soragni et al. 2001). *T. borchii* is an ectomycorrhizal fungus i.e. it can form a symbiotic association with the roots of several species of trees and shrubs. However, *T. borchii* is not an obligate symbiont and is capable of growing in mycelial cultures via exploitation of their limited saprotrophic capabilities (Soragni et al. 2001). Like most $sPLA_2$ enzymes, the phospholipase activity of TbSP1 (M_w 19 kDa) is Ca^{2+} dependent and contains a predicted N-terminal secretion signal peptide with a pre-protein cleavage site, a conserved (Arg-Gly-Asp) motif, and conserved catalytic His, Ca^{2+} binding, and disulfide bonded Cys residues forming a new XIV group within the PLA_2 superfamily (Soragni et al. 2001; Köhler et al. 2006). Expression of *TbSP1* in the symbiotic fungus *T. borchii* was found to be upregulated and activated via autoproteolysis upon nutrient deprivation (carbon and nitrogen) conditions which in turn enhanced the establishment of symbiosis and mycorrhiza formation (Soragni et al. 2001; Cavazzini et al. 2013). Thus, there is a possible signaling role of *TbSP1* in nutrient starved environment which in turn enhances mycorrhiza development of *T. borchii* with a specific host plant (Miozzi et al. 2005; Nakahama et al. 2010).

***Helicosporium sp.* HN1:** The ascomycete *Helicosporium* sp. HN1 encodes a novel 15 kDa secreted protein, p15 that belongs to group XIV and its primary amino acid sequence possess a conserved region that comprises of four Cys residues required for its stability (Wakatsuki et al.1999; 2001). This particular secretory protein induces neurite outgrowth and differentiation of neurons from rat pheochromocytoma cell line PC12 cells via activation of the L-type Ca^{2+} channels that triggers downstream cascade of signaling events (Wakatsuki et al. 1999; 2001). Another $sPLA_2$ that is included in group XIV is Scp15 (Mw: 14 kDa), isolated from *Streptomyces coelicor* and similar to fungal secretory protein, p15, contains four Cys residues and displays neurite stimulating activity in PC12 cells (Nakashima et al. 2003).

***Aspergillus oryzae*:** The genome of the saprotrophic ascomycete *A. oryzae* consists of two novel, putative $sPLA_2$ genes named sPlaA and sPlaB (Machida et al. 2005; Kobayashi et al. 2007; Nakahama et al. 2010). The deduced amino acid sequence of sPlaA is composed of 222 amino acids that contains putative N-terminal signal sequence of 19 amino acids and 6 Cys residues while sPlaB is comprised of 160 amino acids with putative signal sequence of 17 amino acids and 6 Cys (Nakahama et al. 2010). Both sPlaA and sPlaB exhibit distinct physiological properties such as sPlaA shows maximal enzyme activity for Ca^{2+} under acidic pH conditions with extracellular secretion while sPlaB displayed highest enzyme activity for Ca^{2+} at a neutral to alkaline pH and is maintained predominantly in intracellular localization (Nakahama et al. 2010). Only sPlaA expression was found to be strongly upregulated following carbon starvation, oxidative stress, heat shock, and during or after conidiation while sPlaB expression was barely detected in any of the conditions (Nakahama et al. 2010).

1.3.3 Ca^{2+} exchangers

The Ca^{2+} exchangers are Ca^{2+} transporting proteins that functions to reduce high $[Ca^{2+}]_c$ to resting levels by removing the excess cytosolic Ca^{2+} out of the cell, and by transporting Ca^{2+} into the intracellular Ca^{2+} storing organelles with the simultaneous exchange of positive ions across membranes that is driven by ATP hydrolysis (Zelter et al. 2004). The *N. crassa* Ca^{2+} signaling machinery includes six novel Ca^{2+}/H^+ exchangers and two putative Ca^{2+}/Na^+ exchangers (Galagan et al. 2003; Borkovich et al. 2004; Zelter et al. 2004). All the Ca^{2+} exchangers possess conserved Ca^{2+} exchanger domains. However, little is known about the detailed cellular role for any of the Ca^{2+} exchanger in fungi. The vacuolar Ca^{2+}/H^+ exchanger of *S. cerevisiae*, Vcx1p/Hum1p, is negatively regulated by calcineurin and is involved in rapid sequestration of cytosolic Ca^{2+} into vacuoles and also functions to transport cadmium (Cd^{2+}; Cunningham and Fink 1996; Miseta et al. 1999; Pittman et al. 2004). The human pathogenic fungus *C. neoformans* encodes a vacuolar Ca^{2+} exchanger, VCX1, which is involved in calcineurin dependent Ca^{2+} tolerance and is a potential virulence determinant of cryptococcosis (Kmetzsch et al. 2010). The *N. crassa* Ca^{2+}/H^+ exchanger called CAX, a homologue of *S. cerevisiae* Vcx1p/Hum1p, is involved in maintaining intracellular Ca^{2+} levels since strains lacking *cax* accumulates very little Ca^{2+} in the dense vacuolar fraction (Bowman et al. 2011). Out of the six Ca^{2+}/H^+ exchangers in *N. crassa*, NCU06366 encoded Ca^{2+}/H^+ (or Ca^{2+}/proton) exchanger is one of the two Ca^{2+}/H^+ exchangers that differ

significantly from its homologues in *M. grisea*, *S. cerevisiae*, and *Arabidopsis thaliana* in a phylogenetic analysis (Zelter et al. 2004). However, detailed knowledge about the Ca^{2+}/H^{+} exchangers including the NCU06366 encoded Ca^{2+}/H^{+} exchanger (CPE-1) has remained largely unknown in *N. crassa*.

1.4 Objectives of this study

Only a few Ca^{2+} signaling genes have been studied so far in *N. crassa* and detailed knowledge about the Ca^{2+} signaling machinery of *N. crassa* has remained largely unknown. Moreover, little is known about the functions of the homologues of PLC-1, sPLA2, and the Ca^{2+}/H^{+} exchangers including the CPE-1 in *N. crassa*, therefore, I have decided to work on three broad objectives as given below:

1. To understand the cellular roles of the Ca^{2+} signaling genes *phospholipase C-1* (*plc-1*), *secretory phospholipase A2* (*splA2*), and *Ca^{2+}/H^{+} exchanger-1* (*cpe-1*) in *N. crassa*.
2. To study the cell functions regulated by the genetic interactions of the *plc-1*, *splA2*, and *cpe-1* genes in *N. crassa*, and
3. To understand the molecular basis of the *plc-1*, *splA2*, and *cpe-1* functions in *N. crassa*.

Chapter 2

Materials and Methods

2.1 Materials

2.1.1 Chemicals and other materials

Glucose, fructose, sorbose, sucrose, sorbitol, bacto-agar, sodium dodecyl sulphate (SDS), cetyltrimethyl ammonium bromide (CTAB), calcium chloride ($CaCl_2.H_2O$), sodium citrate dehydrate (Na_3citrate.$2H_2O$), potassium phosphate monobasic (KH_2PO_4), potassium phosphate dibasic (K_2HPO_4), ammonium nitrate (NH_4NO_3), magnesium sulphate ($MgSO_4$), citric acid ($C_6H_8O_7.H_2O$), zinc sulphate heptahydrate ($ZnSO_4.7H_2O$), ferrous sulphate heptahydrate ($FeSO_4.7H_2O$), copper sulphate pentahydrate ($CuSO_4.5H_2O$), manganous sulphate ($MnSO_4.H_2O$), boric acid (H_3BO_3), sodium molybdate ($Na_2MoO_4.2H_2O$), potassium nitrate (KNO_3), sodium chloride (NaCl), sodium hydroxide (NaOH), potassium acetate (CH_3COOK), Tris base ($C_4H_{11}NO_3$), ethylenediaminetetra acetic acid disodium salt (EDTA $C_{10}H_{14}N_2O_8Na_2.2H_2O$), skim milk, calcium D-pantothenate ($C_9H_{16}O_5N.1/2Ca$), silica gel (6-12 mesh; Cat No. 214426-1KG), hexane, acetone, Tween 80, glacial acetic acid, absolute ethanol, Phenol:Chloroform:Isoamyl mixture (25:24:1), β-mercaptoethanol, glycerol, chloroform, agarose, ethidium bromide, X-gal (5 bromo-4-chloro-3-indolyl-B-galactoside), IPTG (isopropylthio-β-d-galactoside) and other general laboratory chemicals and glass wares were procured from various manufacturers such as Sigma Aldrich (Mumbai, India), SRL (Mumbai, India), Merck (Mumbai, India), Himedia (Mumbai, India), Borosil (Mumbai, India), Tarsons (Kolkata, India), and Rankem reagents (Faridabad, India). Hygromycin B solution was obtained from Himedia (Cat. No. PCT 1503-20 ML; Mumbai, India), biotin was procured from SRL (Cat. No. 0248120; Mumbai, India), and TRIzol reagent was purchased from Invitrogen (Cat. No. 84602; CA, USA). All restriction enzymes, DNA size markers, and Taq DNA polymerases for PCRs were purchased from New England Biolabs (NEB, USA). High fidelity Taq polymerases were purchased from Thermo Fischer Scientific (Finland). Custom oligonucleotide primers were purchased from Bioserve, India as well as from Integrated DNA Technologies, USA. DNA purification kits were from Nucleospin Gel and PCR Clean-up (Macherey-Nagel, Duren, Germany). All other chemicals were purchased from local manufacturers and were of analytical grade.

2.1.2 *N. crassa* strains

1. *74-OR23-1 A* (FGSC 987), and *OR8-1 a* (FGSC 988)

These are standard wild type *N. crassa* laboratory strains. The wild type strains FGSC 987 and the FGSC 988 were obtained from the Fungal Genetics Stock Center (FGSC; http://www.fgsc.net/, University of Missouri, Kansas City, MO 64110; McCluskey et al. 2010).

2. Knockout mutants of *N. crassa* Ca^{2+} signaling genes used in this study

These strains (Table 2.1) were generated using a high-throughput gene knockout procedure developed by the Neurospora functional genomics project (http://geiselmed.dartmouth.edu/dunlaploros/genome/; Colot et al. 2006) and obtained from the FGSC.

Table 2.1: List of the knockout mutants of *N. crassa* Ca^{2+} signaling genes used in this study

Sl. No.	NCU No.	Mating type	Type of Protein	Reference
1	07075	*mat a*	Ca^{2+}/H^{+} exchanger	FGSC 11248
2	07075	*mat A*	Ca^{2+}/H^{+} exchanger	FGSC 11249
3	0795	*mat a*	Ca^{2+}/H^{+} exchanger	FGSC 12376
4	0795	*mat A*	Ca^{2+}/H^{+} exchanger	FGSC 12375
5	02826	*mat a*	Ca^{2+}/H^{+} exchanger	FGSC 11530
6	02826	*mat A*	Ca^{2+}/H^{+} exchanger	FGSC 11529
7	06366	*mat a*	Ca^{2+}/H^{+} exchanger	FGSC 11407
8	06366	*mat A*	Ca^{2+}/H^{+} exchanger	FGSC 11408

9	08490	*mat a*	Ca^{2+}/H^{+} exchanger	FGSC 12468
10	07605	*mat A*	Ca^{2+} permeable channel	FGSC 11253
11	06703	*mat a*	Ca^{2+} permeable channel	FGSC 11707
12	06703	*mat A*	Ca^{2+} permeable channel	FGSC 11708
13	03305	*mat a*	Ca^{2+} ATPase	FGSC 13287
14	04736	*mat A*	Ca^{2+} ATPase	FGSC 13071
15	05154	*mat a*	Ca^{2+} ATPase	FGSC 13036
16	05154	*mat A*	Ca^{2+} ATPase	FGSC 13037
17	04898	*mat A*	Ca^{2+} ATPase	FGSC 13040
18	07966	*mat a*	Cation-ATPase	FGSC 11410
19	07966	*mat A*	Cation-ATPase	FGSC 11409
20	01266	*mat a*	Phospholipase C	FGSC 12022
21	06245	*mat a*	Phospholipase C	FGSC 11411
22	09655	*mat a*	Phospholipase C	FGSC 11271
23	09655	*mat A*	Phospholipase C	FGSC 11271
24	02175	*mat a*	Phospholipase C	FGSC 12023

25	05225	*mat a*	Ca^{2+} and/or CaM binding protein	FGSC 11405
26	05225	*mat A*	Ca^{2+} and/or CaM binding protein	FGSC 11406
27	02115	*mat a*	Ca^{2+} and/or CaM binding protein	FGSC 13049
28	02738	*mat a*	Ca^{2+} and/or CaM binding protein	FGSC 15890
30	06948	*mat a*	Ca^{2+} and/or CaM binding protein	FGSC 11541
31	06948	*mat A*	Ca^{2+} and/or CaM binding protein	FGSC 11542
32	04379	*mat a*	Ca^{2+} and/or CaM binding protein	FGSC 11403
33	04379	*mat A*	Ca^{2+} and/or CaM binding protein	FGSC 11404
34	03750	*mat a*	Ca^{2+} and/or CaM binding protein	FGSC 11531
35	02283	*mat a*	Ca^{2+} and/or CaM binding protein	FGSC 12448
36	02283	*mat A*	Ca^{2+} and/or CaM binding protein	FGSC 12449
37	09123	*mat a*	Ca^{2+} and/or CaM binding protein	FGSC 12548
38	09123	*mat A*	Ca^{2+} and/or CaM binding protein	FGSC 12549
39	02814	*mat a*	Ca^{2+} and/or CaM binding protein	FGSC 11169
40	02814	*mat A*	Ca^{2+} and/or CaM binding protein	FGSC 11170
41	09212	*mat a*	Ca^{2+} and/or CaM binding protein	FGSC 11545

42	06650	*mat a*	Ca^{2+} and/or CaM binding protein	FGSC 11246
43	06650	*mat A*	Ca^{2+} and/or CaM binding protein	FGSC 11247
44	06177	*mat a*	Ca^{2+} and/or CaM binding protein	FGSC 11537
45	06177	*mat A*	Ca^{2+} and/or CaM binding protein	FGSC 11536

3. *erg-3RIP A* and *erg-3RIP a* strains

The RIP-induced *erg*-3 mutants lack a functional sterol C-14 reductase (Prakash et al. 1999). They have slow growth rate than the wild type and are female sterile. The *erg-3RIP A* and *erg-3RIP a* strains were a kind gift from Dr. D. P. Kasbekar, Centre of Cellular and Molecular Biology, Hyderabad.

4. *his-3 A* strains

The *his-3 mat A* strains (FGSC 6031 and 6032) are deficient for the enzyme histidinol dehydrogenase and requires medium supplemented with histidine for growth. These strains were obtained from the FGSC.

5. Strains generated in this study

For targeted integration of exogenous DNA into the *his-3* locus, the *Δplc-1::hph::his-3 mat A (21)*, *Δplc-1::hph::his-3 mat A (29)*, *Δplc-1::hph::his-3 mat A (36)*, *Δplc-1::hph::his-3 mat A (76)*, *ΔsplA2::hph::his-3 mat A (10)*, *ΔsplA2::hph::his-3 mat A (21)*, *ΔsplA2::hph::his-3 mat A (51)*, *Δcpe-1::hph::his-3 mat A (4)*, *Δcpe-1::hph::his-3 mat A (16)*, *Δcpe-1::hph::his-3 mat A (36)*, *Δcpe-1::hph::his-3 mat A (40)*, *Δcpe-1::hph::his-3 mat A (60)*, and *Δcpe-1::hph::his-3 mat A (65)* recipient strains were generated in this study by crossing the individual knockout strains with the *his-3* strain of the opposite mating types. These recipient strains were selected by scoring for resistance to hygromycin B and histidine auxotrophy and verified by PCR analysis.

The *Δplc-1::hph::P$_{ccg-1}$::plc-1::gfp hop A (1)*, *Δplc-1::hph::P$_{ccg-1}$::plc-1::gfp hop A (13)*, *Δplc-1::hph::P$_{ccg-1}$::plc-1::gfp hop A (23)*, *Δplc-1::hph::P$_{ccg-1}$::plc-1::gfp hop A (24)*, *Δplc-1::hph::P$_{ccg-1}$::plc-1::gfp hop A (39)*, *ΔsplA2::hph::P$_{ccg-1}$::splA2::gfp hop A (72)*, *ΔsplA2::hph::P$_{ccg-1}$::splA2::gfp hop A (73)*, *ΔsplA2::hph::P$_{ccg-1}$::splA2::gfp hop A (74)*, *ΔsplA2::hph::P$_{ccg-1}$::splA2::gfp hop A (76)*, *ΔsplA2::hph::P$_{ccg-1}$::splA2::gfp hop A (78)*, *ΔsplA2::hph::P$_{ccg-1}$::splA2::gfp hop A (83)*, *ΔsplA2::hph::P$_{ccg-1}$::splA2::gfp hop A (90)*, *ΔsplA2::hph::P$_{ccg-1}$::splA2::gfp hop A (91)*, *Δcpe-1::hph::P$_{ccg-1}$::cpe-1::gfp hop A (2)*, *Δcpe-1::hph::P$_{ccg-1}$::cpe-1::gfp hop A (11)*, *Δcpe-1::hph::P$_{ccg-1}$::cpe-1::gfp hop A (12)*, *Δcpe-1::hph::P$_{ccg-1}$::cpe-1::gfp hop A (18)*, *Δcpe-1::hph::P$_{ccg-1}$::cpe-1::gfp hop A (19)*, *Δcpe-1::hph::P$_{ccg-1}$::cpe-1::gfp hop A (35)*, and *Δcpe-1::hph::P$_{ccg-1}$::cpe-1::gfp hop A (40)* homokarotic strains were generated for complementation studies as described in Chapter 3.

For genetic interaction studies, the Δ*cpe-1*; Δ*splA2 mat A (4)*, Δ*cpe-1*; Δ*splA2 mat A (19)*, Δ*cpe-1*; Δ*splA2 mat a (10)*, Δ*cpe-1*; Δ*splA2 mat a (24)*, Δ*plc-1*; Δ*splA2 mat A (17)*, Δ*plc-1*; Δ*splA2 mat A (20)*, Δ*plc-1*; Δ*splA2 mat a (6)*, Δ*plc-1*; Δ*splA2 mat a (15)*, Δ*plc-1*; Δ*cpe-1 mat A (10)*, Δ*plc-1*; Δ*cpe-1 mat A (23)*, Δ*plc-1*; Δ*cpe-1 mat a (14)*, and Δ*plc-1*; Δ*cpe-1 mat a (20)* double mutants were generated by crossing the individual knockout mutant strains of opposite mating types as described in Chapter 4.

2.1.3 Bacterial strain

The *Escherichia Coli DH5α*, genotype *SupE*44 D*lac*U169 (f80*lacZ* DM15) *hsdR*17 *recA*1 *end A*1 *gyrA*96 *thi*-1 *relA*1, is a recombination-deficient amber suppressing strain used for plating and growth of plasmids (Sambrook and Russell 2001). The f80 *lacZ′* DM15 mutation permits α-complementation with the amino terminus of β-galactosidase encoded in pUC vectors. It was used for all routine transformations, plasmid isolation, and selection of recombinants.

2.1.4 Plasmid vectors

(i) pBARGEM7-1

The plasmid vector pBARGEM7-1 is of size 4.5 kb and carries the fungal selectable marker *bar*, polylinker, and *lacZ′* sequence including the T7 and SP6 promoters, bacterial selectable marker ampicillin, and pUC origin (FGSC 19; Pall and Brunelli 1993; Figure 2.1). The expression of *bar* gene is under the control of *A. nidulans trpC* promoter. The *bar* gene encodes a phosphinothricin

acetyl transferase that detoxifies the antibiotic basta present in the selection medium and therefore, serves as a selectable marker for fungal transformants. The polylinker region containing the *lacZ′* sequence is sub cloned from pGEM7Zf (+) vector. Insertion of DNA fragments into the polylinker region disrupt the function of the *lacZ′* gene and recombinant clone can be screened by blue white selection on the concept of α-complementation (Ullmann et al. 1967).

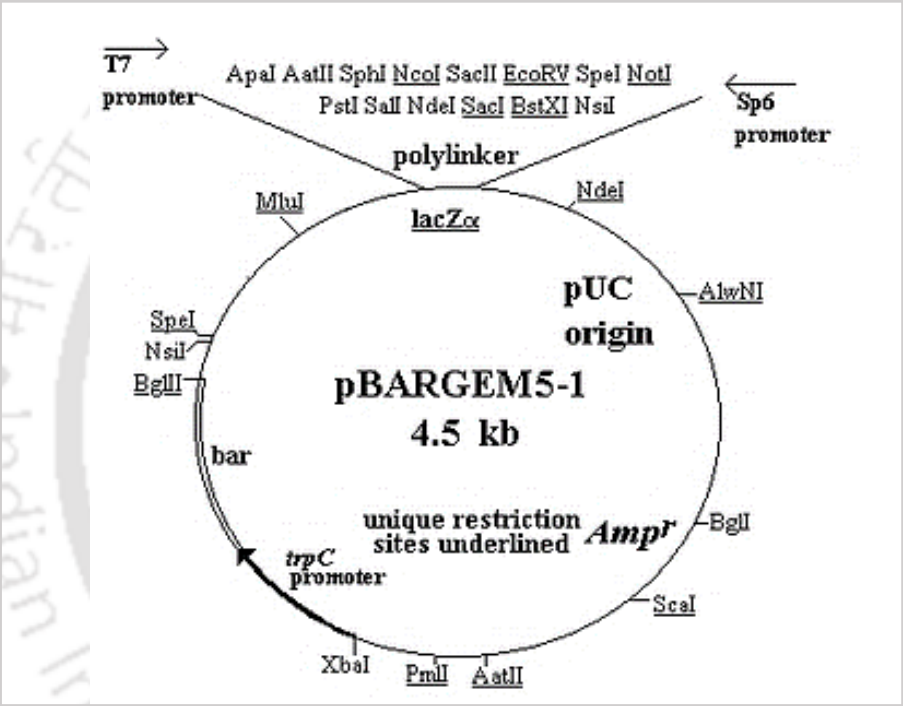

Figure 2.1: Schematic of the pBARGEM7-1 vector. The size of the vector is 4.5 kb. The unique restriction sites are underlined in the polylinker region of *lacZ′* sequence. The plasmid map is adapted from Pall and Brunelli 1993.

(ii) pMF272

The plasmid vector pMF272 (Figure 2.2) of size 8.4 kb, carries the GFP variant gene (*sgfp*), *lacZ′* sequence including the T7 and SP6 promoters, bacterial selectable marker ampicillin, and a multiple cloning site (MCS) for translational fusion of Neurospora genes to *sgfp* (Freitag et al. 2004). The *sgfp* gene is a derivative of GFP with substitution of serine to threonine at position 65 (S65T) which results in increased brightness, and mutations to shift the codon bias closer to that found in humans. It is under the control of inducible *N. crassa ccg-1* promoter, which is strongly

induced by glucose deprivation or stress (McNally and Free 1988). The $P_{ccg\text{-}1}$*::sgfp* cassette was constructed using the pBM60 backbone that allows *his-3* targeting of the transgene by gene replacement (Margolin et al. 1997).

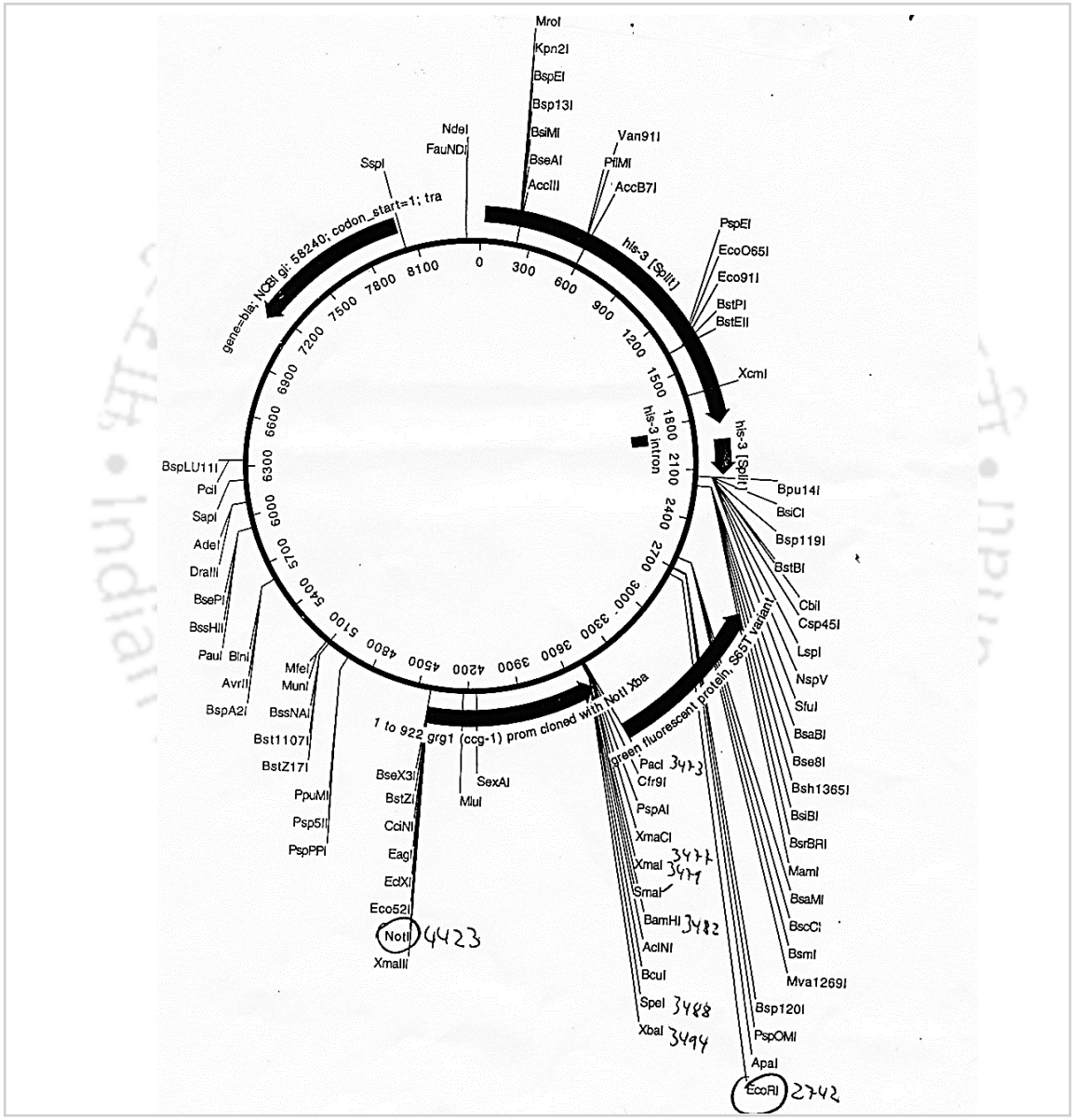

Figure 2.2: Schematic of the pMF272 vector. The size of the vector is 8.4 Kb. It consists of a MCS region with unique restriction sites. The plasmid map is available at www.fgsc.net/plasmid/image/609.jpg.

(iii) pRS426

The pRS526 is a yeast-type episomal shuttle plasmid vector used for gene cloning in host *S. cerevisiae* and *E. coli*. In *E. coli*, it has the pBM1 origin of replication from pBR322 and carries bacterial selectable marker ampicillin resistance gene, polylinker, and *lacZ'* sequence including T7 and T3 promoters. The *lacZ'* gene encodes α peptide of beta-galactosidase, which permits transformed colonies selection through blue-white screening. The unique cloning sites present in the polylinker region of the *lacZ'* sequence are *SacI BxtXI SacII EagI NotI SpeI BamHI SmaI EcoRI HindIII ClaI SalI XhoI I KpnI*. For replication in *S. cerevisae*, the pRS426 carries origin of replication from 2 micron circle plasmid along with the REP3 and FRT sequences necessary for high copy propagation. The yeast auxotrophic marker *URA3* is present for selection of transformed yeast. In *S. cerevisiae*, the copy number is about 20 per haploid cell (Figure 2.3). The pRS426 was used as a host vector in generating various knockout mutants of *N. crassa* including knockout mutants of Ca^{2+} signaling genes through high throughput gene knockout procedure (Colot et al. 2006; described in Chapter 3).

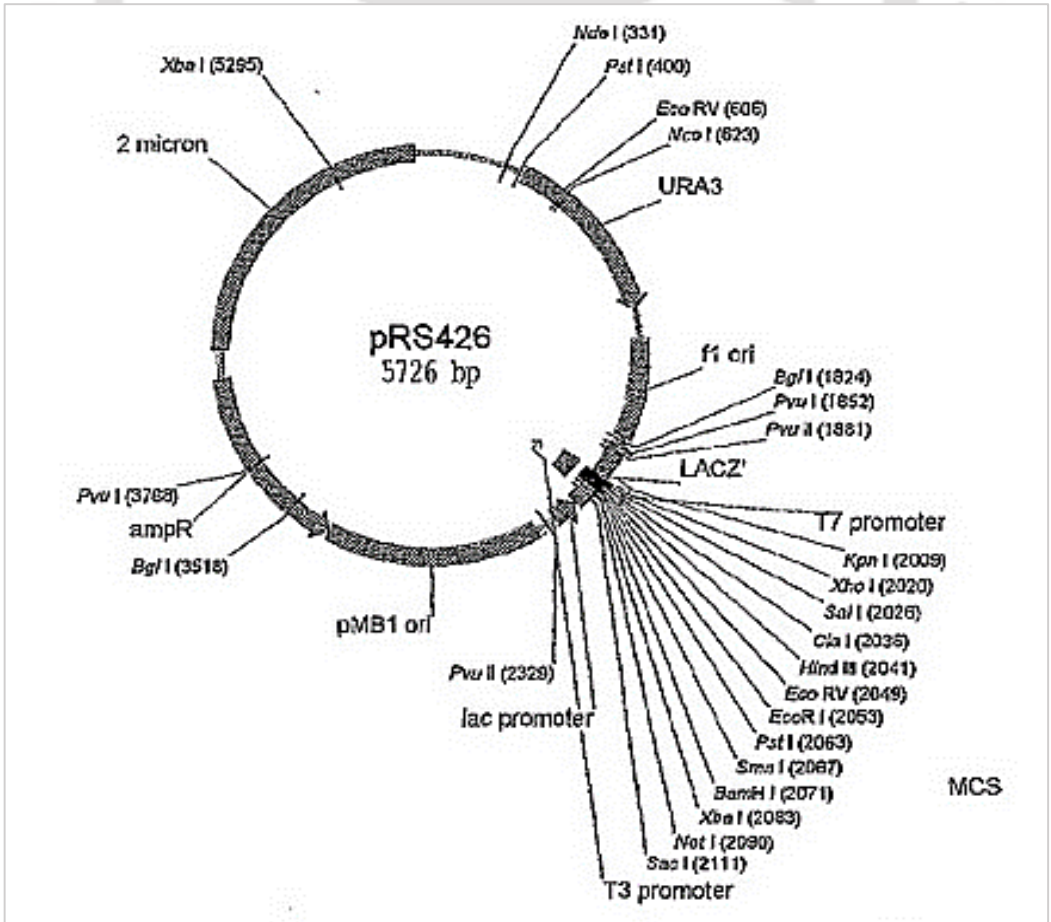

Figure 2.3: Schematic of the pRS426 vector. The size of the vector is 5.726 kb. The unique restriction sites are *Sac*I *Bxt*XI *Sac*II *Eag*I *Not*I *Spe*I *Bam*HI *Sma*I *EcoR*I *Hind*III *Cla*I *Sal*I *Xho*I *Kpn*I are present in the polylinker region of *lacZ'* sequence. The *URA3*, an auxotrophic marker for selection in *S. cerevisae*, and amp^R marker for selection in *E. coli* through blue-white screening. The plasmid map is available at http://www.creativebiogene.com/pRS426-phagemid-in-E.-coli-vector-VET1104-179-16.html.

2.1.5 Bacterial media, antibiotics, and commonly used solutions

Commonly used solutions described below were prepared essentially as described by Sambrook and Russell 2001.

1. Bacterial media: Luria Bertani (LB) broth, LB agar, terrific broth, and SOC medium were purchased from Himedia (Mumbai, India), prepared according to manufacturer's protocol and sterilized by autoclaving.

2. 20% IPTG: IPTG is isopropylthio-β-D-galactoside. A 20 % solution of IPTG was prepared by dissolving 2 g of IPTG in 8 ml of sterile water. The volume of the solution was adjusted to 10 ml and sterilized by passing it through a 0.22-µm disposable filter. The solution was dispensed into 1 ml aliquots and stored at -20ºC.

3. X-gal (20 mg/ml): X-gal is 5 bromo-4-chloro-3-indolyl-B-galactoside. A stock solution of 20 mg/ml X-gal was prepared in N, N-Dimethylformamide (DMF) in an amber Eppendorf tube to prevent damage by light and stored at -20ºC.

4. 5 M NaCl: Dissolved 29.22 g of NaCl in 80 ml of distilled water, and adjusted the volume to 100 ml. The stock was then sterilized by autoclaving and stored at room temperature.

5. 10N NaOH: Dissolved 40 g of NaOH pellet slowly in 80 ml of distilled water, stirring continuously in a plastic beaker placed on ice, adjusted the volume to 100 ml and stored at room temperature.

6. 2 M KCl: Dissolved 14.9 g of KCl in a final volume of 100 ml of distilled water and stored at room temperature.

6. 5 M $CaCl_2.2H_2O$: Amount of 73.5 g of $CaCl_2.2H_2O$ was dissolved in distilled water to a final volume of 100 ml. The solution was sterilized by autoclaving.

7. 0.1% DEPC: DEPC is Diethylpyrocarbonate. 0.1% DEPC solution was prepared in sterile distilled water and sterilized by autoclaving.

8. 8 M LiCl: Amount of 33.9 g of LiCl was dissolved in a final volume of 100 ml of DEPC treated sterile distilled water and sterilized by autoclaving.

9. 1 M Glucose: Amount of 18.016 g of glucose was dissolved in a final volume of 100 ml of distilled water and sterilized by autoclaving.

10. 1 M Sorbitol: Amount of 18.21 g of sorbitol was dissolved in distilled water to a final volume of 100 ml and sterilized by autoclaving.

11. 5 M Sucrose: Amount of 85.575 g of sucrose was dissolved in distilled water to a final volume of 100 ml and sterilized by autoclaving.

12. Ampicillin: A 1000X stock solution of 100 mg/ml ampicillin was made in sterile double-distilled water and stored in aliquots of 200 µl at -20°C.

13. Hygromycin B (100 mg/ml): A stock solution of 100 mg/ml was prepared by dissolving an amount of 100 mg of hygromycin B in 1 ml of sterile water and stored as aliquots of 200 µl at -20°C.

14. Basta (100 mg/ml): Basta is glufosinate ammonium sulphate. A stock solution of 100 mg/ml was prepared by dissolving an amount of 100 mg of basta in 1 ml of sterile distilled water and stored as aliquots of 200 µl at -20°C.

15. Ethidium bromide (10 mg/ml): 50 mg of ethidium bromide was dissolved in 5 ml of distilled water to prepare 10 mg/ml stock.

16. 6X Gel-loading Buffer (Type III): A solution of 0.25% (w/v) bromophenol blue, 0.25% (w/v) xylene cyanol FF, and 30% glycerol (v/v) was made in sterile water and stored at 4°C.

17. 10% SDS: SDS is sodium dodecyl sulphate. Dissolved 10 g of SDS in 90 ml of distilled water, heated to 68ºC, and stirred with a magnetic stirrer to assist dissolution. The volume was adjusted to 100 ml and stored at room temperature.

18. 1 M Tris: Dissolved 121.1 g of Tris base in 800 ml of distilled water, adjusted pH to the desired value by adding concentrated HCl (~ 70 ml, 60 ml, and 42 ml of concentrated HCl was added for pH 7.4, 7.6, and 8.0, respectively), adjusted the volume to 1 liter with distilled water and sterilized by autoclaving.

19. 0.5 M EDTA (pH 8.0): EDTA is disodium ethylenediaminetetra-acetate.$2H_2O$. 186.1g of EDTA was dissolved in 800 ml of distilled water, adjusted pH to 8.0 by NaOH, adjusted volume to 1 liter and sterilized by autoclaving.

20. 0.5 M EGTA (pH 8.0): EGTA is ethylene glycol bis (β-aminoethyl ether) N, N, N′, N′-tetraacetic acid. Amount of 19.017 g of EGTA was dissolved in 60 ml of sterile water and adjusted pH to 8.0 with NaOH pellets. Final volume was adjusted to 100 ml and sterilized by autoclaving.

21. RNAase A: Dissolved pancreatic RNAase (DNAase free, Sigma) at a concentration of 10 mg/ml in 10 mM Tris-Cl (pH 7.5), 15 mM NaCl, and stored at -20°C.

22. Alkaline lysis Solution I: Amount of 50 mM glucose, 25 mM Tris-Cl (pH 8.0), and 10 mM EDTA (pH 8.0) was added from their stock solutions in a final volume of 100 ml distilled water. Sterilized by autoclaving and stored at 4ºC.

23. Alkaline lysis Solution II: Amount of 0.2 N NaOH and 1% SDS were added in a required volume. The solution was freshly prepared just prior to use.

24. Alkaline lysis Solution III: For a volume of 100 ml solution, 60 ml of 5 M potassium acetate, 11.5 ml of glacial acetic acid, and 23.5 ml of distilled water were mixed together. Sterilized by autoclaving and stored at 4ºC.

25. 50X TAE: The stock solution of 50X TAE for one liter contains 242 g Tris base, 57.1 ml of glacial acetic acid, and 100 ml of 0.5 M EDTA (pH 8.0).

26. 1 X TE: The solution was prepared by adding10 mM Tris-HCl (pH 8.0) and 1 mM EDTA (pH 8.0) from their respective stocks.

27. 10X MOPS electrophoresis buffer: MOPS is a 3[N-Morpholino] Propanesulphonic acid. The stock solution of 10X MOPS for 1 litre contains 41.8 g of MOPS (0.2 M), 20 ml sodium acetate solution (20 mM), and 20 ml EDTA (10 mM). After dissolving, 41.8 g of MOPS in DEPC-treated water, pH was adjusted to 7.0 with 2 N NaOH and then added sodium acetate solution and EDTA in an indicated volume. Solution was filter sterilized using 0.45-µm Millipore filter and stored at room temperature protected from light.

28. Lysis buffer for Neurospora genomic DNA isolation: The lysis buffer contains 10 mM Tris HCl (pH 7.5), 0.5 M NaCl, 10 mM EDTA, 1% SDS, and 1% CTAB.

29. Lysis buffer for Neurospora RNA isolation: The lysis buffer contains 100 mM Tris HCl (pH 8.0), 0.6 M NaCl, 10 mM EDTA (pH 8.0), 4.5 % SDS, and 2 % β-mercaptoethanol.

2.1.6 Solutions for growth, maintenance, and crossing of Neurospora strains

Media for culturing Neurospora are prepared essentially as described in Davis and De Serres 1970.

1. Biotin solution

5 mg of biotin was dissolved in 100 ml of 50% (v/v) ethanol, stored at 4°C.

2. Trace element solution

Trace element solution was prepared by adding the following compounds successively, with stirring to 95 ml of distilled water.

Citric acid.1H_2O	5.00 g
$ZnSO_4.7H_2O$	5.00 g
$Fe(NH_4)_2(SO_4)_2.6H_2O$	1.00 g
$CuSO_4.5H_2O$	0.25 g
$MnSO_4.1H_2O$	0.05 g
H_3BO_3	0.05 g
$Na_2MoO_4.2H_2O$	0.05 g

The final volume was adjusted to 100 ml; 1 ml of chloroform was added as a preservative, and stored at room temperature.

3. Vogel's medium N

Vogel's medium N (Vogel, 1964) was prepared as a 50X-strength solution as follows:

To 750 ml of distilled water, the following ingredients were added in order, dissolving each one prior to addition of the next.

Na_3 citrate.$5H_2O$	150 g
KH_2PO_4	250 g
NH_4NO_3	100 g
$MgSO_4.7H_2O$	10 g
$CaCl_2.2H_2O$ (predissolved in 20 ml H_2O)	5 g
Biotin solution	5 ml
Trace element solution	5 ml

The volume of the solution was adjusted to one liter and 3 ml of chloroform was added as a preservative.

4. Vogel's glucose medium (VGM)

Vogel's medium N	1X
Glucose	1.5 % (w/v)

5. VGM agar

Vogel's medium N	1X
Glucose	1.5% (w/v)
Agar	2.0% (w/v)

6. Vogel's sucrose medium (VSM)

Vogel's medium N	1X
Sucrose	2 % (w/v)

7. VSM agar

Vogel's medium N	1X
Sucrose	2 % (w/v)
Agar	2.0% (w/v)

8. 4X Synthetic crossing medium (SCM)

4X strength synthetic crossing medium (SCM) was prepared by adding the following compounds with stirring to 500 ml of water. After adding the following components, the solution was sterilized by autoclaving.

KNO_3	2.0 g
K_2HPO_4	1.4 g
KH_2PO_4	1.0 g
$MgSO_4.7H_2O$	1.0 g
$CaCl_2.2H_2O$	0.2 g
NaCl	0.2 g
Biotin solution	0.2 ml
Trace element solution	0.2 ml

9. SCM agar

SCM	1X
Glucose	1.5% (w/v)
Agar	2.0% (w/v)

10. 10X FGS

Fructose	0.5% (w/v)
Glucose	0.5% (w/v)
Sorbose	20% (w/v)

11. Vogel's sorbose agar medium

FGS	1X
Vogel's medium N	1X
Agar	2.0% (w/v)

12. Top agar

FGS	1X
Vogel's medium N	1X
Agar	2.8% (w/v)

13. Media for circadian clock study

Vogel's medium N	1X
Glucose	0.1 % (w/v)
Arginine	0.17% (w/v)
Biotin	50 ng/ml
Agar	1.5 % (w/v)

14. Skim milk: Sterile milk was prepared by suspending 3.5 g milk powder in 50 ml of deionized water and stored at 4°C.

15. Media supplements

L-Histidine: 2 ml per 100 ml medium from a stock of 50 mg/ml in distilled H_2O. L-Histidine supplement stock solution was autoclaved and stored at 4°C.

16. Sterilization

All glasswares and plasticwares were sterilized by autoclaving at 120°C (250°F) at a steam pressure of 100 kPa (15 psi) for 20 min. Solutions were prepared in double-distilled water and generally sterilized by autoclaving. Heat-sensitive solutions were sterilized by filtering through a sterile 0.45 µm nitrocellulose filter (Millipore). For RNA isolation, all glasswares were first treated with 0.1 % DEPC solution for overnight, dried in oven at 150ºC, and sterilized by autoclaving.

2.2 Methods

2.2.1 Growth conditions

Growth and maintenance of the Neurospora strains were essentially as described in Davis and De Serres (1970). Strains were routinely grown on Vogel's media (Vogel 1964) for vegetative growth and on synthetic crossing medium (Westergaard and Mitchell 1947) for crossing and sexual development.

2.2.2 Crossing and ascospore collection

Crosses between *N. crassa* strains were essentially as described previously (Westergaard and Mitchell 1947; Davis and de Serres 1970). Crosses were performed by confrontation between opposite mating type mycelia inoculated as plugs on synthetic crossing agar medium in 55-mm-Petri dishes. The crosses were incubated at 22°C in a low temperature incubator (usually BOD incubator) for three to four weeks. Ascospores began to shot within 16-18 days, and harvested by washing the lids with ~1 ml of sterile H_2O after 21-25 days. Ascospores were then plated on Vogel's sorbose agar medium, activated by heat shock at 65°C for 30-60 min in a shaking water bath, and picked under dissection microscope by cutting out a small agar block containing the ascospore and transferred onto a slant with minimal or selective media followed by incubation at 30°C for growth.

2.2.3 Stock management

Silica stocks were prepared to store *N. crassa* strains. Strains were grown in Vogel's glucose agar slant for at 30°C for 3 days and then at room-temperature under light for four days. Silica (6-12 Mesh, Grade 40) was sterilized by autoclaving and dried for two-three days at 60°C and further cooled to room temperature before use. Cryo tubes (4.5 ml) were filled with dried silica and kept

in ice for 30 min. For each strain, one ml of 5% autoclaved skimmed milk was added to the culture tube and vortexed vigorously. Spore suspension was drawn up into a Pasteur pipette and dispensed into the pre-chilled silica gel and vigorously vortexed for five min, breaking up any clumps in the process. Tubes were regularly vortexed for eight-ten days. After a week or more, stocks were kept at -20°C until further use.

2.2.4 Colony morphology

For colony morphology, strains were grown in either 90-mm-Petri dishes or 250 ml flasks containing Vogel's glucose agar medium and incubated for three days in the dark at 30°C followed by four days under light at room temperature and photographed (Nikon Coolpix P500).

2.2.5 Growth rate

Growth was measured by placing mycelial plug in the center of 90-mm-Petri dishes containing Vogel's glucose agar medium and incubated at 30°C. Colony growth was marked after 12 h from inoculation point with an interval of 3 h over a period of 24 h to obtain radial growth rate. Strains that showed lower growth rate on Petri dishes were further analyzed by using standard race tube assay (Figure 2.4; Ryan et al. 1943). Race tubes were partially filled with 13 ml of Vogel's glucose agar medium and inoculated with mycelial plug at one end and incubated at 30°C for three days. The apical growth rate of *N. crassa* was determined by mycelial extension rates at every 12 h interval in race tube and the distance of the hyphal growth front from the inoculation point was measured and plotted against time. Radial and apical growth rates were calculated as cm/h.

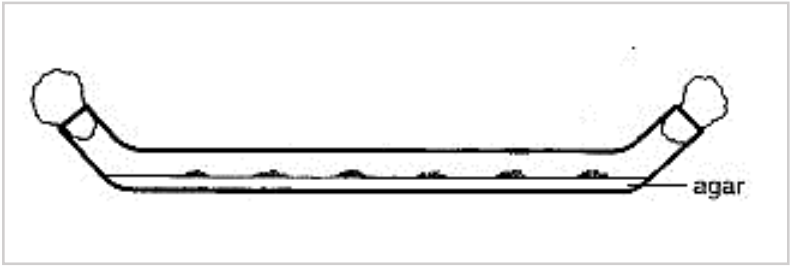

Figure 2.4: Standard race tube (Perkins et al. 2000)

2.2.6 Mycelial mass accumulation analysis

For mass accumulation in solid media, mycelial plug was inoculated at the center of 90-mm-Petri dishes containing Vogel's glucose agar medium overlaid with a cellophane layer and incubated

under the conditions of either 30°C for three days in the dark, or 30°C for two days in the dark followed by illumination at room temperature for one day. Following incubation, cellophane was removed and mycelial mass was taken (Yang et al. 2002). For mass accumulation in liquid media, mycelial plug was inoculated in 250 ml flasks containing VGM for three days at 30°C with shaking at 180 rpm, mycelial mat formed were then dried at 60°C, and dry weight was measured.

2.2.7 Aerial hyphae development analysis

For aerial hyphae, 1×10^6 conidia/ml were inoculated in sterile test tubes containing Vogel's glucose medium and grown in the dark at 30°C for three days and under light at room temperature for four days. Height of aerial hyphae was measured and then photographed (Nikon Coolpix P500).

2.2.8 Hyphal morphology analysis

For hyphal morphology, strains were grown for 12-16 h on a thin layer of Vogel's glucose agar medium on glass slides at 30°C and examined under Trinocular inverted microscope (AxioVert A1 FL, Carl Zeiss) at 20X magnification.

2.2.9 Conidial cell count

For quantification of conidia production, mycelial plug was inoculated in 250 ml flasks containing Vogel's glucose agar medium and incubated at 30°C in the dark for two days followed by incubation under light at 22°C for four days. Conidia were scraped from the agar surface with sterile distilled water and briefly agitated for thorough resuspension of conidia. Conidial counting was performed using a haemocytometer under Trinocular inverted microscope (AxioVert A1 FL, Carl Zeiss).

2.2.10 Time course quantification of conidia

For time course conidia analysis, strains were grown in 55-mm-Petri dishes containing Vogel's glucose agar medium and incubated in complete darkness at 30°C. Conidia were harvested at regular intervals of 12 h for a period of 72 h and quantified using a haemocytometer under Trinocular inverted microscope (AxioVert A1 FL, Carl Zeiss).

2.2.11 Conidial germination assay

Conidial germination was assayed both qualitatively and quantitatively. For qualitative assay, ~1×10^6 conidia/ml were inoculated in sterile test tubes containing Vogel's glucose medium and incubated at 25°C with shaking at 180 rpm. An aliquot of the cultures was observed under the microscope (AxioVert A1 FL, Carl Zeiss) at intervals of 0, 24, 48, and 60 h to determine conidiation efficiency. For quantitative assay, 100 µl from a 1×10^4 conidia/ml conidial suspension of each of the strains were inoculated onto the surface of Vogel's glucose agar medium and incubated at 25°C. Germination of conidia was observed under the Trinocular inverted microscope (AxioVert A1 FL, Carl Zeiss) at intervals of 0, 8, 12, 24, 36, 48, and 60 h. Percent germination was calculated as (germinated conidia/total number of conidia) × 100% (Zhu et al. 2015).

2.2.12 Submerged culture conidiation assay

For conidiation in submerged cultures, ~1×10^6 conidia/ml were inoculated in 250 ml flasks containing Vogel's glucose medium supplemented with or without 2% peptone (w/v) and incubated at 30°C with shaking at 180 rpm for 16 h. Aliquots of these cultures were observed under the microscope (AxioVert A1 FL, Carl Zeiss) to assay formation of conidiophores (Yang et al. 2002).

2.2.13 Carotenoid accumulation estimation

For analysis of carotenoid accumulation, sterile 90-mm-Petri dishes containing Vogel's glucose agar medium supplemented with 0.2% tween 80 were inoculated with conidia at a concentration of ~1×10^6 conidia/ml (Zalokar 1954). Cultures were initially incubated for 48 h in the dark at 30°C and further incubated at three different temperatures of 8, 22, and 30°C either with or without an exposure to white light for 24 h (illuminated with two fluorescent bulbs, Philips TL-D 18W/54 lamp, 18W, 6500 K, 1015 lumens). Mycelia from these cultures were collected, lyophilized, and pulverized into fine powder with mortar and pestle. Subsequently, acetone and hexane were used in consecutive steps for extraction of total carotenoids from 25 mg of dry weight powdered sample. Total carotenoid content was determined by taking the maximum absorbance value at 470 nm and using the formula:

Total carotenoid content (µg/g) = [Total absorbance × Total volume of extract (1 ml) × 10^4] / [Absorption coefficient (2500) × sample weight (g)] as described previously (Rodriguez-Amaya and Kimura 2004).

2.2.14 Time course carotenoid accumulation estimation

For time course analysis of carotenoid accumulation, ~1×10^6 conidia/ml were grown in 90-mm-Petri dishes containing Vogel's glucose medium supplemented with 0.2% tween-80 and incubated at three different temperatures of 8, 22, and 30°C with simultaneous exposure to white light for 0, 1, 3, 6, 9, and 12 h. Carotenoids accumulated in the mycelia were then extracted from the three temperatures at indicated times using acetone and hexane in consecutive steps. Total carotenoid content was determined by taking the maximum absorbance value at 470 nm and using the formula as described in section 2.2.13.

2.2.15 Fertility assay

For fertility assay, strains (female parent) were cultured either on 55-mm-Petri dishes or test tubes containing synthetic crossing medium at room temperature with constant light for seven days and subsequently fertilized with the male parent. After 7 days post fertilization, perithecia formed if any were viewed under Trinocular inverted microscope (AxioVert A1 FL, Carl Zeiss) and images captured. Ascospores were harvested by washing the lids with ~1 ml of sterile H_2O after 21-25 days. Ascospores were then plated on Vogel's sorbose agar medium, activated by heat shock at 65°C for 30-60 min in a shaking water bath and picked. Picking was done under dissection microscope by cutting out a small agar block containing the ascospore and transferred onto a slant with minimal or selective media followed by incubation at 30°C for growth. Ascospores viability was determined by dividing the total number of ascospores by the number of viable ascospores on plates.

2.2.16 Calcium ionophore assay

To test elevated intracellular Ca^{2+} sensitivity on the mutants, mycelial plug was inoculated onto one corner of 90-mm-Petri dishes and 10 µl each of a 9.5 mM stock solution of A23187 (test) or ethanol (control) was spotted onto the other corner on Vogel's glucose agar medium (Lew et al. 2008). Petri dishes were incubated at 30°C for two-three days and colonies were observed under

Trinocular inverted microscope (AxioVertA1FL, Carl Zeiss). Hyphal images were captured with an AxioCam ICc3 CCD camera. The Petri dishes were also photographed after 38 h of growth using a digital camera (Nikon Coolpix P500).

2.2.17 Calcium sensitivity assay

For calcium sensitivity test, mycelial plug ~ 1 cm diameter taken from a three days old culture of each strain was inoculated at the center of 90-mm-Petri dishes containing Vogel's glucose agar medium supplemented with 0.0, 0.2, 0.3, and 0.4 M $CaCl_2$ and incubated at 30°C. Colony diameter was measured after 12 h with an interval of 3 h over a period of 24 h. Radial growth rate was calculated as cm/h.

2.2.18 Osmotic stress assay

For osmotic stress, ~ 1 cm diameter mycelial plug from a three days old culture of each strain was inoculated at the center of 90-mm-Petri dishes containing Vogel's glucose agar medium supplemented with or without the hyperosmotic agents 0.75 M NaCl, 0.75 M KCl, 1.5 M Sucrose, and 1.5 M Sorbitol and incubated at 30°C. Colony diameter was measured after 12 h with an interval of 3 h over a period of 24 h. Radial growth rate was calculated as cm/h.

2.2.19 Temperature sensitivity assay

Temperature sensitivity assay was performed by inoculating ~1 cm diameter mycelial plug at the center of 90-mm-Petri dishes containing Vogel's glucose agar medium and incubated at three different temperatures of 20, 30, and 40°C. Colony diameter was measured after 12 h with an interval of 3 h over a period of 24 h. Radial growth rate was calculated as cm/h.

2.2.20 Oxidative stress assay

For H_2O_2 induced oxidative stress assay, ~1×10^6 conidia/ ml were inoculated in Vogel's glucose medium and germinated with shaking at 200 rpm for 2 h in the dark at 30°C. Germlings obtained were supplemented with (test) or without (control) H_2O_2 at a final concentration of 10 mM and further germinated for 1 h at 30°C. Germlings were plated on Vogel's sorbose agar medium and incubated at 30°C for 24 h. Percent survival was scored by dividing the number of viable colonies

from plates exposed to H_2O_2 (test) by the number of colonies from plates not exposed to H_2O_2 (control) and multiplying by 100.

2.2.21 Thermotolerance assay

For thermotolerance assay, ~1×10^6 conidia/ ml were inoculated in Vogel's glucose medium and germinated with shaking at 200 rpm for 2 h in the dark at 30°C. The 2 h germlings obtained were held at 30°C (control), 30°C (uninduced thermotolerance), and 44°C (induced thermotolerance). Both 30°C (uninduced) and 44°C (induced) germlings were then given a 52°C lethal heat shock for 20 minutes. Germlings were finally plated on Vogel's sorbose agar medium followed by incubation at 30°C for 24 h (Yang and Borkovich 1999). Percent survival was calculated by dividing the number of viable colonies from plates subjected to heat-treatment (induced or uninduced) by the number of colonies on plates held at 30°C (control) and multiplying by 100.

2.2.22 Phytosphingosine sensitivity assay

For phytosphingosine (PHS) assay, ~1×10^6 conidia/ ml were inoculated in Vogel's glucose medium and germinated with shaking at 200 rpm for 2 h in the dark at 30°C. The 2 h germlings obtained were exposed to 10 µg/ml PHS for 0, 30, 60, 90, and 120 min. Germlings were finally plated on Vogel's sorbose agar medium followed by incubation at 30°C for 24 h. Percent survival was calculated by dividing the number of viable colonies from plates exposed to PHS by the number of colonies on plates with a 0 min exposure to PHS (control) and multiplying by 100.

2.2.23 Ultraviolet sensitivity assay

For UV sensitivity assay, conidia were grown in 250 ml flasks containing Vogel's glucose agar medium at 30°C in the dark for 48 h and then at room temperature with constant light for three days. For quantitative analysis, ~1000 conidia were plated on Vogel's sorbose agar medium and irradiated with 50, 100, 150, and 200 J/m^2 of UV (253 nm wavelength) in a UVC 500 cross linker (Hoefer, UK). The plates were incubated at 30°C in the dark for 48 h and number of colonies on each plate counted.

2.2.24 UV sensitivity assay relative to carotenoid accumulation

For UV sensitivity assay relative to carotenoid accumulation, conidia were grown in 250 ml flasks containing Vogel's glucose agar medium at 30°C in the dark for 48 h and then at 8, 22, and 30°C with or without white light illumination (illuminated with two fluorescent bulbs, Philips TL-D 18W/54 lamp, 18W, 6500 K, 1015 lumens). For quantitative analysis, ~1000 conidia were plated on Vogel's sorbose agar medium and irradiated with 50, 100, 150, and 200 J/m^2 of UV (253 nm wavelength) in a UVC 500 cross linker (Hoefer, UK). The plates were incubated at 30°C in the dark for 48 h and number of colonies on each plate was counted.

2.2.25 Membrane potential assay

For membrane potential assay, ~1×10^6 conidia/ ml were germinated at 200 rpm for 2 h at 30°C in Vogel's glucose medium. The 2 h germlings were treated either with ionophore (test) or toluene (control) and further incubated with 3.87 µM DiBAC (Alcántara-Sánchez et al. 2004). After 30 minutes of incubation, observations were made under microscope (AxioVertA1FL, Carl Zeiss) with a 450-490 nm excitation filter and 515 nm emission filter and cells were photographed.

2.2.26 Antioxidative assay

For antioxidative assay, ~1×10^6 conidia/ml were inoculated in Vogel's glucose agar medium supplemented with 0.2% tween-80 and incubated at 30°C for 48 h. Cultures were further incubated for 2 h in the presence of 1 mM N-acetyl-L-cysteine (NAC), and then exposed to white light at 8, 22, and 30°C for an additional 2 h. Mycelia from these cultures were collected, lyophilized, and pulverized into fine powder with mortar and pestle. Subsequently, acetone and hexane were used in consecutive steps for extraction of total carotenoids from 25 mg of dry weight powdered sample. Total carotenoid content was determined by taking the maximum absorbance value at 470 nm and using the formula described in section 2.2.13. N-acetylglycine (NAG) was used as a negative control.

2.2.27 Reactive oxygen species estimation

For qualitative assay for ROS, strains were grown in Vogel's glucose agar medium for two days in the dark and either exposed to white light or kept in the dark for one day at 8, 22, and 30°C. Conidia were harvested and inoculated in Vogel's glucose medium containing 25 µM 2', 7'-

dichlorofluorescein-diacetate (DCFH-DA) for 60 min. Treated conidia were further washed with sterile distilled H_2O. An aliquot of the cultures was taken and observed by fluorescence microscopy (AxioVert A1 FL, Carl Zeiss) with a 450-490 nm excitation filter and 515 nm emission filter. Conidia that showed green fluorescence was captured.

2.2.28 Assay for visualization of internal septation of germlings and hyphae

For visualization of internal septation of germlings, ~1×10^6 conidia/ml were inoculated in Vogel's glucose medium and germinated with shaking at 200 rpm for 2 h in the dark at 30°C. 2 h germlings were then stained with calcoflour white (CFW; 0.1% in 0.05 M PBS). For visualization of internal septation of vegetative hyphae, strains were grown in Vogel's glucose agar medium for 12 h in the dark at 30°C. 12 h growing hyphae were then stained with CFW (0.1% in 0.05 M PBS). The sample slides of germlings and hyphae were incubated in the dark for 20 minutes and observed under a Trinocular inverted fluorescence microscope (AxioVert A1 FL, Carl Zeiss) under DAPI filters with exposure time of 300-400 ms.

2.2.29 Assay for visualization of intracellular distribution of Ca^{2+}

For visualization of intracellular distribution of Ca^{2+}, strains were grown in Vogel's glucose agar medium for 12 h in the dark at 30°C. The 12 h growing hyphae were then supplemented with 200 µM chlortetracycline hydrochloride (CTC) or 20 µM 1-N-Phenylnaphthylamine (NPN) in 0.1% dimethyl sulphoxide (DMSO). CTC and NPN fluorescence were observed under a Trinocular inverted fluorescence microscope (AxioVert A1 FL, Carl Zeiss) under DAPI filters with exposure time of 300-400 ms.

2.2.30 Isolation of sterols from *N. crassa* strains and analysis by UV spectrophotometry

The *N. crassa* strain of interest was grown in Vogel's glucose medium at 30°C for 3 to 5 days. The mycelial mass was harvested by vacuum filtration and lyophilized. The dried mycelia were ground with glass beads (0.2 mm in diameter) using a mortar and a pestle to a fine powder. About 50 mg of the powdered mycelia was taken in a 1.5 ml microfuge tube and 750 µl each of methanol and chloroform was added to the tube and kept on a rotary shaker overnight. The mycelial mass was removed by centrifugation at 12,000 rpm for 10 minutes. The chloroform-methanol extract which contains the lipids was washed once with 0.9 % NaCl and twice with 2 M KCl to remove the

saponifiable lipids. The aqueous and organic phases were separated by centrifugation and the bottom organic phase was transferred to a fresh tube. This step separates the saponifiable lipids from non-saponifiable lipids like sterols. The organic phase containing the sterols was air-dried and the sterols were dissolved in about 20 ml of chloroform. This sample was diluted 1: 200 in ethanol and its UV absorption spectrum (200 to 300 nm) was recorded in a Cary 100 Bio UV-visible spectrophotometer (Agilent technologies, USA).

2.2.31 Scoring for antibiotic resistance

Antibiotic resistance was scored by streaking conidia onto 1.5% agar plate's containing Vogel's sorbose agar medium and supplemented with the antibiotic. The antibiotics used were hygromycin B (220 µg /ml from 100 mg/ml stock in water), and basta (400 µg/ml from 100 mg/ml stock in water).

2.2.32 Preparation of ultracompetent cells

Ultracompetent cells were prepared essentially as described by Inoue et al. 1990. A single colony of *E. coli DH5α* maintained on a fresh LB agar plate was inoculated into 5 ml of LB and incubated at 37°C at 200 rpm for 16 h. One ml of this overnight culture was inoculated into 100 ml of LB medium and incubated at 18°C at 200 rpm, till the OD600 reached 0.750. The culture was chilled on ice and centrifuged at 1,500 g for 15 min at 4°C to pellet the cells. The cells were then resuspended in 32 ml of ice cold Transformation Buffer (TB: 10 mM PIPES of pH 6.7, 15 mM $CaCl_2$, 250 mM KCl, 55 mM $MnCl_2$) and incubated on ice for 10 min. The centrifugation was treated and the cells were resuspended in 8 ml of TB containing 7% DMSO, distributed into 100 ml aliquots, frozen in liquid nitrogen, and stored at -80 °C. Ultracompetent cells were used for cloning experiments involving ligation of DNA fragments with blunt-ended termini.

2.2.33 Transformation of ultracompetent *E. coli* cells by heat shock

Competent cells were removed from the -80°C freezer and thawed on ice. Ligated DNA sample (~50-100 ng) was added to the competent cells and mixed gently. The cells were incubated on ice for 30 min, following which they were subjected to heat shock at 42°C in water bath (Julabo GmbH, Germany) for 90 sec. After the heat shock 800 ml of SOC was added to the cells and the tubes were incubated at 37°C with shaking at 250 rpm for 1 h. Cultures were centrifuged at 8000

rpm for 5 min to pellet down the cells. Supernatant was removed and pellet was resuspended in 200 µl of SOC broth. The cells were plated on 90-mm-LB agar plates containing 100 mg/ml of ampicillin. The plates were incubated at 37°C for 12-14 h.

2.2.34 Isolation of plasmid DNA from bacterial culture

2.2.34.1 Small-scale isolation of plasmid DNA from bacterial culture

Small-scale or minipreparation of plasmid was made by alkaline lysis with SDS (Sambrook and Russell 2001). Briefly, 5 ml of overnight bacterial culture was centrifuged in microfuge tube for 2 min at 6000 rpm. Pellet was resuspended in 100 ml alkaline lysis solution I with vigorous vortexing. After mixing the contents, 200 ml of freshly alkaline lysis solution II was added to the bacterial suspension, contents were mixed by inverting the tubes 4-5 times, and kept on ice for 10 min. To the viscous bacterial lysate, 150 ml alkaline lysis solution III was added, mixed by inverting the tube, and kept on ice for 3-5 min. The tube was centrifuged for 10 min at 12,000 rpm and 4°C. The supernatant was transferred to the fresh microfuge tube and equal volume of phenol: chloroform: isoamyl alcohol (25:24:1) was added, centrifuged for 10 min at 12,000 rpm and 4°C. The aqueous phase was taken in a fresh microfuge tube (1.5 ml) and plasmid DNA precipitated by adding 1.5 volumes of absolute ethanol. The tube was gently inverted few times and the DNA was pelleted by centrifuging the tube for 10 min at 12,000 rpm. The supernatant was discarded and the pellet was washed with 70% ethanol by centrifuging for 2 min at 12,000 rpm. The ethanol trace was completely removed and the DNA pellet was allowed to dry at room temperature for 15 min. Finally, the pellet was dissolved in about 30 µl of 1X TE buffer (pH 8.0) and stored at 4ºC.

2.2.34.2 Large scale isolation of plasmid DNA from bacterial culture

Large-scale preparation of plasmid DNA (~500 mg) was made by alkaline lysis method (Sambrook and Russell 2001). Briefly, centrifuged overnight (250 ml with antibiotic) at 6,000 rpm for 10 min. The pellet was suspended in 9 ml of alkaline lysis solution I, 1 ml of a freshly prepared solution of 10 mg/ml lysozyme, and 20 ml of freshly prepared alkaline lysis solution II. The contents were thoroughly mixed by gently inverting the bottle several times and incubated for 5-10 min at room temperature. 10 ml of alkaline lysis solution III was added to the contents and gently mixed by swirling several times and placed the mixtures on ice for 5-10 min. The bacterial lysate was centrifuged for 15 min at 12,000 rpm at 4°C. The supernatant was transferred to the fresh tube and

0.6 volume of isopropanol was added and stored the tube at room temperature for 10 min. The precipitated nucleic acid was recovered by centrifugation at 12,000 rpm at room temperature and washed once with 70% ethanol. The pellet was dried at room temperature and then dissolved in 200 ml of TE buffer. RNAase A treatment was given to the plasmid solution and then stored at -20°C for further use.

2.2.35 Transformation of the *N. crassa* strain by electroporation

The protocol was based on the method as described previously (Margolin et al. 1997; Bhat et al. 2004). The recipient strain was grown in six to eight 250 ml conical flasks on Vogel's glucose agar medium for a week at 30°C. The conidia were harvested in sterile water and separated from the mycelium by passing the suspension through cheesecloth attached to a 250 ml conical flask (the mouth of a 250 ml conical flask was covered with cheesecloth and sterilized by autoclaving beforehand). The conidial suspension was taken in a 30 ml Corex tube and centrifuged at 800 rpm for 6 min in a Sorvall HB-4 rotor in 4°C. The conidial mass was washed twice in 30 ml water and resuspended in 1 M sorbitol at a concentration of $3x10^9$ spores/ml. About 40 µl of the conidial suspension was mixed with the transforming DNA and the mixture was placed in a pre-chilled 0.2 cm gap sterile electroporation cuvette (BioRad Laboratories, Hercules, CA). Electroporation was performed using a BioRad Gene Pulser apparatus (BioRad Laboratories, Hercules, CA). The conditions for electroporation were 1.5 KV, 25 µF, and 600 W. The time constant varied from 13 to 15 ms. Immediately, after the pulse, 600 ml of chilled 1 M sorbitol was added, kept in ice for 5 min, and the transformant conidial suspension was mixed with top agar and plated on a Vogel's sorbose agar plate. Usually about 4-5 transformants were obtained per plate and were 'pickable' under a dissection microscope after 2 days. A control transformation was done without adding DNA to eliminate the possibility of any contamination.

2.2.36 Neurospora genomic DNA isolation

The strain of interest was grown in Vogel's glucose medium at 30°C for 2 to 3 days with shaking at 200 rpm. The mycelial mass was harvested by vacuum filtration and lyophilized. The dried mycelia were ground with glass beads (0.2 mm in diameter) using a mortar and a pestle to a fine powder. Approximately, 150 mg of the powdered mycelia was taken in a 1.5 ml microfuge tube and 1 ml of lysis buffer added to it. Complete mixing of the mycelia and lysis buffer was achieved

using a pipette tip or a toothpick. The tube was incubated at 65°C for 30 min, followed by centrifugation at 15,000 rpm for 10 min. The supernatant was taken in a fresh microfuge tube and 500 µl of phenol: chloroform: isoamyl alcohol mixture (25:24:1) was added. The tube was rotated in a cell mixer for 15 min and centrifuged at 15,000 rpm for 10 min. The aqueous phase was carefully removed and the phenol: chloroform: isoamyl alcohol treatment repeated. The aqueous phase was taken in a fresh microfuge tube and washed with 600 µl of chloroform to remove the last traces of phenol. The aqueous phase was taken in a fresh tube and genomic DNA precipitated by adding 1.5 volumes of absolute ethanol. The tube was gently inverted few times and the genomic DNA pelleted by centrifuging the tube for 10 min at 15,000 rpm. The supernatant was discarded and the pellet was washed with 70% ethanol by centrifuging for 2 min at 15,000 rpm. The traces of ethanol were completely removed and the genomic DNA pellet was allowed to dry at room temperature for 15 min. Finally, the pellet was dissolved in about 60 µl of 1X TE buffer (pH 8.0) and stored at 4ºC. All centrifugations were carried out at 25ºC.

2.2.37 Neurospora RNA isolation

RNA was isolated from *N. crassa* strains as described previously (http://www.fgsc.net/fgn37/sokol.html). The conidia of the strain of interest were grown in 250 ml flasks in Vogel's glucose medium at 30°C with shaking at 180 rpm for 12 to 16 h. The mycelial mass was harvested by vacuum filtration and immediately frozen in liquid nitrogen. The frozen tissue was ground to a fine powder using a mortar and a pestle. The powder (~25 mg) was immediately transferred into a 2 ml microfuge tube containing 300 µl TRIzol reagent (Invitrogen, CA) to protect RNA from degradation by RNAase followed by further addition of the mixture of 750 µl lysis buffer (0.6 M NaCl, 10 mM EDTA, 100 mM Tris HCl, pH 8.0, 4% SDS) and 750 µl phenol (saturated with 0.1 M Tris HCl, pH 8.0). The tube was rotated in a cell mixer for 20 min and centrifuged at 10,000 rpm for 10 min. The upper aqueous phase was carefully removed and transferred to a fresh 2 ml microfuge tube containing an equal volume of phenol (saturated with 0.1 M Tris HCl, pH 8.0). The mixture was vortexed for few seconds and centrifuged for 10 min at 10,000 rpm. The upper aqueous phase was transferred to a fresh 2 ml microfuge tube and 750 µl of 8 M LiCl was added. The mixture was stored overnight at 4°C for 16-20 h. The next day mixture was vortexed briefly and centrifuge for 10 min at 10,000 rpm. The pellet was resuspended, which is not always visible, in 0.3 ml double distilled water, mixed with 0.03 ml 3 M Na-acetate (pH 5.2)

and 750 µl ethanol. The mixture was stored at -20°C for 2 h and centrifuged for 10 min at 10,000 rpm. The supernatant was discarded and the precipitate was washed with 70% ethanol. The RNA pellet was dried in room temperature for 10 to 15 min and re-dissolved in 30 µl DEPC treated or RNAase free water. The RNA solution was stored at -80°C.

2.2.38 Quantitation of nucleic acids

The concentration of nucleic acids was estimated by measuring the OD at 260 nm in nanodrop spectrophotometer (eppendorf, Germany). The following empirical relationships were used to calculate the concentrations. An OD_{260} of 1 corresponds to ~50 µg/ml for double stranded DNA, 40 µg/ml for single-stranded DNA and RNA, ~20 µg/ml for single-stranded oligonucleotides. The purity of nucleic acids was estimated by calculating the OD_{260}/OD_{280} ratio. Pure preparations of DNA and RNA have OD_{260}/OD_{280} values of 1.8 and 2.0, respectively.

2.2.39 Polymerase Chain Reaction

The routine polymerase chain reaction (PCR) reaction was carried out using *Taq* DNA polymerase and according to the manufacturer's protocol (Cat no. M0273S, NEB, USA). *Taq* DNA polymerase isolated from *Thermus aquaticus* and has no proofreading ability. Therefore, for subsequent cloning purposes, Phusion High-Fidelity DNA polymerase was used (Cat no. F-530S, Thermo Scientific, USA). The enzyme possesses proofreading activity (3′-5′ exonuclease activity). The enzyme isolated from *Pyroccocus furiosus* was further processed by Phusion DNA Technology to bring a novel *Pyroccocus*-like enzyme with a processivity enhanced domain. Ordinarily, the PCR conditions were varied with respect to the product size and annealing temperature of the primers. All PCRs were performed with Arktik Thermal Cycler (Thermo Fisher Scientific, Finland).

2.2.40 Reverse transcriptase PCR

For reverse transcriptase PCR (RT-PCR) based gene expression study, total RNA was isolated from the mycelia using the procedure as described in Neurospora RNA isolation. cDNA was synthesized from two µg of total RNA template using Thermo Scientific Verso cDNA synthesis kit (Cat no. AB-1453/A, USA). The cycling condition for cDNA synthesis was 50°C for 45 min followed by 95°C for 2 min for one cycle. The cDNA template was further subjected to PCR

cycling with gene specific primers to analyze the expression of gene. The PCR amplicons were analyzed in 1.2 % agarose gel with 100 bp DNA ladder for size comparison of amplicons.

2.2.41 Quantitative real time PCR

Pure RNA preparation isolated from *N. crassa* was used for quantitative real time PCR (qRT-PCR). One µg of total RNA was used to synthesize cDNA using Thermo Scientific Verso cDNA synthesis kit as described in section 2.2.40. qRT-PCR was performed in an ABI 7500 Fast Real time PCR system (Applied Biosystems, USA) with the SYBR® select master mix (Applied Biosystems, USA) by using 100 ng of cDNA and 10 mM each of primer in a final reaction volume of 15 µl. In general, 15 µl reaction mixture contained 7 µl of cDNA (100 ng), 0.5 µl of forward and reverse primer and 7 µl sybr green. The PCR cycle was as follows: 95°C for 10 min followed by 40 cycles of 95°C for 15 s and 60°C for 1 min. The $2^{-\Delta\Delta C}{}_{T}$ quantification method was used to calculate the fold change expression of each gene, using the β-tubulin gene as an endogenous control and wild type as calibrator (Livak and Schmittgen 2001).

2.2.42 Digestion of DNA with restriction endonuclease

For analytical and preparative purposes, plasmid DNA were digested with specific restriction endonucleases (NEB, USA). An aliquot of ~50-100 ng of DNA was digested with 5 units of restriction endonuclease in a final volume of 30 µl. The reaction was carried out for 3 h using suitable buffers and assay conditions as specified by manufacturer's protocol. The digested DNA fragments were analyzed by agarose gel electrophoresis. Digestion with two enzymes was done after consulting the enzyme compatibility chart present in the NEB.

2.2.43 Ligation reactions

Ligation reactions were carried out using Quick Ligation TM Kit (Cat no. M2200S, NEB). The 20 µl ligation reaction volume contained ~50 ng of a linearized DNA vector, a 3-fold molar excess of insert, 10 µl of 2X ligation buffer (132 mM Tris-HCL, 20 mM $MgCl_2$, 2 mM dithiothreitol, 2 mM ATP, 15 % polyethylene glycol 6000), and 1 µl quick T4 DNA ligase enzyme. The ligation was performed for 15-20 min at 25°C in cooling water bath (MRC Scientific Instruments).

2.2.44 Agarose gel electrophoresis

The DNA samples were loaded with one-sixth the volume of 6X DNA loading dye (0.25% bromophenol blue, 0.25% xylene cyanol, 30% glycerol). Depending upon the size of the fragments to be resolved, the samples were loaded on 0.7% to 1.5% agarose gels cast on 1X TAE containing 0.5 µg/ml ethidium bromide. Electrophoresis was carried out in 1X TAE at 5 V/cm. Standard DNA size markers were run alongside for estimation of DNA fragment sizes. The ethidium bromide stained DNA samples were visualized on a gel doc (Image 4.1, Bio-Rad, USA, or Mega Bio print, Vilbert Lormat, France). RNA samples were resolved in 1.2% agarose gel containing 2.2 M formaldehyde and 1X MOPS buffer and 0.5 µg/ml ethidium bromide.

2.2.45 Purification of DNA fragments from agarose gels

PCR amplified DNA subsequently used for cloning, sequencing, and transformation was purified from agarose gels using Nucleospin Gel and PCR Clean-up (Macherey-Nagel, Duren, Germany). The sample containing DNA was resolved on a 1% high purity agarose gel. The DNA bands were visualized on a gel doc and the DNA band to be eluted was excised and transferred to a weighed 1.5 ml centrifuge tube. DNA from the gel slice was eluted according to the instructions provided by the manufacturer.

2.2.46 Sequence analysis

Basic local alignment search tool (BLAST; Altschul et al. 1990; 1997) was performed using software tools available from NCBI and Conserved Domain Database (CDD; Marchler-Bauer and Bryant 2004; Marchler-Bauer et al. 2009) was used to identify conserved domains in the protein. Protein sequences were aligned with Clustal X (Thompson et al. 1997) then transferred to GeneDoc for visualization (Nicholas et al. 1997). Phylogenetic trees (Felsenstein 1985; Rzhetsky and Nei 1992) were constructed from these alignments using the software Molecular Evolutionary Genetic Analysis version 5 (MEGA 5; Tamura et al. 2007).

2.3 Databases and software programs used

1. Basic Local Alignment Search Tool (BLAST): BLAST program (Altschul et al. 1990; 1997; 2005) was used to compare nucleotide or protein sequences to sequence databases. This is available at http://blast.ncbi.nlm.nih.gov/Blast.cgi.

2. Clustal W: The Clustal W software was used for multiple alignment of DNA and protein sequence. It is available at http://www.ebi.ac.uk./clustal or commonly used offline software is Clustal X (Thompson et al. 1997).

3. Conserved Domain Database (CDD): CDD (Marchler-Bauer and Bryant 2004; Marchler-Bauer et al. 2009) was used to identify conserved domains in the proteins. This is available at http://www.ncbi.nlm.nih.gov/Structure/cdd/wrpsb.cgi.

4. ExPasy Translate tool: The ExPasy Translate tool was used for translating DNA sequences to protein sequences. It is available at http://web.expasy.org/tools/DNA.

5. GeneDoc: GeneDoc software (Nicholas et al. 1997) was used for finding conserved domains among aligned sequences of DNA or protein. It is available at http://www.nrbsc.org/gfx/genedoc/.

6. Genomatix software: The Genomatix software (Quandt et al. 1995) was used for promoter analysis of genomic DNA sequence. It is available at http://www.genomatix.de/cgi-bin//matinspector_prof/mat_fam.

7. Maps sites for restriction enzymes: This was used for restriction analysis of DNA sequences. It is available at http://www.restrictionmapper.org/.

8. Molecular Evolutionary Genetic Analysis Version 5 (MEGA 5) tool: The MEGA software (Tamura et al. 2007) was used to depict the evolutionary relationship among the organisms or gene sequences. It is available at http://www.megasoftware.net/.

9. *N. crassa* genome databases: Genome resource for Neurospora is available at http://fungidb.org. The web site for Fungal Genetics Stock Center is http://www.fgsc.net/.

10. NCBI/EMBL: NCBI at http://www.ncbi.nlm.nih.gov/ or EMBL at http://embl.org/ is used to retrieve the primary sequence of proteins or nucleic acid.

11. Primer3: Primer3 was used for analysis of the secondary structure of oligonucleotide primers. It is available at http://bioinfo.ut.ee/primer3-4.0/.

12. Prediction of putative calmodulin (CaM) binding site: To predict putative CaM binding site in the protein a previously described software program (http://calcium.uhnres.utoronto.ca/ctdb/ctdb/sequence.html; Yap et al. 2000) was used.

13. Site for reverse-complement: To convert a DNA sequence into reverse-complement counterpart, sequence manipulation suite (SMS) software package was used. It is available at http://www.bioinformatics.org/sms/index.html.

14. Search Tool For The Retrieval Of Interacting Genes/Proteins (STRING): STRING version 10.0 (Szklarczyk et al. 2015) available at http://string-db.org/ was used to predict functional protein association networks.

Chapter 3

Understanding the cellular roles of homologues of phospholipase C-1, secretory phospholipase A2, and calcium proton exchanger-1 in Neurospora crassa

3.1 Introduction

The genome of *N. crassa* is ~40 Mb in size and contains ~10,082 protein coding genes including a set of 48 genes that encode for Ca^{2+} channel proteins, Ca^{2+}/cation-ATPases, Ca^{2+}/H^{+} exchangers, Ca^{2+}/Na^{+} exchangers, PLC-δ subtype proteins, CaM, and Ca^{2+} and/or CaM binding proteins (Galagan et al. 2003; Borkovich et al. 2004). The *Neurospora* functional genomics project (http://geiselmed.dartmouth.edu/dunlaploros/genome/) aimed to generate knockout mutants for all the ~10,082 genes for functional analysis using a high-throughput gene knockout procedure (Colot et al. 2006). This knockout procedure essentially used a gene targeting cassette that contains ~1-1.5 kb of 5′ flanking sequence of the target ORF followed by the selectable marker *hph* (gene for hygromycin B phosphotransferase) under the *trpC* promoter that confers resistance to antibiotic hygromycin and flanked by the engineered *Mme*I restriction site, and ~1-1.5 kb of 3′ flanking sequence of the target ORF (Figure 3.1; Gritz and Davies 1983; Staben et al. 1989).

We have obtained 43 knockout, including 31 homokaryotic and 12 heterokaryotic mutants of the Ca^{2+} signaling genes from the FGSC. The generation of the knockout mutant for the remaining five Ca^{2+} signaling genes were not successful indicating that these genes could be essential for viability. I had initially screened 28 Ca^{2+} signaling knockout mutants (Table 3.1) for their hyphal morphology in response to increased intracellular free Ca^{2+}. The Ca^{2+} ion is a universal messenger that plays a central role in intracellular signaling in eukaryotes and its concentration varies with space, time, and amplitude (Berridge et al. 1998; Clapham 2007). The target protein undergoes changes in its conformation and charge upon Ca^{2+} binding and thus governs protein functions (Clapham 2007). The Ca^{2+} concentration in the extracellular fluid is ~10^{-3} M, whereas the resting $[Ca^{2+}]_c$ is ~100 nm, however, transient increase in $[Ca^{2+}]_c$ upto 1µM or more either due to entry of extracellular Ca^{2+} or release of Ca^{2+} from intracellular stores triggers Ca^{2+} signaling (Chin and Means 2000; Bootman et al. 2001). The increase in $[Ca^{2+}]_c$ is detected by multiple Ca^{2+} sensing proteins triggering a versatile Ca^{2+} signaling events. High $[Ca^{2+}]_c$ is toxic to cells and therefore, $[Ca^{2+}]_c$ is effectively regulated in *N. crassa* using active transport mechanisms across plasma membrane, Ca^{2+} buffering in organelles, and vacuolar Ca^{2+} sequestration (Bowman et al. 2011). The Ca^{2+} signaling machinery regulates numerous physiological processes and also plays an important role in perceiving extracellular environmental changes to thrive in diverse environments in *N. crassa* (Galagan et al. 2003; Borkovich et al. 2004).

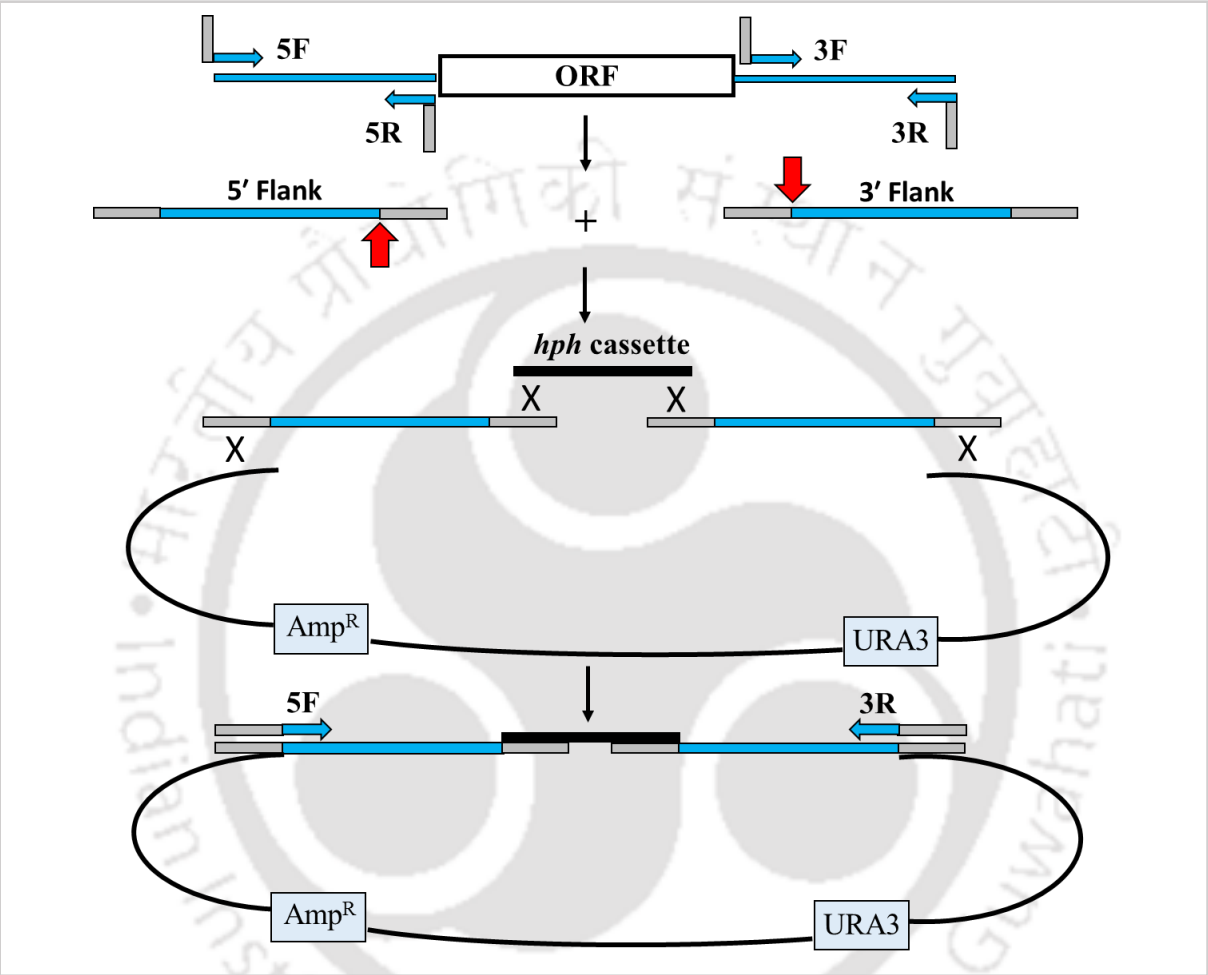

Figure 3.1: Strategy for generating the knockout constructs. The primer pairs 5F and 5R, and 3F and 3R, were used to PCR amplify the 5′ and 3′ flank fragments, respectively, from the wild type. The 5′ tails of 5R and 3F primers are homologous to the *hph* cassette and incorporate *Mme*I sites (M), whereas, the 5′ tails of 5F and 3R are homologous to the yeast shuttle vector pRS426 vector (Christianson et al. 1992). Homologous recombination allows the formation of circular constructs and using the primers 5F and 3R, the final linear deletion cassette is amplified from the yeast pooled DNA. The *hph* is transcribed in the antisense direction relative to the transcription of the target gene. Adapted from Colot et al. 2006.

3.2 Results

3.2.1 Calcium ionophore assay

3.2.1.1 Effect of increased cytosolic Ca^{2+} levels on hyphal morphology of the *N. crassa* knockout mutants of Ca^{2+} signaling genes

The universal second messenger Ca^{2+} regulates a wide range of signal transduction pathways in eukaryotes including filamentous fungi (Gadd 1994; Berridge et al. 1998). In *N. crassa*, Ca^{2+} is mainly stored in the intracellular stores such as vacuoles (>90% of Ca^{2+} is sequestered in the vacuoles), Golgi, endoplasmic reticulum; however, only a small amount of Ca^{2+} (~100 nM) is present freely in the cytosol indicated as $[Ca^{2+}]_c$ (Bowman et al. 2011). The low levels of $[Ca^{2+}]_c$ is tightly regulated by various Ca^{2+} signaling proteins and efficient interaction between these signaling proteins is essential for maintaining Ca^{2+} homeostasis and generating appropriate cellular responses in *N. crassa*. Therefore, to identify the Ca^{2+} signaling genes important for maintaining Ca^{2+} homeostasis in *N. crassa*, I studied hyphal morphology of knockout mutants of 28 Ca^{2+} signaling genes in response to elevated intracellular Ca^{2+} caused by the addition of the ionophore A23187 in Vogel's glucose agar medium in Petridishes (100 mm diameter; Table 3.1). Ionophores are mobile ion carriers that facilitates simultaneous exchange of protons and divalent metal ions across biological membranes (Babcock et al. 1976). The ionophore A23187 is directly involved in Ca^{2+} transport across membranes of cells and organelles either by activation of Ca^{2+} influx through native Ca^{2+} channels or phospholipase C dependent mobilization of Ca^{2+} from intracellular stores or activation of Ca^{2+} influx through store regulated mechanism (Figure 3.2 A; Dedkova et al. 2004; Nelson et al. 2004). In *N. crassa*, A23187 causes an increase in $[Ca^{2+}]_c$ by facilitating the release of Ca^{2+} from intracellular Ca^{2+} stores (Nelson et al. 2004). To test the effect of A23187 on hyphal growth, mycelial plugs of the wild type and the Ca^{2+} signaling mutant strains were inoculated onto one corner of Petri dish containing Vogel's glucose agar medium and A23187 (test) or ethanol (control) was spotted onto the other corner as described in Chapter 2 (Lew et al. 2008). Plates were incubated at 30°C for two-three days and colonies were observed under the Trinocular inverted microscope (AxioVert A1 FL, Carl Zeiss). Among the 28 Ca^{2+} signaling knockout mutants studied, three mutants ΔNCU06245, ΔNCU06650, and ΔNCU06366 showed morphological defects on Vogel's medium containing the divalent ionophore A23187 (Figure 3.2 B). In presence of the ionophore, the ΔNCU06245 mutant exhibited characteristics spherical sac like structures at the apex of hyphae with reduced branching while compact branching with similar apical sac like

structures was observed in the ΔNCU06650 mutant (Figure 3.2 B). The ΔNCU06366 mutant displayed apical hyper branching phenomenon in presence of the ionophore (Figure 3.2 B). The remaining 25 Ca^{2+} signaling knockout mutants exhibited similar hyphal morphology like the wild type strain. I also studied the apical growth rate of the strains using the standard race tube assay (Ryan et al. 1943; Ryan 1950). Mycelial plugs of the wild type and the three single mutants were inoculated at one end of the race tube containing Vogel's glucose agar medium and incubated at 30°C for 72 h. The hyphal growth front was marked periodically at an interval of 12 h for 72 h, and the distance of the hyphal growth front from the inoculation point was plotted against time (discussed in Chapter 2). Interestingly, hyphal extension rates of ΔNCU06245, ΔNCU06650, and ΔNCU06366 mutants on normal Vogel's glucose agar medium without the addition of ionophore were similar to the wild type strain (Figure 3.2 C; Table 3.2). Therefore, the aberrant morphological defects in response to increased $[Ca^{2+}]_c$ prompted me to study ΔNCU06245, ΔNCU06650, and ΔNCU06366 mutants in detail.

Table 3.1: List of the *N. crassa* strains

Sl. No.	FGSC No. (a/A) or Strain No.	NCU no. or Strain Type	Type of Protein	Source
1	988/997	Wild type	-	FGSC
2	11248/11249	7075.2	Ca^{2+}/H^{+} exchanger	FGSC
3	12376/12375	795.2	Ca^{2+}/H^{+} exchanger	FGSC
4	11530/11529	2826.2	Ca^{2+}/H^{+} exchanger	FGSC
5	11407/11408	6366.2	Ca^{2+}/H^{+} exchanger	FGSC
6	12468/NA	8490.2	Ca^{2+}/H^{+} exchanger	FGSC

7	NA/11253	7605.2	Ca^{2+} permeable channel	FGSC
8	11707/11708	6703.2	Ca^{2+} permeable channel	FGSC
9	13287/NA	3305.2	Ca^{2+} ATPase	FGSC
10	NA/13071	4736.2	Ca^{2+} ATPase	FGSC
11	13036/13037	5154.2	Ca^{2+} ATPase	FGSC
12	NA/13040	4898.2	Ca^{2+} ATPase	FGSC
13	11410/11409	7966.2	Cation- ATPase	FGSC
14	12022/NA	1266.2	Phospholipase C	FGSC
15	11411/NA	6245.2	Phospholipase C	FGSC
16	11271/11271	9655.2	Phospholipase C	FGSC
17	12023/NA	2175.2	Phospholipase C	FGSC
18	11405/11406	5225.2	Ca^{2+} and/or CaM binding protein	FGSC
19	13049/NA	2115.2	Ca^{2+} and/or CaM binding protein	FGSC
20	15890/NA	2738.2	Ca^{2+} and/or CaM binding protein	FGSC
21	11541/11542	6948.2	Ca^{2+} and/or CaM binding protein	FGSC

22	11403/11404	4379.2	Ca^{2+} and/or CaM binding protein	FGSC
23	11531/NA	3750.2	Ca^{2+} and/or CaM binding protein	FGSC
24	12448/12449	2283.2	Ca^{2+} and/or CaM binding protein	FGSC
25	12548/12547	9123.2	Ca^{2+} and/or CaM binding protein	FGSC
26	11169/11170	2814.2	Ca^{2+} and/or CaM binding protein	FGSC
27	11545/NA	9212.2	Ca^{2+} and/or CaM binding protein	FGSC
28	11246/11247	6650.2	Ca^{2+} and/or CaM binding protein	FGSC
29	11537/11536	6177.2	Ca^{2+} and/or CaM binding protein	FGSC

(A)

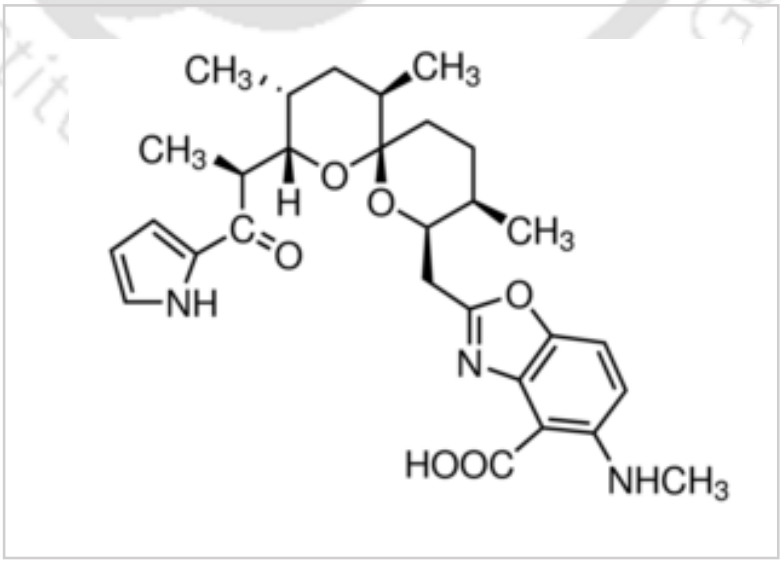

(B)

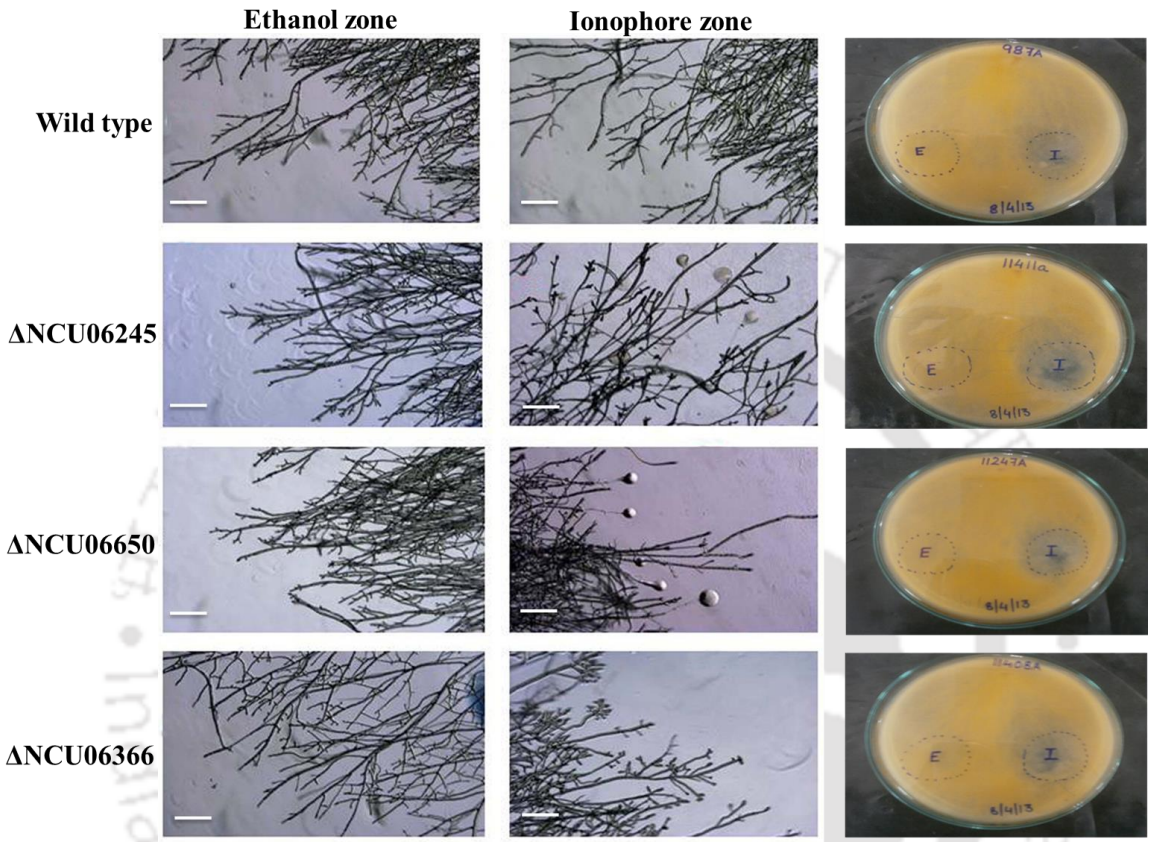

(C)

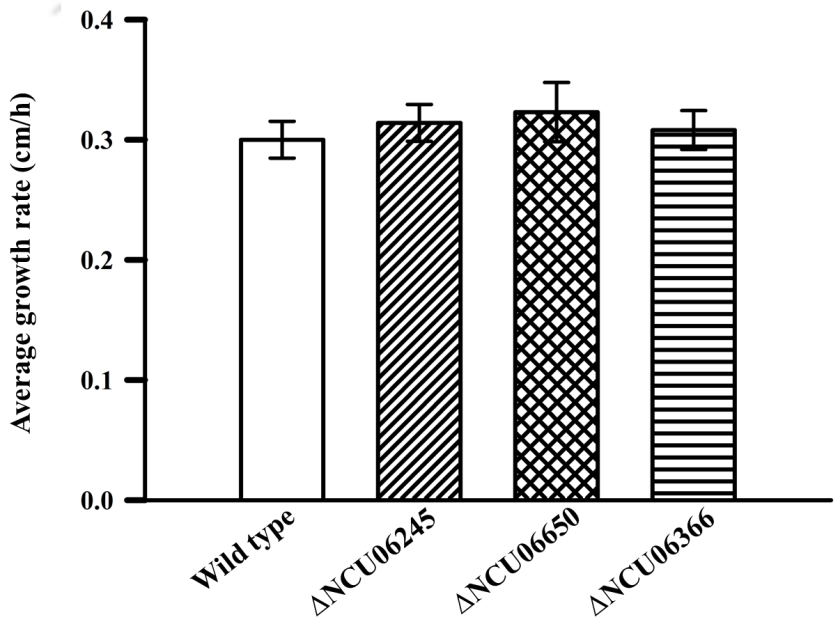

Figure 3.2: Effect of increased $[Ca^{2+}]_c$ on growth phenotype of the *N. crassa* strains. (A) Chemical structure of calcium ionophore A23187. The ionophore A23187 facilitates Ca^{2+} release from intracellular Ca^{2+} stores with simultaneous exchange of positive ions across membranes (Dedkova et al. 2004). Its chemical structure is available at http://www.sigmaaldrich.com/catalog/product/sigma/c7522?lang=en&region=IN. **(B)** Ca^{2+} ionophore assay. The wild type, ΔNCU06245, ΔNCU06650, and ΔNCU06366 mutant strains were grown in Petri dishes containing the ionophore zone (test) and the ethanol zone (control) and incubated at 30°C. Images were captured under a Trinocular inverted microscope (AxioVert A1 FL, Carl Zeiss) when hyphae of the strains touched both the zones (38 h of growth at 30°C). Ten images for each strain is captured and a representative image is shown. Scale bar 20 µm. **(C)** Growth phenotype of the *N. crassa* strains. The apical growth of the wild-type, ΔNCU06245, ΔNCU06650, and ΔNCU06366 mutant strains were measured at 30ºC using 'race tubes' over a period of 72 h containing Vogel's glucose agar medium. Error bars indicate the standard deviations calculated from the data for three independent experiments (n=3).

Table 3.2: Average growth rates of the wild type, ΔNCU06245, ΔNCU06650, and ΔNCU06366 mutant strains in race tubes

Strains	Average growth rates (cm/h)
Wild type	0.300 ± 0.0153
ΔNCU06245	0.314 ± 0.0153
ΔNCU06650	0.323 ± 0.0246
ΔNCU06366	0.308 ± 0.0162

3.2.1.2 Confirmation of the ΔNCU06245, ΔNCU06650, and ΔNCU06366 knockout mutants by PCR analysis

The ΔNCU06245, ΔNCU06650, and ΔNCU06366 knockout mutants were generated by the NIH Neurospora functional genomics project (http://geiselmed.dartmouth.edu/dunlaploros/genome/; Colot et al. 2006) and confirmed using Southern analysis (http://borkovichlims.ucr.edu/southern/). I verified ΔNCU06245, ΔNCU06650, and ΔNCU06366 knockout mutants using the forward primers HI-NCU06245-F, HI-NCU06650-F, and HI-NCU06366-F specific for upstream of the 5′ flanks of the genes *plc-1*, *splA2*, and *cpe-1* respectively, along with the common reverse primer

5HPHR that is specific for the *hph* cassette used to generate the knockout mutants (Figure 3.3 A; Table 3.3; Entry 1-4; Colot et al. 2006; Deka et al. 2011). Amplicons of sizes 2 kb, 2.044 kb, and 1.981 kb, respectively, indicated presence of the Δ*plc-1*, Δ*splA2*, and Δ*cpe-1* alleles in the mutants (Figure 3.3 B).

Table 3.3: Primers used for knockout confirmation and complementation analysis

Sl. No.	Primer	Sequence (5′→3′)	Source
1	HI-NCU06245-F	AGTTGGTCGCCTCCTAGAAC	This study
2	HI-NCU06650-F	GCCGGACGGCAACTGAATAT	This study
3	HI-NCU06366-F	CTG CAA GGA GGC TAA TTC GG	This study
4	5HPHR	ATCCACTTAACGTTACTGAAATC	Deka et al. 2011
5	PLC-1-GFP-5F	ATGCCAGCAGCTGTCCATGG	This study
6	PLC-1-GFP-5R	CAACCTCAACTTCTTGCTTATC	This study
7	SPLA2-GFP-5F	ATGAAGTTCTTCTCTGCCCTC	This study
8	SPLA2-GFP-5R	ATAATACAACGGATCCTCGCC	This study
9	CPE-1-GFP-5F	ATGACATCGCCCTACCATGC	This study
10	CPE-1-GFP-5R	ATGATGACCACCCTCCGACC	This study
11	Pccg-1-Fw	CCATCATCAGCCAACAAAGC	This study
12	GFP-Rv	AACTTGTGGCCGTTTACGTC	This study

(A)

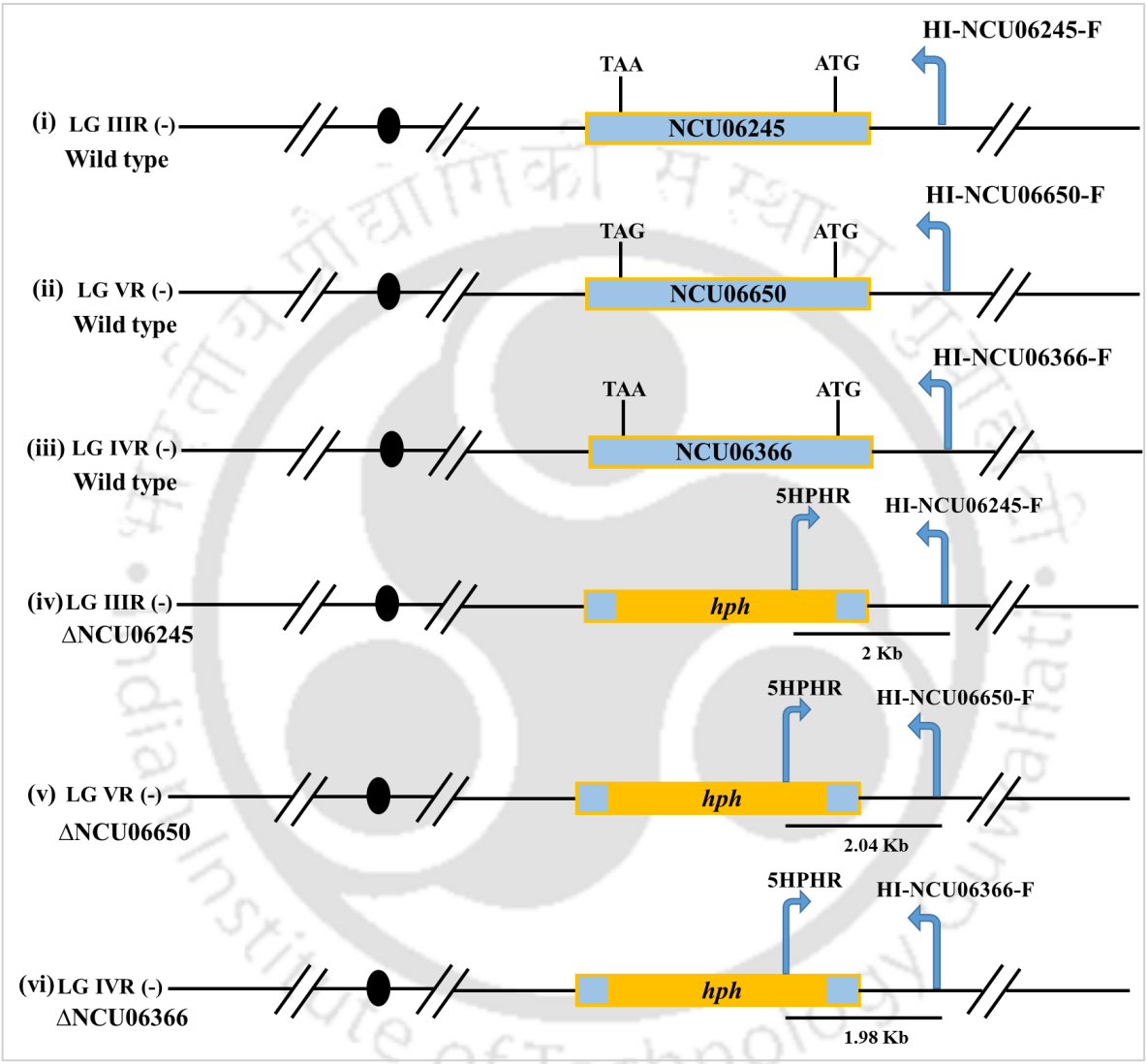

(B)

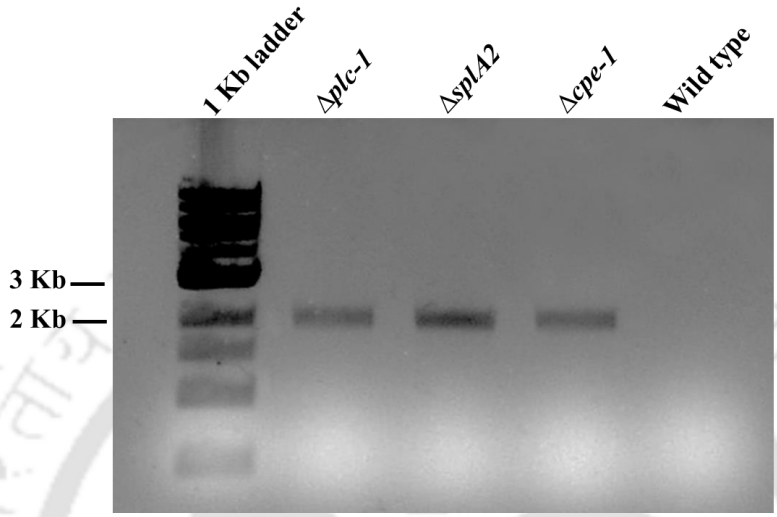

Figure 3.3: Confirmation of knockout mutants of NCU06245, NCU06650, and NCU06366. **(A)** Primer design for PCR verification of the ΔNCU06245, ΔNCU06650, and ΔNCU06366 knockout mutants. **(B)** Confirmation of the ΔNCU06245, ΔNCU06650, and ΔNCU06366 knockouts using PCR. The ΔNCU06245, ΔNCU06650, and ΔNCU06366 mutants were verified using the forward primers HI-NCU06245-F 5′-AGT TGG TCG CCT CCT AGA AC-3′, HI-NCU06650-F 5′-GCC GGA CGG CAA CTG AAT AT-3′ and HI-NCU06366-F 5′- CTG CAA GGA GGC TAA TTC GG -3′ specific for upstream of the open reading frame of the genes *plc-1*, s*plA2*, and *cpe-1*, respectively, along with the common reverse primer 5HPHR 5′-ATC CAC TTA ACG TTA CTG AAA TC-3′ that is specific for the *hph* cassette used to generate the knockout mutants (Colot et al. 2006; Deka et al. 2011). Amplification of PCR products of size 2 kb, 2.044 kb, and 1.981 kb, respectively, indicate presence of the Δ*plc-1*, Δ*splA2*, and Δ*cpe-1* alleles in the mutants. PCR products of the Δ*plc-1* (lane 1), Δ*splA2* mutant (lane 2), Δ*cpe-1* mutant (lane 3), and wild type (lane 4; used as negative control) were visualized in a 0.8% agarose gel. M: 1 kb DNA ladder (NEB).

3.2.2 Sequence analysis

3.2.2.1 The NCU06245, NCU06650, and NCU06366 genes encode the phospholipase C-1 (PLC-1), secretory phospholipase A2 (sPLA2), and Ca^{2+}/H^{+} exchanger-1 (CPE-1), respectively, in *N. crassa*

The NCU06245, NCU06650, and NCU06366 genes encode three distinct types of Ca^{2+} signaling proteins. The analysis of homologous sequences of NCU06245, NCU06650, and NCU06366 were performed using information obtained from fungal genome database (http://geiselmed.dartmouth.edu/dunlaploros/genome/; http://fungidb.org). The NCU06245 is genetically mapped in supercontig three from position 2027776-2031034 (-) at the right arm of linkage group three (LG IIIR; Figure 3.4 A), the NCU06650 is mapped in supercontig five from position 4123065-4123980 (-) at the LG VR (Figure 3.4 B), and the NCU06366 is mapped in supercontig four from position 2765568-2768250 (-) at the LG IVR (Figure 3.4 C). The genomic sequence of NCU06245 (Figure 3.5 A) and NCU06650 (Figure 3.5 B) contains two exons and one intron each, while NCU06366 possesses three exons and two introns (Figure 3.5 C). The NCU06245, NCU06650, and NCU06245 encoded proteins contain several conserved domains (Figure 3.6 A-C). The NCU06245 gene is predicted to encode a 711 amino acid residues phospholipase C-1 (PLC-1; GenBank accession no. AAZ23795.1; http://fungidb.org/fungidb/app/record/gene/NCU06245) protein sharing sequence similarity with the PLC homologues of *A. capsulatus*, *C. higginsianum*, and *MoPLC2* and *MoPLC3* proteins of *M. oryzae* with *e*-values 9*e*-171, 0, 0 and 6*e*-171, 43, 52, 51, and 43% identities, and 96, 97, 97, and 97% similarities, respectively (Figure 3.6 A). Sequence analysis of the NCU06245 homologues revealed important Ca^{2+} and H^{+} binding residues essential for its catalytic activity similar to PLC homologues of *Cryphonectria parasitica*, *M. grisea*, and *Arabidopsis thaliana* (Figure 3.6 A; Chung et al. 2006). The NCU06650 gene is predicted to encode a conserved hypothetical secretory phospholipase A2 (sPLA2; GenBank accession no. XP_960883.1; http://fungidb.org/fungidb/app/record/gene/NCU06650) of 186 amino acid residues that shares sequence similarity to sPLA2 homologues of *A. capsulatus*, *A. oryzae*, *T. borchii* and *V. alfalfa* with *e*-values 7*e*-35, 5*e*-31, 2*e*-31, and 1*e*-51; 55, 41, 50, and 57% identities; 66, 88, 58, and 77% similarities, respectively (Figure 3.6 B). The NCU06650 encoded sPLA2 protein possesses an N-terminal signal peptide residue (residues 1-30) presumably for secretion, a highly conserved region (residues 122–153) that contains a catalytic histidine residue, and two disulphide-bonded Cys

residues similar to the sPLA2 homologue of *T. borchii* and belongs to the group XIV (GXIV) $sPLA_2$ group of enzymes (Figure 3.6 B; Soragni et al. 2001; Takayanagi et al. 2015). In addition, the NCU06366 gene encodes a Ca^{2+}/H^+ exchanger (calcium proton exchanger-1; CPE-1; GenBank accession no. ESA42901.1; http://fungidb.org/fungidb/app/record/gene/NCU06366) of 505 amino acid residues with a high degree of similarity to the *A. capsulatus*, *A. niger*, *C. higginsianum* and *M. oryzae homologues* of CPE with *e*-values 4*e*-153, 6*e*-143, 0, and 8*e*-141; 50, 52, 59, and 68% identities; 93, 89, 95, and 67% similarities, respectively (Figure 3.6 C). The NCU06366 gene product contains nine transmembrane domains as predicted by the TMHMM program possibly for Ca^{2+} transport (Figure 3.6 C; http://www.cbs.dtu.dk/services/TMHMM/; Zelter et al. 2004; Guttery et al. 2013). Moreover, a phylogenetic analysis with a subset of homologues of different fungi revealed that NCU06245, NCU06650, and NCU06366 proteins of *N. crassa* were clustered within the Sordariomycetes clade (Figure 3.7). Therefore, the NCU06245, NCU06650, and NCU06366 genes encode the *N. crassa* homologues of the PLC-1, sPLA2, and CPE-1, respectively.

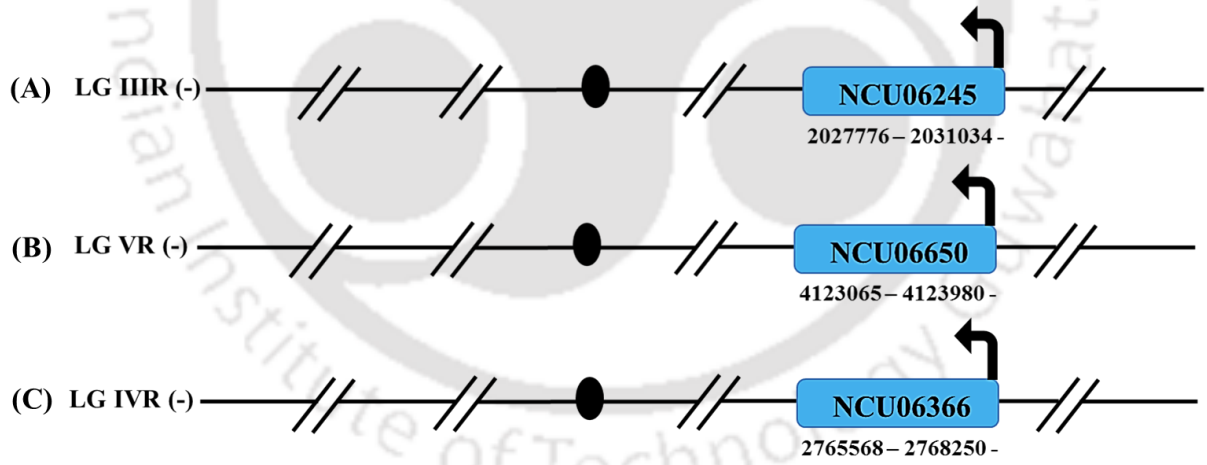

Figure 3.4: Genomic location of NCU06245, NCU06650, and NCU06366 in *N. crassa*. (A) Genetic map of NCU06245 localized at the right arm of supercontig three from position 2027776-2031034 (-). **(B)** Genetic map of NCU06650 localized at the right arm of supercontig five from position 4123065-4123980(-). **(C)** Genetic map of NCU06366 localized at the right arm of supercontig four from position 2765568-2768250 (-).

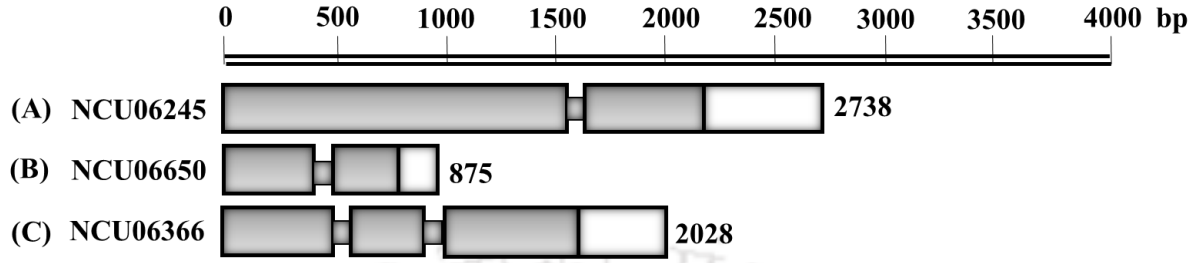

Figure 3.5: Genetic organization of NCU06245, NCU06650, and NCU06366 in *N. crassa*. (A) NCU06245 gene possesses two exons and one intron **(B)** NCU06650 contains two exons and one intron **(C)** NCU06366 possesses three exons and two introns.

(A)

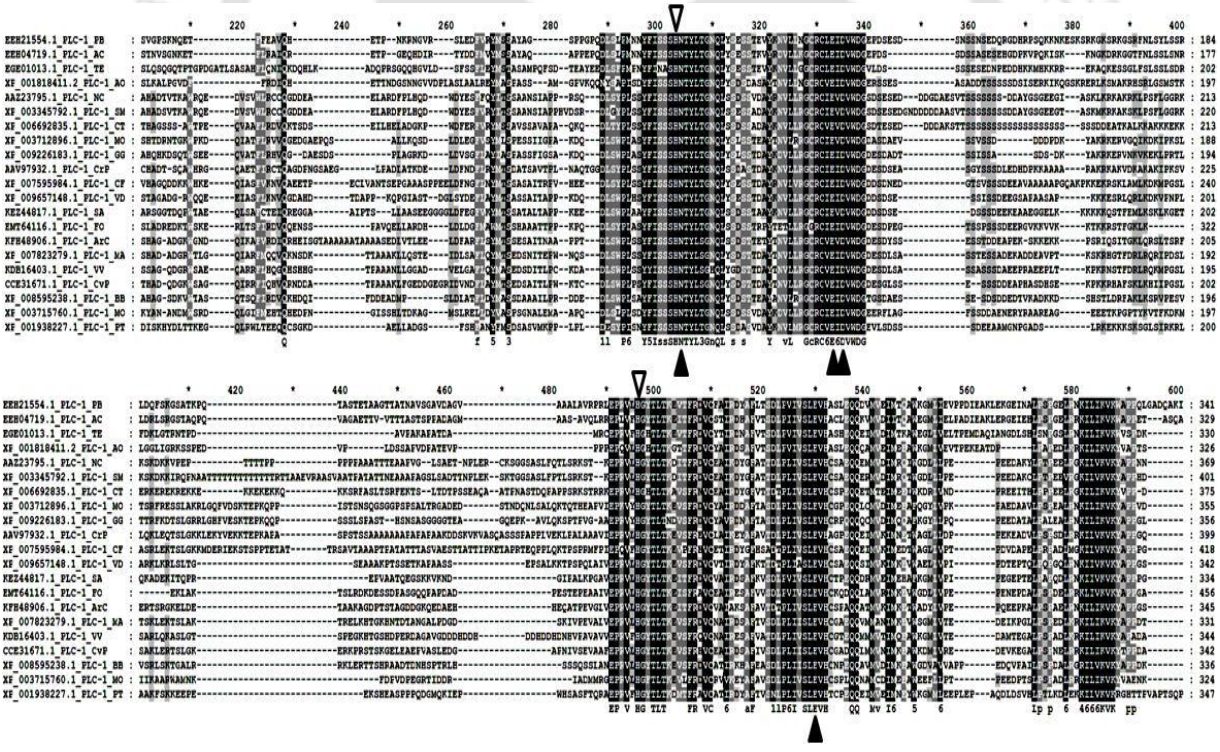

(B)

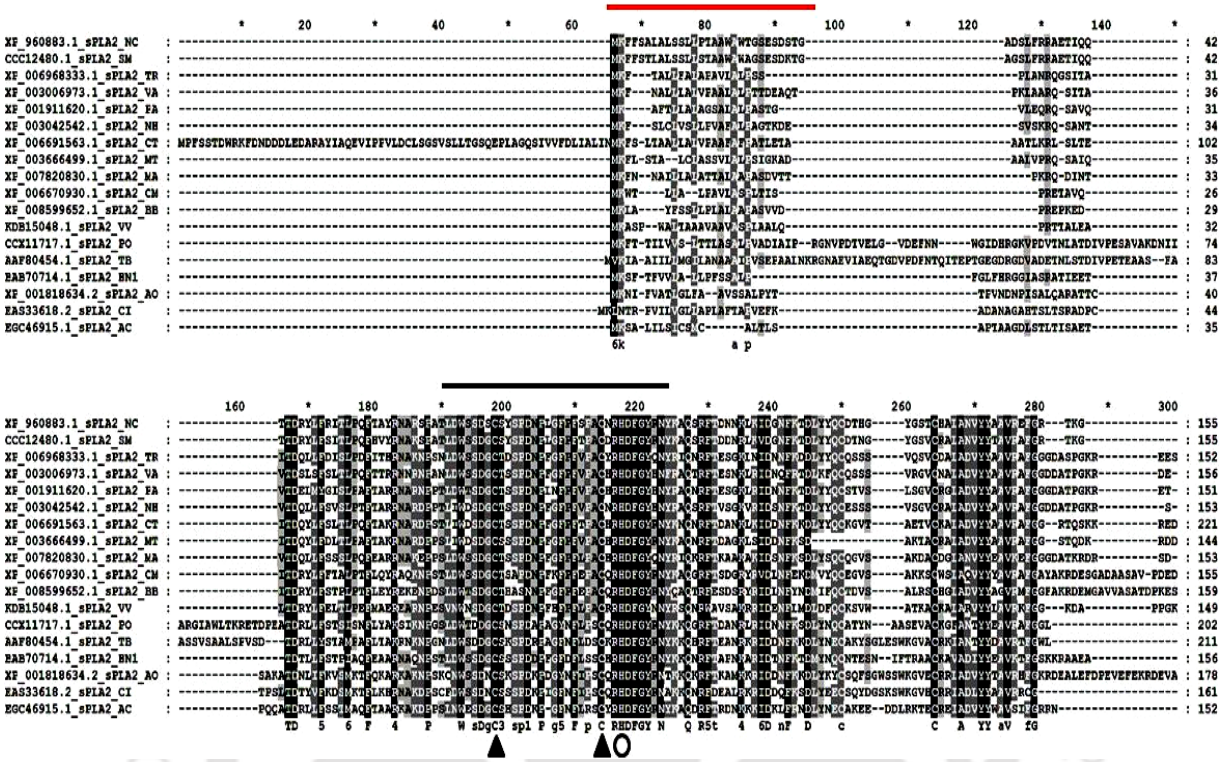

(C)

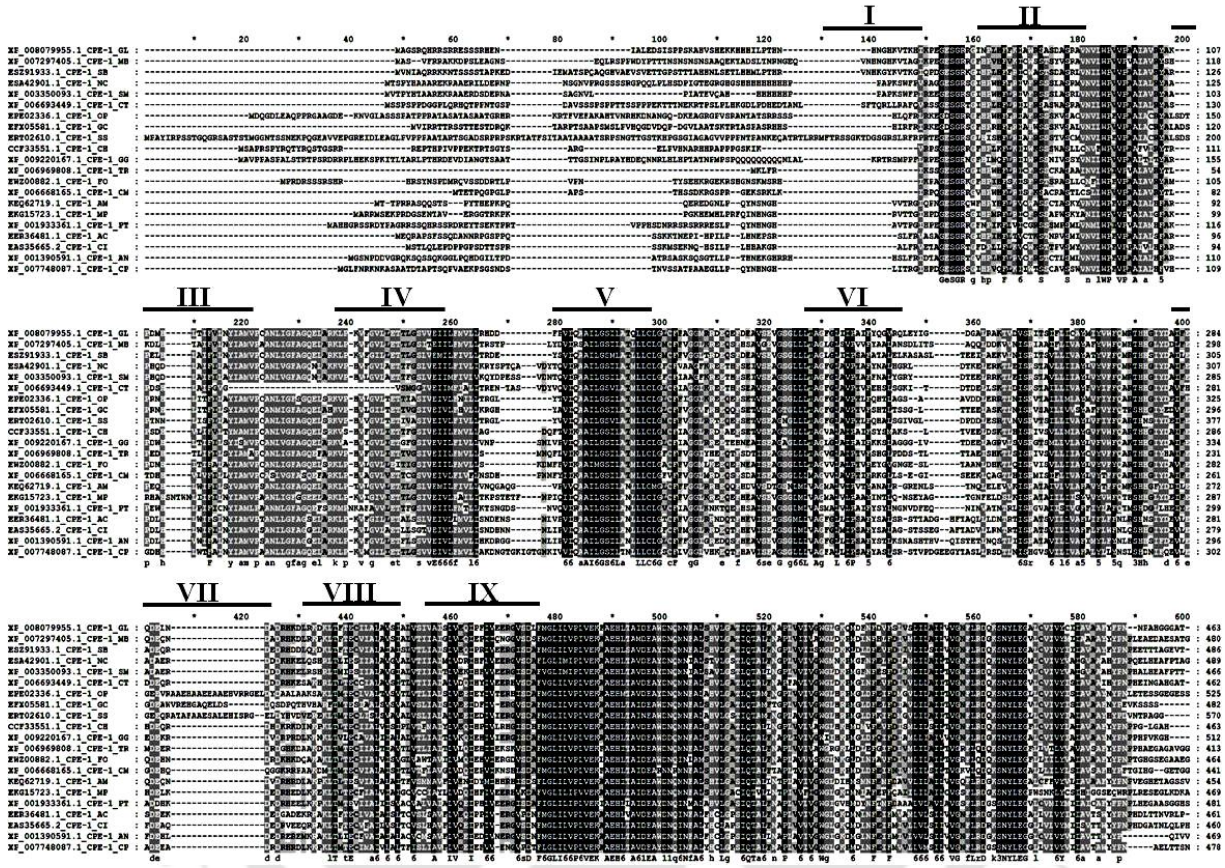

Figure 3.6: Sequence analysis. (A) Sequence alignment of PLC-1 homologues. The positions of the hydrogen binding residues (inverted triangles), and the Ca^{2+} binding residues (filled triangles) are indicated above and below the alignment, respectively (Chung et al. 2006). **(B)** Sequence alignment of sPLA2 homologues. The predicted secretion signal peptide is underlined in red. The highly conserved portion of sPLA2 is underlined in black. The positions of the catalytic histidine residue (open circle) and disulphide bonded cysteine residues (filled triangles) are indicated below the alignment (Soragni et al. 2008). **(C)** Sequence alignment of CPE-1 homologues. The sequence corresponds to transmembrane segments (I to IX) as predicted with TMHMM program are shown underlined (http://www.cbs.dtu.dk/services/TMHMM/; Zelter et al. 2004; Guttery et al. 2013). The sequences used in the analyses are AC, *A. capsulatus*; ArC, *Acremonium chrysogenum*; AM, *Aureobasidium melanogenum*, AN, *A. niger*; AO, *A. oryzae*; BB, *Beauveria bassiana*; CF, *C. fioriniae*, CH, *C. higginsianum*; CI, *Coccidioides immitis*; CM, *C. militaris*; CP, *Cladophialophora*

psammophila; CrP, *C. parasitica*; CvP, *Claviceps purpurea*, CT, *Chaetomium thermophilum*, FO, *Fusarium oxysporum*; GC, *G. clavigera*; GG, *Gaeumannomyces graminis*; HN1, *Helicosporium sp.*, GL, *Glarea lozoyensis*, MA, *M. anisopliae*; MB, *Marssonina brunnea*; MO, *M. oryzae*; MP, *Macrophomina phaseolina*; MT, *Myceliophthora thermophila*; NC, *N. crassa*; NH, *N. haematococca*, OP, *Ophiostoma piceae*; PA, *Podospora anserine*, PB, *Paracoccidioides brasiliensis*; PO, *Pyronema omphalodes*, PT, *Pyrenophoratritici-repentis*; SA, *Scedosporium apiospermum*, SB, *S. borealis*; SM, *S. macrospora*; SS, *S. schenckii*; TB, *T. borchii*; TE, *T. equinum*; TR, *T. reesei*; VA, *V. alfalfa*e; VD, *V. dahliae*, VV, *Villosiclava virens*. X2 program was used to produce the alignments. Conserved amino acids are indicated in black (100%), dark grey (>80%) and light grey (>60%) in the alignments. The proteins are described by GenBank accession number, organism, and class.

(A)

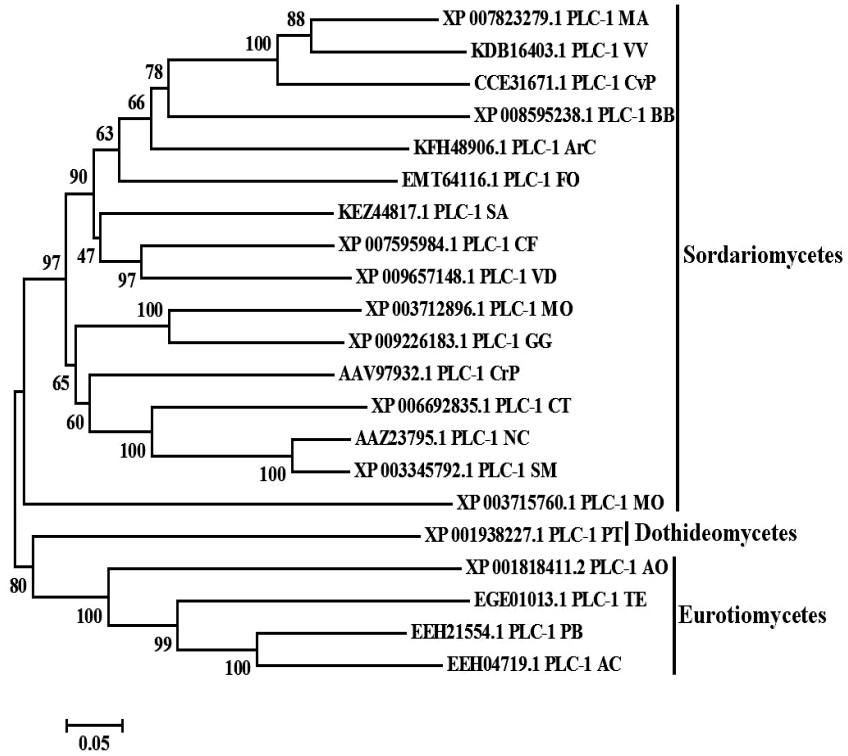

(B)

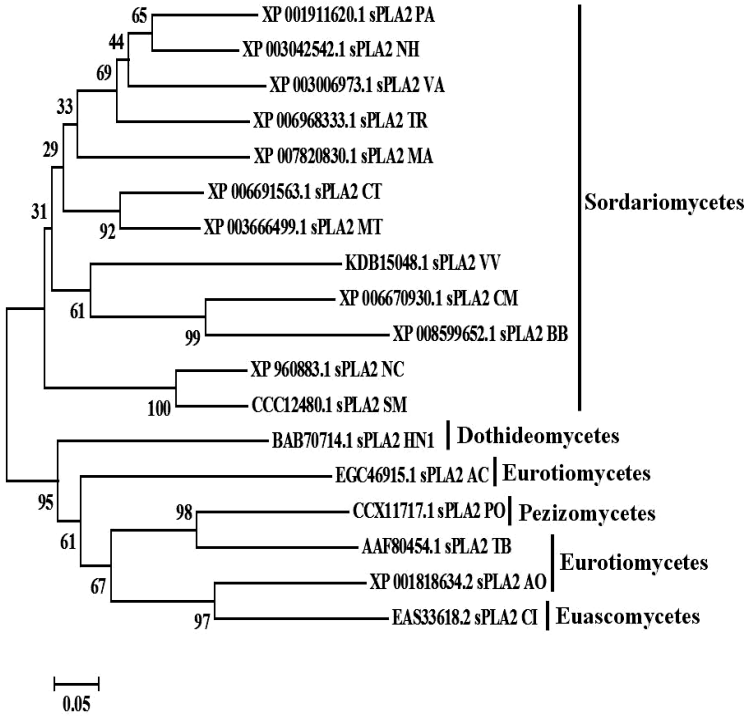

(C)

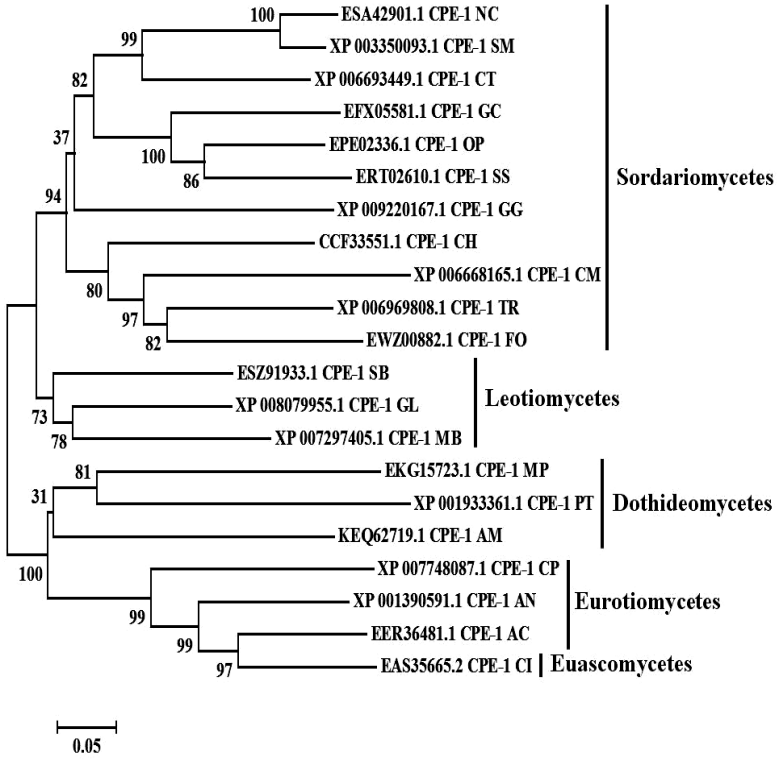

Figure 3.7: Phylogenetic analysis. Phylogenetic analysis of PLC-1 **(A)**, sPLA2 **(B)**, and CPE-1 **(C)** homologues, respectively. The sequences used in the analyses are AC, *A. capsulatus*; ArC, *A. chrysogenum*; AM, *A. melanogenum*, AN, *A niger*; AO, *A. oryzae*; BB, *B. bassiana*; CF, *C. fioriniae*, CH, *C. higginsianum*; CI, *C. immitis*; CM, *C. militaris*; CP, *C. psammophila*; CrP, *C. parasitica*; CvP, *C. purpurea*, CT, *C. thermophilum*, FO, *F. oxysporum*; GC, *G. clavigera*; GG, *G. graminis*; HN1, *Helicosporium sp.*, GL, *G. lozoyensis*, MA, *M. anisopliae*; MB, *M. brunnea*; MO, *M. oryzae*; MP, *M. phaseolina*; MT, *M. thermophila*; NC, *N. crassa*; NH, *N. haematococca*, OP, *O. piceae*; PA, *P. anserine*, PB, *P. brasiliensis*; PO, *P. omphalodes*, PT, *P. tritici-repentis*; SA, *S. apiospermum*, SB, *S. borealis*; SM, *S. macrospora*; SS, *S. schenckii*; TB, *T. borchii*; TE, *T. equinum*; TR, *T. reesei*; VA, *V. alfalfa*e; VD, *V. dahliae*, VV, *V. virens*. Phylogenetic analyses were performed using the minimum evolution method, 500 Bootstrap replications (bootstrap values are indicated in the point as nodes) as test of phylogeny, and the software MEGA5. The proteins are described by GenBank accession number, organism, and class.

3.2.3 The hyphal growth defect of the Δ*plc-1*, Δs*plA2,* and Δ*cpe-1* mutants on ionophore treatment was not due to the dissipation of membrane potential

In addition to the electroneutral exchange of positive ions, ionophores are also capable of disrupting plasma membrane potentials by causing depolarization of intact cells (Nicholls 2006). Therefore, in order to test if the hyphal growth defects of the ΔNCU06245, ΔNCU06650, and ΔNCU06366 mutants upon ionophore treatment was due to dissipation of membrane potential, I used the fluorescent membrane potential indicator bis(1,3-dibutylbarbituric acid) (DiBAC) that fluoresces when membranes are depolarized (Figure 3.8 A; Alćantara-Sánchez et al. 2004). The voltage sensitive probe DiBAC can enter depolarized yet intact cells where it interacts with cytoplasmic proteins or membrane and exhibits slow but enhanced fluorescence (Yamada et al. 2001). I inoculated conidia of the wild type and the three mutant strains at a concentration of ~1×10^6 conidia/ml in Vogel's glucose medium and incubated at 30°C for 2 h with shaking at 200 rpm. Germlings obtained were then treated with either the ionophore A23187 or toluene, used as a control, incubated further with the fluorophore DiBAC, and observed under a Trinocular inverted fluorescence microscope (AxioVert A1FL, Carl Zeiss). The A23187 treated germlings of ΔNCU06245, ΔNCU06650, and ΔNCU06366 were not stained at all by DiBAC, whereas the germlings treated with toluene followed by DiBAC incubation produced enhanced green

fluorescence (Figure 3.8 B). Therefore, this result suggested that the hyphal growth defect of the ΔNCU06245, ΔNCU06650, and ΔNCU06366 mutants was not due to dissipation of membrane potential.

(A)

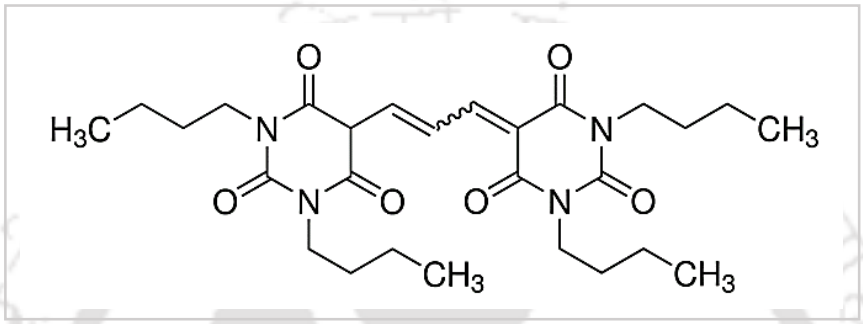

(B)

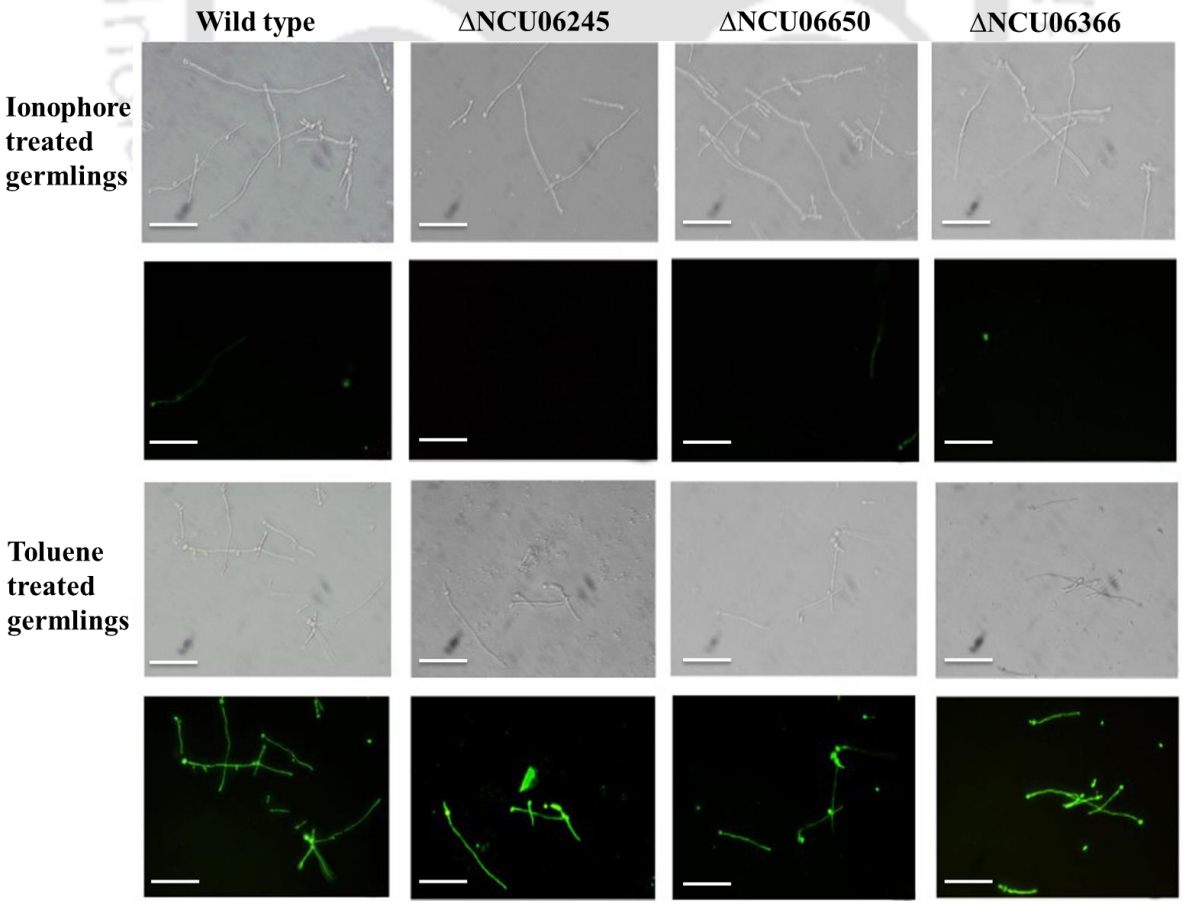

Figure 3.8: Effect of A23187 ionophore on membrane potential of the *N. crassa* strains. (A) Chemical structure of DiBAC [bis (1,3-dibutylbarbituric acid) trimethine oxonol; λ_{ex} = 485 nm, and λ_{em}= 515 nm]. The membrane potential sensitive fluorophore DiBAC fluoresces when membranes are depolarized (Alćantara-Sánchez et al. 2004). Its chemical structure is available at http://www.sigmaaldrich.com/catalog/product/sial/d8189?lang=en&region=IN. **(B)** Membrane potential assay. Germlings of the wild type, ΔNCU06245, ΔNCU06650, and ΔNCU06366 mutant strains were treated either with ionophore (test) or toluene (control) and incubated with 3.87 µM DiBAC at 30°C. Post-incubation observations were made under a Trinocular inverted microscope with a 450-490 nm excitation filter and 515 nm emission filter, observed under a microscope (AxioVert A1 FL, Carl Zeiss), and photographed using a CCD camera (AxioCam ICc3, Carl Zeiss). Ten images for each strain is captured and a representative image is shown. Scale bar 20 µm.

3.2.4 Oxidative stress assay

3.2.4.1 The Δ*plc-1*, Δs*plA2*, and Δ*cpe-1* mutants showed increased sensitivity to hydrogen peroxide induced oxidative stress

Oxidative stress causes an increased production of ROS with a significant decrease in the cell's anti-oxidative defense mechanisms causing imbalance in the normal redox state of the cells and eventually results in irreversible oxidative damage to lipids, proteins, and DNA including apoptosis (Figure 3.9; Scheiber and Chandel 2014; Zorov et al. 2014; Görlach et al. 2015). Various environmental factors and external cues induces oxidative stress in fungal cells that causes generation of high intracellular ROS and disruption of Ca^{2+} homeostasis (Belozerskaya and Gessler 2006). Regulation of cellular ROS concentration is needed during various stages of fungal development and also for generating appropriate physiological responses (Gessler et al. 2006). Therefore, to determine if the *plc-1*, s*plA2*, and *cpe-1* genes play any role in survival of *N. crassa* in oxidative stress, I tested the viability of Δ*plc-1*, Δs*plA2*, and Δ*cpe-1* mutants in hydrogen peroxide (H_2O_2) induced oxidative stress. H_2O_2 is a deleterious agent capable of generating ·OH radicals via the Haber Weiss reaction and eventually lipid peroxides derived from H_2O_2 can cause irreversible damage to cell membranes (Haber and Weiss 1934; Halliwell and Gutteridge 1984). To test the effect of H_2O_2 on viability, conidia of the wild type and the mutant strains were germinated in the dark and supplemented with or without (control) H_2O_2. Percent survival was

determined and the number of viable colonies were counted (discussed earlier in chapter 2). The Δ*plc-1*, Δs*plA2*, and Δ*cpe-1* mutants showed reduced survival percentage as compared to wild type and the resistance to H_2O_2 induced oxidative stress tolerance followed the trend wild type>*Δcpe-1*>*ΔsplA2*>*Δplc-1* (Figure 3.10; Table 3.4). Therefore, the Δ*plc-1*, Δs*plA2*, and Δ*cpe-1* mutants showed an increased sensitivity to H_2O_2 induced oxidative stress indicating that the *plc-1*, s*plA2*, and *cpe-1* genes play a role in oxidative stress tolerance.

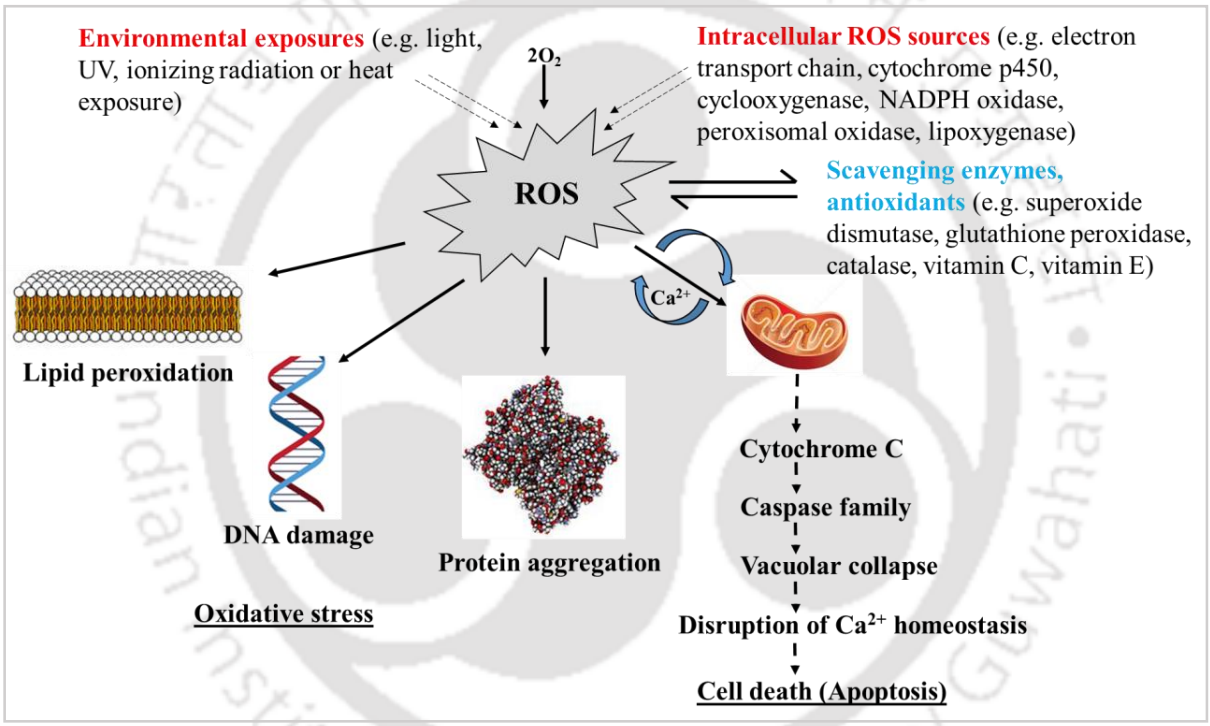

Figure 3.9: A schematic representation of effects of increased intracellular ROS production. Oxidative stress refers to overall increase in cellular ROS formed in response to a number of environmental and external stressors (e.g. light, UV, ionizing radiation or heat exposure) including endogenous sources causing damage to lipids (lipid peroxidation), proteins (protein aggregation), and DNA (DNA damage) (Scheiber and Chandel 2014; Zorov et al. 2014). Increased accumulation of ROS and accumulated Ca^{2+} also causes mitochondrial dysfunction and damages mitochondrial membrane potential that triggers cytoplasmic release of cytochrome C which activates the caspase family of proteases and ultimately leads to apoptosis (Zorov et al. 2014; Görlach et al. 2015). Various scavenging enzymes and antioxidants balances the redox state of a cell minimizing harmful oxidative damage (Görlach et al. 2015).

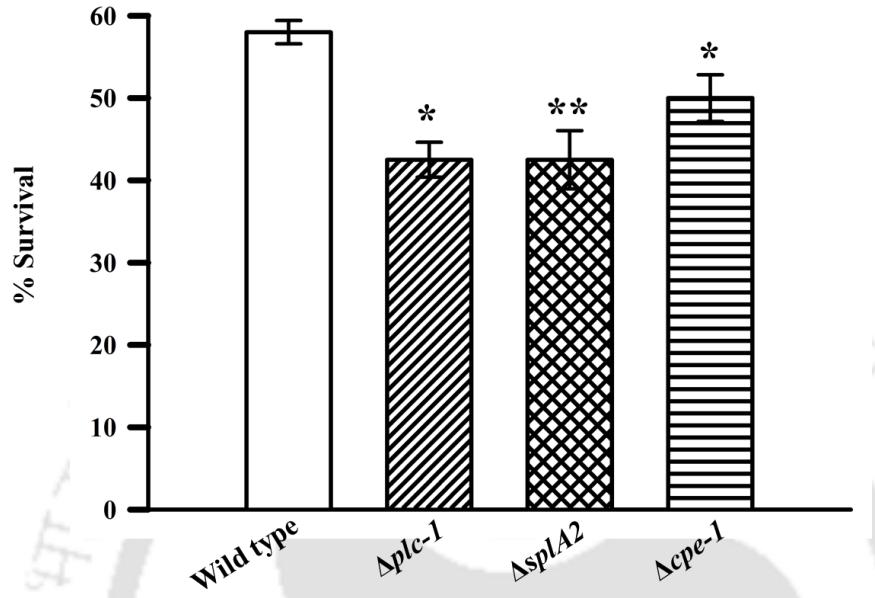

Figure 3.10: Oxidative stress assay. Germlings of wild type, Δ*plc-1*, Δs*plA2*, and Δ*cpe-1* mutant strains were incubated at 10 mM H_2O_2 at 30°C and percent survival determined. Error bars indicate the standard deviations calculated from the data for three independent experiments (n=3) with *P-values* < 0.05 (*), <0.01 (**), and < 0.001 (***) compared with the wild type strain as measured by one-way ANOVA test.

Table 3.4: Percent survival of the wild type, Δ*plc-1*, Δs*plA2*, and Δ*cpe-1* mutants at 10 mM H_2O_2

Strains	Percent survival at 10 mM H_2O_2[†]
Wild type	58 ± 1.41
Δ*plc-1*	43 ± 2.12 (*)
Δs*plA2*	43 ± 3.53 (**)
Δ*cpe-1*	50 ± 2.82 (*)

[†]Results are shown as mean ± standard deviation for three independent experiments (n=3) with *P values* < 0.05 (*), < 0.01 (**), and < 0.001 (***) compared with the wild type strain as measured by one-way ANOVA test.

3.2.4.2 The *plc-1*, *splA2*, and *cpe-1* null mutations contributed to ROS production upon exposure to H_2O_2

The increased sensitivity of the Δ*plc-1*, Δs*plA2*, and Δ*cpe-1* mutants to oxidative stress induced by H_2O_2 suggested an increased ROS level in these mutants. Therefore, I measured the endogenous amounts of ROS using the non-fluorescent dye 2', 7'- dichlorofluorescein-diacetate (DCFH-DA; Figure 3.11 A; Radman et al. 2004). The oxidant sensitive probe DCFH-DA passes through the cell membrane, where it is hydrolyzed by the intracellular esterases to 2′, 7′-dichlorodihydrofluorescein (DCFH). DCFH is further oxidized to the highly fluorescent molecule 2′, 7′-dichlorofluorescein (DCF) in the presence of ROS inside the cells (Figure 3.11 B). Fluorescence of DCF is therefore considered as an indicator of ROS production. I detected ROS levels in conidia treated with or without H_2O_2 using DCFH-DA. I observed conidial counts for the Δ*plc-1*, Δs*plA2*, and Δ*cpe-1* mutants stained with DCFH-DA were more than those from the wild type, indicating an increased amounts of ROS were produced in Δ*plc-1*, Δs*plA2*, and Δ*cpe-1* mutants treated with exogenous H_2O_2 (Figure 3.11B).

(A)

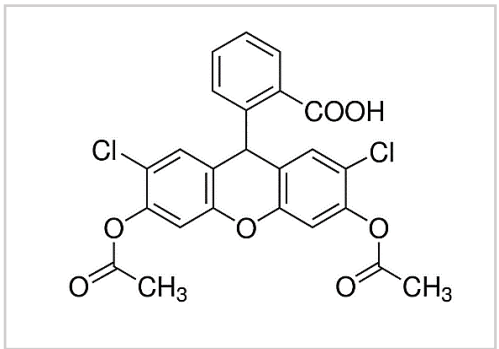

(B)

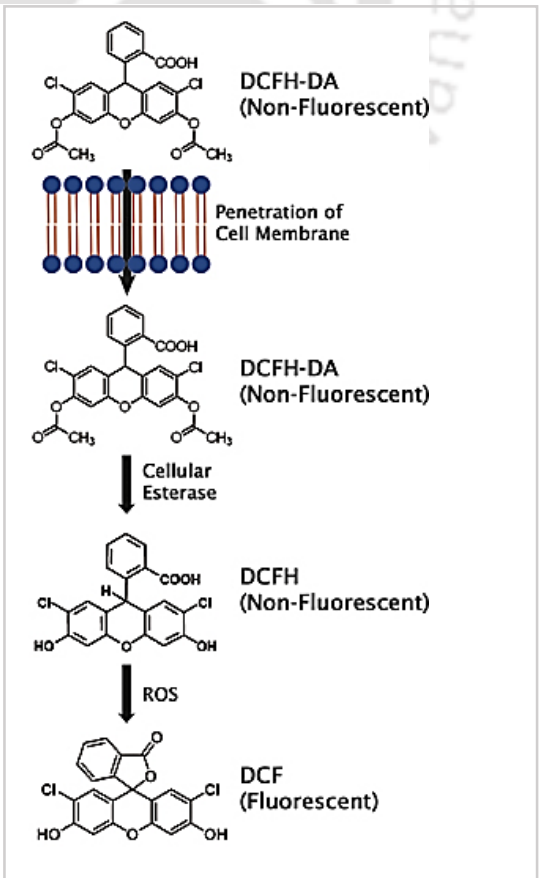

(C)

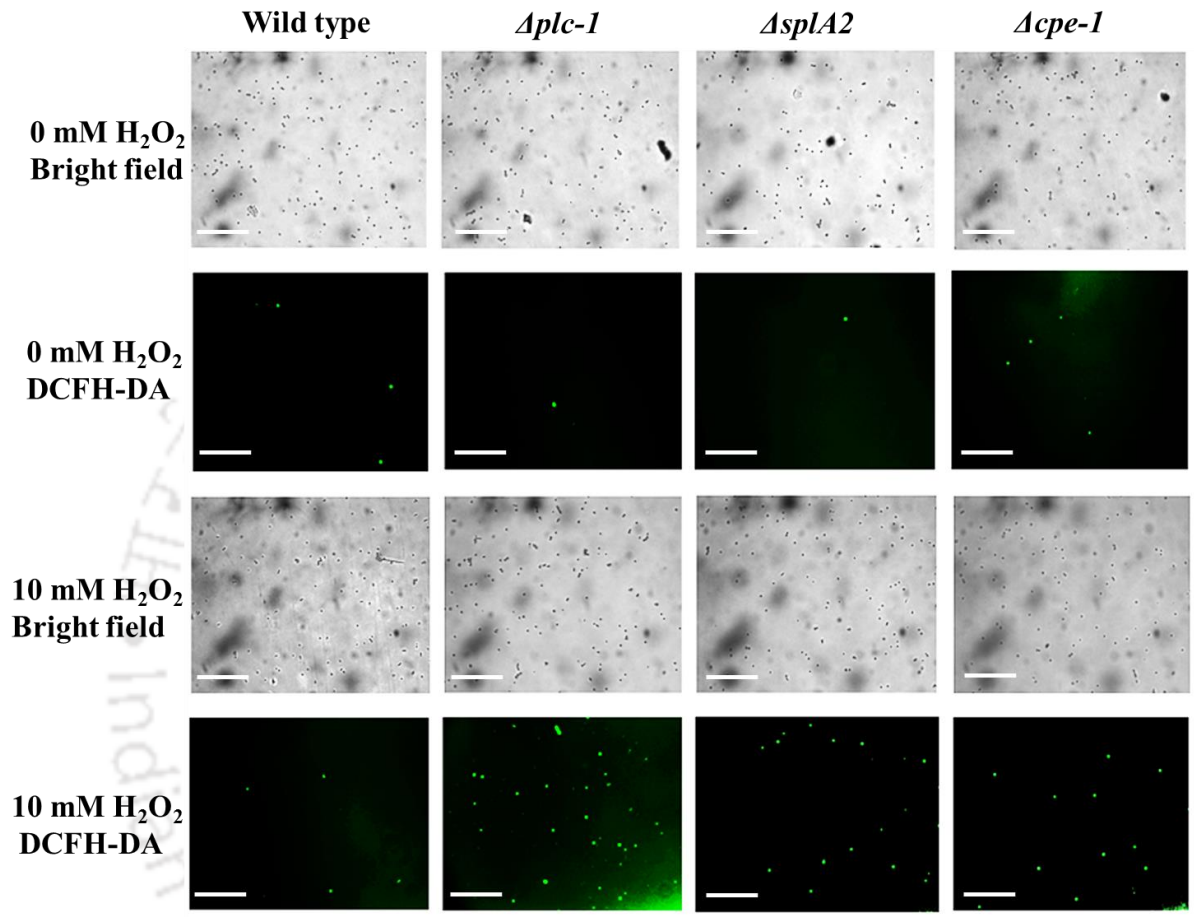

Figure 3.11: Estimation of ROS production of the *N. crassa* strains. (A) Chemical structure of DCFH-DA (2', 7'- dichlorofluorescein-diacetate; λ_{ex}= 485 nm and λ_{em}= 515 nm). The fluorophore DCFH-DA fluoresces in the presence of intracellular ROS, therefore, its fluorescence is considered as an indicator of degree of oxidative stress (Radman et al. 2004). Its chemical structure is available at http://www.sigmaaldrich.com/catalog/product/sigma/d6883?lang=en&region=IN. **(B)** Mechanism of action of DCFH-DA is available at https://www.cellbiolabs.com/reactive-oxygen-species-ros-assay#details. **(C)** DCFH-DA assay. Approximately, 1000 conidia of the wild type, Δ*plc-1*, Δ*splA2*, and Δ*cpe-1* mutant strains were incubated with 10 µM DCFH-DA for 30 min and further treated with 10 mM H_2O_2 for 90 min. Fluorescence signal were captured using a Trinocular inverted microscope (AxioVert A1 FL, Carl Zeiss) with a 450-490 nm excitation filter and 515 nm emission filter. Each image is representative of ten different microscopic fields. Scale bar 20 µm.

3.2.5 Thermotolerance assay

3.2.5.1 The Δ*plc-1*, Δs*plA2*, and Δ*cpe-1* mutants showed an increased sensitivity to heat shock

Since the response pathway to oxidative stress, heat shock, and thermotolerance are interrelated in *N. crassa* (Kapoor et al. 1990), therefore, I also investigated the roles for *plc-1*, s*plA2*, and *cpe-1* genes in thermotolerance-to a lethal temperature. Induced thermotolerance is the increased survival of cells pre-incubated at a sub-lethal (heat shock) temperature after subsequent exposure to a lethal temperature, whereas, uninduced thermotolerance is the survival of cells after exposure to a lethal temperature, without pre-incubation at a heat shock temperature (Kapoor et al. 1990). Incubation of *N. crassa* cells at sub-lethal heat shock temperatures leads to synthesis of heat shock proteins which subsequently protects the cells from lethal temperature (Kapoor et al. 1995; Yang and Borkovich 1999). To determine thermotolerance of Δ*plc-1*, Δs*plA2*, and Δ*cpe-1* mutants, I determined viability of the mutant colonies after exposure to a lethal temperature with or without pre-exposure to a sublethal heat shock temperature of 44°C. Percent survival was determined and the number of viable colonies were counted (discussed earlier in chapter 2). The Δ*plc-1*, Δs*plA2*, and Δ*cpe-1* mutants showed decreased survival percentage relative to the wild type under induced thermotolerance, whereas, survival of the Δs*plA2* and Δ*cpe-1* was slightly higher than the wild type, and no viable colony was observed in the Δ*plc-1* mutant in uninduced thermotolerance (Figure 3.12; Table 3.5). These results suggested that *plc-1*, s*plA2*, and *cpe-1* genes might play a role in survival at lethal temperatures mediated by prior expression of heat shock proteins, indicating a role of these genes in acquisition of thermotolerance induced by heat shock.

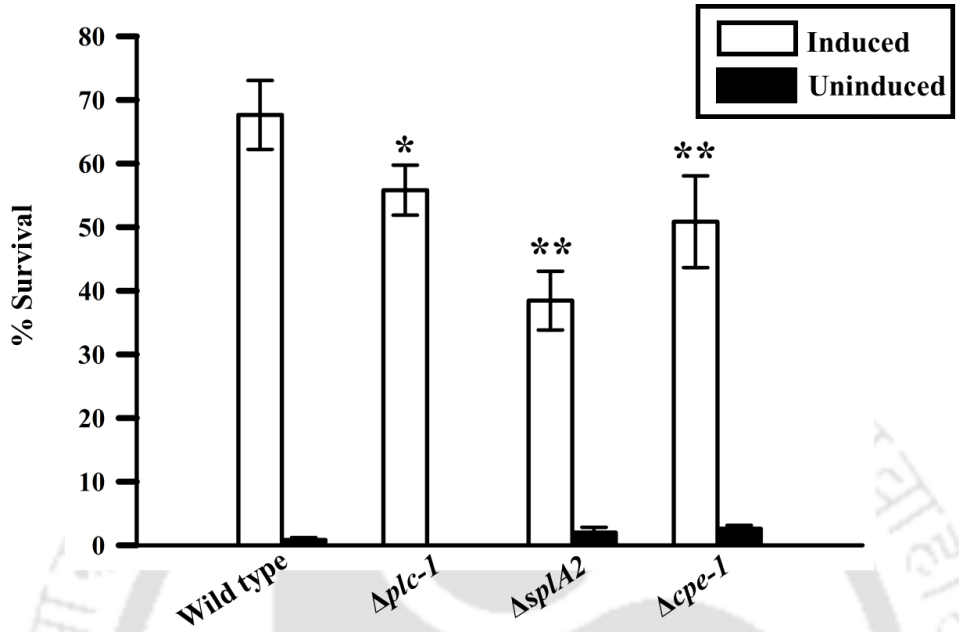

Figure 3.12: Thermotolerance assay. Germlings of wild type, Δ*plc-1*, Δs*plA2*, and Δ*cpe-1* mutant strains were exposed to 52°C lethal temperature with (induced) or without (uninduced) pre-exposure to a sublethal heat shock temperature at 44°C and percent survival determined. Error bars indicate the standard deviations calculated from the data for three independent experiments (n=3) with *P-values* < 0.05 (*), <0.01 (**), and < 0.001 (***) compared with the wild type strain as measured by one-way ANOVA test.

Table 3.5: Percent survival of the wild type, Δ*plc-1*, Δs*plA2*, and Δ*cpe-1* mutants upon heat shock

Strains	Percent survival upon exposure to heat shock (52°C)†	
	Induced (44°C)	Uninduced (30°C)
Wild type	67.63 ± 5.41	0.83 ± 0.37
Δ*plc-1*	55.80 ± 3.93 (*)	0.00 ± 0.00
Δs*plA2*	38.44 ± 4.62 (**)	2.00 ± 0.82
Δ*cpe-1*	50.84 ± 7.21 (**)	2.59 ± 0.53

† Results are shown as mean ± standard deviation for three independent experiments (n=3) with *P-values* < 0.05 (*), < 0.01 (**), and < 0.001 (***) compared with the wild type strain as measured by one-way ANOVA test.

3.2.6 Phytosphingosine assay

3.2.6.1 The Δ*plc-1*, Δs*plA2*, and Δ*cpe-1* mutants showed an increased sensitivity to phytosphingosine

Programmed cell death (PCD) is a characteristics cell suicidal phenomenon of both prokaryotic and eukaryotic systems in which cells in response to various external or endogenous stimuli undergo a unique genetic programme leading to death, thereby, maintaining homeostasis in multicellular organisms (Cheng et al. 2003; Green and Kroemer 2004; Hamann et al. 2008; Madeo et al. 2004; Castro et al. 2008; Vidiera et al. 2009). Therefore, to determine if the *plc-1*, s*plA2*, and *cpe-1* genes in *N. crassa* have any role in PCD, I used phytosphingosine (PHS), a natural phospholipid widely distributed in plants and animals including humans, which causes PCD in *N. crassa* (Figure 3.13 A; Castro et al. 2008). Conidia from the wild type, Δ*plc-1*, Δs*plA2*, and Δ*cpe-1* mutants were exposed to PHS in different time periods and their percent survival was determined (discussed earlier in Chapter 2). I observed that conidia from the Δ*plc-1*, Δs*plA2*, and Δ*cpe-1* mutants showed similar sensitivity to PHS exposure as they showed upon exposure to H_2O_2 or heat shock (Figure 3.13 B; Table 3.6). Therefore, I concluded that Δ*plc-1*, Δs*plA2*, and Δ*cpe-1* mutants are more sensitive to PHS indicating a role of the *plc-1*, s*plA2*, and *cpe-1* genes in survival under the PHS-induced PCD.

(A)

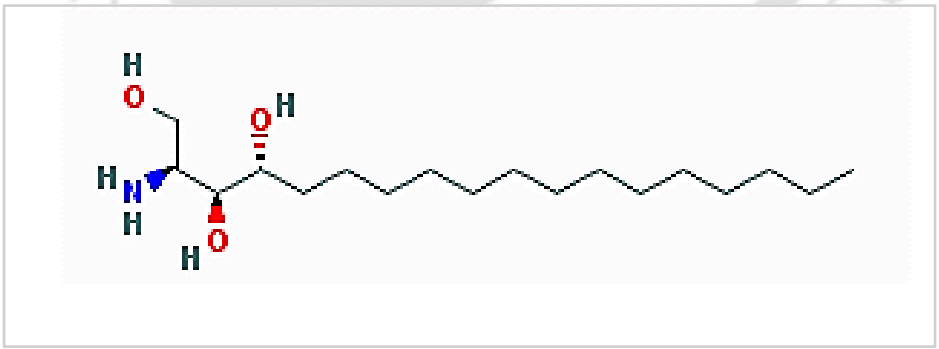

(B)

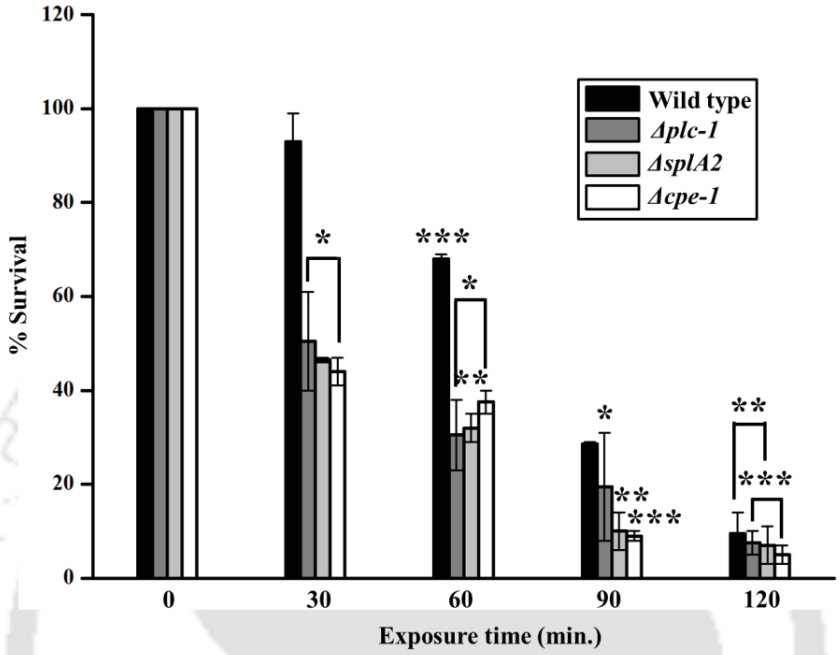

Figure 3.13: Structure of phytosphingosine and its effect on the *N. crassa* strains. (A) Chemical structure of PHS (Phytosphingosine). The natural phospholipid PHS is responsible for causing apoptotic like cell death in filamentous fungi (Cheng et al. 2003; Castro et al. 2008). Its chemical structure is available at http://www.chemspider.com/Chemical-Structure.108921.html. **(B)** The PHS sensitivity assay. Conidia of wild type, Δ*plc-1*, Δ*splA2*, and Δ*cpe-1* mutant strains were exposed to 10 µg/ml PHS at different time intervals and percent survival determined. Error bars indicate the standard deviations calculated from the data for three independent experiments (n=3) with *P-values* < 0.05 (*), <0.01 (**), and < 0.001 (***) compared with the wild type strain as measured by one-way ANOVA test.

Table 3.6: Percent survival of the wild type, Δ*plc-1*, Δ*splA2*, and Δ*cpe-1* mutants upon exposure to PHS

Strains	Percent survival upon exposure to PHS†				
	0 min	**30 min**	**60 min**	**90 min**	**120 min**
Wild type	100 ± 0.00	93 ± 6.00	68 ± 1.00 (***)	28.5 ± 0.50	9.5 ± 4.50 (**)
Δ*plc-1*	100 ± 0.00	50.5 ± 10.50 (*)	30.5 ± 7.50 (*)	19.5 ± 11.50 (*)	7.5 ± 2.50 (***)
Δ*splA2*	100 ± 0.00	46.5 ± 0.50 (*)	32 ± 3.00 (**)	10 ± 4.00 (**)	7 ± 4.00 (**)
Δ*cpe-1*	100 ± 0.00	44 ± 3.00 (*)	37.5 ± 2.50 (*)	9 ± 1.00 (***)	5 ± 2.00 (***)

†Results are shown as mean ± standard deviation for three independent experiments (n=3) with *P-values* < 0.05 (*), < 0.01 (**), and < 0.001 (***) compared with the wild type strain as measured by one-way ANOVA test.

3.2.7 Carotenoid analysis

3.2.7.1 The Δ*plc-1*, Δ*splA2*, and Δ*cpe-1* mutants showed higher carotenoid accumulation

Carotenoid amounts in Δ*plc-1*, Δ*splA2*, and Δ*cpe-1* mutants were examined to test the effect of these mutations in carotenoid biosynthesis. Carotenoids are the most widespread and naturally occurring pigment i.e. characteristic of organisms for all major taxa and play significant roles in certain important biological processes including photosynthesis, vision, and quenching of free radicals and singlet oxygen (Vershinin 1999). Cultures of *N. crassa* strains shows characteristics orange pigmentation mainly due to the accumulation of the xanthophyll neurosporoxanthin and variable amounts of carotenoid precursors in mycelia and air-borne conidia (Zalokar 1954; Avalos et al. 2013). Light and temperature are two important factors that affect carotenoid biosynthesis with neurosporoxanthin biosynthesis greatly enhanced upon illumination at low temperature, whereas illumination at normal temperature results in the accumulation of carotenoid precursors (Harding et al. 1969; Harding 1974; Estrada et al. 2008; Diaz-Sanchez et al. 2011). Therefore, I determined carotenoid content in Δ*plc-1*, Δ*splA2*, and Δ*cpe-1* mutants in both light and dark and also at three different temperatures of 8, 22, and 30°C. The three mutants showed higher carotenoid content than wild type at all three temperatures of 8, 22, and 30°C in light and also showed marginally increased amounts of carotenoid in dark relative to the wild type (Figure 3.14 A-C; Table 3.7). Therefore, this result suggested that *plc-1*, *splA2*, and *cpe-1* genes might be involved in carotenoid accumulation in *N. crassa*. I also assessed conidiation in Δ*plc-1*, Δ*splA2*, and Δ*cpe-*

1 mutants, however, conidia amount in the three mutants were found to be similar to the wild type strain suggesting that these mutations do not affect asexual sporulation in *N. crassa* (Figure 3.15).

(A)

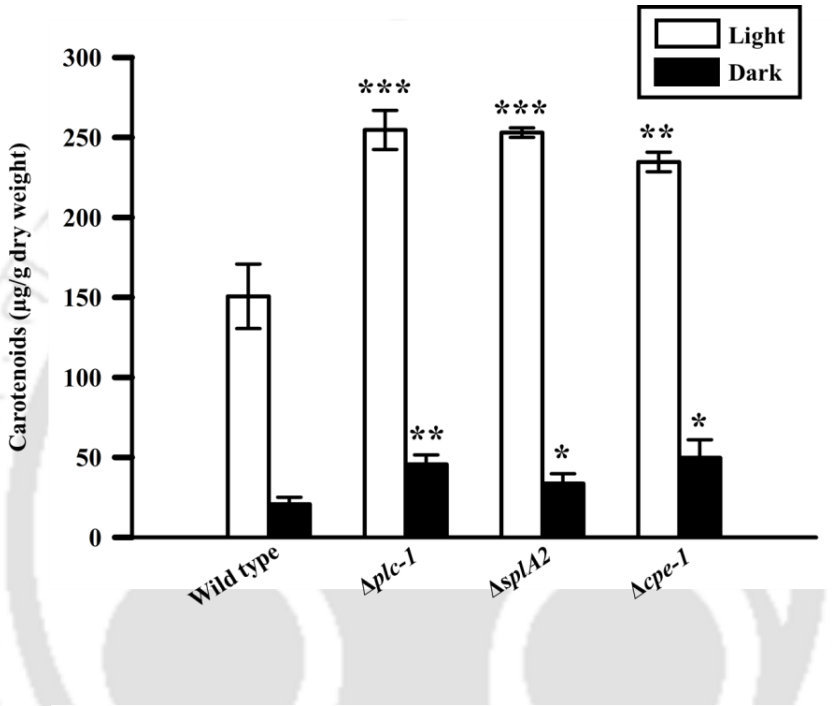

(B)

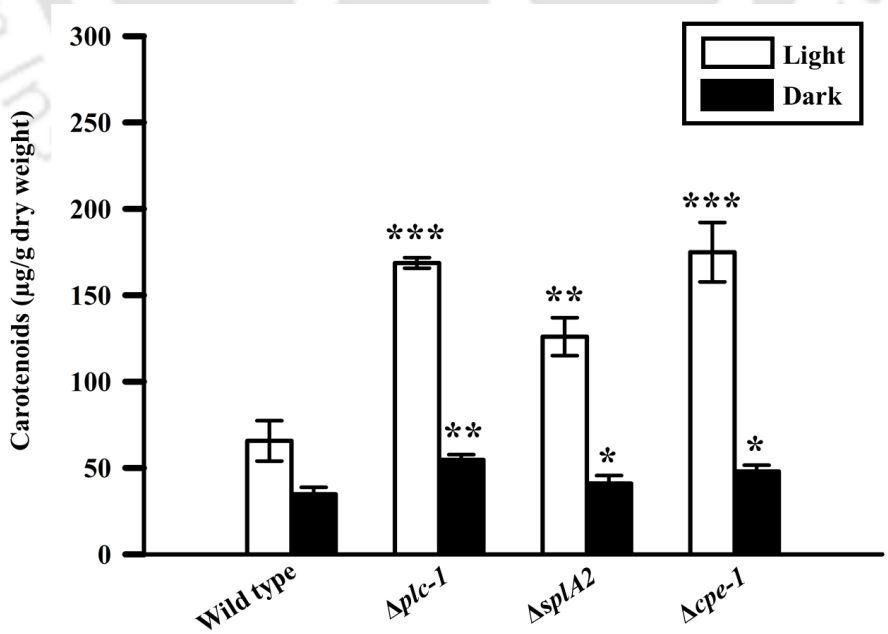

(C)

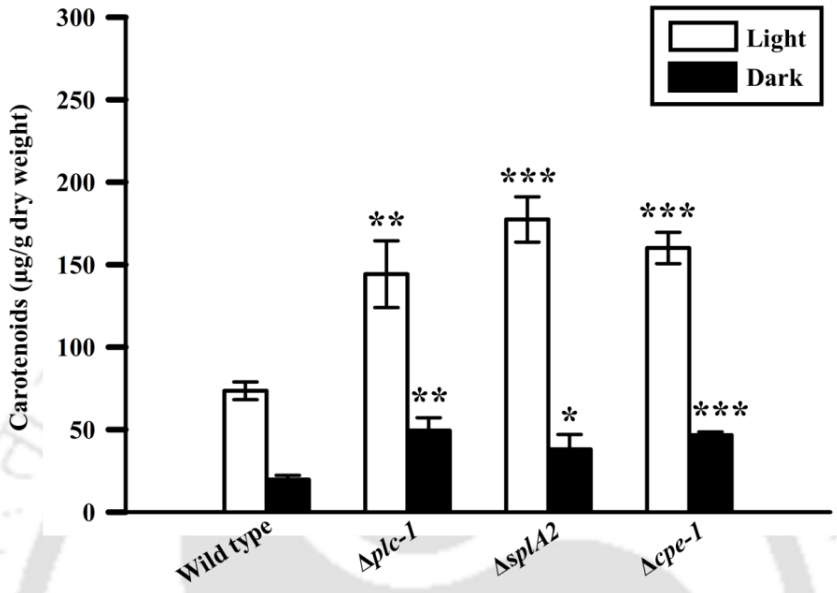

Figure 3.14: Carotenoid accumulation in the *N. crassa* strains. The wild type, Δ*plc-1*, Δs*plA2*, and Δ*cpe-1* mutant strains were grown in Petri dishes containing Vogel's glucose agar medium and incubated at 30°C in the dark for 48 h followed by with or without exposure to white light at 8°C **(A)**, 22°C **(B)**, and 30°C **(C)** for 24 h. Error bars indicate the standard deviations calculated from the data for three independent experiments (n=3) with *P-values* < 0.05 (*), <0.01 (**), and < 0.001 (***) compared with the wild type strain as measured by one-way ANOVA test.

Table 3.7: Carotenoid content of the wild type, Δ*plc-1*, Δ*splA2,* and Δ*cpe-1* mutants at three different temperatures

Strains	Carotenoids (µg/g dry weight)†					
	8°C		22°C		30°C	
	Light	Dark	Light	Dark	Light	Dark
Wild type	151 ± 20.1	21 ± 4.3	66 ± 12	35 ± 4	74 ± 5.4	18 ± 3
Δplc-1	253 ± 3 (***)	34 ± 6.1 (**)	126 ± 11(***)	55 ± 3.1 (**)	144.2 ± 20.2 (**)	49.4 ± 8 (**)
ΔsplA2	255 ± 12.2 (***)	46 ± 6 (*)	169 ± 3.1 (**)	41 ± 5 (*)	177.4 ± 14 (***)	38.1 ± 9 (*)
Δcpe-1	235 ± 6.1 (**)	50 ± 11.2 (*)	175 ± 17.2 (***)	48 ± 4 (*)	160.1 ± 10 (***)	47 ± 2 (***)

†Results are shown as mean ± standard deviation for three independent experiments (n=3) with *P-values* < 0.05 (*), < 0.01 (**), and < 0.001 (***) compared with the wild type strain as measured by one-way ANOVA test.

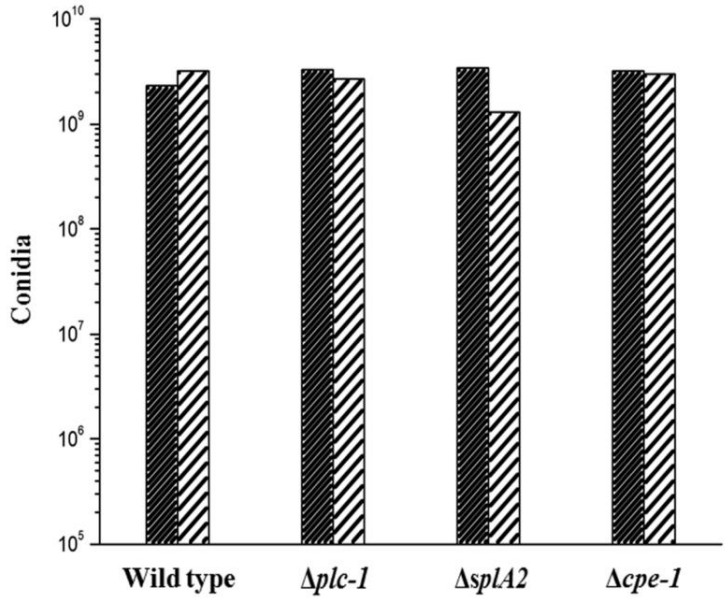

Figure 3.15: Conidiation of the *N. crassa* strains. Conidia of *Δplc-1*, *ΔsplA2* and *Δcpe-1* mutants were quantified after 48 h incubation in the dark at 30°C followed by continuous exposure to light at 22°C for 96 h. The bars indicate two independent determinations for each strain.

3.2.8 Ultraviolet sensitivity assay

3.2.8.1 The Δ*plc-1*, Δ*splA2*, and Δ*cpe-1* mutants showed increased ultraviolet survival

Carotenoids are known to be powerful antioxidants that protects cells and tissues from harmful UV damage in fungi and humans (Luque et al. 2012). Carotenoids are capable of quenching singlet oxygen species thereby neutralizes several attacks of ROS. Therefore, in order to test whether the increased carotenoid accumulation in Δ*plc-1*, Δ*splA2*, and Δ*cpe-1* mutants could provide protection against harmful UV radiation, I performed the UV sensitivity assay. To test this, conidia of the wild type and the three mutant strains at a concentration of ~1×10^6 conidia/ml were inoculated in Vogel's glucose agar medium and incubated at 30°C for 48 h in the dark and then either at 8, 22, and 30°C with or without illumination. Subsequently, conidia were harvested, washed with sterile water, and finally re-suspended in sterile water. Approximately, 1000 conidia were then plated on Vogel's sorbose agar medium and irradiated with UV doses of 100, 200, and 300 J/m^2 in a UVC 500 cross linker (Hoefer, UK). The results from the UV dose response curves indicated that conidia from the three mutants produced at 8, 22, and 30°C in both light and dark had increased UV survival relative to the wild type (Figure 3.16 A-F). However, when grown in conditions not inducing carotenoids accumulation, which is incubation at 30ºC for 48 h followed by illumination under light at room temperature for 96 h, the UV-dose response curves of *Δplc-1*, *ΔsplA2* and *Δcpe-1* mutants were similar to wild type (Figure 3.17). Taken together, these results suggested that the increased carotenoid content in Δ*plc-1*, Δ*splA2*, and Δ*cpe-1* mutants might have contributed to their increased UV survival at the three temperatures.

(A)

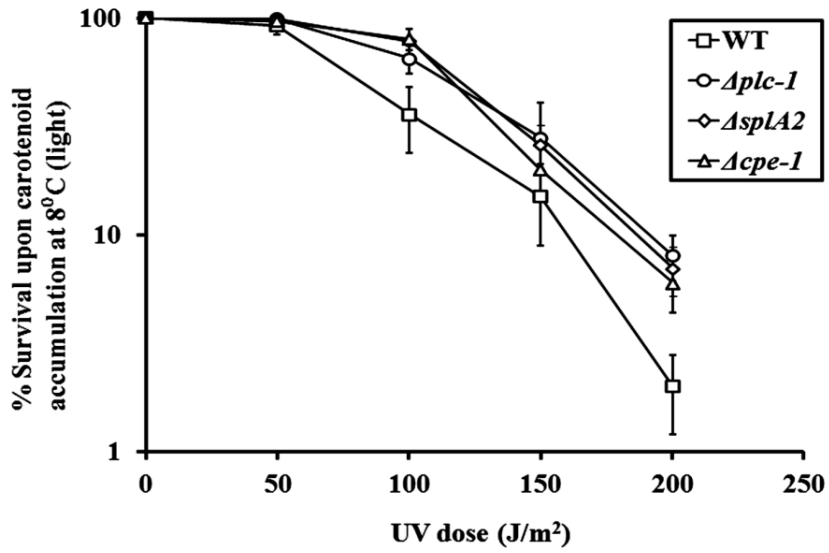

(B)

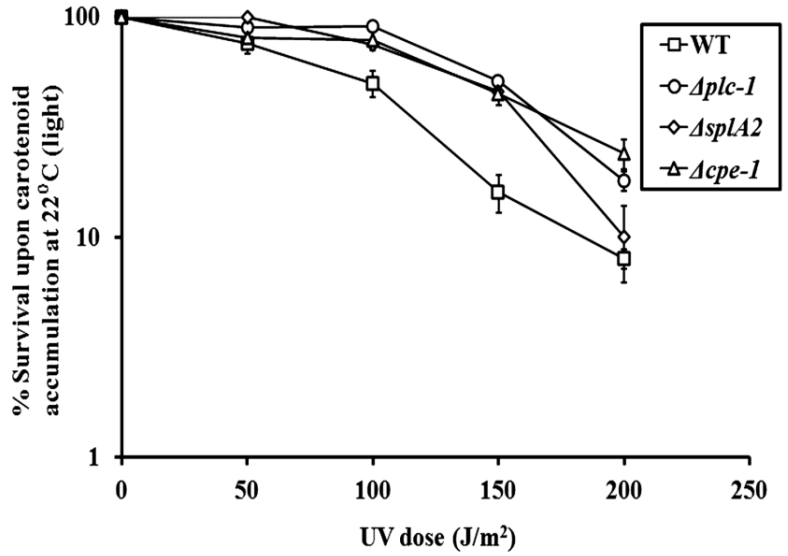

(C)

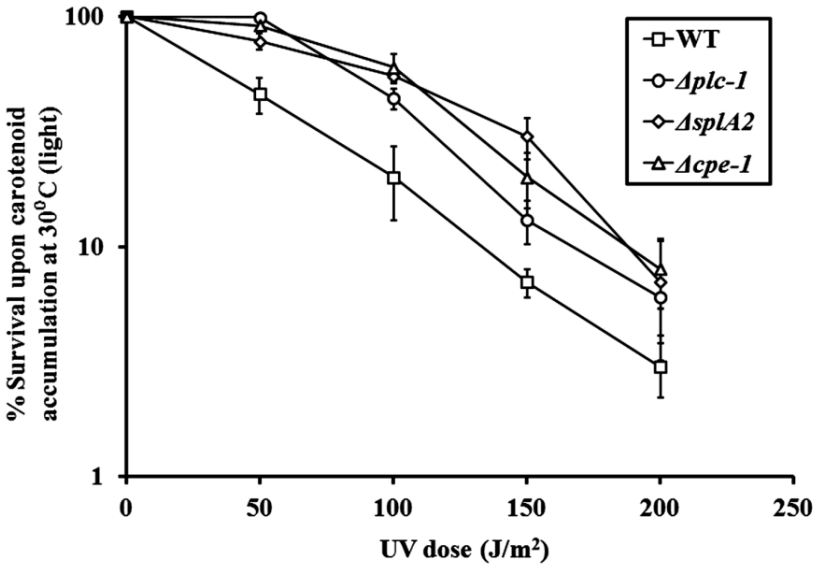

(D)

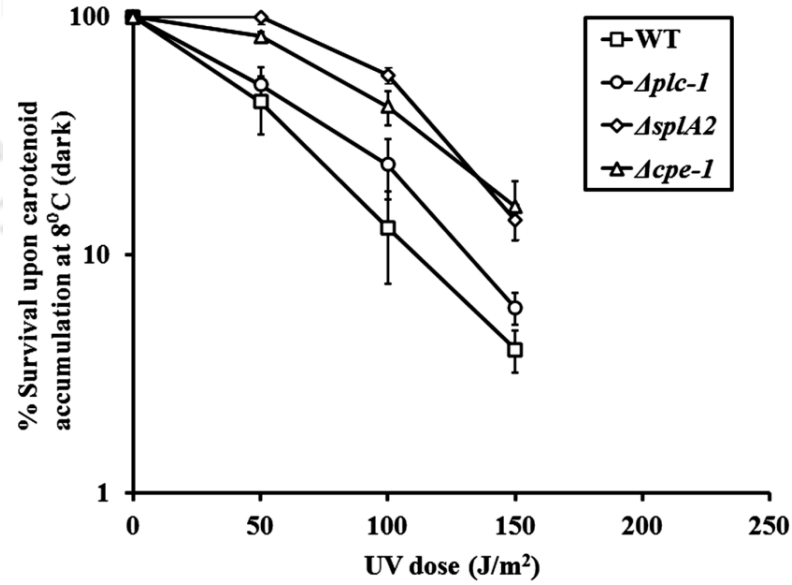

(E)

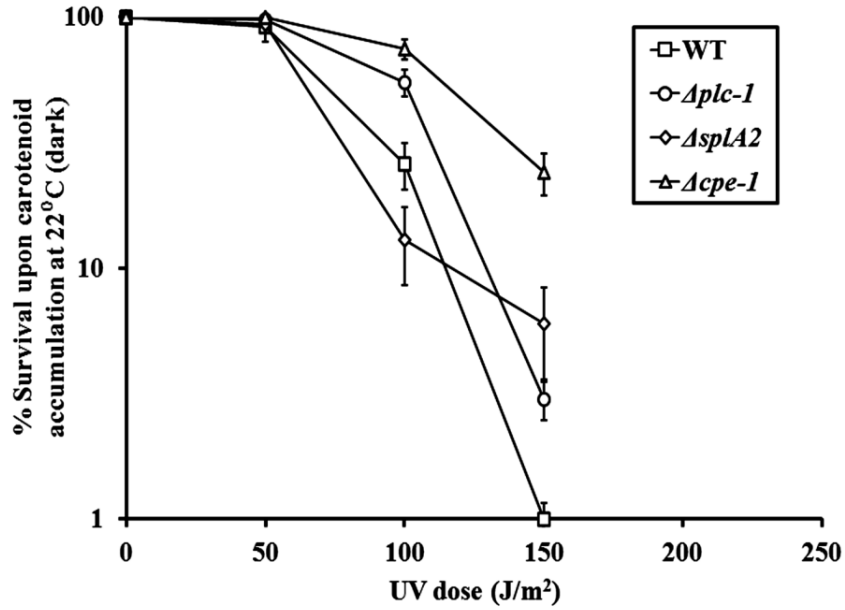

(F)

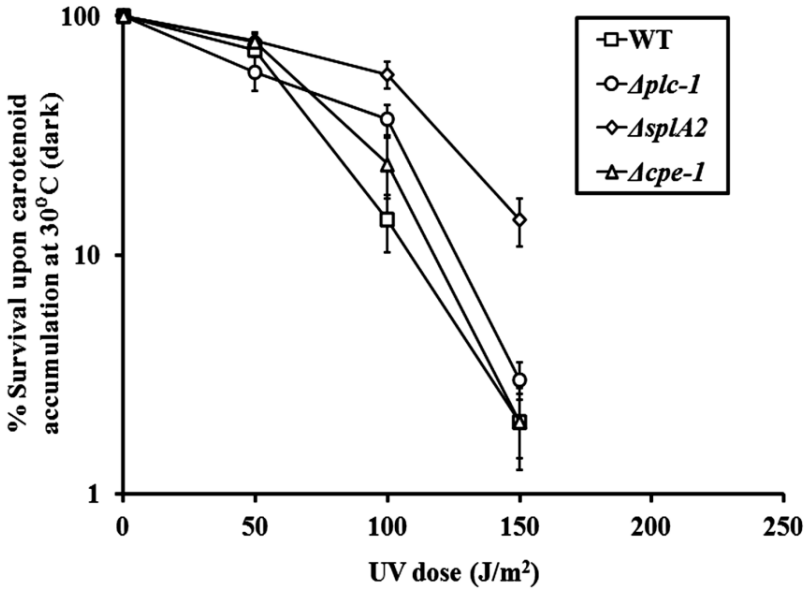

Figure 3.16: UV sensitivity assay relative to carotenoid accumulation. Dose-response curves of the wild-type and mutant strains after exposure to UV radiation after carotenoid accumulation for 48 h in the dark at 30°C followed by incubation at 8, 22, or 30°C for 24 h either in light illumination **(A-C)**, or in continuous darkness **(D-F)**. Percent survival was obtained by dividing

the number of colonies from plates irradiated with UV by the number of colonies on plates with no UV irradiation (control). Error bars indicate standard deviations calculated from the data for three independent experiments (n=3).

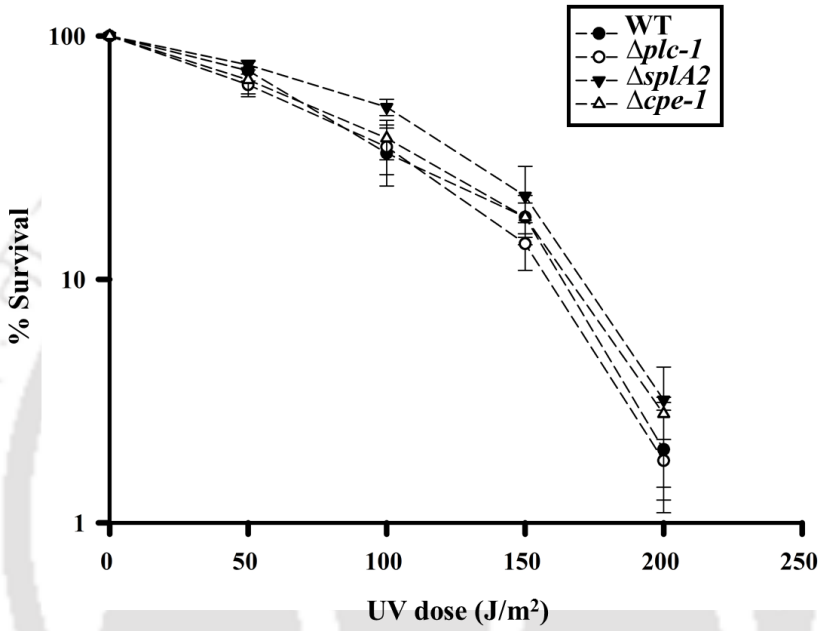

Figure 3.17: UV sensitivity assay. Dose-response curves of the wild-type and mutant strains after incubation at 30ºC for 48 h followed by illumination under light at room temperature for 96 h and irradiated with different doses of UV. Percent survival was obtained by dividing the number of colonies from plates irradiated with UV by the number of colonies on plates with no UV irradiation (control). Error bars indicate standard deviations calculated from the data for three independent experiments (n=3).

3.2.9 Cloning of *plc-1*, *splA2*, and *cpe-1* gene products from the wild type for complementation analysis

To complement the Δ*plc-1*, Δ*splA2*, and Δ*cpe-1* mutants, I PCR amplified *plc-1*, *splA2*, and *cpe-1* genes of sizes 2,192, 762, and 1,656 bp, respectively, from the wild type using the gene specific primers, and ligated into the *Sma* I site of pMF272 vector (Figure 3.18 A-C; Table 3.3; Entry 5-10). The ligated products were transformed into the *E. coli DH5α* ultra-competent cells, and plasmids constructs were isolated. I verified the correct clones using PCR and restriction digestion

using *Xba*I and *Pac*I enzymes, and isolated three recombinant plasmids pAB-1, pAB-2, and pAB-3 containing the *plc-1*, s*plA2*, and *cpe-1* genes, respectively (Figure 3.18 D-G).

(A)

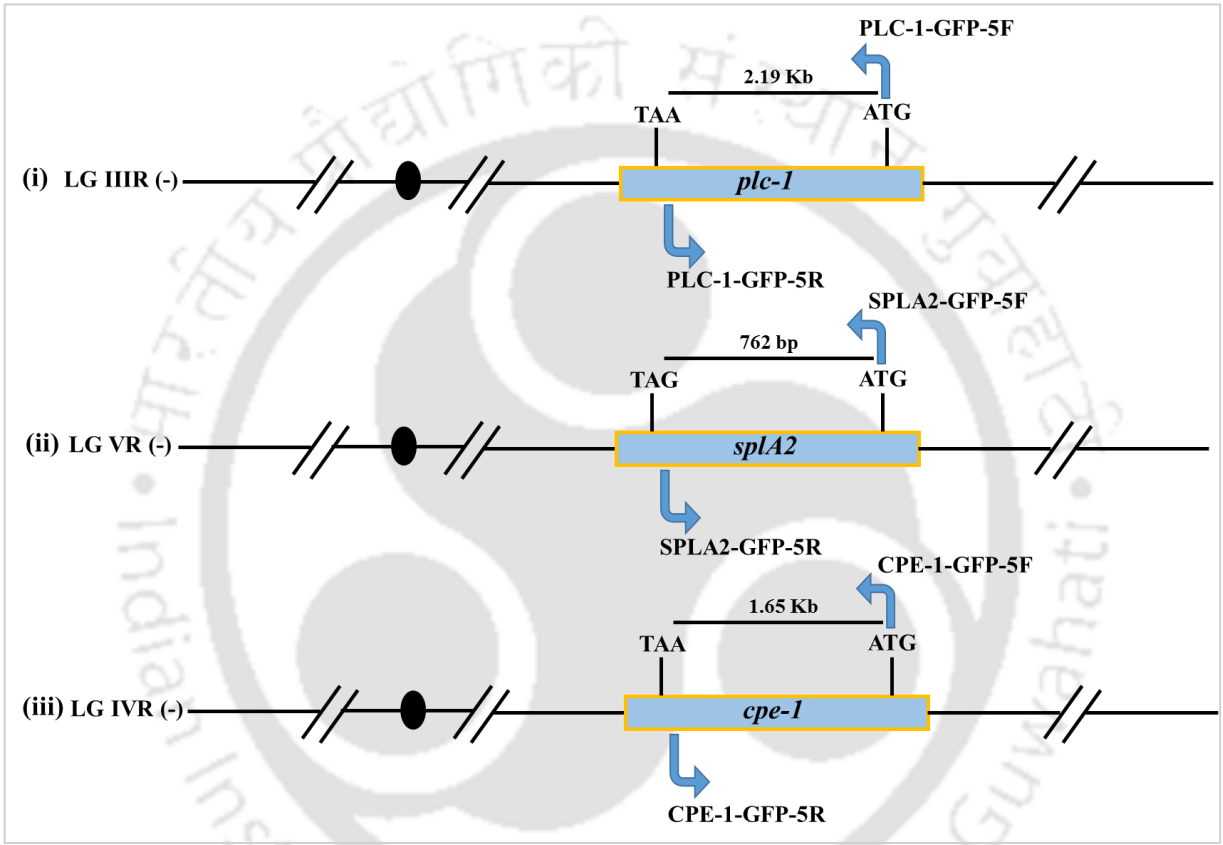

(B)

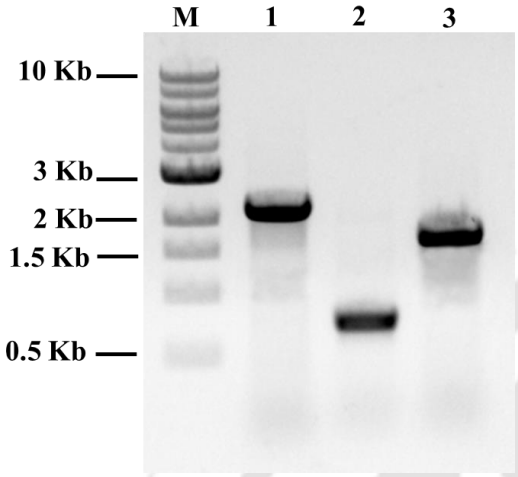

(C)

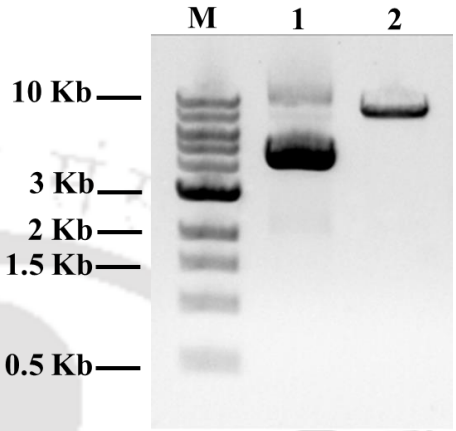

(D)

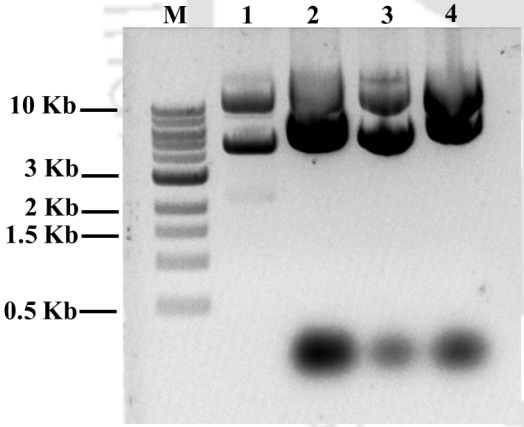

(E)

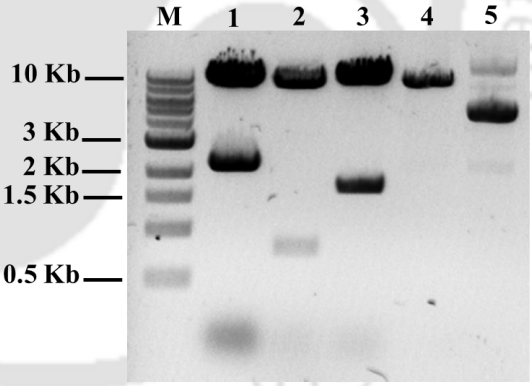

(F)

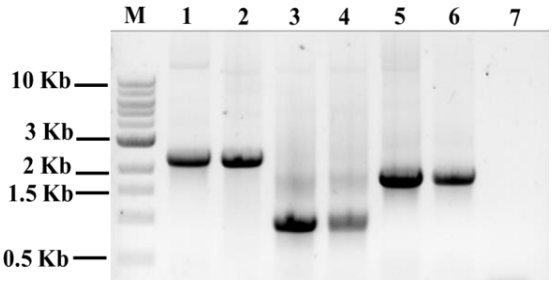

(G)

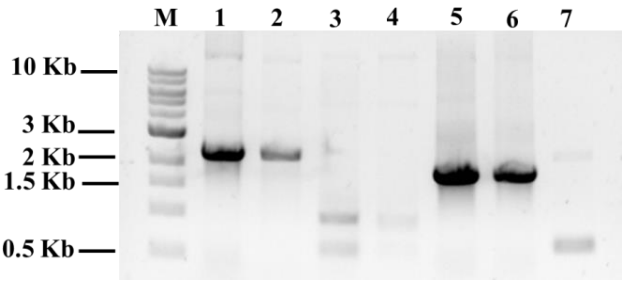

Figure 3.18: Cloning of *plc-1*, *splA2*, and *cpe-1* fragments from the wild type for complementation analysis. (**A**) Schematics showing the primers to PCR amplify the *plc-1*, *splA2*, and *cpe-1* fragments. The primer pairs PLC-1-GFP-5F and PLC-1-GFP-5R, SPLA2-GFP-5F and SPLA2-GFP-5R, CPE-1-GFP-5F and CPE-1-GFP-5R (Table 3.3), used to amplify the *plc-1*, *splA2*, and *cpe-1* fragments respectively (~2.19, 0.762, and 1.65 kb in sizes) from the wild-type, are indicated. The relative positions of the start (ATG) and the stop (TAA) codons are shown. The sizes of the PCR amplified product is shown below. (**B**) Visualization of the PCR amplicons of the *plc-1*, *splA2*, and *cpe-1*. The *plc-1*, *splA2*, and *cpe-1* fragments of size ~2.19 (lane 1), 0.762 (lane 2), and 1.65 (lane 3) kb, respectively, were resolved in a 0.8 % agarose gel; M, 1 kb DNA ladder (NEB). (**C**) Visualization of the vector. The pMF272 undigested (lane 1) and *Sma*I digested (lane 2) plasmid DNA of 8.4 kb was visualized using a 0.8 % agarose gel; M, 1 kb DNA ladder (NEB). (**D**) Plasmid constructs. The plasmid constructs isolated from *E. coli* DH5α transformants, M, 1 kb DNA ladder (NEB); lane 1, pMF272 vector (uncut); lane 2, pMF272 vector containing the *plc-1* insert and designated as pAB-1 (~10.59 kb); lane 3, pMF272 vector containing the *splA2* insert (~9.162 kb) and designated as pAB-2; lane 4, pMF272 vector containing the *cpe-1* insert (~10.05 kb) and designated as pAB-3. (**E**) Restriction digestion analysis of pAB-1, pAB-2, and pAB-3 plasmid constructs. The pAB-1, pAB-2, and pAB-3 plasmid constructs were digested with *Xba*I and *Pac*I restriction enzymes and resolved in 0.8 % agarose gel. Digestion with *Xba*I and *Pac*I restriction enzymes resulted in release of inserts of sizes ~2.19, 0.762, and 1.65 kb from pAB-1, pAB-2, and pAB-3 constructs, respectively. M, 1 kb DNA ladder (NEB); lane 1, digested pAB-1 (release of 2.19 kb fragment); lane 2, digested pAB-2 (release of 0.762 kb fragment); lane 3, digested pAB-1 (release of 1.65 kb fragment); lane 4, digested pMF272 vector (negative control); lane 5, undigested pMF272 vector (negative control). (**F**) PCR amplification of pAB-1, pAB-2, and pAB-3 plasmid constructs using Pccg-1-Fw primer and the gene specific reverse primer (Table 3.3; Entry 5-11). PCR products were resolved in 0.8 % agarose gel. M, 1 kb DNA ladder (NEB); lane 1, PCR amplified product for verifying *plc-1* insert in the pAB-1 construct using Pccg-1-Fw and PLC-1-GFP-R (~2.28 kb); lane 2, another PCR amplified product for verifying *plc-1* insert in the pAB-1 construct using Pccg-1-Fw and PLC-1-GFP-R (~2.28 kb); lane 3, PCR amplified product for verifying *splA2* insert in the pAB-2 construct using Pccg-1-Fw and SPLA2-GFP-R (0.852 kb); lane 4, another PCR amplified product for verifying *splA2* insert in the pAB-2 construct using Pccg-1-Fw and SPLA2-GFP-R (0.852 kb); lane 5, PCR amplified product for verifying *cpe-*

1 insert in the pAB-3 construct using Pccg-1-Fw and CPE-1-GFP-R (1.74 kb); lane 6, PCR amplified product for verifying *cpe-1* insert in the pAB-3 construct using Pccg-1-Fw and CPE-1-GFP-R (1.74 kb); lane 7, PCR amplification was not observed for the pMF272 plasmid control using the Pccg-1-Fw and gene specific primer pairs. (**G**) PCR amplification of pAB-1, pAB-2, and pAB-3 plasmid constructs using gene specific forward primer and GFP-Rv primer (Table 3.3; Entry 5-10 and 12). PCR products were resolved in 0.8 % agarose gel. M, 1 kb DNA ladder (NEB); lane 1, PCR amplified product for verifying *plc-1* insert in the pAB-1 construct using PLC-1-GFP-F and GFP-Rv (~2.273 kb); lane 2, another PCR amplified product for verifying *plc-1* insert in the pAB-1 construct using PLC-1-GFP-F and GFP-Rv (~2.273 kb); lane 3, PCR amplified product for verifying *splA2* insert in the pAB-2 construct using SPLA2-GFP-F and GFP-Rv (~0.845 kb); lane 4, another PCR amplified product for verifying *splA2* insert in the pAB-2 construct using SPLA2-GFP-F and GFP-Rv (~0.845 kb); lane 5, PCR amplified product for verifying *cpe-1* insert in the pAB-3 construct using CPE-1-GFP-F and GFP-Rv (~1.733 kb); lane 6, another PCR amplified product for verifying *cpe-1* insert in the pAB-3 construct using CPE-1-GFP-F and GFP-Rv (~1.733 kb).

3.2.10 Transformation of the pAB-1, pAB-2, and pAB-3 constructs into the *Δplc-1::hph::his-3 mat A*, *ΔsplA2::hph::his-3 mat A*, and *Δcpe-1::hph::his-3 mat A* strains, respectively

The *Δplc-1::hph*::*his-3 mat A* (4), *ΔsplA2::hph*::*his-3 mat A* (D), and *Δcpe-1::hph*::*his-3 mat A* (d) recipient strains were generated by crossing the *Δplc-1::hph mat a* with *plc-1::his-3 mat A*, *ΔsplA2::hph mat a* with *splA2*::*his-3 mat A*, and *Δcpe-1::hph mat a* with *cpe-1*::*his-3 mat A* (Figure 3.19 A). The f_1 progenies from these crosses were screened on minimal media containing 220 µg/ml of hygromycin B, and genotype of the recipient strains was PCR verified (Figure 3.19 B). The *his-3* targeted gene replacement allows for the generation of functional and non-functional version of *his-3* with the targeted sequences lying between *his-3*$^{+}$*::gene::his-3* (Aramayo and Metzenberg 1996). The pAB-1, pAB-2, and pAB-3 constructs containing the *plc-1*, *splA2*, and *cpe-1* fragments were transformed into the *Δplc-1::hph*::*his-3 mat A*, *ΔsplA2::hph*::*his-3 mat A* and *Δcpe-1::hph*::*his-3 mat A* recipient strains, respectively, by electroporation (described in Chapter 2). The heterokaryotic transformants were selected on sorbose containing minimal media and were further crossed with the *Δplc-1*, *ΔsplA2*, and *Δcpe-1* mutants of opposite mating type to

obtain the homokaryotic progenies. I verified the presence of the *plc-1*, *splA2*, and *cpe-1* transgenes in the homokaryotic progenies using PCR (Figure 3.19 C-D).

(A)

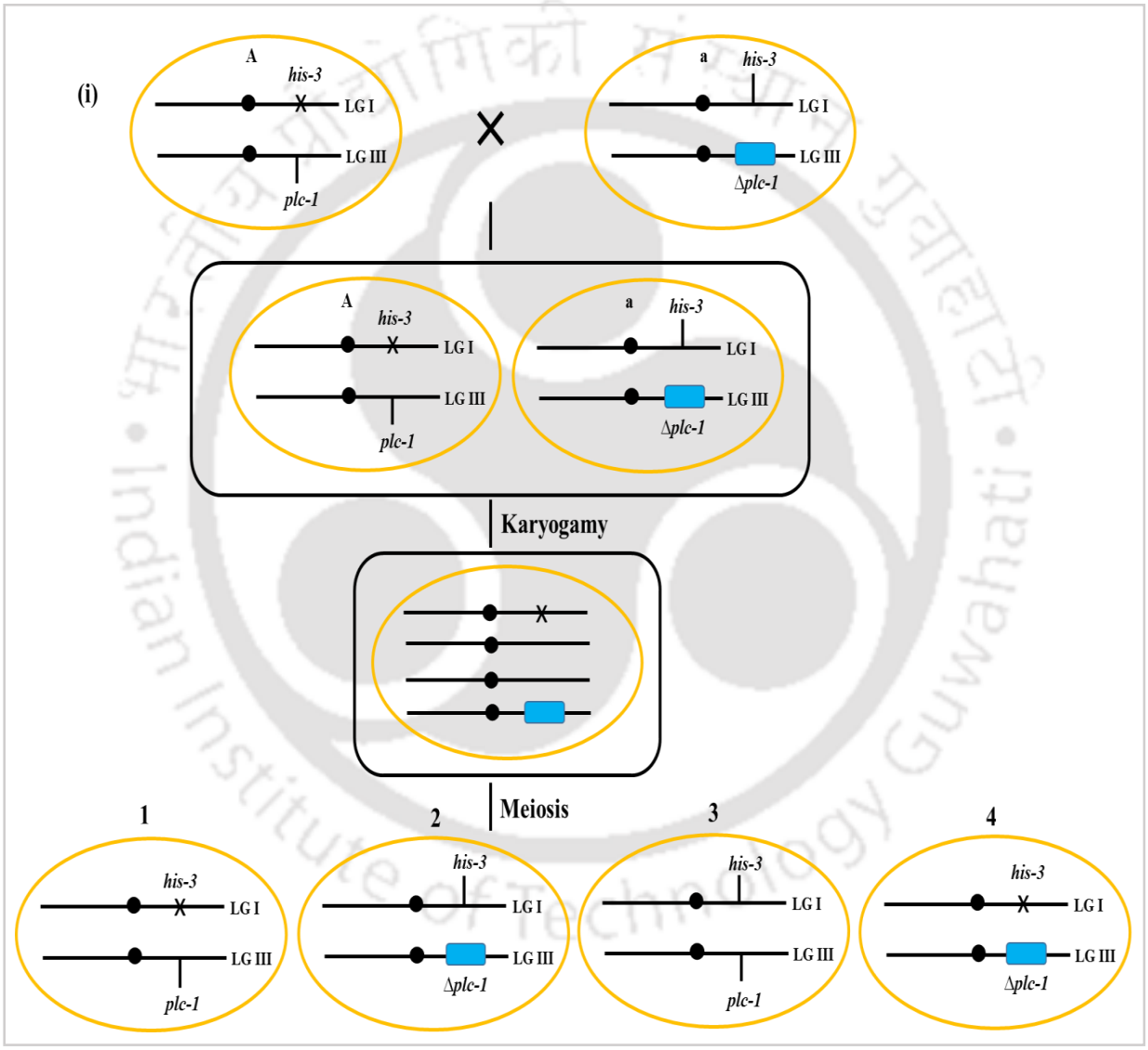

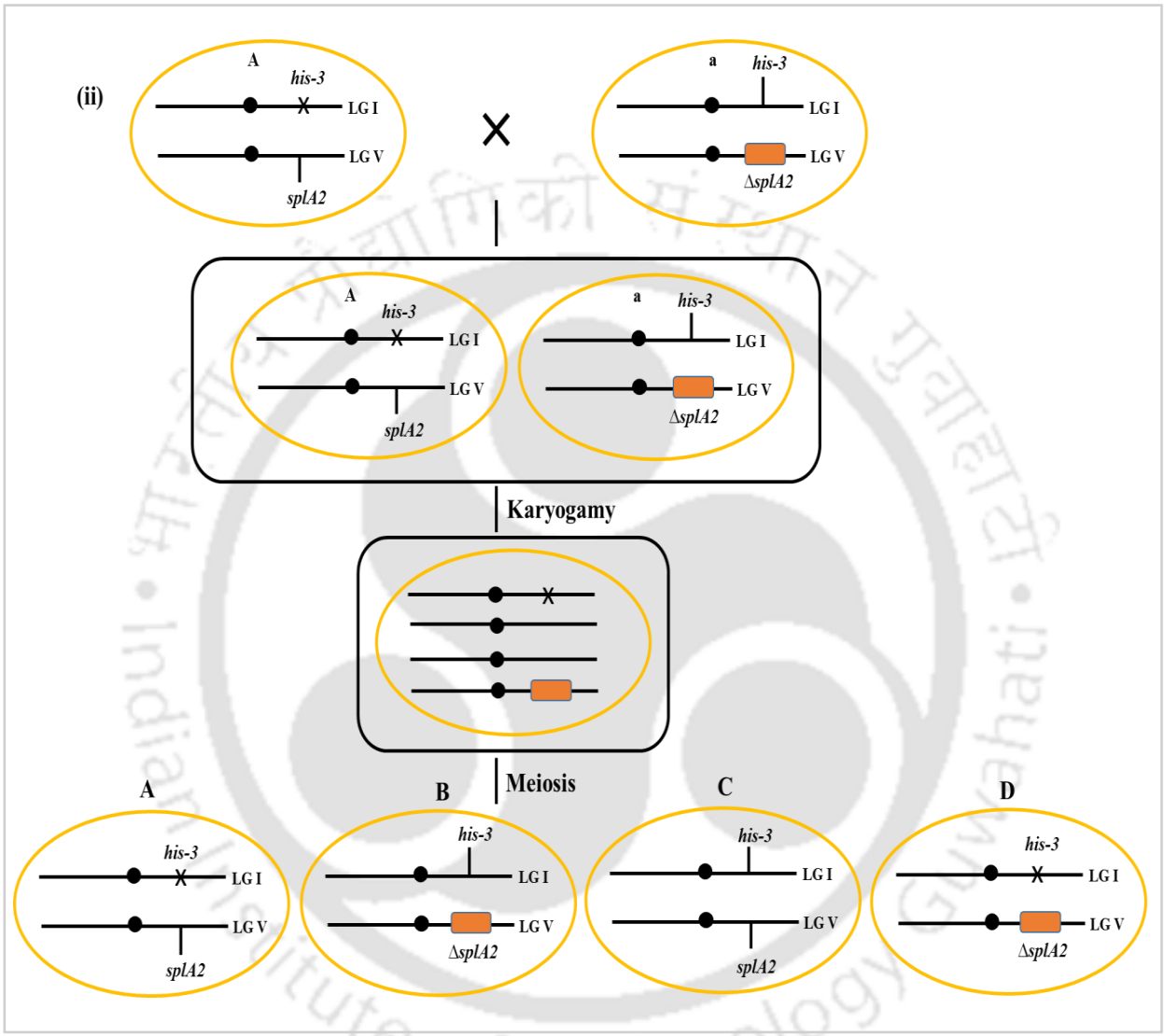

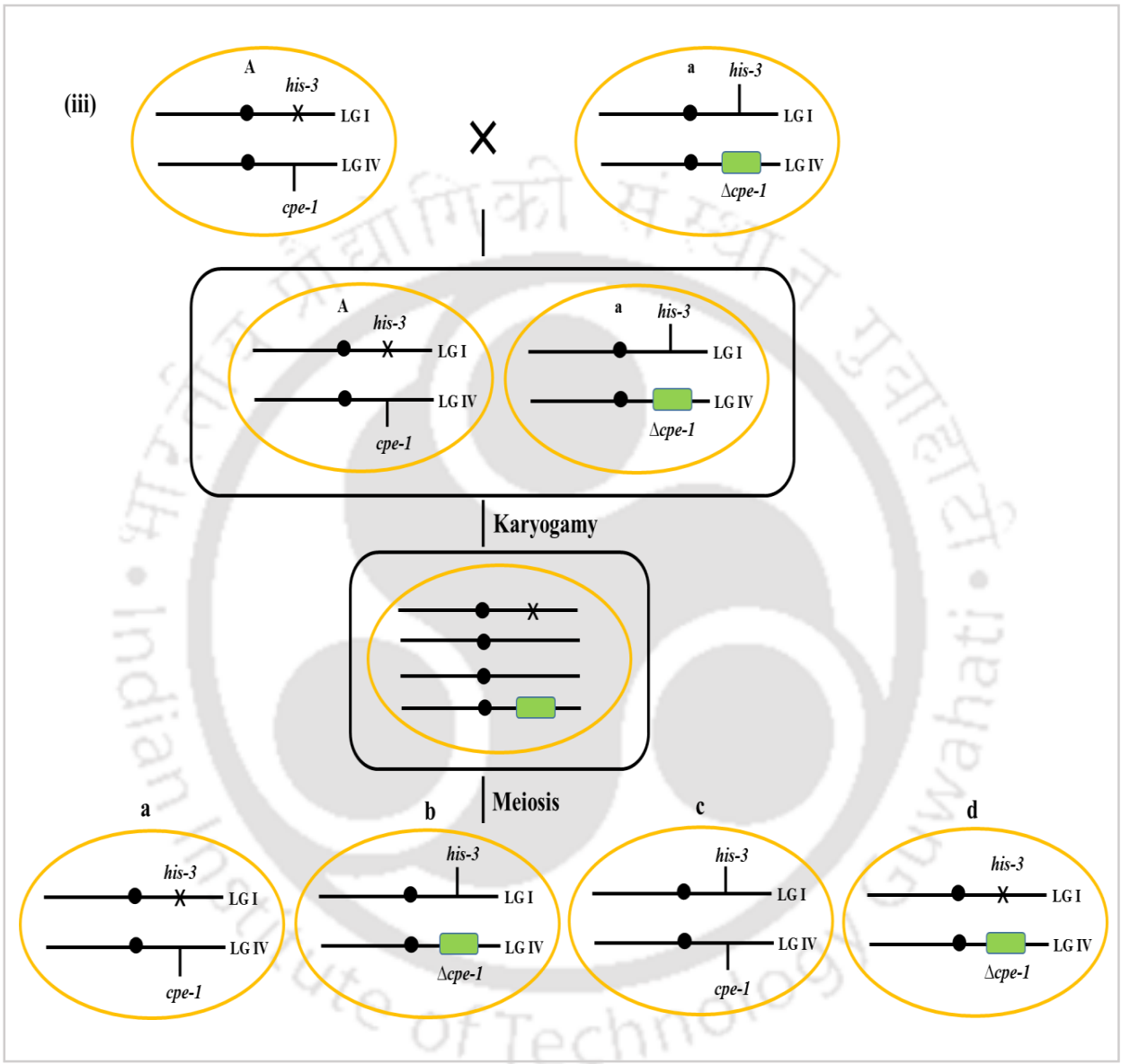

(B)

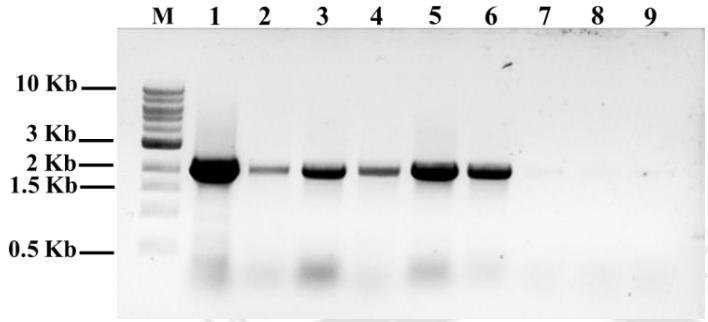

(C)

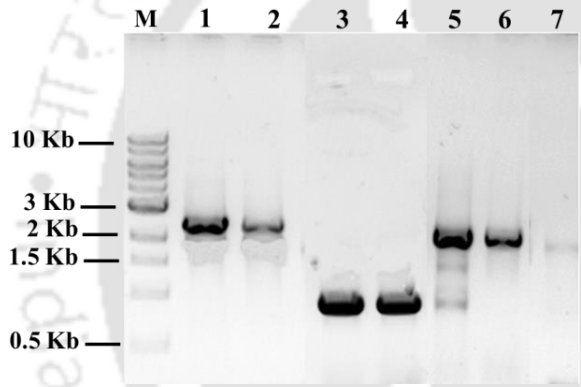

(D)

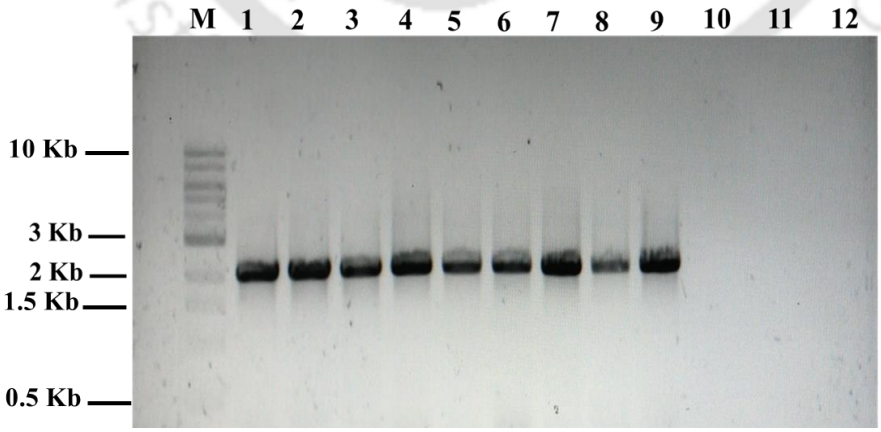

Figure 3.19: Transformation of the pAB-1, pAB-2, and pAB-3 constructs into the hyg^R *his-3 mat A* recipient strains. (**A**) A schematic representation of crosses for generation of hyg^R *his-3 mat A* recipient strains. The *Δplc-1::hph::his-3 mat A* (4), *ΔsplA2::hph::his-3 mat A* (D), and *Δcpe-*

1::hph::his-3 mat A (d) strains were generated by crossing the single mutants with *his-3 mat A* strain (i-iii). **(B)** PCR verification of the recipient strains of *N. crassa* for complementation analysis. The *Δplc-1::hph::his-3 mat A*, *ΔsplA2::hph::his-3 mat A*, and *Δcpe-1::hph::his-3 mat A* strains were confirmed using the gene specific forward primers specific for upstream of the open reading frame of the genes *plc-1*, s*plA2*, and *cpe-1*, respectively, along with the common reverse primer 5HPHR (Figure 3.8 A; Table 3.3; Entry 1-4). PCR products were resolved in a 0.8% agarose gel. M, 1 kb DNA ladder (NEB); lane 1, PCR amplification verifying the presence of the knockout allele (~2 kb in size) in the *Δplc-1* mutant (control); lane 2, PCR amplification to verify the *Δplc-1* mutant allele (~2 kb in size) in *Δplc-1::hph::his-3 mat A*; lane 3, PCR amplification verifying the presence of the knockout allele (~2.044 kb in size) in the *ΔsplA2* mutant (control), lane 4, PCR amplification to verify the *ΔsplA2* mutant allele (~2.044 kb in size) in *ΔsplA2::hph::his-3 mat A*; lane 5, PCR amplification verifying the presence of the knockout allele (~1.98 kb in size) in the *Δcpe-1* mutant (control); lane 6, PCR amplification to verify the *Δcpe-1* mutant allele (~1.98 kb in size) in *Δcpe-1::hph::his-3 mat A*; lanes 7, 8, 9, wild type control (no PCR product as target sequence for 5HPHR primer is absent in the wild type). **(C)** PCR verification of the homokaryotic transformants. The *Δplc-1::hph::*$P_{ccg\text{-}1}$*::plc-1::gfp*; *ΔsplA2::hph::*$P_{ccg\text{-}1}$*::splA2::gfp*, and *Δcpe-1::hph::*$P_{ccg\text{-}1}$*::cpe-1::gfp* homokaryotic transformants were confirmed using the Pccg-1-Fw primer and GFP-Rv primer (Table 3.3; Entry 11-12). PCR products were resolved in a 0.8% agarose gel. M, 1 kb DNA ladder (NEB); lane 1, PCR amplified product for verifying *plc-1* allele in *Δplc-1::hph::*$P_{ccg\text{-}1}$*::plc-1::gfp* HoP-1 (~2.364 kb in size); lane 2, PCR amplified product for verifying *plc-1* allele in *Δplc-1::hph::*$P_{ccg\text{-}1}$*::plc-1::gfp* HoP-13 (~2.364 kb in size); lane 3, PCR amplified product for verifying *splA2* allele in *ΔsplA2::hph::*$P_{ccg\text{-}1}$*::splA2::gfp* HoP-72 (~945 bp in size); lane 4, PCR amplified product for verifying *splA2* allele in *ΔsplA2::hph::*$P_{ccg\text{-}1}$*::splA2::gfp* HoP-74 (~945 bp in size); lane 5, PCR amplified product for verifying *cpe-1* allele in *Δcpe-1::hph::*$P_{ccg\text{-}1}$*::cpe-1::gfp* HoP-2 (~1.8 kb in size); lane 6, PCR amplified product for verifying *cpe-1* allele in *Δcpe-1::hph::*$P_{ccg\text{-}1}$*::cpe-1::gfp* HoP-11 (~1.8 kb in size); lane 7, wild type control (no PCR product) **(D)** PCR verification of the Δ*plc-1*, Δs*plA2*, and Δ*cpe-1* mutant alleles in the homokaryotic transformants. Presence of the *hph* allele in the *Δplc-1::hph::*$P_{ccg\text{-}1}$*::plc-1::gfp*; *ΔsplA2::hph::*$P_{ccg\text{-}1}$*::splA2::gfp*, and *Δcpe-1::hph::*$P_{ccg\text{-}1}$*::cpe-1::gfp* homokaryotic transformants were confirmed using the gene specific forward primers specific for upstream of the open reading frame of the genes *plc-1*, s*plA2*, and *cpe-1*, respectively, along with the common

reverse primer 5HPHR (Figure 3.8 A; Table 3.3; Entry 1-4). PCR products were resolved in a 0.8% agarose gel. M, 1 kb DNA ladder (NEB); lane 1, PCR amplification verifying the presence of the knockout allele (~2 kb in size) in the *Δplc-1* mutant (control); lane 2, PCR amplification verifying the *Δplc-1* mutant allele (~2 kb in size) in *Δplc-1::hph::P$_{ccg-1}$::plc-1::gfp* HoP-1; lane 3, PCR amplification verifying the *Δplc-1* mutant allele (~2 kb in size) in *Δplc-1::hph::P$_{ccg-1}$::plc-1::gfp* HoP-13; lane 4, PCR amplification verifying the *ΔsplA2* mutant allele (~2.044 kb in size) in *ΔsplA2* mutant (control); lane 5, PCR amplification verifying the *ΔsplA2* mutant allele (~2.044 kb in size) in *ΔsplA2::hph::P$_{ccg-1}$::splA2::gfp* HoP-72; lane 6, PCR amplification verifying the *ΔsplA2* mutant allele (~2.044 kb in size) in *ΔsplA2::hph::P$_{ccg-1}$::splA2::gfp* HoP-74; lane 7, PCR amplification verifying the presence of the knockout allele (~1.98 kb in size) in the *Δcpe-1* mutant (control); lane 8, PCR amplification verifying the *Δcpe-1* mutant allele (~1.98 kb in size) in *Δcpe-1::hph::P$_{ccg-1}$::cpe-1::gfp* HoP-2; lane 9, PCR amplification verifying the *Δcpe-1* mutant allele (~1.98 kb in size) in *Δcpe-1::hph::P$_{ccg-1}$::cpe-1::gfp* HoP-11; lanes 10, 11, 12, wild type control (no PCR product as target sequence for 5HPHR primer is absent in the wild type).

3.2.11 Complementation of the Δ*plc-1*, Δ*splA2*, and Δ*cpe-1* mutants

I tested four homokaryotic transformants each containing the *plc-1*, s*plA2*, and *cpe-1* transgenes, for their ability to complement the oxidative stress, thermotolerance, and carotenoid accumulation phenotypes of the corresponding knockout mutants. I found that the homokaryotic transformants complements viability in exposure to oxidative stress (Figure 3.20; Table 3.8), thermotolerance (Fig. 3.21; Table 3.9), and carotenoid accumulation at all three temperatures of 8, 22, and 30°C (Figure 3.22 A-C; Table 3.10), of the Δ*plc-1,* Δ*plc-1*, and Δ*cpe-1* mutants. Therefore, I concluded that *plc-1*, *splA2*, and *cpe-1* genes play a role in carotenoid accumulation at all the three different temperatures tested, survival in oxidative stress, and thermotolerance.

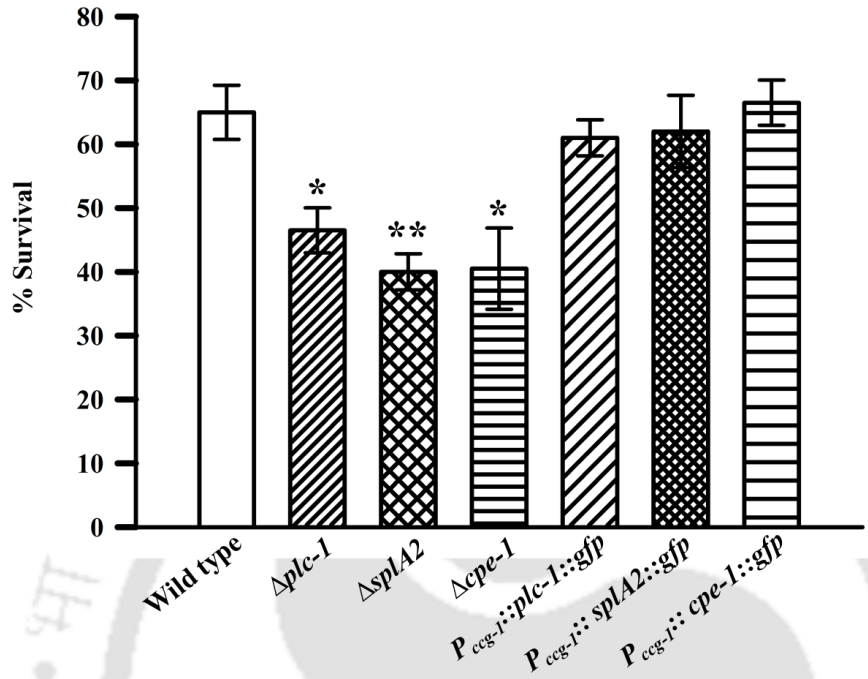

Figure 3.20: Complementation of oxidative stress sensitivity phenotype of Δ*plc-1*, Δ*splA2*, and Δ*cpe-1* mutants. Germlings of wild type, Δ*plc-1*, Δ*splA2*, Δ*cpe-1* mutants, and the homokaryotic transformants were incubated at 10 mM H_2O_2 at 30°C and percent survival determined. Error bars indicate the standard deviations calculated from the data for three independent experiments (n=3) with *P-values* < 0.05 (*), <0.01 (**), and < 0.001 (***) compared with the wild type strain as measured by one-way ANOVA test.

Table 3.8: Percent survival of the wild type, Δ*plc-1*, Δ*splA2*, Δ*cpe-1* mutants, and the homokaryotic transformants at 10 mM H_2O_2

Strains	Percent survival at 10 mM H_2O_2†
Wild type	65 ± 4.24
Δ*plc-1*	47 ± 3.53 (*)
Δ*splA2*	40 ± 2.83 (**)
Δ*cpe-1*	41 ± 6.36 (*)
P_{ccg-1}::*plc-1*::*gfp*	61 ± 2.82
P_{ccg-1}::*splA2*::*gfp*	62 ± 5.66
P_{ccg-1}::*cpe-1*::*gfp*	67 ± 3.54

†Results are shown as mean ± standard deviation for three independent experiments (n=3) with *P values* < 0.05 (*), < 0.01 (**), and < 0.001 (***) compared with the wild type strain as measured by one-way ANOVA test.

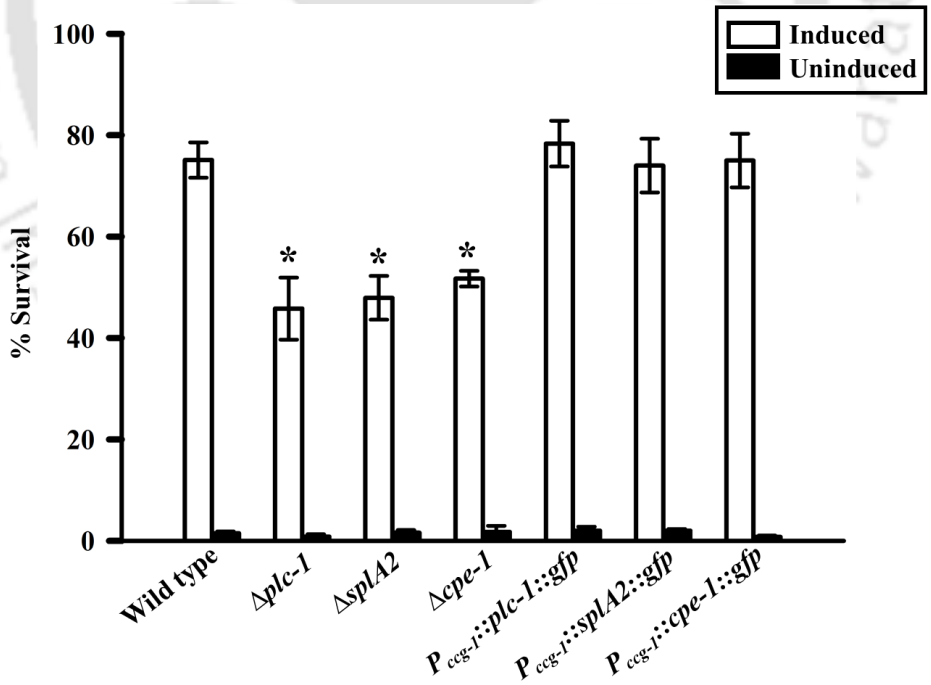

Figure 3.21: Complementation of heat shock sensitivity phenotype of Δ*plc-1*, Δ*splA2*, and Δ*cpe-1* mutants. Germlings of wild type, Δ*plc-1*, Δ*splA2*, Δ*cpe-1* mutants, and the homokaryotic transformants were exposed to 52°C lethal temperature with (induced) or without (uninduced) pre-

exposure to a sublethal heat shock temperature at 44°C and percent survival determined. Error bars indicate the standard deviations calculated from the data for three independent experiments (n=3) with *P-values* < 0.05 (*), <0.01 (**), and < 0.001 (***) compared with the wild type strain as measured by one-way ANOVA test.

Table 3.9: Percent survival of the wild type, Δ*plc-1*, Δ*splA2*, Δ*cpe-1* mutants, and the homokaryotic transformants upon heat shock

Strains	Percent survival upon exposure to heat shock (52°C)†	
	Induced (44°C)	**Uninduced (30°C)**
Wild type	75.10 ± 3.48	1.51 ± 0.32
Δ*plc-1*	46 ± 6.12 (*)	0.81 ± 0.48
Δ*splA2*	48 ± 4.32 (*)	1.59 ± 0.53
Δ*cpe-1*	52 ± 1.55 (*)	1.75 ± 1.20
$P_{ccg\text{-}1}$::*plc-1*::*gfp*	78.33 ± 4.51	1.99 ± 0.77
$P_{ccg\text{-}1}$::*splA2*::*gfp*	74 ± 5.29	1.99 ± 0.32
$P_{ccg\text{-}1}$::*cpe-1*::*gfp*	75 ± 5.29	0.76 ± 0.28

†Results are shown as mean ± standard deviation for three independent experiments (n=3) with *P-values* < 0.05 (*), < 0.01 (**), and < 0.001 (***) compared with the wild type strain as measured by one-way ANOVA test.

(A)

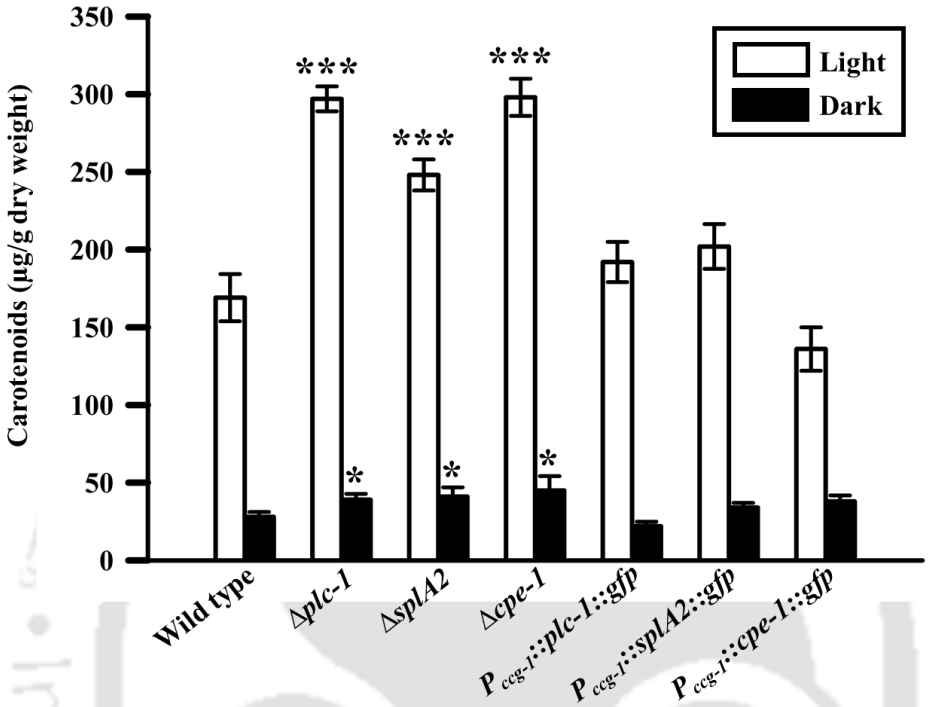

(B)

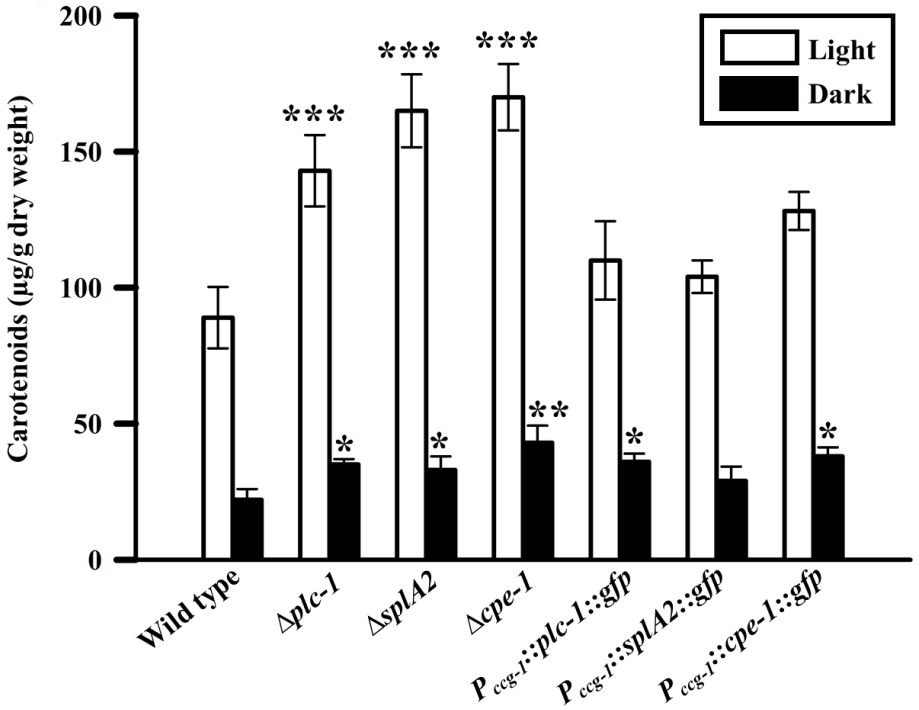

(C)

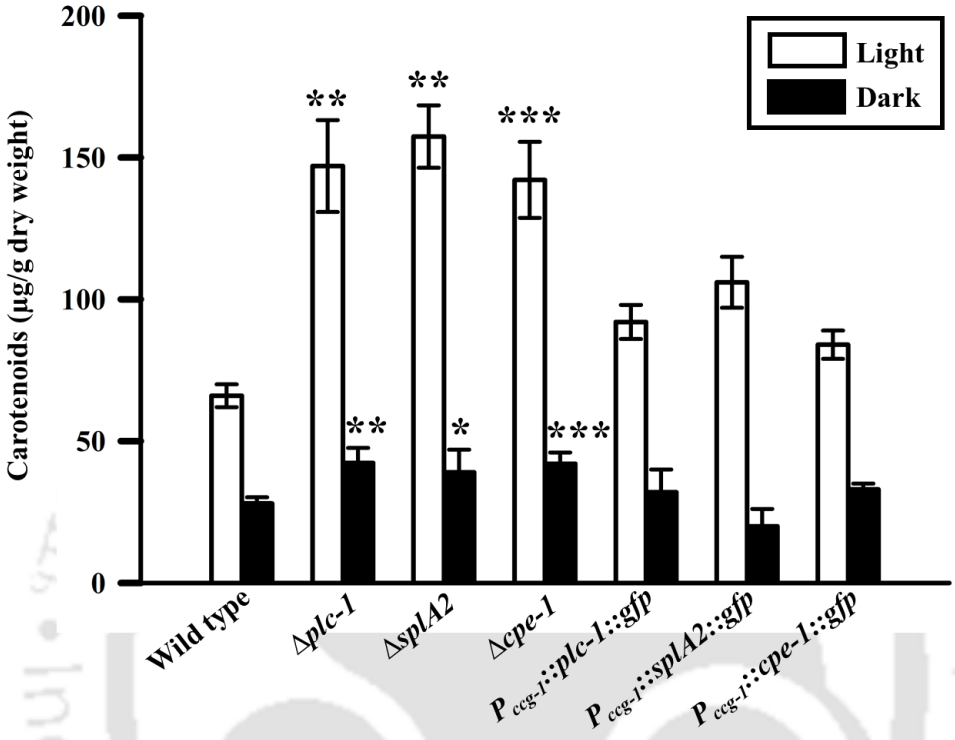

Figure 3.22: Complementation of increased carotenoid accumulation phenotype of Δ*plc-1*, Δ*splA2*, and Δ*cpe-1* mutants. The wild type, Δ*plc-1*, Δ*splA2*, Δ*cpe-1* mutants, and the homokaryotic transformants were grown in Petri dishes containing Vogel's glucose agar medium and incubated at 30°C in the dark for 48 h followed by with or without exposure to white light at 8°C **(A)**, 22°C **(B)**, and 30°C **(C)** for 24 h. Error bars indicate the standard deviations calculated from the data for three independent experiments (n=3) with *P-values* < 0.05 (*), <0.01 (**), and < 0.001 (***) compared with the wild type strain as measured by one-way ANOVA test.

Table 3.10: Carotenoid content of the wild type, Δ*plc-1*, Δ*splA2*, Δ*cpe-1* mutants, and the homokaryotic transformants at three different temperatures

Strains	Carotenoids (µg/g dry weight)†					
	8°C		22°C		30°C	
	Light	Dark	Light	Dark	Light	Dark
Wild type	169 ± 15.2	28 ± 3.1	89 ± 11.3	22 ± 4	66 ± 4	28 ± 2.2
Δplc-1	297 ± 8 (***)	39 ± 3.8 (*)	143 ± 13.1 (***)	35 ± 2 (*)	147 ± 16.2 (**)	42.3 ± 5.3 (**)
ΔsplA2	248 ± 10 (***)	41 ± 6 (*)	165 ± 13.4 (***)	33 ± 5 (*)	157.4 ± 11 (**)	39 ± 8 (*)
Δcpe-1	298 ± 12 (***)	45 ± 9.2 (*)	170 ± 12.2 (***)	43 ± 6.3 (**)	142.1 ± 13.4 (***)	42 ± 4 (***)
$P_{ccg\text{-}1}$::*plc-1::gfp*	192 ± 13	22 ± 2.9	110 ± 14.4	36 ± 3 (*)	92 ± 6	32 ± 8
$P_{ccg\text{-}1}$::*splA2::gfp*	202 ± 4.4	34 ± 3	104 ± 6	29 ± 5.2	106 ± 9	20 ± 6.1
$P_{ccg\text{-}1}$::*cpe-1::gfp*	136 ± 14	38 ± 3.8	98.2 ± 7	38 ± 3.3 (*)	84 ± 5	33 ± 2

†Results are shown as mean ± standard deviation for three independent experiments (n=3) with *P-values* < 0.05 (*), < 0.01 (**), and < 0.001 (***) compared with the wild type strain as measured by one-way ANOVA test.

3.3 Discussion

The universal signaling molecule Ca^{2+} modulates numerous physiological processes in *N. crassa* such as Ca^{2+} stress tolerance (Deka et al. 2011; Laxmi and Tamuli 2015; Gohain et al. 2016), circadian clock (Deka and Tamuli 2013), cytoskeletal organization (Gadd 1994), growth (Deka et al. 2011; Gohain et al. 2016), hyphal branching (Barman and Tamuli 2015), infection structure differentiation (Shaw and Hoch 2000), secretion (Shaw and Hoch 2000), sexual development (Tamuli et al. 2011, 2016; Kumar and Tamuli 2014), sporulation (Barman and Tamuli 2015), and UV survival (Deka et al. 2011; Gohain et al. 2016; Laxmi and Tamuli 2016). The Ca^{2+} signaling machinery of *N. crassa* consists of 48 Ca^{2+} signaling proteins including novel PLC, Ca^{2+} and/or CaM binding $sPLA_2$, and Ca^{2+} exchangers (Galagan et al. 2003; Borkovich et al. 2004). The PLC and $sPLA_2$ proteins belong to the phospholipase superfamily. PLC catalyses the hydrolysis of PIP_2 into second messengers IP_3 and DAG. IP_3 diffuses through the cytosol and binds to IP_3 receptors inducing Ca^{2+} release from intracellular Ca^{2+} stores, and DAG activates protein kinase C (PKC), thereby, triggers a range of cellular activities (Rhee and Bae 1997). Eukaryotic PLCs consists of two catalytic domains X and Y, an N-terminal phospholipid interacting pleckstrin homology (PH) domain, a Ca^{2+} binding EF-hand motif for interaction of PH with membrane phospholipid and a C-terminal Ca^{2+} dependent C2 domain for binding with phospholipid (Bristol et al. 1988; Watson and Arkinstall 1994; Sutton et al. 1995; Yamamoto et al. 1999). The $sPLA_2$ enzymes, which are Ca^{2+} dependent extracellular secretory enzymes with relatively low molecular weight (13-19 kDa), hydrolyze the *sn-2* ester linkage of glycerophospholipids releasing two potential signaling molecules FFAs and 1-acyl-lysophospholipid (1-acyl-LPL) that are capable of controlling a range of biological functions in various organisms (Ghannoum 2000; Cavazzini et al. 2013). A majority of eukaryotic $sPLA_2$ have a highly conserved region containing a His-Asp dyad sequence responsible for catalytic activity and a number of unique disulfide bonded cysteine residues required for its stability (Murakami and Kudo 2004; Schaloske and Dennis 2006). Another group of Ca^{2+} signaling molecules are the Ca^{2+} exchangers that maintain Ca^{2+} homeostasis during steep rises in intracellular Ca^{2+} due to environmental changes, or following signal transduction caused by events such as hyperosmotic shock, hormone response, and response to mating pheromones. Ca^{2+} exchangers act as Ca^{2+} pumps removing excess $[Ca^{2+}]_c$ by transporting Ca^{2+} out of the cell and into the intracellular Ca^{2+} stores with the simultaneous exchange of positive ions across membranes (Zelter et al. 2004; Tamuli et al. 2013). All the Ca^{2+} exchangers possess conserved

Ca^{2+} exchanger domains for transport of Ca^{2+} across intracellular membranes (Galagan et al. 2003; Borkovich et al. 2004; Zelter et al. 2004; Tamuli et al. 2013).

The genome of *N. crassa* possesses four PLC-δ subtype proteins, two distinct $sPLA_2$ proteins, and six novel Ca^{2+}/H^+ exchangers and two putative Ca^{2+}/Na^+ exchangers (Galagan et al. 2003; Borkovich et al. 2004; Zelter et al. 2004). The NCU06245 gene designated *plc-1* (Figure 3.6 A) encodes a homologue of PLC-δ that is highly divergent among the natural isolates of *N. crassa*. The NCU06245 gene exhibits high incidence of polymorphisms resulting in a coding sequence changes for amino acid positions 200-250 unique to *N. crassa* (Gavric et al. 2007). In *N. crassa*, the NCU06650 and NCU09423 genes encode for two distinct $sPLA_2$ proteins possessing Ca^{2+}-dependent lipolytic activity with preferential cleavage of *sn-2* ester linkage of substrates to produce 1-acyl lysophospholipids (Takayanagi et al. 2015). The NCU06650 was designated *splA2* (Figure 3.6 B), and contains a putative CaM binding site from the amino acid residues 135 to 158 of sequence TCHALANVYYAAVREFGRTKGELQ, which was absent in the NCU09423, with normalized scores 1 to 9 (http://calcium.uhnres.utoronto.ca/ctdb/ctdb/sequence.html; Yap et al. 2000) and also classified as a Ca^{2+} and/or calmodulin (CaM) protein (Borkovich et al. 2004). The NCU06366 gene designated *cpe-1* (Figure 3.6 C) encodes a putative Ca^{2+}/H^+ exchanger involved in maintaining intracellular levels of Ca^{2+} and is found to be significantly different from homologues found in *S. cerevisiae* and *M. grisea* in a phylogenetic analysis (Zelter et al. 2004).

In this chapter, I investigated the functions of *plc-1*, *splA2*, and *cpe-1* genes in *N. crassa*. Strains lacking *plc-1*, *splA2*, and *cpe-1* displayed growth defects in response to increase in $[Ca^{2+}]_c$ induced by the Ca^{2+} ionophore A23187 (Figure 3.2 B). The Δ*plc-1*, Δ*splA2*, and Δ*cpe-1* mutants showed sensitivity to H_2O_2 induced oxidative stress (Figure 3.10; Table 3.4). The deletion of *plc-1*, *splA2*, and *cpe-1* was also associated with an increased amount of ROS on exposure to exogenous H_2O_2 (Figure 3.11 B). Moreover, the Δ*plc-1*, Δ*splA2*, and Δ*cpe-1* mutants displayed a reduction in induced thermotolerance (Figure 3.12; Table 3.5), and an increase in sensitivity to PHS (Figure 3.13; Table 3.6). The Δ*plc-1*, Δ*splA2*, and Δ*cpe-1* mutants also exhibited an altered carotenoid profile (Figure 3.14; Table 3.7) and the increase in the amounts of carotenoid was linked to UV-survival of the strains (Figure 3.16 A-F). In addition, fragments carrying the *plc-1*, *splA2*, and *cpe-1* transgenes complemented the sensitivity to oxidative stress (Figure 3.20; Table 3.8), reduced thermotolerance (Figure 3.21; Table 3.9), and increased carotenoid accumulation (Figure 3.22 A-C; Table 3.10) phenotypes of the Δ*plc-1*, Δ*splA2*, and Δ*cpe-1* mutants. Therefore, the *plc-*

1, *splA2*, and *cpe-1* genes regulates multiple cellular pathways possibly via maintaining Ca^{2+} homeostasis in *N. crassa*.

I published results described in this Chapter in Journal of Microbiology (Barman and Tamuli 2015), and also presented as posters in (i) "International Consultative Meeting on Seribiotechnology, 2012" held at Institute of Bioresources and Sustainable Development, Imphal, Manipur, (ii) "8th International Conference on Yeast Biology, 2013" held at Industrial Microbial Technology, Chandigarh, India, (iii) "International conference on Disease Biology and Therapeutics, 2014" held at Institute of Advanced Study in Science and Technology, Guwahati, Assam, and (iv) "Molecular Intricacies of Plant Pathogenic Micro-organisms, an Alternative Meet, 2015" held at Department of Molecular Biology and Biotechnology, Tezpur University, Tezpur, Assam.

In the next Chapter, I describe the phenotypic analysis of the *plc-1*, *splA2*, and *cpe-1* double mutants to determine the cellular processes controlled by the genetic interactions between their loci.

Chapter 4

Genetic interaction studies of phospholipase C-1, secretory phospholipase A2, and calcium proton exchanger-1 in Neurospora crassa

4.1 Introduction

Genetic interactions of Ca^{2+} signaling genes regulate numerous cell functions in *N. crassa* (Deka and Tamuli 2013). Genetic interaction can be either negative or positive, if the observed phenotype of a double mutant is stronger or less severe, respectively, than the phenotypes of the single mutant (Baryshnikova et al. 2013). Possible genetic interactions have been shown to occur between loci that controls or affects the same phenotype. Such genetic interactions can be either additive or multiplicative whereby the two loci act independent of each other. Genetic interactions can also occur between two loci that are dependent on each other and such genetic interactions can be either epistatic, where mutation in one locus masks the effects of mutation at the second locus, or it can be intergenic suppression (novelty), where mutation in one locus reverses the effects of mutation at the other locus such that a wild type phenotype is observed, or it can also be synergistic whereby the phenotype is affected due to interactive communications between the two loci (Lakin-thomas and Brody 1985; Morgan and Feldman 2001). Antagonistic interaction, a type of novel interaction, is the one where the phenotype of the double mutant is far severely affected than the single mutants alone and can be either sub-lethal or lethal (Gavric and Griffiths 2003).

The complex Ca^{2+} signaling machinery of *N. crassa* consists of 48 Ca^{2+} signaling proteins that effectively interact in coordination for triggering a range of Ca^{2+} signaling responses and to maintain Ca^{2+} homeostasis (Borkovich et al. 2004; Barman and Tamuli 2015). In the previous chapter, I described the role of *N. crassa* homologues of *plc-1*, s*plA2*, and *cpe-1* genes in regulation of $[Ca^{2+}]_c$, carotenoid accumulation, oxidative stress, and thermotolerance (Barman and Tamuli 2015). However, cell function regulated by the interactions of *plc-1*, s*plA2*, and *cpe-1* remains largely unknown in *N. crassa*. Therefore, to gain deeper insight into the genetic interactions of *plc-1*, s*plA2*, and *cpe-1* in regulating various cell functions, I have generated and studied the double mutants of *plc-1*, *splA2*, and *cpe-1* genes.

4.2 Results

4.2.1 Generation of the Δ*cpe-1*; Δ*splA2*, Δ*plc-1*; Δ*splA2*, and Δ*plc-1*; Δ*cpe-1* double mutants

The Δ*plc-1*, Δs*plA2*, and Δ*cpe-1* single mutants were generated and confirmed by the Neurospora functional genomics project (**https://www.broadinstitute.org/fungal-genome-initiative/neurospora-crassa-genome-project**; **http://geiselmed.dartmouth.edu/dunlaploros/genome/**; Colot et al. 2006). I described the

genetic loci of *plc-1*, *splA2*, and *cpe-1* genes, and their individual knockout mutants in Chapter 3 (Figures 3.3 A-B; 3.4 A-C; Barman and Tamuli 2015). To generate the Δ*cpe-1*; Δ*splA2*, Δ*plc-1*; Δ*splA2*, and Δ*plc-1*; Δ*cpe-1* double mutants, the single mutant strains of opposite mating types were crossed (Figure 4.1 A i-iii), ascospores from these crosses were harvested after 21 days, and germinated on Vogel's sorbose agar medium after heat shock at 60°C for 50 min. Progenies were then transferred to Vogel's glucose agar medium and incubated for two days at 30°C and one day under light. The f_1 progenies were then screened for the resistance to hygromycin B (Hyg^R) phenotype, and presence of the knockout alleles were then confirmed using the gene specific primers HI-NCU06245-F, HI-NCU06650-F, and HI-NCU06366-F for the Δ*plc-1*, Δ*splA2*, and Δ*cpe-1* mutant strains, respectively, along with the common reverse primer 5HPHR specific for the *hph* cassette used to generate the knockout mutants (Figure 3.3 A; Table 3.3; Entry 1-4). PCR amplified products of size 2, 2.044, and 1.981 kb indicated presence of the Δ*plc-1*, Δ*splA2*, and Δ*cpe-1* alleles, respectively, in the corresponding mutant strains (Figure 4.1 B). I obtained four double mutants of each of Δ*cpe-1*; Δ*splA2*, Δ*plc-1*; Δ*splA2*, and Δ*plc-1*; Δ*cpe-1* and studied their phenotypes.

(A)

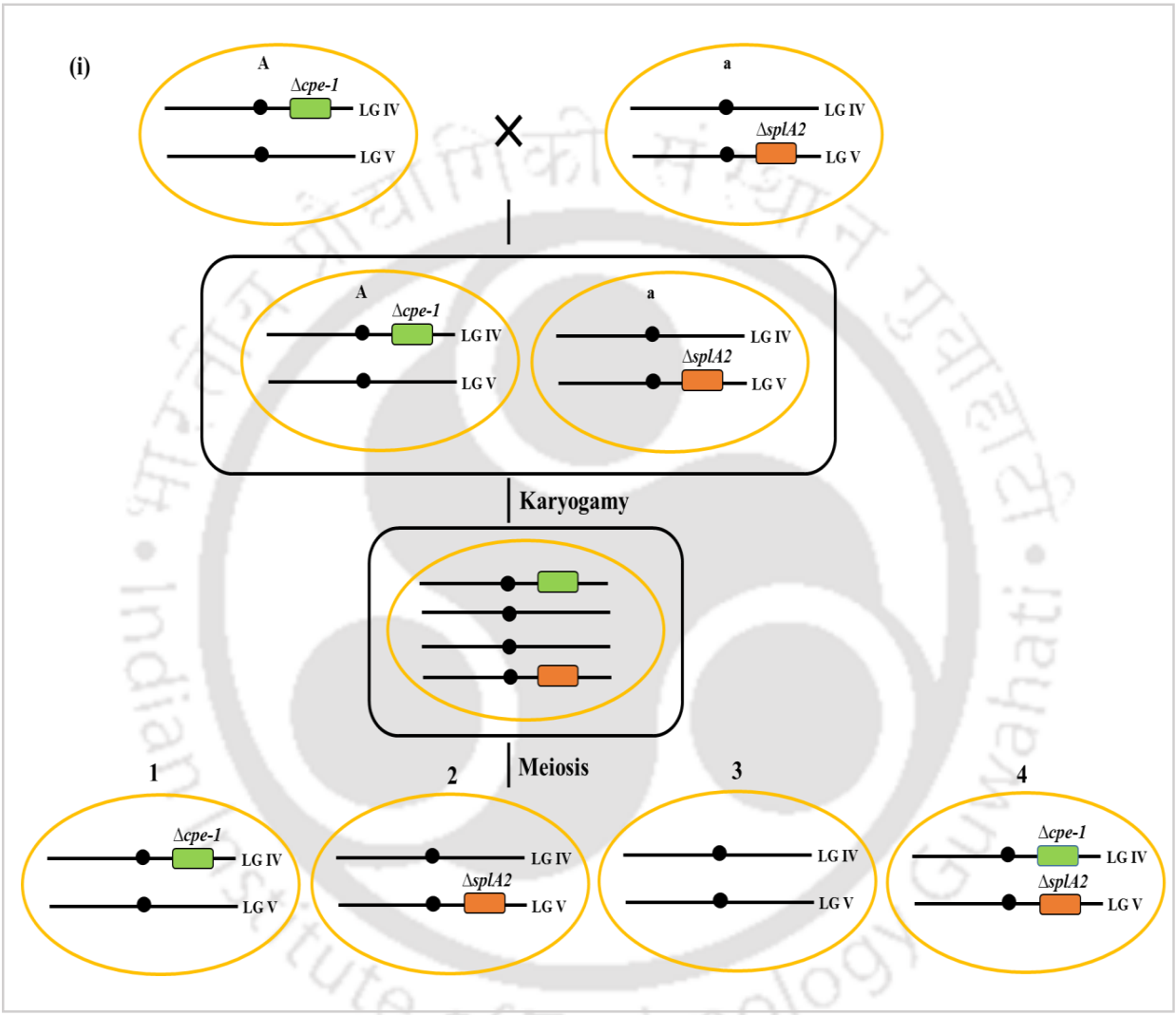

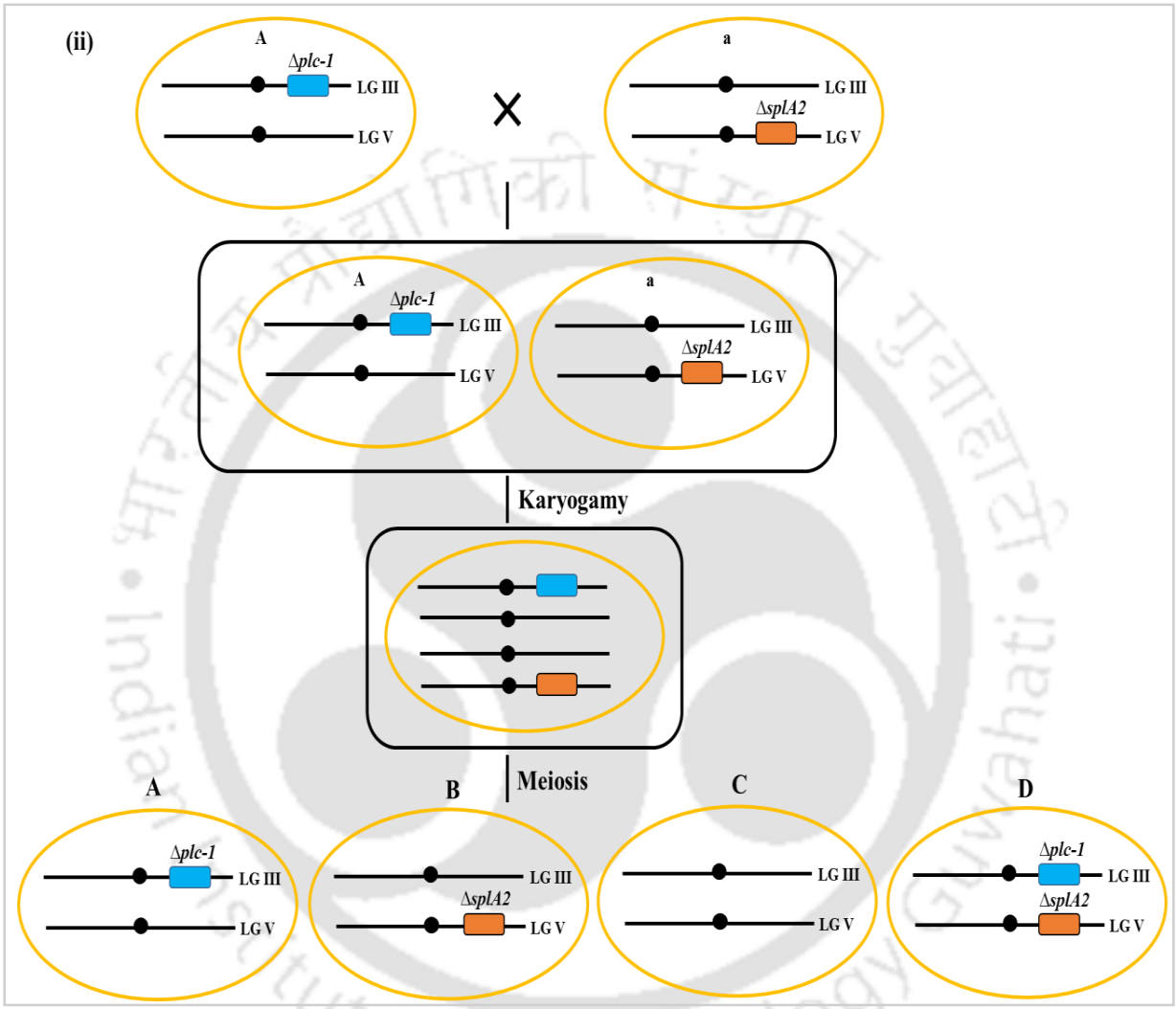

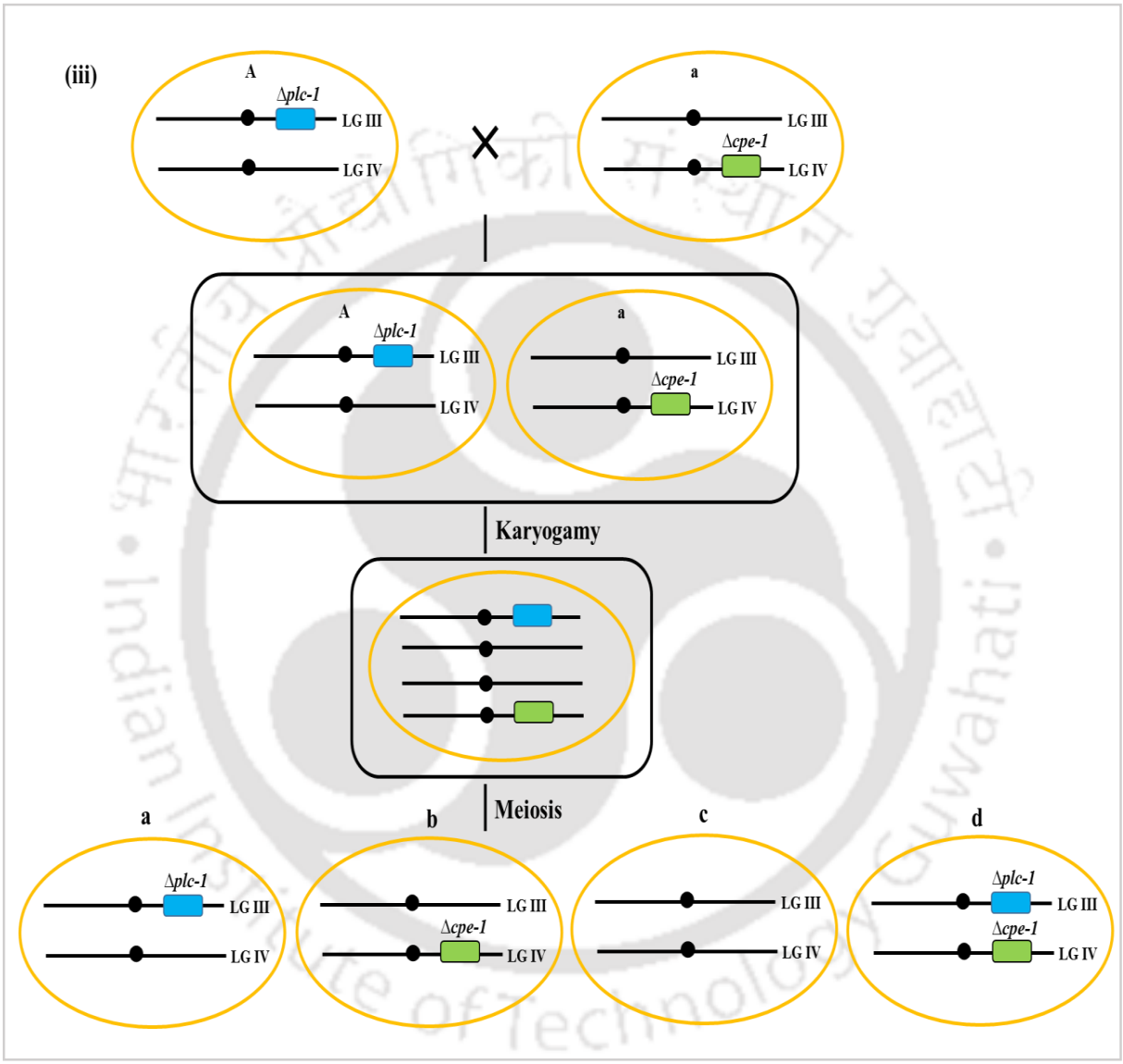

(B)

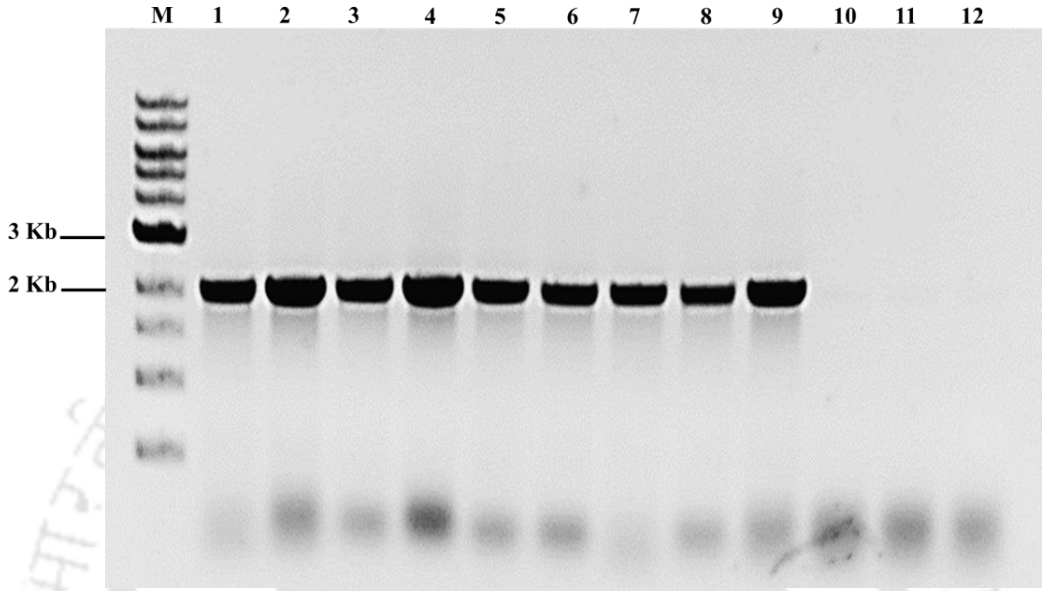

Figure 4.1: Generation and confirmation of Δ*plc-1*, Δ*splA2*, and Δ*cpe-1* double mutants. (A) A schematic representation of crosses of (i) Δ*plc-1*, (ii) Δ*splA2*, and (iii) Δ*cpe-1* single mutants for generating the double mutants. The Δ*cpe-1*; Δ*splA2* (4), Δ*plc-1*; Δ*splA2* (D), and Δ*plc-1*; Δ*cpe-1* (d) double mutants were generated by crossing the single mutant strains of opposite mating type. **(B)** Confirmation of Δ*plc-1*, Δ*splA2*, and Δ*cpe-1* double mutants by PCR analysis. The Δ*cpe-1*; Δ*splA2*, Δ*plc-1*; Δ*splA2*, and Δ*plc-1*; Δ*cpe-1* double mutants were verified by using the forward primers HI-NCU06245-F, HI-NCU06650-F, and HI-NCU06366-F (Table 3.3), specific for upstream of the open reading frame of the genes *plc-1*, *splA2*, and *cpe-1* respectively, along with the common reverse primer that is specific for the *hph* cassette used to generate the knockout mutants (Colot et al. 2006; Deka et al. 2011). Amplification of PCR products of size 2 kb, 2.044 kb, and 1.981 kb, respectively, indicate presence of the Δ*plc-1*, Δ*splA2*, and Δ*cpe-1* alleles in the mutants. PCR products of the Δ*plc-1* (lane 1), Δ*plc-1* allele from the Δ*plc-1*; Δ*splA2* mutant (lane 2), Δ*plc-1* allele from the Δ*plc-1*; Δ*cpe-1* mutant (lane 3), Δ*splA2* (lane 4), Δ*splA2* allele from the Δ*cpe-1*; Δ*splA2* mutant (lane 5), Δ*splA2* allele from the Δ*plc-1*; Δ*splA2* mutant (lane 6), Δ*cpe-1* (lane 7), Δ*cpe-1* allele from the Δ*plc-1*; Δ*cpe-1* mutant (lane 8), Δ*cpe-1* allele from the Δ*cpe-1*; Δ*splA2* mutant (lane 9), and wild type (lanes 10, 11, 12; used as negative control for all three single mutant alleles) were visualized in a 0.8% agarose gel. M: 1 Kb DNA ladder (NEB). The single

mutants were generated by the *N. crassa* genome project (Colot et al. 2006) and previously PCR-verified (Chapter 3; Figure 3.3 B; Barman and Tamuli 2015).

4.2.2 The Δ*plc-1*; Δ*splA2* and Δ*plc-1*; Δ*cpe-1* double mutants showed distinct colony and hyphal morphology

To study morphology of the wild type, Δ*plc-1*, Δ*splA2*, Δ*cpe-1*, Δ*cpe-1*; Δ*splA2*, Δ*plc-1*; Δ*splA2*, and Δ*plc-1*; Δ*cpe-1*, mycelial plugs of the strains were inoculated in Vogel's glucose agar medium and incubated at 30°C for four days in the dark followed by three days under light. The Δ*plc-1*; Δ*splA2* and Δ*plc-1*; Δ*cpe-1* double mutants showed a distinct colonial morphology from that of the parental single mutants and wild type, with reduced mycelial pigmentation (Figure 4.2 A-B). The morphological phenotype exhibited by the two double mutants was found to be different than either of the parental single mutants and wild type.

To study hyphal morphology, strains were incubated at 30°C in Vogel's glucose agar medium for one day and observed by microscopy. The Δ*plc-1*; Δ*splA2* double mutant displayed slightly reduced branching with numerous bud-like structures at the apex of the hyphae, and the Δ*plc-1*; Δ*cpe-1* double mutant displayed severely reduced hyphal branching (Figure 4.2 C). The single and the Δ*cpe-1*; Δ*splA2* double mutants exhibited normal hyphal morphology and branching pattern like the wild type.

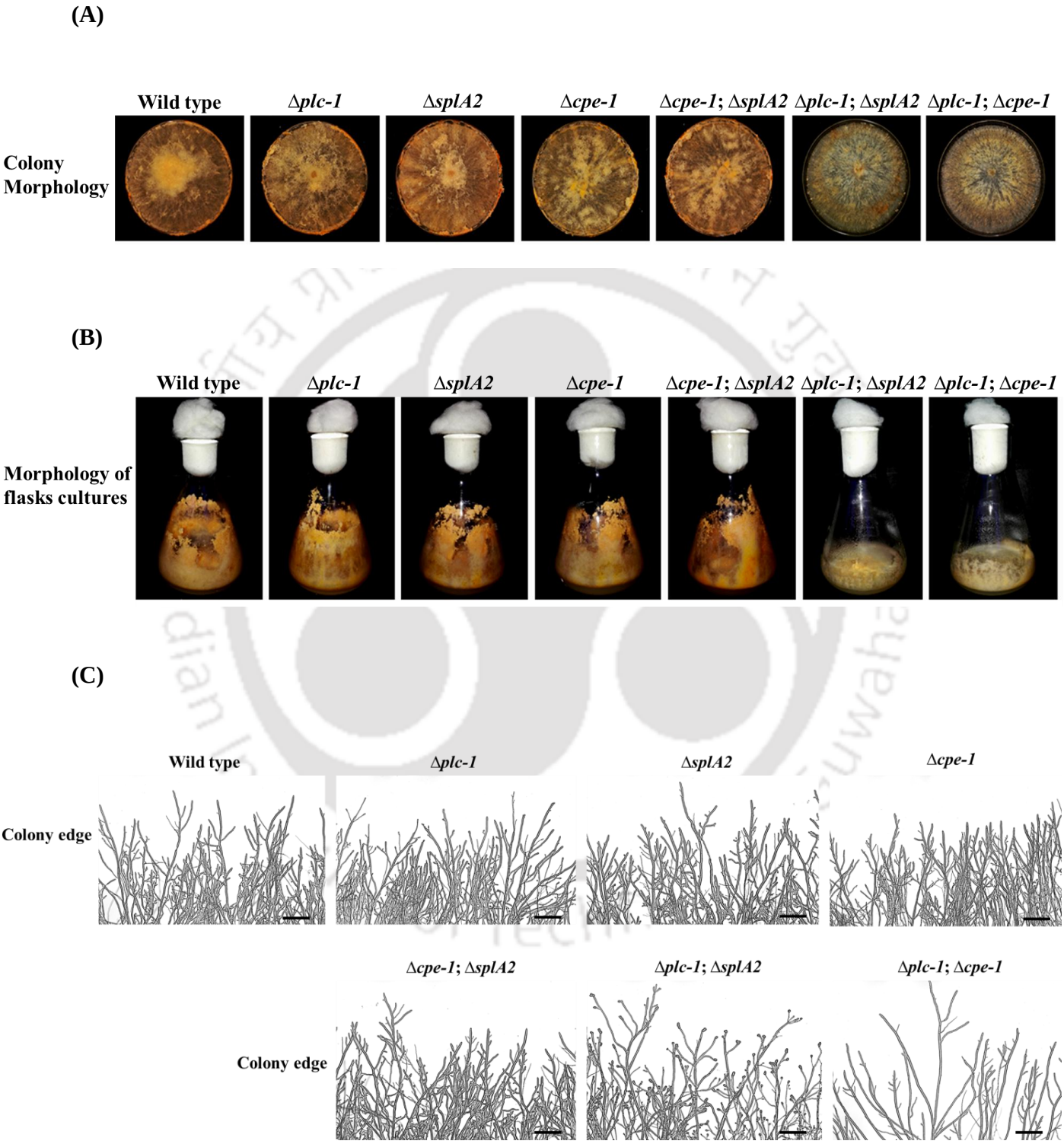

Figure 4.2: Morphology and growth of the wild type, Δ*plc-1*, Δ*splA2*, Δ*cpe-1* single and double mutant strains. (A) Colony morphology of the strains on Vogel's glucose agar medium

in Petri dishes. Images were captured using a digital camera (Nikon Coolpix P500). **(B)** Colony morphology of the strains on Vogel's glucose agar medium in flasks. For colony morphology, the *N. crassa* strains were incubated for three days in the dark at 30°C followed by four days under light at room temperature. Images were captured using a digital camera (Nikon Coolpix P500). **(C)** Hyphal morphology of the strains on Vogel's glucose agar medium after a 12 h incubation at 30°C was examined under a Trinocular inverted microscope (AxioVert A1 FL, Carl Zeiss). Scale bar 20 µm.

4.2.3 The Δ*plc-1*; Δ*splA2* and Δ*plc-1*; Δ*cpe-1* double mutants showed slower growth rate and reduced biomass accumulation

The mycelial plugs of wild type, Δ*plc-1*, Δ*splA2*, and Δ*cpe-1* single mutants, Δ*cpe-1*; Δ*splA2*, Δ*plc-1*; Δ*splA2*, and Δ*plc-1*; Δ*cpe-1* double mutants were also inoculated in sterile race tubes containing Vogel's glucose agar medium and incubated at 30°C to measure the mycelial extension rates. Hyphal growth fronts were measured after every 12 h till 72 h and plotted against time (same as described in Chapter 3). Growth rates of both the Δ*plc-1*; Δ*splA2* and Δ*plc-1*; Δ*cpe-1* double mutants were slower than their parental single mutants and wild type (Figure. 4.3 A-B; Table 4.1). However, all the three single mutants and the Δ*cpe-1*; Δ*splA2* double mutant displayed growth rate similar to the wild type (Figure 4.3 A-B; Table 4.1). I also studied accumulation of mycelial mass of the strains in both solid and liquid growth conditions. For solid media, mycelial plugs of the strains were inoculated in Vogel's glucose agar medium either at 30°C for 3 days in the dark, or 30°C for two days in the dark followed by light exposure for one day and mycelial mass was measured. For liquid media, mycelial plugs of the strains were incubated in Vogel's glucose medium at 30°C for 3 days in the dark and mycelial mass accumulation was determined. I observed a reduction of ~53-28% and 50-26% of the mycelial mass in the Δ*plc-1*; Δ*splA2* and Δ*plc-1*; Δ*cpe-1* double mutants in both the growth conditions, respectively, as compared to the wild type (Figure 4.4 A-B; Table 4.2). Thus, the slower growth rates of Δ*plc-1*; Δ*splA2* and Δ*plc-1*; Δ*cpe-1* double mutants were further supported by a reduction in accumulation of mycelial mass. In addition, mycelia of the Δ*plc-1*; Δ*splA2* and Δ*plc-1*; Δ*cpe-1* double mutants displayed dispersed growth, and did not form aggregates in liquid growth conditions unlike their single mutant and the wild type strains, which suggested a defect in hyphal fusion and hyphal network formation in the double

mutants (Figure 4.4 C). Therefore, these results indicated that *plc-1* interactions with *splA2* and *cpe-1* is essential for normal vegetative growth in *N. crassa*.

(A)

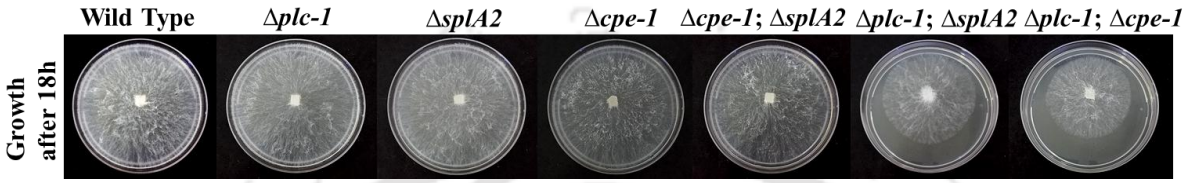

(B)

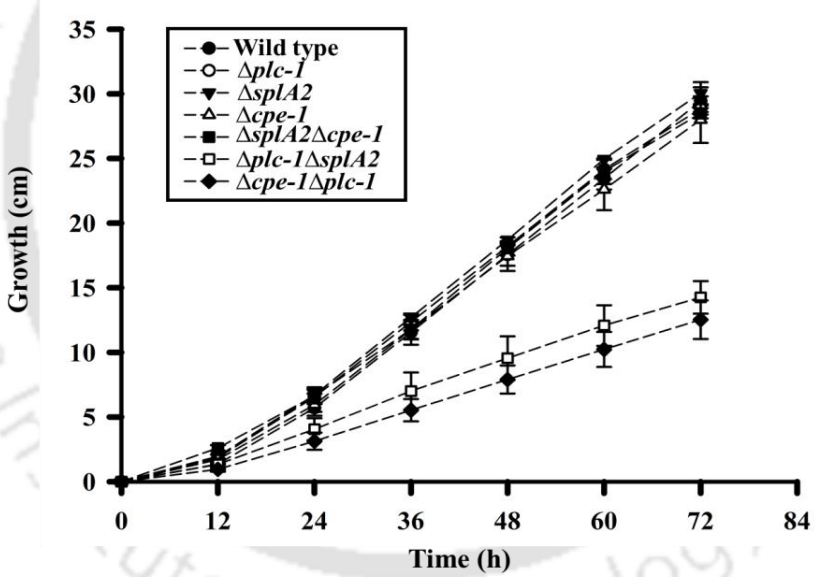

Figure 4.3: Growth phenotype of the wild type, Δ*plc-1*, Δ*splA2*, Δ*cpe-1* single and double mutant strains. (A) Colony growth. The colony growth was determined for the *N. crassa* strains at 30ºC in Petri dishes containing Vogel's glucose agar medium for 18 h, and photographed using a digital camera (Nikon Coolpix P500). **(B)** Apical growth. The apical growth rates of the strains were measured at 30ºC using 'race tubes' over a period of 72 h containing Vogel's glucose agar medium. Error bars indicate the standard deviations calculated from the data for three independent experiments (n=3).

Table 4.1: Average apical extension rates of the wild type, Δ*plc-1*, Δ*splA2*, Δ*cpe-1* single and double mutant strains in race tubes

Strains	Average growth rates (cm/h)†
Wild type	0.305 ± 0.013
Δ*plc-1*	0.320 ± 0.011
Δ*splA2*	0.321 ± 0.005
Δ*cpe-1*	0.308 ± 0.034
Δ*cpe-1*; Δ*splA2*	0.309 ± 0.025
Δ*plc-1*; Δ*splA2*	0.153 ± 0.006 (**)
Δ*plc-1*; Δ*cpe-1*	0.139 ± 0.018 (**)

†Results are shown as mean ± standard deviation for three independent experiments (n=3) with *P-values* < 0.05 (*), < 0.01 (**), and < 0.001 (***) compared with the wild type strain as measured by one-way ANOVA test.

(A)

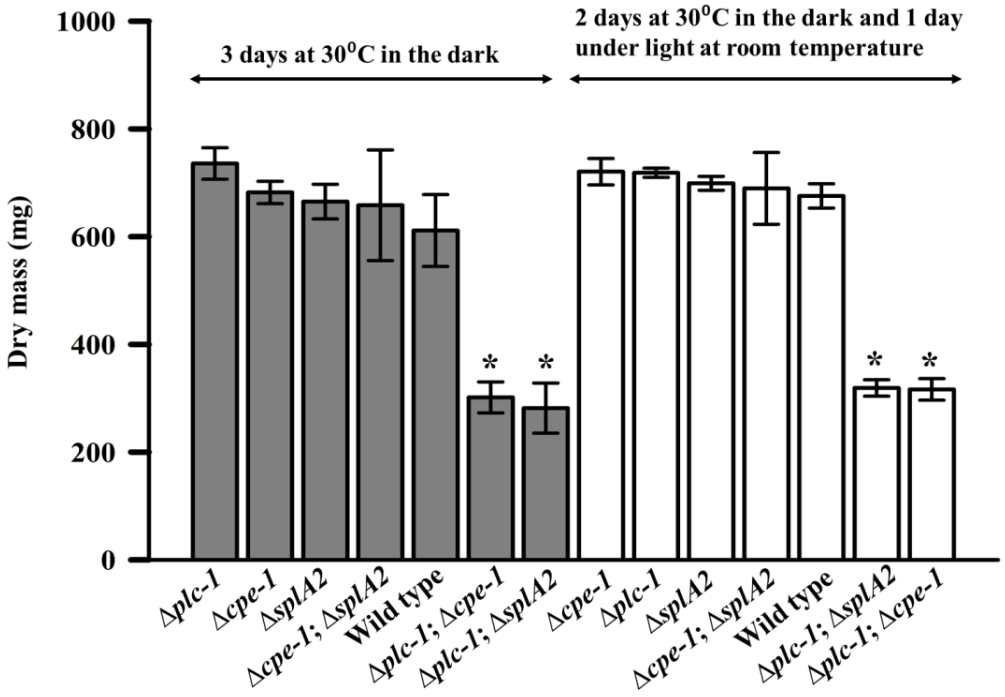

(B)

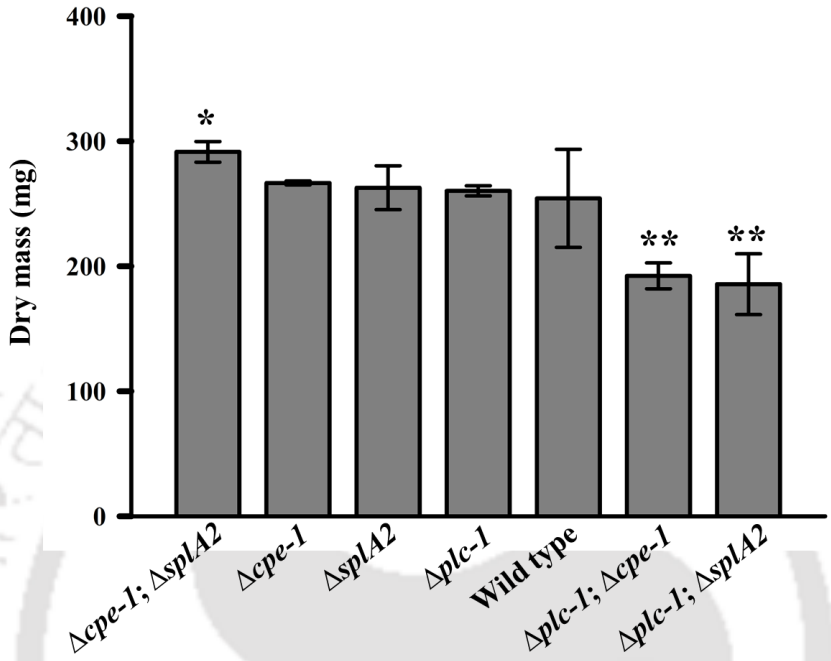

(C)

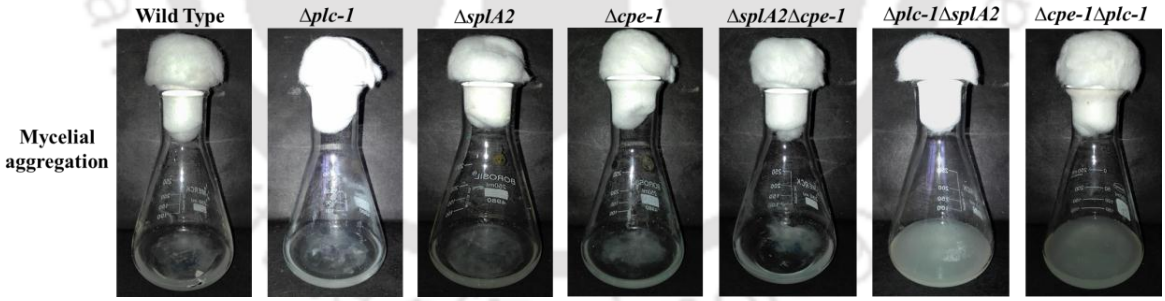

Figure 4.4: Mycelial mass accumulation in the wild type, Δ*plc-1*, Δ*splA2*, Δ*cpe-1* single and double mutant strains in both solid and liquid media. (A) Accumulation of mycelial mass of the strains in Vogel's glucose agar medium. In the first set (filled bars), strains were incubated in complete darkness at 30°C for three days, while in the latter set (empty bars), strains were kept in the dark for two days at 30°C and then one day under light for conidiation. Error bars indicate the standard deviations calculated from the data for three independent experiments (n=3) with *P-values* < 0.05 (*), < 0.01 (**), and < 0.001 (***) compared with the wild type strain as measured by one-way ANOVA test. **(B)** Accumulation of mycelial mass of the strains in Vogel's glucose

medium. Strains were incubated for three days at 30°C with shaking at 180 rpm. Error bars indicate the standard deviations calculated from the data for three independent experiments (n=3) with *P-values* < 0.05 (*), < 0.01 (**), and < 0.001 (***) compared with the wild type strain as measured by one-way ANOVA test **(C)** Accumulation of mycelial mass of the strains in Vogel's glucose medium. Strains were incubated for three days at 30°C in dark and photographed (Nikon Coolpix P500).

Table 4.2: Mass accumulation of the wild type, Δ*plc-1*, Δ*splA2*, Δ*cpe-1* single and double mutant strains

Strains	**Solid media (mg/dry weight)†**		**Liquid media (mg/dry weight)†**
	Dark, 30°C	**Light, RT**	**Dark, 30°C, 180 rpm**
Wild type	611 ± 94.4	676 ± 23	260 ± 4.1
Δ*plc-1*	736 ± 29.3	719 ± 9	254 ± 39.3
Δ*splA2*	665 ± 46	699 ± 13	263 ± 18
Δ*cpe-1*	682 ± 40	721 ± 25	267 ± 2
Δ*cpe-1*; Δ*splA2*	658 ± 119	690 ± 67	291 ± 8.3
Δ*plc-1*; Δ*splA2*	282 ± 54 (*)	319 ± 15.2 (*)	186 ± 24.3 (*)
Δ*plc-1*; Δ*cpe-1*	302 ± 33.1 (*)	316 ± 20 (*)	192 ± 10.4 (*)

†Results are shown as mean ± standard deviation for three independent experiments (n=3) with *P-values* < 0.05 (*), < 0.01 (**), and < 0.001 (***) compared with the wild type strain as measured by one-way ANOVA test.

4.2.3.1 The slow growth phenotypes of the Δ*plc-1*; Δ*splA2* and Δ*plc-1*; Δ*cpe-1* double mutants were not due to a defect in ergosterol biosynthesis

Ergosterol, one of the major constituent of fungal plasma membrane, is synthesized from a central metabolite acetyl CoA (Paltauf et al. 1992; Parks and Casey 1995). The biosynthetic pathway of ergosterol is catalyzed by several different enzymes. In *N. crassa*, the *erg-3* gene encodes the sterol C-14 reductase that catalyses the reduction of the $\Delta^{14,15}$ double bond in intermediates of the sterol biosynthetic pathway using NADPH as a cofactor (Prakash et al. 1999). The RIP (Selker and Garrett 1988; Cambareri et al. 1989) induced *erg-3* mutant grows slowly due to a defect in

ergosterol biosynthesis (Prakash et al. 1999). To test if the slow growth phenotypes of Δ*plc-1*; Δ*splA2* and Δ*plc-1*; Δ*cpe-1* double mutants were due to a defect in ergosterol biosynthesis, I analyzed the ergosterol profiles of the wild type, Δ*plc-1*, Δ*splA2*, and Δ*cpe-1* single mutants, Δ*cpe-1*; Δ*splA2*, Δ*plc-1*; Δ*splA2*, and Δ*plc-1*; Δ*cpe-1* double mutants by UV spectrophotometry (discussed in Chapter 2; Deka et al. 2011). Ergosterol has UV absorption maxima at 272, 282, and 293 nm whereas the *erg-3* mutant absorbs maximally at ~250 nm, typical of $\Delta^{8,14}$ sterols, indicating absence of ergosterol in the *erg-3* mutant (Prakash et al. 1999). Analysis of UV spectra of sterols extracted from the wild type, Δ*plc-1*, Δ*splA2*, Δ*cpe-1*, Δ*cpe-1*; Δ*splA2*, Δ*plc-1*; Δ*splA2*, and Δ*plc-1*; Δ*cpe-1* indicated presence of ergosterol in these strains (Figure 4.5). In addition, the Δ*plc-1*; Δ*splA2*, and Δ*plc-1*; Δ*cpe-1* double mutants showed absorption maxima at 272, 282, and 293 nm like the wild type (Figure 4.5), suggesting no defect in ergosterol biosynthesis in these double mutants. Therefore, the slow growth phenotypes of Δ*plc-1*; Δ*splA2*, and Δ*plc-1*; Δ*cpe-1* double mutants were not due to a defect in ergosterol biosynthesis.

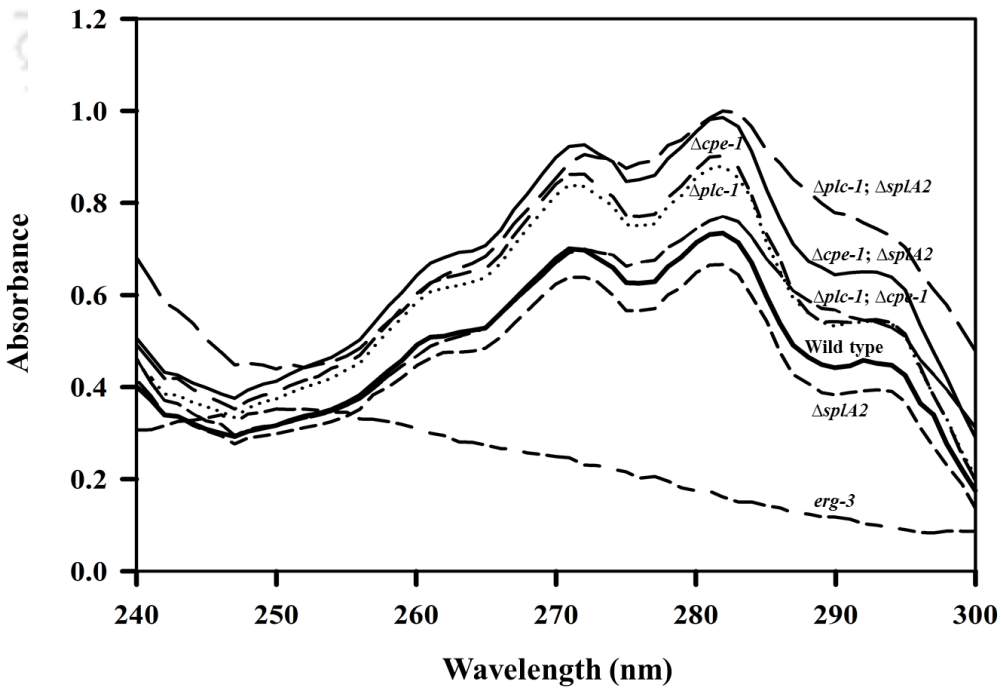

Figure 4.5: Ergosterol profile of the wild type, Δ*plc-1*, Δ*splA2*, Δ*cpe-1* single and double mutant strains. Profile of the sterols extracted from the wild type, Δ*plc-1*, Δ*splA2*, Δ*cpe-1*, Δ*cpe-1*; Δ*splA2*, Δ*plc-1*; Δ*splA2*, and Δ*plc-1*; Δ*cpe-1* mutants and the *erg-3* mutant were analyzed by

UV spectrophotometry. Ergosterol has UV absorption maxima at 272, 282, and 293 nm whereas the *erg-3* mutant absorbs maximally at ~250 nm, typical of $\Delta^{8, 14}$ sterols, indicating absence of ergosterol in the *erg-3* mutant (Prakash et al. 1999). Ergosterol is present in the wild type, Δ*plc-1*, Δ*splA2*, Δ*cpe-1*, Δ*cpe-1*; Δ*splA2*, Δ*plc-1*; Δ*splA2*, and Δ*plc-1*; Δ*cpe-1* mutant strains.

4.2.4 The Δ*plc-1*; Δ*splA2* and Δ*plc-1*; Δ*cpe-1* double mutants showed reduced aerial hyphae and conidiation

I also studied if the double deletions affect the aerial hyphal development and conidiation in the mutant strains. To study aerial hyphae, ~1×10^6 conidia/ml of the wild type, all the single and the double mutants were inoculated in Vogel's glucose medium and incubated at 30°C for four days in the dark followed by three days under light for conidiation. The Δ*plc-1*; Δ*splA2* and Δ*plc-1*; Δ*cpe-1* double mutants produced significantly shorter aerial hyphae as compared to wild type and the parental single mutants (Figure 4.6 A; Table 4.3). To determine conidiation, mycelial plugs of the wild type, the three single mutants, and the double mutants were inoculated in Vogel's glucose agar medium and incubated for two days in the dark at 30°C, and four days under light at 22°C. After thorough resuspension of conidia in sterile distilled water counting of conidia was done using a haemocytometer. The Δ*plc-1*; Δ*splA2* and Δ*plc-1*; Δ*cpe-1* double mutants produced fewer conidia and showed ~50% reduction in conidiation relative to individual single mutants and wild type (Figure 4.6 B; Table 4.4). Another double mutant, the Δ*cpe-1*; Δ*splA2* strain showed morphology, hyphal branching, pigmentation, aerial hyphae, and conidia production similar to those of wild type and the individual single mutants. Therefore, these results indicated that interactions of *plc-1* with *splA2* and *cpe-1* play an important role for normal aerial hyphae development and conidiation in *N. crassa*.

(A)

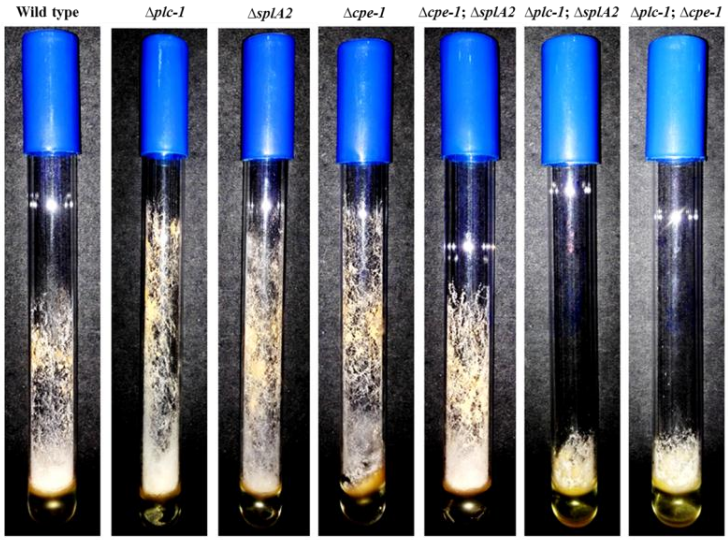

(B)

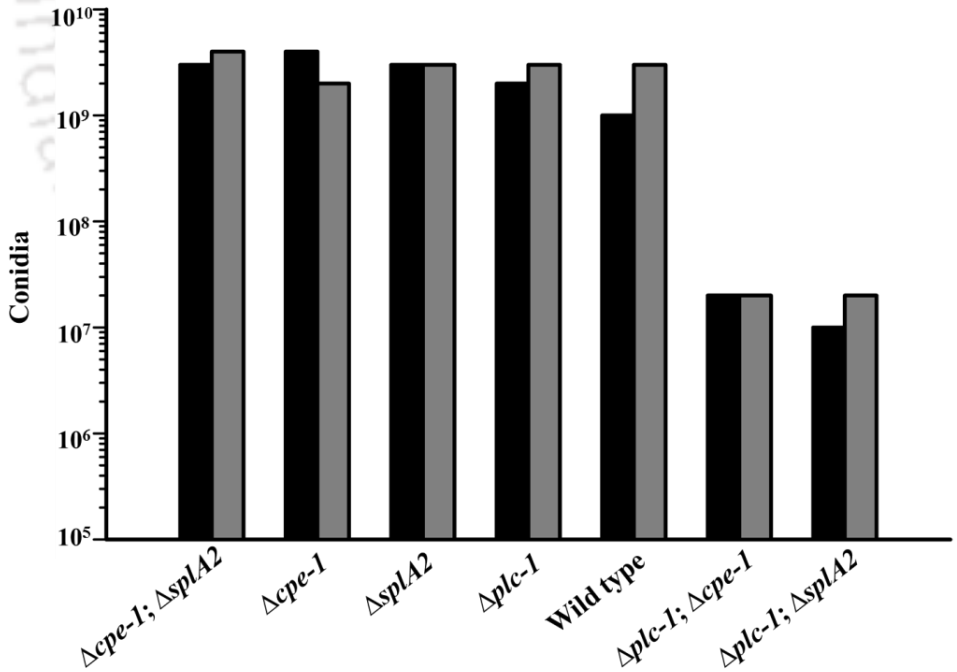

Figure 4.6: Analysis of aerial hyphae and conidiation of the wild type, Δ*plc-1*, Δ*splA2*, Δ*cpe-1* single and double mutant strains. **(A)** Aerial hyphae of the strains in Vogel's glucose medium. Strains were incubated at 30°C for three days in the dark and further kept under light for four days at room temperature and photographed (Nikon Coolpix P500). **(B)** Conidia produced by the strains

were quantified after two days incubation in the dark at 30°C followed by continuous exposure to light at 22°C for four days. The bars indicate two independent determinations for each strain.

Table 4.3: Average aerial hyphae height of the wild type, Δ*plc-1*, Δ*splA2*, Δ*cpe-1* single and double mutant strains

Strains	Average aerial hyphae height (cm)†
Wild type	6 ± 0.173
Δ*plc-1*	9 ± 0.710 (*)
Δ*splA2*	9 ± 0.208 (***)
Δ*cpe-1*	9 ± 0.251 (***)
Δ*cpe-1*; Δ*splA2*	7 ± 0.242 (**)
Δ*plc-1*; Δ*splA2*	2 ± 0.606 (**)
Δ*plc-1*; Δ*cpe-1*	2 ± 0.296 (***)

†Results are shown as mean ± standard deviation for three independent experiments (n=3) with *P-values* < 0.05 (*), < 0.01 (**), and < 0.001 (***) compared with the wild type strain as measured by one-way ANOVA test.

Table 4.4: Conidial count of the wild type, Δ*plc-1*, Δ*splA2*, Δ*cpe-1* single and double mutant strains

Strains	Average count of conidia (conidia/ml)
Wild type	3×10^9
Δ*plc-1*	3×10^9
Δ*splA2*	3×10^9
Δ*cpe-1*	4×10^9
Δ*cpe-1*; Δ*splA2*	4×10^9
Δ*plc-1*; Δ*splA2*	2×10^7
Δ*plc-1*; Δ*cpe-1*	2×10^7

4.2.5 The Δ*plc-1*; Δ*splA2* and Δ*plc-1*; Δ*cpe-1* double mutants displayed early conidiation with reduced conidial germination

In previous independent studies, formation of shorter aerial hyphae was found to be linked to premature and constitutive or non-repressing conidiation as seen in a putative histidine kinase *development and carotenogenesis control-1* (*dcc-1*), and a non-repressing conidiation protein *nonrepressible conidiation gene-1* (*nrc-1*) mutant, respectively (Kothe and Free 1998; Barba-Ostria et al. 2011). I found that the Δ*plc-1*; Δ*splA2* and Δ*plc-1*; Δ*cpe-1* double mutants also produced shorter aerial hyphae. Therefore, to test if the reduced aerial hyphae phenotype of the Δ*plc-1*; Δ*splA2* and Δ*plc-1*; Δ*cpe-1* double mutants was linked to premature conidiation, I did a time course analysis of conidia in glucose-rich medium under complete darkness, which is a growth-repressing condition. Approximately, 10^3 conidia of the single and double mutants and the wild type strains were inoculated in Vogel's glucose agar medium and incubated at 30°C in the dark, and conidia produced were counted after every 12 h till 72 h. The Δ*plc-1*; Δ*splA2* and Δ*plc-1*; Δ*cpe-1* double mutants produced conidia as early as 12 h, whereas, the Δ*cpe-1*; Δ*splA2* double mutant, individual single mutants, and the wild type produced conidia only after 48 h post inoculation (Figure 4.7). Therefore, I concluded that both Δ*plc-1*; Δ*splA2* and Δ*plc-1*; Δ*cpe-1* double mutants enter the asexual developmental program earlier than either the parental single mutants or the wild type. I further tested germination efficiency of the conidia produced by the wild type, the three single mutants, and the double mutants both qualitatively and quantitatively. For qualitative analysis, ~1×10^6 conidia/ml of wild type, Δ*plc-1*, Δ*splA2*, Δ*cpe-1*, Δ*cpe-1*; Δ*splA2*, Δ*plc-1*; Δ*splA2*, and Δ*plc-1*; Δ*cpe-1* mutant strains were germinated in Vogel's glucose medium and viewed by microscopy at regular intervals of time. Conidial germination was not observed in the Δ*plc-1*; Δ*splA2* and Δ*plc-1*; Δ*cpe-1* double mutants after 8 h and 12 h post inoculation, but abundant germinating conidia with long germ tubes were seen in Δ*cpe-1*; Δ*splA2* double mutant, individual single mutants, and the wild type strain (Figure 4.8 A). In addition, only ~1-2 germ tubes were seen till 48 h in the Δ*plc-1*; Δ*splA2* and Δ*plc-1*; Δ*cpe-1*double mutants; however, conidia with well-developed germ tubes were seen in the other strains (Figure 4.8 A). For quantitative analysis, ~10^3 conidia of wild type, Δ*plc-1*, Δ*splA2*, Δ*cpe-1*, Δ*cpe-1*; Δ*splA2*, Δ*plc-1*; Δ*splA2*, and Δ*plc-1*; Δ*cpe-1* mutant strains were inoculated in Vogel's glucose agar medium and incubated at 25°C. Germination of conidia was observed under the microscope at regular time period. Percent germination was calculated as (germinated conidia/total number of conidia)

×100%. Approximately, 100% conidia from the Δ*plc-1*; Δ*splA2* and Δ*plc-1*; Δ*cpe-1* double mutants were germinated after 60 h post inoculation, whereas, almost all the conidia from the Δ*cpe-1*; Δ*splA2* double mutant, individual single mutants, and the wild type were germinated as early as 24 h post inoculation (Figure 4.8 B). Therefore, it might be possible that the early conidiation in the Δ*plc-1*; Δ*splA2* and Δ*plc-1*; Δ*cpe-1* strains subsequently produced pre-matured conidia causing a delay in conidial germination in these two double mutant strains. Thus, these results suggested that the genetic interactions of *plc-1* with *splA2* and *cpe-1* play an important role in the production and germination of conidia in *N. crassa* under favorable conditions.

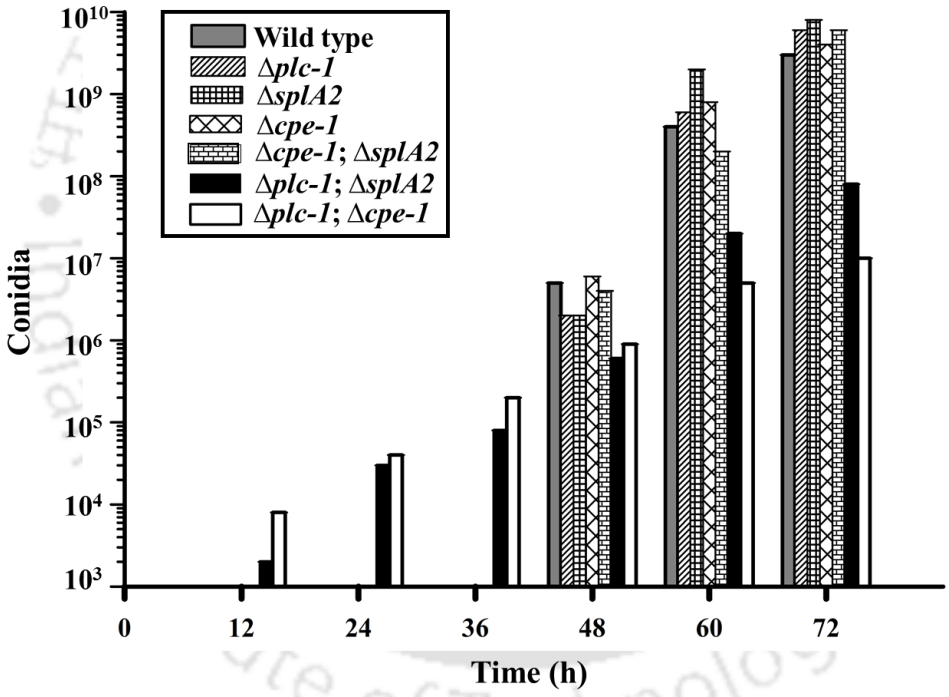

Figure 4.7: Time course analysis of conidiation of the wild type, Δ*plc-1*, Δ*splA2*, Δ*cpe-1* single and double mutant strains. Strains were grown on Petri dishes containing Vogel's glucose agar medium and incubated at 30°C in complete darkness. Conidia were harvested and quantified at regular intervals using a haemocytometer.

(A)

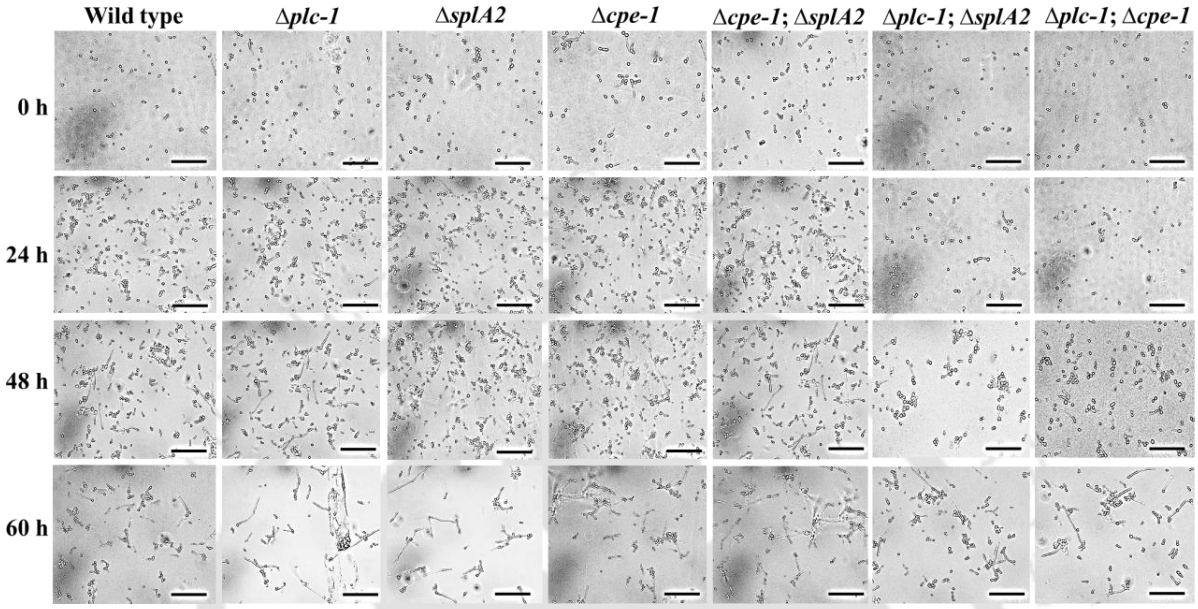

(B)

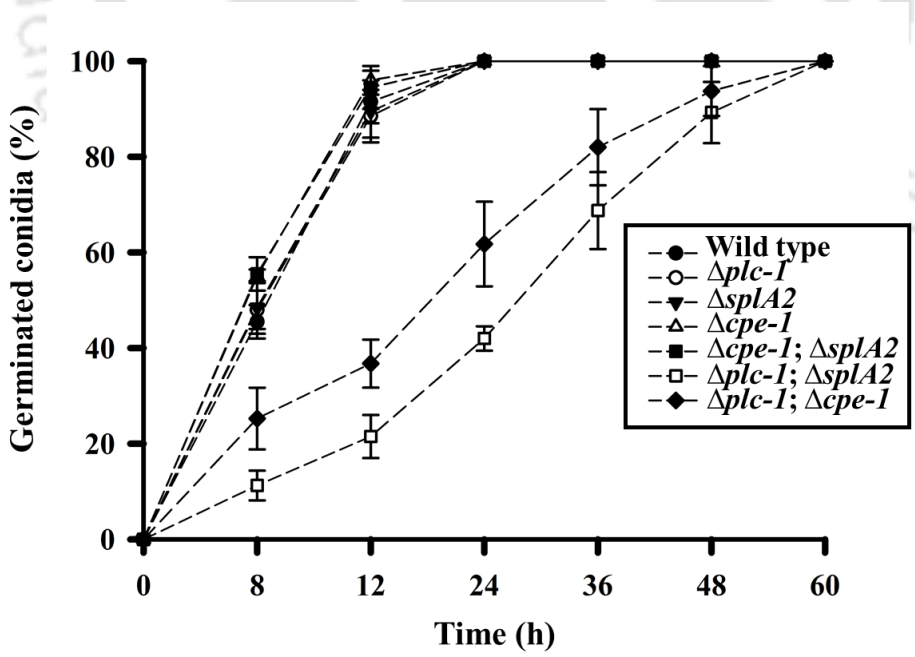

Figure 4.8: Time course analysis of conidial germination of the wild type, Δ*plc-1*, Δ*splA2*, Δ*cpe-1* single and double mutant strains. (A) Qualitative analysis. Conidia at a concentration of ~10^6 conidia/ml were inoculated in Vogel's glucose medium and incubated at 25°C with shaking at 180 rpm. An aliquot of the cultures was taken and formation of germ tubes were viewed under

the Trinocular inverted microscope (AxioVert A1FL, Carl Zeiss) at intervals of 0, 24, 48, and 60 h. Images of germinated conidia were captured. Delayed germination of conidia were seen in the Δ*plc-1*; Δ*splA2* and Δ*plc-1*; Δ*cpe-1* double mutant strains. Scale bar 20 µm. **(B)** Quantitative analysis. Conidial suspensions of the strains were inoculated on Petri dishes containing Vogel's glucose agar medium and incubated at 25°C. Germination of conidia was observed under the under the Trinocular inverted microscope (AxioVert A1FL, Carl Zeiss) at regular interval of indicated times and percent germination was determined. Error bars indicate standard deviations calculated from the data for three independent experiments (n=3).

4.2.6 The Δ*plc-1*; Δ*splA2* and Δ*plc-1*; Δ*cpe-1* double mutants showed inappropriate conidiation in submerged cultures

In *N. crassa*, formation of aerial hyphae and subsequent conidiation occurs under nutrient limiting conditions and in presence of an air-water interface (Springer 1993). Thus, in general, conidiation does not occur in submerged cultures. However, carbon or nitrogen limitations, heat shock or cellular stress can induce conidiation in submerged cultures of *N. crassa* wild type (Cortat and Turian 1974; Guignard et al. 1974; That and Turian 1978; Plesofsky-Vig et al. 1985; Madi et al. 1997). The Δ*plc-1*; Δ*splA2* and Δ*plc-1*; Δ*cpe-1* double mutant strains exhibited early conidiation in growth-repressing conditions (Figure 4.7), indicating that these mutants could conidiate in condition that is unfavorable for conidiation. Therefore, I also investigated if these two double mutants produce conidia in submerged cultures. To test submerged culture conidiation phenotype, conidia from the wild type, Δ*plc-1*, Δ*splA2*, Δ*cpe-1*, Δ*cpe-1*; Δ*splA2*, Δ*plc-1*; Δ*splA2*, and Δ*plc-1*; Δ*cpe-1* mutant strains were inoculated at a concentration of ~10^6 conidia/ml in Vogel's glucose medium and incubated at 30°C with shaking for 16 h, and aliquots of the cultures were observed under the microscope to assay formation of conidiophores. Abundant conidiophores were observed in 16 h-submerged cultures of the Δ*plc-1*; Δ*splA2* and Δ*plc-1*; Δ*cpe-1* double mutants (Figure 4.9). In contrast, the Δ*cpe-1*; Δ*splA2* double mutant, individual single mutants, and the wild type did not produce conidiophores or conidia and maintained vegetative non-conidiating hyphae in submerged cultures. In previous independent studies, supplementation of the rich nutrient peptone was shown to suppress conidiation in submerged cultures of the *cr-1* adenylyl cyclase, *gna-1* and *gna-3* Gα subunits, *gnb-1* Gβ subunit, and *rco-3* glucose transporter mutants (Ivey et al. 2002; Kays et al. 2000; Madi et al. 1997; Yang et al. 2002). Therefore, I tested if addition of peptone in

submerged cultures of Δ*plc-1*; Δ*splA2* and Δ*plc-1*; Δ*cpe-1* mutant strains could suppress conidiophores development. Supplementation of 2% peptone resulted in complete suppression of conidiophores formation in submerged cultures of Δ*plc-1*; Δ*splA2* and Δ*plc-1*; Δ*cpe-1* mutant strains, and showed normal vegetative hyphal growth similar to wild type (Figure 4.9). These results further supported the genetic interactions of *plc-1* with *splA2* and *cpe-1*, and indicated a role of these Ca^{2+}-signaling genes in normal conidiation.

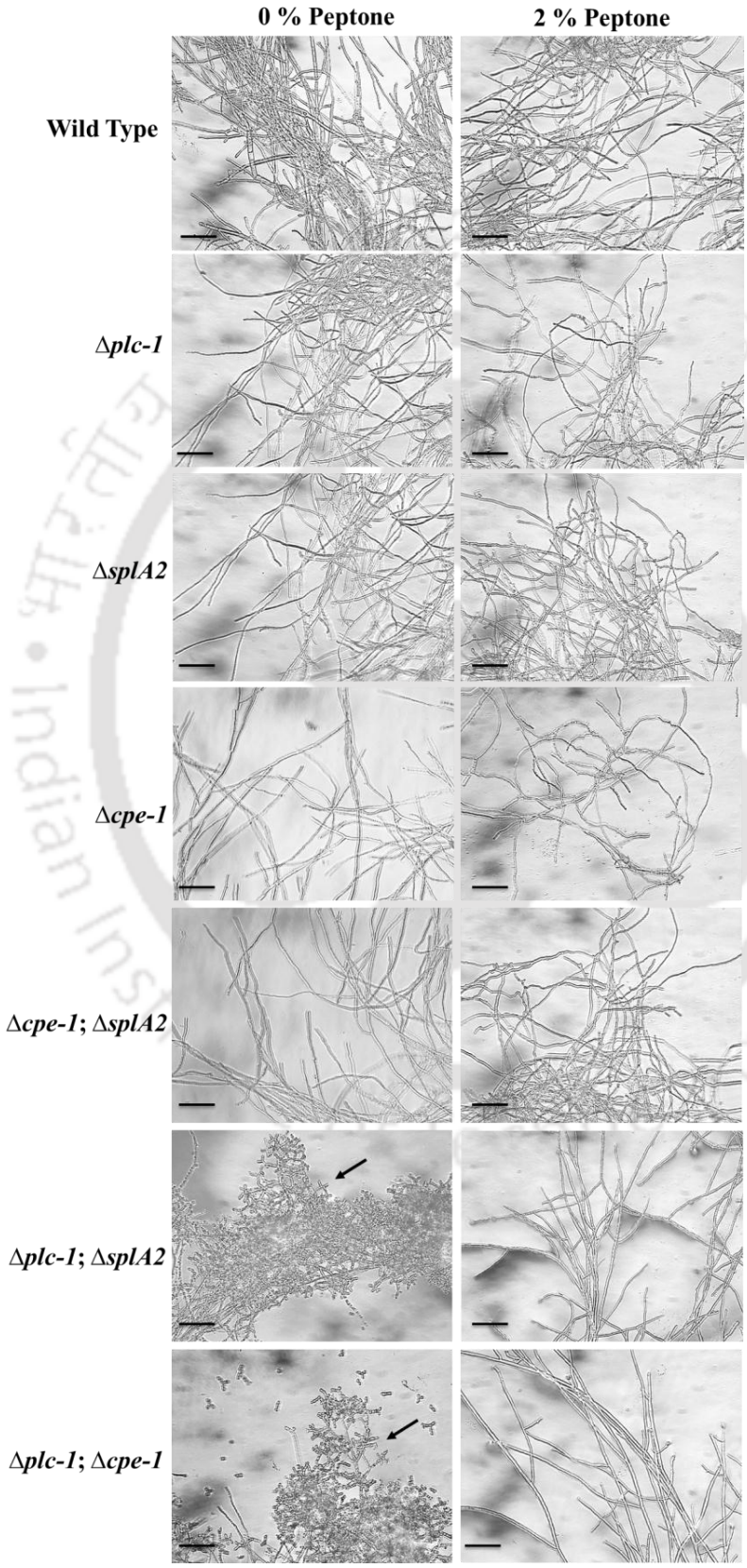

Figure 4.9: Conidiophore formation in submerged cultures of the wild type, Δ*plc-1*, Δ*splA2*, Δ*cpe-1* single and double mutant strains. Strains were inoculated in Vogel's glucose medium at a concentration of ~10^6 conidia/ml and supplemented with or without 2% w/v peptone, and incubated in dark at 30°C with shaking at 180 rpm for 16 h. Conidiophore development was assessed by microscopy (Trinocular inverted microscope; AxioVert A1FL, Carl Zeiss) and photographed. Black arrows indicate conidiophores. Scale bar 20 µm.

4.2.7 Carotenoid accumulation was affected in the Δ*plc-1*; Δ*splA2* and Δ*plc-1*; Δ*cpe-1* double mutants

Conidial suspensions of the Δ*plc-1*; Δ*splA2* and Δ*plc-1*; Δ*cpe-1* double mutants appeared light yellow in color as compared to dark orange color observed for the individual single and the Δ*cpe-1*; Δ*splA2* double mutant and the wild type, indicating reduced carotenoid accumulation in these two double mutants (Figure 4.10). Therefore, I measured the carotenoid content in the wild type, *Δplc-1*, *ΔsplA2*, and *Δcpe-1* single as well as Δ*cpe-1*; Δ*splA2*, Δ*plc-1*; Δ*splA2*, and Δ*plc-1*; Δ*cpe-1* double mutant strains in both light and dark conditions at three different temperatures of 8, 22, and 30°C, using the procedure described in Chapters 2 and 3. The Δ*plc-1*; Δ*splA2* and Δ*plc-1*; Δ*cpe-1* double mutants showed significantly lower carotenoid accumulation at all three temperatures, whereas, the *Δplc-1*, *ΔsplA2*, *Δcpe-1*, and Δ*cpe-1*; Δ*splA2* mutants showed higher carotenoid accumulation than the wild type at 8, 22, and 30°C (Figure 4.11 A-C; Table 4.5). I also analyzed carotenoid accumulation in the wild type, single and double mutants of *Δplc-1*, *ΔsplA2*, and *Δcpe-1* at 8, 22, and 30°C in a time dependent manner with an exposure to light for 0 to 12 h. Carotenoid accumulation in the *Δplc-1*, *ΔsplA2*, *Δcpe-1*, and Δ*cpe-1*; Δ*splA2* mutants at different time points were higher than the wild type, however, the Δ*plc-1*; Δ*splA2* and Δ*plc-1*; Δ*cpe-1* double mutants showed a slower carotenoid accumulation than the individual single mutants and the wild type at different time points (Figure 4.12 A-C). Therefore, these results indicated that cultures of Δ*plc-1*; Δ*splA2* and Δ*plc-1*; Δ*cpe-1* double mutants exhibited lower carotenoid accumulation after a 24 h illumination at three different temperatures of 8, 22, and 30°C due to a slower rate of carotenoid accumulation at different time points, causing reduced mycelial pigmentation. Therefore, I concluded that genetic interactions between *plc-1* with *splA2*, and *cpe-1* play an important role in carotenoid accumulation in turn for the characteristics orange colored mycelial pigmentation in *N. crassa*.

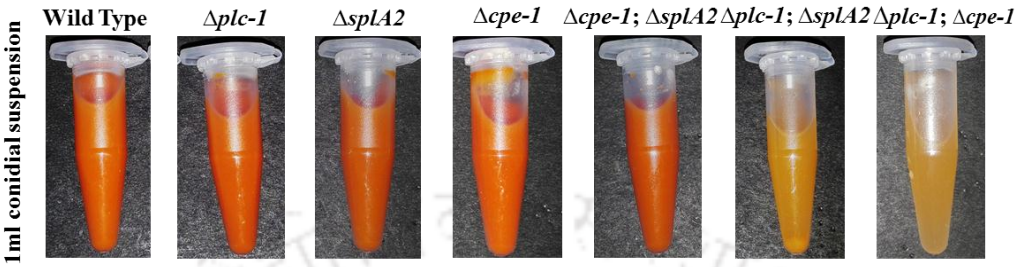

Figure 4.10: Carotenoid accumulation. Representative images of 1 ml conidial suspensions showing the carotenoid accumulation in the wild type, and Δ*plc-1*, Δ*splA2*, Δ*cpe-1* single and double mutants (Nikon Coolpix P500).

(A)

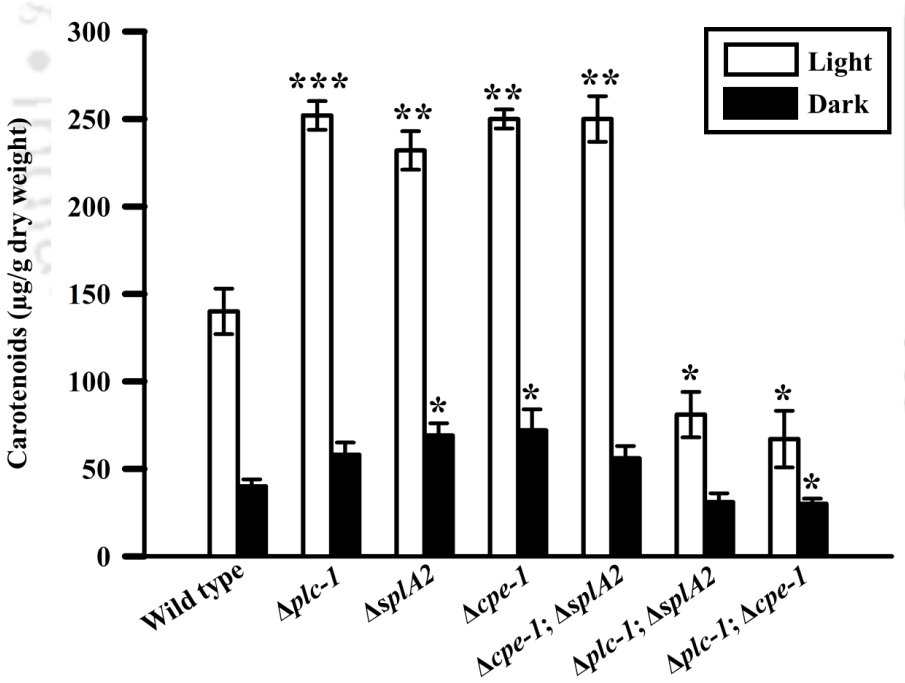

(B)

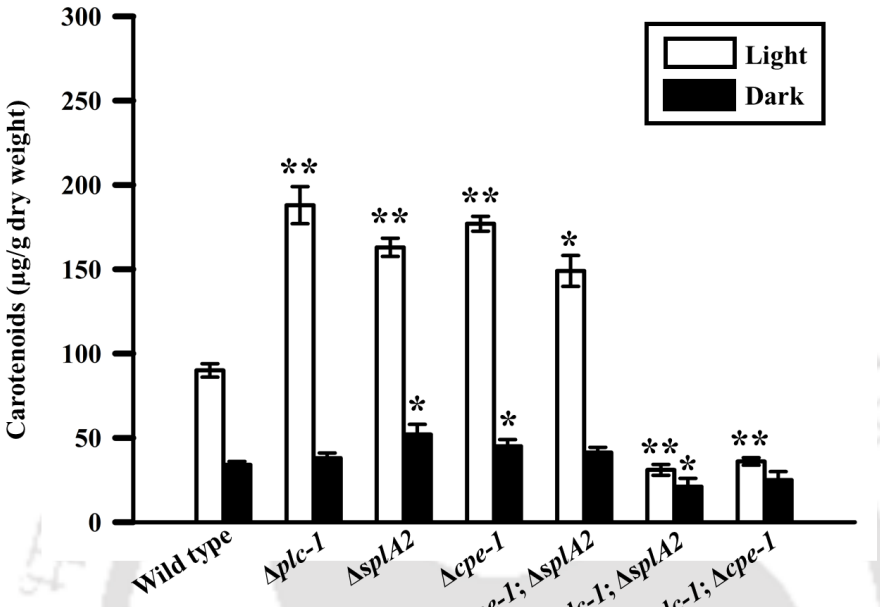

(C)

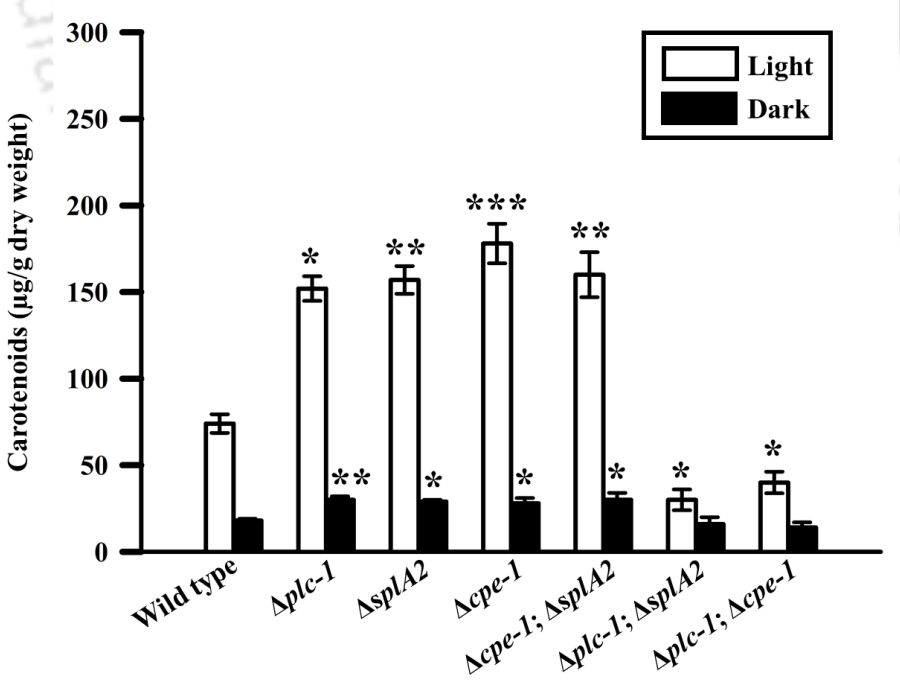

Figure 4.11: Carotenoid accumulation of the wild type, Δ*plc-1*, Δ*splA2*, Δ*cpe-1* single and double mutant strains. Strains were grown in Vogel's glucose medium supplemented with 0.2%

tween-80 and incubated initially at 30°C in dark for 48 h and then at three different temperatures of **(A)** 8°C, **(B)** 22°C, and **(C)** 30°C with simultaneous exposure to white light for 24 h. Carotenoids accumulated in the mycelia were then extracted from the three temperatures at indicated times. Accumulated carotenoids are expressed as μg carotenoid per gram of dry weight. Error bars indicate standard deviations calculated from the data for three independent experiments (n=3) with *P-values* < 0.05 (*), < 0.01 (**), and < 0.001 (***) compared with the wild type strain as measured by one-way ANOVA test.

Table 4.5: Carotenoid content of the wild type, Δ*plc-1*, Δ*splA2*, Δ*cpe-1* single and double mutant strains at three different temperatures

Strains	**Carotenoids (µg/g dry weight)†**					
	8°C		**22°C**		**30°C**	
	Light	**Dark**	**Light**	**Dark**	**Light**	**Dark**
Wild type	140 ± 13	40 ± 4	90 ± 4	34 ± 2	74 ± 5.4	18 ± 1
Δ*plc-1*	252 ± 8.2 (***)	58 ± 7	188 ± 11(**)	38 ± 3	152 ± 7.1 (*)	30 ± 2 (**)
Δ*splA2*	232 ± 11 (**)	69 ± 7 (*)	163 ± 5.4 (**)	52 ± 6 (*)	157 ± 8 (**)	29 ± 1 (*)
Δ*cpe-1*	240 ± 5.4 (**)	72 ± 12 (*)	177 ± 4.4 (**)	45 ± 4 (*)	178 ± 11.4 (***)	28 ± 3 (*)
Δ*cpe-1*; Δ*splA2*	250 ± 13 (**)	56 ± 7	149 ± 9.2 (*)	41.3 ± 3.1	160 ± 13 (**)	30 ± 4 (*)
Δ*plc-1*; Δ*splA2*	81 ± 13 (*)	31 ± 5	31 ± 3.2 (**)	21 ± 5 (*)	30 ± 6 (*)	16 ± 4
Δ*plc-1*; Δ*cpe-1*	67 ± 16.2 (*)	30 ± 3 (*)	36 ± 2.2 (**)	25 ± 5	40 ± 6.2(*)	14 ± 3

†Results are shown as mean ± standard deviation for three independent experiments (n=3) with *P-values* < 0.05 (*), < 0.01 (**), and < 0.001 (***) compared with the wild type strain as measured by one-way ANOVA test.

(A)

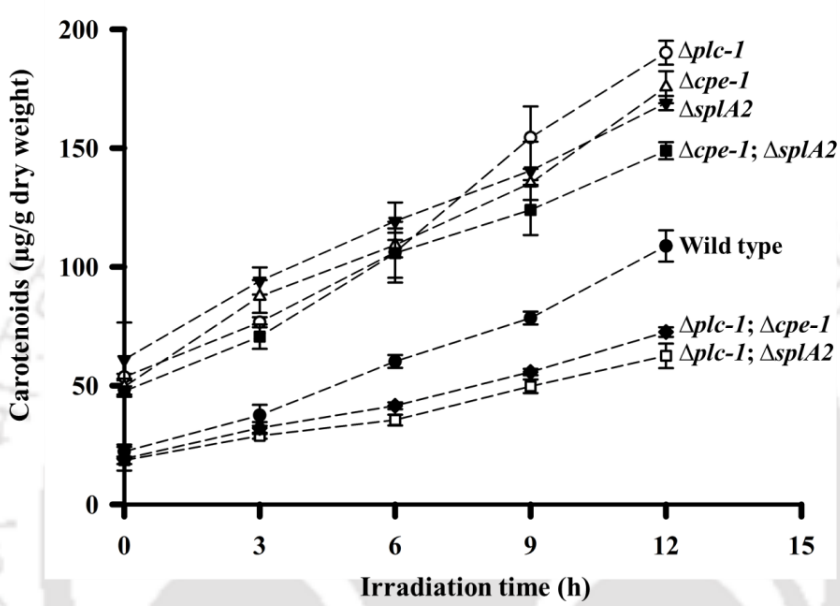

(B)

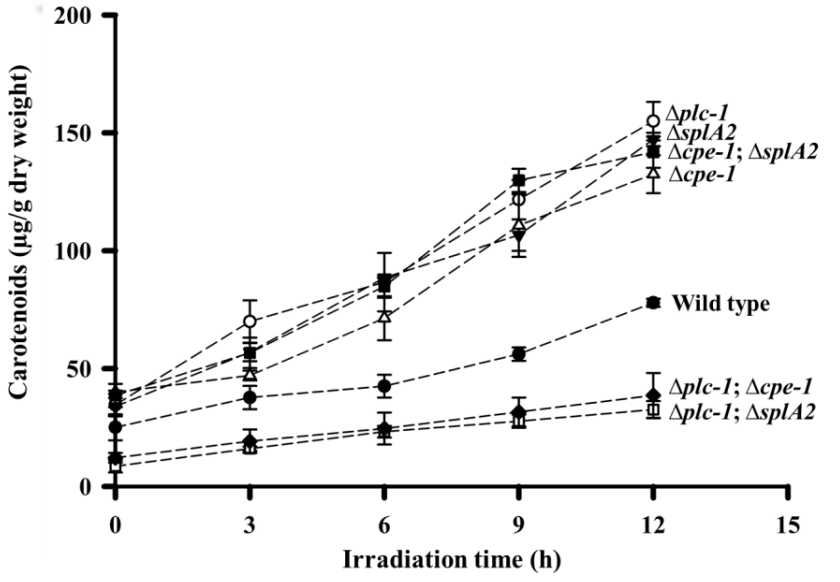

(C)

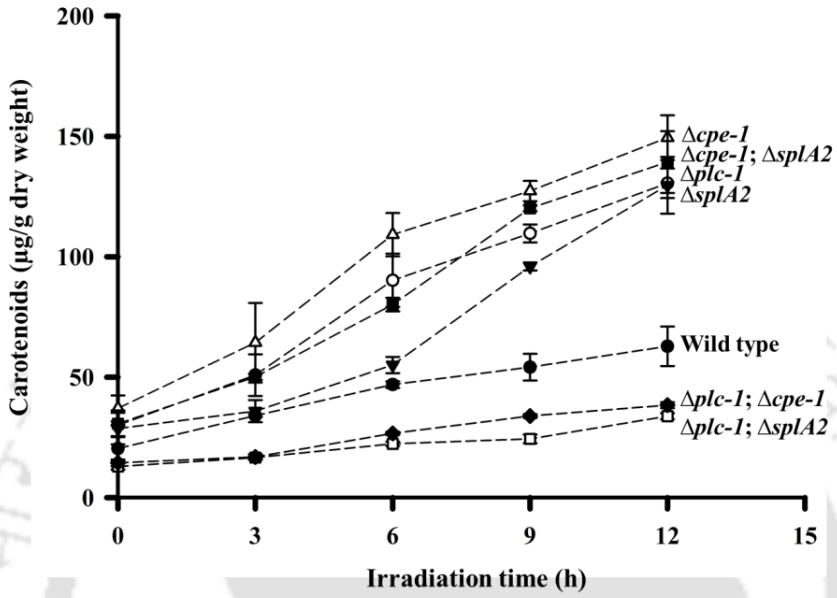

Figure 4.12: Time course analysis of carotenoid accumulation of the wild type, Δ*plc-1*, Δ*splA2*, Δ*cpe-1* single and double mutant strains. Strains were grown in Vogel's glucose medium supplemented with 0.2% tween-80 and incubated initially at 30°C in dark for 48 h and then at three different temperatures of **(A)** 8°C, **(B)** 22°C, and **(C)** 30°C with simultaneous exposure to white light for 0, 3, 6, 9, and 12 h. Carotenoids accumulated in the mycelia were then extracted from the three temperatures at indicated times. Accumulated carotenoids are expressed as μg carotenoid per gram of dry weight. Error bars indicate standard deviations calculated from the data for three independent experiments (n=3).

4.2.7.1 Increased carotenoid accumulation in the Δ*plc-1*, Δ*splA2*, Δ*cpe-1*, and Δ*cpe-1*; Δ*splA2* mutants could be linked to production of high intracellular ROS

In *N. crassa*, carotenoid biosynthesis induced by light was shown to be related with production of intracellular ROS (Yoshida and Hasunuma 2004). ROS has also been reported to regulate carotenoid synthesis in other organisms including *Phaffia rhodozyma*, where carotenoid synthesis was induced by singlet oxygen, and *Fusarium aquaeductuum*, where increased carotenoid accumulation in the mycelia was observed upon treatment with redox dyes under red light (Sundquist et al. 1994; Schroeder and Johnson 1995). Therefore, I tested if carotenoid accumulation in the single and double mutants of *Δplc-1*, *ΔsplA2*, and *Δcpe-1* was affected by

generation of intracellular ROS using the antioxidant N-acetyl-L-cysteine (NAC; Figure 4.13) that reduces high intracellular ROS level, and N-acetylglycine (NAG; Figure 4.13), an analog of NAC but without any antioxidative activity, as a control. I found that treatment with 1 mM NAC followed by white light illumination for 2 h resulted in lower carotenoid accumulation in the *Δplc-1*, *ΔsplA2*, *Δcpe-1*, and Δ*cpe-1*; Δ*splA2* mutants, whereas, carotenoid accumulation was similar in both NAC and NAG treated cultures of the wild type, Δ*plc-1*; Δ*splA2*, and Δ*plc-1*; Δ*cpe-1* double mutants at all the three temperatures of 8, 22, and 30°C (Figure 4.14). I also tested intracellular ROS production by using the DCFH-DA (Chapter 3; Figure 3.11 A) dye that fluoresces green in the presence of intracellular ROS. Conidia from the *Δplc-1*, *ΔsplA2*, *Δcpe-1*, and Δ*cpe-1*; Δ*splA2* double mutant strains, when stained with 25 µM of DCFH-DA, showed an increased fluorescence than the wild type, Δ*plc-1*; Δ*splA2*, and Δ*plc-1*; Δ*cpe-1* after a 24 h illumination at 8, 22, and 30°C (Figure 4.15 A-C). In addition, even the unilluminated conidia from the *Δplc-1*, *ΔsplA2*, and *Δcpe-1* mutants stained with 25 µM DCFH-DA showed slightly enhanced fluorescence than the wild type at 8, 22, and 30°C (Figure 4.15 A-C). Therefore, these results suggested that increased carotenoid accumulation in the *Δplc-1*, *ΔsplA2*, *Δcpe-1*, and Δ*cpe-1*; Δ*splA2* mutants could be linked to an overall increase in intracellular ROS generation in these mutants.

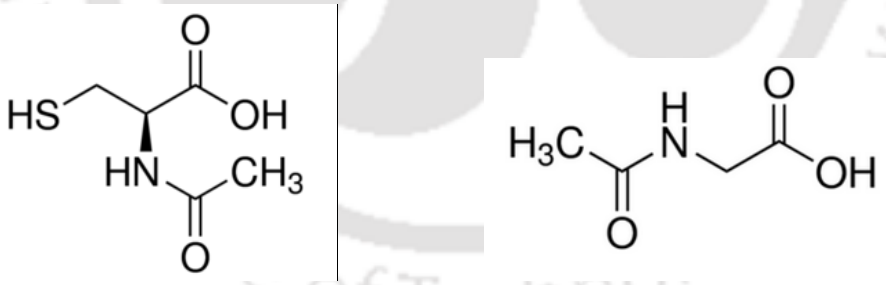

N-acetyl-L-cysteine (NAC) (Antioxidative activity)

N-acetylglycine (NAG) (No antioxidative activity)

Figure 4.13: Chemical structures of N-acetyl-L-cysteine and N-acetylglycine. N-acetyl-L-cysteine (NAC) is an antioxidant while N-acetylglycine (NAG), an analogue of NAC, has no antioxidative activity. NAC increases the cellular pools of free radical scavengers. Both the chemical structures are available at http://www.sigmaaldrich.com/catalog/product/sial/a7250?lang=en&region=IN & http://www.sigmaaldrich.com/catalog/product/aldrich/a16300?lang=en&region=IN

(A)

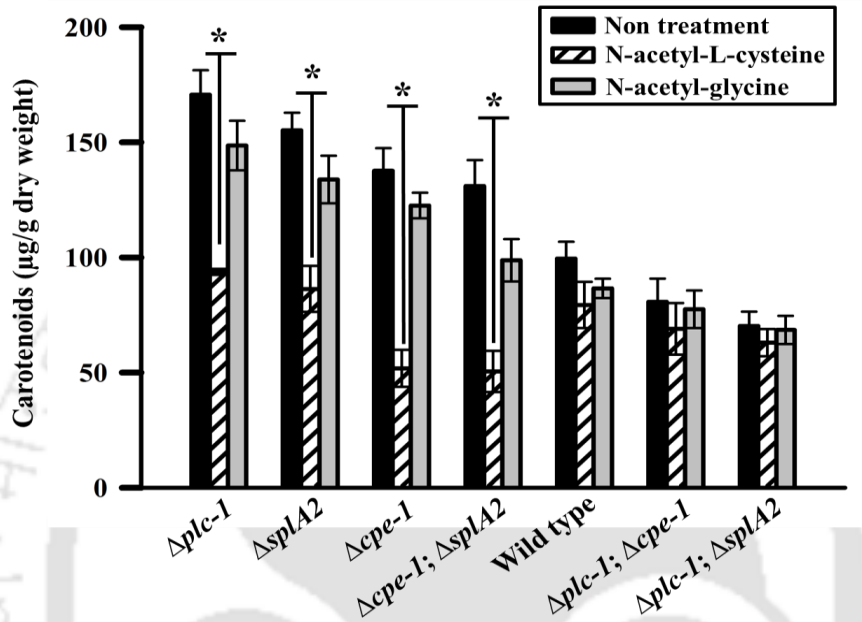

(B)

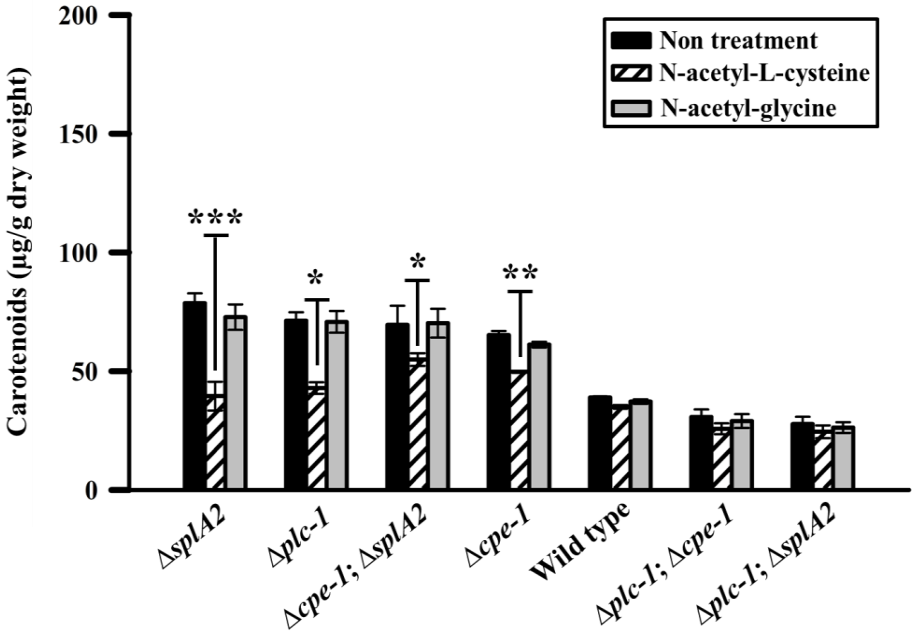

(C)

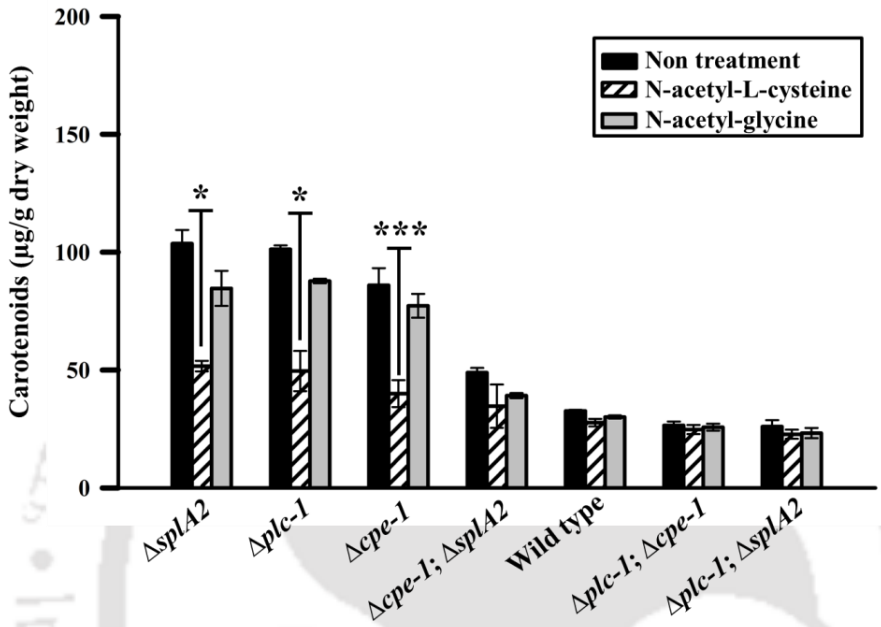

Figure 4.14: Effect of antioxidant on carotenoid accumulation in the wild type, Δ*plc-1*, Δ*splA2*, Δ*cpe-1* single and double mutant strains. Cultures were incubated for 2 h in the presence of 1 mM N-acetyl-L-cysteine (NAC), and then exposed to white light at **(A)** 8°C, **(B)** 22°C, and **(C)** 30°C for an additional 2 h. Carotenoids extracted from the indicated *N. crassa* strains are expressed as μg carotenoid per gram of dry weight. N-acetylglycine (NAG) was used as a negative control. Error bars indicate standard deviations calculated from the data for three independent experiments (n=3) with *P-values* < 0.05 (*), <0.01 (**), and < 0.001 (***) compared with the wild type strain as measured by one-way ANOVA test.

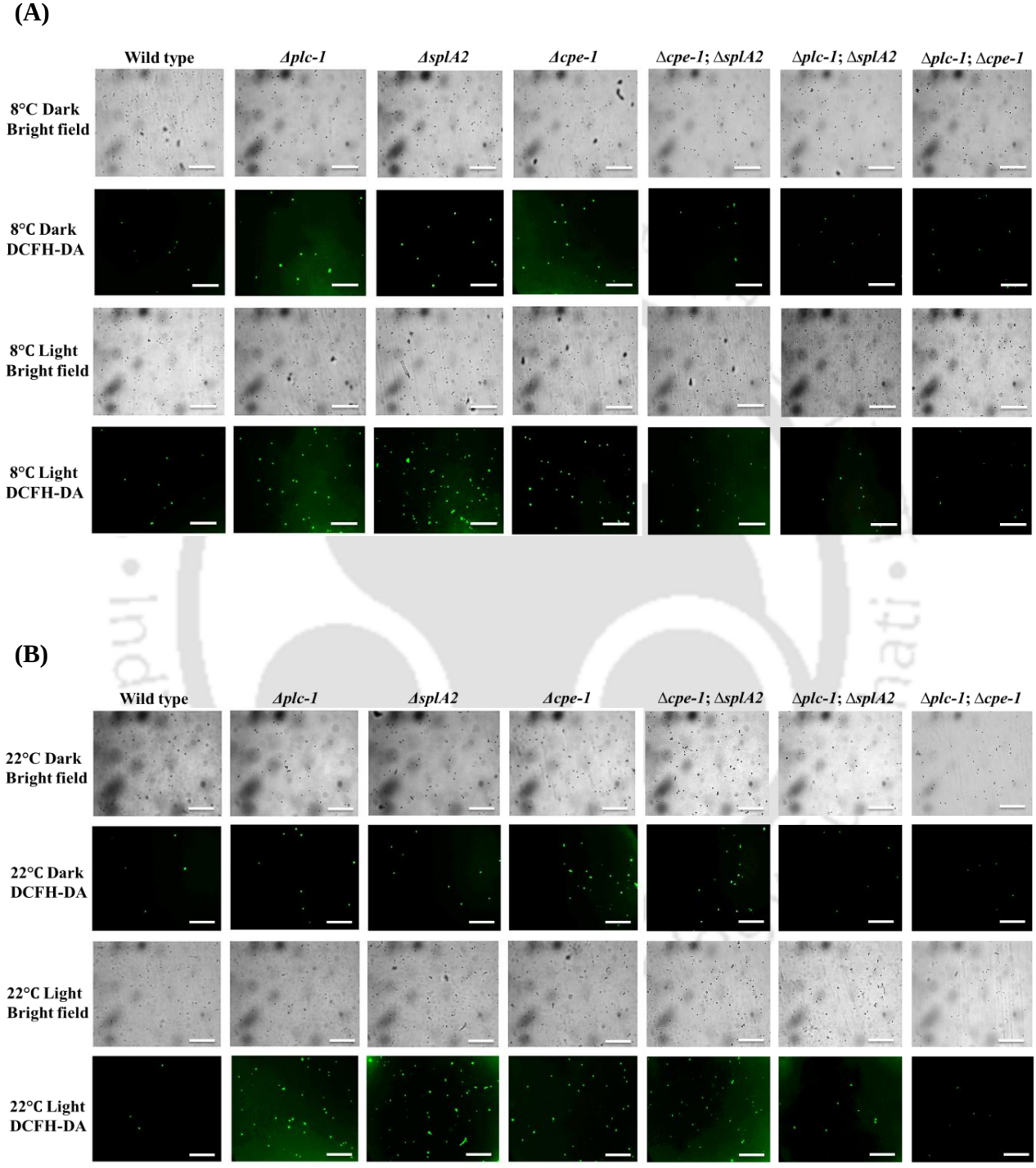

(C)

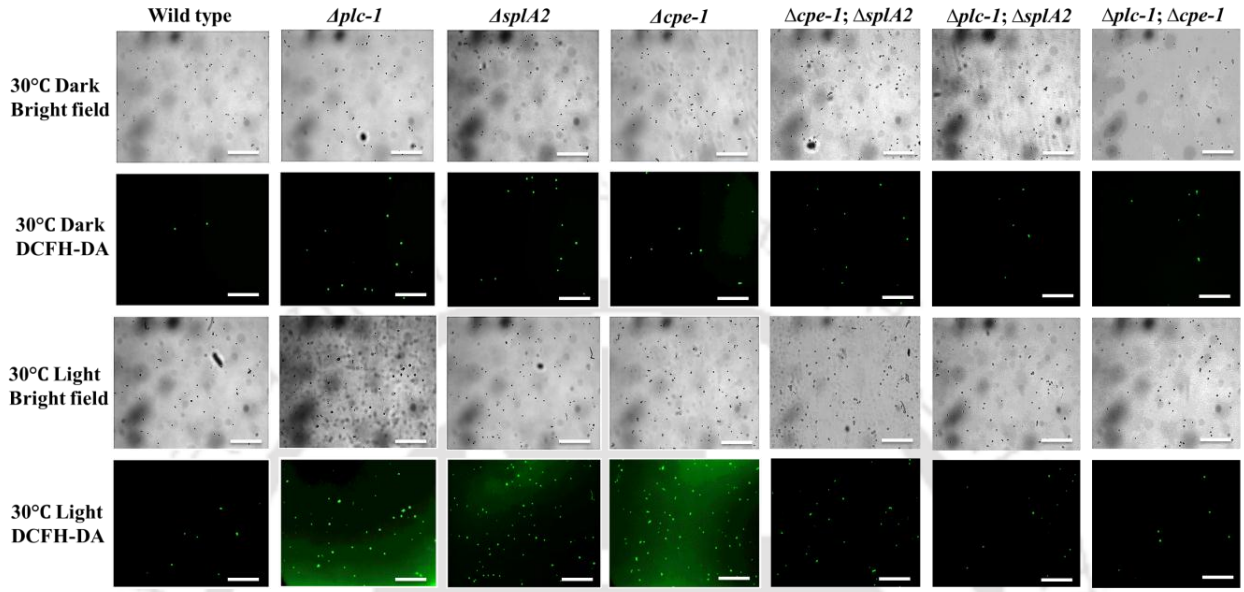

Figure 4.15: Estimation of ROS using DCFH-DA. Strains were grown in Vogel's glucose agar medium for 2 days in the dark and either exposed to white light or kept in the dark for 1 day at 8°C **(A)**, 22°C **(B)**, and 30°C **(C)**. Conidia were harvested and inoculated in Vogel's glucose medium containing 25 µM DCFH-DA for 60 min. An aliquot of the cultures was taken and observed by fluorescence microscopy. Conidia that showed green fluorescence was captured. Scale bar 20 µm.

4.2.3 Ca[l]cium sensitivity assay to test the effect of the mutations on maintaining Ca^{2+} homeostasis

4.2.3.1 Effect of increase in intracellular Ca^{2+} levels

The $[Ca^{2+}]_c$ and the Ca^{2+} gradient in fungal hyphae plays an important role in establishing and maintaining apical organization, morphogenesis, and growth (Jackson and Heath 1989). The Ca^{2+} ionophore A23187 (or Calcimycin) is a highly selective Ca^{2+} binding hydrophobic molecule (that forms a dimer complex with 2:1 stoichiometry), and facilitates Ca^{2+} transport across plasma membrane (Chapter 3; Figure 3.2 A; Chaney et al. 1974; Verma et al. 2011). The *N. crassa* Ca^{2+} signaling gene *mid-1*, a homolog of the *S. cerevisiae mating-induced death* (*MID-1*) gene, was shown to exhibit inhibited growth at elevated intracellular Ca^{2+} levels induced by the ionophore A23187 (Lew et al. 2008). I described about apical sac like structures in Δ*plc-1* and Δ*splA2*, and apical hyperbranching in Δ*cpe-1* single mutant when grown on media treated with the ionophore

A23187 in Chapter 3 (Chapter 3; Figure 3.2 B; Barman and Tamuli 2015). Here, I further studied the effect of elevated intracellular Ca^{2+} levels induced by the ionophore A23187 on hyphal morphology of the double mutants. The Δ*plc-1*; Δ*splA2* and Δ*plc-1*; Δ*cpe-1* double mutants exhibited aberrant hyphal morphology on A23187 added Vogel's glucose agar media and showed severe reduction in normal branching pattern (Figure 4.16). Another double mutant, the Δ*cpe-1*; Δ*splA2* did not show any apparent morphological defect and only showed slightly reduced branching in A23187 treated media (Figure 4.16). In all the mutants, no hyphal defect was observed in the ethanol treated control zone (Figure 4.16). Therefore, this result suggested that *plc-1*, *splA2*, and *cpe-1* genes and their interactions could be involved in maintaining $[Ca^{2+}]_c$ which in turn helps in normal *N. crassa* hyphal growth.

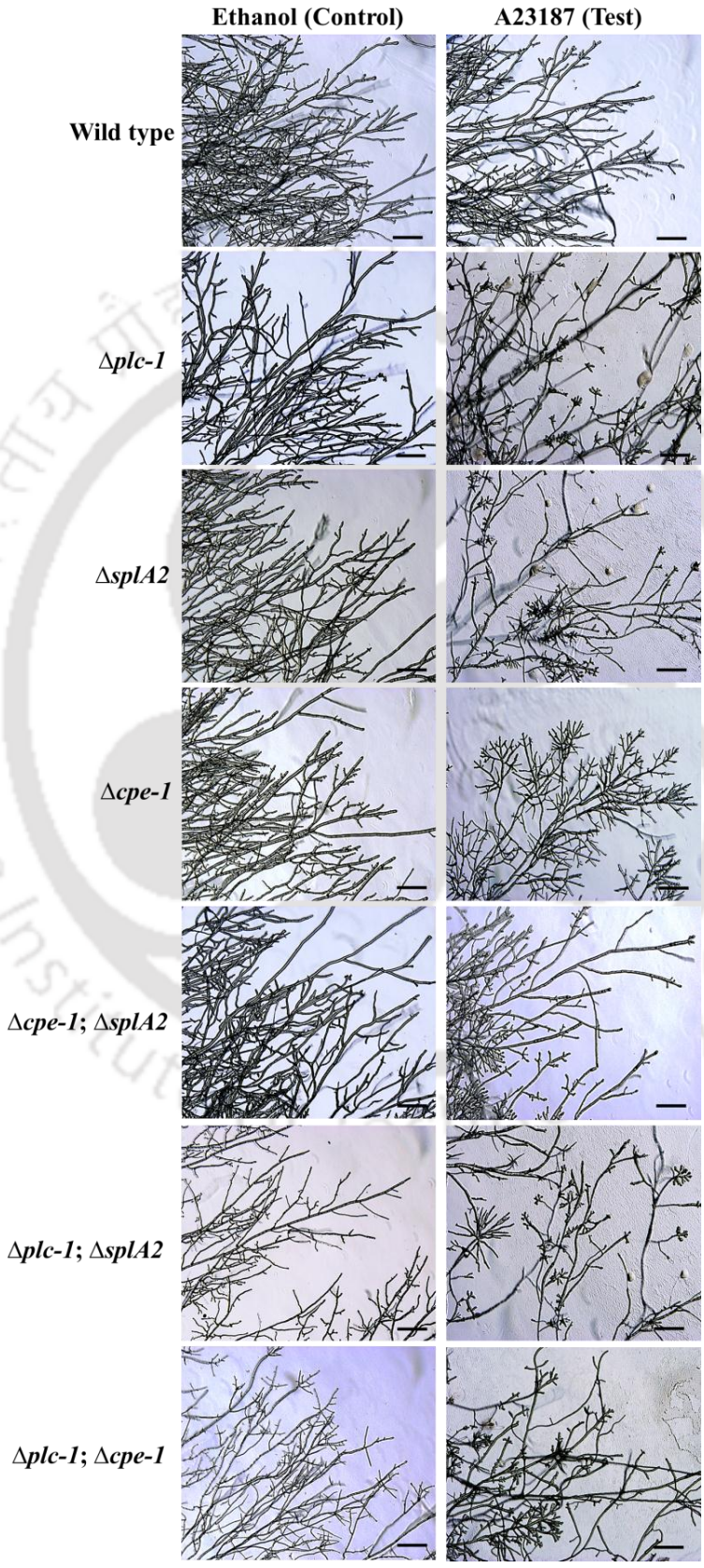

Figure 4.16 Calcium ionophore assay. The wild type, Δ*plc-1*, Δ*splA2*, Δ*cpe-1* single mutant, and double mutant strains were grown in Petri dishes containing the ionophore A23187 zone (test) and the ethanol zone (control). Images were taken when hyphae of the strains touched both the zones (38 h of growth at 30°C). Ten images were captured for each strain and a representative image is shown. Scale Bar 20 µm.

4.2.3.2 Effect of increase in extracellular Ca^{2+} levels

To test if Ca^{2+} stress tolerance is affected by the interactions of *plc-1*, *splA2-1*, and *cpe-1*, I studied sensitivity of the mutants to various concentrations of $CaCl_2$. To assay Ca^{2+}-sensitivity, I performed the growth analysis of the wild type, Δ*plc-1*, Δ*splA2*, Δ*cpe-1*, Δ*cpe-1*; Δ*splA2*, Δ*plc-1*; Δ*splA2*, and Δ*plc-1*; Δ*cpe-1* double mutants on medium supplemented with various concentrations of $CaCl_2$ (0, 0.2, 0.3, and 0.4 M). Interestingly, at 0.2 M $CaCl_2$, the growth of Δ*plc-1*; Δ*splA2* and Δ*plc-1*; Δ*cpe-1* was stimulated, however, at 0.3, and 0.4 M $CaCl_2$, growth was gradually reduced for both the double mutants (Figure 4.17). The growth of another double mutant Δ*cpe-1*; Δ*splA2* and all the individual single mutants was similar to the wild type (Figure 4.17). In addition, I also calculated the average colony growth rate by plotting colony growth rate against different concentrations of $CaCl_2$. The Δ*plc-1*; Δ*splA2* and Δ*plc-1*; Δ*cpe-1* double mutants displayed a lower colony growth rate than the wild type, all the single and Δ*cpe-1*; Δ*splA2* double mutants (Table 4.6). Therefore, interaction of *plc-1* with *splA2* and *cpe-1* might play a role in decreasing $[Ca^{2+}]_c$ by stimulating Ca^{2+} efflux to promote hyphal growth and development in *N. crassa*.

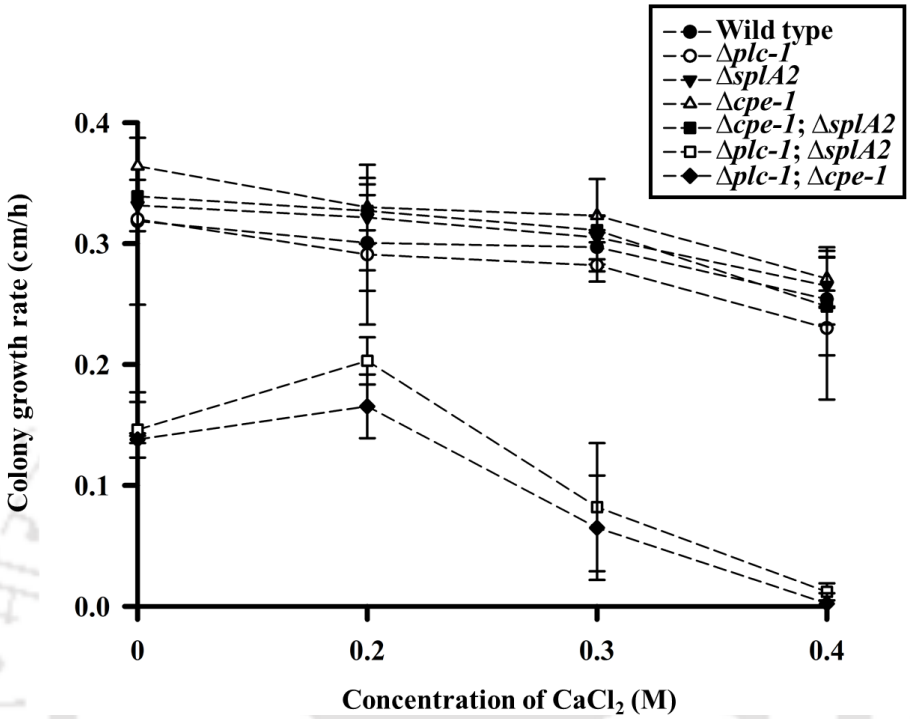

Figure 4.17 Calcium sensitivity assay. Strains were grown in Petri dishes containing Vogel's glucose agar medium supplemented with various concentrations of $CaCl_2$ (0.0, 0.2, 0.3, 0.4 M). Plates were incubated at 30ºC for 24 h. Colony growth rate (cm/h) was calculated by plotting colony growth rate against different concentrations of $CaCl_2$. Error bars indicate the standard deviations calculated from the data for three independent experiments (n=3).

Table 4.6: Average colony growth rate of the wild type, Δ*plc-1*, Δ*splA2*, Δ*cpe-1* single and double mutant strains at different concentrations of $CaCl_2$

Strains	Average colony growth rate (cm/h) at different concentrations of $CaCl_2$ (M)			
	0	**0.2**	**0.3**	**0.4**
Wild type	0.318 ± 0.069	0.301 ± 0.039	0.297 ± 0.014	0.254 ± 0.007
Δ*plc-1*	0.320 ± 0.143	0.291 ± 0.058	0.282 ± 0.005	0.230 ± 0.059
Δ*splA2*	0.332 ± 0.021	0.322 ± 0.044	0.305 ± 0.004	0.265 ± 0.032
Δ*cpe-1*	0.364 ± 0.221	0.330 ± 0.019	0.323 ± 0.003	0.271 ± 0.023
Δ*cpe-1*; Δ*splA2*	0.339 ± 0.000	0.327 ± 0.027	0.311 ± 0.042	0.248 ± 0.040
Δ*plc-1*; Δ*splA2*	0.146 ± 0.023	0.203 ± 0.019	0.082 ± 0.053	0.012 ± 0.007
Δ*plc-1*; Δ*cpe-1*	0.138 ± 0.003	0.165 ± 0.026	0.065 ± 0.043	0.002 ± 0.008

4.2.4 Osmotic sensitivity analysis

Osmotic stress that inhibits fungal growth is caused due to high concentrations of salts. In most eukaryotes, Ca^{2+} acts as one of the primary regulators of osmotic stress. There is an increase in intracellular Ca^{2+} levels during hypo-osmotic and hyper-osmotic stresses (Kader and Lindberg 2010). Therefore, I tested the growth characteristics of wild type, Δ*plc-1*, Δ*splA2*, and Δ*cpe-1* single mutants, Δ*cpe-1*; Δ*splA2*, Δ*plc-1*; Δ*splA2*, and Δ*plc-1*; Δ*cpe-1* double mutants on hyperosmotic media. In addition, to determine whether the Ca^{2+} sensitivity of the Δ*plc-1*; Δ*splA2*, and Δ*plc-1*; Δ*cpe-1* was specific to $CaCl_2$ or due to a mere sensitivity to osmotic stress, I studied the growth of the wild type, Δ*plc-1*, Δ*splA2*, Δ*cpe-1*, Δ*cpe-1*; Δ*splA2*, Δ*plc-1*; Δ*splA2*, and Δ*plc-1*; Δ*cpe-1* mutants grown on Vogel's glucose agar medium supplemented with elevated levels of KCl (Figure 4.18 A, Table 4.7), NaCl (Figure 4.18 B, Table 4.7), and sucrose (Figure 4.18 C, Table 4.7). I found that the Δ*plc-1*; Δ*splA2* and Δ*plc-1*; Δ*cpe-1* mutants were not sensitive to either KCl, NaCl, or sucrose stress. The percent apical extension rate inhibition of the Δ*plc-1*; Δ*splA2* and Δ*plc-1*; Δ*cpe-1* mutants on medium supplemented with 0.75 M KCl, 0.75 M NaCl, and 1.5 M sucrose was relatively similar to the wild type and parental single mutants. The Δ*cpe-1*; Δ*splA2* double mutant also showed similar apical extension rate inhibition as compared to wild type and parental single mutants on medium supplemented with 0.75 M KCl, 0.75 M NaCl, and 1.5 M sucrose. These results suggested that the sensitivity of Δ*plc-1*; Δ*splA2* and Δ*plc-1*; Δ*cpe-1* mutants to $CaCl_2$ stress was not due to a mere osmotic effect.

(A)

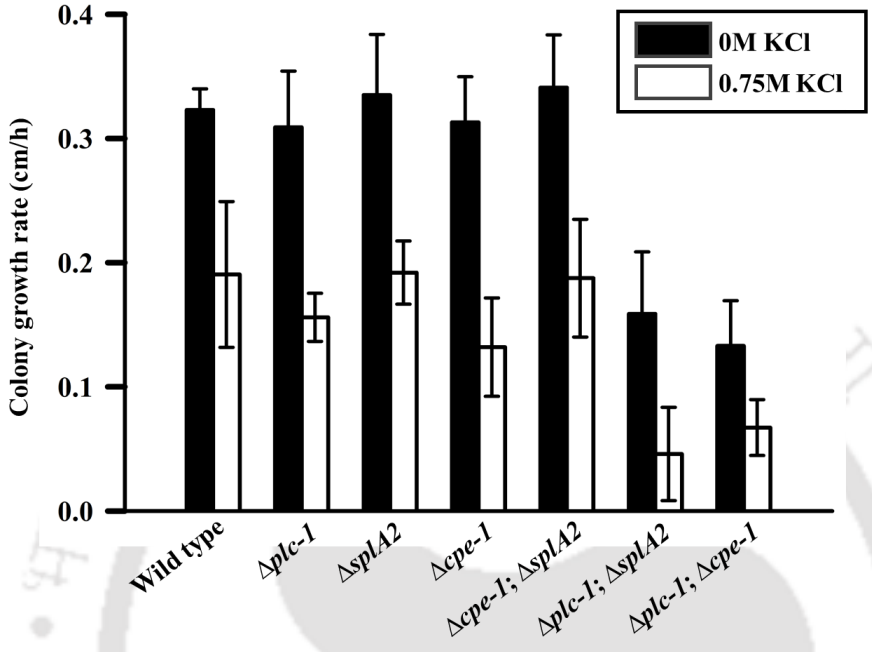

(B)

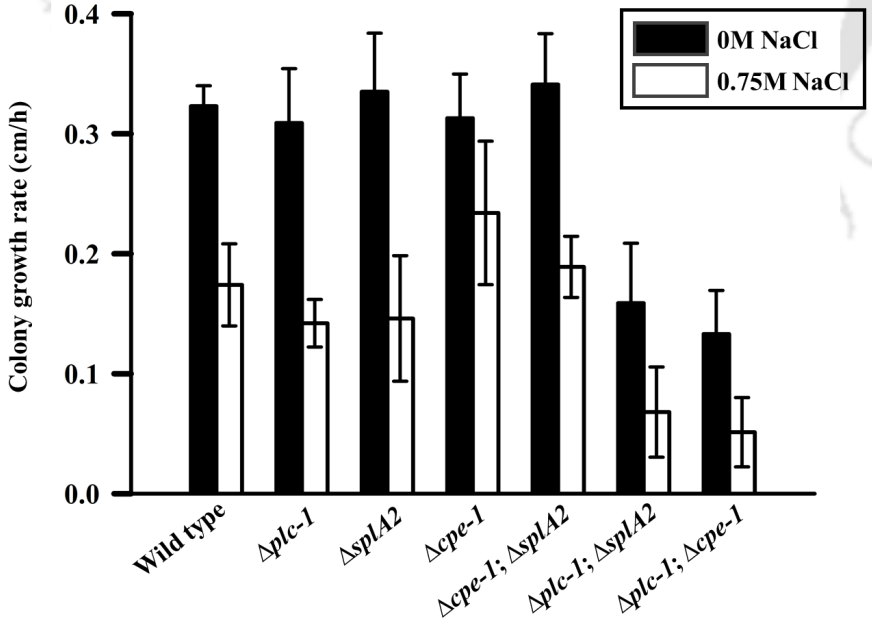

(C)

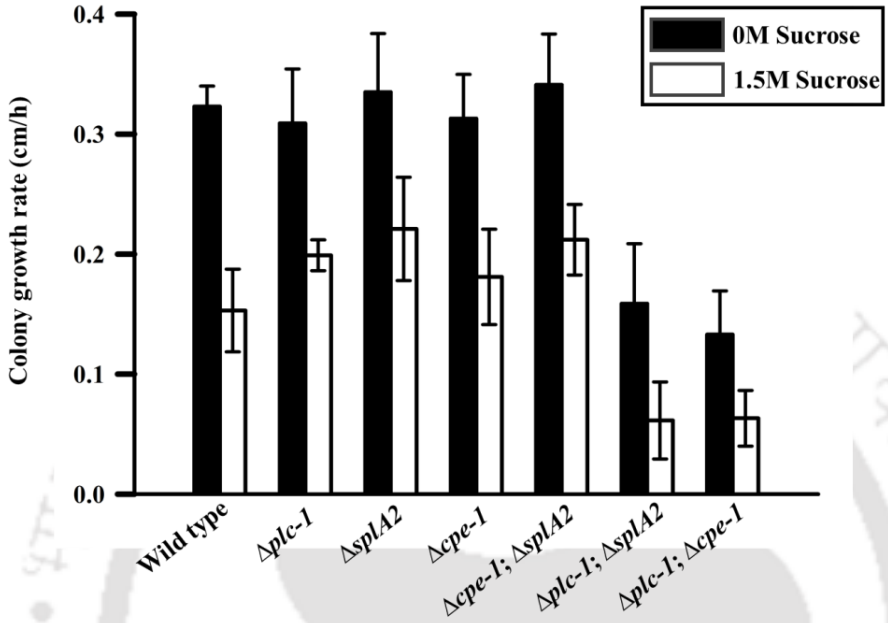

Figure 4.18: Osmotic sensitivity assay. Relative colony growth rate of the wild type, Δ*plc-1*, Δ*splA2*, Δ*cpe-1* single mutant, and double mutant strains grown on Vogel's glucose agar medium supplemented with various osmotic agents **(A)** 0.75 M KCl, **(B)** 0.75 M NaCl, and **(C)** 1.5 M sucrose. Plates were incubated at 30ºC for 24 h. Error bars indicate the standard deviations calculated from the data for three independent experiments (n=3).

Table 4.7: Average colony growth rate of the wild type, Δ*plc-1*, Δ*splA2*, Δ*cpe-1* single and double mutant strains at indicated concentrations of KCl, NaCl, and sucrose

Strains	Average colony growth rate (cm/h) at different concentrations of osmotic agents (M)			
	0 KCl/NaCl/sucrose	0.75 KCl	0.75 NaCl	1.5 M Sucrose
Wild type	0.323 ± 0.017	0.191 ± 0.058	0.174 ± 0.034	0.153 ± 0.035
Δ*plc-1*	0.3090 ± 0.0453	0.156 ± 0.019	0.142 ± 0.019	0.199 ± 0.013
Δ*splA2*	0.3350 ± 0.048	0.192 ± 0.026	0.146 ± 0.052	0.221 ± 0.043
Δ*cpe-1*	0.313 ± 0.036	0.132 ± 0.039	0.234 ± 0.059	0.181 ± 0.039
Δ*cpe-1*; Δ*splA2*	0.341 ± 0.042	0.187 ± 0.047	0.189 ± 0.025	0.212 ± 0.029
Δ*plc-1*; Δ*splA2*	0.158 ± 0.049	0.046 ± 0.038	0.068 ± 0.038	0.061 ± 0.032
Δ*plc-1*; Δ*cpe-1*	0.133 ± 0.036	0.067 ± 0.022	0.051 ± 0.029	0.063 ± 0.023

4.2.5 Temperature sensitivity analysis

In *N. crassa*, development occurs in response to various environmental stimuli and stressors (Ivey et al. 2002). Apart from light and abundant nutrients, temperature is also an important environmental cue for vegetative growth followed by hyphal extension and fusion to form the multicellular mycelium, and accumulation of mycelial carotenoids in *N. crassa* (Springer 1993). While vegetative growth occurs in normal ambient temperature, the sexual development occurs at lower temperature. The Δ*plc-1*; Δ*splA2* and Δ*plc-1*; Δ*cpe-1* double mutants showed numerous phenotypes including colonial growth, stunted aerial hyphae, reduced carotenoid accumulation, and female sterility (Figures 4.2, 4.6, 4.11, and 4.23). Since the growth rates of Δ*plc-1*; Δ*splA2* and Δ*plc-1*; Δ*cpe-1* double mutants were significantly slower than the wild type and the single mutants at normal 30°C ambient temperature (Figure 4.3), I also determined growth rate of the strains at lower (20°C) and elevated (40°C) temperatures. To perform the temperature sensitivity assay, mycelial plugs of the wild type, single, and double mutant strains were inoculated at the center of Petri dishes containing Vogel's glucose agar medium and incubated at 20, 30, and 40°C for 24 h. The hyphal growth front was marked after 12 h and then periodically marked after every 3 h till 24 h. The Δ*plc-1*; Δ*splA2* and Δ*plc-1*; Δ*cpe-1* double mutants showed decreased colony growth rate at all the three temperatures in comparison to the wild type, individual single, and the

Δ*cpe-1*; Δ*splA2* double mutant (Figure 4.19; Table 4.8). Therefore, genetic interaction of *plc-1* with *splA2* and *cpe-1* plays a key role in normal vegetative growth in *N. crassa*.

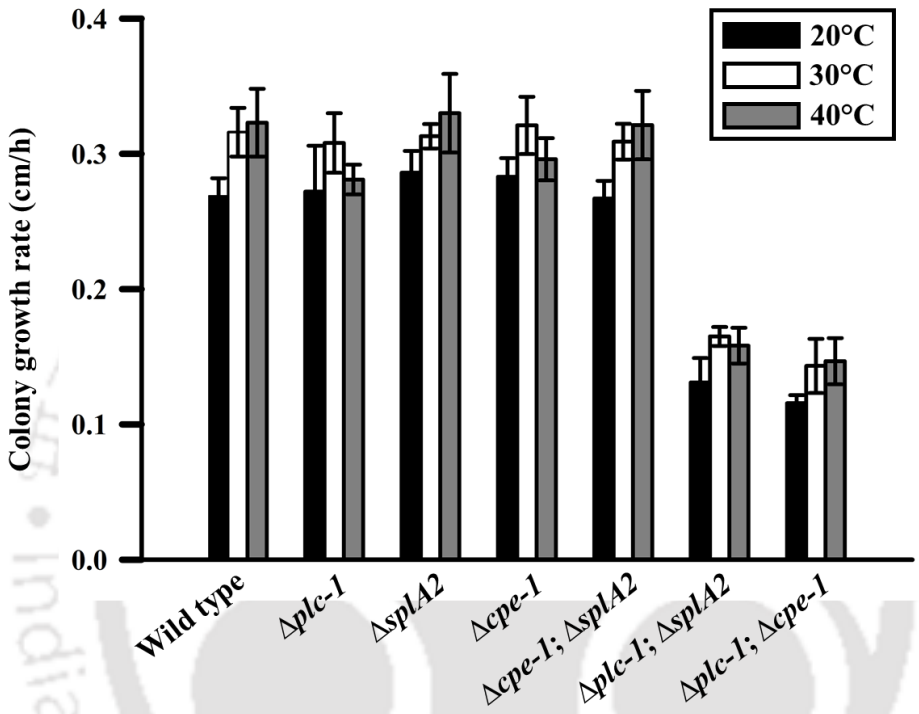

Figure 4.19: Temperature sensitivity assay. Relative colony growth rate of the wild type, the Δ*plc-1*, Δ*splA2*, Δ*cpe-1* single and double mutant strains grown on Vogel's glucose agar medium and incubated at 20, 30, and 40ºC for 24 h. Error bars indicate the standard deviations calculated from the data for three independent experiments (n=3).

Table 4.8: Average colony growth rate of the wild type, Δ*plc-1*, Δ*splA2*, Δ*cpe-1* single and double mutant strains at three different temperatures

Strains	Average colony growth rate (cm/h)		
	20°C	30°C	40°C
Wild type	0.269 ± 0.013	0.316 ± 0.018	0.323 ± 0.025
Δ*plc-1*	0.272 ± 0.034	0.308 ± 0.022	0.281 ± 0.011
Δ*splA2*	0.286 ± 0.016	0.313 ± 0.009	0.330 ± 0.029
Δ*cpe-1*	0.283 ± 0.014	0.321 ± 0.021	0.296 ± 0.016
Δ*cpe-1*; Δ*splA2*	0.267 ± 0.013	0.309 ± 0.013	0.321 ± 0.025
Δ*plc-1*; Δ*splA2*	0.131 ± 0.018	0.165 ± 0.007	0.158 ± 0.013
Δ*plc-1*; Δ*cpe-1*	0.116 ± 0.006	0.143 ± 0.020	0.146 ± 0.017

4.2.6 Oxidative stress and thermotolerance assay

I also determined the viability of Δ*plc-1*; Δ*splA2* and Δ*plc-1*; Δ*cpe-1* double mutants in exposure to H_2O_2 induced oxidative stress. The Δ*plc-1*, Δ*splA2*, and Δ*cpe-1* single mutants were previously found sensitive to the H_2O_2 induced oxidative stress (Chapter 3; Figure 3.10; Table 3.4). I also found that the Δ*plc-1*; Δ*splA2* and Δ*plc-1*; Δ*cpe-1* double mutants showed a decreased survival percentage than the wild type after exposure to H_2O_2, however, survival percentage of both the double mutants was similar to their parental single mutants (Figure 4.20; Table 4.9). The survival percentage of Δ*cpe-1*; Δ*splA2* double mutant was similar to wild type strain (Figure 4.20; Table 4.9).

Loss of *plc-1*, *splA2*, and *cpe-1* genes were previously shown to have lower levels of induced thermotolerance than wild type (Chapter 3; Figure 3.12). Additionally, I studied the ability of Δ*plc-1*; Δ*splA2* and Δ*plc-1*; Δ*cpe-1* double mutants in acquisition of induced thermotolerance. Both the Δ*plc-1*; Δ*splA2* and Δ*plc-1*; Δ*cpe-1* double mutants showed severe reduction in survival percentage in both induced and uninduced thermotolerance conditions as compared to parental single mutants (Figure 4.21; Table 4.10). However, survival percentage of Δ*cpe-1*; Δ*splA2* double mutant at heat shock temperature was comparable to the wild type (Figure 4.21; Table 4.10). It was shown previously that the pre exposure of *N. crassa* germinating spores to 44°C induces synthesis of heat shock proteins and subsequently protects spores from lethal heat shock 52°C temperature (Kapoor et al. 1995; Yang and Borkovich 1999). Therefore, interaction of *plc-1* with

splA2 and *plc-1* with *cpe-1* might play an essential role in acquisition of induced thermotolerance at heat shock temperatures.

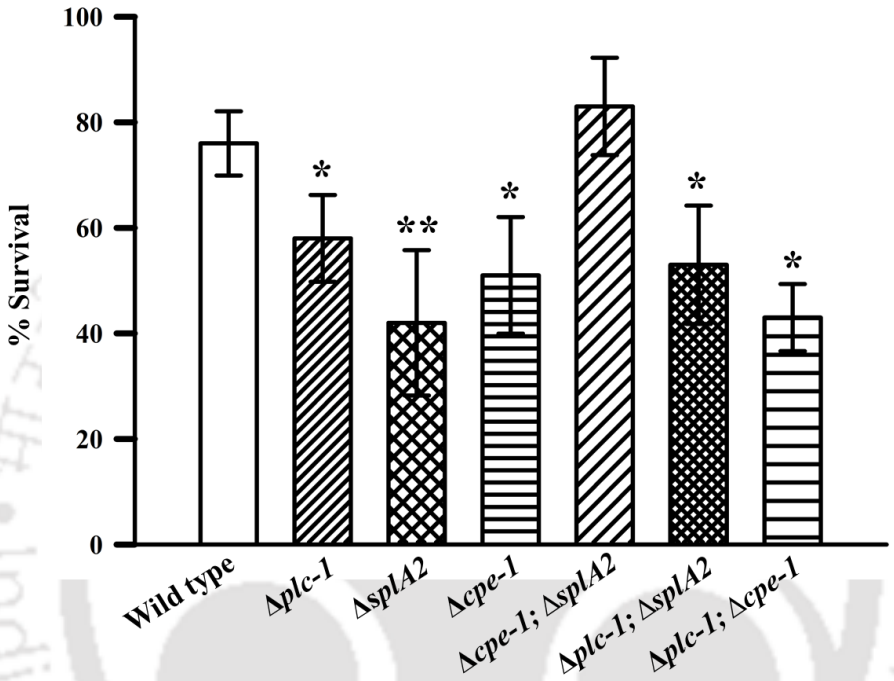

Figure 4.20: Oxidative stress assay. Germlings (2 h old) of the wild type, Δ*plc-1*, Δ*splA2*, Δ*cpe-1* single mutant, and double mutant strains were incubated in medium containing 10 mM H_2O_2 at 30°C and percent survival was determined. Error bars indicate the standard deviations calculated from the data for three independent experiments (n=3). Statistically significant values are indicated by asterisks, **P*<0.05, ***P*<0.01, ****P*<0.001.

Table 4.9: Percent survival of the wild type, Δ*plc-1*, Δ*splA2*, Δ*cpe-1* single and double mutant strains at 10 mM H_2O_2

Strains	Percent survival (%)	
	0 mM H_2O_2	10 mM H_2O_2
Wild type	100 ± 0	76 ± 6.10
Δ*plc-1*	100 ± 0	58 ± 8.22
Δ*splA2*	100 ± 0	42 ± 13.77
Δ*cpe-1*	100 ± 0	51 ± 11.04
Δ*cpe-1*; Δ*splA2*	100 ± 0	83 ± 9.23
Δ*plc-1*; Δ*splA2*	100 ± 0	53 ± 11.21
Δ*plc-1*; Δ*cpe-1*	100 ± 0	43 ± 6.36

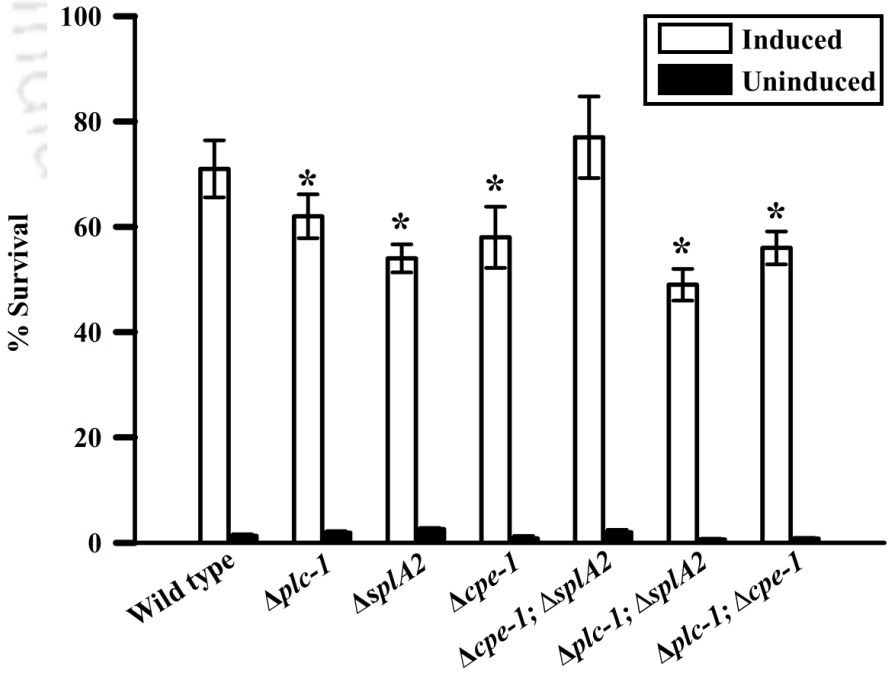

Figure 4.21: Thermotolerance assay. Viability of 2 h old germlings of the wild type, Δ*plc-1*, Δ*splA2*, Δ*cpe-1* single mutant, and double mutant strains after exposure to 52°C lethal temperature with (induced) or without (uninduced) pre-exposure to a sublethal heat shock temperature of 44°C. Error bars indicate the standard deviations calculated from the data for three independent

experiments (n=3). Statistically significant values are indicated by asterisks, *P<0.05, **P<0.01, ***P<0.001.

Table 4.10: Percent survival of the wild type, Δ*plc-1*, Δ*splA2*, Δ*cpe-1* single and double mutant strains in induced and uninduced temperatures

Strains	Percent survival (%)	
	Induced (44°C)	**Uninduced (30°C)**
Wild type	71 ± 5.42	1.30 ± 0.31
Δ*plc-1*	62 ± 4.16	1.90 ± 0.31
Δ*splA2*	54 ± 2.66	2.60 ± 0.22
Δ*cpe-1*	58 ± 5.81	0.82 ± 0.48
Δ*cpe-1*; Δ*splA2*	77 ± 7.74	2.00 ± 0.46
Δ*plc-1*; Δ*splA2*	49 ± 3.01	0.61 ± 0.16
Δ*plc-1*; Δ*cpe-1*	56 ± 3.12	0.77 ± 0.18

4.2.7 UV sensitivity analysis

In Chapter 3, I described the UV-protective role of *plc-1*, *splA2*, and *cpe-1* genes linked to higher carotenoid accumulation (Chapter 3; Figure 3.16). In this chapter, I tested the sensitivity of the double mutants and the parental single mutants to UV irradiation. The Δ*plc-1*; Δ*splA2* and Δ*plc-1*; Δ*cpe-1* double mutants showed an increased sensitivity to UV as compared to wild type and the parental single mutants (Figure 4.22; Table 4.11). However, the Δ*cpe-1*; Δ*splA2* double mutant was more tolerant to UV than either of the parental single mutants (Figure 4.22; Table 4.11). Therefore, these results suggested that interactions of *plc-1* with *splA2* and *cpe-1* affect UV survival in *N. crassa*.

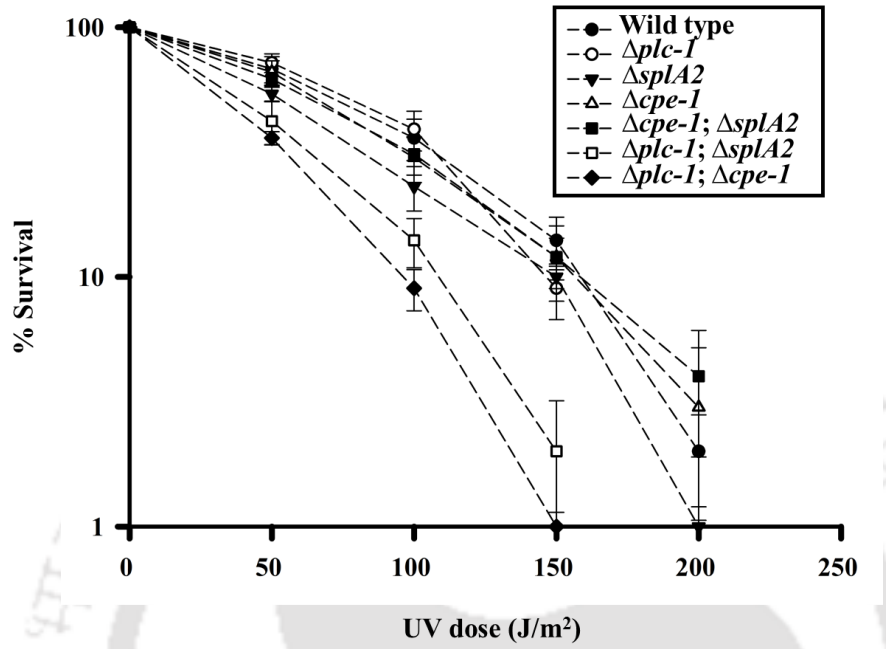

Figure 4.22: UV sensitivity assay. Dose response curves of the wild type, Δ*plc-1*, Δ*splA2*, Δ*cpe-1* single mutant, and double mutant strains after exposure to different doses of UV radiation. Each data point represents the mean of atleast three independent experiments (n=3).

Table 4.11: Relative UV sensitivity of the wild type, Δ*plc-1*, Δ*splA2*, Δ*cpe-1* single and double mutant strains

Strains	Percent survival (%) at indicated UV doses (J/m^2)					
	0	**50**	**100**	**150**	**200**	**250**
Wild type	100 ± 0.00	68 ± 8.17	36 ± 6.81	14 ± 3.33	2 ± 0.80	0 ± 0.00
Δ*plc-1*	100 ± 0.00	72 ± 6.20	39 ± 7.07	9 ± 2.26	0 ± 0.00	0 ± 0.00
Δ*splA2*	100 ± 0.00	54 ± 3.47	23 ± 4.64	10 ± 1.03	1 ± 0.06	0 ± 0.00
Δ*cpe-1*	100 ± 0.00	66 ± 7.37	30 ± 6.13	12 ± 4.01	3 ± 2.22	0 ± 0.00
Δ*cpe-1*; Δ*splA2*	100 ± 0.00	62 ± 3.81	31 ± 5.43	12 ± 2.28	4 ± 2.10	0 ± 0.00
Δ*plc-1*; Δ*splA2*	100 ± 0.00	42 ± 8.26	14 ± 3.13	2 ± 1.19	0 ± 0.00	0 ± 0.00
Δ*plc-1*; Δ*cpe-1*	100 ± 0.00	36 ± 2.14	9 ± 1.69	1 ± 0.14	0 ± 0.00	0 ± 0.00

4.2.8 The Δ*plc-1*; Δ*splA2* and Δ*plc-1*; Δ*cpe-1* double mutants were female sterile

I next evaluated the role of *plc-1*, *splA2*, and *cpe-1* genes in sexual development of *N. crassa*. The sexual development in *N. crassa* is initiated by the formation of specialized multicellular female reproductive structures termed protoperithecia in response to low levels of nitrogen, light, and low temperature (Perkins and Barry 1977; Nelson and Metzenberg 1992; Nelson 1996; Coppin et al. 1997). The chemotropic polarized growth of female specific specialized hyphae called trichogynes towards male cells (vegetative cells of opposite mating type) results in fertilization, a process mediated by pheromones, and forms perithecia (fertilized protoperithecia) that encloses multiple asci each containing eight ordered ascospores (Raju 1992; Kim and Borkovich 2006). To assay fertility, I cultured the female parent on synthetic crossing medium with low nitrogen content at room temperature, incubated under constant light for seven days, and subsequently fertilized with the male parent. After seven days of post-fertilization, I observed the crossing plates under the microscope and harvested the ascospores produced. Loss of the *plc-1*, *splA2*, and *cpe-1* genes did not affect the sexual cycle, and crosses involving the Δ*plc-1*, Δ*splA2*, and Δ*cpe-1* single mutants either as male or female parent with the wild type strains of opposite mating type were fully fertile (Figure 4.23 A-B; Table 4.12). In contrast, crosses involving the Δ*plc-1*; Δ*splA2* and Δ*plc-1*; Δ*cpe-1* double mutants as the female parent with the respective double or parental single mutants and wild type strains of opposite mating type as the male parent showed complete absence of perithecia and resulted in a sterile phenotype (Figure 4.23 A; Table 4.12). However, crosses involving the Δ*plc-1*; Δ*splA2* and Δ*plc-1*; Δ*cpe-1* double mutant as a male parent were fertile and showed matured perithecia with abundant ascospores (Figure 4.23 B; Table 4.12). Another double mutant, the Δ*cpe-1*; Δ*splA2* did not show any defect in sexual cycle and crosses involving the Δ*cpe-1*; Δ*splA2* either as male or female parent were fully fertile and formed normal perithecia with abundant ascospores (Figure 4.23 A-B; Table 4.12). I also examined survival score of the ascospores produced from the different crosses. The ascospores produced from crosses of Δ*plc-1*, Δ*splA2*, Δ*cpe-1*, and Δ*cpe-1*; Δ*splA2* as a male or female parent and Δ*plc-1*; Δ*splA2* and Δ*plc-1*; Δ*cpe-1* double mutants as a male parent had a similar survival percentage like the ascospores produced in the crosses involving the wild types (Figure 4.24; Table 4.13). Therefore, these results indicated that genetic interaction of *plc-1* with *splA2* and *cpe-1* plays a critical role in normal sexual development in *N. crassa*.

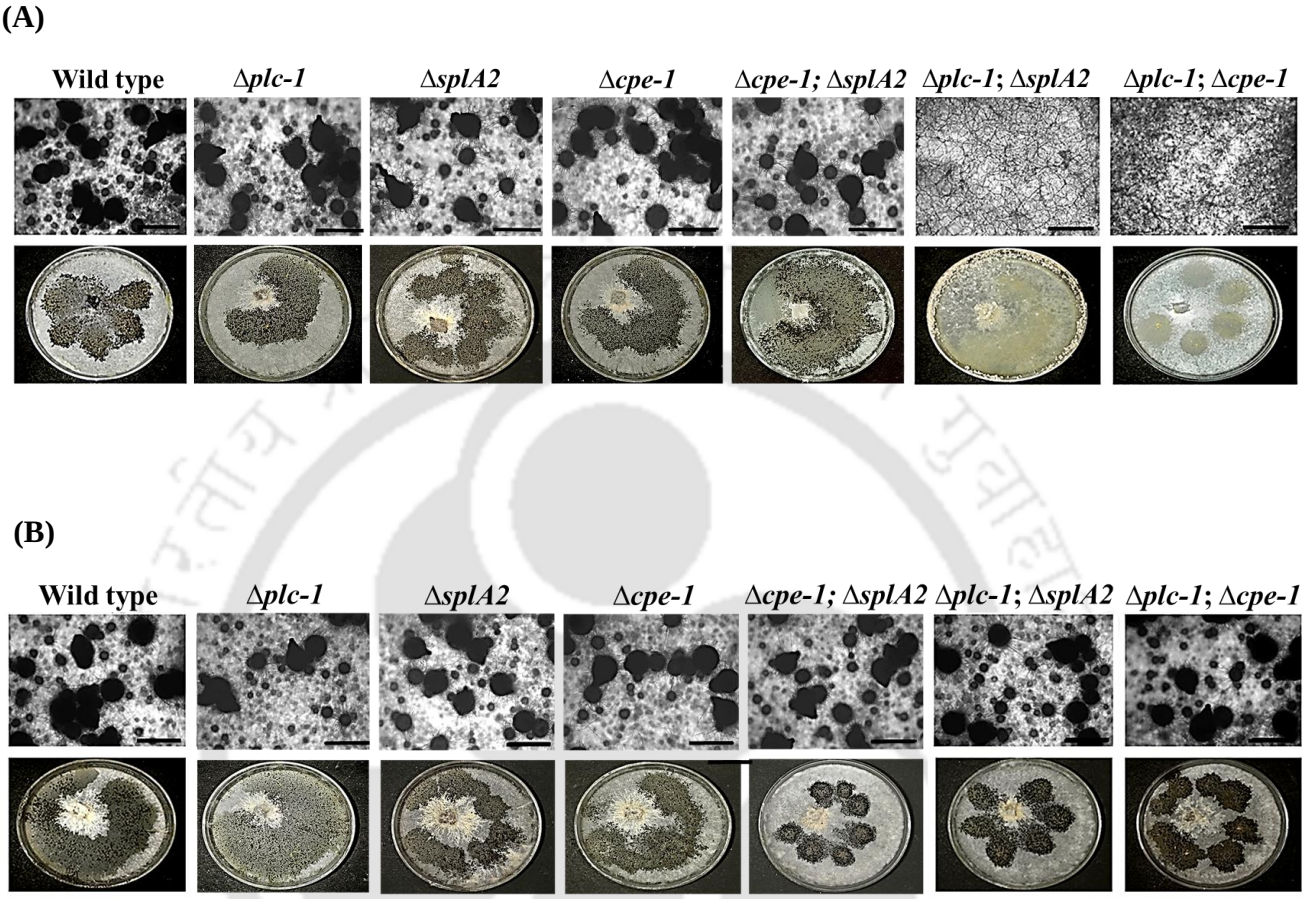

Figure 4.23: Sexual fertility assay of the wild type, Δ*plc-1*, Δ*splA2*, Δ*cpe-1* single and double mutant strains. Strains were cultured on synthetic crossing agar medium (SCM) at room temperature with constant light for seven days and subsequently fertilized with wild type (74 A or 74 a) conidia. **(A)** Absence of perithecia in the SCM cultures of Δ*plc-1*; Δ*splA2* and Δ*plc-1*; Δ*cpe-1* strains when inoculated as female parent. **(B)** Black enlarged perithecia with matured ascospores were seen in SCM cultures of Δ*plc-1*; Δ*splA2* and Δ*plc-1*; Δ*cpe-1* strains when inoculated as male parent. Scale bar 20 µm.

Table 4.12: Sexual fertility of the wild type, Δ*plc-1*, Δ*splA2*, Δ*cpe-1* single and double mutant strains

Sl.No.	Female Parent	Male Parent	Perithecia formed	Ascospores produced	Phenotype
1	OR A	OR a	Yes	Abundant	Fertile
2	OR a	OR A	Yes	Abundant	Fertile
3	Δ*plc-1::hph A*	OR a	Yes	Abundant	Fertile
4	Δ*plc-1::hph a*	OR A	Yes	Abundant	Fertile
5	Δ*splA2::hph A*	OR a	Yes	Abundant	Fertile
6	Δ*splA2::hph a*	OR A	Yes	Abundant	Fertile
7	Δ*cpe-1::hph A*	OR a	Yes	Abundant	Fertile
8	Δ*cpe-1::hph a*	OR A	Yes	Abundant	Fertile
9	Δ*cpe-1::hph*; Δ*splA2::hph A*	OR a	Yes	Abundant	Fertile
10	Δ*cpe-1::hph*; Δ*splA2::hph a*	OR A	Yes	Abundant	Fertile
11	Δ*plc-1::hph*; Δ*splA2::hph A*	OR a	No	None	Sterile
12	Δ*plc-1::hph*; Δ*splA2::hph a*	OR A	No	None	Sterile
13	Δ*plc-1::hph*; Δ*cpe-1::hph A*	OR a	No	None	Sterile
14	Δ*plc-1::hph*; Δ*cpe-1::hph a*	OR A	No	None	Sterile
15	Δ*plc-1::hph A*	Δ*plc-1::hph a*	Yes	Abundant	Fertile
16	Δ*plc-1::hph a*	Δ*plc-1::hph A*	Yes	Abundant	Fertile
17	Δ*splA2::hph A*	Δ*splA2::hph a*	Yes	Abundant	Fertile
18	Δ*splA2::hph a*	Δ*splA2::hph A*	Yes	Abundant	Fertile
19	Δ*cpe-1::hph A*	Δ*cpe-1::hph a*	Yes	Abundant	Fertile
20	Δ*cpe-1::hph a*	Δ*cpe-1::hph A*	Yes	Abundant	Fertile
21	Δ*cpe-1::hph*; Δ*splA2::hph A*	Δ*cpe-1::hph*; Δ*splA2::hph a*	Yes	Abundant	Fertile
22	Δ*cpe-1::hph*; Δ*splA2::hph a*	Δ*cpe-1::hph*; Δ*splA2::hph A*	Yes	Abundant	Fertile
23	Δ*plc-1::hph*; Δ*splA2::hph A*	Δ*plc-1::hph*; Δ*splA2::hph a*	No	None	Sterile
24	Δ*plc-1::hph*; Δ*splA2::hph a*	Δ*plc-1::hph*; Δ*splA2::hph A*	No	None	Sterile
25	Δ*plc-1::hph*; Δ*cpe-1::hph A*	Δ*plc-1::hph*; Δ*cpe-1::hph a*	No	None	Sterile
26	Δ*plc-1::hph*; Δ*cpe-1::hph a*	Δ*plc-1::hph*; Δ*cpe-1::hph A*	No	None	Sterile

27	Δ*cpe-1::hph*; Δ*splA2::hph A*	Δ*cpe-1::hph a*	Yes	Abundant	Fertile
28	Δ*cpe-1::hph a*	Δ*cpe-1::hph*; Δ*splA2::hph A*	Yes	Abundant	Fertile
29	Δ*cpe-1::hph*; Δ*splA2::hph a*	Δ*cpe-1::hph A*	Yes	Abundant	Fertile
30	Δ*cpe-1::hph A*	Δ*cpe-1::hph*; Δ*splA2::hph a*	Yes	Abundant	Fertile
31	Δ*cpe-1::hph*; Δ*splA2::hph A*	Δ*splA2::hph a*	Yes	Abundant	Fertile
32	Δ*splA2::hph a*	Δ*cpe-1::hph*; Δ*splA2::hph A*	Yes	Abundant	Fertile
33	Δ*cpe-1::hph*; Δ*splA2::hph a*	Δ*splA2::hph A*	Yes	Abundant	Fertile
34	Δ*splA2::hph A*	Δ*cpe-1::hph*; Δ*splA2::hph a*	Yes	Abundant	Fertile
35	Δ*plc-1::hph*; Δ*splA2::hph A*	Δ*plc-1::hph a*	No	None	Sterile
36	Δ*plc-1::hph a*	Δ*plc-1::hph*; Δ*splA2::hph A*	Yes	Abundant	Fertile
37	Δ*plc-1::hph*; Δ*splA2::hph a*	Δ*plc-1::hph A*	No	None	Sterile
38	Δ*plc-1::hph A*	Δ*plc-1::hph*; Δ*splA2::hph a*	Yes	Abundant	Fertile
39	Δ*plc-1::hph*; Δ*splA2::hph A*	Δ*splA2::hph a*	No	None	Sterile
40	Δ*splA2::hph a*	Δ*plc-1::hph*; Δ*splA2::hph A*	Yes	Abundant	Fertile
41	Δ*plc-1::hph*; Δ*splA2::hph a*	Δ*splA2::hph A*	No	None	Sterile
42	Δ*splA2::hph A*	Δ*plc-1::hph*; Δ*splA2::hph a*	Yes	Abundant	Fertile
43	Δ*plc-1::hph*; Δ*cpe-1::hph A*	Δ*plc-1::hph a*	No	None	Sterile
44	Δ*plc-1::hph a*	Δ*plc-1::hph*; Δ*cpe-1::hph A*	Yes	Abundant	Fertile
45	Δ*plc-1::hph*; Δ*cpe-1::hph a*	Δ*plc-1::hph A*	No	None	Sterile
46	Δ*plc-1::hph A*	Δ*plc-1::hph*; Δ*cpe-1::hph a*	Yes	Abundant	Fertile
47	Δ*plc-1::hph*; Δ*cpe-1::hph A*	Δ*cpe-1::hph a*	No	None	Sterile
48	Δ*cpe-1::hph a*	Δ*plc-1::hph*; Δ*cpe-1::hph A*	Yes	Abundant	Fertile
49	Δ*plc-1::hph*; Δ*cpe-1::hph a*	Δ*cpe-1::hph A*	No	None	Sterile
50	Δ*cpe-1::hph A*	Δ*plc-1::hph*; Δ*cpe-1::hph a*	Yes	Abundant	Fertile
51	OR a	Δ*plc-1::hph A*	Yes	Abundant	Fertile
52	OR A	Δ*plc-1::hph a*	Yes	Abundant	Fertile
53	OR a	Δ*splA2::hph A*	Yes	Abundant	Fertile
54	OR A	Δ*splA2::hph a*	Yes	Abundant	Fertile
55	OR a	Δ*cpe-1::hph A*	Yes	Abundant	Fertile
56	OR A	Δ*cpe-1::hph a*	Yes	Abundant	Fertile
57	OR a	Δ*cpe-1::hph*; Δ*splA2::hph A*	Yes	Abundant	Fertile

58	OR A	Δ*cpe-1::hph*; Δ*splA2::hph a*	Yes	Abundant	Fertile
59	OR a	Δ*plc-1::hph*; Δ*splA2::hph A*	Yes	Abundant	Fertile
60	OR A	Δ*plc-1::hph*; Δ*splA2::hph a*	Yes	Abundant	Fertile
61	OR a	Δ*plc-1::hph*; Δ*cpe-1::hph A*	Yes	Abundant	Fertile
62	OR A	Δ*plc-1::hph*; Δ*cpe-1::hph a*	Yes	Abundant	Fertile

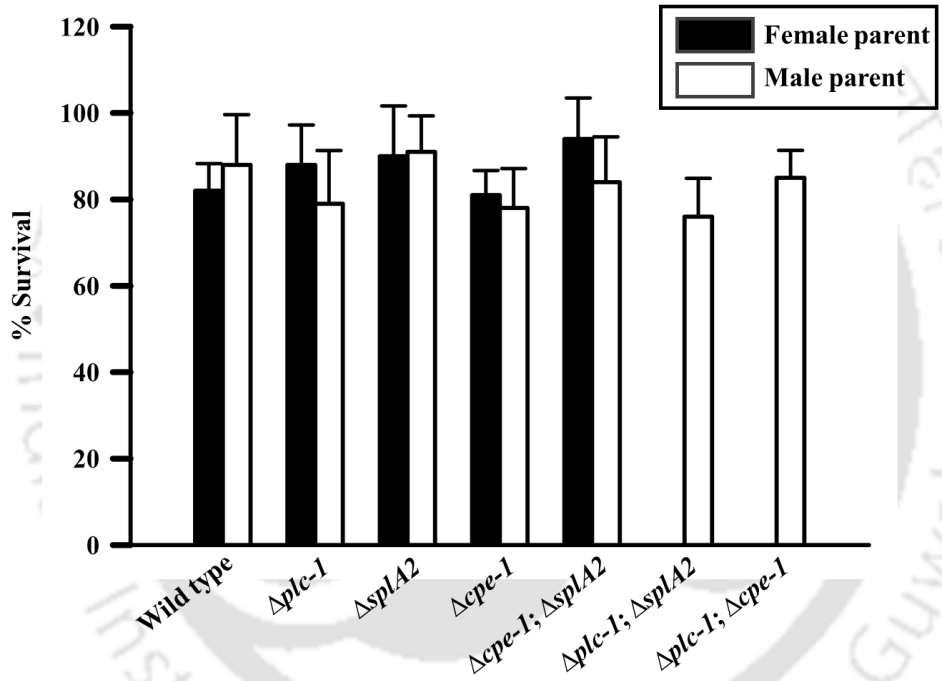

Figure 4.24: Survival percentage of the ascospores of the wild type, Δ*plc-1*, Δ*splA2*, Δ*cpe-1* single and double mutant strains. Ascospores of the strains were germinated on Petri dishes containing Vogel's sorbose agar medium after heat shock at 60°C for 50 min. Germination of ascospores was observed under the microscope after 12 h and percent survival was determined. Error bars indicate standard deviations calculated from the data for three independent experiments (n=3).

Table 4.13: Percent survival of the ascospores of the wild type, Δ*plc-1*, Δ*splA2*, Δ*cpe-1* single and double mutant strains

Strains	Percent survival (%) female parent	Percent survival (%) male parent
Wild type	82 ± 6.29	88 ± 11.63
Δ*plc-1*	88 ± 9.22	79 ± 12.31
Δ*splA2*	90 ± 11.62	91 ± 8.34
Δ*cpe-1*	81 ± 5.68	78 ± 9.13
Δ*cpe-1*; Δ*splA2*	94 ± 9.47	84 ± 10.48
Δ*plc-1*; Δ*splA2*	0 ± 0.00	76 ± 8.88
Δ*plc-1*; Δ*cpe-1*	0 ± 0.00	85 ± 6.36

4.2.8.2 Analysis of promoter region of the *plc-1*, *splA2*, and *cpe-1* genes

Transcription factor binding elements are known to regulate the expression of a gene, therefore, I analyzed the transcription factor binding sites in the putative promoter regions of the *plc-1*, *splA2*, and *cpe-1* genes using the MatInspector program (Quandt et al. 1995). In the promoter regions of the *plc-1*, *splA2*, and *cpe-1* genes, I found putative binding sequences for several transcription factors including pheromone response elements, yeast cell cycle and metabolic regulator, yeast mating factors, and yeast stress response elements (Figure 4.25; Table 4.14). Presence of these regulatory sequences further supported the hypothesis that the *plc-1*, *splA2*, and *cpe-1* are required during the sexual development in *N. crassa*.

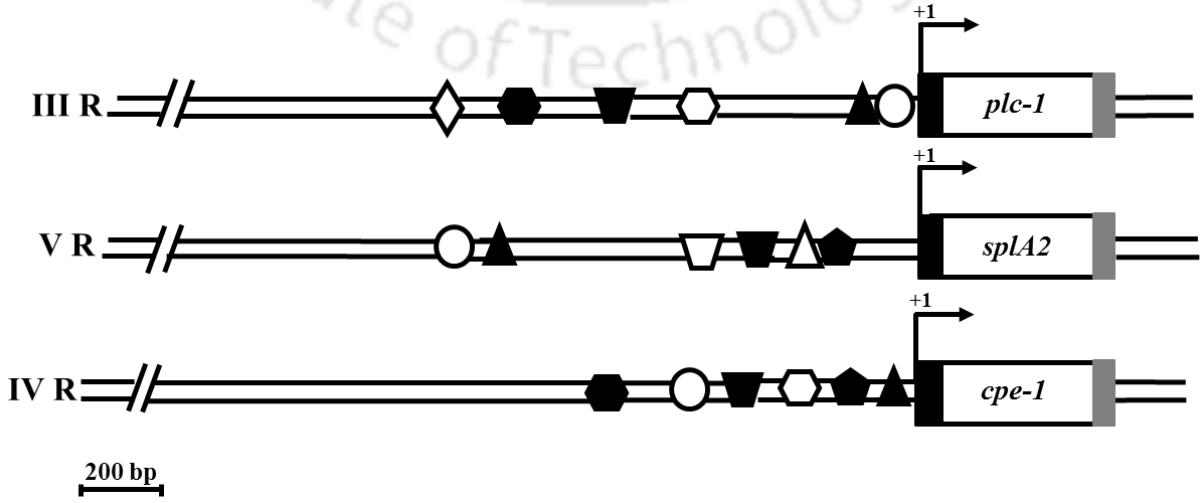

Figure 4.25: Transcription regulators of the *plc-1*, *splA2*, and *cpe-1* genes. Transcriptional regulatory sequences of the *plc-1*, *splA2*, and *cpe-1* genes were predicted and analyzed using the Mat Inspector program (Quandt et al. 1995). Some of the important regulatory elements identified for each gene are represented and are listed in table 4.14 with their specific role. White boxes and double lines represent exons and introns respectively. Arrows indicate transcription start site at +1.

Table 4.14: Functions of regulatory sequences in the promoter region of the *plc-1*, *splA2*, and *cpe-1* genes in *N. crassa*

Transcriptional Regulatory Sequence	Role
Aspergillus/*Neurospora* nitrogen regulator	Transcriptional activator of nitrogen regulated genes.
cAMP-element responsive binding proteins	Regulation of cellular DNA-dependent transcription.
Carbon source-responsive elements	Zinc cluster transcriptional activator binding to carbon source responsive elements (CSRE).
Fungal basic leucine zipper family	Transcriptional regulation of growth and development, nutrient utilization, pathogenicity, and stress responses (Kong et al. 2015).
Fungal GATA binding factors	Transcriptional regulation of nitrogen metabolism, sidephore biosynthesis, light induction, and mating type-switching (Scazzocchio 2000).
Pheromone response element	Transcriptional activator for genes involved in mating or pseudohyphal/invasive growth pathways via a MAP kinase signaling cascade.
Yeast cell cycle and metabolic regulator	Yeast multifunctional global regulator MCM-1 that acts as transcriptional regulator of *Mat α* factors, cell type-specific genes, cell cycle-specific genes, and arginine metabolic genes (Chen and Tye 1995).

Yeast heat shock factors	Transcriptional activator of genes for survival in stress conditions (Ruis and Schüller 1995).
Yeast mating factor	Transcriptional regulation of *Mat α*2 gene involved in mating.
Yeast stress response elements	Transcriptional activator of genes for survival in stress conditions (Ruis and Schüller 1995).

4.3 Discussion

Mutations in two different genes could result in a significantly different phenotype than the individual mutations. Such a genetic interaction predicts functional relationship between genes or their corresponding gene products and pathways and provides theoretical explanations for the selective advantage of sexual reproduction and recombination (Boone et al. 2007; Mani et al. 2007). Genetic interactions can be broadly classified into two models- a 'between pathway model' depicting bidirectional genetic redundancy, where one pathway compensates for defects in the other and a 'within pathway model' in which both genes functions in the same essential pathway, the function of which is diminished by each mutation (Boone et al. 2007).

In this chapter, I generated and analyzed the double mutants of Ca^{2+} signaling genes *plc-1*, *splA2*, and *cpe-1* to understand the numerous phenotypic alterations regulated by their genetic interactions. The Δ*plc-1*; Δ*splA2*, Δ*plc-1*; Δ*cpe-1*, and Δ*cpe-1*; Δ*splA2* double mutants were generated by crossing the single mutant strains of opposite mating type (Figure 4.1) and phenotypes of the double mutants were studied to determine genetic interaction of the *plc-1*, *splA2*, and *cpe-1* genes in *N. crassa*. The Δ*plc-1*; Δ*splA2* and Δ*plc-1*; Δ*cpe-1* double mutants synthetically showed numerous phenotypes such as colonial growth (Figure 4.2), slower growth rate (Figure 4.3; Table 4.1), reduced biomass accumulation with failure to form aggregates in liquid growth conditions (Figure 4.4; Table 4.2), reduced aerial hyphae with decreased conidiation (Figure 4.6; Tables 4.3; 4.4), premature conidiation with reduced germination efficiency (Figures 4.7; 4.8), inappropriate conidiation in submerged culture (Fig. 4.9), reduced carotenoid accumulation (Figures 4.10; 4.11; 4.12; Table 4.5), and female sterility (Fig. 4.23; Table 4.12). In addition, the Δ*plc-1*; Δ*splA2* and Δ*plc-1*; Δ*cpe-1* double mutants showed hyphal defect upon increase in intracellular [Ca^{2+}] induced by the Ca^{2+} ionophore A23187 (Figure 4.16) and decreased colony growth upon increase in extracellular [Ca^{2+}] (Figure 4.17; Table 4.6). Furthermore, the Δ*plc-1*;

Δ*splA2* and Δ*plc-1*; Δ*cpe-1* double mutants displayed increased sensitivity to oxidative stress, and reduced thermotolerance in comparison to the single mutants (Figures 4.20; 4.21; Tables 4.9; 4.10). Moreover, the Δ*plc-1*; Δ*splA2* and Δ*plc-1*; Δ*cpe-1* double mutants exhibited increased sensitivity to UV than the wild type or the parental single mutants (Figure 4.22; Table 4.11). However, another double mutant, the Δ*cpe-1*; Δ*splA2* showed no phenotypic defect which indicated that the Ca^{2+} signaling genes do not interact randomly. The increased carotenoid accumulation in the three single mutants was linked to increased intracellular ROS generation (Figures 4.14; 4.15).

In shaking liquid cultures, Δ*plc-1*; Δ*splA2* and Δ*plc-1*; Δ*cpe-1*double mutants failed to produce mycelial aggregates like the parental single mutants and the wild type, which could be due to loss of vegetative hyphal fusion resulting in a defect in the hyphal network formation in the double mutants (Figure 4.4 C). Similar observations was also reported in the *so* mutants of *F. verticillioides* (*fvso*), *F. oxysporum* (*fso1*) and *fmk1*, a MAPK mutant of *F. oxysporum* (Prados Rosales and Di Pietro 2008; Guo et al. 2015). Hyphal fusion in *N. crassa* is under the control of a putative transmembrane protein HAM-2 and hyphal fusion protein SO (Xiang et al. 2001; Fleißner et al. 2005). Both *so* and *ham-2* mutants showed phenotypes such as shorter aerial hyphae, lesser conidiation, and female sterility similar to those observed for the Δ*plc-1*; Δ*splA2* and Δ*plc-1*; Δ*cpe-1* double mutants. The sterol profile Δ*plc-1*; Δ*splA2* and Δ*plc-1*; Δ*cpe-1* double mutants showed UV absorption maxima at 272, 282, and 293 nm, indicating presence of ergosterol in these strains, and therefore, slow growth phenotype of these mutants was not due to a defect in ergosterol biosynthesis (Figure 4.5; Prakash et al. 1999).

The standing liquid cultures of Δ*plc-1*; Δ*splA2* and Δ*plc-1*; Δ*cpe-1* double mutants formed short and densed aerial hyphae, with significant reduction in conidia production (Figure 4.6 A-B; Tables 4.3 and 4.4). In addition, the Δ*plc-1*; Δ*splA2* and Δ*plc-1*; Δ*cpe-1* double mutants showed premature conidiation as early as 12 h of growth in repressing conditions (glucose-rich medium and complete darkness), and constitutive conidiation on solid medium even under non-sporulating conditions were also observed (Figure 4.7). Therefore, both Δ*plc-1*; Δ*splA2* and Δ*plc-1*; Δ*cpe-1* double mutants enter the asexual developmental program earlier than either the wild type or parental single mutants and the wild type. Premature or constitutive conidiation could also be linked to characteristic colony morphology and the slow linear growth of the Δ*plc-1*; Δ*splA2* and Δ*plc-1*; Δ*cpe-1* double mutants (Figures 4.2 A-C and 4.3 A-C). Furthermore, at 24 h post

inoculation, 100% of the conidia of the wild type and single mutants were germinated, whereas, conidia from Δ*plc-1*; Δ*splA2* and Δ*plc-1*; Δ*cpe-1* double mutants displayed 100% germination only at 60 h (Figure 4.8 A-B). Therefore, early conidiation in Δ*plc-1*; Δ*splA2* and Δ*plc-1*; Δ*cpe-1* double mutants might not have produced fully developed conidia leading to delayed germination. In previous studies, formation of shorter aerial hyphae was found to be linked to premature and constitutive or non-repressing conidiation as seen in a putative histidine kinase *development and carotenogenesis control-1* (*dcc-1*), and a non-repressing conidiation protein *nonrepressible conidiation gene-1* (*nrc-1*) mutant, respectively (Barba-Ostria et al. 2011, Kothe and Free 1998). Therefore, this study showed that synthetic interaction of *plc-1* and *splA2*, and *cpe-1* and *plc-1* is required for normal asexual development of *N. crassa*.

Asexual sporulation (macroconidiation) in *N. crassa* typically requires the presence of an air/water interface with conidiation normally occurring on a solid surface (Ivey et al. 2002; Yang et al. 2002; Krystofova and Borkovich 2005). The wild type strain of *N. crassa* maintains undifferentiated vegetative hyphal growth in submerged cultures, however, it can be induced to conidiate when subjected to stress such as high temperatures or cellular stress and carbon or nitrogen limitations (Cortat and Turian 1974; Guignard et al. 1974; That and Turian 1978; Plesofsky-Vig et al. 1983; Madi et al. 1997; Ivey et al. 2002; Yang et al. 2002; Kays and Borkovich 2003; Krystofova and Borkovich 2005). Inappropriate conidiation in submerged cultures has been observed in case of certain mutants such as those of Gα subunits (*gna-1* and *gna-3*), Gβ subunit (*gnb-1*) as well as adenylyl cyclase *cr-1* and the putative glucose transporter *rco-3* (Madi et al. 1997; Kays et al. 2000; Ivey et al. 2002; Yang et al. 2002; Krystofova and Borkovich 2005). The Δ*plc-1*; Δ*splA2* and Δ*plc-1*; Δ*cpe-1* double mutants produced abundant conidiophores in submerged cultures and this phenotype was completely suppressed on addition of the rich nutrient peptone (Figure 4.9).

Cultures of *N. crassa* produce characteristic orange pigmentation mainly due to the accumulation of the apocarotenoid neurosporoxanthin and variable amounts of its precursor carotenoid (Zalokar 1954; Avalos et al. 2013; Barman and Tamuli 2015). Accumulation of carotenoid occurs not only in the mycelial masses but also in the asexual spores or conidia that are produced by the illuminated air borne mycelia (Li and Schmidhauser 1995; Lauter et al. 1997; Estrada et al. 2008; Díaz-Sánchez et al. 2011). Carotenoid biosynthesis in *N. crassa* is affected by both light and temperature, illumination at low temperature causes increased neurosporoxanthin

accumulation whereas illumination at normal temperature results in the accumulation of its carotenoid precursors (Harding et al. 1969; Harding 1974; Estrada et al. 2008; Díaz-Sánchez et al. 2011; Barman and Tamuli 2015). I found lower carotenoid content after a 24 h illumination in cultures of Δ*plc-1*; Δ*splA2* and Δ*plc-1*; Δ*cpe-1* double mutants at all three temperatures of 8, 22, and 30°C due to a slower carotenoid accumulation rate and this could explain their reduced mycelial pigmentation (Figures 4.11 A-C; 4.12 A-C; Table 4.5). In contrast, Δ*plc-1,* Δ*splA2*, and Δ*cpe-1* as well as Δ*cpe-1*; Δ*splA2* showed an increased rate of carotenoid accumulation that resulted in their increased carotenoid content after a 24 h illumination as compared to the wild type strain (Figures 4.11 A-C; 4.12 A-C; Table 4.5). Previously, VVD, a blue light photoreceptor protein, and SOD-1, a copper-zinc -superoxide dismutase protein were shown to regulate carotenoid biosynthesis in *N. crassa* (Schwerdtfeger and Linden 2003; Yoshida and Hasunuma //2004). Both *vvd* and *sod-1* mutant showed light induced increased carotenoid accumulation in the mycelia (Schwerdtfeger and Linden 2003; Yoshida and Hasunuma 2004). Enhanced carotenoid accumulation was also observed for catalase-3 deficient mutant, *cat-3* (Michán et al. 2003). Increased carotenoid accumulation in the *sod-1* mutant was related to intracellular generation of ROS (Yoshida and Hasunuma 2004). ROS has also been reported to regulate carotenoid synthesis in other organisms such as *Phaffia rhodozyma*, where singlet oxygen induced carotenoid synthesis, and *F. aquaeductuum*, where increased carotenoid accumulation in the mycelia was observed upon treatment with redox dyes under red light (Sundquist et al. 1994; Schroeder and Johnson 1995). Therefore, increased carotenoid accumulation in Δ*plc-1*, Δ*splA2*, Δ*cpe-1* and also in Δ*cpe-1*; Δ*splA2* could be due to intracellular concentration of ROS as revealed by reduction of carotenoid accumulation by the antioxidant NAC and the increased fluorescence signal with DCFH-DA (Figures 4.14 A-C; 4.15 A-C). In *N. crassa*, ROS generation mainly occurs during the process of aerobic respiration in mitochondria and following light exposure (harmful UV-radiations; Iigusa et al. 2005). Carotenoids are known to be powerful antioxidants that protects the cells from elevated levels of ROS (Darvin et al. 2011). In Chapter 3, I have reported increased UV survival in Δ*plc-1,* Δ*splA2*, and Δ*cpe-1* than the wild type strain (Figure 3.16; Barman and Tamuli 2015). Therefore, it is possible that light induced enhanced intracellular ROS generation in the Δ*plc-1,* Δ*splA2* and Δ*cpe-1* single mutants that resulted in increased carotenoids accumulation contributing to higher survival of the mutants upon UV irradiation. Several cell functions in *N. crassa* including UV induced DNA damage and repair were also found to be regulated by the genetic interactions

of some of Ca^{2+} signaling genes such as *ncs-1*, *mid-1*, and *nca-2* encoding for the neuronal calcium sensor-1, a Ca^{2+}-permeable channel, and a PMCA-type Ca^{2+}-ATPase, respectively, in *N. crassa* (Deka and Tamuli 2013). In addition, interaction of *plc-1* with *splA2* and *plc-1* with *cpe-1* might play an important role in acquisition of induced thermotolerance in *N. crassa (*Figure 4.21; Table 4.10). The pre exposure of *N. crassa* germinating spores to 44°C induces synthesis of heat shock proteins to protect spores from lethal heat shock 52°C temperature (Kapoor et al. 1995; Yang and Borkovich 1999).

The double deletion mutant strains Δ*plc-1*; Δ*splA2* and Δ*plc-1*; Δ*cpe-1* when used as a female parent in a cross, showed defect in the early stage of the sexual development resulting in complete absence of perithecia formation (Figure 4.23 A; Table 4.12). However, crosses involving Δ*plc-1*; Δ*splA2* and Δ*plc-1*; Δ*cpe-1* as a male parent were fully fertile with formation of enlarged black pigmented perithecia and fully developed ascospores (Figure 4.23 B; Table 4.12). Furthermore, crosses involving Δ*plc-1,* Δ*splA2*, Δ*cpe-1*, and Δ*cpe-1*; Δ*splA2* mutants were fully fertile either as female or male parent (Figure 4.23 A-B; Table 4.12). Important transcription regulatory sequences were identified in the upstream of the promoter regions of *plc-1, splA2*, and *cpe-1* genes including pheromone response elements, yeast cell cycle and metabolic regulator, yeast mating factors and yeast stress response elements (Figure 4.25; Table 4.14).

Thus, the Δ*plc-1*; Δ*splA2* and Δ*plc-1*; Δ*cpe-1* double mutants displayed several defects in vegetative and sexual phases in *N. crassa*. Therefore, effect of the Δ*plc-1*; Δ*splA2* and Δ*plc-1*; Δ*cpe-1* double mutants in vegetative growth and sexual development in *N. crassa* consistently suggested pleiotropic nature of these double mutants. Genetic interactions of the *plc-1*, *splA2*, and *cpe-1* genes might be involved in modulating cellular pathways controlled by Ca^{2+} signaling machinery in *N. crassa*. Therefore, several synthetic phenotypes of the Δ*plc-1*; Δ*splA2* and Δ*plc-1*; Δ*cpe-1* double mutants were identified, which indicated novel genetic interaction of these genes in controlling numerous cell functions in *N. crassa*.

A part of this chapter was published in Current Genetics (Barman and Tamuli 2017) and presented in "Research Conclave, 2016" held at Indian Institute of Technology, Guwahati, Assam.

In the next chapter, I describe the regulators of *plc-1*, *splA2*, and *cpe-1* genes and propose a possible mechanistic model for the Ca^{2+} signaling responses mediated by the *plc-1*, *splA2*, and *cpe-1* genes in *N. crassa*.

Chapter 5

Understanding the molecular basis of phospholipase C-1, secretory phospholipase A2, and calcium proton exchanger-1 functions in Neurospora crassa

5.1 Introduction

Ca^{2+} signaling machinery acts in coordination with other signaling pathways for regulation of cellular processes that results in 'molecular crosstalk' between the signaling pathways (Sanders et al. 2002; Berridge et al. 2003). Such crosstalk enables cells to recognize, process, and interpret different stimuli to generate appropriate cellular responses (Siso-Nadal et al. 2009). Intracellular signaling in *N. crassa* is complex and comprises of three principle signaling components that includes the MAPK pathway, the heterotrimeric G protein-cAMP signaling pathway, and the Ca^{2+} mediated signaling pathway (Chapter 1; Figure 1.2; Galagan et al. 2003). Cross talks between the three pathways enables coordination of signal transduction in *N. crassa*. The crosstalk between the cAMP and Ca^{2+} signaling pathways has been well studied in plant and animal cells including the filamentous fungus *A. niger* (DeBernardi and Brooker 1996; Moore et al. 1998; Volotovski et al. 1998; Gorbunova and Spitzer 2002; Zaccolo and Pozzan 2003; Benčina et al. 2005). Additionally, protein-protein interaction networks are essential for system level understanding of all fundamental processes including cell growth, cell proliferation, morphology, intercellular communication, metabolic pathways, and signal transduction (Phizicky and Fields 1995).

In this chapter, I analyzed the influence of cAMP on the Ca^{2+} signaling genes *plc-1*, *splA2*, and *cpe-1* in *N. crassa* and report few interacting partners for each of the PLC-1, sPLA2, and CPE-1 protein. In Chapters 3 and 4, I described cell functions of the *plc-1*, *splA2*, and *cpe-1* genes and also reported genetic interactions between their loci based on the phenotypic analysis of the double mutants. The *plc-1*, *splA2*, and *cpe-1* genes were shown to regulate multiple cellular functions such as growth, carotenoid accumulation, oxidative stress, thermotolerance, and fertility (Barman and Tamuli 2015; 2017). In this chapter, I report that some of the important developmental and biosynthetic genes regulate the conidiation, carotenoid accumulation, and pheromone signaling of the *plc-1*, *splA2*, and *cpe-1* and also describe the molecular mechanism of Ca^{2+} mediated signaling responses of *plc-1*, *splA2*, and *cpe-1* genes.

5.2 Results

5.2.1 Prediction about interacting partners using the STRING analysis

The search tool for the retrieval of interacting genes/proteins (STRING; http://string-db.org/; Szklarczyk et al. 2015) is a biological database of known and predicted protein-protein interactions, and currently covers 9,643,763 proteins from 2,031 organisms and derives

information from sources like text-mining, gene fusion, co-occurrence, co-expression, high throughput experimental data, automated text collections, and computational predictions. The interactions include both direct (physical) and indirect (functional) associations and such interactions provides system level understanding of cellular processes including structural, functional, and evolutionary properties of proteins. SPRING data analysis revealed a number of interacting partners of PLC-1, sPLA2 and CPE-1 proteins. Among the predicted functional partners of PLC-1 include the heterotrimeric guanine nucleotide binding Gα proteins GNA-1, GNA-2, and GNA-3 (Figure 5.1 A). The G proteins GNA-1, GNA-2, and GNA-3 functions as transducers or modulators in various transmembrane signaling systems and are also capable of activating other second messengers such as membrane associated adenylate cyclase enzyme stimulation causing cAMP production, which stimulates and activates PKA. Further, PKA triggers a number of downstream signaling events. In the SPRING network, the sPLA2 protein was shown to interact with lower stringency with aldose epimerase-2, an enzyme that participates in glycolysis and gluconeogenesis, the lyase enzymes pectate lyase A and alpha amylase A, and the proteinase enzyme metalloprotese-14 (Figure 5.1 B). *N. crassa* has four putative P-type Ca^{2+} ATPases that functions as Ca^{2+} pumps transporting excess Ca^{2+} from the cytosol. SPRING analysis predicted a number of functional partners of CPE-1 including the Plasma membrane Ca^{2+} ATPase (PMCA) type proteins NCA-2 and NCA-3 that are localized primarily in the plasma membrane and functions as Ca^{2+} pumps removing excess $[Ca^{2+}]_c$ into the vacuoles (Bowman et al. 2011). CPE-1 protein was also shown to interact with SPCA type (Secretory pathway Ca^{2+} ATPase) PMR-1 which functions in the Golgi bodies (Figure 5.1 C; Bowman et al. 2011). However, in the SPRING network, no interaction was predicted between CPE-1 and the NCA-1, a smooth endoplasmic reticulum Ca^{2+} type ATPase (SERCA), which predominantly functions in the ER (Figure 5.1 C). Thus, SPRING analysis predicted different interacting partners of PLC-1, sPLA2, and CPE-1, including proteins involved in Ca^{2+} and other signaling pathways, indicating an interconnection of Ca^{2+} and other signaling proteins for appropriate coordination of cellular responses.

(A)

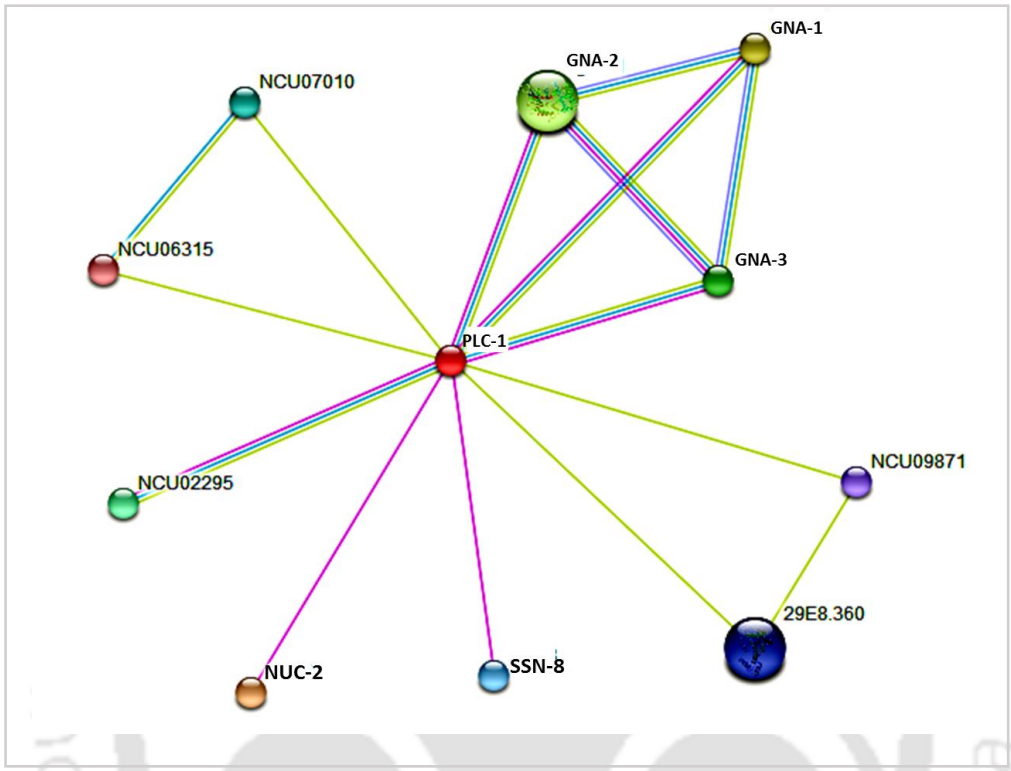

(B)

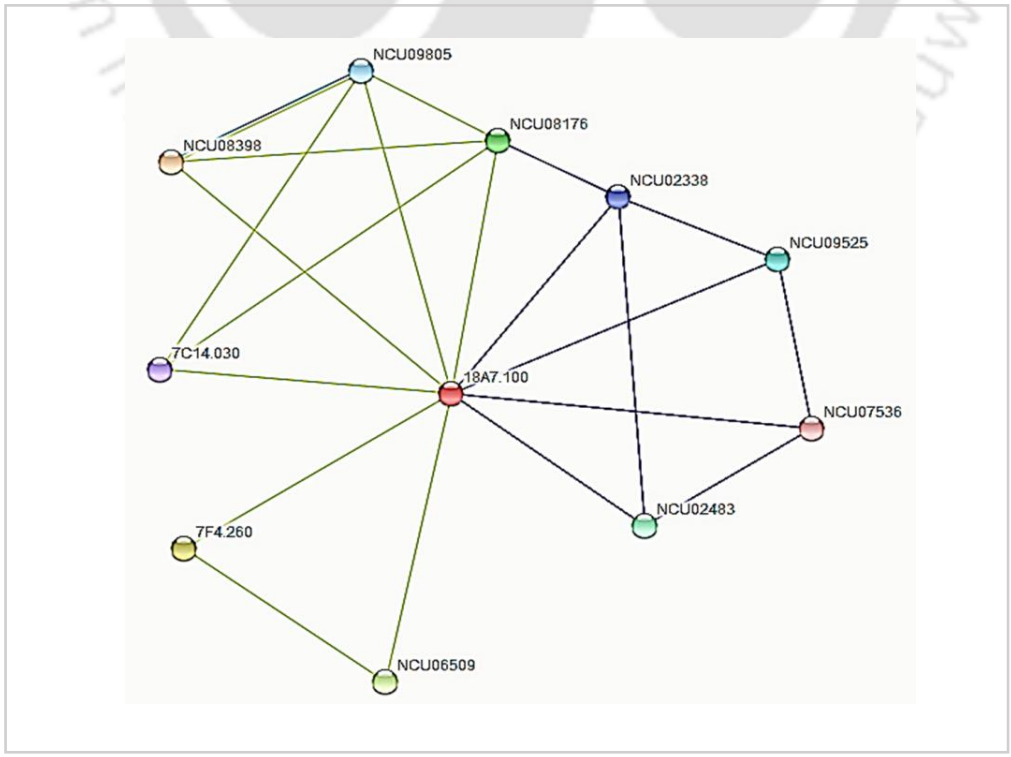

(C)

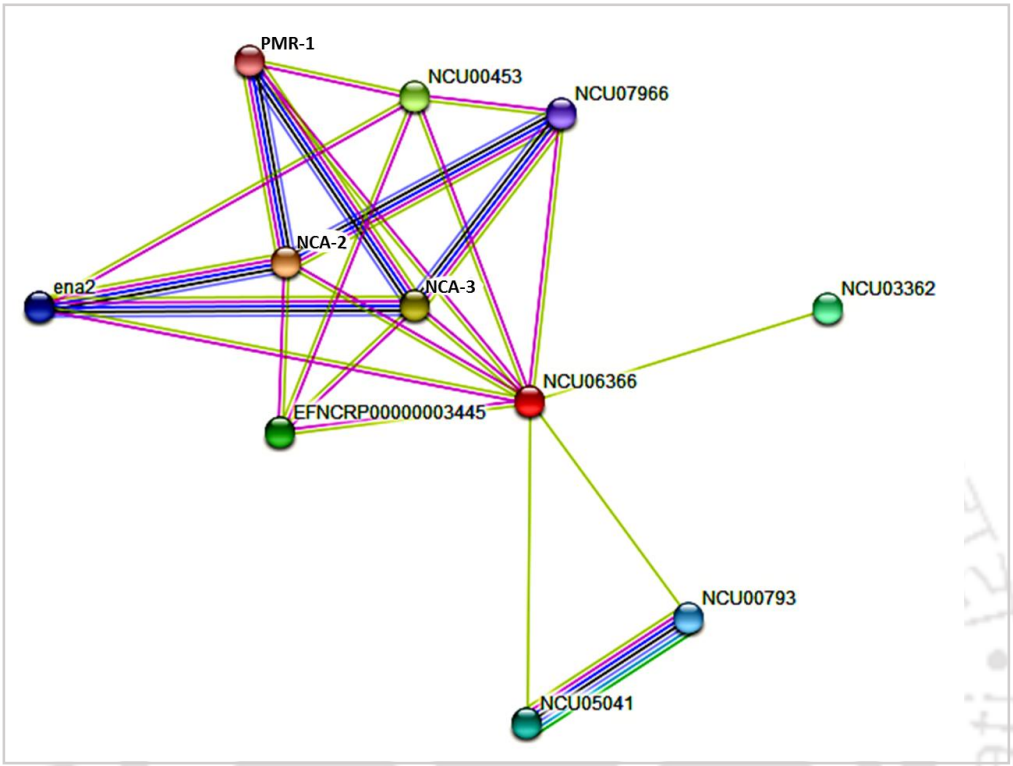

Figure 5.1: Schematic representation of the interacting network of the *N. crassa* PLC-1, sPLA2, and CPE-1 protein predicted using the STRING analysis. The edges in the network represent protein-protein associations that are specific and meaningful, indicating proteins jointly contribute to a shared function, which does not necessarily mean direct physical binding with each other. Small nodes represent protein of unknown 3D structure, and large nodes indicate protein with solved or predited 3D structure. Colored nodes represent query proteins and first shell of interactors, while white nodes represent second shell of interactors. **(A)** STRING based analysis of interacting partners of PLC-1 protein. In the STRING network, the interaction of PLC-1 protein with NUC-2 (ankyrin repeat protein), heterotrimeric Gα proteins (GNA-1, GNA-2, and GNA-3), NCU02295 (phosphatidylinositol-4-phosphate-5-kinase its3), NCU07010 (cortical actin cytoskeleton protein), SSN-8 (RNA polymerase II holoenzyme cyclin like subunit), 29E8.360 (probable regulator of phosphatidylinositol-4-OH kinase protein), NCU09871 (centrin 3 protein), NCU06315 (inositol-8) is shown. **(B)** STRING based analysis of interacting partners of sPLA2 protein. In the STRING network, sPLA2 protein with lower stringency is shown to interact with NCU08398 (aldose epimerase-2), 7F4.260 (predicted protein), NCU06509 (hypothetical protein),

NCU08176 (pectate lyase A), NCU02483 (hypothetical protein), NCU09525 (secretory protein), NCU09805 (alpha-amylase A), NCU02338 (secretory protein), 7C14.030 (putative uncharacterized protein), NCU07536 (metalloprotease-14). **(C)** STRING based analysis of interacting partners of CPE-1 protein. In the STRING network, the interactions of the CPE-1 protein with NCA-2 (a SERCA type Ca^{2+} type ATPase), NCA-3 (putative P-type calcium ATPase), NCU00453 (Na^{+}/H^{+} exchanger), EFNCRP00000003445 (calcineurin subunit B), NCU03362 (steroid alpha reductase), NCU05041 (trehalose phosphatase), NCU00793 (trehalose phosphate synthase), ena2 (putative uncharacterized protein), NCU07966 (calcium transporting ATPase 3), PMR-1 (calcium transporting ATPase type 2C member) are shown.

5.2.2 cAMP assay

5.2.2.1 Interaction of *plc-1* with *splA2* and *cpe-1* controls *N. crassa* development independent of cAMP

In fungi, cAMP (Figure 5.2 A) regulates a wide variety of processes including cellular organization, morphogenesis, metabolism, sexual development, and virulence (Pall 1981; Kronstad 1997; Borges-Walmsley and Walmsley 2000; Lengeler et al. 2000; D'Souza and Heitman 2001; Lee et al. 2003). In the yeast *S. cerevisiae*, cAMP signal transduction pathway plays an important role in stress resistance, carbon source utilization, glycogen accumulation, cell cycle progression, sporulation, and pseudohyphal growth (Matsumoto et al. 1982a; 1982b; Thevelein 1994; Tokiwa et al. 1994; Lorenz and Heitman 1997; Thevelein and de Winde 1999). In *N. crassa*, cAMP signaling is known to regulate hyphal tip growth, asexual differentiation, and carbon metabolism (Terenzi et al. 1974; 1979; Bruno et al. 1996; Banno et al. 2005). In Chapter 4, I described that the Δ*plc-1*; Δ*splA2* and Δ*plc-1*; Δ*cpe-1* double mutants showed a few pleiotropic phenotypes such as colonial growth, stunted aerial hyphae, early macroconidiation, and submerged conidiation (Barman and Tamuli 2017). These phenotypes were similar to the adenylate cyclase deficient *crisp-1* (*cr-1*) and the Gα subunit *gna-3* mutants (Terenzi et al. 1974; Kays et al. 2000). Furthermore, *gna-3* was shown to be a predicted functional interacting partner of *plc-1* (Figure 5.1 A). It was found that the addition of exogenous cAMP could partially rescue the colonial growth, aerial hyphae, and premature conidiation phenotypes of the *cr-1* and *gna-3* mutants (Kays et al. 2000; Ivey et al. 2002). Therefore, I tested if the addition of cAMP could also rescue defects of the Δ*plc-1*; Δ*splA2* and Δ*plc-1*; Δ*cpe-1* mutants. Addition of exogenous cAMP at a concentration

of 2 mM in cultures of *N. crassa* strains could not rescue the vegetative growth defect, reduced aerial hyphal elongation, early conidiation, and submerged conidiation phenotypes of Δ*plc-1*; Δ*splA2* (Figure 5.2 B-G; Tables 5.1-5.4). However, the Δ*plc-1*; Δ*splA2* double mutant showed a slight increase in mycelial carotenoid accumulation (Figure 5.2 H; Table 5.4), while crosses involving Δ*plc-1*; Δ*splA2* as a female parent produced a few aberrant perithecia in presence of 2 mM cAMP (Figure 5.2 I). Similar aberrant perithecia were also observed in the Δ*plc-1*; Δ*cpe-1* mutant (Figure 5.2 I), however, none of the other phenotypes was rescued by cAMP supplementation (Figure 5.2 B-H; Tables 5.1-5.4). Therefore, these results indicated that interaction of *plc-1* with *splA2* and *cpe-1* plays a pivotal role in controlling developmental processes such as apical growth, aerial hyphae, conidiation, carotenogenesis, and perithecia formation during the sexual cycle, and these genes function independent to that of the cAMP pathway unlike the *cr-1* and *gna-3*.

(A)

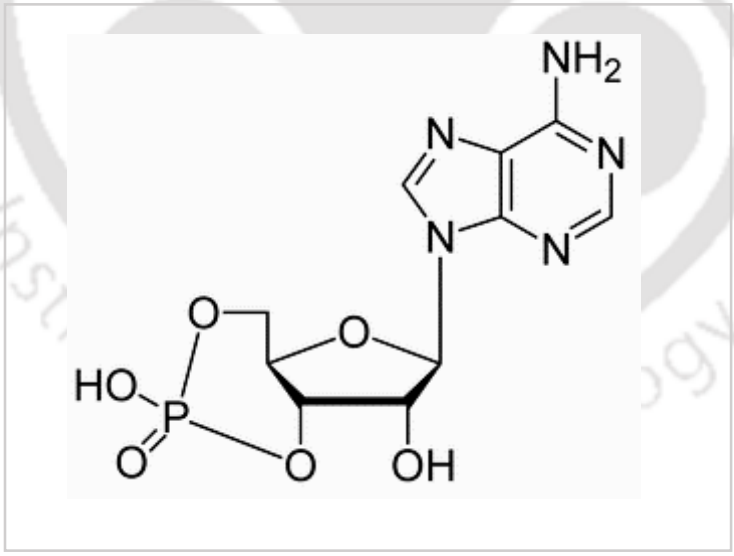

(B)

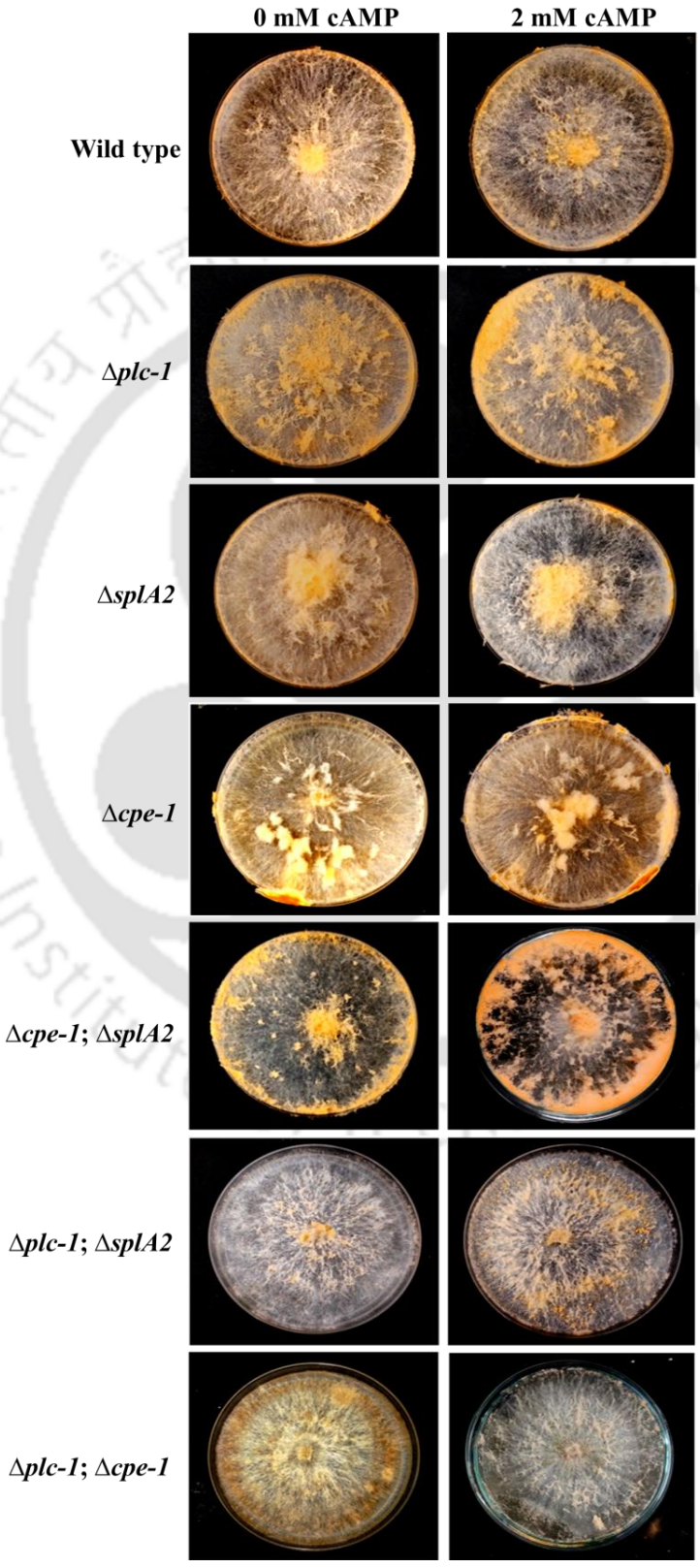

(C)

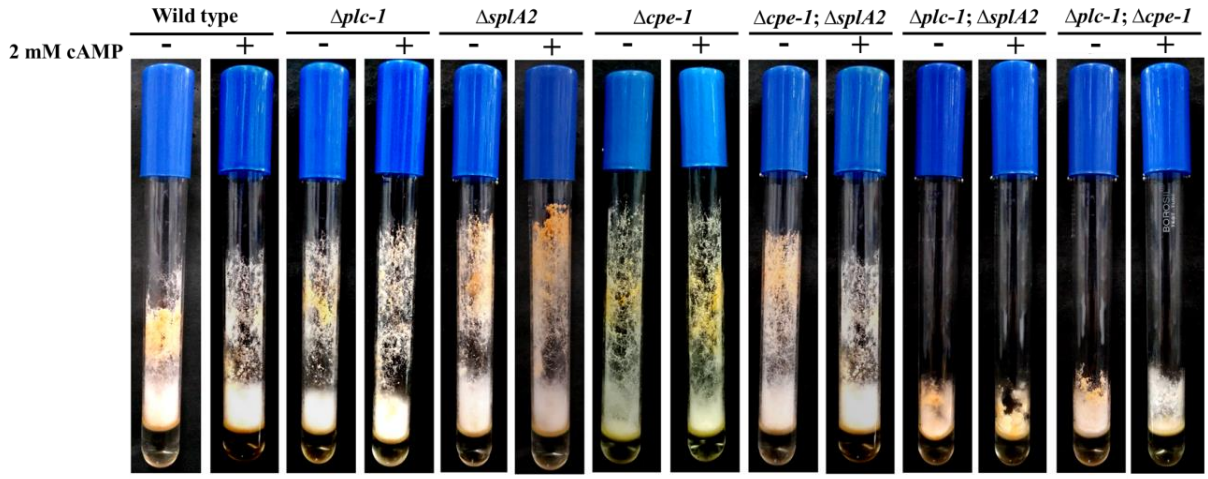

(D)

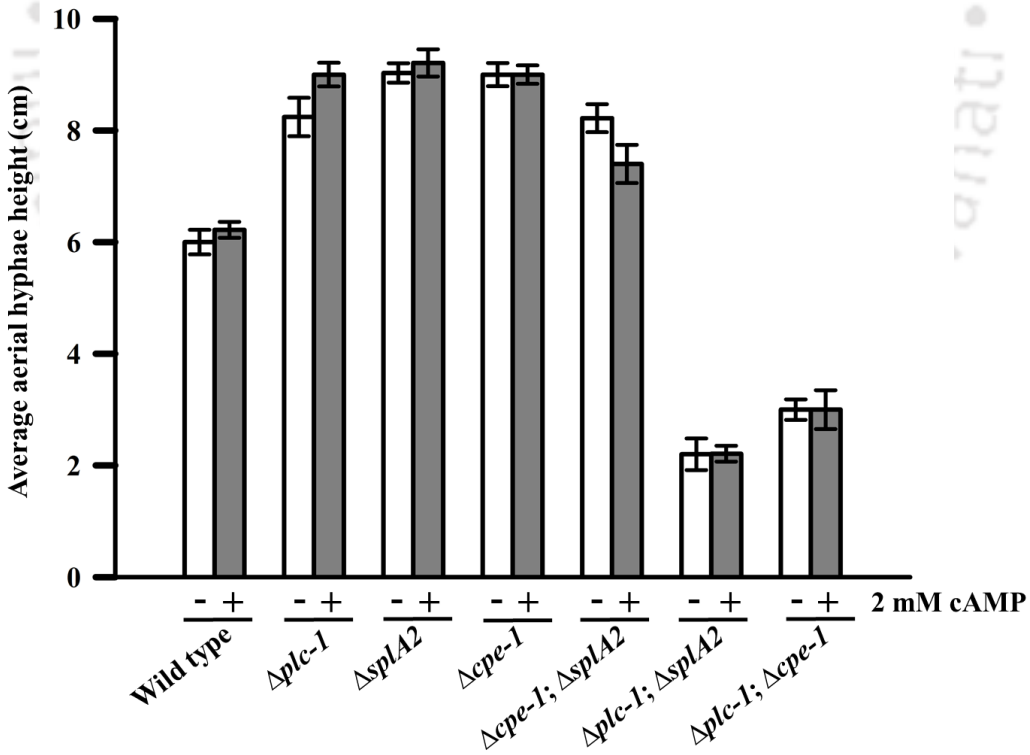

(E)

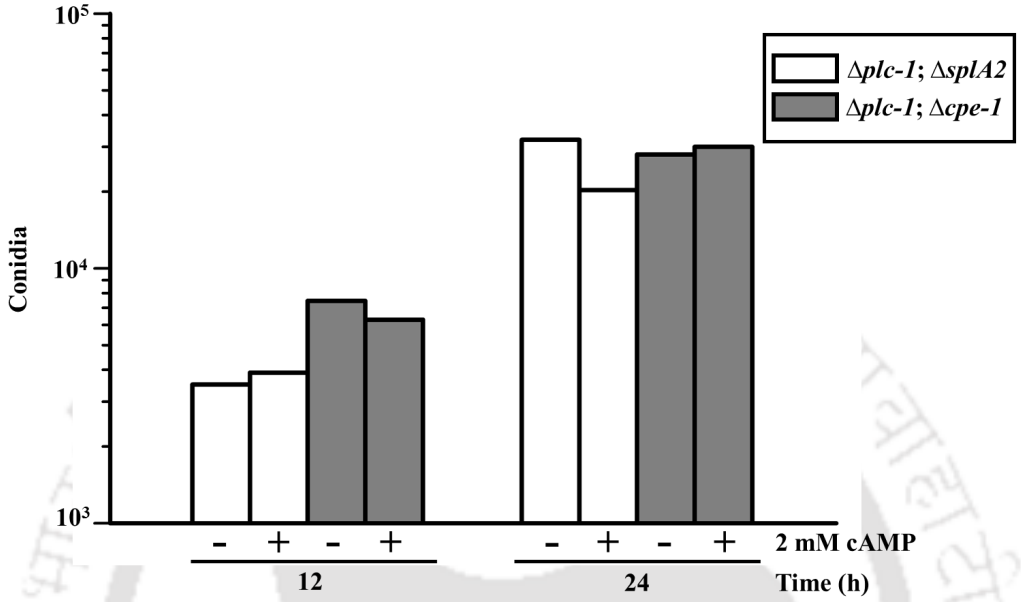

(F)

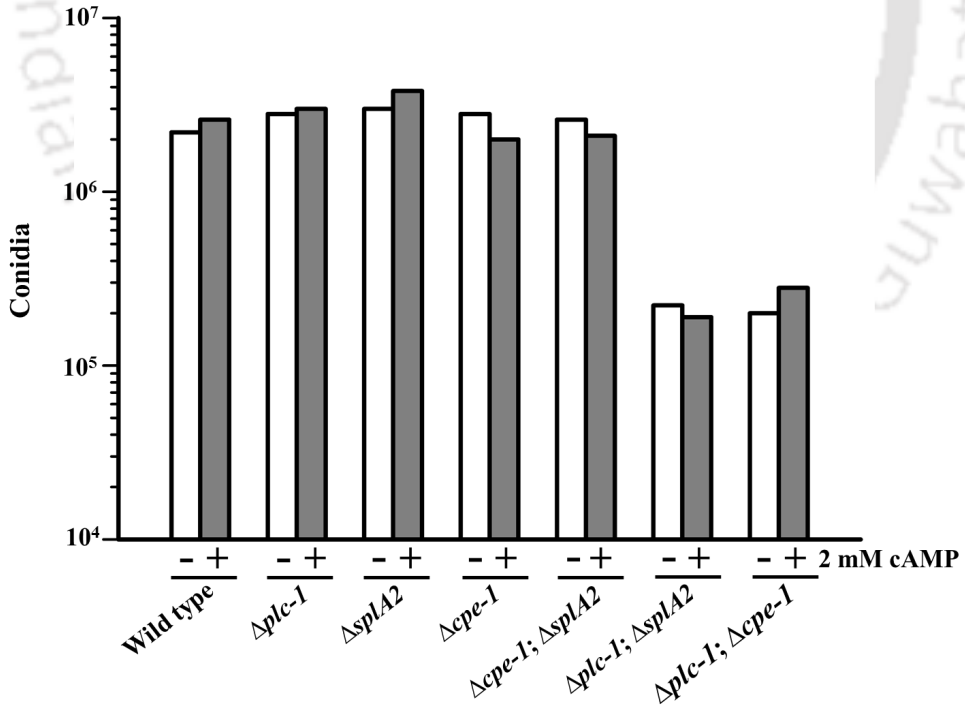

(G)

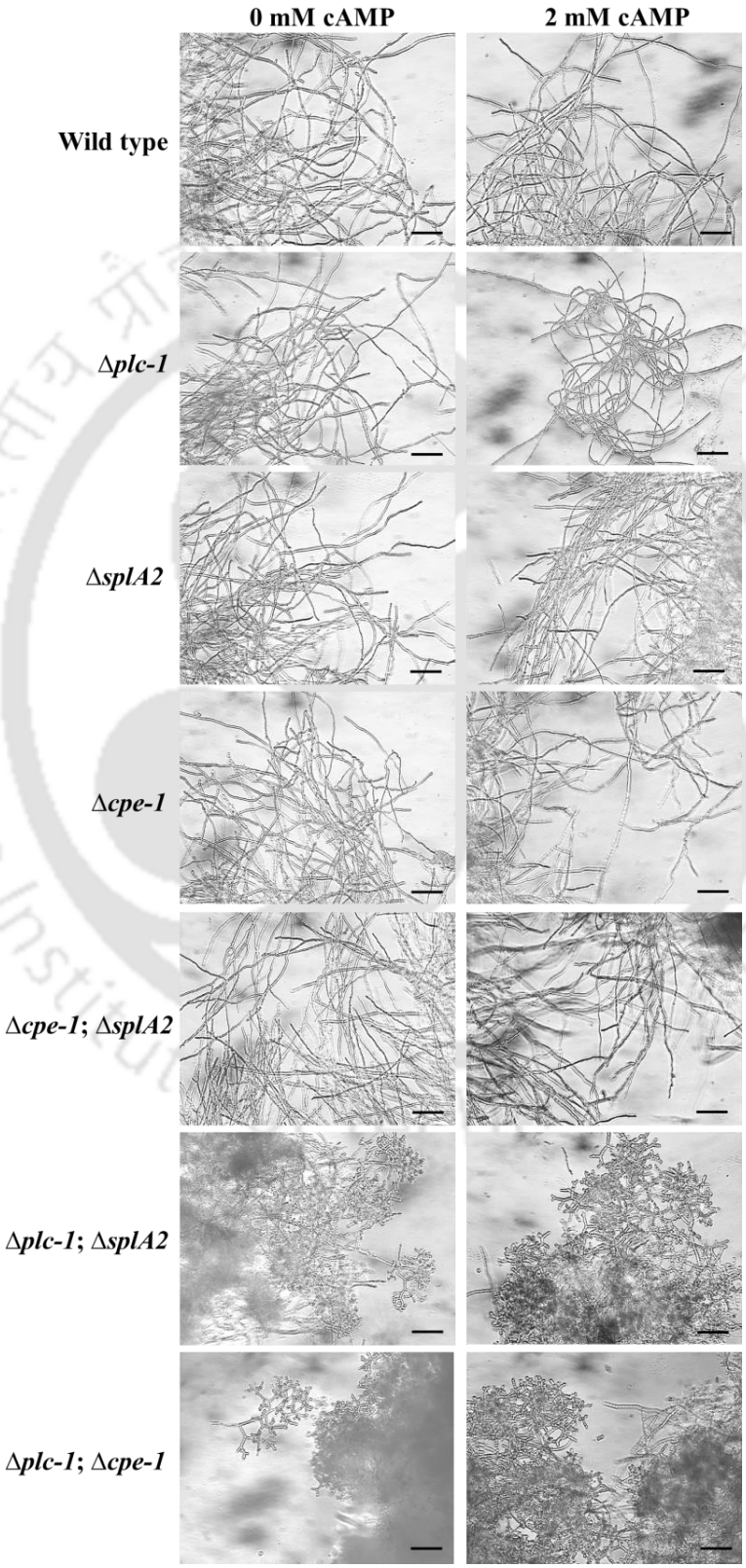

(H)

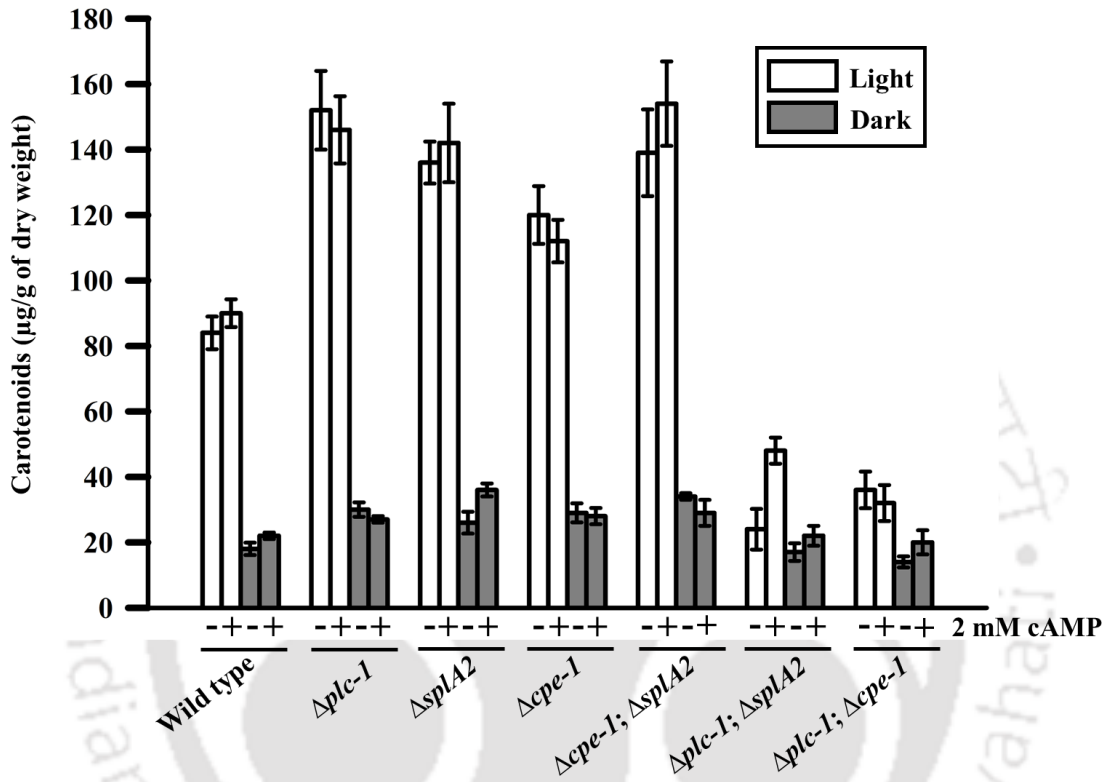

(I)

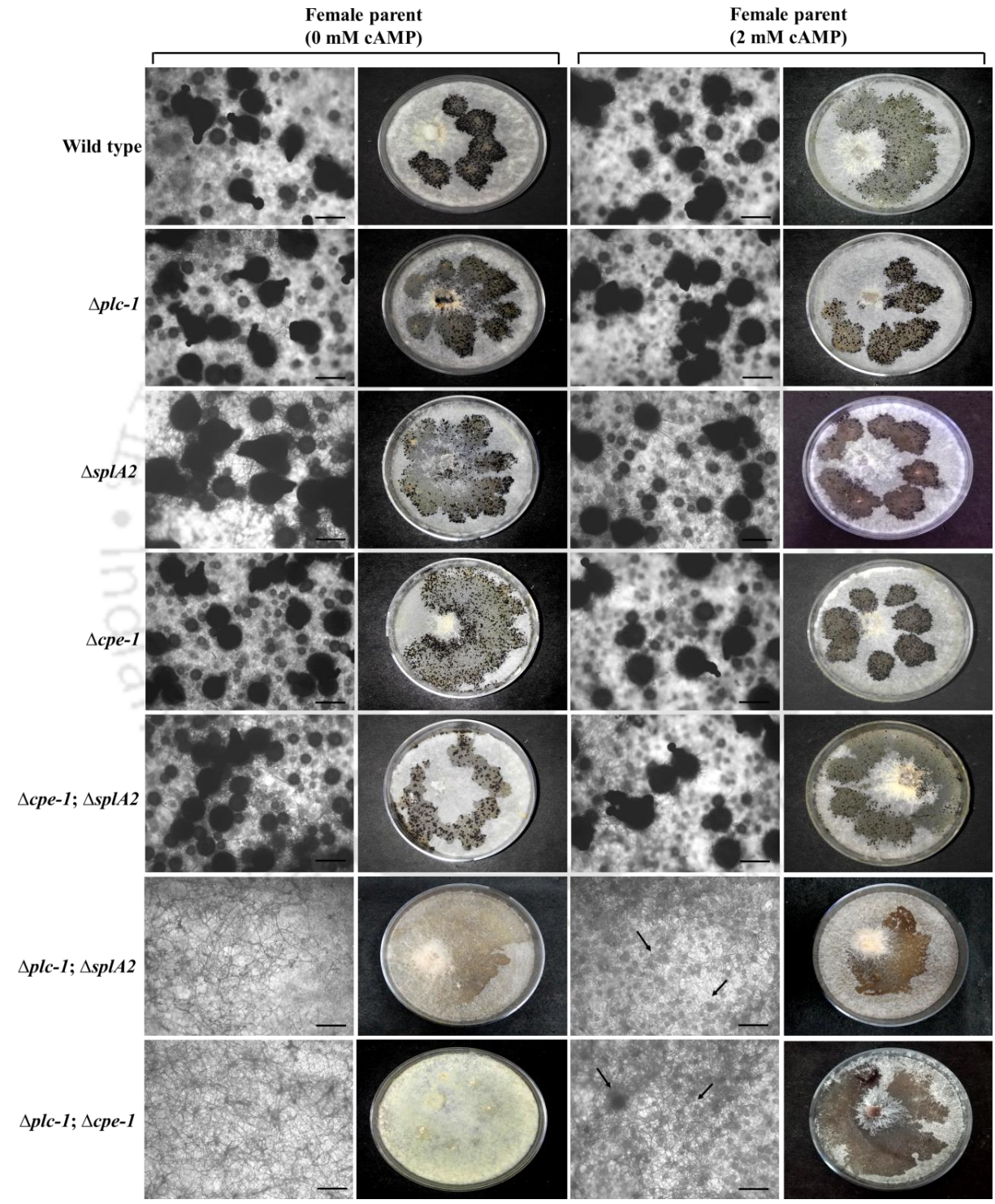

Figure 5.2: cAMP assay. (A) Chemical structure of 3′, 5′ cyclic adenosine monophosphate (cAMP). Its chemical structure is available at http://www.wikidoc.org/index.php/Cyclic_nucleotide. **(B)** Colony growth of the *N. crassa* strains on Petri dishes containing Vogel's glucose agar medium or with addition of 2 mM cAMP. Cultures were incubated for three days in the dark at 30°C and four days under light at room temperature and photographed (Nikon Coolpix P500). **(C)** Growth of aerial hyphae of the *N. crassa* strains on test tubes containing Vogel's glucose medium or with addition of 2 mM cAMP. Cultures were incubated for three days in the dark at 30°C followed by four days under light at room temperature and photographed (Nikon Coolpix P500). **(D)** Average height of the aerial hyphae of the *N. crassa* strains grown on test tubes (as described for **B** above) containing Vogel's glucose medium or with addition of 2 mM cAMP. Error bars indicate standard deviations calculated from the data for three independent experiments (n=3). **(E)** Conidiation in *N. crassa* strains grown in complete darkness at 30°C on Vogel's glucose agar medium or with 2 mM cAMP. Conidia were harvested and quantified at 12 and 24 h time period. **(F)** Conidiation of *N. crassa* strains grown in complete darkness at 30°C on Vogel's glucose agar medium or with 2 mM cAMP for 48 h followed by continuous exposure to light at 22°C for 96 h. Conidia were harvested and quantified. **(G)** *N. crassa* strains were inoculated in Vogel's glucose medium or with 2 mM cAMP, and incubated for 16 h in the dark at 30°C with shaking at 180 rpm. Aliquots of the cultures were viewed under the Trinocular inverted microscope (AxioVert A1FL, Carl Zeiss) and photographed. **(H)** *N. crassa* strains were grown in Vogel's glucose medium or with 2 mM cAMP, supplemented with 0.2% tween-80 and exposed to white light at 30°C or kept in the dark as control. Carotenoids were extracted from 0.25 g of mycelia using acetone and hexane while absorbance was taken at 470 nm. Accumulated carotenoids are expressed as μg carotenoid per gram of dry weight. Error bars indicate standard deviations calculated from the data for three independent experiments (n=3). **(I)** *N. crassa* strains were inoculated as a female parent in synthetic crossing agar medium or with 2 mM cAMP and incubated under light at room temperature for seven days. Cultures were subsequently fertilized with a male parent after 7 days of post-inoculation and were later photographed (AxioVert A1FL, Carl Zeiss; Nikon Coolpix P500). Black arrows indicate aberrant perithecia in cAMP added cultures of Δ*plc-1*; Δ*splA2* and Δ*plc-1*; Δ*cpe-1* strains. Scale bar 20 µm.

Table 5.1: Average aerial hyphae height of the *N. crassa* strains

Strains	Average aerial hyphae height (cm)	Average aerial hyphae height (cm)
	0 cAMP (mM)	**2 cAMP (mM)**
Wild type	6 ± 0.221	6.22 ± 0.142
Δ*plc-1*	8.24 ± 0.344	9 ± 0.212
Δ*splA2*	9.03 ± 0.173	9.21 ± 0.243
Δ*cpe-1*	9 ± 0.208	9 ± 0.165
Δ*cpe-1*; Δ*splA2*	8.22 ± 0.251	7.4 ± 0.341
Δ*plc-1*; Δ*splA2*	2.2 ± 0.283	2.21 ± 0.142
Δ*plc-1*; Δ*cpe-1*	3 ± 0.184	3 ± 0.348

Table 5.2: **Conidial count of the *N. crassa* strains**

Strains	Conidial count (conidia/ml)			
	12 h		**24 h**	
	0 cAMP (mM)	**2 cAMP (mM)**	**0 cAMP (mM)**	**2 cAMP (mM)**
Δ*plc-1*; Δ*splA2*	3.5×10^3	3.9×10^3	3.2×10^4	2×10^4
Δ*plc-1*; Δ*cpe-1*	7.5×10^3	6.3×10^3	2.8×10^4	3×10^4

Table 5.3: Average conidial count of the *N. crassa* strains

Strains	Average count of conidia (conidia/ml)	
	0 cAMP (mM)	**2 cAMP (mM)**
Wild type	2.2×10^6	2.6×10^6
Δ*plc-1*	2.8×10^6	3×10^6
Δ*splA2*	3×10^6	3.8×10^6
Δ*cpe-1*	2.8×10^6	2×10^6
Δ*cpe-1*; Δ*splA2*	2.6×10^6	2.1×10^6
Δ*plc-1*; Δ*splA2*	2.2×10^5	1.9×10^5
Δ*plc-1*; Δ*cpe-1*	2.2×10^5	2.8×10^5

Table 5.4: Carotenoid content of the *N. crassa* strains

Strains	Carotenoids (µg/g dry weight)†			
	Light		Dark	
	0 cAMP (mM)	2 cAMP (mM)	0 cAMP (mM)	2 cAMP (mM)
Wild type	84 ± 5	90 ± 4.23	18 ± 2	22 ± 1
Δ*plc-1*	152 ± 12	146 ± 10.3	30 ± 2.2	27 ± 1
Δ*splA2*	136 ± 6.42	142 ± 12	26 ± 3.4	36 ± 2
Δ*cpe-1*	120 ± 9	112 ± 7	29 ± 3	28 ± 3
Δ*cpe-1*; Δ*splA2*	139 ± 13.23	154 ± 13	34 ± 1	29 ± 4
Δ*plc-1*; Δ*splA2*	24 ± 6.2	48 ± 4	17 ± 3	22 ± 3.03
Δ*plc-1*; Δ*cpe-1*	36 ± 6	32 ± 6	14 ± 2	20 ± 4

5.2.3 Growth defect in the Δ*plc-1*; Δ*splA2* and Δ*plc-1*; Δ*cpe-1* double mutants were not due to a defect in septation

5.2.3.1 Assay for visualization of internal septation of germlings and hyphae

One of the mutant of the GTP-binding proteins (GTPase) in *Botrytis cinerea*, *Rho3*, a member of Rho superfamily, was shown to exhibit suppressed vegetative growth and conidiation and also increased distance between septa of individual hyphae (Bang et al. 2015). The slender vegetative hyphae of *N. crassa* also consists of numerous internal cross-walls called septa that partition each hypha into individual cells. Similar to the *Rho3* RIP mutant, the Δ*plc-1*; Δ*splA2* and Δ*plc-1*; Δ*cpe-1* double mutants were reported to have a few pleiotropic phenotypes including colonial morphology with slower apical extension rate and reduced conidiation (Barman and Tamuli 2017). Since the Δ*plc-1*; Δ*splA2* and Δ*plc-1*; Δ*cpe-1* double mutants showed a few pleiotropic phenotypes including reduced vegetative growth and slower apical extension rate, I tested if the growth defect of these two strains was due to improper septation in the growing vegetative hyphae using the calcoflour white (CFW; Figure 5.3 A), a fluorescent probe that specifically binds to cell walls composed of cellulose and chitin. The Δ*plc-1*; Δ*splA2* and Δ*plc-1*; Δ*cpe-1* double mutants showed abnormal hyphal branching pattern and conidial germination efficiency, however, germlings and vegetative hyphae of Δ*plc-1*; Δ*splA2* and Δ*plc-1*; Δ*cpe-1* after staining with CFW and visualization by fluorescence microscopy showed proper septa similar to wild type, individual single mutants,

and Δ*cpe-1*; Δ*splA2* double mutant strain (Figure 5.3 B). However, the septa and cell walls of the fewer vegetative hyphae of Δ*plc-1*; Δ*splA2* and Δ*plc-1*; Δ*cpe-1* did not stain as deeply with CFW as those of wild type, individual single mutants, and Δ*cpe-1*; Δ*splA2* double mutant strain which indicated deposition of cell wall cellulose and chitin was affected in the two double mutants (Figure 5.3 B). Therefore, loss of *plc-1* together with *splA2* or *cpe-1* resulted in various morphological defects including colonial growth morphology, however, these defects were not due to lack of proper septation.

(A)

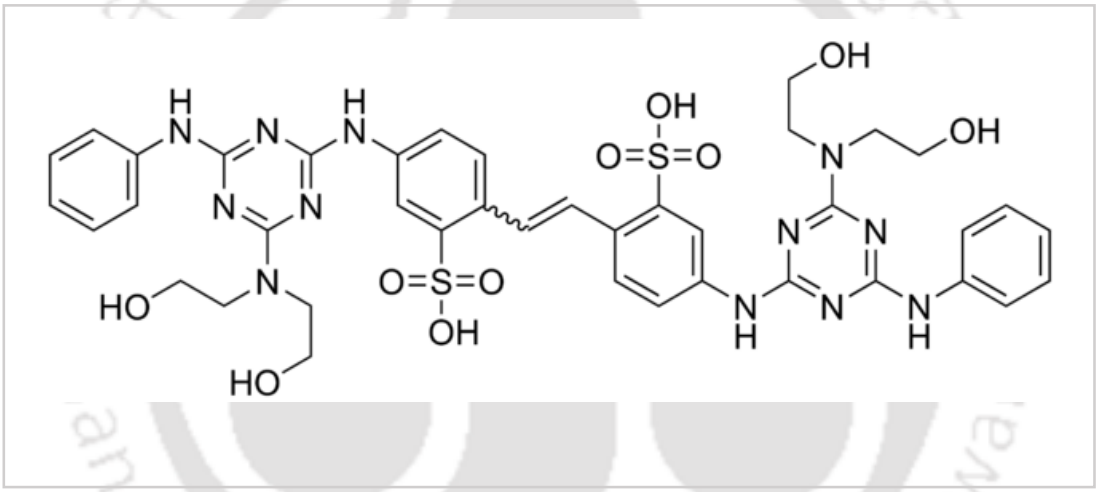

(B)

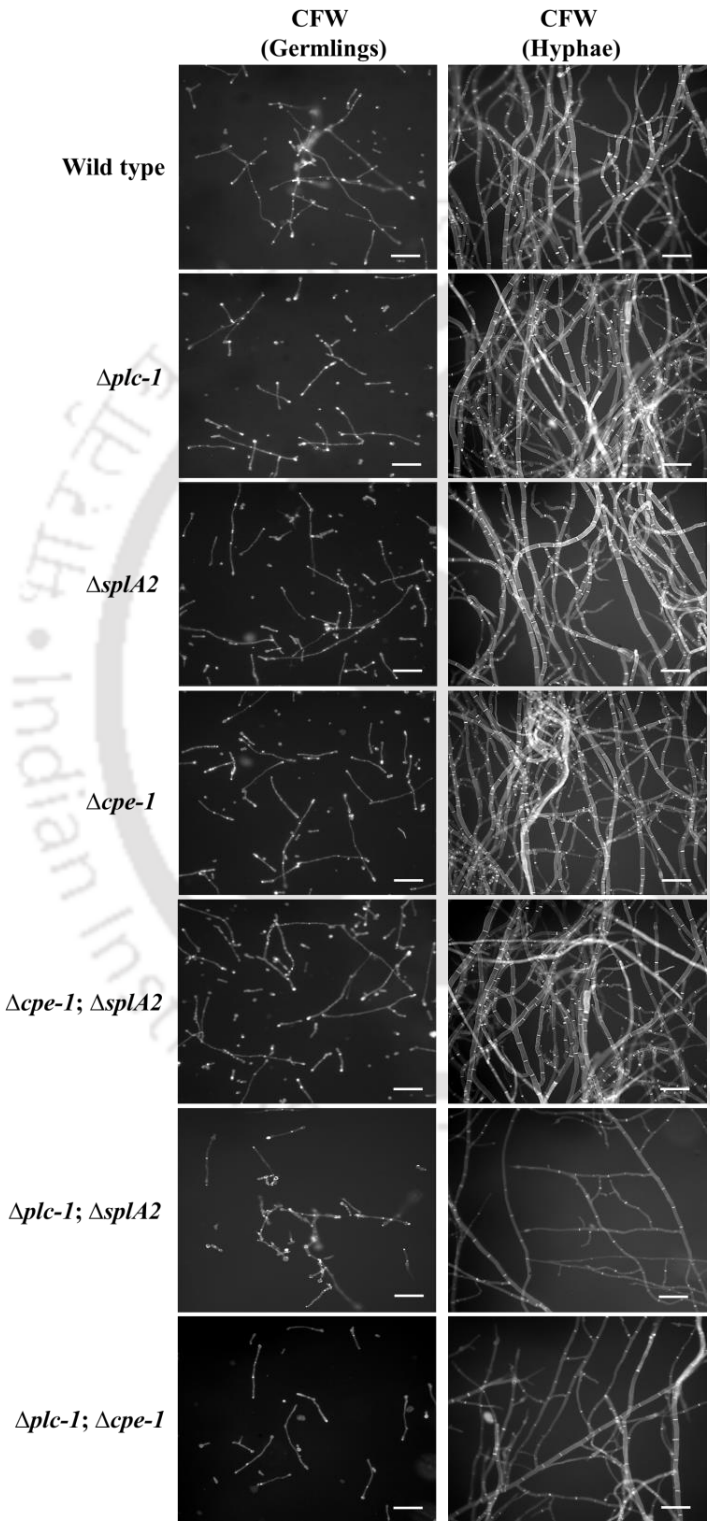

Figure 5.3: Assay for visualization of internal septation of germlings and hyphae. (A) Chemical structure of calcoflour white (CFW; λ_{ex}= 355 nm; λ_{em}= 420 nm). CFW a non-specific fluorochrom that binds with cellulose and chitin contained in the cell walls of fungi and other organisms. Its chemical structure is available at http://www.sigmaaldrich.com/catalog/product/sigma/f3543?lang=en&region=IN. **(B)** Germlings and hyphae of the wild type, Δ*plc-1*, Δ*splA2*, and Δ*cpe-1* single mutant and Δ*cpe-1*; Δ*splA2* strains stained with CFW (0.1% in 0.05 M PBS) showed bright staining at septa and cell walls whereas Δ*plc-1*; Δ*splA2* and Δ*plc-1*; Δ*cpe-1* showed reduced CFW staining at septa and cell walls. The sample slides were incubated in the dark for 20 minutes and observed under a Trinocular inverted fluorescence microscope (AxioVert A1 FL, Carl Zeiss) under DAPI filters with exposure time of 300-400 ms. Scale bar 20 µm.

5.2.3.2 Assay for visualization of intracellular distribution of Ca^{2+}

N. crassa maintains a tip high Ca^{2+} gradient during hyphal extension and sequestration of Ca^{2+} occurs in the storage vesicles immediately behind the apex (Schmid and Harold 1988; Silverman-Gavrila and Lew 2000). The tip high Ca^{2+} gradient is generated and maintained internally by the IP_3 activated Ca^{2+} channels (Silverman-Gavrila and Lew 2002). The RIP mutant of vacuolar H^+-ATPase, *vma-1*, exhibited altered vacuolar morphology, depleted Ca^{2+} vacuolar stores affecting Ca^{2+} homeostasis, and showed severe morphological defects including colony morphology, shorter aerial hyphae, and female sterility (Bowman et al. 2000). I, therefore, visualized the internal stores such as Ca^{2+} storing vesicles of the wild type, Δ*plc-1,* Δ*splA2*, Δ*cpe-1* single and double mutant strains using chlortetracycline (CTC), a dye that binds to $Ca^{2+}$and forms a fluorescent complex (Figure 5.4 A; Schmid and Harold 1988). Intensity of fluorescence increases upon binding of complex to membranes that enables visualization of Ca^{2+} accumulation in vesicles and organelles (Schmid and Harold 1988; Bowman et al. 2000). Microscopic analysis showed enhanced fluorescence in the internal Ca^{2+} storing vesicles in the growing hyphae of the wild type, Δ*plc-1*, Δ*splA2*, Δ*cpe-1*, and Δ*cpe-1*; Δ*splA2* strains (Figure 5.4 C). However, significantly fewer Ca^{2+} storing vesicles were observed in the young growing hyphae of Δ*plc-1*; Δ*splA2* and Δ*plc-1*; Δ*cpe-1* double mutants (Figure 5.4 C). This indicated that loss of *plc-1* with *splA2* and *plc-1* with *cpe-1* caused disruption of Ca^{2+} homeostasis which lead to various morphological defects as observed in these two strains (discussed in Chapter 4).

Apart from Ca^{2+}, CTC fluorescence is also affected by intracellular distribution of membranes and Mg^{2+} ions (Caswell 1979; Blinks et al. 1982). I further visualized the growing hyphae in the presence of 1-N-Phenylnaphthylamine (NPN), a fluorescent probe that binds to cell membranes (Figure 5.4 B). I did not observe enhanced fluorescence in the Ca^{2+} storing vesicles in the hyphae of any of the strains which ruled out the possibility that the fluorescence of CTC was contributed by membrane density or Mg^{2+} ions (Figure 5.4 C).

(A)

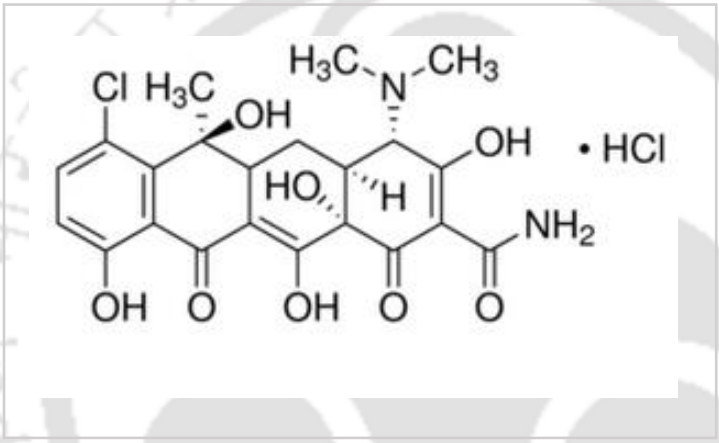

(B)

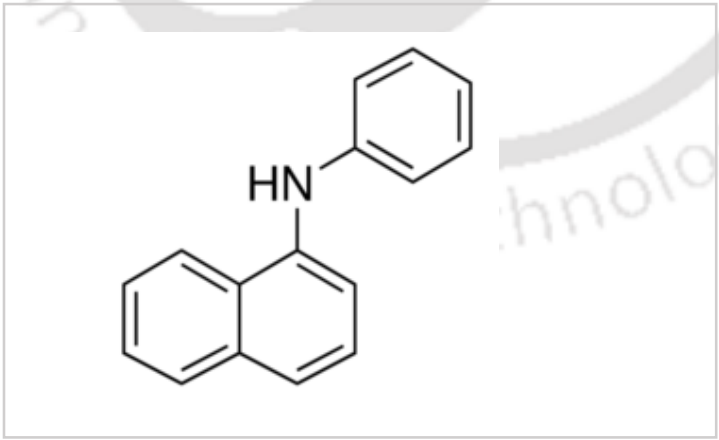

(C)

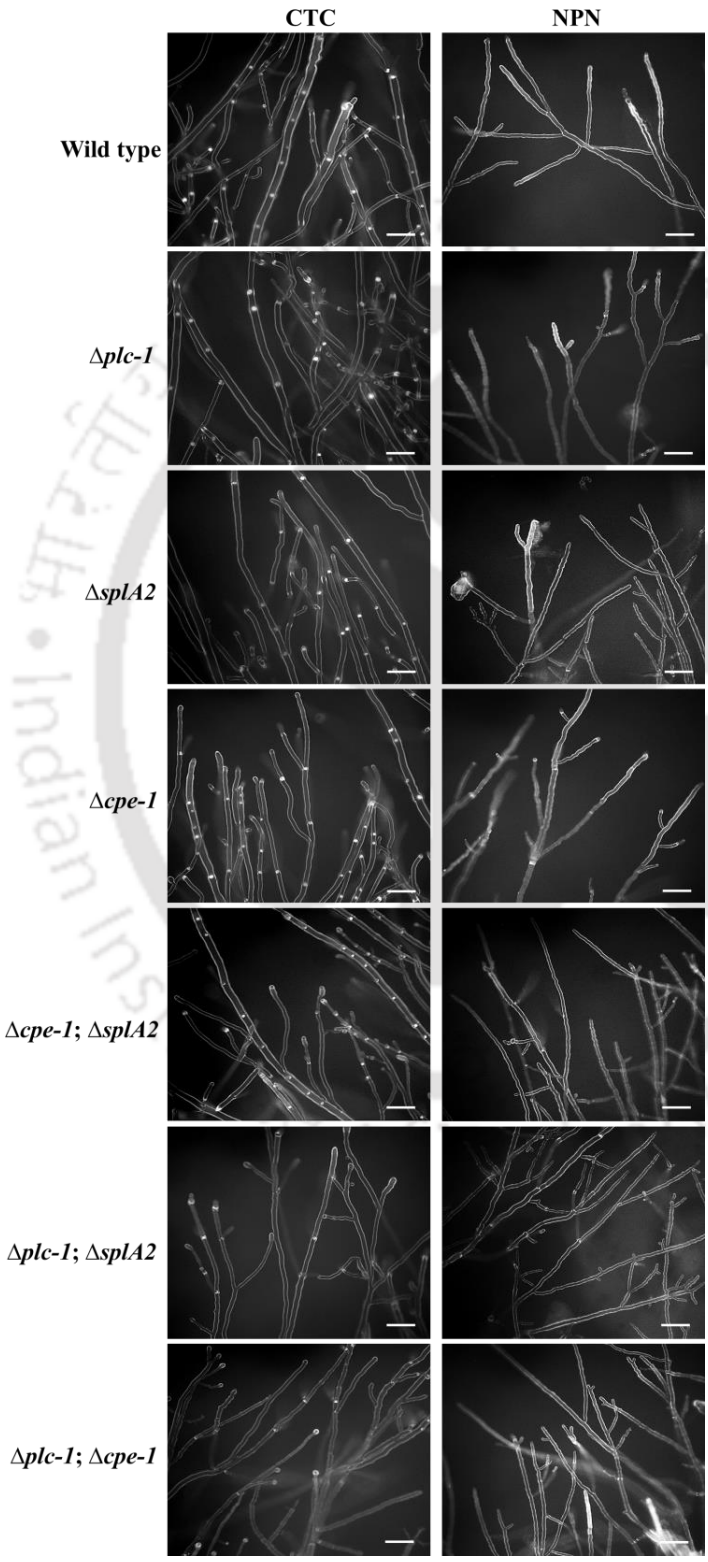

Figure 5.4: Assay for visualization of intracellular distribution of Ca^{2+}. (A) Chemical structure of chlortetracycline hydrochloride (CTC; λ_{ex}= 400 nm; λ_{em}= 470 nm). Its chemical structure is available at http://www.sigmaaldrich.com/catalog/product/sigma/c4881?lang=en&region=IN. **(B)** Chemical structure of 1-N-Phenylnaphthylamine (NPN; λ_{ex}= 380 nm; λ_{em}= 470 nm). Its chemical structure is available at http://www.sigmaaldrich.com/catalog/product/sial/104043?lang=en&region=IN&utm_term=n-phenylnaphthylamine&utm_medium=cpc&utm_content=sial/104043&utm_source=bing&utm_campaign=Top%20Product%20Replacements%20(Bing%20ebizpfs). **(C)** Hyphae of the wild type, Δ*plc-1*, Δ*splA2*, and Δ*cpe-1* single and double mutant strains were grown in Vogel's glucose agar medium supplemented with 200 µM CTC or 20 µM NPN in 0.1% dimethyl sulphoxide (DMSO). CTC and NPN fluorescence was observed under a Trinocular inverted fluorescence microscope (AxioVert A1 FL, Carl Zeiss) under DAPI filters with exposure time of 300-400 ms. Scale bar 20 µm.

5.2.4 Transcriptional analysis of biosynthetic and developmental genes

5.2.4.1 The Δ*plc-1*, Δ*splA2*, and Δ*cpe-1* mutants showed an increase in expression of carotenoid biosynthetic genes *albino-1 (al-1)*, *albino-2 (al-2)*, and *albino-3 (al-3)*

In Chapters 3 and 4, I reported higher carotenoid accumulation in the Δ*plc-1,* Δ*splA2*, and Δ*cpe-1* single mutants as compared to wild type, and the increased carotenoid amounts was shown to be linked with increased intracellular ROS generation in all the three mutants (Chapter 3; Figure 3.14 A-C; Table 3.7; Chapter 4; Figures 4.14 A-C; 4.15 A-C). The *N. crassa* carotenoid biosynthetic pathway is regulated by the neurosporoxanthin biosynthetic genes *albino-1* (*al-1*) that encodes a phytoene dehydrogenase, the bi-functional gene *albino-2* (*al-2*) that encodes a phytoene synthase and a carotene cyclase, and the *albino-3* (*al-3*) that encodes geranylgeranyl pyrophosphate synthetase (Figure 5.5 A; Dián-Sánchez et al. 2011; Luque et al. 2012). I examined the expression of the *al-1*, *al-2*, and *al-3* genes in the wild type, Δ*plc-1,* Δ*plc-1*, and Δ*cpe-1* mutants by quantitative real time PCR (qRT-PCR) using RNA obtained from mycelia exposed to either white light at 30°C or incubated in the dark as control (discussed in chapter 2). I found that the high carotenoid accumulation in the Δ*plc-1* mutant correlated with the higher expression of the *al-1* and *al-2* genes in the mutant (Figure 5.5 B; Table 5.5; Entry 1-6). In addition, increased expression of the *al-1* followed by *al-3* and *al-2* was observed in the Δ*splA2* mutant, whereas, expression of only

al-1 gene was found to be enhanced in the Δ*cpe-1* mutant (Figure 5.5 B). Thus, these results indicated that increased carotenoid accumulation in the Δ*plc-1,* Δ*splA2*, and Δ*cpe-1* mutants correlated with the increased expression of the *al-1*, *al-2*, and *al-3* genes that are involved in the *N. crassa* carotenoid biosynthesis pathway.

Table 5.5: Primers used for qRT-PCR analysis

Sl. No.	Primer	Sequence (5′→3′)	Source
1	Qal-1-Fw	ACCGACAACGCCACCATGAA	This study
2	Qal-1-Rv	AGTTGCGGTGCAGAACGTGT	This study
3	Qal-2-Fw	AAGGTTACCGGCCAGGTAGT	This study
4	Qal-2-Rv	GAGGGTCCAGATAGCCAGTA	This study
5	Qal-3-Fw	AACCCAGACCGATTTGCGAC	This study
6	Qal-3-Rv	GTCGAAGGCCTTGACCATCT	This study
7	Qcon10-Fw	CCAAGGAAGAGGTTCAGGCC	This study
8	Qcon10-Rv	TTGCCGCCCTTGGAAGCAAT	This study
9	Qccg-4-Fw	CAGCCTCCAAGAGAAGTTCG	This study
10	Qccg-4-Rv	CACGCTTCTTCCAGCACGAT	This study
11	Qmfa-1-Fw	ATGCCTTCCACCGCTGCTTC	This study
12	Qmfa-1-Rv	CATAACAACGCAGTAGCCGT	This study
13	Qfmf-1-Fw	CGGACAAGACAGCAGTTCCT	This study
14	Qfmf-1-Rv	TTTCGGTGGTTGCTGTTCATC	This study
15	Qtub-Fw	CCCAAGAACATGATGGCTGC	This study
16	Qtub-Rv	TTGTTCTGAACGTTGCGCATC	This study

(A)

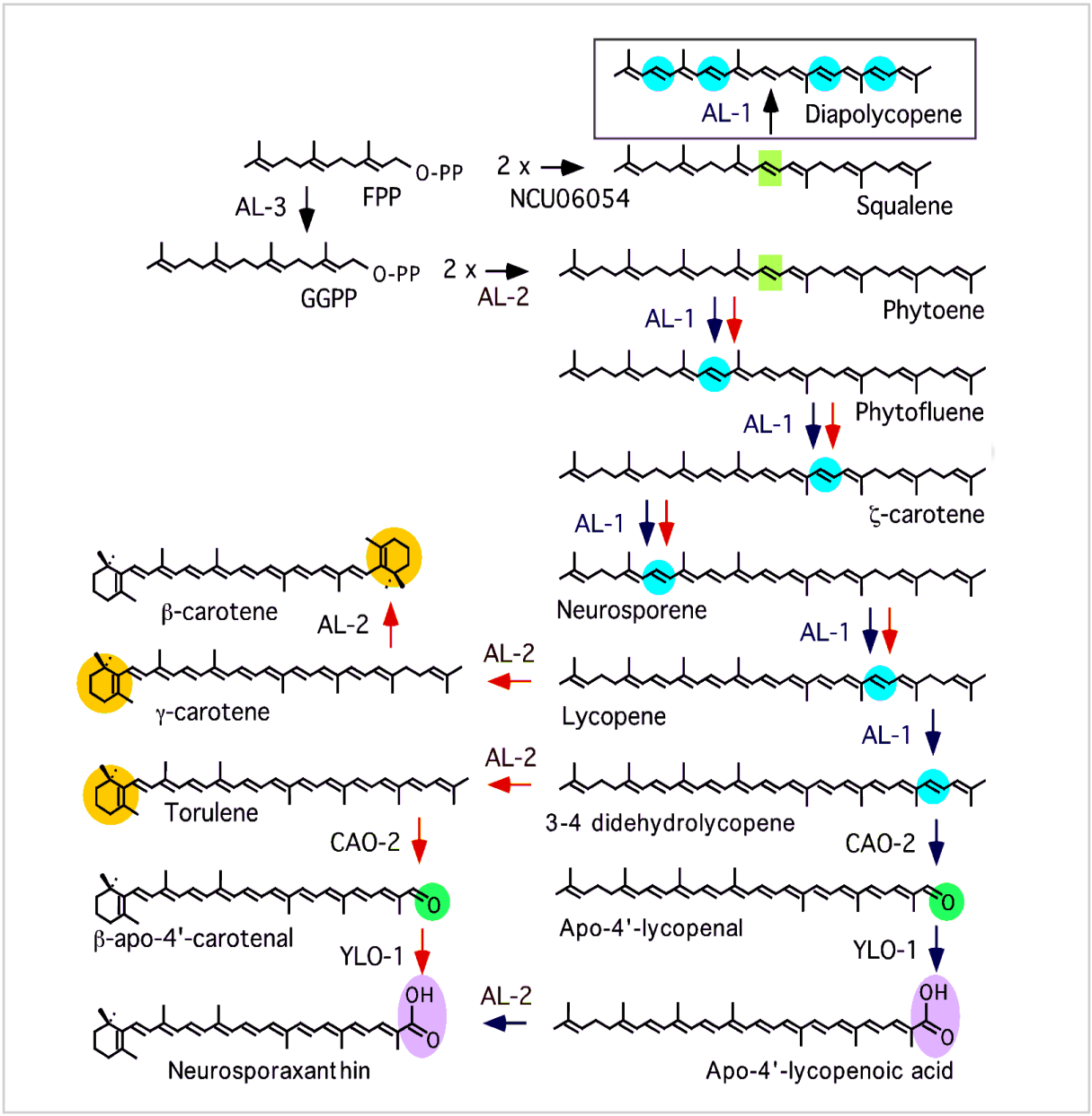

(B)

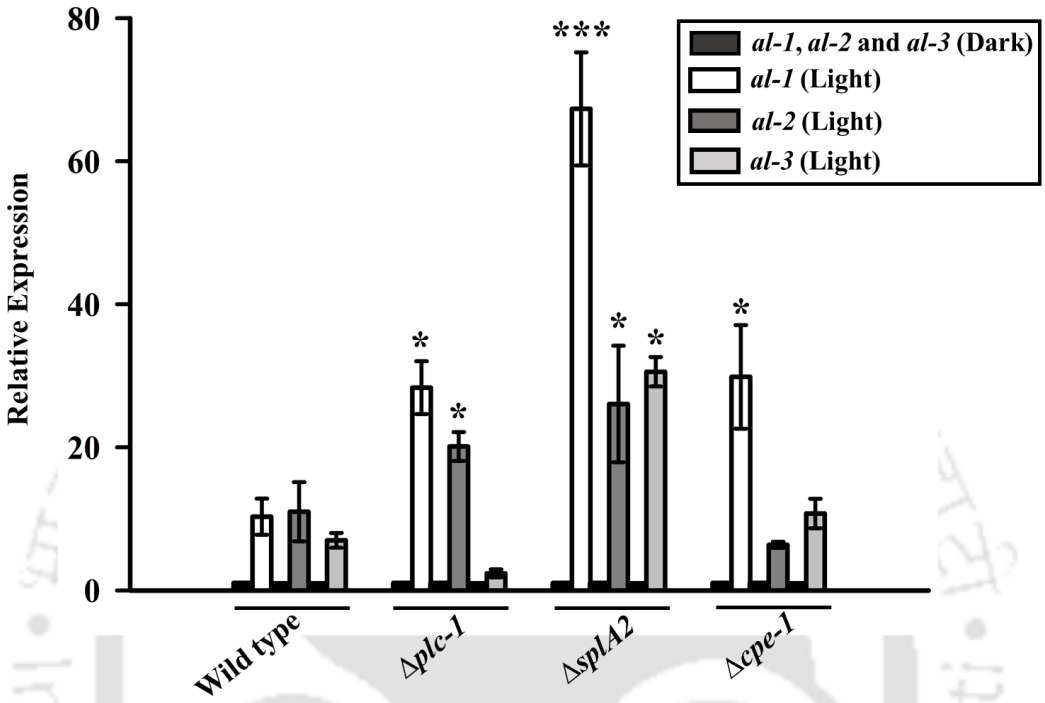

Figure 5.5: Carotenoid biosynthetic pathway and neurosporaxanthin biosynthetic gene expression in carotenoid inducing cultures of wild type, Δ*plc-1*, Δ*splA2*, and Δ*cpe-1* single mutant strains. (A) Neurosporoxanthin biosynthetic pathway in *N. crassa*. Neurosporoxanthin biosynthesis is greatly enhanced upon illumination at low temperature (predominant steps from phytoene upon illumination at 8°C), whereas illumination at normal temperature results in the accumulation of carotenoid precursors (predominant steps from phytoene upon illumination at 30°C). The light inducible genes *al-1*, *al-2*, and *al-3* encode enzymes that regulate biosynthesis of neurosporoxanthin. Adapted from Diáz-Sánchez et al. 2011. **(B)** RNA was extracted from Vogel's glucose medium carotenoid cultures and expression of neurosporoxanthin biosynthetic genes *al-1*, *al-2*, and *al-3* were studied by qRT-PCR on three biological replicates for each of the *N. crassa* strain indicated. The relative expression of each gene was normalized to the expression of β-tubulin gene and expression values were compared with that of wild type. Error bars indicate standard deviations calculated from the data for three independent experiments (n = 3) with P values <0.05 (*), <0.01 (**), and <0.001 (***) compared with the wild type strain as measured by one-way ANOVA test.

5.2.4.2 Submerged cultures of the Δ*plc-1*; Δ*splA2* and Δ*plc-1*; Δ*cpe-1* double mutants showed inappropriate expression of conidiation specific gene *con-10*

In Chapter 4, I described a few phenotypic abnormalities of the Δ*plc-1*; Δ*splA2* and Δ*plc-1*; Δ*cpe-1* double mutant strains including early conidiation in growth-repressing conditions and inappropriate conidiation in submerged cultures (Chapter 4; Figures 4.7; 4.9). Inappropriate expression of the conidiation specific gene *con-10* was found to correlate with conidiation in submerged cultures (Madi et al. 1997; Kays et al. 2000; Ivey et al. 2002; Yang et al. 2002). Therefore, to test if the conidiation observed in submerged cultures of the Δ*plc-1*; Δ*splA2* and Δ*plc-1*; Δ*cpe-1* double mutants also correlated with the expression of *con-10*, transcript level of *con-10* was determined by qRT-PCR using the RNA isolated from submerged cultures and the *con-10* primers (Table 5.5; Entry 7-8). The 16 h submerged cultures of Δ*plc-1*; Δ*splA2* and Δ*plc-1*; Δ*cpe-1* double mutants showed seven and four-fold increase in the transcription level of *con-10* respectively, relative to wild type, *Δplc-1*, *ΔsplA2*, *Δcpe-1*, and Δ*cpe-1*; Δ*splA2* (Figure 5.6). However, addition of 2% peptone in submerged cultures resulted in similar transcript level of *con-10* in the Δ*plc-1*; Δ*splA2* and Δ*plc-1*; Δ*cpe-1* double mutants as compared to wild type, *Δplc-1*, *ΔsplA2*, *Δcpe-1*, and Δ*cpe-1*; Δ*splA2* (Figure 5.6). Therefore, I concluded that inappropriate expression of the *con-10* correlated with the inappropriate conidiation in the Δ*plc-1*; Δ*splA2* and Δ*plc-1*; Δ*cpe-1* double mutants and that the interaction between *plc-1* and *splA2*, and also *plc-1* and *cpe-1*, plays a critical role in normal conidiation in *N. crassa*.

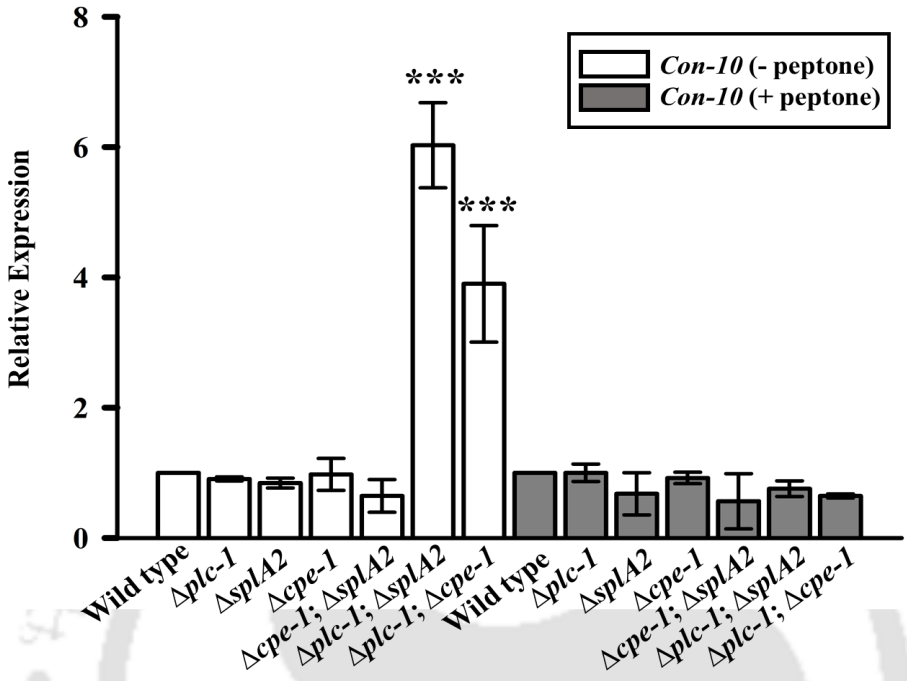

Figure 5.6: Expression of conidiation specific gene in submerged cultures of wild type, Δ*plc-1*, Δ*splA2*, and Δ*cpe-1* single and double mutant strains. RNA was extracted from submerged cultures and conidiation specific *con-10* gene expression was studied by qRT-PCR on three biological replicates of each strain. The relative expression of the *con-10* gene was normalized with the β-tubulin gene and expression values were compared with that of wild type. Error bars indicate standard deviations calculated from the data for three independent experiments (n = 3) with P values <0.05 (*), <0.01 (**), and <0.001 (***) compared with the wild type strain as measured by one-way ANOVA test.

5.2.4.3 The Δ*plc-1*; Δ*splA2* and Δ*plc-1*; Δ*cpe-1* double mutants showed decreased expression of *clock-controlled gene-4 (ccg-4)*, *mating factor a-1* (*mfa-1)*, and *female and male fertility-1 (fmf-1)* genes

In addition to the low levels of nitrogen, light, and low temperature, sexual development in *N. crassa* is also regulated by a few sexual development and pheromone related genes. The *N. crassa mat A* cells express the pheromone receptor gene *pre-1* and the corresponding pheromone precursor gene *clock-controlled gene-4* (*ccg-4*), while *mat a* cells express the *pre-2* pheromone receptor gene and the predicted pheromone precursor *mating factor a-1 (mfa-1)* gene (Bobrowicz

et al. 2002). The chemotropic polarized growth of female specific trichogyne towards a fertilizing male cell is regulated by PRE-1 and PRE-2 that recognize and bind to MFA-1 and CCG-4 pheromones, respectively (Bobrowicz et al. 2002; Kim et al. 2002; 2012; Kim and Borkovich 2004; 2006; Deka et al. 2016). Another pheromone related gene *fmf-1*, which encodes the female and male fertility gene, play a role in pheromone signaling for mating in *N. crassa*. Since the Δ*plc-1*; Δ*splA2* and Δ*plc-1*; Δ*cpe-1* double mutants failed to produce matured perithecia as a female parent (Chapter 4; Figure 4.23 A-B; Table 4.12), therefore, I examined the transcription levels of pheromone related genes *ccg-4*, *mfa-1*, and *fmf-1* in the Δ*plc-1*; Δ*splA2* and Δ*plc-1*; Δ*cpe-1* considering an incubation period of 18-20 h to avoid conidiation induced by starvation in liquid cultures for nitrogen or glucose limitation in *N. crassa* (Müller and Russo 1989; Bobrowicz et al. 2002). RNA was isolated from the nitrogen starved tissues of each of the strain, and subsequently expression of the *ccg-4*, *mfa-1*, and *fmf-1* was determined by qRT-PCR using the *ccg-4*, *mfa-1*, and *fmf-1* primers (Table 5.5; Entry 9-14). As consistent with the female sterility phenotype, liquid cultures of Δ*plc-1*; Δ*splA2* and Δ*plc-1*; Δ*cpe-1* showed significantly reduced expression of *ccg-4*, *mfa-1*, and *fmf-1* in comparison to the wild type, individual single mutants and Δ*cpe-1*; Δ*splA2* (Figure 5.7 A-C). Therefore, these results further indicated that interaction of the *plc-1* with *splA2* and *cpe-1* play an important role in sexual development that could involve normal expression of pheromone signaling genes in *N. crassa*.

(A)

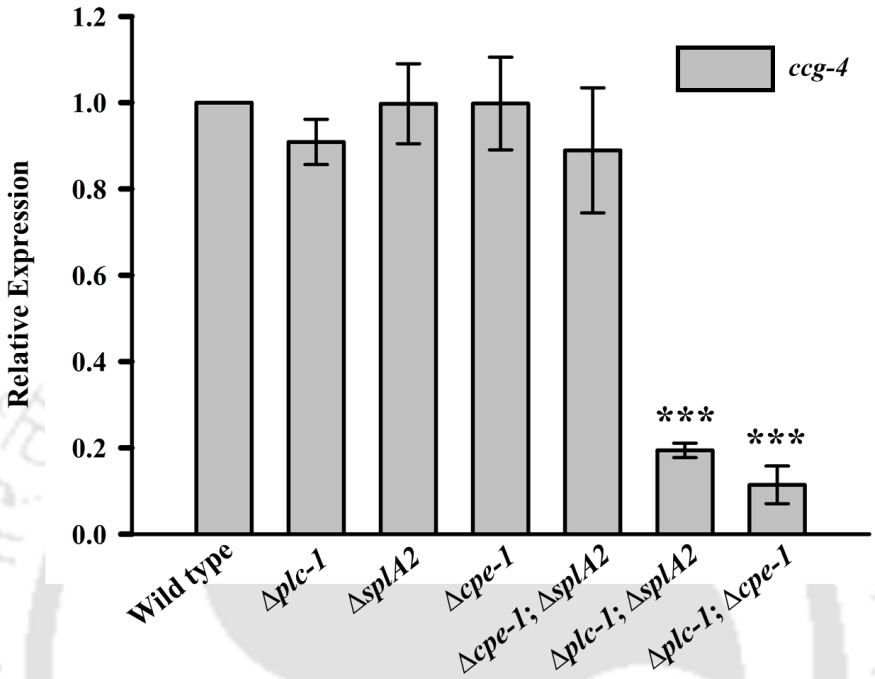

(B)

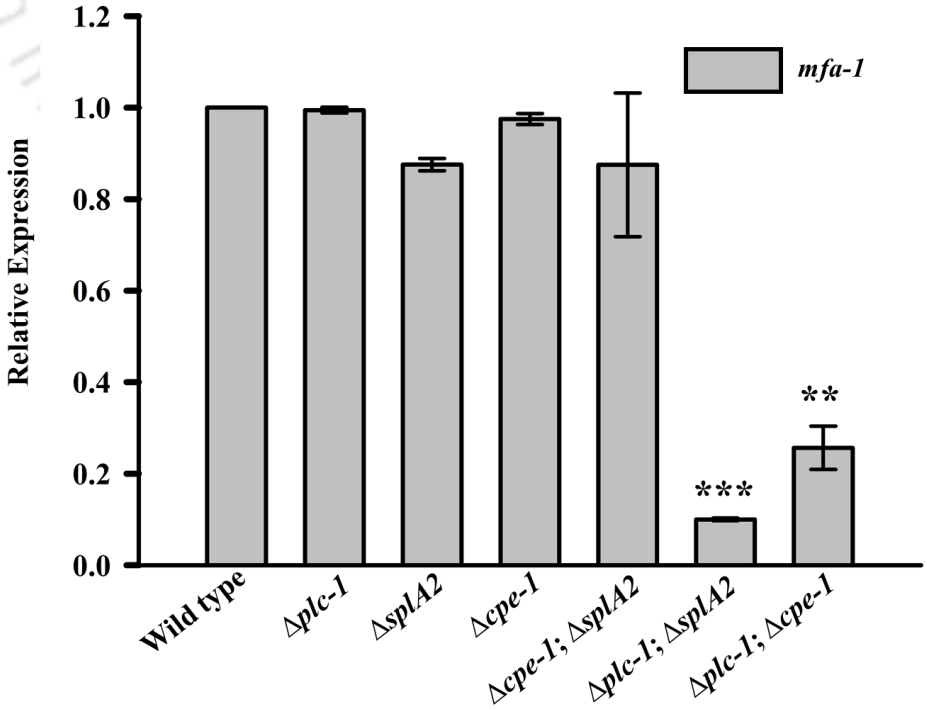

(C)

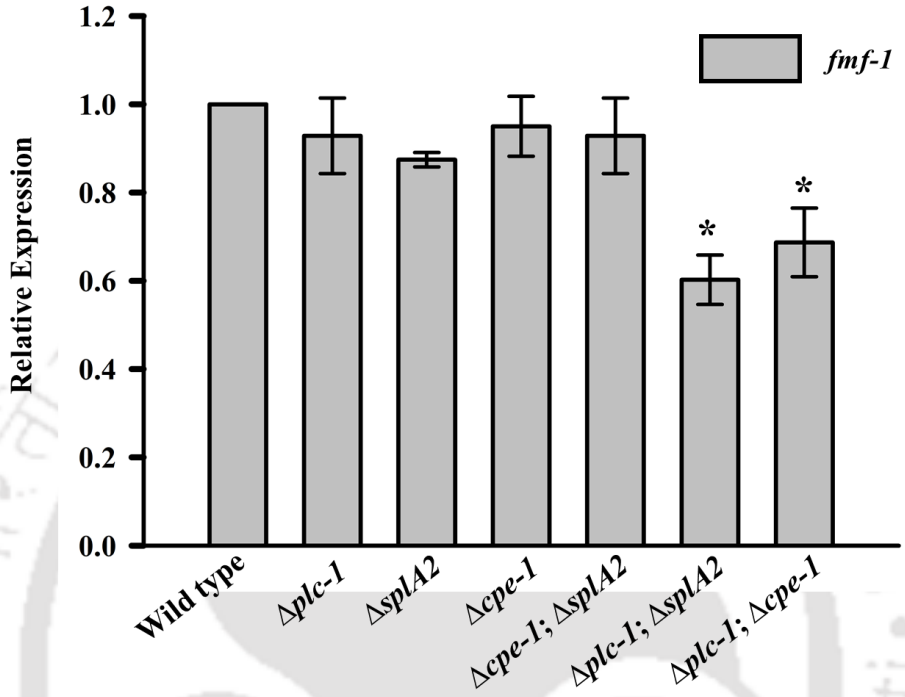

Figure 5.7: Expression of the pheromone signaling genes in the wild type, Δ*plc-1*, Δ*splA2*, Δ*cpe-1* single and double mutant strains. RNA was extracted from SCM cultures and the expression of mating pheromone signaling genes **(A)** *ccg-4*, **(B)** *mfa-1*, and **(C)** *fmf-1* were studied by qRT-PCR on three replicates for each of the *N. crassa* strains indicated. The relative expression of each gene was normalized to the expression of *β*-tubulin gene and expression values were compared with that of wild type. Error bars indicate standard deviations calculated from the data for three independent experiments (n = 3) with P values <0.05 (*), <0.01 (**), and <0.001 (***) compared with the wild type strain as measured by one-way ANOVA test.

5.2.4.4 Expression analysis of the *plc-1*, *splA2*, and *cpe-1* genes

I examined *plc-1*, *splA2*, and *cpe-1* transcript level in the wild type and the single mutants by qRT-PCR using the RNA extracted from the cultures of 16 h conidia of the corresponding strains. I observed decreased transcript level of *cpe-1* in both Δ*plc-1* and Δ*splA2* mutants, while *plc-1* transcription level was decreased only in the Δ*cpe-1* mutant (Figure 5.8). Similarly, transcription of *splA2* gene was only moderately affected in the Δ*plc-1* and Δ*cpe-1* mutants (Figure 5.8).

Therefore, this result suggested a possible transcriptional control feedback between *plc-1* and *cpe-1*, and regulation of *cpe-1* transcription by *splA2*.

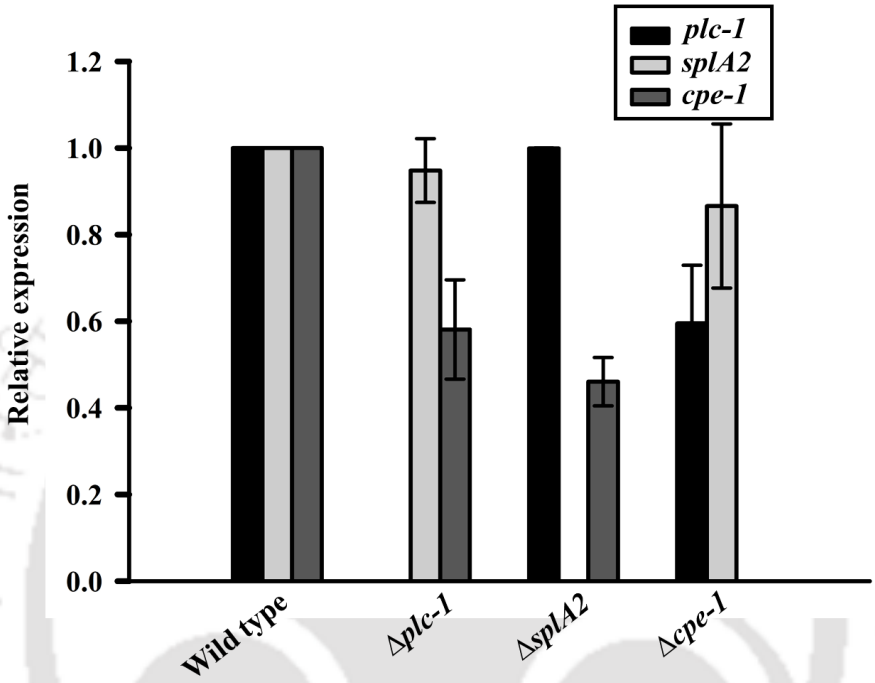

Figure 5.8 Expression analysis of *plc-1*, *splA2*, and *cpe-1* genes in the *N. crassa* strains. Approximately 10^6 conidia/ml were inoculated in Vogel's glucose medium and incubated at 30°C with shaking at 180 rpm for 16 h in complete darkness. RNA was extracted from the cultures and relative expression of *plc-1*, *splA2*, and *cpe-1* genes were normalized with the *N. crassa* β-tubulin gene expression. Expression values were compared with that of wild type.

5.2.5 Molecular mechanism of Ca^{2+} mediated signaling responses of *plc-1*, *splA2*, and *cpe-1* genes

In response to appropriate stimuli, PLC-1 generates IP_3 which induces release of Ca^{2+} from intracellular Ca^{2+} stores causing an increase in $[Ca^{2+}]_c$ and also releases DAG that activates PKC. Increased $[Ca^{2+}]_c$ and/or activated PKC acts as a signal for the $Ca^{2+}$and/CaM binding sPLA2 protein. The Ca^{2+} and PKC modulated sPLA2 protein in turn regulates *N. crassa* growth and development. On the other hand, CPE-1 regulates fertility possibly through regulation of a pheromone response cascade by the Ca^{2+} buffering activity of CPE-1 (Figure 5.9). Therefore,

genetic interactions between the *plc-1*, *splA2*, and *cpe-1* generates appropriate Ca^{2+} signaling that mediates *N. crassa* growth and development.

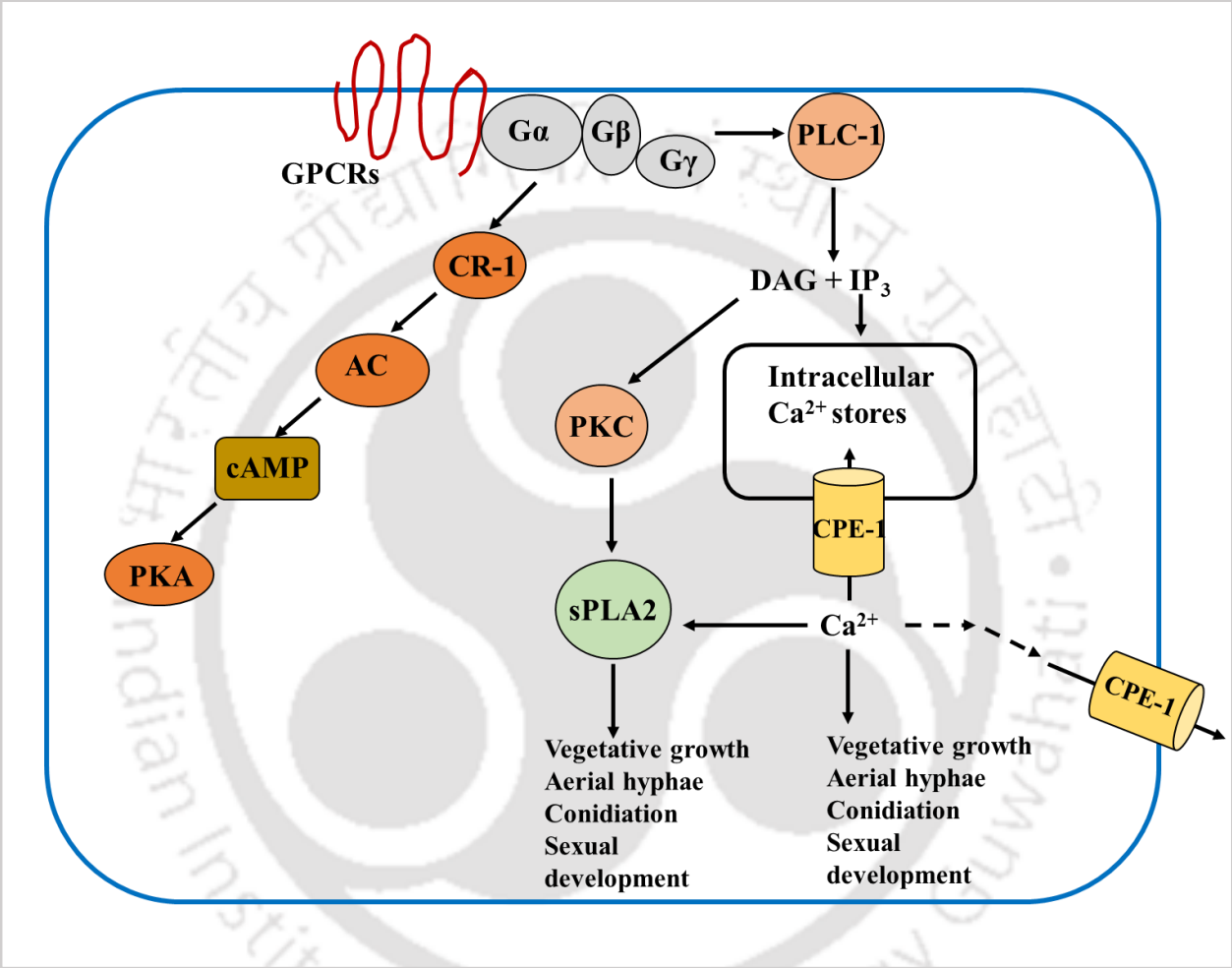

Figure 5.9: A possible mechanistic model behind the Ca^{2+} mediated signaling responses of *plc-1*, *splA2*, and *cpe-1* genes. The *plc-1*, *splA2*, and *cpe-1* genes act in coordination for maintaining cellular Ca^{2+} homeostasis. Imbalance or disruption of Ca^{2+} homeostasis triggers a number of morphological and physiological changes. AC: adenylyl cyclase; cAMP: 3′, 5′- cyclic adenosine monophosphate; CPE-1: Ca^{2+}/H^{+} exchanger-1; CR-1: crisp-1; DAG: diacylglycerol; GPCR: G-protein-coupled receptor; Gα: G-protein α subunit; Gβ: G-protein β subunit; Gγ: G-protein γ subunit; IP_3: inositol-1, 4, 5-trisphosphate; PKA: protein kinase A; PLC-1: phospholipase C-1; PKC: protein kinase C; sPLA2: secretory phospholipase A2.

5.3 Discussion

Intracellular signaling pathways are complex and are regulated by the two fundamental second messengers, cAMP and Ca^{2+}. A variety of extracellular stimuli activates specific GPCRs and the activated G protein stimulates adenylyl cyclase, which in turn converts ATP to cAMP. Increased cAMP concentration further activates cAMP-dependent PKA and thereby phosphorylates a number of target proteins. Dephosphorylation of cAMP to AMP by cAMP phosphodiesterases shuts off the cAMP signaling pathway (Moore et al. 1998). Activated G protein is also known to stimulate membrane associated PLC that in turn catalyses hydrolysis of PIP_2 into IP_3 and DAG. The polar molecule IP_3 induces Ca^{2+} release from endoplasmic reticulum and other intracellular Ca^{2+} stores into the cytosol and increased $[Ca^{2+}]_c$ activates target proteins such as kinases and phosphatases (Berridge 1987; 1993; Cornelius 1989). Ca^{2+} influences cAMP levels by regulating the activities of adenylate cyclase, an enzyme that synthesizes cAMP and phosphodiesterase, an enzyme that catalyses breakdown of cAMP (DeBernardi and Brooker 1996; Moore et al. 1998; Hanoune and Defer 2001). On the other hand, phosphorylation of target proteins by PKA triggered by cAMP has been shown to regulate cellular Ca^{2+} homeostasis via activation of Ca^{2+} channels or Ca^{2+} ATPases (Carafoli 1992; Gray et al. 1998; Negash et al. 2000; Sorrentino and Rizzuto 2001; Wetzel et al. 2001; Yang et al. 2001). Thus, the Ca^{2+} and cAMP signaling pathways are tightly interconnected and effectively regulates a wide array of target proteins thus controlling a myriad of cell functions (DeBernardi and Brooker 1996; Zaccolo and Pozzan 2003). *N. crassa* is the first filamentous fungus, where G protein encoding genes were identified (Turner and Borkovich 1993; Galagan et al. 2003). The *N. crassa* Gα protein possesses 10 predicted seven-transmembrane helix proteins that includes three putative cAMP receptor proteins and three essential proteins adenylyl cyclase, cyclase associated protein, and putative cAMP phosphodiesterases for the synthesis and degradation of cAMP (Turner and Borkovich 1993; Galagan et al. 2003). The cAMP signaling plays a critical role in asexual differentiation of aerial hyphae to proconidial chain formation (Greenwald et al. 2010). It also regulates branching as observed in the colonial mutants of *N. crassa* (Reissig and Kinney 1983). The cAMP-PKA signaling in *N. crassa* is activated by the glucose sensor GPR-4 (GPCR) that interacts with the Gα subunit GNA-1 protein and activates adenylate cyclase, regulating growth and development via cAMP signaling (Ivey et al. 2002). The adenylate cyclase mutant *cr-1* and the G protein α subunit *gna-1* and *gna-3* mutants exhibited colonial growth and rapid conidiation, phenotypic defects that were overcome by the addition of

exogenous cAMP (Kays et al. 2000; Ivey et al. 2002). The Ca^{2+} signaling PLC-1 protein was predicted to interact with the G α subunit proteins GNA-1, GNA-2, and GNA-3 (Figure 5.1 A). The two double mutant Δ*plc-1*; Δ*splA2* and Δ*plc-1*; Δ*cpe-1* exhibited similar abnormal morphologies like the *cr-1* and *gna-1* (discussed in Chapter 4). However, I found that the addition of exogenous cAMP does not fully restore the phenotypes of the Δ*plc-1*, Δ*splA2*, and Δ*cpe-1* and their double mutants (Figures 5.2 A-I; Table 5.1-5.4). This result suggested that the Ca^{2+} signaling responses mediated by the *plc-1*, *splA2*, and *cpe-1* genes occur through a cAMP independent pathway.

The Δ*plc-1*, Δ*splA2*, and Δ*cpe-1* and their double mutants showed normal cell wall and septa formation similar to the wild type strain (Figure 5.3). Therefore, morphological defects observed in the Δ*plc-1*; Δ*splA2* and Δ*plc-1*; Δ*cpe-1* double mutants were not due to lack of proper septation, indicating other physiological defects in these double mutants. In addition, CTC staining of Δ*plc-1*; Δ*splA2* and Δ*plc-1*; Δ*cpe-1* double mutants showed depleted Ca^{2+} stores, indicating that the deletion of both the *plc-1* together with *splA2* or *cpe-1* causes disruption of Ca^{2+} homeostasis causing various phenotypic abnormalities exhibited by the two double mutants (Figure 5.4).

I also performed qRT-PCR and determined fold change expression of some of the important genes such as carotenoid biosynthetic genes *al-1*, *al-2*, and *al-3*, conidiation specific gene *con-10*, and the pheromone signaling genes *ccg-4*, *mfa-1*, and *fmf-1*, in the wild type, single, and double mutant strains. Carotenoid biosynthetic pathway in *N. crassa* comprises of phytoene synthase, dehydrogenase, cyclase, and oxidase enzyme activities and is regulated by a number of neurosporoxanthin biosynthetic genes including the albino genes *al-1*, *al-2*, and *al-3* that encode for a phytoene dehydrogenase, a phytoene synthase, and a geranylgeranyl pyrophosphate synthetase, respectively (Zalokar 1954; Arrach et al. 2002). I observed differentially increased expression of the three albino genes in the Δ*plc-1*, Δ*splA2*, and Δ*cpe-1* mutants that further supported the increased carotenoid amounts as reported in these mutants (Figure 5.5). During the asexual phase of *N. crassa*, subset of genes are differentially expressed and few of them participate in the conidial development process (Roberts et al. 1988). One such gene is conidiation specific *con-10* expressed during the later stages of conidiation (Roberts et al. 1988). The double mutants Δ*plc-1*; Δ*splA2* and Δ*plc-1*; Δ*cpe-1* showed enhanced transcript level of *con-10* in submerged cultures which confirmed further that genetic interactions between the *plc-1*, *splA2*, and *cpe-1* genes is important for normal asexual sporulation in *N. crassa* (Figure 5.6). The process of sexual

development in *N. crassa* is regulated by a few sexual development and pheromone related genes. The polarized chemotropic growth of trichogynes, which originates from a female cell towards a fertilizing male cell, is regulated by the GPCRs PRE-1 and PRE-2 that recognize and bind to their respective pheromones MFA-1 and CCG-4, respectively (Bobrowicz et al. 2002; Kim et al. 2002, 2012; Kim and Borkovich 2004, 2006; Deka et al. 2016). PRE-1 and PRE-2 are homologous to the pheromone receptors Ste3p and Ste2p, and MFA-1 and CCG-4 are homologous to the pheromone precursor a- and α-mating factors of *S. cerevisiae*, respectively (Pöggeler and Kück 2001; Bobrowicz et al. 2002; Kim et al. 2002; Kim and Borkovich 2006; Deka et al. 2016). The pheromone precursor genes *ccg-4* and *mfa-1* are under circadian clock control and shows rhythms in mRNA accumulation with the average peak occurring at the subjective early morning (Loros et al. 1989; Bell-Pederson et al. 1996). The female and male fertility gene *fmf-1*, homologue of *S. pombe* transcription factor *ste11*, regulator of sexual development, plays a corresponding role in mating pheromone signaling in *N. crassa* (Qin et al. 2003; Iyer et al. 2009). Presence of pheromone response elements in the upstream of the promoter region of *plc-1*, *splA2*, and *cpe-1* further confirmed the requirement of these genes during the sexual development in *N. crassa* (Figure 4.25; Table 4.14; discussed in Chapter 4). The Δ*plc-1*; Δ*splA2* and Δ*plc-1*; Δ*cpe-1* double mutants exhibited decreased transcript levels of all three pheromone signaling genes in particular *ccg-4* and *mfa-1* (Figure 5.7 A-C). Thus, I found that the product of the *plc-1*, *splA2*, and *cpe-1* genes affects expression of the albino genes for carotenoid accumulation, *con-10* gene for conidiation in the vegetative phase, and pheromone signaling genes during sexual phase for fertility in *N. crassa*.

Ca^{2+} plays a central role in the polarized apical growth of tip growing organisms (Schmid and Harold 1988). *N. crassa* maintains a tip high $[Ca^{2+}]_c$ gradient at the apex of growing hyphae and Ca^{2+} is sequestered in the storage vesicles behind the apex (Schmid and Harold 1988; Silverman-Gavrila and Lew 2000). However, unlike other tip growing organisms such as pollen tubes (Pierson et al. 1994) and root hairs (Felle and Hepler 1997) of plants, *Saprolegnia ferax* (Lew 1999), fucoid algae (Kuhtreiber and Jaffe 1990), where the tip high $[Ca^{2+}]_c$ gradient during growth is generated due to tip-localized Ca^{2+} influx from the external medium, the tip high $[Ca^{2+}]_c$ gradient in *N. crassa* is generated and maintained internally (Silverman-Gavrila and Lew 2000). In *N. crassa*, Ca^{2+} is mainly stored in the intracellular stores such as vacuoles (>90% of Ca^{2+} is sequestered in the vacuoles), Golgi, ER; however, only a small amount of Ca^{2+} (~100 nM) is present freely $[Ca^{2+}]_c$ in the cytosol. The low levels of $[Ca^{2+}]_c$ is maintained via Ca^{2+}/cation-

ATPases and the Ca^{2+}/H^+ and Ca^{2+}/Na^+ exchangers localized in the plasma membrane and intracellular Ca^{2+} stores (Tamuli et al. 2013). Ca^{2+} is re-sequestered from intracellular Ca^{2+} stores via IP_3 activated Ca^{2+} permeable channels, cADP-ribose activated Ca^{2+} permeable channels, vacuolar voltage activated Ca^{2+} permeable channels or Ca^{2+} permeable channels in the ER (Allen et al. 1995; Calvert and Sanders 1995; Klusener et al. 1995; Muir and Sanders 1997; Silverman-Gavrila and Lew 2000). One of the Ca^{2+} sensing protein, PLC-1 catalyses the hydrolysis of PIP_2 to IP_3 which induces Ca^{2+} release from the intracellular stores, and DAG that activates PKC (Rhee and Bae 1997; discussed in Chapter 3). The $sPLA_2$ is a secretory enzyme which cleaves at the *sn-2* ester linkage of glycerophospholipids in a Ca^{2+} dependent manner and regulates a range of biological functions (Ghannoum 2000; Dennis et al. 2011; Cavazzini et al. 2013). *N. crassa* possesses two $sPLA_2$ proteins encoded by NCU06650 and NCU09423 (Takayanagi et al. 2015). NCBI BLAST analysis revealed 37% sequence identity (*e*-value 1e-38) between the two $sPLA_2$ proteins (https://blast.ncbi.nlm.nih.gov/Blast.cgi; Altschul et al. 1990; Barman and Tamuli 2017). The $sPLA_2$ protein encoded by NCU06650 and not NCU09423 contains a putative calmodulin (CaM) binding site with the amino acid sequence TCHALANVYYAAVREFGRTKGELQ (http://calcium.uhnres.utoronto.ca/ctdb/ctdb/sequence.html) and is classified as a member of the Ca^{2+} and/or CaM binding proteins (Borkovich et al. 2004; Barman and Tamuli 2017). CPE-1 is a low -affinity Ca^{2+}/H^+ exchanger activated in the presence of high $[Ca^{2+}]_c$ (also designated as $[Ca^{2+}]_i$), requires a H^+ or pH gradient maintained by a H^+-transporting ATPase and also a functional synaptic vesicular protein synaptotagmin-1 (SYT-1) that contains two C2 domains for Ca^{2+}-binding for buffering the $[Ca^{2+}]_c$ level in the rat pheochromocytoma PC12 cells (Cordeiro et al. 2013; Barman and Tamuli 2017). The release of Ca^{2+} from the intracellular stores, which is induced by IP_3 generated by the PLC-1, and/or activated PKC is necessary for the $sPLA_2$ mediated signaling for normal growth and development in *N. crassa*. In addition, under the conditions inducing sexual development, release of Ca^{2+} mediated by the PLC-1 and the $[Ca^{2+}]_c$ buffering activity of the CPE-1 Ca^{2+}/H^+ exchanger might play an important role in the regulation of the pheromone signaling genes necessary for fertility (Figure 5.9).

Thus, genetic interactions of the *plc-1*, *splA2*, and *cpe-1* genes regulate multiple cell functions in *N. crassa*. The *plc-1*, *splA2*, and *cpe-1* mediated Ca^{2+} signaling, which appears to be independent of the cAMP, is regulated by few structural genes *al-1*, *al-2*, and *al*-3, and developmentally important genes such as *con-10*, *ccg-4*, *mfa-1*, and *fmf-1*. This study also explains

a possible mechanistic model for the Ca^{2+} signaling responses mediated by the *plc-1*, *splA2*, and *cpe-1*. Therefore, this study revealed the cell functions, genetic interactions, and molecular targets of the *plc-1*, *splA2*, and *cpe-1* genes in *N. crassa*.

Discussions and future perspectives

Major conclusions of the study

In this work, I have studied the cellular roles of three Ca^{2+} signaling genes in *N. crassa* using their knockout mutant strains. Sequence analysis has revealed that NCU06245 encodes a protein of 711 amino acid residues that shows significant similarity to homologues of phospholipase C-1 (PLC-1), NCU06650 encodes a conserved hypothetical secretory phospholipase A_2 (sPLA2) protein, and NCU06366 encodes a 505 amino acid residues protein that shows sequence similarity to homologues of Ca^{2+}/H^+ exchanger-1 (CPE-1). All three encoded proteins are found to be highly conserved among the members of fungal species. Therefore, NCU06245, NCU06650, and NCU06366 encodes homologues of PLC-1, sPLA2, and CPE-1 in *N. crassa*. I found that the *plc-1*, *splA2*, and *cpe-1* genes are involved in the regulation of $[Ca^{2+}]_c$, carotenoid accumulation, survival under stress conditions, and acquisition of induced thermotolerance in *N. crassa*.

I generated double mutants of Δ*cpe-1*; Δ*splA2*; Δ*plc-1*; Δ*splA2*, and Δ*plc-1*; Δ*cpe-1* to study genetic interactions between *plc-1*, *splA2*, and *cpe-1* genes in *N. crassa*. Studies on the double mutants revealed that they synthetically regulate growth, aerial hyphae, biomass accumulation, conidial germination, carotenoid accumulation, fertility, Ca^{2+} stress tolerance, UV survival, oxidative stress survival, and acquisition of thermotolerance induced by heat shock. Therefore, a complex genetic interaction of *plc-1*, *splA2*, and *cpe-1* genes regulate multiple cell functions in *N. crassa*.

In addition, I have shown that the signaling functions of the *plc-1*, *splA2*, and *cpe-1* genes are independent of cAMP mechanism. The double mutants of the *plc-1*, *splA2*, and *cpe-1* genes showed depleted Ca^{2+} stores and disruption of Ca^{2+} homeostasis resulted in the various morphological changes of the double mutants. Some of the important developmental and biosynthetic genes were shown to regulate the conidiation, carotenoid accumulation, and pheromone signaling of the *plc-1*, *splA2*, and *cpe-1* genes. I hypothesized a possible mechanistic model for the Ca^{2+} signaling responses mediated by the *plc-1*, *splA2*, and *cpe-1* genes. The *plc-1*, *splA2*, and *cpe-1* act in co-ordination for regulating $[Ca^{2+}]_c$ which further promotes growth and development. Thus, this study revealed that the *plc-1*, *splA2*, and *cpe-1* genes synthetically play an important role in both asexual and sexual development in *N. crassa*.

Future perspectives

Future directions will be to study the PLC-1, sPLA2, and CPE-1 localizations and their molecular targets in response to various stress conditions to understand molecular pathways of these Ca^{2+} signaling proteins in *N. crassa*. Moreover, using techniques such as Fluorescence Resonance Energy transfer (FRET) and Yeast two hybrid systems will help us to determine the molecular mechanisms of PLC-1, sPLA2, and CPE-1 functions. In addition, studies using Nuclear Magnetic Resonance (NMR) and X-ray crystallography will help us in understanding the structure function relationship of these Ca^{2+} signaling proteins, specifically for the low molecular weight protein sPLA2. Therefore, detailed information about the mechanisms of PLC-1, sPLA2, and CPE-1 is expected to emerge in the future.

References

Akhtar N, Påhlman AK, Larsson K, Corbett AH, Adler L (2000) *SGD1* encodes an essential nuclear protein of *Saccharomyces cerevisiae* that affects expression of the *GPD1* gene for glycerol 3-phosphate dehydrogenase. FEBS Lett 483:87-92

Akimitsu K, Peever TL, Timmer LW (2003) Molecular, ecological and evolutionary approaches to understanding *Alternaria* diseases of citrus. Mol Plant Pathol 4:435-46

Alcántara-Sánchez F, Reynaga-Peña CG, Salcedo-Hernández R, Ruiz-Herrera J (2004) Possible role of ionic gradients in the apical growth of *Neurospora crassa*. Antonie van Leeuwenhoek 86:301-311

Allen GJ, Muir SR, Sanders D (1995) Release of Ca^{2+} from individual plant vacuoles by both InsP3 and cyclic ADP-ribose. Science 268:735-737

Altschul SF, Gish W, Miller W, Myers EW, Lipman DJ (1990) Basic local alignment search tool. J Mol Biol 215:403-410

Altschul SF, Madden TL, Schäffer AA, Zhang J, Zhang Z, Miller W, Lipman DJ (1997) Gapped BLAST and PSI-BLAST: a new generation of protein database search programs. Nucleic Acids Res 25:3389-3402

Altschul SF, Wootton JC, Gertz EM, Agarwala R, Morgulis A, Schäffer AA, Yu YK (2005) Protein database searches using compositionally adjusted substitution matrices. FEBS Journal 272:5101-5109

Anagnostakis SL (1982) Biological control of chestnut blight. Science 215:466-471

Andaluz E, Coque JJ, Cueva R, Larriba G (2001) Sequencing of a 4.3 kbp region of chromosome 2 of *Candida albicans* reveals the presence of homologues of *SHE9* from *Saccharomyces cerevisiae* and of bacterial phosphatidylinositol-phospholipase C. Yeast 18:711-721

Ansari K, Martin S, Farkasovsky M, Ehbrecht IM, Küntzel H (1999) Phospholipase C binds to the receptor-like *GPR1* protein and controls pseudohyphal differentiation in *Saccharomyces cerevisiae*. J Biol Chem 274:30052-30058

Aramayo R, Metzenberg RL (1996) Meiotic transvection in fungi. Cell 86:103-113

Arioka M, Cheon SH, Ikeno Y, Nakashima S, Kitamoto K (2005) A novel neurotrophic role of

secretory phospholipases A2 for cerebellar granule neurons. FEBS Lett 579:2693-2701

Arrach N, Schmidhauser TJ, Avalos J (2002) Mutants of the carotene cyclase domain of *al-2* from *Neurospora crassa*. Mol Genet Genomics 266:914-921

Avalos J, Corrochano LM (2013) Carotenoid Biosynthesis in *Neurospora*. In: Kasbekar DP, McCluskey K (eds) Neurospora: genomics and molecular biology, Caister Academic Press, Norfolk, UK, pp 227-241

Babcock DF, First NL, Lardy HA (1976) Action of ionophore A23187 at the cellular level. Separation of effects at the plasma and mitochondrial membranes. J Biol Chem 251:3881-3886

Bang An, Boqiang Li, Guozheng Qin, Shiping Tian (2015) Function of small GTPase Rho3 in regulating growth, conidiation and virulence of *Botrytis cinerea*. Fungal Genet Biol 75:46-55

Banno S, Ochiai N, Noguchi R, Kimura M, Yamaguchi I, Kanzaki S, Murayama T, Fujimura M (2005) A catalytic subunit of cyclic AMP-dependent protein kinase, PKAC-1, regulates asexual differentiation in *Neurospora crassa*. Genes Genet Syst 80:25-34

Barba-Ostria C, Lledías F, Georgellis, D (2011) The *Neurospora crassa* DCC-1 protein, a putative histidine kinase, is required for normal sexual and asexual development and carotenogenesis. Eukaryot Cell 12:1733-1739

Barman A, Tamuli R (2015) Multiple cellular roles of *Neurospora crassa plc-1*, s*plA2*, and *cpe-1* in regulation of cytosolic free calcium, carotenoid accumulation, stress responses, and acquisition of thermotolerance. J Microbiol 53:226-235

Barman A, Tamuli R (2017) The pleiotropic vegetative and sexual development phenotypes of *Neurospora crassa* arise from double mutants of the calcium signaling genes *plc-1*, *splA2*, and *cpe-1*. Current Genet DOI 10.1007/s00294-017-0682-y

Baryshnikova A, Costanzo M, Myers CL, Andrews B, Boone C (2013) Genetic interaction networks: toward an understanding of heritability. Annu Rev Genomics Hum Genet 14:111-133

Beadle GW, Tatum EL (1941) Genetic control of chemical reactions in *Neurospora*. Proc Natl Acad Sci 27:499-506

Bell-Pederson D, Shinohara ML, Loros JJ, Dunlap JC (1996) Circadian clock-controlled genes isolated from *Neurospora crassa* are late night- to early morning-specific. Proc Natl Acad Sci USA 93:13096-13101

Belozerskaia TA, Gessler NN (2006) Oxidative stress and cell differentiation in *Neurospora crassa*. Mikrobiologiia 75:497-501

Benčina M, Legiša M, Read ND (2005) Cross-talk between cAMP and calcium signalling in *Aspergillus niger*. Mol Microbiol 56:268-281

Benito B, Garciadeblas B, Rodriguez-Navarro A (2000) Molecular cloning of the calcium and sodium ATPases in *Neurospora crassa*. Mol Microbiol 35:1079-1088

Bennett DE, McCreary CE, Coleman DC (1998) Genetic characterization of a phospholipase C gene from *Candida albicans:* presence of homologous sequences in *Candida* species other than *Candida albicans*. Microbiology 144:55-72

Bennett JW, Klich M (2003) Mycotoxins. Clin Microbiol Revs 16:497-516

Berridge MJ, Irvine RF (1984) Inositol trisphosphate, a novel second messenger in cellular signal transduction. Nature 312:315-321

Berridge MJ (1987) Inositol trisphosphate and diacylglycerol: two interacting second messengers. Annu Rev Biochem 56:159-193

Berridge MJ (1993) Inositol trisphosphate and calcium signalling. Nature 361:315-325

Berridge MJ, Bootman MD, Lipp P (1998) Calcium—a life and death signal. Nature 395:645-648

Berridge MJ, Lipp P, Bootman MD (2000) The versatility and universality of calcium signaling. Nat Rev Mol Cell Biol 1:11-21

Berridge MJ, Bootman MD, Roderick HL (2003) Calcium signalling: dynamics, homeostasis, and remodeling. Nat Rev Mol Cell Biol 4:517-529

Bhat A, Tamuli R, Kasbekar DP (2004) Genetic transformation of *Neurospora tetrasperma*, demonstration of repeat-induced point mutation (RIP) in self-crosses and a screen for recessive RIP defective mutants. Genetics 167:1155-1164

Blinks JR, Gil Wier W, Hess P, Prendergast FG (1982) Measurement of Ca^{2+} concentrations in living cells. Prog Biophys Mol Biol 40:1-114

Bobrowicz P, Pawlak R, Correa A, Bell-Pedersen D, Ebbole DJ (2002) The *Neurospora crassa* pheromone precursor genes are regulated by the mating type locus and the circadian clock. Mol Microbiol 45:795-804

Boilard E, Lai Y, Larabee K, Balestrieri B, Ghomashchi F, Fujioka D, Gobezie R, Coblyn JS, Weinblatt ME, Massarotti EM, Thornhill TS, Divangahi M, Remold H, Lambeau G, Gelb MH, Arm JP, Lee DM (2010) A novel anti-inflammatory role for secretory phospholipase A2 in immune complex-mediated arthritis. EMBO Mol Med 2:172-187

Borges-Walmsley MI, Walmsley AR (2000) cAMP signalling in pathogenic fungi: control of dimorphic switching and pathogenicity. Trends Microbiol 8:133-141

Borkovich KA, Alex LA, Yarden O, Freitag M, Turner GE, Read ND, Seiler S, Bell-Pedersen D,Paietta J, Plesofsky N, Plamann M, Goodrich-Tanrikulu M, Schulte U, Mannhaupt G, Nargang FE, Radford A, Selitrennikoff C, Galagan JE, Dunlap JC, Loros JJ, Catcheside D, Inoue H, Aramayo R, Polymenis M, Selker EU, Sachs MS, Marzluf GA, Paulsen I, Davis R, Ebbole DJ, Zelter A, Kalkman ER, O'Rourke R, Bowring F, Yeadon J, Ishii C, Suzuki K, Sakai W, Pratt R (2004) Lessons from the genome sequence of *Neurospora crassa*: tracing the path from genomic blueprint to multicellular organism. Microbiol Mol Biol Rev 68:1-108

Boone C, Bussey H, Andrews BJ (2007) Exploring genetic interactions and networks with yeast. Nat Rev Genet 8:437-449

Bootman MD, Collins TJ, Peppiatt CM, Prothero LS, Mac-Kenzie L, De Smet P, Travers M, Tovey SC, Seo JT, Berridge MJ, Ciccolini F, Lipp P (2001) Calcium signalling–an overview. Semin Cell Dev Biol 12:3-10

Bowman BJ, Abreu S, Margolles-Clark E, Draskovic M, Bowman EJ (2011) Role of four calcium transport proteins, encoded by *nca-1*, *nca-2*, *nca-3*, and *cax*, in maintaining intracellular calcium levels in *Neurospora crassa*. Eukaryot Cell 10:654-661

Bowman EJ, Kendle R, Bowman BJ (2000) Disruption of vma-1, the gene encoding the catalytic subunit of the vacuolar H (+)-ATPase, causes severe morphological changes in *Neurospora crassa*. J Biol Chem 275:167-176

Bristol A, Hall SM, Kriz RW, Stahl ML, Fan YS, Byers MG, Eddy RL, Shows TB, Knopf JL, (1988) Phospholipase C-148: chromosomal location and deletion mapping of functional domains. Cold Spring Harb Symp Quant Biol 53:915-920

Brown EM, Gamba G, Riccardi D, Lombardi M, Butters R, Kofor O, Sun A, Hediger MA, Lytton J, Hebert SC (1993) Cloning and characterization of an extracellular Ca(2+)-sensing receptor from bovine parathyroid. Nature 366:575-580

Bruno KS, Aramayo R, Minke PF, Metzenberg RL, Plamann M (1996) Loss of growth polarity and mislocalization of septa in a Neurospora mutant altered in the regulatory subunit of cAMP-dependent protein kinase. EMBO J 15:5772-5782

Burns C, Stajich JE, Rechtsteiner A, Casselton L, Hanlon SE, Wilke SK, Savytskyy OP, Gathman AC, Lilly WW, Lieb J.D, Zolan ME, Pukkila PJ (2010) Analysis of the basidiomycete *Coprinopsis cinerea* reveals conservation of the core meiotic expression program over half a billion years of evolution. PLoS Genet 6:e1001135

Calvert CM, Sanders D (1995) Inositol trisphosphate-dependent and independent Ca^{2+} mobilization pathways at the vacuolar membrane of *Candida albicans*. J Biol Chem 270:7272-7280

Cambareri EB, Jensen BC, Schabtach E, Selker EU (1989) Repeat induced G-C to A-T mutations in Neurospora. Science 244:1571-1575

Capelli N, van Tuinen D, Ortega Perez R, Arrighi JF, Turian G (1993) Molecular cloning of a cDNA encoding calmodulin from *Neurospora crassa*. FEBS Lett 321:63-68

Carafoli E (1992) The Ca^{2+} pump of the plasma membrane. J Biol Chem 267:2115-2118

Carneiro P, Duarte M, Videira A (2007) The external alternative NAD(P)H dehydrogenase NDE3 is localized both in the mitochondria and in the cytoplasm of *Neurospora crassa*. J Mol Biol 368:1114-1121

Carugo O, Djinovic K, Rizzi M (1993) Comparison of co-ordinative behaviour of calcium(II) and magnesium(II) from crystallographic data. J Chem Soc Dalton Trans 1993:2127-2135

Castro A, Lemos C, Falcão A, Glass NL, Videira A (2008) Increased resistance of complex I mutants to phytosphingosine-induced programmed cell death. J Biol Chem 283:19314-19321

Caswell AH (1979) Methods of measuring intracellular calcium. Int Rev Cytol 56:145-181

Cavazzini D, Meschi F, Corsini R, Bolchi A, Rossi GL, Einsle O, Ottonello S (2013) Autoproteolytic activation of a symbiosis-regulated truffle phospholipase A2. J Biol Chem 288:1533-1547

Chafouleas JG, Bolton WE, Means AR (1984) Potentiation of bleomycin lethality by anti-calmodulin drugs: a role for calmodulin in DNA repair. Science 224:1346-1348

Chaney MO, Demarco PV, Jones ND, Occolowitz JL (1974) The structure of A23187, a divalent cation ionophore. J American Chem Society 96:1932-1933

Chard PA (1987) DNA repair in human cells: methods for the determination of calmodulin involvement. Methods Enzymol 139:715-730

Chayakulkeeree M, Perfect J (2006) Cryptococcosis. Infectious Dis Clin North Am 20:507-544

Chen Y, Tye B (1995) The yeast Mcm1 protein is regulated posttranscriptionally by the flux of glycolysis. Mol Cell Biol 15:4631-4639

Cheng J, Park TS, Chio LC, Fischl AS, Ye XS (2003) Induction of apoptosis by sphingoid long-chain bases in *Aspergillus nidulans*. Mol Cell Biol 23:163-177

Chin D, Means AR (2000) Calmodulin: a prototypical calcium sensor. Trends Cell Biol 10:322-328

Choi J, Kim KS, Rho HS, Lee YH (2011) Differential roles of the phospholipase C genes in fungal development and pathogenicity of *Magnaporthe oryzae*. Fungal Genet Biol 48:445-455

Christianson TW, Sikorski RS, Dante M, Shero JH, Hieter P (1992) Multifunctional yeast high-copy-number shuttle vectors. Gene110:119-122.

Chung HJ, Kim MJ, Lim JY, Park SM, Cha BJ, Kim YH,Yang MS, Kim DH (2006) A gene encoding phosphatidylinositol-specific phospholipase C from *Cryphonectria parasitica* modulates the *lac*1 expression. Fungal Genet Biol 43:326-336

Clapham DE (2007) Calcium Signaling Cell 131:1047-1058

Coccetti P, Tisi R, Martegani E, Teixeira LS, Brandão RL, Castro IM, Thevelein JM (1998) The *PLC1* encoded phospholipase C in the yeast *Saccharomyces cerevisiae* is essential for glucose-induced phosphatidylinositol turnover and activation of plasma membrane H^+-ATPase. Biochim Biophys Acta 1405:147-154

Colot HV, Park G, Turner GE, Ringelberg C, Crew CM, Litvinkova L, Weiss RL, Borkovich KA, Dunlap JC (2006) A highthroughput gene knockout procedure for Neurospora reveals functions for multiple transcription factors. Proc Natl Acad Sci USA 103:10352-10357

Cooper KF, Mallory MJ, Strich R (1999) Oxidative stress-induced destruction of the yeast C-type cyclin Ume3p requires phosphatidylinositol-specific phospholipase C and the 26S proteasome. Mol Cell Biol 19:3338-3348

Coppin E, Debuchy R, Arnaise S, Picard M (1997) Mating types and sexual development in filamentous ascomycetes. Microbiol Mol Biol Rev 61:411-428

Cordeiro JM, Boda B, Gonçalves PP, Dunant Y (2013) Synaptotagmin 1 is required for vesicular Ca^{2+}/H^+-antiport activity. J Neurochem 126:37-46

Cornelius G, Nakashima H (1987) Vacuoles play a decisive role in calcium homeostasis in *Neurospora crassa*. J Gen Microbiol 133:2341-2347

Cornelius G, Gebauer G, Techel D (1989) Inositol trisphosphate induces calcium release from *Neurospora crassa* vacuoles. Biochem Biophys Res Commun 162:852-856

Cortat M, Turian G (1974) Conidiation of *Neurospora crassa* in submerged culture without mycelial phase. Arch Microbiol 95:305-309

Cunningham KW, Fink JR (1996) Calcineurin inhibits VCX1-dependent H^+/Ca^{2+} exchange and induces Ca^{2+} ATPases in *Saccharomyces cerevisiae*. Mol Cell Biol 16:2226-2237

Darvin M.E, Sterry W, Lademann J, Vergou T (2011) The role of carotenoids in human skin. Molecules 16:10491-10506

Davis RH, De Serres FJ (1970) Genetic and microbiological research techniques for *Neurospora crassa*. Methods Enzymol 71:79-143

Davis RH (2000) Neurospora: contributions of a model organism. Oxford University Press, New York

Davis RH, Perkins DD (2002) *Neurospora*: a model of model microbes. Nat Rev Genet 3:397-403

DeBernardi MA, Brooker G (1996) Single cell Ca^{2+}/cAMP cross-talk monitored by simultaneous Ca^{2+}/cAMP fluorescence ratio imaging. Proc Natl Acad Sci USA 93:4577-4582

Dedkova EN, Ji X, Lipsius SL, Blatter LA (2004) Mitochondrial calcium uptake stimulates nitric oxide production in mitochondria of bovine vascular endothelial cells. Am J Physiol Cell Physiol 286:C406-C415

Deka R, Kumar R, Tamuli R (2011) *Neurospora crassa* homologue of Neuronal Calcium Sensor-1 has a role in growth, calcium stress tolerance, and ultraviolet survival. Genetica 139:885-894

Deka R, Tamuli R (2013) *Neurospora crassa ncs-1*, *mid-1* and *nca-2* double-mutant phenotypes suggest diverse interaction among three Ca^{2+}-regulating gene products. J Genetics 92:559-563

Deka R, Ghosh A, Tamuli R, Borkovich KA (2016) Heterotrimeric G proteins. In: Drik H (ed) The mycota IV, Springer-Verlag, Berlin, Germany

Dennis EA, Cao J, Hsu YH, Magrioti V, Kokotos G (2011) Phospholipase A2 enzymes: physical structure, biological function, disease implication, chemical inhibition, and therapeutic intervention. Chem Rev 111:6130-6185.

Díaz-Sánchez V, Estrada AF, Trautmann D, Limón MC, Al-Babili S, Avalos J (2011) Analysis of *al-2* mutations in *Neurospora*. PLoS One 6:e21948

Dodd AN, Kudla J, Sanders D (2010) The language of calcium signaling. Annu Rev Plant Biol 61:593-620

Dodge BO (1939) Some problems in the genetics of the fungi. Science 90:379-85

D'Souza CA, Heitman J. (2001) Conserved cAMP signaling cascades regulate fungal development and virulence. FEMS Microbiol Rev 25:349-364

Essen LO, Perisic O, Cheung R, Katan M, Williams RL (1996) Crystal structure of a mammalian phosphoinositide-specific phospholipase C delta. Nature 380:595-602

Estrada AF, Youssar L, Scherzinger D, Al-Babili S, Avalos J (2008) The ylo-1 gene encodes an aldehyde dehydrogenase responsible for the last reaction in the *Neurospora* carotenoid pathway. Mol Microbiol 69:1207-1220

Fankhauser H, Schweingruber AM, Edenharter E, Schweingruber ME (1995) Growth of a mutant defective in a putative phosphoinositide-specific phospholipase C of *Schizosaccharomyces pombe* is restored by low concentrations of phosphate and inositol. Curr Genet 28:199-203

Flick JS, Thorner J (1993) Genetic and biochemical characterization of a phosphatidylinositol-specific phospholipase C in *Saccharomyces cerevisiae*. Mol Cell Biol 13:5861-5876

Felle HH, Hepler PK (1997) The cytosolic Ca^{2+} concentration gradient of *Sinapis alba* root hairs as revealed by Ca^{2+}-sensitive microelectrode tests and fura-dextran ratio imaging. Plant Physiol 114:39-45

Felsenstein J (1985) Confidence limits on phylogenies: an approach using the bootstrap. Evolution 39:783-791

Fleißner A, Sarkar S, Jacobson DJ, Roca MG, Read N.D, Glass NL (2005) The *so* locus is required for vegetative cell fusion and postfertilization events in *Neurospora crassa*. Eukaryot Cell 4:920-930

Freitag M, Hickey PC, Raju NB, Selker EU, Read ND (2004) GFP as a tool to analyze the organization, dynamics and function of nuclei and microtubules in *Neurospora crassa*. Fungal Genet Biol 41:897-910

Gadd GM (1994) Signal transduction in fungi. In: Gow NAR, Gadd GM (eds.) The growing fungus. Chapman and Hall, London, pp 183-210

Galagan JE, Calvo SE, Borkovich KA, Selker EU, Read ND, Jaffe D, FitzHugh W, Ma LJ, Smirnov S, Purcell S, Rehman B, Elkins T, Engels R, Wang S, Nielsen CB, Butler J, Endrizzi M, Qui D, Ianakiev P, Bell-Pedersen D, Nelson MA, Werner-Washburne M, Selitrennikoff CP, Kinsey JA, Braun EL, Zelter A, Schulte U, Kothe GO, Jedd G, Mewes W, Staben C, Marcotte E, Greenberg D, Roy A, Foley K, Naylor, J., Stange-Thomann N, Barrett R, Gnerre S, Kamal M, Kamvysselis M, Mauceli E, Bielke C, Rudd S, Frishman D, Krystofova S, Rasmussen C, Metzenberg RL, Perkins DD, Kroken S, Cogoni C, Macino G, Catcheside D, Li W, Pratt RJ, Osmani SA, DeSouza CP, Glass L, Orbach MJ, Berglund JA, Voelker R, Yarden O, Plamann M, Seiler S, Dunlap J, Radford A, Aramayo R, Natvig DO, Alex LA, Mannhaupt G, Ebbole DJ, Freitag M, Paulsen I, Sachs MS, Lander ES, Nusbaum C, Birren B (2003) The genome sequence of the filamentous fungus *Neurospora crassa*. Nature 422:859-868

Garnjobst L, Tatum EL (1967) A survey of new morphological mutants in *Neurospora crassa*. Genetics 57:579-604

Gavric O, Griffiths AJ (2003) Interaction of mutations affecting tip growth and branching in *Neurospora*. Fungal Genet Biol 40:261-270

Gavric O, dos Santos DB, Griffiths A (2007) Mutation and divergence of the phospholipase C gene in *Neurospora crassa*. Fungal Genet Biol 44:242-249

Gessler NN, Leonovich OA, Rabinovich IaM, Rudchenko MN, Belozerskaia TA (2006) A comparative study of the components of the antioxidant defense system during growth of the mycelium of a wild-type *Neurospora crassa* strain and mutants, white collar-1 and white collar-2. Prikl Biokhim Mikrobiol 42:332-337

Ghannoum MA (2000) Potential role of phospholipases in virulence and fungal pathogenesis. Clin Microbiol Rev 13:122-143

Gohain D, Deka R, Tamuli R (2016) Identification of critical amino acid residues and functional conservation of the *Neurospora crassa* and *Rattus norvegicus* orthologues of neuronal calcium sensor-1. Genetica 144:665-674

Gorbunova YV, Spitzer NC (2002) Dynamic interactions of cyclic AMP transients and spontaneous Ca^{2+} spikes. Nature 418:93-96

Görlach A, Bertram K, Hudecova S, Krizanova O (2015) Calcium and ROS: A mutual interplay. Redox Biol 6:260-271

Goswami RS, Kistler HC (2004) Heading for disaster: *Fusarium graminearum* on cereal crops. Mol Plant Pathol 5:515-525

Gray PC, Scott JD, Catterall WA (1998) Regulation of ion channels by cAMP-dependent protein kinase and A-kinase anchoring proteins. Curr Opin Neurobiol 8:330-334

Green DR, Kroemer G (2004) The pathophysiology of mitochondrial cell death. Science 305:626-629

Greenwald CJ, Kasuga T, Glass NL, Shaw BD, Ebbole DJ, Wilkinson HH (2010) Temporal and spatial regulation of gene expression during asexual development of *Neurospora crassa*. Genetics 186:1217-1230

Gritz L, Davies J (1983) Plasmid-encoded hygromycin B resistance: the sequence of hygromycin B phosphotransferase gene and its expression in *Escherichia coli* and *Saccharomyces cerevisiae*. Gene 25:179-188

Guignard R, Grange F, Turian G (1974) Microcycle conidiation induced by partial nitrogen deprivation in *Neurospora crassa*. Can J Microbiol 30:1210-1215

Guo L, Wenner N, Kuldau GA (2015) *FvSO* regulates vegetative hyphal fusion, asexual growth, fumonisin B1 production, and virulence in *Fusarium verticillioides*. Fungal Biol 119: 1158-1169

Guttery DS, Pittman JK, Freñal K, Poulin B, McFarlane LR, Slavic K, Wheatley SP, Soldati-Favre D, Krishna S, Tewari R, Staines HM (2013) The *Plasmodium berghei* Ca^{2+}/H^{+} exchanger,

PbCAX, is essential for tolerance to environmental Ca^{2+} during sexual development. PLoS Pathog 9:e1003191

Haber F, Weiss J (1934) The catalytic decomposition of hydrogen peroxide by iron salts. Proc R Soc Lond A 147:332-351

Halliwell B, Gutteridge JM (1984) Oxygen toxicity, oxygen radicals, transition metals and disease. Biochem J 219:1-14

Hamann A, Brust D, Osiewacz HD (2008) Apoptosis pathways in fungal growth, development and ageing. Trends Microbiol 16:276-283

Hanoune J, Defer N (2001) Regulation and role of adenylyl cyclase isoforms. Annu Rev Pharmacol Toxicol 41:145-174

Hong Y, Zhao J, Guo L, Kim SC, Deng X, Wang G, Zhang G, Li M, Wang X (2016) Plant phospholipases D and C and their diverse functions in stress responses. Prog Lipid Res 62:55-74

Harding RW, Huang PC, Mitchell HK (1969) Photochemical studies of the carotenoid biosynthetic pathway in *Neurospora crassa.* Arch Biochem Biophys 129:696-707

Harding RW (1974) The Effect of temperature on photo-induced carotenoid biosynthesis in *Neurospora crassa*. Plant Physiol 54:142-147

Inoue H, Nojima H, Okayama H (1990) High efficiency transformation of Escherichia coli with plasmids. Gene 96:23-28

Ivey FD, Hodge PN, Turner GE, Borkovich KA (1996) The $G\alpha_i$ homologue *gna-1* controls multiple differentiation pathways in *Neurospora crassa*. Mol Biol Cell 7:1283-1297

Ivey FD, Kays AM, Borkovich KA (2002) Shared and independent roles for a $G\alpha_i$ protein and adenylate cyclase in regulating development and stress responses in *Neurospora crassa*. Eukaryot Cell 1:634-642

Iyer SV, Ramakrishnan M, Kasbekar DP (2009) *Neurospora crassa fmf-1* encodes the homologue of the *Schizosaccharomyces pombe* Ste11p regulator of sexual development. J Genet 88:33-39

Jackson SL, Heath IB (1989) Effects of exogenous calcium ions on tip growth, intracellular Ca^{2+} concentration, and actin arrays in hyphae of the fungus *Saprolegnia ferax*. Experimental Mycol 13:1-12

Jaiswal JK (2001) Calcium- how and why? J Biosci 26:357-363

Johnson TE (1979) A Neurospora mutation that arrests perithecial development as either male or female parent. Genetics 92:1107-1120

Kader A, Lindberg S (2010) Cytosolic calcium and pH signaling in plants under salinity stress. Plant Signal Behavior 5:233-238

Kapoor M, Sreenivasan GM, Goel N, Lewis J (1990) Development of thermotolerance in *Neurospora crassa* by heat shock and other stresses eliciting peroxidase induction. J Bacteriol 172:2798-2801

Kapoor M, Curle CA, Runham C (1995) The hsp70 gene family of *Neurospora crassa*: cloning, sequence analysis, expression, and genetic mapping of the major stress-inducible member. J Bacteriol 177:212-221

Kays AM, Rowley PS, Baasiri RA, Borkovich KA (2000) Regulation of conidiation and adenylyl cyclase levels by the Gα protein GNA-3 in *Neurospora crassa*. Mol Cell Biol 20:7693-7705

Kays AM, Borkovich KA (2003) Severe impairment of growth and differentiation in *Neurospora crassa* mutant lacking all heterotrimeric Gα proteins. Genetics 166:1229-1240

Kim H, Metzenberg RL, Nelson MA (2002) Multiple functions of *mfa-1*, a putative pheromone precursor gene of *Neurospora crassa*. Eukaryot Cell 1:987-989

Kim H, Borkovich KA (2004) A pheromone receptor gene, *pre-1*, is essential for mating type-specific directional growth and fusion of trichogynes and female fertility in *Neurospora crassa*. Mol Microbiol 52:1781-1798

Kim H, Borkovich KA (2006) Pheromones are essential for male fertility and sufficient to direct chemotropic polarized growth of trichogynes during mating in *Neurospora crassa*. Eukaryot Cell 5:544-554

Kim H, Wright SJ, Park G, Ouyang S, Krystofova S, Borkovich KA (2012) Roles for receptors, pheromones, G proteins, and mating type genes during sexual reproduction in *Neurospora crassa*. Genetics 190:1389-1404

Klee CB, Crouch TH, Krinks MH (1979) Calcineurin: a calcium- and calmodulin-binding protein of the nervous system. Proc Natl Acad Sci USA 76:6270-6273

Klusener B, Boheim G, Lib H, Engelberth J, Weiler EW (1995) Gadolinium-sensitive, voltage-dependent calcium release channels in the endoplasmic reticulum of a higher plant mechanoreceptor organ. EMBO J 14:2708-2714

Kmetzsch L, Staats CC, Simon E, Fonseca FL, de Oliveira DL, Sobrino L, Rodrigues J, Leal AL, Nimrichter L, Rodrigues ML, Schrank A, Vainstein MH (2010) The vacuolar Ca^{2+} exchanger Vcx1 is involved in calcineurin-dependent Ca^{2+} tolerance and virulence in *Cryptococcus neoformans*. Eukaryot Cell 9:1798-1805

Knechtle P, Goyard S, Brachat S, Ibrahim-Granet O, d'Enfert C (2005) Phosphatidylinositol-dependent phospholipases C Plc2 and Plc3 of Candida albicans are dispensable for morphogenesis and host-pathogen interaction. Res Microbiol 156:822-829

Kobayashi T, Abe K, Asai K, Gomi K, Juvvadi PR, Kato M, Kitamoto K, Takeuchi M, Machida M (2007) Genomics of *Aspergillus oryzae*. Biosci Biotechnol Biochem 71: 646-670

Köhler GA, Brenot A, Haas-Stapleton E, Agabian N, Deva R, Nigam S (2006) Phospholipase A2 and phospholipase B activities in fungi. Biochim Biophys Acta 1761:1391-1399

Kothe GO, Free SJ (1998) The isolation and characterization of *nrc-1* and *nrc-2*, two genes encoding protein kinases that control growth and development in *Neurospora crassa*. Genetics 149:117-130

Kong S, Park SY, Lee YH (2015) Systematic characterization of the bZIP transcription factor gene family in the rice blast fungus, *Magnaporthe oryzae.* Environ Microbiol 17:1425-1443

Kronstad JW, Staben C (1997) Mating type in filamentous fungi. Annu Rev Genet 31:245-276

Krystofova S, Borkovich KA (2005) The heterotrimeric G-protein subunits GNG-1 and GNB-1 form a Gβγ dimer required for normal female fertility, asexual development, and Gα protein levels in *Neurospora crassa*. Eukaryot Cell 4:365-378

Kuhtreiber WM, Jaffe LF (1990) Detection of extracellular calcium gradients with a calcium-specific vibrating electrode. J Cell Biol 110:1565-1573

Kumar R, Tamuli R (2014) Calcium/calmodulin-dependent kinases are involved in growth, thermotolerance, oxidative stress survival, and fertility in *Neurospora crassa*. Arch Microbiol 196:295-305

Kunze D, Melzer I, Bennett D, Sanglard D, MacCallum D, Nörskau J, Coleman DC, Odds FC, Schäfer W, Hube B (2005) Functional analysis of the phospholipase C gene CaPLC1 and two unusual phospholipase C genes, *CaPLC2* and *CaPLC3*, of *Candida albicans*. Microbiol 151:3381-3394

Lakin-Thomas PL, Brody S (1985) Circadian rhythms in *Neurospora crassa*: interactions between clock mutations. Genetics109:49-66

Larson TG, Choi GH, Nuss DL (1992) Regulatory pathways governing modulation of fungal gene expression by a virulence-attenuating mycovirus. EMBO J 11:4539-4548

Lauter FR, Yamashiro CT, Yanofsky C (1997) Light stimulation of conidiation in *Neurospora crassa*: studies with the wild-type strain and mutants *wc-1*, *wc-2* and *acon-2*. J Photochem Photobiol 37:203-211

Laxmi V, Tamuli R (2015) The *Neurospora crassa cmd*, *trm-9*, and *nca-2* play a role in growth, development, and survival in stress conditions. Gen App Biol 6:1-12

Laxmi V, Tamuli R (2016) The calmodulin gene in *Neurospora crassa* is required for normal vegetative growth, ultraviolet survival, and sexual development. Arch Micro Biol 199:531-542

Lee N, D'Souza CA, Kronstad JW (2003) Of smuts, blasts, mildews, and blights: cAMP signaling in phytopathogenic fungi. Annu Rev Phytopathol 41:399-427

Lengeler KB, Davidson RC, D'souza C, Harashima T, Shen WC, Wang P, Pan X, Waugh M, Heitman J. (2000) Signal transduction cascades regulating fungal development and virulence. Microbiol Mol Biol Rev 64:746-785

Lew RR (1999) Comparative analysis of Ca^{2+} and H^{+} flux magnitude and location along growing hyphae of *Saprolegnia ferax* and *Neurospora crassa*. Eur J Cell Biol 78:892-902

Lew RR, Abbas Z, Anderca MI, Free SJ (2008) Phenotype of a mechanosensitive channel mutant, *mid-1*, in a filamentous fungus, *Neurospora crassa*. Eukaryot Cell 7:647-655

Lew RR, Giblon RE, Lorenti MS (2015) The phenotype of a phospholipase C (*plc-1*) mutant in a filamentous fungus, *Neurospora crassa*. Fungal Genet Biol 82:158-167.

Li C, Schmidhauser TJ (1995) Developmental and photoregulation of *al-1* and *al-2*, structural genes for two enzymes essential for carotenoid biosynthesis in *Neurospora*. Dev Biol 169:90-95

Li L, Borkovich KA (2006) GPR-4 is a predicted G-protein-coupled receptor required for carbon source-dependent asexual growth and development in *Neurospora crassa*. Eukaryot Cell 5:1287-300

Ligusa H, Yoshida Y, Hasunuma K (2005) Oxygen and hydrogen peroxide enhance light-induced carotenoid synthesis in *Neurospora crassa*. FEBS Lett 579:4012-4016

Lindegren CC (1936) A six-point map of the sex chromosome of *Neurospora crassa*. J Genet 32:243-256

Lin H, Choi JH, Vancura A (1998) Phosphoinositide-specific phospholipase C interacts with phosphatidylinositol kinase homolog TOR2. Biochem Biophys Res Commun 18:285-289

Lin H, Choi JH, Hasek J, DeLillo N, Lou W, Vancura A (2000) Phospholipase C is involved in kinetochore function in *Saccharomyces cerevisiae*. Mol Cell Biol 20:3597-3607

Lin H, Nguyen P, Vancura A (2002) Phospholipase C interacts with Sgd1p and is required for expression of *GPD1* and osmoresistance in *Saccharomyces cerevisiae*. Mol Genet Genomics 267:313-320

Liu W, Xie Y, Ma J, Luo X, Nie P, Zuo Z, Lahrmann U, Zhao Q, Zheng Y, Zhao Y, Xue Y, Ren J (2015) IBS: an illustrator for the presentation and visualization of biological sequences. Bioinformatics 31:3359-3361

Livak KJ, Schmittgen TD (2001) Analysis of relative gene expression data using real-time quantitative PCR and the $2^{-\Delta\Delta Ct}$ method. Methods 25:402-408

Lorenz MC, Heitman J (1997) Yeast pseudohyphal growth is regulated by GPA2, a G protein alpha homolog. EMBO J 16:7008-7018

Loros JJ, Dunlap JC (2001) Genetic and molecular analysis of circadian rhythms in *Neurospora*. Annu Rev Physiol 63:757-794

Luque EM, Gutierrez G, Navarro-Sampedro L, Olmedo M, Rodríguez-Romero J, Ruger-Herreros C, Tagua VG, Corrochano LM (2012) A relationship between carotenoid accumulation and the distribution of species of the fungus *Neurospora* in Spain. *PLoS ONE* 7:e33658

Lytton J (2007) Na^+/Ca^{2+} exchangers: three mammalian gene families control Ca^{2+} transport. Biochem J 406:365-382

MacDonald WL, Fulbright DW (1991) Biological control of chestnut blight: use and limitations of transmissible hypovirulence. Plant Disease 75:656-661

Machida M, Asai K, Sano M, Tanaka T, Kumagai T, Terai G, Kusumoto K, Arima T, Akita O, Kashiwagi Y, Abe K, Gomi K, Horiuchi H, Kitamoto K, Kobayashi T, Takeuchi M, Denning DW, Galagan JE, Nierman WC, Yu J, Archer DB, Bennett JW, Bhatnagar D, Cleveland TE, Fedorova ND, Gotoh O, Horikawa H, Hosoyama A, Ichinomiya M, Igarashi R, Iwashita K, Juvvadi PR, Kato M, Kato Y, Kin T, Kokubun A, Maeda H, Maeyama N, Maruyama J, Nagasaki H, Nakajima T, Oda K, Okada K, Paulsen I, Sakamoto K, Sawano T, Takahashi M, Takase K, Terabayashi Y, Wortman JR, Yamada O, Yamagata Y, Anazawa H, Hata Y, Koide Y, Komori T, Koyama Y, Minetoki T, Suharnan S, Tanaka A, Isono K, Kuhara S, Ogasawara N, Kikuchi H (2005) Genome sequencing and analysis of *Aspergillus oryzae*. Nature 438:1157-1161

Madeo F, Herker E, Wissing S., Jungwirth H, Eisenberg T, Frohlich K-U (2004) Apoptosis in yeast. Curr Opin Microbiol 7:655-660

Madi L, McBride SA, Bailey LA, Ebbole DJ (1997) *rco-3*, a gene involved in glucose transport and conidiation in *Neurospora crassa*. Genetics 146:499-508

Mani R, St. Onge RP, Hartman JL, Giaever G, Roth FP (2007) Defining genetic interaction. PNAS 105:3461-3466

Marchler-Bauer A, Bryant SH (2004) CD-Search: protein domain annotations on the fly. Nucleic Acids Res 32:W327-W331

Marchler-Bauer A, Anderson JB, Chitsaz F, Derbyshire MK, DeWeese-Scott C, Fong JH, Geer LY, Geer RC, Gonzales NR, Gwadz M, He S, Hurwitz DI, Jackson JD, Ke Z, Lanczycki CJ, Liebert CA, Liu C, Lu F, Lu S, Marchler GH, Mullokandov M, Song JS, Tasneem A, Thanki N, Yamashita RA, Zhang D, Zhang N, Bryant SH (2009) CDD: specific functional annotation with the Conserved Domain Database. Nucleic Acids Res 37:D205-D210

Margolin BS, Freitag M, Selker EU (1997) Improved plasmids for gene targeting at the *his-3* locus of *Neurospora crassa* by electroporation. Fungal Genet Newslett 44:34-36

Matsumoto K, Uno I, Oshima Y, Ishikawa T (1982a) Isolation and characterization of yeast mutants deficient in adenylate cyclase and cAMP-dependent protein kinase. Proc Natl Acad Sci USA 79:2355-2359

Matsumoto K, Uno I, Toh-E A, Ishikawa T, Oshima Y (1982b) Cyclic AMP may not be involved in catabolite repression in *Saccharomyces cerevisiae*: evidence from mutants capable of utilizing it as an adenine source. J Bacteriol 150:277-285

McCluskey K, Wiest A, Plamann M (2010) The Fungal Genetics Stock Center: a repository for 50 years of fungal genetics research. J Biosci 35:119-126

McNally MT, Free SJ (1988) Isolation and characterization of a Neurospora glucose-repressible gene. Curr Genet 14:545-551

Melo AM, Duarte M, Videira A (1999) Primary structure and characterisation of a 64 kDa NADH dehydrogenase from the inner membrane of *Neurospora crassa* mitochondria. Biochim Biophys Acta 1412:282-287

Melo AM, Duarte M, Moller IM, Prokisch H, Dolan PL, Pinto L, Nelson MA, Videira A (2001) The external calcium-dependent NADPH dehydrogenase from *Neurospora crassa* mitochondria. J Biol Chem 276:3947-3951

Michán S, Lledías F, Hansberg W (2003) Asexual development is increased in *Neurospora crassa cat-3* null mutant strains. Eukaryot Cell 2:798-808

Miller AJ, Vogg G, Saunders D (1990) Cytostolic calcium homeostasis in fungi: roles of plasma membrane transport and intracellular sequestration of calcium. Proc Natl Acad Sci USA 87:9348-9352

Miozzi L, Balestrini R, Bolchi A, Novero M, Ottonello S, Bonfante P (2005) Phospholipase A_2 up-regulation during mycorrhiza formation in *Tuber borchii*. New Phytol 167:229-238

Mirzayans R, Famulski KS, Enns L, Fraser M, Paterson MC (1995) Characterization of the signal transduction pathway mediating gamma ray-induced inhibition of DNA synthesis in human cells: indirect evidence for involvement of calmodulin but not protein kinase C nor p53. Oncogene 11:1597-1605

Miseta A, Kellermayer R, Ajello DF, Fu L, Bedwell DM (1999) The vacuolar Ca^{2+}/H^{+} exchanger Vcx1p/Hum1p tightly controls cytosolic Ca^{2+} levels in *S. cerevisiae*. FEBS Lett 451:132-136

Montagne C (1843) Quatrième centurie de plantes cellulaires exotiques nouvelles. Ann Sci Nat Bot 2e Sér 20:352-379

Moore TM, Chetham PM, Kelly JJ, Stevens T (1998) Signal transduction and regulation of lung endothelial cell permeability. Interaction between calcium and cAMP. Lung Cell Mol Physiol 19:L203-L222

Morgan LW, Feldman J F (2001) Epistatic and synergistic interactions between circadian clock mutations in *Neurospora crassa*. Genetics 159:537-543

Muir SR, Sanders D (1997) Inositol-1, 4, 5-trisphosphate-sensitive Ca^{2+} release across nonvacuolar membranes in cauliflower. Plant Physiol 114:1511-1521

Müller BT, Russo VRA (1989) Nitrogen starvation or glucose limitation induces conidiation in constantly shaken liquid cultures of *Neurospora crassa*. Fungal Genet Newslett 36:58-60

Murakami M, Kudo I (2004) Secretory phospholipase A_2. Biol Pharm Bull 27:1158-1164

Nakahama T, Nakanishi Y, Viscomi AR, Takaya K, Kitamoto K, Ottonello S, Arioka M (2010) Distinct enzymatic and cellular characteristics of two secretory phospholipases A_2 in the filamentous fungus *Aspergillus oryzae*. Fungal Genet Biol 47:318-331

Nakajima M, Akutsu K (2014) Virulence factors of *Botrytis cinerea*. J Gen Plant Pathol 80:15-23

Nakashima S, Ikeno Y, Yokoyama T, Kuwana M, Bolchi A, Ottonello S, Kitamoto K, Arioka M (2003) Secretory phospholipases A_2 induce neurite outgrowth in PC12 cells. Biochem J 376:655-666

Negash S, Yao Q, Sun H, Li J, Bigelow DJ, Squier TC (2000) Phospholamban remains associated with the Ca^{2+}- and Mg^{2+}-dependent ATPase following phosphorylation by cAMP-dependent protein kinase. Biochem J 351:195-205

Nelson MA, Metzenberg RL (1992) Sexual development genes of *Neurospora crassa*. Genetics 132:149-162

Nelson MA (1996) Mating systems in ascomycetes: a romp in the sac. Trends Genet 12:69-74

Nelson G, Kozlova-Zwinderman O, Collis AJ, Knight MR, Fincham JR, Stanger CP, Renwick A, Hessing JG, Punt PJ, van den Hondel CAMJJ, Read ND (2004) Calcium measurement in living filamentous fungi expressing codon-optimized aequorin. Mol Microbiol 52:1437-1450

Nevalainen TJ, Cardoso JC, Riikonen PT (2012) Conserved domains and evolution of secreted phospholipases A_2. 279:636-649

Nevalainen TJ, Morgado I, Cardoso JC (2013) Identification of novel phospholipase A_2 group IX members in metazoans. Biochimie 95:1534-1543

Nicholas KB, Nicholas HB, Deerfield DW (1997) GeneDoc: analysis and visualization of genetic variation. EMBnet News 4:1-4

Nicholls DG (2006) Simultaneous monitoring of ionophore- and inhibitor-mediated plasma and mitochondrial membrane potential changes in cultured neurons. J Biol Chem 281:14864-14874

Nishizuka Y (1984) The role of protein kinase C in cell surface signal transduction and tumour promotion. Nature 308:693-698

Nuss DL (1992) Biological control of chestnut blight: an example of virus-mediated attenuation of fungal pathogenesis. Microbiol Rev 56:561-576

Oh YT, Ahn CS, Lee KJ, Kim JG, Ro HS, Kim JW, Lee CW (2012) The activity of phosphoinositide-specific phospholipase C is required for vegetative growth and cell wall regeneration in *Coprinopsis cinerea*. J Microbiol 50:689-692

Osborne LE, Stein JM (2007) Epidemiology of Fusarium head blight on small-grain cereals. Int J Food Microbiol 119:103-108

Ou SH (1985) Rice Disease, second ed. Commonwealth Mycological Institute, Kew, UK

Pall ML (1981) Adenosine 3', 5'-phosphate in fungi. Microbiol Rev 45:462-480

Pall ML, Brunelli JP (1993) A series of six compact fungal transformation vectors containing polylinkers with multiple unique restriction sites. Fungal Genet Newslett 40:59-62

Paltauf F, Kohlwein S, Henry SA (1992) Regulation and compartmentalization of lipid synthesis in yeast. In: Jones EW, Pringle JR, Broach JR (eds) The molecular and cellular biology of the yeast Saccharomyces: gene expression, Cold Spring Harbor Laboratory Press, New York, pp 415-500

Parks LW, Casey WM (1995) Physiological implications of sterol biosynthesis in yeast. Ann Rev Microbiol 49: 95-116

Pavelic K (1987) Calmodulin antagonist W 13 prevents DNA repair after bleomycin treatment of human urological tumor cells growing on extracellular matrix. Int J Biochem 19:1091-1095

Payen A (1843) Extrain d'un rapport addresse' a' M. Le Marechal Duc de Dalmatie, Ministre de la Guerre, President du Conseil, sur une alteration extraordinaire du pain du munition. Ann Chim Phys 9:5-21

Payne WE, Fitzgerald-Hayes M (1993) A mutation in *PLC1*, a candidate phosphoinositide-specific phospholipase C gene from *Saccharomyces cerevisiae*, causes aberrant mitotic chromosome segregation. Mol Cell Biol 13:4351-4364

Perkins DD, Barry EG (1977) The cytogenetics of *Neurospora*. Adv Genet 19:133-285

Perkins DD (1992) *Neurospora*: the organism behind the molecular revolution. Genetics 130:687-701

Perkins DD, Radford A, Sachs MS (2000) The Neurospora Compendium: Chromosomal Loci. Academic Press, San Diego

Phizicky EM, Fields S (1995) Protein-protein interactions: methods for detection and analysis. Microbiol Rev 59:94-123

Pickard RT, Chiou XG, Strifler BA, DeFelippis MR, Hyslop PA, Tebbe AL, Yee YK, Reynolds LJ, Dennis EA, Kramer RM, Sharp JD (1996) Identification of essential residues for the catalytic function of 85-kDa cytosolic phospholipase A_2. Probing the role of histidine, aspartic acid, cysteine, and arginine. J Biol Chem 271:19225-19231

Pierson ES, Miller DD, Callaham DA, Shipley AM, Rivers BA, Cresti M, Hepler PK (1994) Pollen tube growth is coupled to the extracellular calcium ion flux and the intracellular calcium gradient, effect of BAPTA-type buffers and hypertonic media. Plant Cell 6:1815-1828

Pittman JK, Cheng NH, Shigaki T, Kunta M, Hirschi KD (2004) Functional dependence on calcineurin by variants of the *Saccharomyces cerevisiae* vacuolar Ca^{2+}/H^{+} exchanger Vcx1p Mol Microbiol 54:1104-1116

Plesofsky-Vig N, Brambl R (1985) Heat shock response of *Neurospora crassa*: protein synthesis and induced thermotolerance. J Bacteriol 162:1083-1091

Pöggeler S, Kück U (2001) Identification of transcriptionally expressed pheromone receptor genes in filamentous ascomycetes. Gene 280:9-17

Prados Rosales RC, Pietro AD (2008) Vegetative hyphal fusion is not essential for plant infection by *Fusarium oxysporum*. Eukaryot Cell 7:162-171

Prakash A, Sengupta S, Aparna K, Kasbekar DP (1999) The erg-3 (sterol D14, 15-reductase) gene of *Neurospora crassa*: generation of null mutants by repeat-induced point mutation and complementation by proteins chimeric for human lamin B receptor sequences. Microbiol 145:1443-1451

Prokisch H, Yarden O, Dieminger M, Tropschug M, Barthelmess IB (1997) Impairment of calcineurin function in *Neurospora crassa* reveals its essential role in hyphal growth, morphology and maintenance of the apical Ca^{2+} gradient. Mol Gen Genet 256:104-114

Pukkila PJ (2011) *Coprinopsis cinerea*. Curr Biol 21:R616-R617

Quandt K, Frech K, Karas H, Wingender E (1995) MatInd and MatInspector: new fast and versatile tools for detection of consensus matches in nucleotide sequence data. Nuclei Acids Res 23:4878-84

Qin J, Kang W, Leung B, McLeod M (2003) Ste11p, a high-mobility-group box DNA-binding protein, undergoes pheromone-and nutrient-regulated nuclear cytoplasmic shuttling. Mol Cell Biol 23:3253-3264

Radman R, Bucke C, Keshavarz T (2004) Elicitor effects on reactive oxygen species in liquid cultures of *Penicillium chrysogenum*. Biotechnol Lett 26:147-152

Raju NB (1980) Meiosis and ascospore genesis in Neurospora. Eur J Cell Biol 23:208-223

Raju NB (1992) Genetic control of the sexual cycle in *Neurospora*. Mycol Res 96:241-262

Reissig JL, Kinney SG (1983) Calcium as a branching signal in *Neurospora crassa*. J Bacteriol 154:1397-1402

Rhee SG, Bae YS (1997) Regulation of phosphoinositide-specific phospholipase C isozymes. J Biol Chem 272:15045-15048

Rho HS, Jeon J, Lee YH (2009) Phospholipase C-mediated calcium signalling is required for fungal development and pathogenicity in *Magnaporthe oryzae*. Mol Plant Pathol 10:337-346

Roberts AN, Berlin V, Hager KM, Yanofsky C (1988) Molecular analysis of a *Neurospora crassa* gene expressed during conidiation. Mol Cell Biol 8:2411-2418

Rodriguez-Amaya DB, Kimura M **(**2004) Harvest plus handbook for carotenoid analysis. *Harvest Plus Technical Monograph 2*. International Food Policy Research Institute (IFPRI) and International Center for Tropical Agriculture (CIAT), Washington, DC, USA

Romano N, Macino G (1992) Quelling: transient inactivation of gene expression in *Neurospora crassa* by transformation with homologous sequences. Mol Microbiol 6:3343-3353

Ruis H, Schüller C (1995) Stress signaling in yeast. Bioessays 17:959-965

Ryan FJ, Beadle GW, Tatum EL (1943) The tube method of measuring the growth rate of Neurospora. Am J Bot 30:784-799

Ryan FJ (1950) Selected methods of Neurospora genetics. Methods Med Res 3:51-75

Rzhetsky A, Nei M (1992) Statistical properties of the ordinary leastsquares, generalized least-squares, and minimum-evolution methods of phylogenetic inference. J Mol Evol 35:367-375

Sadakane Y, Nakashima H (1996) Light-induced phase shifting of the circadian conidiation rhythm is inhibited by calmodulin antagonists in *Neurospora crassa*. J Biol Rhythms 11:234-240

Salo PM, Arbes SJ Jr, Sever M, Jaramillo R, Cohn RD, London SJ, Zeldin DC (2006) Exposure to *Alternaria alternata* in US homes is associated with asthma symptoms. J Allergy Clin Immunol 118:892-898

Sambrook J, Russell DW (2001) Molecular cloning: A laboratory manual. Cold spring harbor laboratory press, Cold spring harbor, New York

Sanders D, Pelloux J, Browniee C, Harper JF (2002) Calcium at the crossroads of signaling. Plant Cell 14:S401-S417

Scazzocchio C (2000) The fungal GATA factors. Curr Opin Microbiol 3:126-131

Schaloske RH, Dennis EA (2006) The phospholipase A2 superfamily and its group numbering system. Biochim Biophys Acta 1761:1246-1259

Schieber M, Chandel NS (2014) ROS function in redox signaling and oxidative stress. Curr Biol 24:R453-R462

Schmid J, Harold FM (1988) Dual roles for calcium ions in apical growth of *Neurospora crassa*. J Gen Microbiol 134:2623-2631

Schroeder WA, Johnson EA (1995) Singlet oxygen and peroxyl radicals regulate carotenoid biosynthesis in *Phaffia rhodozyma*. J Biol Chem 270:18374-18379

Schumacher J, Viaud M, Simon A, Tudzynski B (2008) The Ga subunit BCG1, the phospholipase C (BcPLC1) and the calcineurin phosphatase co-ordinately regulate gene expression in the grey mould fungus *Botrytis cinerea*. Mol Microbiol 67:1027-1050

Schwerdtfeger C, Linden H (2003) VIVID is a flavoprotein and serves as a fungal bluelight photoreceptor for photoadaptation. EMBO J 22:4846-4855

Scott DL, White SP, Otwinowski Z, Yuan W, Gelb MH, Sigler PB (1990) Interfacial catalysis: the mechanism of phospholipase A2. Science 250:1541-1546

Selker EU, Garrett PW (1988) DNA sequence duplications trigger gene inactivation in *Neurospora crassa*. Proc Natl Acad Sci USA 85:6870-6874

Shaw BD, Hoch HC (2000) Ca^{2+} regulation of *Phyllosticta ampelicida* pycnidiospore germination and appressorium formation. Fungal Genet Biol 31:43-53

Shear CL, Dodge BO (1927) Life histories and heterothallism of the red bread-mold fungi of the *Monilia sitophila* group. J Agric Res 34:1019-1042

Shiu PK, Raju NB, Zickler D, Metzenberg RL (2001) Meiotic silencing by unpaired DNA. Cell 107:905-916

Silverman-Gavrila LB, Lew RR (2000) Regulation of the tip-high [Ca^{2+}] gradient in growing hyphae of the fungus *Neurospora crassa*. Eur J Cell Biol 80:379-390

Silverman-Gavrila LB, Lew RR (2002) An IP3-activated Ca^{2+} channel regulates fungal tip growth. J Cell Sci 115:5013-5025

Siso-Nadal F, Fox JJ, Laporte SA, Hébert TE, Swain PS (2009) Cross-talk between signaling pathways can generate robust oscillations in calcium and cAMP. 4:e7189

Soragni E, Bolchi A, Balestrini R, Gambaretto C, Percudani R, Bonfante P, Ottonello S (2001) A nutrient-regulated, dual localization phospholipase A_2 in the symbiotic fungus *Tuber borchii*. EMBO J 20:5079-5090

Sorrentino V, Rizzuto R (2001) Molecular genetics of Ca^{2+} stores and intracellular Ca^{2+} signaling. Trends Pharmacol Sci 22:459-464

Springer, ML (1993) Genetic control of fungal differentiation: the three sporulation pathways in *Neurospora crassa*. Bioessays 15:365-374

Staben C, Jensen B, Singer M, Pollock J, Schechtman M , Kinsey J, Selker E (1989) Use of a bacterial Hygromycin B resistance gene as a dominant selectable marker in *Neurospora crassa* transformation. Fungal Genet Newslett 36:79-81

Sundquist AR, Briviba K, Sies H (1994) Singlet oxygen quenching by carotenoids. Methods Enzymol 234:384-388

Suresh K, Subramanyam C (1997) A putative role for calmodulin in the activation of *Neurospora crassa* chitin synthase. FEMS Microbiol Lett 150:95-100

Sutton RB, Devletov BA, Berghuis SM, Sudhof TS, Sprang SR (1995) Structure of the first C2 domain of synaptotagmin I; a novel Ca^{2+}/phospholipids-binding fold. Cell 80:929-938

Swain AL, Amma EL (1989) The coordination polyhedron of Ca^{2+}, Cd^{2+} in parvalbumin. Inorg Chim Acta 163:5-7

Szklarczyk D, Franceschini A, Wyder S, Forslund K, Heller D, Huerta-Cepas J, Simonovic M, Roth A, Santos A, Tsafou KP, Kuhn M, Bork P, Jensen LJ, von Mering C (2015) STRING v10: protein-protein interaction networks, integrated over the tree of life. Nucleic Acids Res 43:D447-D452

Takayanagi A, Miyakawa T, Asano A, Ohtsuka J, Tanokura M, Arioka M (2015) Expression, purification, refolding, and enzymatic characterization of two secretory phospholipases A_2 from *Neurospora crassa*. Protein Expr Purif 115:69-75

Tamuli R, Kumar R, Deka R (2011) Cellular roles of neuronal calcium sensor-1 and calcium/calmodulin-dependent kinases in fungi. J Basic Microbiol 51:120-128

Tamuli R, Kumar R, Srivastava DA, Deka R (2013) Calcium signaling. In: Kasbekar DP, McCluskey K (eds) Neurospora: genomics and molecular biology, Caister Academic Press, Norfolk, UK, pp 35-57

Tamuli R, Deka R, Borkovich KA (2016) Calcineurin subunits A and B interact to regulate growth and asexual and sexual development in *Neurospora crassa*. PLoS One 11:e0151867

Tamura K, Dudley J, Nei M, Kumar S (2007) MEGA4: molecular evolutionary genetics analysis (MEGA) software version 4.0. Mol Biol Evol 24:1596-1599

Terenzi HF, Flawiá MM, Torres HN (1974) A *Neurospora crassa* morphological mutant showing reduced adenylate cyclase activity. Biochem Biophys Res Commun 58:990-996

Terenzi HF, Jorge JA, Roselino JE, Migliorini RH (1979) Adenylyl cyclase deficient cr-1 (Crisp) mutant of *Neurospora crassa*: cyclic AMP-dependent nutritional deficiencies. Arch Microbiol 123:251-258

That T C, Turian G (1978) Ultrastructural study of microcyclic macroconidiation in *Neurospora crassa*. Arch Microbiol 116:279-288

Thevelein JM (1994) Signal transduction in yeast. Yeast 10:1753-1790

Thevelein JM, de Winde JH (1999) Novel sensing mechanisms and targets for the cAMP-protein kinase A pathway in the yeast *Saccharomyces cerevisiae*. Mol Microbiol 33:904-918

Thompson JD, Gibson TJ, Plewniak F, Jeanmougin F, Higgins DG (1997) The CLUSTAL-X windows interface: flexible strategies for multiple sequence alignment aided by quality analysis tools. Nucleic Acids Res 25:4876-4882

Tisi R, Baldassa S, Belotti F, Martegani E (2002) Phospholipase C is required for glucose-induced calcium influx in budding yeast. FEBS Lett 520:133-138

Tokiwa G, Tyers M, Volpe T, Futcher B (1994) Inhibition of G1 cyclin activity by the Ras/cAMP pathway in yeast. Nature 371:342-345

Tsai HC, Chung KR (2014) Calcineurin phosphatase and phospholipase C are required for developmental and pathological functions in the citrus fungal pathogen *Alternaria alternata*. Microbiol 160:1453-1465

Turner GE, Borkovich KA (1993) Identification of a G protein alpha subunit from *Neurospora crassa* that is a member of the Gi family. J Biol Chem 268:14805-14811

Ullmann A, Jacob E, Monod J (1967) Characterization by in vitro complementation of a peptide corresponding to an operator-proximal segment of the beta-galactosidase structural gene of *Escherichia coli.* J Mol Biol 24:339-343

Van Alfen NK, Jaynes RA, Anagnostakis SL, Day PR (1975) Chestnut blight: biological control by transmissible hypovirulence in *Endothia parasitica*. Science 189:890-891

Verheij HM, Volwerk JJ, Jansen EH, Puyk WC, Dijkstra BW, Drenth J, de Haas GH (1980) Methylation of histidine-48 in pancreatic phospholipase A_2. Role of histidine and calcium ion in the catalytic mechanism. Biochemistry 19:743-750

Verma A, Bhatt AN, Farooque A, Dwarakanath B (2011) Calcium ionophore A23187 reveals calcium related cellular stress as "I bodies": An old actor in a new role. Cell Calcium 50:510-522

Vershinin A (1999) Biological function of carotenoids – diversity and evolution. BioFactors 10:99-104

Videira A, Kasuga T, Tian C, Lemos C, Castro A, Glass NL (2009) Transcriptional analysis of the response of *Neurospora crassa* to phytosphingosine reveals links to mitochondrial function. Microbiol 155:3134-3141

Vogel HJ (1964) Distribution of lysine pathways among fungi: evolutionary implications. Am. Naturalist 98:435-446

Volotovski ID, Sokolovsky SG, Molchan OV, Knight MR (1998) Second messengers mediate increases in cytosolic calcium in tobacco protoplasts. Plant Physiol 117:1023-1030

Wakatsuki S, Arioka M, Dohmae N, Takio K, Yamasaki M, Kitamoto K (1999) Characterization of a novel fungal protein, p15, which induces neuronal differentiation of PC12 cells. J Biochem 126:1151-1160

Wakatsuki S, Yokoyama T, Nakashima S, Nishimura A, Arioka M, Kitamoto K (2001) Molecular cloning, functional expression and characterization of p15, a novel fungal protein with potent neurite-inducing activity in PC12 cells. Biochim Biophys Acta 1522:74-81

Watson S, Arkinstall S (1994) G protein linked effector and second messenger systems. In the G Protein Linked Receptor Factsbook Academic Press, London, pp 358-387

Westergaard M, Mitchell HK (1947) Neurospora V. A synthetic medium favoring sexual reproduction. Am J Botany 34:573-577

Wetzel CH, Spehr M, Hatt H (2001) Phosphorylation of voltage-gated ion channels in rat olfactory receptor neurons. Eur J Neurosci 14:1056-1064

Winkler MA, Merat DL, Tallant EA, Hawkins S, Cheung WY (1984) Catalytic site of calmodulin-dependent protein phosphatase from bovine brain resides in subunit A. Proc Natl Acad Sci USA 81:3054-3058

Wright SJ, Inchausti R, Eaton CJ, Krystofova S, Borkovich KA (2011) RIC8 is a guanine-nucleotide exchange factor for Gα subunits that regulates growth and development in *Neurospora crassa*. Genetics 189:165-176

Xiang Q, Rasmussen C, Glass NL (2001) The *ham-2* Locus, encoding a putative transmembrane protein, is required for hyphal fusion in *Neurospora crassa*. Genetics 160:169-180

Yamada A, Gaja N, Ohya S, Muraki K, Narita H, Ohwada T, Imaizumi Y (2001) Usefulness and limitation of DiBAC4(3), a voltage-sensitive fluorescent dye, for the measurement of membrane potentials regulated by recombinant large conductance Ca^{2+}-activated K^{+} channels in HEK293 Cells. Jpn J Pharmacol 86:342-350

Yamamoto T, Takeuchi H, Kanematsu T, Allen V, Yagisawa H, Kikkawa U, Watanabe Y, Nakasima A, Katan M, Hirata M (1999) Involvement of EF hand motifs in the Ca^{2+}-dependent binding of the pleckstrin homology domain to phosphoinositides. Eur J Biochem 265:481-490

Yang Q, Borkovich KA **(**1999) Mutational activation of a Gαi causes uncontrolled proliferation of aerial hyphae and increased sensitivity to heat and oxidative stress in *Neurospora crassa*. Genetics 151:107-117

Yang S-N, YuJ, Mayr GW, Hofmann F, Larsson O, Berggren P-O (2001) Inositol hexakisphosphate increases 1-type Ca^{2+} channel activity by stimulation of adenylyl cyclase. FASEB J 15:1753-1763

Yang Y, Cheng P, Zhi G, Liu Y (2001) Identification of a calcium/calmodulin-dependent protein kinase that phosphorylates the *Neurospora* circadian clock protein FREQUENCY. J Biol Chem 276:41064-41072

Yang Q, Poole SI, Borkovich KA (2002) A G-protein β subunit required for sexual and vegetative development and maintenance of normal G alpha protein levels in *Neurospora crassa*. Eukaryot Cell 1:378-390

Yap KL, Kim J, Truong K, Sherman M, Yuan T, Ikura M (2000) Calmodulin target database. J Struct Funct Genom 1:8-14

Yoko-o T, Matsui Y, Yagisawa H, Nojima H, Uno I, Toh-e A (1993) The putative phosphoinositide-specific phospholipase C gene, *PLC1*, of the yeast *Saccharomyces cerevisiae* is important for cell growth. Proc Natl Acad Sci USA 90:1804-1808

York JD, Odom AR, Murphy R, Ives EB, Wente SR (1999) A phospholipase C-dependent inositol polyphosphate kinase pathway required for efficient messenger RNA export. Science 285:96-100

Yoshida Y, Hasunuma K (2004) Reactive oxygen species affect photomorphogenesis in *Neurospora crassa*. J Biol Chem 279:6986-6993

Zaccolo M, Pozzan T (2003) cAMP and Ca^{2+} interplay: a matter of oscillation pattern. Trends Neurosci 26:53-55

Zalokar M (1954) Studies on biosynthesis of carotenoids in *Neurospora crassa*. Arch Biochem Biophys 50:71-80

Zelter A, Bencina M, Bowman BJ, Yarden O, Read ND (2004) A comparative genomic analysis of the calcium signaling machinery in *Neurospora crassa*, *Magnaporthe grisea*, and *Saccharomyces cerevisiae*. Fungal Genet Biol 41:827-841

Zhu C, Wang W, Wang M, Ruan R, Sun X, He M, Mao C, Li H (2015) Deletion of *PdMit1*, a homolog of yeast *Csg1*, affects growth and Ca^{2+} sensitivity of the fungus *Penicillium digitatum*, but does not alter virulence. Res Microbiol 166:153-152

Zorov DB, Juhaszova M, Sollott SJ (2014) Mitochondrial reactive oxygen species (ROS) and ROS-induced ROS release. Physiol Rev 94:909-950

Publications, Conferences, Seminars, and workshops

Total Publications:

1. **Barman A, Tamuli R (2015)** Multiple cellular roles of *Neurospora crassa plc-1*, s*plA2*, and *cpe-1* in regulation of cytosolic free calcium, carotenoid accumulation, stress responses, and acquisition of thermotolerance. J Microbiol 53:226-235.
2. **Barman A, Tamuli R (2017)** The pleiotropic vegetative and sexual development of *Neurospora crassa* arise from the double mutants of the calcium signaling genes *plc-1*, *splA2*, and *cpe-1*. Curr Genet doi: 10.1007/s00294-017-0682-y.
3. **Barman A, Gohain D, Bora U, Tamuli R (2017)** Phospholipases in fungi (Submitted).

Total Conference presentations:

1. **Barman A, Tamuli R (2012)** Poster presentation on Comparative analysis of cell signaling pathways and methylation patterns in *Bombyx mori* and *Neurospora crassa*" presented at "International Consultative meeting on Seribiotechnology-5th to 7th December 2012" held at Institute of Bioresources and Sustainable Development, Imphal, Manipur, India **(Received Best Poster Presentation Award)**.
2. **Barman A, Tamuli R (2013)** Poster presentation on "Role of Ca^{2+}/H^{+} exchanger and secretory phospholipase A2 in regulating C^{2+} homeostasis in *Neurospora crassa*" presented at "Yeast conference-4th to 7th December 2013" held at Institute of Microbial Technology, Chandigarh, India.
3. **Barman A, Gohain D, Tamuli R (2014)** Poster presentation on "Reactive oxygen species and cell signaling in *Neurospora crassa*" presented at "International Conference on Disease Biology and Therapeutics-3rd to 5th December 2014" held at Institute of Advanced Study in Science and Technology, Guwahati, Assam, India **(Received Best Poster Presentation Award)**.
4. Participation on "Recent advances in Cancer biology and Therapeutics-5th December 2014" held at Indian Institute of Technology-Guwahati, Assam, India.
5. **Barman A, Gohain D, Laxmi V, Deka R, Kumar R, Tamuli R (2015)** Poster presentation on "Cellular functions of calcium signaling machinery in the model filamentous fungus *Neurospora crassa*" presented at "Molecular Intricacies of Plant Pathogenic Micro-organisms (MIPPM), an Alternative Meet-21st to 22nd February 2015"

held at Department of Molecular Biology and Biotechnology, Tezpur University, Assam, India.

6. **Barman A, Gohain D, Tamuli R (2015)** Poster presentation on "Functional analysis of calcium signaling genes and a novel approach to study direct protein-protein interaction in *Neurospora crassa*" presented at "Research Conclave-23rd to 26th March 2015" held at Indian Institute of Technology, Guwahati, Assam, and India.
7. **Barman A, Nagar M, Tamuli R (2016)** Poster presentation on "Calcium signaling and regulation of cell function in *Neurospora crassa*" presented at "Research Conclave-17th to 20th March 2016" held at Indian Institute of Technology, Guwahati, Assam, India **(Received Best Poster Presentation Award)**.

Total Seminars:

1. DBT sponsored National seminar on "Prospects of Molecular Biological and Biotechnological Applications for Human Welfare" organized by Department of Biotechnology, Pandu College, Pandu, Guwahati, India from 11th to 12th May, 2012..

Total Workshops:

1. DBT sponsored workshop on "Training on Molecular Techniques in Biological Research" organized by State Biotech Hub, College of Veterinary Sciences, Assam Agricultural University, Khanapara, Guwahati, India from 8th to 10th September, 2011.
2. DBT sponsored workshop on "Basic Techniques in Bioinformatics" organized by Bioinformatics Facility, Department of Biotechnology, Indian Institute of Technology, Guwahati, Assam, India from 12th to 14th October, 2011.
3. DBT and BCIL sponsored workshop on "Capacity building in grant writing skills and effective management of Intellectual Property Rights (IPR) in Biotechnology by universities and research institutions in the North East Region" held at College of Veterinary Sciences, Assam Agricultural University, Khanapara, Guwahati, India from 28th to 30th December, 2016.

Barman A, Tamuli R (2012) Understanding of cell signalling pathways in *Bombyx mori*. Seribiotechnology (5th-7th December 2012). Organized by Institute of Bioresources and Sustainable development (IBSD), Imphal, Manipur.

Understanding of cell signalling pathways in *Bombyx mori*

Ananya Barman and Ranjan Tamuli

Department of Biotechnology, Indian Institute of Technology, Guwahati-781 039, Assam, India

Abstract

We have studied the calcium/calmodulin (Ca^{2+}/CaM) dependent protein kinase type I and type II proteins (BmCaMKI and BmCaMKII) of silkworm *Bombyx mori*, a model insect of the Lepidopteran species for which the draft genome sequence became available in 2004. The ORFs for the BmCaMKI and BmCaMKII are 1455, and 1532 bps in length and these ORFs encoded proteins contain 360 and 510 amino acid residues, respectively. Both, BmCaMKI and BmCaMKII share 44 and 40% sequence identities with the Ca^{2+}/CaM-dependent protein kinase type I (Ca^{2+}/CaMKI, encoded by NCU09123 gene) and the Ca^{2+}/CaM-dependent protein kinase type II (Ca^{2+}/CaMKII, encoded by NCU02283 gene) of *Neurospora crassa*, respectively. Previous work in our lab had shown that Ca^{2+}/CaMKI and Ca^{2+}/CaMKII are necessary for full fertility in *N. crassa*. The Ca^{2+}/CaM dependent protein kinase II in *B. mori* mediates sex pheromone biosynthesis. Additionally, we have also studied the comparative methylation of *B. mori* and *N. crassa*. The *B. mori* has about 0.11% of the genomic cytosine methylated, occurring in CG dinucleotides and is much lower as compared to *N. crassa* where 2-3% of the cytosines are methylated and methylation is not preferentially in the CpG dinucleotides.

Barman A, Tamuli R (2013) Role of Ca^{2+}/H^{+} exchanger and secretory phospholipase A2 in regulating Ca^{2+} homeostasis in *Neurospora crassa*. Yeast conference (4^{th}-7^{th} December 2013). Organized by Industrial Microbial Technology (IMTECH), Chandigarh, India.

Role of Ca^{2+}/H^{+} exchanger and secretory phospholipase A2 in regulating Ca^{2+} homeostasis in *Neurospora crassa*

[1]Ananya Barman and Ranjan Tamuli

Fungal Research Group, Department of Biotechnology, Indian Institute of Technology, Guwahati-781 039, India. [1]E-mail: b.ananya@iitg.ernet.in

Abstract

In this study, we describe cellular roles of calcium (Ca^{2+})-signaling genes NCU06366 and NCU06650, encodes for a Ca^{2+}/H^{+} exchanger and a secretory phospholipase A2, respectively, in regulating Ca^{2+} homeostasis in the filamentous fungus *Neurospora crassa*. In *N. crassa*, Ca^{2+} is mainly stored in the intracellular stores such as vacuoles (>90% of Ca^{2+} is sequestered in the vacuoles), Golgi, endoplasmic reticulum; however, only a small amount of Ca^{2+} (~100 nM) is present freely in the cytosol ($[Ca^{2+}]_c$). The Ca^{2+} ionophore A23187 increases the $[Ca^{2+}]_c$ level by releasing Ca^{2+} from the intracellular stores. Here we have investigated the cellular roles of NCU06366 and NCU06650 in *N. crassa* using the Ca^{2+} ionophore A23187. The ΔNCU06366.2 and ΔNCU06650.2 mutants showed a growth defect on the medium containing the ionophore, indicating that NCU06366 and NCU06650 genes might play a role in the maintenance of Ca^{2+} homeostasis. Moreover, in the ionophore region, the ΔNCU06366.2 mutant showed apical hyper bursting of the hyphae, the ΔNCU06650.2 mutant showed profuse branching with characteristic spherical sac like structures at the apex of the growing hyphae, and ΔNCU06366.2 ΔNCU06650.2 double mutant showed both apical hyper bursting and spherical sac like structures. The ORFs for NCU06366 and NCU06650 genes are 2597 and 916 bps in length and encode for a Ca^{2+}/H^{+} exchanger and a secretory phospholipase A2 of 505 and 186 amino acid residues, respectively. In addition, bioinformatics analysis revealed the presence of a conserved Ca^{2+} exchanger domain in NCU06366 and a catalytic domain in NCU06650 encoded proteins. Thus, our study had showed that NCU06366 and NCU06650 play a role in regulation of Ca^{2+} homeostasis in *N. crassa*.

Barman A, Gohain D, Tamuli R. (2014) Reactive oxygen species and cell signaling in *Neurospora crassa*. International conference on Disease Biology and Therapeutics (3rd-5th December 2014). Organised by Institute of Advanced Study in Science and Technology (IASST), Guwahati, Assam.

Reactive oxygen species and cell signaling in *Neurospora crassa*

Ananya Barman, Dibakar Gohain and Ranjan Tamuli

Department of Biotechnology, Indian Institute of Technology, Guwahati-781 039, India.

E-mail: b.ananya@iitg.ernet.in

Abstract

Reactive oxygen species (ROS) generated as by-products of cellular metabolism or environmental factors can act as second messengers thereby playing important role in cell signaling and homeostasis [1]. However, enhanced ROS production also referred to as oxidative stress results in a series of events which deregulate cellular functions leading to various pathological conditions such as cancer, atherosclerosis, neurodegenerative diseases, gastroduodenal pathogenesis, metabolic dysfunction and premature aging [2]. In biological systems, light exposure (UV radiations or ionizing radiations) as well as elevated sublethal temperatures (thermal stress or heat shock) can act as inducers of over production of ROS [3]. Carotenoids are known to be powerful antioxidants that are capable of quenching singlet oxygen species thereby neutralizing several attacks of ROS [4]. In this study we have used the filamentous fungi *Neurospora crassa* as a model system to understand the links between cell signaling, oxidative stress and carotenoids production. We have taken three calcium (Ca^{2+})-signaling genes NCU06245, NCU06650 and NCU06366 that encodes, respectively, the *N. crassa* homologues of *plc-1*, s*plA2*, and *cpe-1*. The *Δplc-1*, *ΔsplA2*, and *Δcpe-1* mutants showed reduced survival rate than the wild type in H_2O_2 and PHS induced oxidative stress and in acquiring thermotolerance induced by heat shock temperature. However the *Δplc-1*, *ΔsplA2*, and *Δcpe-1* mutants showed increased carotenoids accumulation thereby more ROS production than the wild type. Interestingly, carotenoids accumulation in the *Δplc-1*, *ΔsplA2* and *Δcpe-1* mutants showed increased ultraviolet (UV)-survival percentage of these strains, suggesting that carotenoids play a UV-protective role in these mutants. Thus, this study revealed

multiple cellular roles of *plc-1*, s*plA2*, and *cpe-1* genes in regulation of carotenoids accumulation promoting UV-survival, oxidative stress tolerance, and acquisition of thermotolerance induced by heat shock temperature.

Barman A, Gohain D, Laxmi V, Deka R, Kumar R, Tamuli R (2015) Cellular functions of calcium signaling machinery in the model filamentous fungus *Neurospora crassa*. Molecular Intricacies of Plant Pathogenic Micro-organisms (MIPPM), an Alternative Meet (21st-22nd February 2015). Organized by Department of Molecular Biology and Biotechnology (MBBT), Tezpur University, Tezpur, Assam.

Cellular functions of calcium signaling machinery in the model filamentous fungus *Neurospora crassa*

Ananya Barman[1, 2], Dibakar Gohain[1, 2], Vijya Laxmi[1], Rekha Deka, Ravi Kumar and RanjanTamuli[1,]

[1]*Correspondence*: Department of Biosciences and Bioengineering, Indian Institute of Technology Guwahati**,** Guwahati 781 039**,** Assam, India.

[1]*Presnting Authors*

Abstract

Calcium ion (Ca^{2+}) is a ubiquitous second messenger molecule that plays a versatile role in intracellular signaling processes including fungal virulence and pathogenicity. We studied several Ca^{2+}-signaling genes that encode for calcineurin (CNA), calmodulin (CaM), phospholipase C-1 (PLC-1), neuronal calcium sensor 1 (NCS-1), Ca^{2+}/CaM-dependent protein kinases (Ca^{2+}/CaMK) etc. using the model filamentous fungus *Neurospora crassa*. Studies in our laboratory have revealed multiple cellular roles of Ca^{2+}-signaling genes including growth, development, fertility, thermotolerance, circadian clocks, tolerance to Ca^{2+} and oxidative stress, and ultraviolet (UV) survival in *N. crassa*. Studies on the components of the Ca^{2+}-signaling machinery may lead to the identification of novel antifungal drug targets.

Barman A, Nagar M, Tamuli R (2016) Calcium signaling and regulation of cell function in *Neurospora crassa*. Research Conclave (18^{th}-20^{th} March 2016). Organized by Indian Institute of Technology (IIT), Guwahati, Assam.

Calcium signaling and regulation of cell function in *Neurospora crassa*

Ananya Barman, Manju Nagar and Ranjan Tamuli

Department of Biosciences and Bioengineering, Indian institute of Technology Guwahati, Guwahati -781039, Assam, India.

E-mail: b.ananya@iitg.ernet.in, manju.nagar@ iitg.ernet.in

Abstract

Calcium ion (Ca^{2+}) is a ubiquitous second messenger molecule that plays a versatile role in intracellular signaling in all cell types and tissues. Particularly in *Neurospora crassa*, Ca^{2+} signaling regulates numerous physiological processes such as secretion, sporulation, infection structure differentiation, cytoskeletal organization, growth, hyphal branching, Ca^{2+} stress tolerance, UV survival, sexual development and circadian clock etc. The *N. crassa* Ca^{2+} signaling machinery is unique and differ significantly from that of plants and animals with respect to second messenger systems involved in Ca^{2+} release from internal stores. The complex Ca^{2+} signaling machinery of *N. crassa* consists of 48 Ca^{2+} signaling proteins including four novel phospholipase C-δ subtype proteins PLC-δ, a Ca^{2+} and/or CaM binding protein sPLA2 and a Ca^{2+}/H^{+} exchanger CPE-1. In this study we have used the filamentous fungi *Neurospora crassa* as a model system to understand the various cellular processes regulated by these proteins. Also genetic interactions between PLC-δ, sPLA2 and CPE-1 were shown to regulate diverse signal transduction pathways in this fungi.

Journal of Microbiology (2015)
DOI 10.1007/s12275-015-4465-1

Multiple cellular roles of *Neurospora crassa plc-1*, *splA2*, and *cpe-1* in regulation of cytosolic free calcium, carotenoid accumulation, stress responses, and acquisition of thermotolerance[§]

Ananya Barman and RanjanTamuli*

Department of Biotechnology, Indian Institute of Technology Guwahati Guwahati 781 039, India

(Received Aug 12, 2014 / Revised Dec 12, 2014 / Accepted Dec 15, 2014)

Phospholipase C1 (PLC1), secretory phospholipase A2 (sPLA2) and Ca^{2+}/H^{+} exchanger proteins regulate calcium signaling and homeostasis in eukaryotes. In this study, we investigate functions for phospholipase C1 (*plc-1*), sPLA2 (*splA2*) and a Ca^{2+}/H^{+} exchanger (*cpe-1*) in the filamentous fungus *Neurospora crassa*. The *Δplc-1*, *ΔsplA2*, and *Δcpe-1* mutants exhibited a growth defect on medium supplemented with the divalent ionophore A23187, suggesting that these genes might play a role in regulation of cytosolic free Ca^{2+} concentration ($[Ca^{2+}]_c$) in *N. crassa*. The strains lacking *plc-1*, *splA2*, and *cpe-1* possessed higher carotenoid content than wild type at 8°C, 22°C, and 30°C, and showed increased ultraviolet (UV)-survival under conditions that induced carotenoid accumulation. Moreover, *Δplc-1*, *ΔsplA2*, and *Δcpe-1* mutants showed reduced survival rate under hydrogen peroxide-induced oxidative stress and induced thermotolerance after exposure to heat shock temperatures. Thus, this study revealed multiple cellular roles for *plc-1*, *splA2*, and *cpe-1* genes in regulation of $[Ca^{2+}]_c$, carotenoid accumulation, survival under stress conditions, and acquisition of thermotolerance induced by heat shock.

Keywords: calcium signaling, Ca^{2+}/H^{+} exchanger, phospholipase C-1, secretory phospholipase A2, *Neurospora crassa*

Introduction

Cell signaling requires messengers including calcium ion (Ca^{2+}) whose concentration varies with space, time and amplitude (Berridge *et al*., 1998; Clapham, 2007). Binding of Ca^{2+} to target proteins changes their conformation, charge, and thereby, governs protein functions (Clapham, 2007). Thus, Ca^{2+} has evolved as a universal messenger that plays a versatile role in intracellular signaling in all cell types and tissues (Berridge *et al*., 1998; Kazmierczak *et al*., 2013). Ca^{2+}-signaling is typically triggered by a transient increase in cytosolic free Ca^{2+} concentration ($[Ca^{2+}]_c$). The resting $[Ca^{2+}]_c$ is ~100 nM; however, when Ca^{2+}-signaling is triggered, $[Ca^{2+}]_c$ rises transiently upto 1 μM or more (Chin and Means, 2000; Bootman *et al*., 2001).

In the filamentous fungus *Neurospora crassa*, low $[Ca^{2+}]_c$ is maintained using active transport mechanisms across the plasma membrane and buffering Ca^{2+} in organelles (Bowman *et al*., 2011). In *N. crassa*, Ca^{2+}-signaling is known to be involved in regulating a variety of processes such as Ca^{2+} stress tolerance, the circadian clock, growth, hyphal tip branching, ion transport, sexual development and UV survival (Deka *et al*., 2011; Deka and Tamuli, 2013; Tamuli *et al*., 2011, 2013; Kumar and Tamuli, 2014). The predicted Ca^{2+}-signaling machinery of *N. crassa* is complex and contains many different proteins including four novel phospholipase C-δ subtype (PLC-δ) proteins (Galagan *et al*., 2003; Borkovich *et al*., 2004). The PLC protein cleaves phosphotidylinositol -4, 5-bisphosphate (PIP2) into second messengers, namely, inositol 1, 4, 5-trisphosphate (IP_3) and diacylglycerol (DAG) (Chae *et al*., 2007). In animal cells, IP_3 diffuses through the cytosol and binds to the IP_3 receptors, inducing Ca^{2+} release from vacuoles, whereas DAG activates protein kinase C (PKC), triggering a range of cellular activities (Cornelius and Nakashima, 1987; Chae *et al*., 2007). Interestingly, no recognizable IP_3 receptors has been identified in *N. crassa* and both of its PKC proteins lack a C2 domain with Ca^{2+} binding sites (Galagan *et al*., 2003; Borkovich *et al*., 2004).

PLC proteins are involved in diverse cell functions in different organisms. In the budding yeast *Saccharomyces cerevisiae*, Plc1p, a phosphatidylinositol-specific phospholipase C (PI-PLC) shows sequence homology to the mammalian PI-PLC-δ isoforms and is involved in nutritional and stress-related responses (Flick and Thorner, 1993). In *S. cerevisiae*, Plc1p is necessary for growth at nonpermissive temperatures (above 35°C), survival under hyperosmotic stress, and utilization of galactose, raffinose, or glycerol as a carbon source at permissive temperatures (23 to 30°C) (Flick and Thorner, 1993). In the grey mold fungus *Botrytis cinerea*, a necrotrophic plant pathogen, PLC1 homologue *BcPLC1* functions in growth, conidiation, germination and virulence (Schumacher *et al*., 2008). In *Magnaporthe oryzae*, the rice blast fungus, the *MoPLC1* gene encodes a fungal PI-PLC-δ isoform that regulates intracellular Ca^{2+} fluxes essential for fungal development, appressorium formation and pathogenicity (Rho *et al*., 2009). Moreover, two other PLC isozymes *MoPLC2* and *MoPLC3* exhibit, respectively, 58% and 49% identity to the *PLC1* gene of *N. crassa* (NCU06245), and play distinct roles in *M. oryzae* including regulating development and appres-

*For correspondence. E-mail: ranjantamuli@iitg.ernet.in, ranjan.tam@gmail.com; Tel.: +91-361-258-2220; Fax: +91-361-258-2249
[§]Supplemental material for this article may be found at http://www.springerlink.com/content/120956.

sorium-mediated penetration (Choi *et al.*, 2011). In *Alternaria alternata*, the citrus fungal pathogen, the *PLC1* homologue plays an important role in vegetative growth, conidial formation, Ca^{2+} homeostasis, and virulence (Tsai and Chung, 2014). In the encapsulated yeast and human pathogen *Cryptococcus neoformans*, *CnPlc1*, a homologue of the mammalian PI-PLC-δ, supplies the IP3 substrate required for the catalytic activity of the major IP3 kinase, Arg1, which is essential for cellular homeostasis and virulence (Lev *et al.*, 2013).

In contrast to these other fungi, little is known about the *N. crassa* homologues of PLC homologs. The NCU06245 gene encodes a homologue of PLC-δ that is highly divergent among the natural isolates of *N. crassa*. The NCU06245 gene exhibits high incidence of polymorphisms resulting in a coding sequence changes for amino acid positions 200–250 unique to *Neurospora* (Gavric *et al.*, 2007).

The *N. crassa* Ca^{2+}-signaling machinery also includes 23 members of Ca^{2+} and/or CaM binding protein families (Galagan *et al.*, 2003; Borkovich *et al.*, 2004; Tamuli *et al.*, 2013). One member of this group shows sequence similarity to secretory phospholipase A2 (sPLA2). sPLA2, comprises a diverse family of low-molecular weight secretory enzymes possessing the ability to hydrolyze the ester bond at the *sn-2* position of glycerophospholipids in a Ca^{2+} dependent manner, thereby, liberating fatty acids and lysophospholipids (Murakami and Kudo, 2002). Various sPLA2 proteins play roles in numerous biological processes such as atherosclerosis, host defense, inflammation, and regulation of eicosanoid synthesis (Murakami and Kudo, 2002; Boilard *et al.*, 2010). A novel secretory protein, p15, isolated from *Helicosporium sp.* HN1 has been shown to induce outgrowth of neurites and neuronal differentiation from rat pheochromocytoma PC12 cells (Wakatsuki *et al.*, 1999; 2001). Another sPLA2 homologue Scp15 isolated from *Streptomyces coelicolor* displays similar neurite inducing activity in PC12 cells (Nakashima *et al.*, 2003). Fungi possesses a heterogeneous group of PLA_2 proteins with a variety of structural domains that could play an important role in nutrient acquisition and interaction with the host (Köhler *et al.*, 2006). In the symbiotic fungus *Tuber borchii*, the phospholipase A TbSP1 is strongly up-regulated and activated via autoproteolysis that may enhance establishment of symbiosis and mycorrhiza formation in response to nutrient starvation (Soragni *et al.*, 2001; Cavazzini *et al.*, 2013). In the filamentous ascomycete *Aspergillus oryzae*, two distinct $sPLA_2$s, sPlaA and sPlaB exhibit distinct physiological properties such as pH optimum for enzyme activity, Ca^{2+} requirement, substrate preferences, expression profile, and cellular localization (Nakahama *et al.*, 2010). In mice, sPLA2 regulates phagocytosis and contributes to the innate immune response against *Candida albicans* (Balestrieri *et al.*, 2009). Furthermore, in humans, a group of sPLA2 enzymes

Table 1. ***Neurospora crassa*** **strains used in this study**

Sl. No.	FGSC no. (a/A) or strain no.	NCU no. or strain type	Type of protein	Source
1	11248/11249	7075.2	Ca^{2+}/H^+ exchanger	FGSC
2	12376/12375	795.2	Ca^{2+}/H^+ exchanger	FGSC
3	11530/11529	2826.2	Ca^{2+}/H^+ exchanger	FGSC
4	11407/11408	6366.2	Ca^{2+}/H^+ exchanger	FGSC
5	12468/NA	8490.2	Ca^{2+}/H^+ exchanger	FGSC
6	NA/11253	7605.2	Ca^{2+} permeable channel	FGSC
7	11707/11708	6703.2	Ca^{2+} permeable channel	FGSC
8	13287/NA	3305.2	Ca^{2+} ATPase	FGSC
9	NA/13071	4736.2	Ca^{2+} ATPase	FGSC
10	13036/13037	5154.2	Ca^{2+} ATPase	FGSC
11	NA/13040	4898.2	Ca^{2+} ATPase	FGSC
12	11410/11409	7966.2	Cation- ATPase	FGSC
13	12022/NA	1266.2	Phospholipase C	FGSC
14	11411/NA	6245.2	Phospholipase C	FGSC
15	11271/11271	9655.2	Phospholipase C	FGSC
16	12023/NA	2175.2	Phospholipase C	FGSC
17	11405/11406	5225.2	Ca^{2+} and/or CaM binding protein	FGSC
18	13049/NA	2115.2	Ca^{2+} and/or CaM binding protein	FGSC
19	15890/NA	2738.2	Ca^{2+} and/or CaM binding protein	FGSC
20	11541/11542	6948.2	Ca^{2+} and/or CaM binding protein	FGSC
21	11403/11404	4379.2	Ca^{2+} and/or CaM binding protein	FGSC
22	11531/NA	3750.2	Ca^{2+} and/or CaM binding protein	FGSC
23	12448/12449	2283.2	Ca^{2+} and/or CaM binding protein	FGSC
24	12548/12547	9123.2	Ca^{2+} and/or CaM binding protein	FGSC
25	11169/11170	2814.2	Ca^{2+} and/or CaM binding protein	FGSC
26	11545/NA	9212.2	Ca^{2+} and/or CaM binding protein	FGSC
27	11246/11247	6650.2	Ca^{2+} and/or CaM binding protein	FGSC
28	11537/11536	6177.2	Ca^{2+} and/or CaM binding protein	FGSC
29	988/987	Wild type		FGSC

possibly plays a novel anti-inflammatory role in immune complex-mediated arthritis (Boilard *et al.*, 2010). However, little is known about the sole sPLA2 protein identified in *N. crassa*.

The high $[Ca^{2+}]_c$ is reduced to the resting level by another group of Ca^{2+}-signaling proteins, Ca^{2+} exchangers that pump Ca^{2+} out of the cell and transport Ca^{2+} into the intracellular Ca^{2+} storage organelles with the simultaneous exchange of positive ions across membranes (Zelter *et al.*, 2004; Tamuli *et al.*, 2013). The *N. crassa* Ca^{2+}-signaling machinery possesses six novel Ca^{2+}/H^+ exchangers and two putative Ca^{2+}/Na^+ exchangers, and all of these exchangers contain conserved Ca^{2+} exchanger domains (Galagan *et al.*, 2003; Borkovich *et al.*, 2004; Zelter *et al.*, 2004). One of the *N. crassa* Ca^{2+}/H^+ exchangers called CAX is homologous to Vcx1p from *S. cerevisiae*. The *Δcax* mutant accumulates very little Ca^{2+} in the dense vacuolar fraction, and therefore, CAX could be involved in maintaining intracellular Ca^{2+} levels in *N. crassa* (Bowman *et al.*, 2011). Phylogenetic analysis has revealed that one of the *N. crassa* Ca^{2+}/H^+ exchangers, encoded by NCU06366, is significantly different from homologues found in *S. cerevisiae* and *M. grisea* (Zelter *et al.*, 2004). However, detailed knowledge about the NCU06366-encoded Ca^{2+}/H^+ exchanger has remained largely unknown.

In this work, we describe the cellular roles of *plc-1*, *splA2*, and NCU06366 in regulation of $[Ca^{2+}]_c$, carotenoid accumulation, survival under stress conditions, and acquisition of thermotolerance.

Materials and Methods

Strains, media, and growth conditions

N. crassa wild type strains 74-OR23-1 A (FGSC 987) and OR8-1 a (FGSC 988), Ca^{2+} signaling mutants ΔNCU06245.2 a (FGSC 11411), ΔNCU06650.2 A (FGSC11247), ΔNCU06650.2 a (FGSC11247), ΔNCU06366.2 A (FGSC 11408), ΔNCU06366.2 a (FGSC 11407), and other strains (Table 1) were obtained from the Fungal Genetics Stock Center (FGSC; University of Missouri, Kansas city, MO 64110) (McCluskey, 2010). We verified knockout mutants using the gene-specific primers along with the common reverse *hph* primer in polymerase chain reactions (Supplementary data Fig. S1). Media and procedures for growth and maintenance of *N. crassa* strains were essentially as described (Davis and DeSerres, 1970). For vegetative growth, strains were routinely cultured on 1X Vogel's (Vogel, 1964) glucose medium (VGM) with 1.5% D-glucose as a carbon source and 1.5% Bacto Grade Agar (SRL).

Sequence analysis

The sequences of *N. crassa* NCU06245, NCU06650 and NCU06366 proteins were downloaded from Broad Institute Neurospora database version 7 (http://www.broadinstitute.org/annotation/genome/neurospora/MultiHome.html) and used as queries to search against the non-redundant protein sequence databases at the NCBI using BLASTP (http://blast.ncbi.nlm.nih.gov/Blast.cgi; Altschul *et al.*, 1990) with the default parameters. Proteins were selected based on % identities, % similarities and *E* values. Multiple sequence alignments of the selected proteins were built using CLUSTALX 1.83 (Thompson *et al.*, 1997) and alignments visualized using the GeneDoc program (Nicholas and Nicholas, 1997). These alignments were used for constructing phylogenetic trees using the minimum-evolution method (Rzhetsky and Nei, 1992), 500 bootstrap replication as test of phylogeny (Felsenstein, 1985) and the software MEGA5 (Tamura *et al.*, 2011).

Calcium ionophore assay

To test for elevated intracellular Ca^{2+} sensitivity in the mutants, an agar block was inoculated onto one corner of petri dishes and 10 µl each of a 9.5 mM stock solution of A23187 (test) or ethanol (control) was spotted onto the other corner on the VGM media as described previously (Lew *et al.*, 2008). Plates were incubated at 30°C for 2–3 days and colonies were observed under a Trinocular inverted microscope (Axio Vert.A1 FL, Carl Zeiss). Hyphal images were captured with an AxioCam ICc3 CCD camera. The petri dishes were also photographed after 38 h of growth using a digital camera (Nikon Coolpix P500).

Carotenoid analysis

For carotenoid analysis, sterile petri dishes containing liquid VGM supplemented with 0.2% tween 80 were inoculated with conidia at a concentration of ~1×10^6 conidia/ml (Zalokar, 1954). Cultures were initially incubated for 48 h in the dark at 30°C and further incubated at the indicated temperature either with or without an exposure to white light for 24 h (illuminated with two fluorescent bulbs, Philips TL-D 18W/54 lamp, 18W, 6500 K, 1015 lumens). Mycelia from these cultures were collected, lyophilized and pulverized into fine powder with mortar and pestle. Subsequently, acetone and hexane were used in consecutive steps for extraction of total carotenoids from 25 mg (dry weight) of the powdered sample. Total carotenoid content was determined by measuring the absorbance value at 470 nm and using the formula:

Total carotenoid content (µg/g) = [Total absorbance × Total volume of extract (1 ml) × 10^4] / [Absorption coefficient (2500) × sample weight (g)] as described previously (Rodriguez-Amaya and Kimura, 2004).

UV sensitivity assay

Conidia were grown in flasks containing VGM (without tween 80 supplement) agar medium at 30°C in the dark for 48 h and then at the indicated temperature with or without illumination as described for the carotenoid analysis above. For quantitative analysis, conidia were plated on FGS (0.05% fructose, 0.05% glucose, 0.05% sorbose plus 2% agar) medium and irradiated with different doses of UV in a UVC 500 cross linker (Hoefer, UK). The plates were incubated at 30°C in the dark for 48 h and number of colonies on each plate counted.

Oxidative stress resistance and thermotolerance studies

For hydrogen peroxide induced oxidative stress assay, conidia of *N. crassa* strains were inoculated at a concentration of

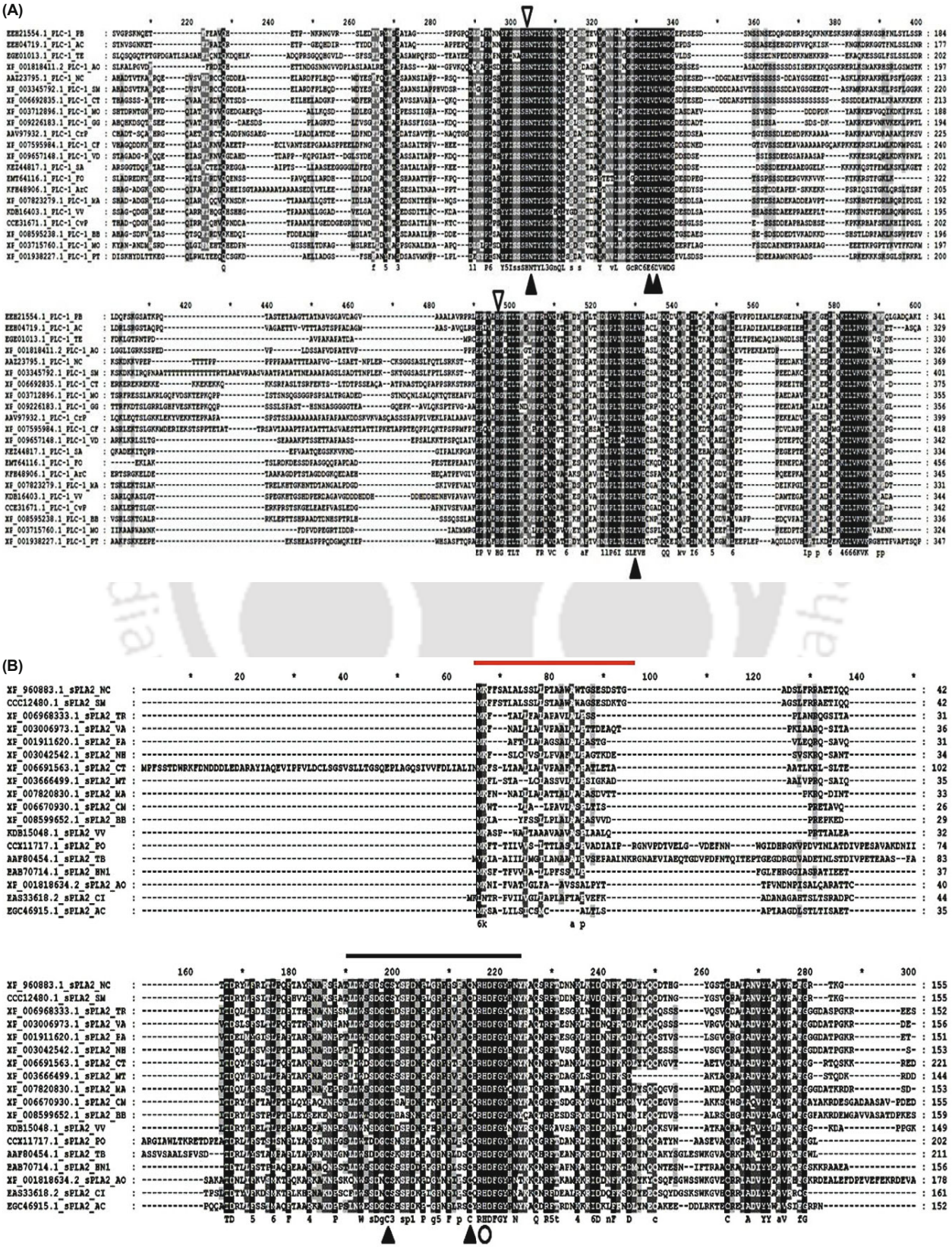

Fig. 1. Continued

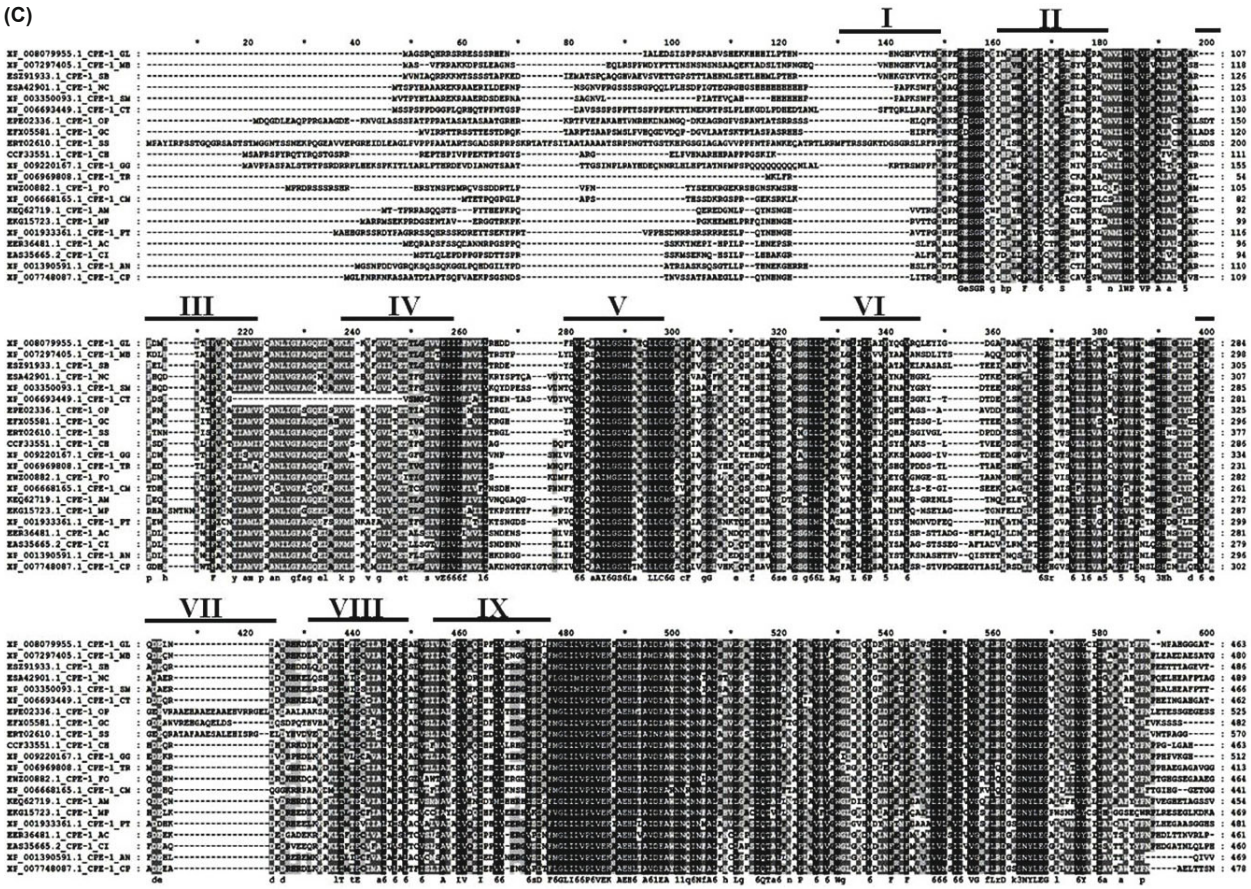

Fig. 1. Sequence analysis of *plc-1*, *splA2*, and *cpe-1* homologues. (A) Sequence alignment of PLC-1 homologues. The positions of the hydrogen binding residues are indicated above the sequence (inverted triangles) and the Ca^{2+} binding residues are indicated below the sequence (filled triangles) (Chung *et al*., 2006). (B) Sequence alignment of sPLA2 homologues. The predicted secretion signal peptide is underlined in red. The highly conserved portion of sPLA2 (positions 122-153) is underlined in black. The positions of the catalytic histidine residue (open circle) and disulphide bonded cysteine residues (filled triangles) are indicated below the sequences (Soragni *et al*., 2001). (C) Sequence alignment of CPE-1 homologues. The sequence corresponds to transmembrane segments (I to IX) as predicted with TMHMM program are shown underlined (http://www.cbs.dtu.dk/services/TMHMM/) (Zelter *et al*., 2004; Guttery *et al*., 2013). The sequences used in the analyses are AC, *A. capsulatus*; ArC, *Acremonium chrysogenum*; AM, *Aureobasidium melanogenum*; AN, *Aspergillus niger*; AO, *A. oryzae*; BB, *Beauveria bassiana*; CF, *Colletotrichum fioriniae*; CH, *C. higginsianum*; CI, *Coccidioides immitis*; CM, *Cordyceps militaris*; CP, *Cladophialophora psammophila*; CrP, *C. parasitica*; CvP, *Claviceps purpurea*; CT, *Chaetomium thermophilum*; FO, *Fusarium oxysporum*; GC, *Grosmannia clavigera*; GG, *Gaeumannomyces graminis*; HN1, *Helicosporium* sp.; GL, *Glarea lozoyensis*; MA, *Metarhizium anisopliae*; MB, *Marssonina brunnea*; MO, *M. oryzae*; MP, *Macrophomina phaseolina*; MT, *Myceliophthora thermophila*; NC, *N. crassa*; NH, *Nectria haematococca*; OP, *Ophiostoma piceae*; PA, *Podospora anserine*, PB, *Paracoccidioides brasiliensis*; PO, *Pyronema omphalodes*; PT, *Pyrenophoratritici-repentis*; SA, *Scedosporium apiospermum*; SB, *Sclerotinia borealis*; SM, *Sordaria macrospora*; SS, *Sporothrix schenckii*; TB, *T. borchii*; TE, *Trichophyton equinum*; TR, *Trichoderma reesei*; VA, *Verticillium alfalfae*; VD, *Verticillium dahliae*; VV, *Villosiclava virens*. Conserved amino acids are indicated in black (100%), dark grey (>80%) and light grey (>60%) in the alignments.

~1×10^6 conidia/ ml into liquid VGM and germinated with shaking at 200 rpm for 2 h in the dark at 30°C. Germlings were supplemented with hydrogen peroxide (test) or without (control) at a final concentration of 10 mM and further germinated for 1 h at 30°C. Germlings were plated on FGS medium and incubated at 30°C for 24 h. Percent survival was scored by dividing the number of viable colonies from plates exposed to H_2O_2 (test) by the number of colonies from plates not exposed to H_2O_2 (control) and multiplying by 100.

Similarly, for thermotolerance assays, 2 h germlings obtained as mentioned above were held at 30°C (control), 30°C (uninduced thermotolerance), and 44°C (induced thermotolerance). Both 30°C (uninduced) and 44°C (induced) germlings were then given a 52°C lethal heat shock for 20 min. Germlings were finally plated on FGS media followed by incubation at 30°C for 24 h (Yang and Borkovich, 1999). Percent survival was calculated by dividing the number of viable colonies from plates subjected to heat-treatment (induced or uninduced) by the number of colonies on plates held at 30°C (control) and multiplying by 100.

Statistical analysis

Statistical analysis was carried out using the data obtained from at least three independent replicates by one-way ANOVA (Microsoft Excel).

Results and Discussion

Sequence analysis of NCU06245, NCU06650 and NCU06366

N. crassa NCU06245, NCU06650, and NCU06366 encode three distinct types of Ca^{2+}signaling proteins. The NCU06245 gene is predicted to encode a 711 amino acid residues phospholipase C-1 (PLC-1) with similarity to PLC homologues in *Ajellomyces capsulatus*, *Colletotrichum higginsianum*, and *MoPLC2* and *MoPLC3* of *M. oryzae* (43, 52, 51, and 43% identities; Fig. 1A). Sequence alignment of NCU06245 homologues revealed important Ca^{2+} and H^{+} binding residues similar to PLC homologues from *Cryphonectria parasitica*, *M. grisea*, and *Arabidopsis thaliana* (Chung *et al*., 2006). The NCU06650 gene is predicted to encode a conserved hypothetical secretory phospholipase A2 (sPLA2) of 186 amino acid residues that shares sequence similarity with *A. capsulatus*, *A. oryzae*, *T. borchii*, and *Verticillium alfalfa* sPLA2 proteins (55, 41, 50, and 57% identities; Fig. 1B). The protein encoded by the NCU06650 gene also possesses conserved signal peptide residues (positions 1–30) and a highly conserved region (positions 122–153) that possesses catalytic histidine residues and disulphide-bonded cysteine residues similar to the sPLA2 homologue of *T. borchii* (Soragni *et al*., 2001). The NCU06366 gene encodes a Ca^{2+}/H^{+} exchanger (calcium proton exchanger-1; CPE-1) of 505 amino acid residues sharing sequence similarity with *A. capsulatus*, *A. niger*, *C. higginsianum* and *M. oryzae* homologues of CPE (50, 52, 59, and 68% identities; Fig. 1C). The NCU06366 gene product contains nine transmembrane helices as predicted by the TMHMM program (http://www. cbs.dtu.dk/services/TMHMM/; Zelter *et al*., 2004; Guttery *et al*., 2013). These results indicate that NCU06245, NCU06650 and NCU06366 correspond to *N. crassa* homologues of the *plc-1*, *splA2*, and *cpe-1*genes, respectively. In addition, the PLC-1, sPLA2, and CPE-1 proteins from *N. crassa* were found clustered within the Sordariomycetes clade during phylogenetic analysis with a subset of homologues from other fungi (Supplementary data Fig. 2).

Δplc-1, *ΔsplA2* and *Δcpe-1* mutants show growth defects in response to increased intracellular free Ca^{2+}

We found that growth rates of the *Δplc-1*, *ΔsplA2*, and *Δcpe-1* mutants on VGM were similar to the wild-type (Supplementary data Table S1). However, the *Δplc-1*, *ΔsplA2*, and *Δcpe-1* mutants exhibited morphological defects when cultured on VGM containing the divalent ionophore A23187 (Fig. 2). The A23187 ionophore causes an increase in cytosolic free Ca^{2+} concentration ($[Ca^{2+}]_c$; Nelson *et al*., 2004). In the ionophore zone, the *Δplc-1* mutant exhibited reduced branching with characteristic spherical sac-like structures at the apex of the growing hyphae. Similar sac like structures and more compact hyphal branching was observed in the *ΔsplA2* mutant. In case of the *Δcpe-1*mutant, apical hyper branching of hyphae was observed. These results indicate that the *plc-1*, s*plA2*, and *cpe-1* genes may play a role in the regulation of $[Ca^{2+}]_c$ in *N. crassa*. We also studied growth of 25 additional knockout mutants lacking predicted Ca^{2+} signaling on medium containing the A23187 ionophore, but, these mutants were similar to wild-type (Supplementary data Table S2).

To test whether the hyphal growth defect of *Δplc-1*, *ΔsplA2*, and *Δcpe-1* mutants upon ionophore treatment was due to dissipation of membrane potential, we used the membrane potential sensitive fluorescent dye DiBAC that fluoresces when membranes are depolarized (Alcántara-Sánchez *et al*., 2004). Germlings of *Δplc-1*, *ΔsplA2*, and *Δcpe-1*mutants

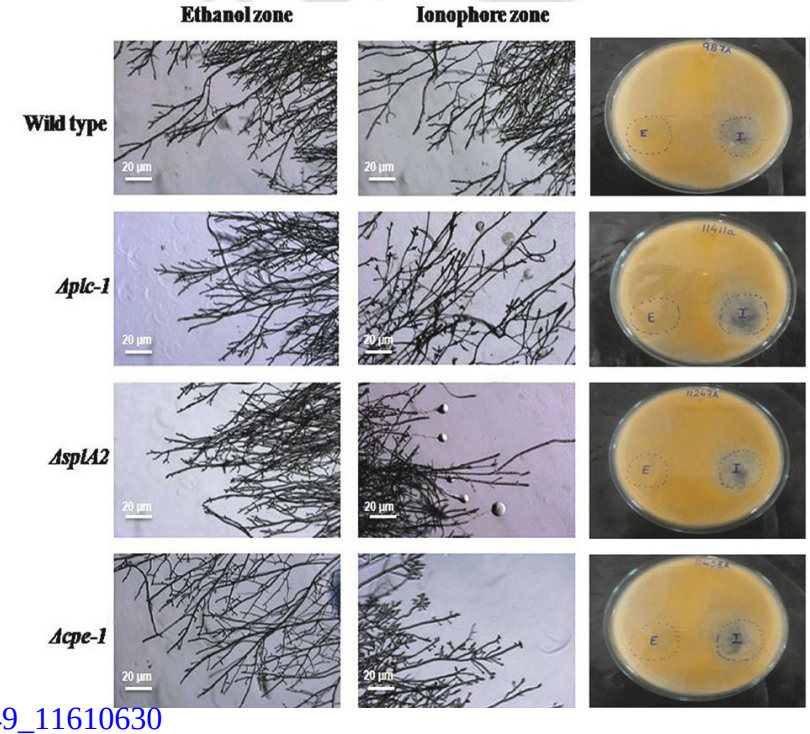

Fig. 2. Calcium ionophore assay. *N. crassa* wild type and the three mutant strains were grown in petri dishes containing the ionophore A23187 zone (test) and the ethanol zone (control). Images were taken when hyphae of the strains touched both the zones (38 h of growth at 30°C). Ten images were captured for each strain and a representative image is shown.

Table 2. Carotenoid content of *N. crassa* strains at three different temperatures.

Strains	Carotenoids (μg/g dry wt.)[a]					
	8°C		22°C		30°C	
	Light	Dark	Light	Dark	Light	Dark
Wild type	151 ± 20.1	21 ± 4.3	66 ± 12	35 ± 4	74 ± 5.4	18 ± 3
Δplc-1	253 ± 3 (***)	34 ± 6.1 (**)	126 ± 11(***)	55 ± 3.1 (**)	144.2 ± 20.2 (**)	49.4 ± 8 (**)
ΔsplA2	255 ± 12.2 (***)	46 ± 6 (*)	169 ± 3.1 (**)	41 ± 5 (*)	177.4 ± 14 (***)	38.1 ± 9 (*)
Δcpe-1	235 ± 6.1 (**)	50 ± 11.2 (*)	175 ± 17.2 (***)	48 ± 4 (*)	160.1 ± 10 (***)	47 ± 2 (***)

[a] Results are shown as mean ± standard deviation for three independent experiments (n=3) with *P-values* < 0.05 (*), < 0.01 (**), and < 0.001 (***) compared with the wild type strain as measured by one-way ANOVA test.

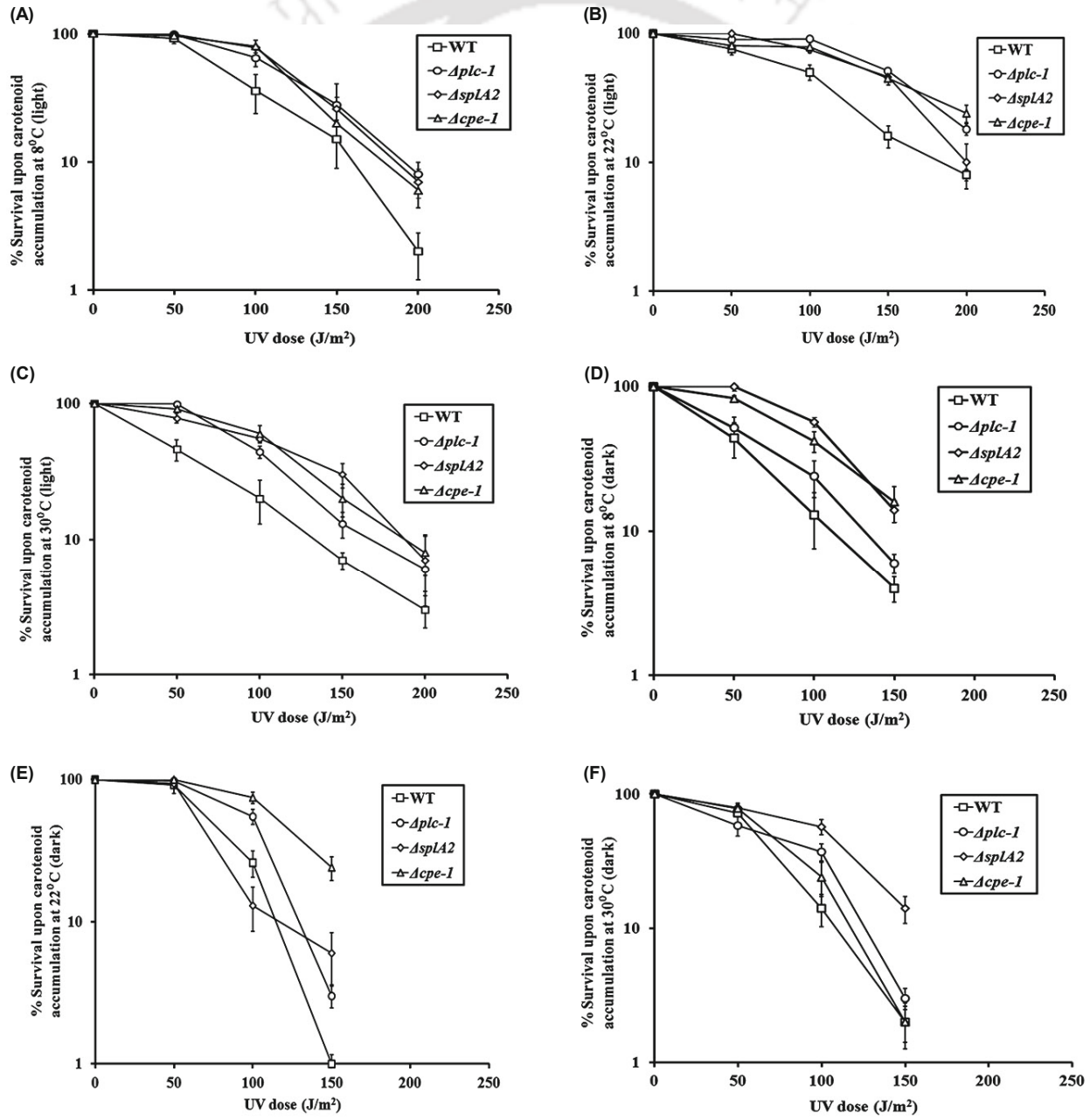

Fig. 3. Assay for UV sensitivity relative to carotenoid accumulation. Dose-response curves of the wild-type and mutant strains after exposure to UV radiation after carotenoid accumulation for 48 h in the dark at 8°C, 22°C or 30°C followed by 24 h either in light illumination (A), (B), and (C) or in continuous darkness (D), (E), and (F). Error bars indicate standard deviations calculated from the data for three independent experiments.

treated with 5 μM A23187, followed by DiBAC incubation showed no fluorescence, suggesting that the effect of A23187 on the germlings of *Δplc-1*, *ΔsplA2*, and *Δcpe-1* mutants was not due to dissipation of membrane potential (Supplementary data Fig. S3).

Assessment of conidiation, carotenoid accumulation, and survival after exposure to UV light in *Δplc-1*, *ΔsplA2*, and *Δcpe-1*

Conidia amounts in the *Δplc-1*, *ΔsplA2*, and *Δcpe-1* mutants were similar to the wild-type, suggesting that these mutations do not affect asexual sporulation in *N. crassa* (Supplementary data Fig. S4). We also measured carotenoid amounts in the three mutants. The characteristic orange pigmentation of *N. crassa* strains is caused by the accumulation of the xanthophyll neurosporoxanthin and variable amounts of carotenoid precursors (Zalokar, 1954; Avalos *et al*., 2013). Carotenoid biosynthesis is affected by light and temperature, with neurosporoxanthin biosynthesis greatly enhanced upon illumination at low temperature whereas illumination at normal temperature results in the accumulation of carotenoid precursors (Harding *et al*., 1969; Harding, 1974; Estrada *et al*., 2008; Díaz-Sánchez *et al*., 2011). Based on this, we determined carotenoid contents in light and dark at three different temperatures, 8°C, 22°C, and 30°C in the three mutants. Our results demonstrated that the three mutants had higher carotenoid content than wild type at all three temperatures, and this was statistically significant (ANOVA, $P < 0.05$) (Table 2).

It has been reported in the literature that the antioxidant activity of carotenoids against reactive oxygen species provides protection against UV damage in fungi and humans (Luque *et al*., 2012). Therefore, we tested whether the increased carotenoid accumulation in the *Δplc-1*, *ΔsplA2*, and *Δcpe-1* mutants was linked to protection against harmful UV radiation. To test this, *N. crassa* strains were grown under conditions similar to those used for the carotenoid analysis. We found that conidia from these mutants produced at 8°C, 22°C, or 30°C in light or dark, showed increased survival relative to wild type after UV irradiation (Fig. 3). Extrapolating from our analysis of carotenoids profile, the increased UV survival of these mutants at 8°C, 22°C, and 30°C in light illumination could be due to higher carotenoid accumulation. In contrast, the UV-dose response curves of *Δplc-1*, *ΔsplA2*, and *Δcpe-1* mutants were similar to wild type under conditions that did not induce carotenoid accumulation (i.e. incubation at 30°C for 48 h followed by illumination under light at room temperature for 96 h; data not shown). These results support the notion that the increase in carotenoid content in the *N. crassa* mutants of *plc-1*, *splA2*, and *cpe-1* is contributing to their increased UV survival.

Effects of the *Δplc-1*, *ΔsplA2*, and *Δcpe-1* mutations on survival under oxidative stress and acquisition of thermotolerance

We tested the viability of the Δ*plc-1*, *ΔsplA2*, and Δ*cpe-1* mutants upon exposure to10 mM hydrogen peroxide-induced oxidative stress and found that all had reduced survival percentage compared to the wild type that was statistically significant (ANOVA, $P < 0.05$) (Fig. 4A). The resistance to hydrogen peroxide-induced oxidative stress tolerance followed the trend wild type>*Δcpe-1*>*ΔsplA2*>*Δplc-1*. These results are supported by results in *A. oryzae* for splA2 homologs demonstrating that *ΔsplaB* displays increased sensitivity to peroxide and *splaA* is strongly upregulated by oxidative stress (Nakahama *et al*., 2010).

We also investigated roles for *plc-1*, *splA2* and *cpe-1* in thermotolerance-to a lethal temperature. Previous work has shown that incubation of cells at a sublethal (heat shock) temperature leads to increased survival after subsequent exposure to a lethal temperature and this phenomenon has been called induced thermotolerance (Kapoor *et al*., 1990). *N. crassa* cells when incubated at sub lethal heat shock temperatures leads to synthesis of heat shock proteins which in turn protects the cells from lethal temperature (Kapoor *et al*., 1995; Yang and Borkovich, 1999). In contrast, uninduced thermotolerance refers to survival of cells after exposure to a lethal temperature, without preincubation at a heat shock tempera-

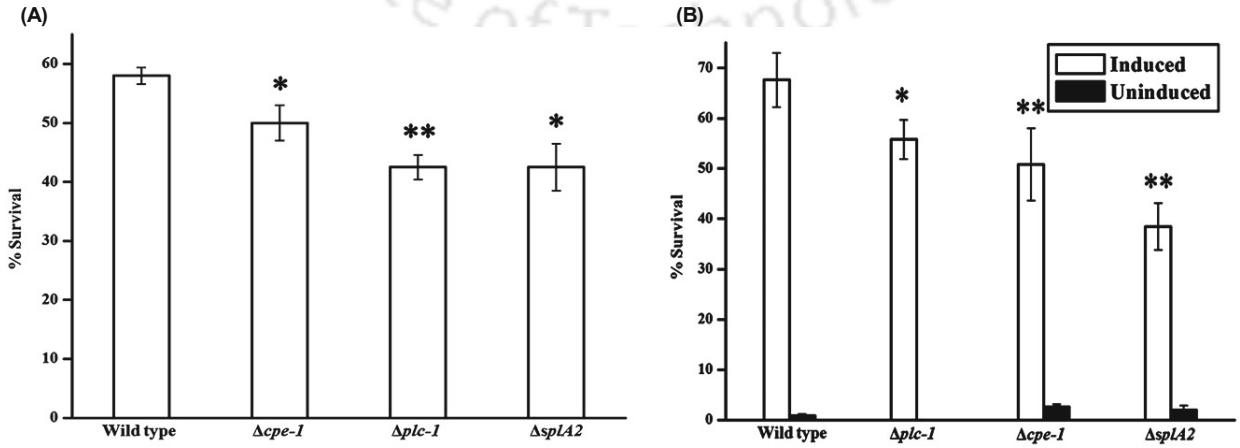

Fig. 4. Oxidative stress and thermotolerance assay. (A) Germlings (2 h old) were incubated in medium containing 10 mM H_2O_2 at 30°C and percent survival determined. (B) Viability of 2 h old germlings after exposure to 52°C lethal temperature with (induced) or without (uninduced) pre-exposure to a sublethal heat shock temperature of 44°C. Error is calculated as the standard deviations, using data from three independent experiments (n=3). Statistically significant values are indicated by asterisks, $^{*}P < 0.05$; $^{**}P < 0.01$.

ture. The *Δplc-1*, *ΔsplA2*, and *Δcpe-1* mutants had decreased survival relative to wild type under induced thermotolerance. In contrast survival was slightly greater than wild type for the *ΔsplA2* and *Δcpe-1* mutants under uninduced thermotolerance conditions (Fig. 4B). In addition, statistical significance was achieved for the thermotolerance assay, according to variance analysis (ANOVA, $P < 0.05$). Interestingly, no viable colony was observed in the *Δplc-1* mutant under uninduced thermotolerance conditions. These results suggested that *plc-1*, *splA2*, and *cpe-1* may play a role in survival at lethal temperatures mediated by prior expression of heat shock proteins. Of interest, *splaB* in *A. oryzae* is weakly upregulated by heat shock (Nakahama *et al.*, 2010).

Conclusion

The *N. crassa* strains lacking *plc-1*, *splA2*, and *cpe-1* displayed growth defects in response to increases in $[Ca^{2+}]_c$ induced by the Ca^{2+}ionophore A23187. Moreover, the carotenoid profile in the *plc-1*, *splA2*, and *cpe-1* mutants was altered and the increased carotenoid amount was linked to UV-survival of the strains. Furthermore, *plc-1*, *splA2*, and *cpe-1* mutants had decreased survival after exposure to hydrogen peroxide-induced oxidative stress and in induced thermotolerance experiments. These phenotypes may result from a disruption in calcium homeostasis in the mutants, suggesting that calcium signaling regulates numerous cellular pathways in *N. crassa*.

Acknowledgements

AB was supported by a Research Fellowship from the Ministry of Human Resource Development, Government of India. We thank Prof. Katherine A. Borkovich (University of California Riverside) for critical reading and valuable suggestions during the preparation of this manuscript. This work was supported partially by a grant (BT/PR3635/BCE/8/892/2012) to RT from the Department of Biotechnology, Government of India. The Fungal Genetic Stock Center (FGSC) generously waived charges for strains and race tubes. The FGSC was supported by NSF grant BIR-9222772.

References

Alcántara-Sánchez, F., Reynaga-Peña, C.G., Salcedo-Hernández, R., and Ruiz-Herrera, J. 2004. Possible role of ionic gradients in the apical growth of *Neurospora crassa*. *Antonie van Leeuwenhoek* **86**, 301–311.

Altschul, S.F., Gish, W., Miller, W., Myers, E.W., and Lipman, D.J. 1990. Basic local alignment search tool. *J. Mol. Biol.* **215**, 403–410.

Avalos, J., Luis, M., and Corrochano, L.M. 2013. Carotenoid Biosynthesis in *Neurospora*, pp. 227–241. *In* Kasbekar, D.P. McCluskey, K. (eds.), Neurospora: genomics and molecular biology. Caister Academic Press, Norfolk, UK.

Balestrieri, B., Maekawa, A., Xing, W., Gelb, M.H., Katz, H.R., and Arm, J.P. 2009. Group V secretory phospholipase A2 modulates phagosome maturation and regulates the innate immune response against *Candida albicans*. *J. Immunol.* **182**, 4891–4898.

Berridge, M.J., Bootman, M.D., and Lipp, P. 1998. Calcium–a life and death signal. *Nature* **395**, 645–648.

Boilard, E., Lai, Y., Larabee, K., Balestrieri, B., Ghomashchi, F., Fujioka, D., Gobezie, R., Coblyn, J.S., Weinblatt, M.E., Massarotti, E.M., *et al.* 2010. A novel anti-inflammatory role for secretory phospholipase A_2 in immune complex-mediated arthritis. *EMBO Mol. Med.* **2**, 172–187.

Bootman, M.D., Collins, T.J., Peppiatt, C.M., Prothero, L.S., MacKenzie, L., De Smet, P., Travers, M., Tovey, S.C., Seo, J.T., Berridge, M.J., *et al.* 2001. Calcium signalling–an overview. *Semin. Cell Dev. Biol.* **12**, 3–10.

Borkovich, K.A., Alex, L.A., Yarden, O., Freitag, M., Turner, G.E., Read, N.D., Seiler, S., Bell-Pedersen, D., Paietta, J., Plesofsky, N., *et al.* 2004. Lessons from the genome sequence of *Neurospora crassa*: tracing the path from genomic blueprint to multicellular organism. *Microbiol. Mol. Biol. Rev.* **68**, 1–108.

Bowman, B.J., Abreu, S., Margolles-Clark, E., Draskovic, M., and Bowman, E.J. 2011. Role of four calcium transport proteins, encoded by *nca-1*, *nca-2*, *nca-3*, and *cax*, in maintaining intracellular calcium levels in *Neurospora crassa*. *Eukaryot. Cell* **10**, 654–661.

Cavazzini, D., Meschi, F., Corsini, R., Bolchi, A., Rossi, G.L., Einsle, O., and Ottonello, S. 2013. Autoproteolytic activation of a symbiosis-regulated truffle phospholipase A_2. *J. Biol. Chem.* **288**, 1533–1547.

Chae, S.W., Kim, J.M., Yun, Y.P., Lee, W.K., Kim, J.S., Kim, Y.H., Lee, K.S., Ko, Y.J., Lee, K.H., and **Rha, H.K.** 2007. Identification and analysis of the promoter region of the human PLC-δ4 gene. *Mol. Biol. Rep.* **34**, 69–77.

Chin, D. and Means, A R. 2000. Calmodulin: a prototypical calcium sensor. *Trends Cell Biol.* **10**, 322–328.

Choi, J., Kim, K.S., Rho, H.S., and Lee, Y.H. 2011.Differential roles of the phospholipase C genes in fungal development and pathogenicity of *Magnaporthe oryzae*. *Fungal Genet. Biol.* **48**, 445–455.

Chung, H.J., Kim, M.J., Lim, J.Y., Park, S.M., Cha, B.J., Kim, Y.H., Yang, M.S., and **Kim, D.H.** 2006. A gene encoding phosphatidyl inositol-specific phospholipase C from *Cryphonectria parasitica* modulates the *lac*1 expression. *Fungal Genet. Biol.* **43**, 326–336.

Clapham, D.E. 2007. Calcium signaling. *Cell* **131**, 1047–1058.

Cornelius, G. and Nakashima, H. 1987. Vacuoles play a decisive role in calcium homeostasis in *Neurospora crassa*. *J. Gen. Microbiol.* **133**, 2341–2347.

Davis, R.H. and De Serres, F.J. 1970. Genetic and microbial research techniques for *Neurospora crassa*. *Methods Enzymol.* **17**, 79–143.

Deka, R., Kumar, R., and Tamuli, R. 2011. *Neurospora crassa* homologue of Neuronal Calcium Sensor-1 has a role in growth, calcium stress tolerance, and ultraviolet survival. *Genetica* **139**, 885–894.

Deka. R. and Tamuli, R. 2013. *Neurospora crassa ncs-1*, *mid-1* and *nca-2* double-mutant phenotypes suggest diverse interaction among three Ca^{2+}-regulating gene products. *J. Genet.* **92**, 559–563.

Díaz-Sánchez, V., Estrada, A. F., Trautmann, D., Limón, M. C., Al-Babili, S., and Avalos, J. 2011. Analysis of *al-2* mutations in *Neurospora*. *PLoS ONE* **6**, e21948.

Estrada, A.F., Youssar, L., Scherzinger, D., Al-Babili, S., and Avalos, J. 2008. The *ylo-1* gene encodes an aldehyde dehydrogenase responsible for the last reaction in the *Neurospora* carotenoid pathway. *Mol. Microbiol.* **69**, 1207–1220.

Felsenstein, J. 1985. Confidence limits on phylogenies: an approach using the bootstrap. *Evolution* **39**, 783–791.

Flick, J.S. and Thorner, J. 1993. Genetic and biochemical characterization of a phosphatidyl-inositol specific phospholipase C in *Saccharomyces cerevisiae*. *Mol. Cell Biol.* **13**, 5861–5876.

Galagan, J.E., Calvo, S.E., Borkovich, K.A., Selker, E.U., Read, N.D.,

Jaffe, D., FitzHugh, W., Ma, L.J., Smirnov, S., Purcell, S., *et al*. 2003. The genome sequence of the filamentous fungus *Neurospora crassa*. *Nature* **422**, 859–868.

Gavric, O., Becker dos Santos, D., and Griffiths, A. 2007. Mutation and divergence of the phospholipase C gene in *Neurospora crassa*. *Fungal Genet. Biol.* **44**, 242–249.

Guttery, D.S., Pittman, J.K., Freñal, K., Poulin, B., McFarlane, L.R., Slavic, K., Wheatley, S.P., Soldati-Favre, D., Krishna, S., Tewari, R., *et al.* 2013. The *Plasmodium berghei* Ca^{2+}/H^{+} exchanger, PbCAX, is essential for tolerance to environmental Ca^{2+} during sexual development. *PLoS Pathog.* **9**, e1003191.

Harding, R.W. 1974. The effect of temperature on photo-induced carotenoid biosynthesis in *Neurospora crassa*. *Plant Physiol.* **54**, 142–147.

Harding, R.W., Huang, P.C., and Mitchell, H.K. 1969. Photochemical studies of the carotenoid biosynthetic pathway in *Neurospora crassa*. *Arch. Biochem. Biophys.* **129**, 696–707.

Kapoor, M., Sreenivasan, G.M., Goel, N., and Lewis, J. 1990. Development of thermotolerance in *Neurospora crassa* by heat shock and other stresses eliciting peroxidase induction. *J. Bacteriol.* **172**, 2798–2801.

Kapoor, M., Curle, C.A., and Runham, C. 1995. The *hsp70* gene family of *Neurospora crassa*: cloning, sequence analysis, expression, and genetic mapping of the major stress-inducible member. *J. Bacteriol.* **177**, 212–221.

Kazmierczak, J., Kempe, S., and Kremer, B. 2013. Calcium in the early evolution of living systems: a biohistorical approach. *Curr. Org. Chem.***17**, 1738–1750.

Köhler, G.A., Brenot, A., Haas-Stapleton, E., Agabian, N., Deva, R., and Nigam, S. 2006. Phospholipase A2 and phospholipase B activities in fungi. *Biochim. Biophys. Acta.***1761**, 1391–1399.

Kumar, R. and Tamuli, R. 2014.Calcium/calmodulin-dependent kinases are involved in growth, thermotolerance, oxidative stress survival, and fertility in *Neurospora crassa*. *Arch. Microbiol.* **196**, 295–305.

Lev, S., Desmarini, D., Li, C., Chayakulkeeree, M.,Traven, A., Sorrell, T.C., and Djordjevic, J.T. 2013. Phospholiase C of *Crytococcus neoformans* regulates homeostasis and virulence by providing inositol trisphosphate as a substrate for Arg1 Kinase. *Infect. Immun.* **81**, 1245–1255.

Lew, R.R., Abbas, Z., Anderca, M.I., and Free, S.J. 2008. Phenotype of a mechanosensitive channel mutant, *mid-1*, in a filamentous fungus, *Neurospora crassa*. *Eukaryot. Cell* **7**, 647–655.

Luque, E.M., Gutierrez, G., Navarro-Sampedro, L., Olmedo, M., Rodríguez-Romero, J., Ruger-Herreros, C., Tagua, V.G., and Corrochano, L.M. 2012. A relationship between carotenoid accumulation and the distribution of species of the fungus *Neurospora* in Spain. *PLoS ONE* **7**, e33658.

McCluskey, K., Wiest, A., and Plamann, M. 2010. The fungal genetics stock center: a repository for 50 years of fungal genetics research. *J. Biosci.* **35**, 119–126.

Murakami, M. and Kudo, I. 2002. Phospholipase A2. *J. Biochem.* **131**, 285–292.

Nakahama, T., Nakanishi, Y., Viscomi, A.R., Takaya, K., Kitamoto, K., Ottonello, S., and Arioka, M. 2010. Distinct enzymatic and cellular characteristics of two secretory phospholipases A_2 in the filamentous fungus *Aspergillus oryzae*. *Fungal Genet. Biol.* **47**, 318–331.

Nakashima, S., Wakatsuki, S., Yokoyama, T., Arioka, M., and Kitamoto, K. 2003. Identification and characterization of Scp15, a novel protein from *Streptomyces coelicolor* A3(2) with neurite-inducing activity in PC12 cells. *Biosci. Biotechnol. Biochem.* **67**, 77–82

Nelson, G., Kozlova-Zwinderman, O., Collis, A.J., Knight, M.R., Fincham, J.R., Stanger, C.P., Renwick, A., Hessing, J.G., Punt, P.J., Van den Hondel, C.A., *et al.* 2004. Calcium measurement in living filamentous fungi expressing codon-optimized aequorin. *Mol. Microbiol.* **52**, 1437–1450.

Nicholas, K.B. and Nicholas, H.B. 1997. GeneDoc: a tool for editing and annotating multiple sequence alignments. Distributed by the author. http://www.psc.edu/biomed/genedoc.

Rho, H.S., Jeon, J., and Lee, Y.H. 2009. Phospholipase C-mediated calcium signalling is required for fungal development and pathogenicity in *Magnaporthe oryzae*. *Mol. Plant Pathol.***10**, 337–346.

Rodriguez-Amaya, D.B. and Kimura, M. 2004. Harvest plus handbook for carotenoid analysis. *Harvest Plus Technical Monograph 2*. International Food Policy Research Institute (IFPRI) and International Center for Tropical Agriculture (CIAT), Washington, DC, USA.

Rzhetsky, A. and Nei, M. 1992. Statistical properties of the ordinary least-squares, generalized least-squares, and minimum-evolution methods of phylogenetic inference. *J. Mol. Evol.* **35**, 367–375.

Schumacher, J., Viaud, M., Simon, A., and Tudzynski, B. 2008. The G alpha subunit BCG1, the phospholipase C (BcPLC1) and the calcineurin phosphatase co-ordinately regulate gene expression in the grey mould fungus *Botrytis cinerea*. *Mol. Microbiol.* **67**, 1027–1050.

Soragni, E., Bolchi, A., Balestrini, R., Gambaretto, C., Percudani, R., Bonfante, P., and Ottonello, S. 2001. A nutrient-regulated, dual localization phospholipase A(2) in the symbiotic fungus *Tuber borchii*. *EMBO J.* **20**, 5079–5090.

Tamuli, R., Kumar, R., and Deka, R. 2011. Cellular roles of neuronal calcium sensor-1 and calcium/calmodulin-dependent kinases in fungi. *J. Basic Microbiol.* **51**, 120–128.

Tamuli, R., Kumar, R., Srivastava, D.A., and Deka, R. 2013. Calcium signaling, pp. 35–57. *In* Kasbekar, D.P. and McCluskey, K. (eds.), Neurospora: genomics and molecular biology. Caister Academic Press, Norfolk, UK.

Tamura, K., Peterson, D., Peterson, N., Stecher, G., Nei, M., and Kumar, S. 2011. MEGA5: molecular evolutionary genetics analysis using maximum likelihood, evolutionary distance, and maximum parsimony methods. *Mol. Biol. Evol.* **28**, 2731–2739.

Thompson, J.D., Gibson, T.J., Plewniak, F., Jeanmougin, F., and Higgins, D.G. 1997. The CLUSTAL_X windows interface: flexible strategies for multiple sequence alignment aided by quality analysis tools. *Nucleic Acids Res.* **25**, 4876–4882.

Tsai, H.C. and Chung, K.R. 2014. Calcineurin phosphatase and phospholipase C are required for developmental and pathological functions in the citrus fungal pathogen *Alternaria alternata*. *Microbiology* **160**, 1453–1465.

VogeL, H.J. 1964. Distribution of lysine pathways among fungi: evolutionary implications. *Am. Naturalist* **98**, 435–446.

Wakatsuki, S., Arioka, M., Dohmae, N., Takio, K., Yamasaki, M., and Kitamoto, K. 1999. Characterization of a novel fungal protein, p15, which induces neuronal differentiation of PC12 cells. *J Biochem.* **126**, 1151–1160. Erratum in: *J Biochem.* **127**, 939.

Wakatsuki, S., Yokoyama, T., Nakashima, S., Nishimura, A., Arioka, M., and Kitamoto, K. 2001. Molecular cloning, functional expression and characterization of p15, a novel fungal protein with potent neurite-inducing activity in PC12 cells. *Biochim. Biophys. Acta* **1522**, 74–81.

Yang, Q. and Borkovich, K.A. 1999. Mutational activation of a Gαi causes uncontrolled proliferation of aerial hyphae and increased sensitivity to heat and oxidative stress in *Neurospora crassa*. *Genetics* **151**, 107–117.

Zalokar, M. 1954. Studies on biosynthesis of carotenoids in *Neurospora crassa*. *Arch. Biochem. Biophys.* **50**, 71–80.

Zelter, A., Bencina, M., Bowman, B.J., Yarden, O., and Read, N.D. 2004. A comparative genomic analysis of the calcium signaling machinery in *Neurospora crassa*, *Magnaporthe grisea*, and *Saccharomyces cerevisiae*. *Fungal Genet. Biol.* **41**, 827–841.

Curr Genet
DOI 10.1007/s00294-017-0682-y

ORIGINAL ARTICLE

The pleiotropic vegetative and sexual development phenotypes of *Neurospora crassa* arise from double mutants of the calcium signaling genes *plc-1, splA2*, and *cpe-1*

Ananya Barman[1] · **Ranjan Tamuli**[1]

Received: 23 September 2016 / Revised: 30 January 2017 / Accepted: 7 February 2017

Abstract We investigated phenotypes of the double mutants of the calcium (Ca^{2+}) signaling genes *plc-1, splA2*, and *cpe-1* encoding for a phospholipase C1 (PLC-1), a secretory phospholipase A_2 ($sPLA_2$), and a Ca^{2+}/H^+ exchanger (CPE-1), respectively, to understand the cell functions regulated by their genetic interactions. Mutants lacking *plc-1* and either *splA2* or *cpe-1* exhibited numerous defects including reduced colonial growth, stunted aerial hyphae, premature conidiation on plates with delayed germination, inappropriate conidiation in submerged culture, and lesser mycelial pigmentation. Moreover, the Δ*plc-1;* Δ*splA2* and Δ*plc-1;* Δ*cpe-1* double mutants were female-sterile when crossed with wild type as the male parent. In addition, Δ*plc-1,* Δ*splA2*, and Δ*cpe-1* single mutants displayed higher carotenoid accumulation and an increased level of intracellular reactive oxygen species (ROS). Therefore, the pleiotropic phenotype of the double mutants of *plc-1, splA2*, and *cpe-1* suggested that the genetic interaction of these genes plays a critical role for normal vegetative and sexual development in *N. crassa*.

Keywords Ca^{2+} signaling · Ca^{2+}/H^+ exchanger · Carotenoid · Fertility · Genetic interaction · *Neurospora crassa* · Pheromone response elements · Phospholipase C1 · Secretory phospholipase A_2

Introduction

Calcium (Ca^{2+}) is a universal signaling molecule and Ca^{2+}-mediated signaling occurs in response to various stimuli causing a transient increase in cytosolic free Ca^{2+} concentration ($[Ca^{2+}]_c$) in eukaryotes (Berridge et al. 1998; Bootman et al. 2001; Dodd et al. 2010). The resting $[Ca^{2+}]_c$ is ~100 nm that is maintained by active Ca^{2+}-pumps and Ca^{2+}-transporters, and the Ca^{2+}-buffering capacity of the cytoplasm. However, $[Ca^{2+}]_c$ rises transiently upto 1 µM or more in response to either entry of extracellular Ca^{2+} or its release from intracellular stores, and the increase in $[Ca^{2+}]_c$ is detected by specific Ca^{2+}-sensing proteins (Chin and Means 2000; Bootman et al. 2001). The target Ca^{2+}-sensing protein undergoes a change in conformation and charge upon Ca^{2+}-binding and mediates numerous signaling events (Clapham 2007). Ca^{2+} signaling pathway plays an important role in perceiving extracellular environmental changes to thrive in diverse environments in organisms including the filamentous fungus *Neurospora crassa* (Galagan et al. 2003; Borkovich et al. 2004). In *N. crassa*, Ca^{2+} signaling pathway is a major component of the intracellular signaling network (Galagan et al. 2003). The Ca^{2+} signaling machinery of *N. crassa* is complex and effectively interacts in coordination for triggering a range of cellular responses (Borkovich et al. 2004; Barman and Tamuli 2015). In *N. crassa*, Ca^{2+} signaling proteins are involved in the regulation of numerous physiological processes such as Ca^{2+} stress tolerance (Deka et al. 2011; Laxmi and Tamuli

Communicated by M. Kupiec.

Electronic supplementary material The online version of this article (doi:10.1007/s00294-017-0682-y) contains supplementary material, which is available to authorized users.

✉ Ranjan Tamuli
ranjantamuli@iitg.ernet.in; ranjan.tam@gmail.com

[1] Department of Biosciences and Bioengineering, Indian Institute of Technology Guwahati, Guwahati, Assam 781 039, India

Published online: 06 March 2017

2015; Gohain et al. 2016), circadian clock (Deka and Tamuli 2013), cytoskeletal organization (Gadd 1994), growth (Deka et al. 2011; Gohain et al. 2016), hyphal branching (Barman and Tamuli 2015), infection structure differentiation (Shaw and Hoch 2000), secretion (Shaw and Hoch 2000), sexual development (Tamuli et al. 2011, 2016; Kumar and Tamuli 2014), sporulation (Barman and Tamuli 2015), and ultraviolet (UV) survival (Deka et al. 2011; Gohain et al. 2016; Laxmi and Tamuli 2016). In *N. crassa*, three important classes of Ca^{2+} signaling proteins that are involved in sensing changes in $[Ca^{2+}]_c$ are phospholipase C(PLC), Ca^{2+} and/or CaM binding secretory phospholipase A_2 ($sPLA_2$), and Ca^{2+} exchangers (Galagan et al. 2003; Borkovich et al. 2004).

The PLC and $sPLA_2$ belong to the phospholipase superfamily of proteins. PLC catalyses the hydrolysis of the phospholipid, phosphatidylinositol 4,5-bisphosphate (PIP_2) to inositol 1,4,5-trisphosphate (IP_3) and diacylglycerol (DAG) inducing Ca^{2+} release from intracellular Ca^{2+} stores and activation of protein kinase C (PKC), respectively, triggering a range of cellular activities (Rhee and Bae 1997). Eukaryotic PLCs consist of an N-terminal pleckstrin homology (PH) domain for interaction with the membrane surface by binding to specific phospholipids, an EF-hand domain for Ca^{2+} binding, a catalytic core formed by the X and Y domains, and a C-terminal C2 domain that facilitates Ca^{2+}-dependent binding of the proteins to phospholipids (Rhee and Bae 1997; Williams and Katan 1996; Yamamoto et al. 1999; Rhee 2001). The mammalian PLC isozymes have been grouped into four types β, γ, δ, and ε that differ in their size and primary structure (Williams and Katan 1996; Rhee 2001). *N. crassa* possesses four novel PLC-δ subtype proteins including the PLC-1 that lacks the PH domain but consists of catalytic X and Y domains, and a C2-like domain (Borkovich et al. 2004; Gavric et al. 2007; Barman and Tamuli 2015). The PLC proteins play an important role in regulating various cell functions in different organisms including yeast, filamentous fungi, and mammals.

In addition, the $sPLA_2$ are a group of relatively low molecular weight (13–19 kDa), Ca^{2+} dependent extracellular secretory enzymes that hydrolyze the *sn-2* ester linkage of glycerophospholipids releasing two potential signaling molecules free fatty acids (FFAs) and 1-acyl-lysophospholipid (1-acyl-LPL) that are capable of controlling a range of biological functions in various organisms (Ghannoum 2000; Dennis et al. 2011; Cavazzini et al. 2013; Takayanagi et al. 2015). A majority of eukaryotic $sPLA_2$ have a highly conserved region containing a His-Asp dyad sequence responsible for catalytic activity and a number of unique disulfide bonded cysteine residues required for its stability (Murakami and Kudo 2004; Schaloske and Dennis 2006). This family of enzymes plays diverse roles in a wide range of organisms and tissues and are known to regulate a number of biological processes such as atherosclerosis, eicosanoid biosynthesis, host defense, and inflammation (Murakami and Kudo 2004; Boilard et al. 2010; Dennis et al. 2011).

The first $sPLA_2$ described in fungi was a dual localization protein TbSP1 in the symbiotic fungus *Tuber borchii* (Soragni et al. 2001). The TbSP1 was found both secreted extracellularly and surface associated, and up-regulated by either carbon or nitrogen starvation suggesting its role in nutritional limitation in *T. borchii* (Soragni et al. 2001). The *N. crassa* $sPLA_2$ encoded by the NCU06650 gene has an N-terminal signal peptide residue presumably for secretion, a highly conserved region that contains a catalytic histidine residue, two disulphide bonded cysteine residues, and belongs to the group XIV (GXIV) $sPLA_2$ group of enzymes (Barman and Tamuli 2015; Takayanagi et al. 2015). In *N. crassa*, another secreted protein encoded by the NCU09423 was found to possess the PLA_2 activity (Takayanagi et al. 2015). The NCU06650 and NCU09423 genes in *N. crassa* encode for two distinct $sPLA_2$ proteins possessing Ca^{2+}-dependent lipolytic activity with preferential cleavage of *sn-2* ester linkage of substrates to produce 1-acyl lysophospholipids (Takayanagi et al. 2015). The NCU06650 and NCU09423 encoded proteins and two non-redundant distinct $sPLA_2$ enzymes sPlaA and sPlaB from *Aspergillus oryzae* showed high sequence homology including the conservation of four cysteines residues, except for two additional cysteines present in NCU09423 and sPlaA (Nakahama et al. 2010; Takayanagi et al. 2015). In *A. oryzae*, overexpression of the sPlaA and sPlaB showed a defect in conidiation, which was more distinct for the sPlaB overexpression. However, morphology of the *ΔsplaA*, *ΔsplaB*, or their double knockout mutants did not show any distinct phenotypic defect, although, hyphal growth of the *ΔsplaA*, but not the *ΔsplaB*, mutant was sensitive to hydrogen peroxide (H_2O_2)-induced oxidative stress (Nakahama et al. 2010).

Another group of Ca^{2+} signaling molecules are the Ca^{2+} exchangers involved in maintaining low $[Ca^{2+}]_c$ by transporting Ca^{2+} out of the cells and into the intracellular Ca^{2+} stores with the simultaneous exchange of positive ions across membranes (Zelter et al. 2004; Tamuli et al. 2013). *N. crassa* possesses six novel Ca^{2+}/H^+ exchangers and two putative Ca^{2+}/Na^+ exchangers (Galagan et al. 2003; Borkovich et al. 2004; Zelter et al. 2004). The Ca^{2+}/Na^+ exchanger CPE-1 contains nine putative transmembrane domains for Ca^{2+} transport (Tamuli et al. 2013; Barman and Tamuli 2015).

In a previous study, the *plc-1, splA2*, and *cpe-1* genes were shown to be involved in regulation of $[Ca^{2+}]_c$, carotenoid accumulation, survival under stress conditions, and acquisition of thermotolerance in *N. crassa* (Barman and

Tamuli 2015). Here, we generated double mutants of *plc-1, splA2*, and *cpe-1* genes and studied their phenotypes to determine the possible genetic interactions between these loci. The *Δplc-1; ΔsplA2*, and *Δplc-1; Δcpe-1* double mutants severely affect growth, aerial hyphae, conidiation, conidial germination, carotenoid accumulation, and fertility. Therefore, genetic interactions of *plc-1, splA2*, and *cpe-1* play crucial roles in numerous aspects of vegetative growth and sexual development in *N. crassa*.

Materials and methods

Strains, media, growth, maintenance, crosses, and carotenoid analysis

The *N. crassa* wild type strains 74-OR23-1 A (FGSC 987) and OR8-1 a (FGSC 988), and Ca^{2+} signaling mutant strains *ΔNCU06245. 2::hph mat a* (FGSC 11411), *ΔNCU06650.2::hph mat A* (FGSC11247), *ΔNCU06650.2::hph mat a* (FGSC11246), *ΔNCU06366.2::hph mat A* (FGSC 11408), *ΔNCU06366.2::hph mat a* (FGSC 11407) were obtained from the Fungal Genetics Stock Center (FGSC) University of Missouri, Kansas city, MO 64110 (McCluskey et al. 2010). The NCU06245, NCU06650, and NCU06366 corresponds to *N. crassa* homologues of *plc-1, splA2*, and *cpe-1* genes, respectively (Barman and Tamuli 2015). The *Δcpe-1; ΔsplA2, Δplc-1; ΔsplA2*, and *Δplc-1; Δcpe-1* double mutants were generated by crossing the single mutant strains of opposite mating types. A minimum of four double mutants of each kind was isolated and presence of *Δplc-1, ΔsplA2*, and *Δcpe-1* mutant alleles in the f_1 progenies were confirmed using the gene specific primers HI-NCU06245-F, HI-NCU06650-F, HI-NCU06366-F, respectively, along with the common reverse primer 5HPHR (Table 1; Fig. S1).

Media and procedures for growth, maintenance, and routine crosses of *N. crassa* strains were essentially as described previously (Davis and De Serres 1970). For vegetative growth, strains were routinely cultured on Vogel's (Vogel 1964) glucose (VG) containing 1.5% D-glucose as a carbon source with 1.5% Bacto agar (Himedia, India) for solid medium. Scoring for the selection of progeny that contain hygromycin resistance cassette (*hph*) was done on medium containing 0.05% fructose, 0.05% glucose, 2% sorbose, 2% Bacto agar and supplemented with aqueous solution of hygromycin B (220 µg/ml). Carotenoid analysis was performed as previously described (Barman and Tamuli 2015), cultures were incubated initially at 30 °C for 2 days in the dark followed by incubation at temperatures of 8, 22, and 30 °C under light either for 1 day to determine total carotenoid content, or for the indicated time period of 0–12 h to determine carotenoid accumulation in a time course analysis. Total carotenoid content was determined by measuring the maximum absorbance value at 470 nm and using the formula: Total carotenoid content (µg/g dry weight) = [total absorbance × total volume of extract (1 ml) × 10^4]/[absorption coefficient (2500) × sample weight (g)] essentially as described previously (Rodriguez-Amaya and Kimura 2004).

Vegetative growth, aerial hyphae, conidiation, conidial germination, and fertility assay

Colony morphology, linear growth, mycelial mass accumulation, and quantification of conidia were performed with mycelial plug of ~1 cm diameter taken from a 3 days old culture of each strain. For colony morphology, mycelial plug was inoculated at the center of 250 ml flasks and

Table 1 Primers used in this study

Primer	Sequence (5′ → 3′)	Source
HI-NCU06245-F	AGTTGGTCGCCTCCTAGAAC	Barman and Tamuli (2015)
HI-NCU06650-F	GCCGGACGGCAACTGAATAT	Barman and Tamuli (2015)
HI-NCU06366-F	CTG CAA GGA GGC TAA TTC GG	Barman and Tamuli (2015)
5HPHR	ATCCACTTAACGTTACTGAAATC	Deka et al. (2011)
q-con-10-FW	CCAAGGAAGAGGTTCAGGCC	This study
q-con-10-RV	TTGCCGCCCTTGGAAGCAAT	This study
q-ccg-4-FW	CAGCCTCCAAGAGAAGTTCG	This study
q-ccg-4-RV	CACGCTTCTTCCAGCACGAT	This study
q-mfa-1-FW	ATGCCTTCCACCGCTGCTTC	This study
q-mfa-1-RV	CATAACAACGCAGTAGCCGT	This study
q-fmf-1-FW	CGGACAAGACAGCAGTTCCT	This study
q-fmf-1-RV	TTTCGGTGGTTGCTGTTCATC	This study
q-B-tub-FW	CCCAAGAACATGATGGCTGC	This study
q-B-tub-RV	TTGTTCTGAACGTTGCGCATC	This study

90-mm-Petri dishes containing VG agar and incubated for 3 days in the dark at 30 °C followed by 4 days under light at room temperature. Images were captured using a digital camera (Nikon Coolpix P500). Hyphae formed after a 12 h incubation at 30 °C were observed under a Trinocular inverted microscope (AxioVert A1 FL, Carl Zeiss) and hyphal images were captured with a CCD camera (AxioCam ICc3, Carl Zeiss). For linear growth of strains, mycelial plug was inoculated in sterile race tubes containing VG agar medium and growth front was measured after every 12 h till 72 h (Deka et al. 2011; Deka and Tamuli 2013; Kumar and Tamuli 2014). For mass accumulation in solid media, mycelial plug was inoculated at the center of Petri dishes overlaid with a cellophane layer and incubated under the conditions of either 30 °C for 3 days in the dark, or 30 °C for 2 days in the dark followed by illumination at room temperature for 1 day. Following incubation, cellophane was removed and mycelial mass was taken (Yang et al. 2002). For mass accumulation in liquid media, mycelial plug was inoculated in liquid VG medium for 3 days at 30 °C with shaking at 180 rpm, mycelial mat formed were then dried at 60 °C and dry weight was measured. To study aerial hyphae, ~10^6 conidia/ml were inoculated in sterile test tubes containing liquid VG medium and grown in the dark at 30 °C for 3 days and under light at room temperature for 4 days. Height of aerial hyphae was then measured and photographed using a digital camera (Nikon Coolpix P500, Nikon).

For the quantification of conidia production, mycelial plug was inoculated in 250 ml flasks containing VG agar medium and incubated at 30 °C in the dark for 2 days followed by incubation under light at 22 °C for 4 days. Conidia were scraped from the agar surface with sterile distilled water and briefly agitated for thorough resuspension of conidia. Conidial counting was performed using a haemocytometer.

Conidial germination was assayed both qualitatively and quantitatively. For qualitative assay, ~10^6 conidia/ml were inoculated in sterile test tubes containing liquid VG medium and incubated at 25 °C with shaking at 180 rpm. An aliquot of the cultures was observed under the microscope (AxioVert A1 FL, Carl Zeiss) at intervals of 0, 24, 48, and 60 h to determine conidiation efficiency. For quantitative assay, 100 µl from a ~10^4 conidia/ml conidial suspension of each of the strains were inoculated onto the surface of VG and incubated at 25 °C. Germination of conidia was observed under the microscope (AxioVertA1FL, Carl Zeiss) at intervals of 0, 8, 12, 24, 36, 48, and 60 h. Percent germination was calculated as (germinated conidia/total number of conidia) × 100%.

To determine conidiation in submerged cultures, ~10^6 conidia/ml were inoculated in 250 ml flasks containing liquid VG supplemented with or without 2% peptone (w/v) and incubated at 30 °C with shaking at 180 rpm for 16 h. Aliquots of these cultures were observed under the microscope (AxioVert A1 FL, Carl Zeiss) to assay formation of conidiophores (Yang et al. 2002).

To assay fertility, crosses were performed on synthetic crossing media (SCM) to induce the formation of female reproductive structures (protoperithecia) and incubated at room temperature under constant light. Protoperithecia formed after 7–10 days were fertilized using the desired strains of opposite mating type (Ivey et al. 1996; Yang and Borkovich 1999). After 7 days post-fertilization, perithecia formed were examined under the microscope (AxioVert A1 FL, Carl Zeiss) and images captured.

Antioxidative assay

For antioxidative assay, sterile Petri dishes containing liquid VG supplemented with 0.2% tween 80 were inoculated with conidia at a concentration of ~10^6 conidia/ml (Zalokar 1954). Cultures were initially incubated for 48 h in dark at 30 °C followed by treatment with 1 mM of N-acetyl-L-cysteine (NAC; Himedia, India) at 30 °C in dark for additional 2 h. Cultures were then grown under light either at 8, 22, or 30 °C for another 2 h. Mycelia from these cultures were collected, lyophilized, and pulverized into fine powder with mortar and pestle. Carotenoid was subsequently extracted from the powdered mycelia. Similar conditions were followed while using N-acetylglycine (NAG; Himedia, India), an analogue of NAC, with no antioxidant activity as the control (Yoshida and Hasunuma 2004).

RNA extraction and quantitative real time PCR (qRT-PCR) analysis

For submerged cultures, ~10^6 conidia/ml were inoculated in liquid VG medium and incubated at 30 °C with shaking at 180 rpm for 16 h in complete darkness. To study expression of genes regulating fertility, ~10^6 conidia/ml were inoculated in liquid SCM and incubated at 22 °C under constant light for 18–20 h. Mycelia obtained from these cultures were harvested by vacuum filtration and pulverized into fine powder using liquid nitrogen. Total RNA was isolated from 150 mg of powdered mycelia using TRIzol reagent (Invitrogen, USA). cDNA from total cellular RNA was synthesized using a cDNA synthesis kit (Thermo Scientific, USA) according to manufacturer's protocol. Quantitative Real-Time PCR (qRT-PCR) analyses were done using primer pairs q-con-10-FW and q-con-10-RV, q-ccg-4-FW and q-ccg-4-RV, q-mfa-1-FW and q-mfa-1-RV, q-fmf-1-FW and q-fmf-1-RV, q-B-tub-FW and q-B-tub-RV (Table 1), respectively, for the *con-10, ccg-4, mfa-1, fmf-1*, and *β-tubulin* genes, the SYBR® Select Master Mix (Applied Biosystems, USA), and the 7500 Real-Time PCR

System (Applied Biosystems, USA) according to manufacturer's protocol. Relative expression levels of the target genes were calculated using the $2^{-\Delta\Delta C_T}$ method (Livak and Schmittgen 2001). The expression level of β-tubulin was used as the endogenous control.

Statistical analysis

Statistical analysis was carried out by one-way ANOVA (Microsoft Excel) using the data obtained from at least three independent replicates.

Results

The Δ*plc-1;* Δ*splA2* and Δ*plc-1;* Δ*cpe-1* double mutants displayed defects in morphology, growth, biomass accumulation, mycelial aggregation, aerial hyphae, and sporulation

The Δ*plc-1;* Δ*splA2* and Δ*plc-1;* Δ*cpe-1* double mutants showed distinct colonial morphology with significantly fewer aerial hyphae, reduced pigmentation, and growth (Fig. 1a, b). Growth rates of the wild type, Δ*cpe-1;* Δ*splA2,* Δ*plc-1;* Δ*splA2*, and Δ*plc-1;* Δ*cpe-1* double mutant strains were 0.305 ± 0.013, 0.309 ± 0.025, 0.153 ± 0.006, and 0.139 ± 0.018 cm h^{-1}, respectively (Table S1). In addition, the Δ*plc-1;* Δ*splA2* double mutant displayed slightly reduced branching with numerous bud-like structures at the apex of the hyphae, and the Δ*plc-1;* Δ*cpe-1* double mutant displayed severely reduced hyphal branching (Fig. 1c). The Δ*plc-1;* Δ*splA2* and Δ*plc-1;* Δ*cpe-1* double mutants displayed a slow growth rate, which was not due to a defect in ergosterol biosynthesis (Fig. S2), and this phenotype was further supported by a reduction in the accumulation of mycelial mass. We observed a significant reduction of the mycelial mass accumulation in the Δ*plc-1;* Δ*splA2* and Δ*plc-1;* Δ*cpe-1* double mutants in both solid and liquid growth conditions (Table S2). In addition, mycelia of the Δ*plc-1;* Δ*splA2* and Δ*plc-1;* Δ*cpe-1* double mutants displayed dispersed growth, and did not form aggregates in liquid growth conditions unlike their single mutant and wild type strains (data not shown). Moreover, the Δ*plc-1;* Δ*splA2* and Δ*plc-1;* Δ*cpe-1* double mutants produced significantly shorter aerial hyphae and showed a severe reduction in conidiation (Fig. 1d; Tables S3, S4). Another double mutant, the Δ*cpe-1;* Δ*splA2* strain showed growth, hyphal branching, and pigmentation similar to those of the wild type and individual single mutants (Fig. 1; Tables S1–4). Therefore, interactions of *plc-1* with *splA2* and *cpe-1* play an important role for normal vegetative growth and conidiation in *N. crassa*.

Conidial germination was reduced and inappropriate conidiation in submerged cultures was observed in the Δ*plc-1;* Δ*splA2* and Δ*plc-1;* Δ*cpe-1* double mutants

The Δ*plc-1;* Δ*splA2* and Δ*plc-1;* Δ*cpe-1* double mutants produced shorter aerial hyphae (Fig. 1d), therefore, we tested if this phenotype was linked to premature conidiation as reported previously (Barba-Ostria et al. 2011). Approximately, 10^3 conidia of the mutant and the wild type strains were inoculated in VG agar plates and incubated at 30 °C in complete darkness, and conidia produced were counted after every 12 h till 72 h. We found that Δ*plc-1;* Δ*splA2* and Δ*plc-1;* Δ*cpe-1* double mutants produced conidia as early as 12 h, whereas the Δ*cpe-1;* Δ*splA2* double mutant, individual single mutants, and the wild type produced conidia only after 48 h post inoculation (Fig. 2a). Interestingly, ~100% conidia from the Δ*plc-1;* Δ*splA2* and Δ*plc-1;* Δ*cpe-1* double mutants were germinated after 60 h post inoculation, whereas, almost all the conidia from the Δ*cpe-1;* Δ*splA2* double mutant, individual single mutants, and the wild type were germinated as early as 24 h post inoculation (Fig. 2b). Delayed conidial germination in the Δ*plc-1;* Δ*splA2* and Δ*plc-1;* Δ*cpe-1* double mutants were further supported by microscopy study. We observed no germination in the Δ*plc-1;* Δ*splA2* and Δ*plc-1;* Δ*cpe-1* double mutants after 8 and 12 h post inoculation, but abundant germinating conidia with long germ tubes were seen in the single mutant and the wild type strain (Fig. S3). In addition, only ~1–2 germ tubes were seen till 48 h in the Δ*plc-1;* Δ*splA2* and Δ*plc-1;* Δ*cpe-1*double mutants; however, conidia with well-developed germ tubes were seen in other *N. crassa* strains (Fig. S3). Therefore, genetic interactions between *plc-1* and *splA2*, and also *plc-1* and *cpe-1* are important in the production and germination of *N. crassa* conidia under favorable conditions.

We also studied the role of *plc-1, splA2*, and *cpe-1* genes in regulation of conidiation in *N. crassa* submerged culture conditions. Abundant conidiophores were observed in 16-h-submerged cultures of Δ*plc-1;* Δ*splA2* and Δ*plc-1;* Δ*cpe-1* double mutants. In contrast, the Δ*cpe-1;* Δ*splA2* double mutant, individual single mutants, and the wild type strain did not produce conidiophores or conidia and maintained vegetative non-conidiating hyphae in submerged cultures (Fig. 3a). It was previously shown that the addition of rich nutrient peptone suppressed conidiation in submerged cultures for the mutants of the *cr-1* adenylyl cyclase, *gna-1* and *gna-3* Gα subunits, *gnb-1* Gβ subunit, and *rco-3* glucose transporter (Ivey et al. 2002; Kays et al. 2000; Madi et al. 1997; Yang et al. 2002). Interestingly, the addition of 2% peptone resulted in complete suppression of conidiation in the Δ*plc-1;* Δ*splA2*, and Δ*plc-1;* Δ*cpe-1* double mutants and showed hyphal formation (Fig. 3a). To understand

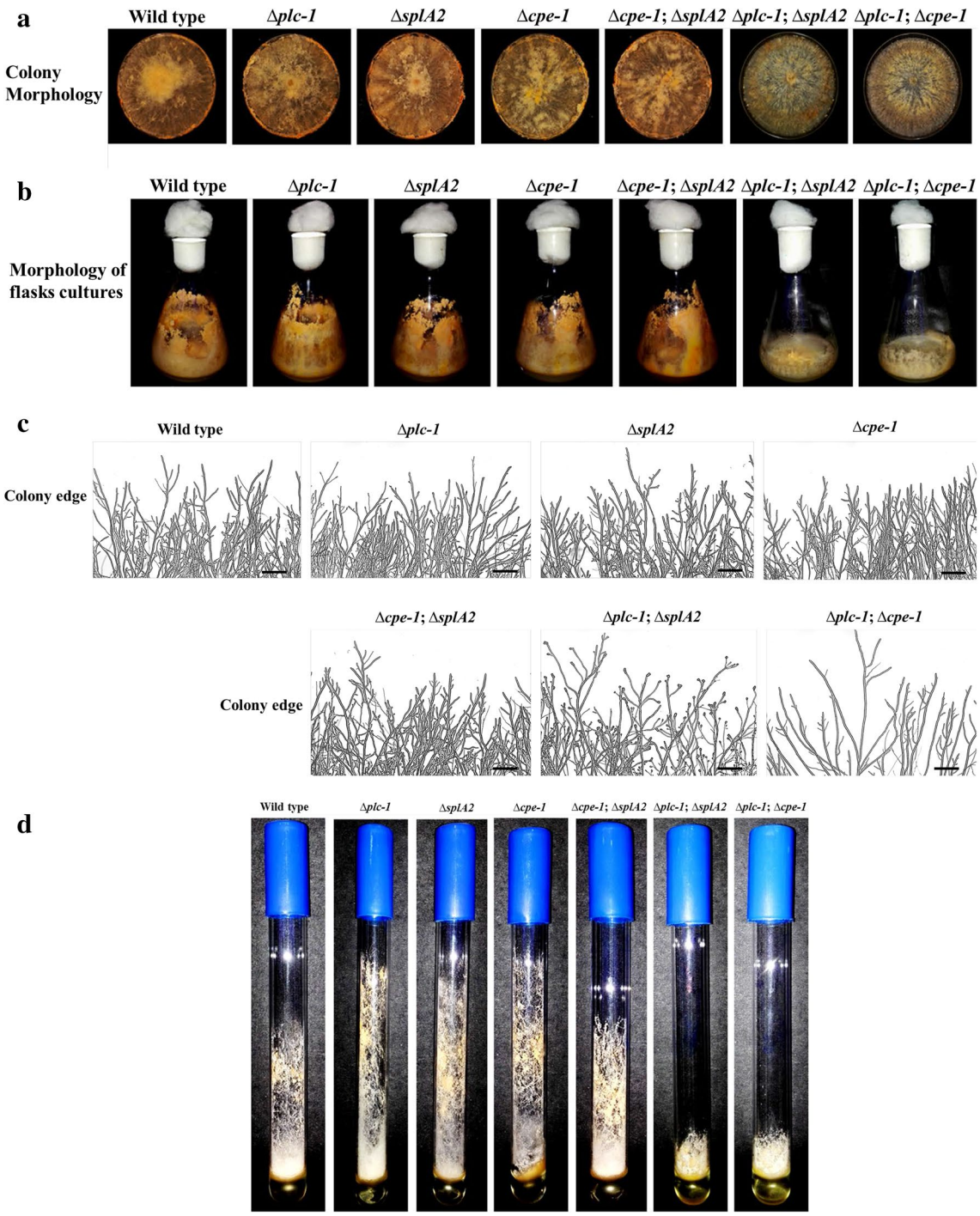

Fig. 1 Morphology and growth of the *N. crassa* strains. **a** Colony morphology of the strains on VG agar medium in Petri dishes. **b** Colony morphology of the strains on VG agar medium in flasks. For colony morphology, the *N. crassa* strains were incubated for 3 days in the dark at 30 °C followed by 4 days under light at room temperature. **c** Hyphal morphology of the strains on VG agar medium after a 12 h incubation at 30 °C was examined under a Trinocular inverted microscope (AxioVert A1 FL, Carl Zeiss). *Scale bar* 20 µm. **d** Aerial hyphae of the strains in VG liquid cultures. Strains were incubated in dark at 30 °C for 3 days and under light at room temperature for 4 days

the molecular players of inappropriate conidiation in submerged cultures of the Δ*plc-1; ΔsplA2* and Δ*plc-1; Δcpe-1* double mutants, we examined the transcription level of the conidiation specific gene, *con-10*, by qRT-PCR. It was shown previously that inappropriate expression of *con-10* correlates with conidiation in submerged cultures (Ivey

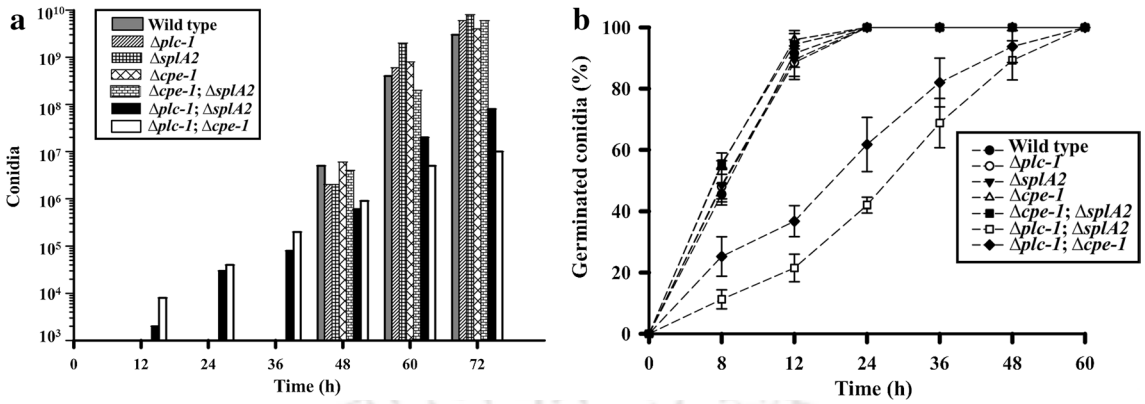

Fig. 2 Time-course analysis of conidia production and germination in the *N. crassa* strains. **a** Conidiation in the strains grown on VG agar plates and incubated at 30 °C in complete darkness. Conidia were harvested and quantified at regular intervals. **b** Germination of conidia. Conidial suspensions of the strains inoculated on VG agar plates and incubated at 25 °C. Germination of conidia was observed under the microscope at regular interval of indicated times and percent germination was determined. *Error bars* indicate standard deviations calculated from the data for three independent experiments

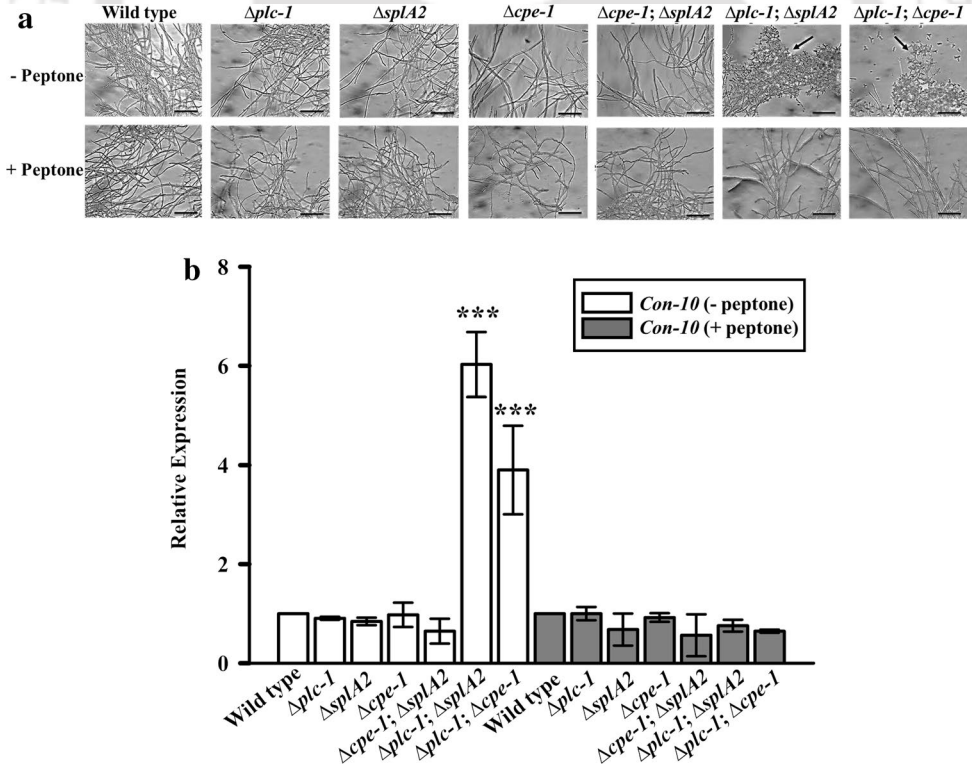

Fig. 3 Conidiophore formation and expression of the conidiation specific *con-10* gene in submerged cultures. **a** Conidiation in submerged culture conditions. The *N. crassa* strains were inoculated in VG liquid medium at a concentration of ~10^6 conidia/ml and supplemented with or without 2% (w/v) peptone, and incubated in dark at 30 °C with shaking at 180 rpm for 16 h, and conidiophore development was observed under the microscope. *Black arrows* indicate conidiophores. *Scale bar* 20 μm. **b** Expression of the *con-10* gene. RNA was extracted from submerged cultures and conidiation specific *con-10* gene expression was studied by qRT-PCR on three biological replicates of each strain. The relative expression of the *con-10* gene was normalized with the β-tubulin gene and expression values were compared with that of wild type. *Error bars* indicate standard deviations calculated from the data for three independent experiments ($n = 3$) with *P*-values <0.05 (*asterisk*), <0.01 (*double asterisk*), and <0.001 (*triple asterisk*) compared with the wild type strain as measured by one-way ANOVA test

et al. 2002; Kays et al. 2000; Madi et al. 1997; Yang et al. 2002). We found expression of *con-10* in Δ*plc-1;* Δ*splA2* and Δ*plc-1;* Δ*cpe-1* double mutants cultured for 16 h under submerged condition were increased by ~seven and four fold, respectively (Fig. 3b). Interestingly, expression of *con-10* in the Δ*plc-1;* Δ*splA2* and Δ*plc-1;* Δ*cpe-1* double mutants was like the wild type on addition of 2% peptone in the submerged cultures (Fig. 3b). Therefore, inappropriate expression of the *con-10* was correlated with the inappropriate conidiation of the Δ*plc-1;* Δ*splA2* and Δ*plc-1;* Δ*cpe-1* double mutants.

The *Δplc-1*, *ΔsplA2*, and *Δcpe-1* mutations affected carotenoid accumulation and production of intracellular reactive oxygen species

Conidial suspensions of the Δ*plc-1;* Δ*splA2* and Δ*plc-1;* Δ*cpe-1* double mutants appeared light yellow in color as compared to dark orange color observed for the individual single mutants and the wild type, indicating reduced carotenoid accumulation in these two strains (data not shown). We, therefore, determined total carotenoid content in the wild type, *Δplc-1, ΔsplA2*, and *Δcpe-1* single as well as Δ*cpe-1;* Δ*splA2,* Δ*plc-1;* Δ*splA2*, and Δ*plc-1;* Δ*cpe-1* double mutant strains in both light and dark conditions at three different temperatures of 8, 22, and 30 °C (Table 2). The *Δplc-1, ΔsplA2, Δcpe-1*, and Δ*cpe-1;* Δ*splA2* strains showed higher carotenoid accumulation than the wild type at 8, 22, and 30 °C (Table 2). In contrast, Δ*plc-1;* Δ*splA2*, and Δ*plc-1;* Δ*cpe-1* double mutant showed significantly lower carotenoid accumulation at all three temperatures (Table 2). We performed a time course analysis of carotenoid accumulation in the wild type, single, and double mutants of *Δplc-1, ΔsplA2*, and *Δcpe-1* at 8, 22, and 30 °C under the exposure to white light for 0–12 h. In the *Δplc-1, ΔsplA2, Δcpe-1*, and Δ*cpe-1;* Δ*splA2* mutants, carotenoid accumulation at different time points were higher than the wild type strain; however, the Δ*plc-1;* Δ*splA2*, and Δ*plc-1;* Δ*cpe-1* double mutants showed a slower carotenoid accumulation than the wild type and individual single mutants at different time points (Fig. 4). In addition, the *Δplc-1,* Δ*splA2*, and *Δcpe-1* mutants consistently showed higher carotenoid accumulation at the 0 h time point, indicating higher carotenoid accumulation in these mutants in the dark.

We also tested generation of intracellular reactive oxygen species (ROS) in *Δplc-1, ΔsplA2*, and *Δcpe-1* strains using the antioxidant N-acetyl-L-cysteine (NAC) that reduces high intracellular ROS levels, and N-acetylglycine (NAG) that is an analog of NAC but without any antioxidative activity as a control. We found that treatment with 1 mM of NAC followed by white light illumination for 2 h had resulted in lower carotenoid accumulation in the *Δplc-1, ΔsplA2, Δcpe-1*, and Δ*cpe-1;* Δ*splA2* mutant strains at all three temperatures (Fig. 5). However, carotenoid accumulation in the wild type, Δ*plc-1;* Δ*splA2*, and Δ*plc-1;* Δ*cpe-1* double mutants were similar in both NAC and NAG treatment (Fig. 5). Therefore, these findings suggest that loss of *plc-1, splA2*, and *cpe-1* genes causes an overall increase in intracellular ROS generation.

The Δ*plc-1;* Δ*splA2* and Δ*plc-1;* Δ*cpe-1* double mutants were female sterile

We also evaluated the role of *plc-1, splA2*, and *cpe-1* genes in sexual development of *N. crassa*. We found that crosses involving the Δ*plc-1,* Δ*splA2*, and Δ*cpe-1* single mutants were fully fertile either as a male or a female parent with the wild type strains of opposite mating type (Fig. S4; Table S5). In contrast, crosses involving the Δ*plc-1;* Δ*splA2* and Δ*plc-1;* Δ*cpe-1* double mutants as the female parent with the respective double or parental single mutants and wild type strains of opposite mating type as the male parent showed complete absence of perithecia and resulted in

Table 2 Carotenoid content of the *N. crassa* strains at three different temperatures

Strains	Carotenoids (μg/g dry weight)[a]					
	8 °C		22 °C		30 °C	
	Light	Dark	Light	Dark	Light	Dark
Wild type	140 ± 13	40 ± 4	90 ± 4	34 ± 2	74 ± 5.4	18 ± 1
Δ*plc-1*	252 ± 8.2 (***)	58 ± 7	188 ± 11(**)	38 ± 3 (**)	152 ± 7.1 (*)	30 ± 2 (*)
Δ*splA2*	232 ± 11 (**)	69 ± 7 (*)	163 ± 5.4 (**)	52 ± 6 (*)	157 ± 8 (**)	29 ± 1 (*)
Δ*cpe-1*	240 ± 5.4 (**)	72 ± 12 (*)	177 ± 4.4 (**)	45 ± 4 (*)	178 ± 11.4 (***)	28 ± 3 (***)
Δ*cpe-1*; Δ*splA2*	250 ± 13 (**)	56 ± 7	149 ± 9.2 (*)	41.3 ± 3.1	160 ± 13 (**)	30 ± 4
Δ*plc-1*; Δ*splA2*	81 ± 13 (*)	31 ± 5	31 ± 3.2 (**)	21 ± 5 (*)	30 ± 6 (*)	16 ± 4
Δ*plc-1*; Δ*cpe-1*	67 ± 16.2 (*)	30 ± 3 (*)	36 ± 2.2 (**)	25 ± 5	40 ± 6.2	14 ± 3

[a]Results are shown as mean ± standard deviation for three independent experiments ($n = 3$) with P values <0.05 (*), <0.01 (**), and <0.001 (***) compared with the wild type strain as measured by one-way ANOVA test

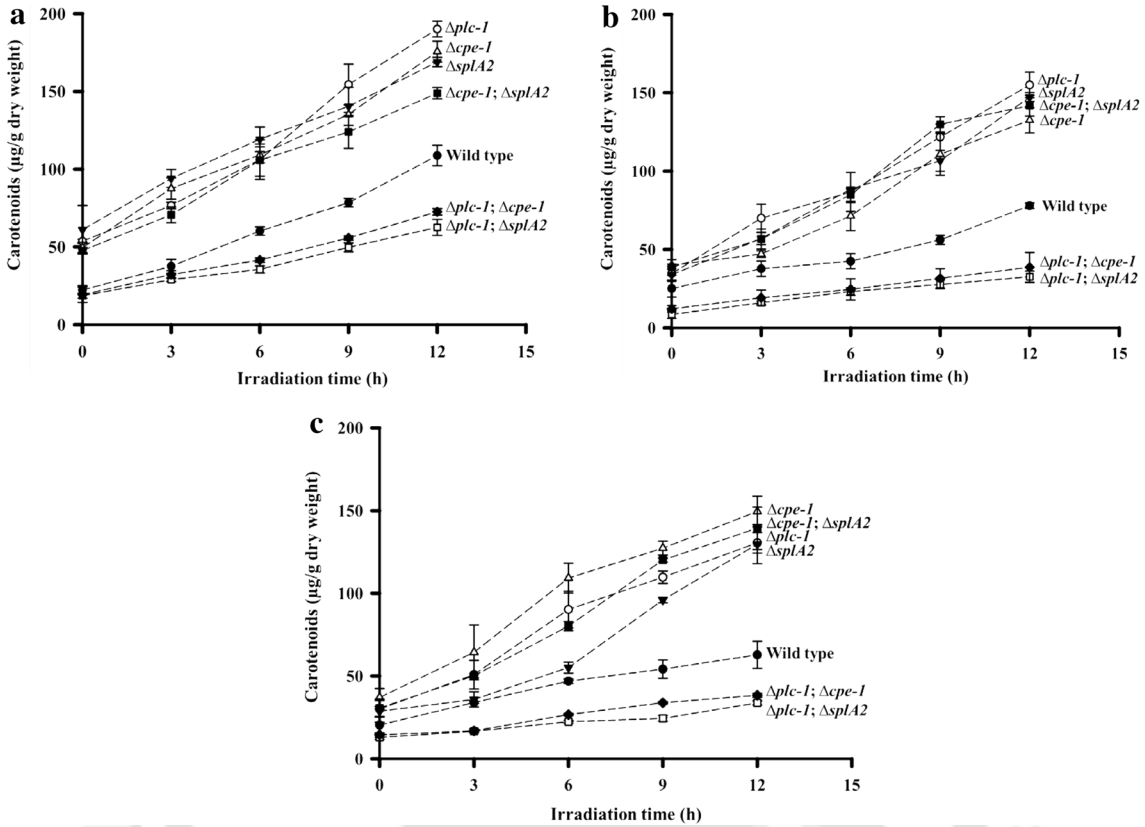

Fig. 4 Time-course analysis of carotenoid accumulation in the *N. crassa* strains. Strains were grown in VG liquid medium supplemented with 0.2% tween-80 and incubated initially at 30 °C in dark for 48 h and then at three different temperatures of **a** 8 °C, **b** 22 °C, and **c** 30 °C with simultaneous exposure to white light for 0, 3, 6, 9, and 12 h. Carotenoids accumulated in the mycelia were then extracted from the three temperatures at indicated times. Accumulated carotenoids are expressed as µg carotenoid per gram of dry weight. *Error bars* indicate standard deviations calculated from the data for three independent experiments ($n = 3$)

a sterile phenotype (Fig. 6a; Table S5). However, crosses involving the Δ*plc-1; ΔsplA2* and Δ*plc-1; Δcpe-1* double mutant as a male parent produced normal perithecia with abundant ascospores and showed a fertile phenotype (Fig. 6b; Table S5). In addition, crosses involving the Δ*cpe-1; ΔsplA2* double mutant produced normal perithecia, either as a male or a female parent and such crosses were fully fertile (Fig. S4). The ascospores produced from the different crosses had a similar survival percentage like the wild type strain (data not shown).

Transcription factor binding elements in the promoter region are known to regulate the expression of a gene; therefore, we analyzed the promoter region of the *plc-1, splA2*, and *cpe-1* by examining ~2 kb of the 5′-flanking genomic region of the respective genes. We identified putative binding sequences for several transcription regulators, including pheromone response elements, yeast cell cycle and metabolic regulator, yeast mating factors, and yeast stress response elements (Fig. 7a; Table S6). These regulatory sequences could be involved in regulating the expression of PLC-1, sPLA2, and CPE-1 during the sexual development of *N. crassa*. Identification of these transcriptional regulatory sequences in the upstream region of *plc-1, splA2*, and *cpe-1* genes prompted us to study the transcription levels of pheromone precursor coding genes such as *clock-controlled gene-4* (*ccg-4*; Bell-Pederson et al. 1996), *mating factor a-1* (*mfa-1*; Kim et al. 2002), and the mating pheromone signaling gene *female* and *male fertility-1* (*fmf-1*; Johnson 1979; Iyer et al. 2009) in the single and double mutants for *plc-1, splA2*, and *cpe-1* genes. We found a severe reduction of both *ccg-4* and *mfa-1* expression in Δ*plc-1; ΔsplA2* and Δ*plc-1; Δcpe-1* double mutants (Fig. 7b). Moreover, expression of *fmf-1* was also decreased in Δ*plc-1; ΔsplA2* and Δ*plc-1; Δcpe-1* double mutants (Fig. 7b). Therefore, these results suggested that interaction of *plc-1* with *splA2* and *cpe-1* might play a role in normal expression of pheromone signaling genes important for sexual development in *N. crassa*.

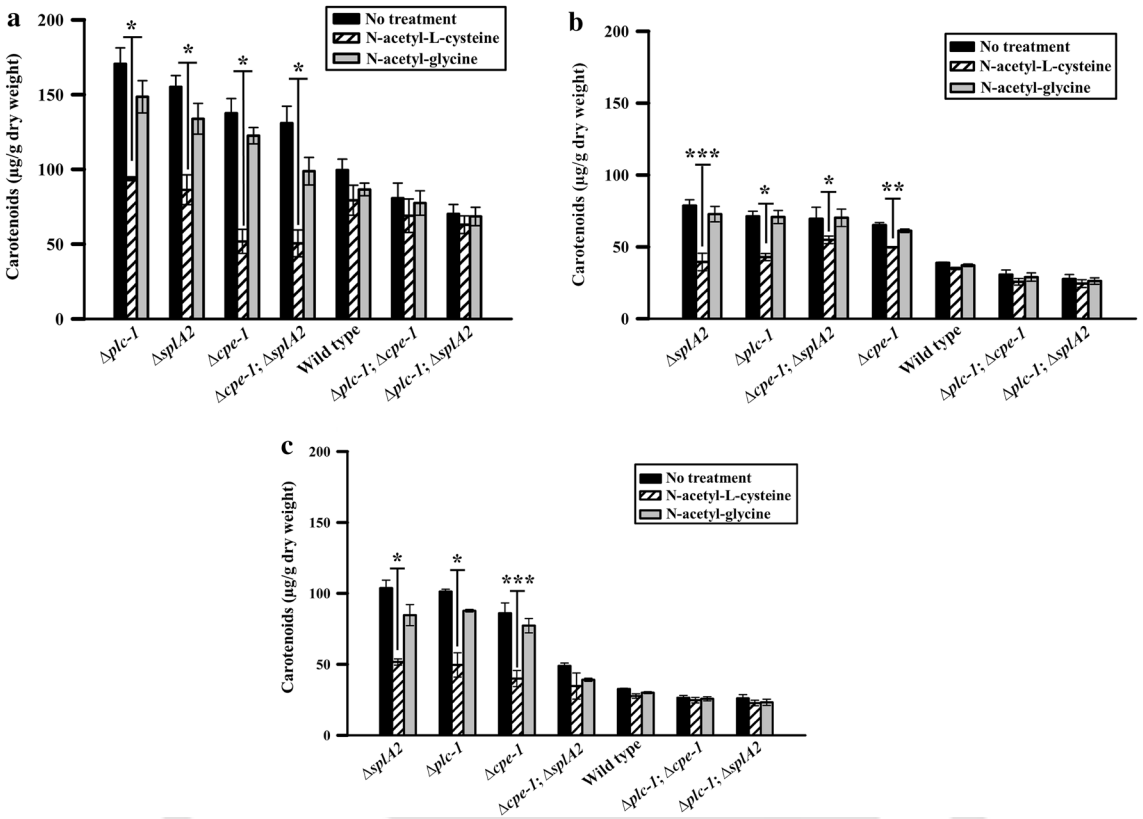

Fig. 5 Effect of antioxidant on carotenoid accumulation of the *N. crassa* strains. Cultures were incubated for 2 h in the presence of 1 mM N-acetyl-L-cysteine (NAC), and then exposed to white light at **a** 8 °C, **b** 22 °C, and **c** 30 °C for an additional 2 h. Carotenoids extracted from the indicated *N. crassa* strains are expressed as µg carotenoid per gram of dry weight. N-acetylglycine was used as a negative control. *Error bars* indicate standard deviations calculated from the data for three independent experiments ($n = 3$) with P values <0.05 (*), <0.01 (**), and <0.001 (***) compared with the wild type strain as measured by one-way ANOVA test

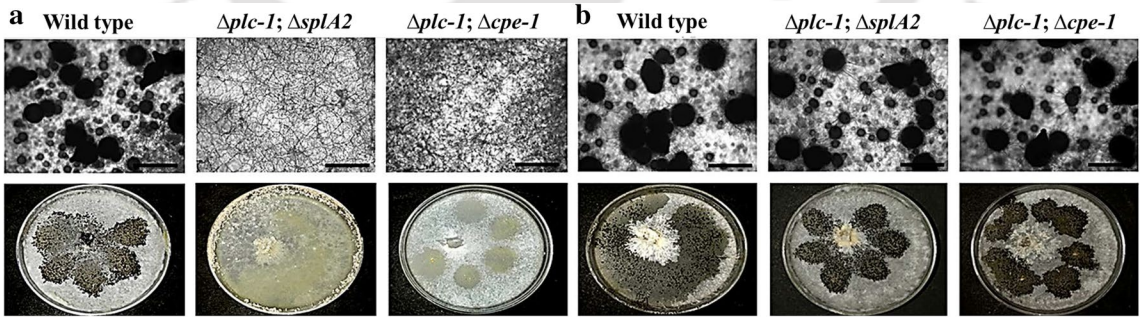

Fig. 6 Fertility assay of the *N. crassa* strains. Female parent was cultured on SCM at room temperature with constant light for 7 days and subsequently fertilized with the male parent. **a** Female fertility assay. Perithecia were absent in the SCM cultures of wild type as the male parent and either Δ*plc-1; ΔsplA2* or Δ*plc-1; Δcpe-1* strains as the female parent. **b** Male fertility assay. Black enlarged perithecia with matured ascospores were seen in SCM cultures of either Δ*plc-1; ΔsplA2* or Δ*plc-1; Δcpe-1* as a male parent and wild type as a female parent. Crosses involving wild type as both male and female parents were fertile. *Scale bar* 20 µm

Expression analysis of *plc-1*, *splA2*, and *cpe-1*

We determined the expression of *plc-1, splA2*, and *cpe-1* genes in the wild type and the mutants by qRT-PCR using the RNA extracted from 16-h-conidia from the corresponding strains. We found that expression of *cpe-1* was decreased in both Δ*plc-1* and Δ*splA2* mutants,

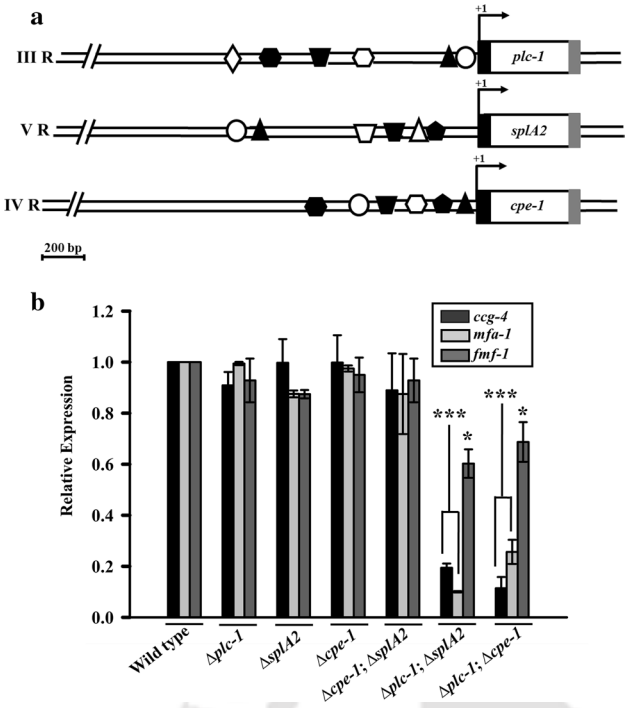

Fig. 7 Regulatory factors for transcription and mating pheromone signaling gene expression in SCM liquid cultures of the *N. crassa* strains. **a** Promoter sequences ~2 kb upstream of transcription start site of the *plc-1, splA2*, and *cpe-1* genes were predicted and analyzed using the Mat Inspector program (Quandt et al. 1995). Regulatory factors identified for each gene are listed in the Table S6 with their respective roles. *Arrows* indicate the transcription start site at +1 in the 5′ UTR (filled in *black*), and the ORFs filled in *grey* indicate the 3′ UTR. *Symbols* that depict different regulatory elements are: *open hexagon Aspergillus*/*Neurospora* nitrogen regulator, *closed hexagon* pheromone response element, *closed triangles* cAMP-element responsive binding proteins, *open triangles* yeast cell cycle and metabolic regulator, *open circles* carbon source responsive element, *closed diamonds* yeast heat shock factors, *closed pentagon* fungal basic leucine zipper family, *open trapezoid* yeast mating factor, *open diamonds* fungal GATA binding factors and *closed trapezoid* yeast stress response elements. **b** expression analysis of the *ccg-4, mfa-1*, and *fmf-1* genes. RNA was extracted from SCM liquid cultures and the expression of mating pheromone precursors were studied by qRT-PCR on three biological replicates for each of the *N. crassa* strain indicated. The relative expression of each gene was normalized to the expression of β-tubulin gene and expression values were compared with that of wild type. *Error bars* indicate standard deviations calculated from the data for three independent experiments ($n=3$) with *P* values <0.05 (*), <0.01 (**) and <0.001 (***) compared with the wild type strain as measured by one-way ANOVA test

while *plc-1* expression was decreased only in the Δ*cpe-1* mutant (Fig. S5). Similarly, expression of *splA2* gene was only moderately changed in Δ*plc-1* and Δ*cpe-1* mutants (Fig. S5). Therefore, this result suggested a possible transcriptional control feedback between *plc-1* and *cpe-1*, and regulation of *cpe-1* transcription by *splA2*.

Discussion

The Ca^{2+} signaling genes *plc-1, splA2*, and *cpe-1* play an important role in the regulation of $[Ca^{2+}]_c$, carotenoid accumulation, survival under stress conditions, and acquisition of thermotolerance in *N. crassa* (Barman and Tamuli 2015). In this study, we generated and analyzed the double mutants of the Ca^{2+} signaling genes *plc-1, splA2*, and *cpe-1* to understand the cell functions regulated by their genetic interactions. The Δ*plc-1;* Δ*splA2* and Δ*plc-1;* Δ*cpe-1* double mutants synthetically showed numerous phenotypic alterations such as growth defect, reduced biomass accumulation, failure to form aggregates in liquid growth conditions, reduced aerial hyphae, premature conidiation with reduced germination efficiency, inappropriate conidiation in submerged culture, reduced carotenoid accumulation, and female sterility. However, another double mutant Δ*cpe-1;* Δ*splA2* and all the parental single mutants showed phenotypes like the wild type strain.

The *plc-1* gene was shown to play a role in normal colony growth, hyphal shape, tip growth, and branching in *N. crassa* using a *plc-1* mutant (RIP *plc-1*) generated by repeat-induce point mutation (RIP; Selker and Garrett 1988; Gavric et al. 2007). However, in contrast to the RIP *plc-1* mutant, the colony and hyphal growth of the Δ*plc-1* mutant were similar to those of the wild type strain (Lew et al. 2015). Therefore, an alternative mechanism or functional redundancy could compensate for the loss of the *plc-1* gene in the Δ*plc-1* knockout mutant, but not in the RIP *plc-1* mutant expressing a dysfunctional gene product (Lew et al. 2015). The existence of the alternative or redundant mechanism is also supported by our findings that the Δ*plc-1;* Δ*splA2* and Δ*plc-1;* Δ*cpe-1* double mutants constantly showed a synthetic defect in morphology, growth, hyphal development, conidiation, and female fertility (Figs. 1, 2, 3, 6). The Δ*plc-1;* Δ*splA2* and Δ*plc-1;* Δ*cpe-1* double mutants also showed reduced accumulation of mycelial mass (Table S2) and failed to produce mycelial aggregates in shaking liquid cultures (data not shown), suggesting a defect in hyphal fusion and hyphal network formation in the double mutants.

The Δ*plc-1;* Δ*splA2* and Δ*plc-1;* Δ*cpe-1* double mutants showed conidiation as early as 12 h under growth-repressing conditions in glucose-rich medium and complete darkness (Fig. 2), and formed conidiophores even under non-sporulating conditions in submerged cultures (Fig. 3). In previous studies, formation of shorter aerial hyphae was found to be linked to premature and constitutive or non-repressing conidiation as seen in a putative histidine kinase *development and carotenogenesis control-1* (*dcc-1*), and a non-repressing conidiation protein *nonrepressible conidiation gene-1* (*nrc-1*) mutant, respectively (Kothe and Free 1998; Barba-Ostria et al. 2011). We found that both Δ*plc-1;*

Δ*splA2* and Δ*plc-1; Δcpe-1* double mutants enter the asexual developmental program earlier than either the wild type or parental single mutants. However, early conidiation in Δ*plc-1; ΔsplA2* and Δ*plc-1; Δcpe-1* double mutants might not have produced fully developed conidia leading to delayed germination. In addition, conidiation in submerged cultures of the Δ*plc-1; ΔsplA2* and Δ*plc-1; Δcpe-1* double mutants were correlated with the expression of conidiation specific gene, *con-10* (Fig. 3). The *con-10* gene was shown to express during conidiation in *N. crassa* (Roberts et al. 1988). These results further support the idea of a possible genetic interaction between *plc-1* and *splA2*, and *plc-1* and *cpe-1*, and indicate a role of these Ca^{2+}-signaling genes in normal conidiation.

Cultures of *N. crassa* produce characteristic orange pigmentation mainly due to the accumulation of the apocarotenoid neurosporoxanthin and variable amounts of its precursor carotenoids in the mycelia and asexual spores or conidia that are produced by the illuminated airborne mycelia (Zalokar 1954; Li and Schmidhauser 1995; Lauter et al. 1997; Estrada et al. 2008; Díaz-Sánchez et al. 2011; Avalos and Corrochano 2013; Barman and Tamuli 2015). Carotenoid biosynthesis in *N. crassa* is affected by both light and temperature, illumination at low temperature causes an increase in neurosporoxanthin accumulation, whereas illumination at normal temperature results in the accumulation of its carotenoid precursors (Harding et al. 1969; Harding 1974; Estrada et al. 2008; Díaz-Sánchez et al. 2011; Barman and Tamuli 2015). We found lower carotenoid accumulation after a 24 h illumination in cultures of Δ*plc-1; ΔsplA2* and Δ*plc-1; Δcpe-1* double mutants at three different temperatures of 8, 22, and 30 °C due to a slower carotenoid accumulation at different time points and this could explain their reduced mycelial pigmentation (Fig. 4; Table 2). In contrast, in a time course analysis, the Δ*plc-1, ΔsplA2, Δcpe-1*, and Δ*cpe-1; ΔsplA2* mutants showed an increased level of carotenoid accumulation after a 24 h illumination as compared to wild type (Fig. 4). Enhanced carotenoid accumulation was also observed in the catalase-3 deficient mutant, *cat-3*, and a Cu, Zn-superoxide dismutase mutant, *sod-1* (Michán et al. 2003; Yoshida and Hasunuma 2004). Increased carotenoid accumulation in the *sod-1* mutant was related to intracellular generation of ROS (Yoshida and Hasunuma 2004). ROS has also been reported to regulate carotenoid synthesis in other organisms, including *Phaffia rhodozyma*, where carotenoid synthesis was induced by singlet oxygen, and *Fusarium aquaeductuum*, where increased carotenoid accumulation in the mycelia was observed upon treatment with redox dyes under red light (Sundquist et al. 1994; Schroeder and Johnson 1995). Therefore, increased carotenoid accumulation in the Δ*plc-1, ΔsplA2, Δcpe-1*, and Δ*cpe-1; ΔsplA2* mutants could be due to an increased intracellular concentration of ROS as revealed by the reduction of carotenoid accumulation by the antioxidant NAC (Fig. 5).

N. crassa cultures when grown in low levels of nitrogen, light, and low temperatures enter the sexual phase of its life cycle and form multicellular female reproductive structures termed as protoperithecia (Perkins and Barry 1977; Nelson and Metzenberg 1992; Nelson 1996; Coppin et al. 1997). Specialized hyphae called trichogynes originate from the protoperithecia and undergo chemotropic growth towards a fertilizing cell of opposite mating type, and after fertilization, protoperithecia develop into perithecia enclosing multiple asci, each containing eight ordered ascospores (Raju 1992; Kim and Borkovich 2006). A few sexual development and pheromone related genes play an important role in the sexual development process in *N. crassa*. The chemotropic attraction of trichogyne towards a male cell is regulated by the G-protein-coupled receptors (GPCRs) PRE-1 and PRE-2 that recognize and bind to their respective pheromones MFA-1 and CCG-4, respectively (Bobrowicz et al. 2002; Kim et al. 2002, 2012; Kim and Borkovich 2004, 2006; Deka et al. 2016). PRE-1 and PRE-2 are homologous to the pheromone receptors Ste3p and Ste2p, and MFA-1 and CCG-4 are homologous to the pheromone precursor a- and α-mating factors of *Saccharomyces cerevisiae*, respectively (Pöggeler and Kück 2001; Bobrowicz et al. 2002; Kim et al. 2002; Kim and Borkovich 2006; Deka et al. 2016). Another pheromone related gene *fmf-1*, that encodes the female and male fertility gene in *N. crassa*, is a homologue of *Schizosaccharomyces pombe* transcription factor *ste11*. Both *fmf-1* and *ste11* play role in pheromone signaling for mating in *N. crassa* and *S. pombe*, respectively (Qin et al. 2003; Iyer et al. 2009). To understand the molecular basis of female sterility of the Δ*plc-1; ΔsplA2* and Δ*plc-1; Δcpe-1* double mutants, we determined the expression of the pheromone related genes *ccg-4, mfa-1*, and *fmf-1* considering an incubation period of 18–20 h to avoid conidiation induced by starvation in liquid cultures for nitrogen or glucose limitation in *N. crassa* (Müller and Russo 1989; Bobrowicz et al. 2002). We found reduced expression of *ccg-4, mfa-1*, and *fmf-1* in SCM liquid cultures of the Δ*plc-1; ΔsplA2* and Δ*plc-1; Δcpe-1* double mutants, and this was consistent with the female sterility phenotype in these two double mutants (Fig. 6; Table S5). In addition, in the promoter regions of the *plc-1, splA2*, and *cpe-1* genes, regulatory sequences for relevant transcription factors, including the pheromone response elements, yeast cell cycle and metabolic regulator, yeast mating factors and yeast stress response elements are found, which further support for the requirement of these genes during sexual development (Fig. 7; Table S6).

Thus, the Δ*plc-1; ΔsplA2* and Δ*plc-1; Δcpe-1* double mutants displayed several defects in vegetative and sexual phases in *N. crassa*. Therefore, effect of the Δ*plc-1; ΔsplA2*

and Δ*plc-1;* Δ*cpe-1* double mutants in vegetative growth and sexual development in *N. crassa* consistently suggested pleiotropic nature of these double mutants. Genetic interactions of the *plc-1, splA2*, and *cpe-1* genes might be involved in modulating cellular pathways controlled by Ca^{2+} signaling machinery in *N. crassa*. The PLC-1 catalyses the hydrolysis of PIP_2 to IP_3 and DAG that induces release of Ca^{2+} from intracellular stores and activation of PKC, respectively (Rhee and Bae 1997). The $sPLA_2$ is a secretory enzyme that hydrolyzes the *sn-2* ester linkage of glycerophospholipids in a Ca^{2+} dependent manner and regulates a range of biological functions (Ghannoum 2000; Dennis et al. 2011; Cavazzini et al. 2013). In *N. crassa*, two $sPLA_2$ proteins encoded by the NCU06650 and NCU09423 genes were characterized (Takayanagi et al. 2015). We found that these two $sPLA_2$ proteins show 37% identity (*e*-value 1e-38) in a BLAST analysis (https://blast.ncbi.nlm.nih.gov/Blast.cgi; Altschul et al. 1990). Moreover, the NCU06650, but not the NCU09423, encoded protein contains a putative calmodulin (CaM) binding site with the amino acid sequence TCHALANVYYAAVREFGRTKGELQ (http://calcium.uhnres.utoronto.ca/ctdb/ctdb/sequence.html; Yap et al. 2000), and the NCU06650 encoded protein was classified as a member of the Ca^{2+} and/or CaM binding proteins (Borkovich et al. 2004). In addition, a low-affinity Ca^{2+}/H^+ exchanger is activated in the presence of high $[Ca^{2+}]_c$ (also designated as $[Ca^{2+}]_i$), requires a H^+ or pH gradient maintained by a H^+-transporting ATPase and a functional synaptic vesicular protein synaptotagmin-1 (SYT-1) that contains two C2 domains for Ca^{2+}-binding, for buffering the $[Ca^{2+}]_c$ level in the rat pheochromocytoma PC12 cells (Cordeiro et al. 2013). Taken together, our findings suggest that the Ca^{2+} release from intracellular stores, which is induced by IP_3 generated by the PLC-1, and/or activated PKC might be necessary for the $sPLA_2$ mediated signaling for normal growth and development in *N. crassa*. In addition, under the conditions inducing sexual development, release of Ca^{2+} mediated by the PLC-1 and the $[Ca^{2+}]_c$ buffering activity of the CPE-1 Ca^{2+}/H^+ exchanger might be important in the regulation of the pheromone signaling genes necessary for fertility. Our current understandings on the functions of the $sPLA_2$ proteins have mainly come from the mammalian enzymes, however, knowledge about their fungal counterparts has remained very limited. Therefore, a detailed insight into the functions of the *N. crassa* $sPLA_2$ encoded by the NCU06650 would be helpful to understand the functions of this largely uncharacterized group in fungi. Similarly, knowledge about the functions of the CPE-1 Ca^{2+}/H^+ exchanger would be helpful to understand the biological role of this unique exchanger. Interestingly, the CPE-1 Ca^{2+}/H^+ exchanger encoded by the NCU06366 was found significantly different from all the Ca^{2+}-transporters identified in *N. crassa, Magnaporthe grisea*, and *S. cerevisiae* in a phylogenetic analysis (Zelter et al. 2004). This study revealed that the *plc-1, splA2*, and *cpe-1* genes synthetically play an important role in both vegetative and sexual development in *N. crassa* that could provide deeper insight into the future understanding of how filamentous fungi are able to respond and adapt to diverse environments.

Acknowledgements The FGSC generously waived charges for strains. The FGSC was supported by NSF Grant BIR-9222772. AB was supported by a Research Fellowship from the Ministry of Human Resource Development, Government of India. We thank IIT Guwahati, and Department of Biotechnology, Government of India (BT/PR3635/BCE/8/892/2012), for partial financial support.

References

Altschul SF, Madden TL, Schäffer AA, Zhang J, Zhang Z, Miller W, Lipman DJ (1990) Gapped BLAST and PSI-BLAST: a new generation of protein database search programs. Nucleic Acids Res 25:3389–3402

Avalos J, Corrochano LM (2013) Carotenoid biosynthesis in *Neurospora*. In: Kasbekar DP, McCluskey K (eds) Neurospora: genomics and molecular biology. Caister Academic Press, Norfolk, pp 227–241

Barba-Ostria C, Lledías F, Georgellis D (2011) The *Neurospora crassa* DCC-1 protein, a putative histidine kinase, is required for normal sexual and asexual development and carotenogenesis. Eukaryot Cell 12:1733–1739

Barman A, Tamuli R (2015) Multiple cellular roles of *Neurospora crassa plc-1*, *splA2*, and *cpe-1* in regulation of cytosolic free calcium, carotenoid accumulation, stress responses, and acquisition of thermotolerance. J Microbiol 53:226–235

Bell-Pederson D, Shinohara ML, Loros JJ, Dunlap JC (1996) Circadian clock-controlled genes isolated from *Neurospora crassa* are late night- to early morning-specific. Proc Natl Acad Sci USA 93:13096–13101

Berridge MJ, Bootman MD, Lipp P (1998) Calcium—a life and death signal. Nature 395:645–648

Bobrowicz P, Pawlak R, Correa A, Bell-Pedersen D, Ebbole DJ (2002) The *Neurospora crassa* pheromone precursor genes are regulated by the mating type locus and the circadian clock. Mol Microbiol 45:795–804

Boilard E, Lai Y, Larabee K, Balestrieri B, Ghomashchi F, Fujioka D, Gobezie R, Coblyn JS, Weinblatt ME, Massarotti EM, Thornhill TS, Divangahi M, Remold H, Lambeau G, Gelb MH, Arm JP, Lee DM (2010) A novel anti-inflammatory role for secretory phospholipase A2 in immune complex-mediated arthritis. EMBO Mol Med 2:172–187. doi:10.1002/emmm.201000072

Bootman MD, Collins TJ, Peppiatt CM, Prothero LS, Mac-Kenzie L, De Smet P, Travers M, Tovey SC, Seo JT, Berridge MJ, Ciccolini F, Lipp P (2001) Calcium signalling—an overview. Semin Cell Dev Biol 12:3–10

Borkovich KA, Alex LA, Yarden O, Freitag M, Turner GE, Read ND, Seiler S, Bell-Pedersen D, Paietta J, Plesofsky N, Plamann M, Goodrich-Tanrikulu M, Schulte U, Mannhaupt G, Nargang FE, Radford A, Selitrennikoff C, Galagan JE, Dunlap JC, Loros JJ, Catcheside D, Inoue H, Aramayo R, Polymenis M, Selker EU, Sachs MS, Marzluf GA, Paulsen I, Davis R, Ebbole DJ, Zelter A, Kalkman ER, O'Rourke R, Bowring F, Yeadon J, Ishii C, Suzuki K, Sakai W, Pratt R (2004) Lessons

from the genome sequence of *Neurospora crassa*: tracing the path from genomic blueprint to multicellular organism. Microbiol Mol Biol Rev 68:1–108
Cavazzini D, Meschi F, Corsini R, Bolchi A, Rossi GL, Einsle O, Ottonello S (2013) Autoproteolytic activation of a symbiosis-regulated truffle phospholipase A2. J Biol Chem 288:1533–1547
Chin D, Means AR (2000) Calmodulin: a prototypical calcium sensor. Trends Cell Biol 10:322–328
Clapham DE (2007) Calcium signaling. Cell 131:1047–1058
Coppin E, Debuchy R, Arnaise S, Picard M (1997) Mating types and sexual development in filamentous ascomycetes. Microbiol Mol Biol Rev 61:411–428
Cordeiro JM, Boda B, Gonçalves PP, Dunant Y (2013) Synaptotagmin 1 is required for vesicular Ca^{2+}/H^{+}-antiport activity. J Neurochem 126:37–46. doi:10.1111/jnc.12278
Davis RH, De Serres FJ (1970) Genetic and microbiological research techniques for *Neurospora crassa*. Methods Enzymol 71:79–143
Deka R, Tamuli R (2013) *Neurospora crassa ncs-1, mid-1* and *nca-2* double-mutant phenotypes suggest diverse interaction among three Ca^{2+}-regulating gene products. J Genet 92:559–563
Deka R, Kumar R, Tamuli R (2011) *Neurospora crassa* homologue of neuronal calcium sensor-1 has a role in growth, calcium stress tolerance, and ultraviolet survival. Genetica 139:885–894
Deka R, Ghosh A, Tamuli R, Borkovich KA (2016) Heterotrimeric G proteins. In: Drik H (ed) The mycota IV. Springer, Berlin
Dennis EA, Cao J, Hsu YH, Magrioti V, Kokotos G (2011) Phospholipase A2 enzymes: physical structure, biological function, disease implication, chemical inhibition, and therapeutic intervention. Chem Rev 111:6130–6185. doi:10.1021/cr200085w
Díaz-Sánchez V, Estrada AF, Trautmann D, Limón MC, Al-Babili S, Avalos J (2011) Analysis of *al-2* mutations in *Neurospora*. PLoS One 6:e21948
Dodd AN, Kudla J, Sanders D (2010) The language of calcium signaling. Annu Rev Plant Biol 61:593–620
Estrada AF, Youssar L, Scherzinger D, Al-Babili S, Avalos J (2008) The *ylo-1* gene encodes an aldehyde dehydrogenase responsible for the last reaction in the *Neurospora* carotenoid pathway. Mol Microbiol 69:1207–1220
Gadd GM (1994) Signal transduction in fungi. In: Gow NAR, Gadd GM (eds) The growing fungus. Chapman and Hall, London, pp 183–210
Galagan JE, Calvo SE, Borkovich KA, Selker EU, Read ND, Jaffe D, FitzHugh W, Ma LJ, Smirnov S, Purcell S, Rehman B, Elkins T, Engels R, Wang S, Nielsen CB, Butler J, Endrizzi M, Qui D, Ianakiev P, Bell-Pedersen D, Nelson MA, Werner-Washburne M, Selitrennikoff CP, Kinsey JA, Braun EL, Zelter A, Schulte U, Kothe GO, Jedd G, Mewes W, Staben C, Marcotte E, Greenberg D, Roy A, Foley K, Naylor J, Stange-Thomann N, Barrett R, Gnerre S, Kamal M, Kamvysselis M, Mauceli E, Bielke C, Rudd S, Frishman D, Krystofova S, Rasmussen C, Metzenberg RL, Perkins DD, Kroken S, Cogoni C, Macino G, Catcheside D, Li W, Pratt RJ, Osmani SA, DeSouza CP, Glass L, Orbach MJ, Berglund JA, Voelker R, Yarden O, Plamann M, Seiler S, Dunlap J, Radford A, Aramayo R, Natvig DO, Alex LA, Mannhaupt G, Ebbole DJ, Freitag M, Paulsen I, Sachs MS, Lander ES, Nusbaum C, Birren B (2003) The genome sequence of the filamentous fungus *Neurospora crassa*. Nature 422:859–868
Gavric O, dos Santos DB, Griffiths A (2007) Mutation and divergence of the phospholipase C gene in *Neurospora crassa*. Fungal Genet Biol 44:242–249
Ghannoum MA (2000) Potential role of phospholipases in virulence and fungal pathogenesis. Clin Microbiol Rev 13:122–143
Gohain D, Deka R, Tamuli R (2016) Identification of critical amino acid residues and functional conservation of the *Neurospora crassa* and *Rattus norvegicus* orthologues of neuronal calcium sensor-1. Genetica 144:665–674
Harding RW (1974) The effect of temperature on photo-induced carotenoid biosynthesis in *Neurospora crassa*. Plant Physiol 54:142–147
Harding RW, Huang PC, Mitchell HK (1969) Photochemical studies of the carotenoid biosynthetic pathway in *Neurospora crassa*. Arch Biochem Biophys 129:696–707
Ivey FD, Hodge PN, Turner GE, Borkovich KA (1996) The $G\alpha_i$ homologue *gna-1* controls multiple differentiation pathways in *Neurospora crassa*. Mol Biol Cell 7:1283–1297
Ivey FD, Kays AM, Borkovich KA (2002) Shared and independent roles for a $G\alpha_i$ protein and adenylate cyclase in regulating development and stress responses in *Neurospora crassa*. Eukaryot Cell 1:634–642
Iyer SV, Ramakrishnan M, Kasbekar DP (2009) *Neurospora crassa fmf-1* encodes the homologue of the *Schizosaccharomyces pombe* Ste11p regulator of sexual development. J Genet 88:33–39
Johnson TE (1979) A Neurospora mutation that arrests perithecial development as either male or female parent. Genetics 92:1107–1120
Kays AM, Rowley PS, Baasiri RA, Borkovich KA (2000) Regulation of conidiation and adenylyl cyclase levels by the Gα protein GNA-3 in *Neurospora crassa*. Mol Cell Biol 20:7693–7705
Kim H, Borkovich KA (2004) A pheromone receptor gene, *pre-1*, is essential for mating type-specific directional growth and fusion of trichogynes and female fertility in *Neurospora crassa*. Mol Microbiol 52:1781–1798
Kim H, Borkovich KA (2006) Pheromones are essential for male fertility and sufficient to direct chemotropic polarized growth of trichogynes during mating in *Neurospora crassa*. Eukaryot Cell 5:544–554
Kim H, Metzenberg RL, Nelson MA (2002) Multiple functions of *mfa-1*, a putative pheromone precursor gene of *Neurospora crassa*. Eukaryot Cell 1:987–989
Kim H, Wright SJ, Park G, Ouyang S, Krystofova S, Borkovich KA (2012) Roles for receptors, pheromones, G proteins, and mating type genes during sexual reproduction in *Neurospora crassa*. Genetics 190:1389–1404
Kothe GO, Free SJ (1998) The isolation and characterization of *nrc-1* and *nrc-2*, two genes encoding protein kinases that control growth and development in *Neurospora crassa*. Genetics 149:117–130
Kumar R, Tamuli R (2014) Calcium/calmodulin-dependent kinases are involved in growth, thermotolerance, oxidative stress survival, and fertility in *Neurospora crassa*. Arch Microbiol 196:295–305
Lauter FR, Yamashiro CT, Yanofsky C (1997) Light stimulation of conidiation in *Neurospora crassa*: studies with the wild-type strain and mutants *wc-1, wc-2* and *acon-2*. J Photochem Photobiol 37:203–211
Laxmi V, Tamuli R (2015) The *Neurospora crassa cmd, trm-9*, and *nca-2* play a role in growth, development, and survival in stress conditions. Genom Appl Biol 6:1–12
Laxmi V, Tamuli R (2016) The calmodulin gene in *Neurospora crassa* is required for normal vegetative growth, ultraviolet survival, and sexual development. Arch Micro Biol. doi:10.1007/s00203-016-1319-0 **(Epub ahead of print)**
Lew RR, Giblon RE, Lorenti MS (2015) The phenotype of a phospholipase C (*plc-1*) mutant in a filamentous fungus, *Neurospora crassa*. Fungal Genet Biol 82:158–167. doi:10.1016/j.fgb.2015.07.007
Li C, Schmidhauser TJ (1995) Developmental and photoregulation of *al-1* and *al-2*, structural genes for two enzymes essential for carotenoid biosynthesis in *Neurospora*. Dev Biol 169:90–95
Livak KJ, Schmittgen TD (2001) Analysis of relative gene expression data using real-time quantitative PCR and the $2^{-\Delta\Delta Ct}$ method. Methods 25:402–408

Madi L, McBride SA, Bailey LA, Ebbole DJ (1997) *rco-3*, a gene involved in glucose transport and conidiation in *Neurospora crassa*. Genetics 146:499–508

McCluskey K, Wiest A, Plamann M (2010) The Fungal Genetics Stock Center: a repository for 50 years of fungal genetics research. J Biosci 35:119–126

Michán S, Lledías F, Hansberg W (2003) Asexual development is increased in *Neurospora crassa cat-3*-null mutant strains. Eukaryot Cell 2:798–808

Müller BT, Russo VRA (1989) Nitrogen starvation or glucose limitation induces conidiation in constantly shaken liquid cultures of *Neurospora crassa*. Fungal Genet Newslett 36:58–60

Murakami M, Kudo I (2004) Secretory phospholipase A_2. Biol Pharm Bull 27:1158–1164

Nakahama T, Nakanishi Y, Viscomi AR, Takaya K, Kitamoto K, Ottonello S, Arioka M (2010) Distinct enzymatic and cellular characteristics of two secretory phospholipases A_2 in the filamentous fungus *Aspergillus oryzae*. Fungal Genet Biol 47:318–331

Nelson MA (1996) Mating systems in ascomycetes: a romp in the sac. Trends Genet 12:69–74

Nelson MA, Metzenberg RL (1992) Sexual development genes of *Neurospora crassa*. Genetics 132:149–162

Perkins DD, Barry EG (1977) The cytogenetics of *Neurospora*. Adv Genet 19:133–285

Pöggeler S, Kück U (2001) Identification of transcriptionally expressed pheromone receptor genes in filamentous ascomycetes. Gene 280:9–17

Qin J, Kang W, Leung B, McLeod M (2003) Ste11p, a high-mobility-group box DNA-binding protein, undergoes pheromone- and nutrient-regulated nuclear-cytoplasmic shuttling. Mol Cell Biol 23:3253–3264

Quandt K, Frech K, Karas H, Wingender E (1995) MatInd and MatInspector: new fast and versatile tools for detection of consensus matches in nucleotide sequence data. Nucleic Acids Res 23:4878–84

Raju NB (1992) Genetic control of the sexual cycle in *Neurospora*. Mycol Res 96:241–262

Rhee SG (2001) Regulation of phosphoinositide-specific phospholipase C. Annu Rev Biochem 70:281–312

Rhee SG, Bae YS (1997) Regulation of phosphoinositide-specific phospholipase C isozymes. J Biol Chem 272:15045–15048

Roberts AN, Berlin V, Hager KM, Yanofsky C (1988) Molecular analysis of a *Neurospora crassa* gene expressed during conidiation. Mol Cell Biol 8:2411–2418

Rodriguez-Amaya DB, Kimura M (2004) Harvest plus handbook for carotenoid analysis. Harvest Plus Technical Monograph 2. International Food Policy Research Institute (IFPRI) and International Center for Tropical Agriculture (CIAT), Washington, DC

Schaloske RH, Dennis EA (2006) The phospholipase A2 superfamily and its group numbering system. Biochim Biophys Acta 1761:1246–1259

Schroeder WA, Johnson EA (1995) Singlet oxygen and peroxyl radicals regulate carotenoid biosynthesis in *Phaffia rhodozyma*. J Biol Chem 270:18374–18379

Selker EU, Garrett PW (1988) DNA sequence duplications trigger gene inactivation in *Neurospora crassa*. Proc Natl Acad Sci USA 85:6870–6874

Shaw BD, Hoch HC (2000) Ca^{2+} regulation of *Phyllosticta ampelicida* pycnidiospore germination and appressorium formation. Fungal Genet Biol 31:43–53

Soragni E, Bolchi A, Balestrini R, Gambaretto C, Percudani R, Bonfante P, Ottonello S (2001) A nutrient-regulated, dual localization phospholipase A_2 in the symbiotic fungus *Tuber borchii*. EMBO J 20:5079–5090

Sundquist AR, Briviba K, Sies H (1994) Singlet oxygen quenching by carotenoids. Methods Enzymol 234:384–388

Takayanagi A, Miyakawa T, Asano A, Ohtsuka J, Tanokura M, Arioka M (2015) Expression, purification, refolding, and enzymatic characterization of two secretory phospholipases A_2 from *Neurospora crassa*. Protein Expr Purif 115:69–75

Tamuli R, Kumar R, Deka R (2011) Cellular roles of neuronal calcium sensor-1 and calcium/calmodulin-dependent kinases in fungi. J Basic Microbiol 51:120–128

Tamuli R, Kumar R, Srivastava DA, Deka R (2013) Calcium signaling. In: Kasbekar DP, McCluskey K (eds) Neurospora: genomics and molecular biology, Caister Academic Press, Norfolk, pp 35–57

Tamuli R, Deka R, Borkovich KA (2016) Calcineurin subunits A and B interact to regulate growth and asexual and sexual development in *Neurospora crassa*. PLoS One 11:e0151867

Vogel HJ (1964) Distribution of lysine pathways among fungi: evolutionary implications. Am Nat 98:435–446

Williams RL, Katan M (1996) Structural views of phosphoinositide-specific phospholipase C: signalling the way ahead. Structure 4:1387–1394

Yamamoto T, Takeuchi H, Kanematsu T, Allen V, Yagisawa H, Kikkawa U, Watanabe Y, Nakasima A, Katan M, Hirata M (1999) Involvement of EF hand motifs in the Ca^{2+}-dependent binding of the pleckstrin homology domain to phosphoinositides. Eur J Biochem 265:481–490

Yang Q, Borkovich KA (1999) Mutational activation of a Gαi causes uncontrolled proliferation of aerial hyphae and increased sensitivity to heat and oxidative stress in *Neurospora crassa*. Genetics 151:107–117

Yang Q, Poole SI, Borkovich KA (2002) A G-protein β subunit required for sexual and vegetative development and maintenance of normal G alpha protein levels in *Neurospora crassa*. Eukaryot Cell 1:378–390

Yap KL, Kim J, Truong K, Sherman M, Yuan T, Ikura M (2000) Calmodulin target database. J Struct Funct Genom 1:8–14

Yoshida Y, Hasunuma K (2004) Reactive oxygen species affect photomorphogenesis in *Neurospora crassa*. J Biol Chem 279:6986–6993

Zalokar M (1954) Studies on biosynthesis of carotenoids in *Neurospora crassa*. Arch Biochem Biophys 50:71–80

Zelter A, Bencina M, Bowman BJ, Yarden O, Read ND (2004) A comparative genomic analysis of the calcium signaling machinery in *Neurospora crassa, Magnaporthe grisea*, and *Saccharomyces cerevisiae*. Fungal Genet Biol 41:827–841